NOAA Technical Report NOS NGS 65

The National Adjustment of 2011

Alignment of Passive GNSS Control with the Three Frames of the North American Datum of 1983 at Epoch 2010.00: NAD83 (2011), NAD83 (PA11), and NAD83 (MA11).

Michael L. Dennis
July 29, 2020

Document version log

Document available at geodesy.noaa.gov/library/pdfs/NOAA_TR_NOS_NGS_0065.pdf

Ver.	Date	Changes
1	07/29/2020	Original release

Executive Summary

Background

Briefly stated, the mission of NOAA's National Geodetic Survey (NGS) is to define, maintain, and provide access to the National Spatial Reference System (NSRS). The NSRS is the official reference system for latitude, longitude, height, scale, gravity, and orientation throughout the United States and its territories. The NSRS is the foundation for the nation's transportation, mapping, and charting infrastructure. It supports a multitude of scientific and engineering applications.

As part of continuing efforts to improve the NSRS, on June 30, 2012, NGS completed the computational and database loading phases of the National Adjustment of 2011 (NA2011) Project. The NA2011 Project concludes with the publication of this report. The project consisted of a nationwide adjustment of over 80,000 NGS *passive* control marks (physical marks, such as brass bench mark discs that can be occupied with survey equipment) positioned using Global Navigation Satellite System (GNSS) technology. The adjustment was constrained to current North American Datum of 1983 (NAD 83) latitude, longitude, and ellipsoid heights of NGS Continuously Operating Reference Stations (CORSs). The NOAA CORS Network is an *active* control system consisting of permanently mounted GNSS antennas, and the network is the *geometric foundation* of the NSRS. Constraining the adjustment to the CORSs optimally aligned the GNSS passive control with the active control, providing a unified reference frame to serve the nation's geometric positioning needs.

All available CORSs data collected from January 1, 1994, through April 16, 2011, were re-processed in the NGS initial *Multi-Year CORS Solution (MYCS1)* project, completed in September 2011. NAD 83 coordinates were determined for 2064 of the MYCS1 CORSs, and these coordinates constituted a new realization of the three NAD 83 reference frames, referred to as *NAD 83 (2011) epoch 2010.00*, *NAD 83 (PA11) epoch 2010.00*, and *NAD 83 (MA11) epoch 2010.00*. The realization names have two parts: the *datum tag* in parentheses following "NAD 83," and the *epoch* in decimal years. The datum tag refers to the year the realization was completed (2011) and the tectonic plate to which the coordinates are referenced (*2011* refers to the North America plate, *PA11* to the Pacific plate, and *MA11* to the Mariana plate). The 2010.00 epoch is a date indicating the location of the control marks on January 1, 2010—an important consideration in tectonically active areas (such as the western United States). Although the marks are referenced to three different tectonic plates, all refer to a common 2010.00 epoch. In this way, the CORS coordinates (and thus the passive marks constrained to the CORSs) are consistent across both space and time.

Summary of results

To compute passive control coordinates, 4267 individual GNSS survey projects stored in the NGS Integrated Data Base were combined to create networks suitable for least squares adjustment. Combining the projects resulted in 81,055 marks interconnected by 424,721 differential vectors computed from GNSS observations made between April 1983 and December 2011, as shown in Figure ES.1. Of these vectors, 21,603 (5.1%) were rejected (disabled) as part

of the network analyses and thus did not contribute to the final computed coordinates. A total of 1195 of the marks in the networks were CORSs with coordinates determined in the MYCS1 realization of the three NAD 83 frames. By constraining the adjustments to the MYCS1 results for these CORSs, all passive marks with NGS-published NAD 83 epoch 2010.00 coordinates are consistent with the NOAA CORS Network and results obtained using the NGS *Online Positioning User Service* (*OPUS*).

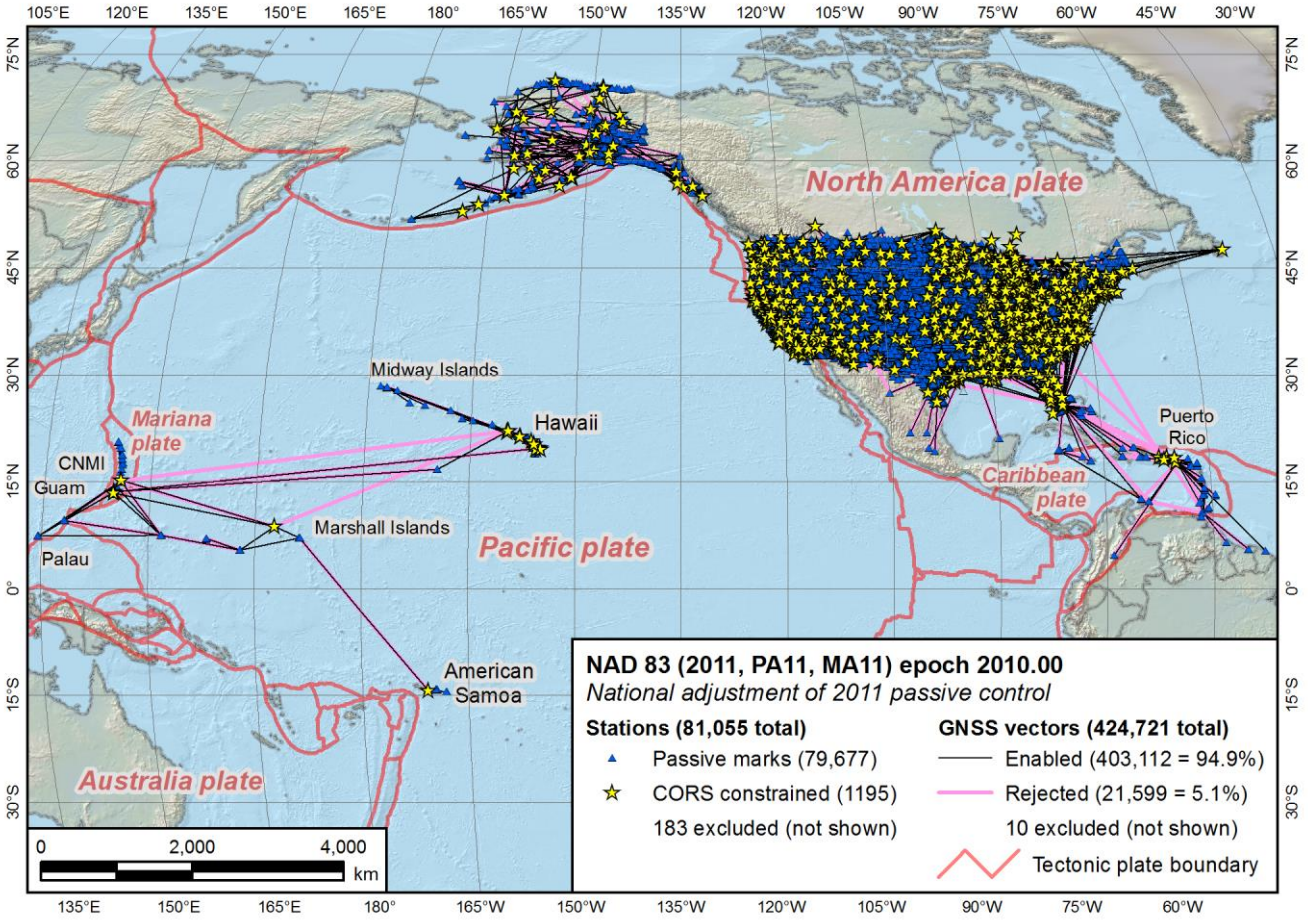

Figure ES.1. GNSS networks and marks in the National Adjustment of 2011 (NA2011) Project.

Because of a lack of vector connections between the conterminous United States (CONUS), Alaska, and the Pacific, these three regions were each adjusted separately, with marks in the Caribbean being both connected to and adjusted with those in CONUS. Marks in CONUS, Alaska, and the Caribbean were referenced to the North America tectonic plate. Pacific marks were referenced to either the Pacific or Mariana tectonic plate, depending on location. Marks in the central Pacific, including Hawaii, American Samoa, and the Marshall Islands, were referenced to the Pacific plate. Western Pacific marks, including those on Guam and the Commonwealth of the Northern Mariana Islands (CNMI), were referenced to the Mariana plate.

The number of marks and vectors for each region is given in Table ES.1, with CONUS split into a Primary and Secondary network. The split was done for the reasons given later in this

summary and was based mainly on the age of the observations, with the Secondary network consisting primarily of vectors observed before 1994. Connection between the Primary and Secondary networks was provided by 5321 marks (including 45 CORSs) that had vectors in both networks. As a consequence of these marks in common, the number in each network is larger than that shown in Table ES.1, with 62,364 marks (including 1097 CORSs) in the Primary network, and 22,503 marks (including only 45 CORSs) in the Secondary network. The large size of the two CONUS networks required using a Helmert blocking strategy for the adjustments. Helmert blocking breaks a large network into separate (but connected) smaller sub-network "blocks" to reduce computation time. The blocks are then each adjusted individually and combined to provide results identical to what would be obtained if the entire adjustment were performed simultaneously.

Table ES.1. Number of projects, marks, and vectors in NA2011 Project.

Network	Number of projects	Number of marks				GNSS vectors		
		Total	CORSs	Passive		Total	Rejected	Percent rejected
				Total	Published			
Overall	**4267**	**81,055**	**1195**	**79,860**	**74,893**	**424,721**	**21,603**	**5.09%**
Referenced to North America tectonic plate (includes marks in the Caribbean)								
CONUS overall	4086	79,546	1113	78,433	73,512	420,023	21,231	5.05%
Primary*	3472	62,172	1096	61,076	56,777	335,530	10,279	3.06%
Secondary*	614	17,374	17	17,357	16,735	84,493	10,952	12.96%
Alaska	142	969	58	911	865	2846	314	11.03%
Referenced to Pacific or Mariana tectonic plate, as indicated								
Pacific overall**	39	540	24	516	516	1852	58	3.13%
Pacific plate	**	363	18	345	345	**	**	**
Mariana plate	**	177	6	171	171	**	**	**

* *Includes 5321 marks in both CONUS Primary and Secondary networks, so actual number of marks in each networks is larger than shown (the network assigned to marks in both networks was based on the source of final coordinates). Total number of marks in the Primary network is 62,364 = 62,172 + 192 Secondary marks, and total number in the Secondary network is 22,503 = 17,374 + 5129 Primary marks.*

** *Entire Pacific network was adjusted for both the Pacific and Mariana plates, with individual marks referenced to different tectonic plates based on location.*

As shown in Table ES.1, results of the 2011 national adjustments are published (publicly available) for 74,893 of the 79,860 passive control marks in the NA2011 networks. Of the 4967 unpublished marks, most (4695, or 94.5%) are airport features, such as runway endpoints determined in Federal Aviation Administration (FAA) surveys, and are not suitable for use as geodetic control. The remaining 272 consist of: one IGS mark; one mark in Hawaii unconnected to any marks in the Pacific (only connected to a mark on Alaska); 88 marks located outside the United States and its territories; and 182 CONUS marks excluded from the final adjustments because they lacked enabled vector connections (due to splitting the CONUS

network into Primary and Secondary). Where possible, these 182 marks will be reconnected to the network in later individual adjustments (100 of these marks are unpublishable FAA features).

Median network accuracy estimates and coordinate shifts are given in Table ES.2 for the final constrained NA2011 adjustments. The median network accuracy for all marks was 0.9 cm horizontal and 1.5 cm vertical (i.e., ellipsoid height) at the 95% confidence level. The accuracies varied by network, with the largest median values in the Alaska network (3.7 cm horizontal and 6.2 cm in ellipsoid height). These large values were due to the Alaska network being dominated by old vectors, a lack of long-established CORSs, and tectonic activity. Note that accuracy values in Table ES.2 do not include so-called "no-check" marks (i.e., mark determined by only a single enabled vector); 2134 passive no-check marks were present in the final set of NA2011 networks. Network and local accuracy estimates for individual marks (including no-check marks) are available through various NGS products, such as Datasheets and control mark shapefiles.

Table ES.2. Summary of NA2011 network final accuracies and marks shifts for passive control.

Network	Median network accuracy at 95% confidence (cm)			Median shift from previous published coordinates (cm)				
	Number*	Horizontal	Ellipsoid ht	Number**	North	East	Up	Horiz
Overall	**77,560**	**0.88**	**1.49**	**79,677*** **	**-0.1**	**+1.8**	**-2.0**	**1.9**
CONUS overall	76,423	0.87	1.47	78,251***	-0.1	+1.8	-2.0	1.9
Primary*	59,979	0.74	1.23	60,928	-0.1	+1.8	-2.1	1.9
Secondary*	16,444	1.63	3.45	17,323***	-0.2	+1.8	-1.8	2.0
Alaska	756	3.67	6.19	910	+1.8	-1.7	+1.0	6.6
Pacific plate	264	1.49	3.99	345	-1.2	+0.7	-1.5	2.3
Mariana plate	117	1.60	3.10	171	+0.8	-1.9	+2.1	2.6

** Does not include no-check marks or CORSs constrained in the adjustment.*

*** Does not include CORSs constrained in the adjustment.*

**** One less mark with height shift due to one mark without a previously published ellipsoid height.*

The median change in coordinates from the previous published values was approximately 2 cm horizontally and vertically. However, some mark coordinates changed by more than 1 meter horizontally and up to 67 cm vertically. Although some of the large coordinate changes resulted from new data and adjustment strategies, most horizontal changes greater than about 6 cm occurred in geologically active areas and were likely due mainly to tectonic motion.

Performing the 2011 national adjustment required appropriate handling of a number of technical challenges. One, as mentioned previously, was that the networks were referenced to three different tectonic plates (North America, Pacific, and Mariana plates). In some cases, marks referenced to one plate were located on a different plate (such as marks in coastal southern California and the Caribbean that were referenced to the North America plate). This situation was handled by transforming the GNSS vectors to the appropriate NAD 83 frame at the common

2010.00 epoch using the NGS *Horizontal Time Dependent Positioning* (*HTDP*) software to model horizontal tectonic motion (including earthquakes). *HTDP* version 3.1.2 was used for CONUS, Alaska, and the Caribbean, and version 3.2.2 was used for the Pacific, including marks on the Mariana and Philippine Sea plates. Other methods used for the NA2011 Project include:

1. Use of stochastic (rather than rigid) constraints for CORSs based on formal error estimates derived from the NGS MYCS1.
2. Scaling of GNSS vector error estimates for all projects to ensure consistent weighting of observations when the projects were combined.
3. Use of downweighting to reject vectors (rather than remove them), to allow an evaluation of whether such vectors should be re-enabled through a series of iterative adjustments. In the final adjustments, over 20,000 previously rejected vectors were re-enabled.
4. Splitting CONUS into a Primary and Secondary network, as mentioned above, allowing the Primary network to be adjusted separately without the problems associated with older observations (including single-frequency receivers, no antenna phase center models, poor orbit accuracy, incomplete satellite constellation, and lack of CORSs).
5. Downweighting the "up" (vertical) component of GNSS vectors to account for (rather than attempt to model) subsidence in the northern Gulf Coast region of CONUS, based on the age of the vectors and estimated subsidence rates.

In addition to the above items, several problems with the GNSS vector data were identified *after* computing final coordinates. These problems include (among others): unrealistically short vectors, erroneous error estimates, duplicate vectors, incorrect date and time, and the presence of a large number of "trivial" (statistically dependent) vectors. Most of the incorrect information issues affected less than about 2% of the vectors, and the problems affecting a large number (such as trivial vectors) had a modest impact on the final coordinates and their accuracies. Nonetheless, such problems should be addressed, and obviously it is much preferable to have done so *before* determining final coordinates. However, identifying them afterward means that action can be taken to remove, correct, or appropriately handle the vector data in future large regional or national adjustments. The errors will also be corrected before the vector data are transferred to the new NSRS database as part of the NSRS Modernization in 2022.

Despite unresolved problems with GNSS vector data, most technical issues were identified and successfully addressed before coordinates and accuracies were published. Considering the magnitude and complexity of the NA2011 Project, the results are overall excellent. Completion of this project is a significant step toward a more integrated, consistent, and accurate NSRS.

Supporting electronic data

Due to the large size of the datasets generated for this project, most of the detailed results are not provided in this report. Instead, the results are provided as electronic data files, mainly in GIS format (as Esri file geodatabases and shapefiles) and Microsoft *Excel* spreadsheets. The files are available for download through the publicly accessible NA2011 folder via anonymous file transfer protocol (FTP) at ftp://geodesy.noaa.gov/pub/NA2011/. A detailed description of the available electronic files is provided in the report appendices.

Acknowledgements

This report has a single author, however, the data, methods, and results described herein are based on the combined contributions of many individuals. The greatest involvement from contributors occurred following the rollout of the National Adjustment Project (NA2011) in April 2011 and continued through the loading of the subsequent results in the National Geodetic Survey's Integrated Database (NGSIDB) in June 2012. Although not every contributor can be listed here, I extend my gratitude to all. That being said, I would be remiss if I did not acknowledge several people individually.

The participation of Jarir Saleh was vital to the success of the NA2011 Project. Jarir prepared and ran the complex *NETSTAT* adjustments. In some sense he also served as the project co-manager by providing valuable input with his unique blend of technical acumen, good judgment, and calm thoughtfulness. Another key contributor was Nagendra Paudel, who performed the many variance factor computations, in addition to a wide variety of technical tasks, with his characteristic good humor. Both Jarir and Nagendra were a pleasure to work with in the day-to-day operations of the project.

Jarir was a member of NGS' NA2011 Steering Committee. Other members also made valuable contributions throughout the life of the project. Included among the committee members were Maralyn Vorhauer, who provided an important link to the 2007 national adjustment and performed detailed analyses in difficult regions such as Alabama; Renee Shields, who gave input from her perspective as the Height Modernization program manager; Jim Tomlin, the NGS Database manager who ensured the work was compatible with the NGSIDB; Dave Minkel and John Ellingson, who provided the local perspective as NGS geodetic advisors; Dru Smith, who gave valuable and insightful contributions on both technical and policy issues; and Dan Roman, who provided input from the perspective of creating a new hybrid geoid model based on the NA2011 results.

Other individuals who were not on the steering committee also contributed to the success of the project. Dale Pursell was the manager of the 2007 national adjustment and had since retired from NGS, but he went on to serve as a contractor for NA2011. At the start of the project, he was the only existing or former NGS employee capable of running *NESTAT*, and his expertise was essential. Mike Potterfield wrote *NETSTAT* for the 2007 adjustment as a contractor, and he provided uniquely valuable assistance on its operation and output. Dave Zilkoski provided input from the distinctive perspective of a retired NGS Director, and he also reviewed an early draft of this report. Dave Doyle provided input related to the history of GPS projects, which in turn assisted in making decisions on how to handle older data. Jake Griffiths offered insight into the technical aspects of the Multiyear CORS Solution (MYCS1), an important contribution to decisions on using CORSs for constraining the adjustments. Richard Snay provided context on the definition of NAD 83 and, importantly, updated Horizontal Time-Dependent Positioning (*HTDP)* by adding the Philippine Sea tectonic plate, which was a great help in performing the Pacific adjustments. Julie Prusky offered input related to receiving and loading the GPS projects that collectively created the NA2011 networks, and she provided insights concerning the NGSIDB.

NGS leadership support proved crucial to the success of both the project and this report. Vicki Childers, as Observations and Analysis Division (OAD) chief and my supervisor, was steadfast in supporting the completion of this report, support that kept me moving forward. Mark Eckl was the OAD Chief during the execution of the project, and he provided the necessary time and resources to complete the adjustments. Although Mark has since passed away, his positive influence on the project persisted throughout the writing of this report. Bobbi Simmons provided an editorial review of the last version of the report before it was delivered for final review; her keen eye and editorial skill improved its readability (of vital importance for such a large work). Lastly, I humbly acknowledge NGS Director Juliana Blackwell for her gracious forbearance over the long period of time required to prepare this report. Her unwavering desire to have the report completed gave me the stamina necessary to finally get it done. I hope it proves worth the wait.

Table of Contents

List of Figures

List of Tables

List of Abbreviations and Acronyms

2D	Two-Dimensional
3D	Three-Dimensional
APC	Antenna Phase Center
ARP	Antenna Reference Point
CBN	Cooperative Base Network
CONUS	CONterminous United States
COOP	COOPerative (for CORSs)
CORS	Continuously Operating Reference Station
DMA	Defense Mapping Agency (now NGA)
DOF	Degrees of Freedom
DORIS	Doppler Orbitography and Radiopositioning Integrated by Satellite
ECEF	Earth-Centered, Earth-Fixed (Cartesian coordinates)
FAA	Federal Aviation Administration
FBN	Federal Base Network
FGCC	Federal Geodetic Control Committee (now FGCS)
FGCS	Federal Geodetic Control Subcommittee (formerly FGCC)
FGDC	Federal Geographic Data Committee
FTP	File Transfer Protocol

GIS	Geographic Information System
GNSS	Global Navigation Satellite System(s)
GPS	Global Positioning System
GRP	Ground Reference Point
HARN	High Accuracy Reference Network
HGSD	Harris-Galveston Subsidence District
HPGN	High Precision Geodetic Network
HTDP	Horizontal Time Dependent Positioning (NGS software)
IERS	International Earth Rotation and Reference Systems Service
IGS	International GNSS Service
ITRF	International Terrestrial Reference Frame
ITRS	International Terrestrial Reference System
LGH	Local Geodetic Horizon
MA11	MAriana adjustment of 2011 (NA2011 marks referenced to Mariana tectonic plate)
mas	milliarcsecond (angle)
MYCS1	Multi-Year CORS Solution 1
MYCS2	Multi-Year CORS Solution 2
NA2011	National Adjustment of 2011 (Project)
NAD 83	North American Datum of 1983
NAVD 88	North American Vertical Datum of 1988
NGA	National Geospatial-Intelligence Agency (formerly DMA and NIMA)
NGS	National Geodetic Survey
NGSIDB	National Geodetic Survey Integrated Data Base
NIMA	National Imagery and Mapping Agency (now NGA)
NSRS	National Spatial Reference System
OP	OPUS-Projects (part of the NGS OPUS online service suite)
OPUS	Online Positioning User Service (NGS online software suite)
PA11	PAcific adjustment of 2011 (NA2011 marks referenced to Pacific tectonic plate)
PAGES	Program for Adjustment of GPS Ephemerides (NGS software); also known as “page5”
PBO	Plate Boundary Observatory
PID	Permanent IDentifier (in NGSIDB)
ppb	Parts per billion
ppm	Parts per million
RINEX	Receiver INdependent EXchange (GNSS data raw data format)
RMSE	Root Mean Square Error
SA	Selective Availability
SECTOR	Scripps Epoch Coordinate Tool and Online Resource (online software)
SINEX	Solution INdependent EXchange (geodetic data solution format)
SLR	Satellite Laser Ranging
USCG	U.S. Coast Guard
VLBI	Very Long Baseline Interferometry
WGS 72	World Geodetic System of 1972
WGS 84	World Geodetic System of 1984

Chapter 1. Introduction and Background

1.1. The National Adjustment of 2011 Project

1.1.1. Project objectives and purpose

The objective of the National Adjustment of 2011 (NA2011) Project was to determine updated North American Datum of 1983 (NAD 83[1]) coordinates on passive control marks with positions determined using Global Navigation Satellite System (GNSS) technology. In general, throughout this report, the abbreviation "GNSS" is used to represent all such satellite systems. "GPS" is usually reserved for explicitly GPS-only applications, and for the name "GPS projects." For historical reasons, that name is still applied to all GNSS-based projects in the NGS Integrated Data Base (IDB), although it is possible some recent ones were performed using other constellations in addition to GPS.

New coordinates were determined for passive GNSS marks with existing coordinates in the NGSIDB. The new passive control coordinates were optimally aligned with the 2011 realization of the Continuously Operating Reference Station (CORS) network by constraining the adjustment to published NAD 83 coordinates of those CORSs.

With this project, NGS sought to improve how the wide range of customer needs are met in providing convenient and efficient access to the National Spatial Reference System (NSRS). Successful completion of this project represents a significant step towards a more integrated suite of NGS products and services, as well as a more coherent strategy for change management.

1.1.2. Background and project summary

The concise version of NOAA's National Geodetic Survey (NGS) mission is to define, maintain, and provide access to the NSRS. A diverse group of users throughout the United States and its territories rely on the NSRS to meet our nation's economic, social, and environmental needs. An integral part of achieving NGS' mission is to make optimal use of GNSS technology. Since the 1980s, NGS has acquired a large body of GNSS data through geodetic observations performed by NGS, as well as through partnerships with federal, state, and local government agencies, and with the private sector. NGS continually strives to properly assimilate these observations into the NSRS to create a more accurate, reliable, and efficient system for all users.

In accordance with the NGS mission, the NA2011 Project updated the NSRS by determining new passive control coordinates, using the existing nationwide dataset of reduced GNSS observations (vectors) connecting passive marks to one another and to CORSs. Updated NAD 83 coordinates were determined through a simultaneous least squares adjustment of 81,055 passive control marks, using a nationwide network of 424,721 GNSS vectors. The GNSS

[1] Since 2003, there have been three distinct global reference frames, all using the name "NAD 83". Each one is, ostensibly, plate fixed, to the three tectonic plates of North America, Pacific and Mariana. The generic use of "NAD 83" anywhere in this report will mean the set of all three frames.

vectors (and associated estimated errors and correlations) used for this project were originally determined in 4267 individual projects and are stored in the NGSIDB.

1.1.3. Project justification

A nationwide adjustment of passive control was necessary to ensure the passive marks with GNSS-derived positions were optimally aligned with the NOAA CORS Network. The CORS network is a GNSS-based system that is the ***geometric*** foundation of the NSRS, and the 2011 realization of the network—referred to as ***Multi-Year CORS Solution 1 (MYCS1)***—was completed in September 2011 (NGS, 2013b). Completion of the NA2011 Project constrained to MYCS1 resulted in a unified realization of both CORSs and passive control referenced to a common epoch of 2010.00 (January 1, 2010). The NA2011 Project benefits NGS customers by ensuring consistency between passive control and other NGS products and services, such as the CORS Network, the *Online Positioning User Service* (*OPUS*), and hybrid geoid model GEOID12B. Consequently, NA2011 is also consistent with the overall aims and objectives of the NGS 2013-2023Ten-Year and 2019-2023 strategic plans (NGS, 2013a and 2019b).

1.1.4. Project scope

The NA2011 Project consisted of the following primary scope items:

1. Perform simultaneous least squares adjustments of GNSS vectors held in the NGSIDB to derive accurate and consistent NAD 83 coordinates (latitude, longitude, and ellipsoid height) for passive marks positioned using these vectors.
2. Constrain the adjustment exclusively to current NAD 83 CORS coordinates (not to passive control coordinates), so that the passive control is optimally aligned with the CORS Network.
3. For each passive mark, publish the NAD 83 coordinates derived from the adjustments. The coordinates each will have a datum tag designating the tectonic plate to which the constrained CORS coordinates were referenced, based on location, and designated as listed below. Note that some locations fall outside the United States and its territories. Although marks in such locations are not formally part of the NSRS (and thus are not publishable), their connecting vectors were not removed from the adjustments. The reason for keeping them was to improve network connectivity, to avoid deconstructing session solutions, to allow ties to important CORSs (such as in Canada), to make them accessible for specific applications outside the United States (such as Federal Aviation Administration airport surveys), and to maintain consistency of results within the NGSIDB for all marks, whether currently publishable or not.
    a. **NAD 83 (2011) epoch 2010.00** (referenced to North America plate). Conterminous United States (CONUS), Alaska, and all marks located in the Caribbean (including Puerto Rico and the U.S. Virgin Islands), as well as in Mexico and South America.
    b. **NAD 83 (PA11) epoch 2010.00** (referenced to Pacific plate). Hawaii, American Samoa, and other marks located on the Pacific plate in the central and southern Pacific Ocean (including Midway, Marshall, Pohnpei, Kosrae, and Chuuk islands).

c. **NAD 83 (MA11) epoch 2010.00** (referenced to Mariana plate). Guam, the Commonwealth of the Northern Mariana Islands (CNMI), and other marks located in the Pacific Ocean on the Mariana and Philippine Sea plates (including Palau and Yap Island).

4. Seamlessly integrate the results of this Project into the NGSIDB and all affected NGS products and services.

Ancillary scope items for the NA2011 Project are listed below:

A1. Update the NGS program *ADJUST* to provide results consistent with NA2011. *ADJUST* (Milbert and Kass, 1987) is used to perform least squares adjustments for a variety of geodetic observations, including GNSS. By NGS policy (NGS, 2012), all horizontal control projects with GNSS or conventional terrestrial observations that are loaded into the NGSIDB must have been adjusted using *ADJUST*.

A2. Perform separate adjustments for islands not referenced to the North America tectonic plate: 1) Hawaii and American Samoa and other central and south Pacific islands located and referenced to the Pacific tectonic plate, and 2) Guam and the Commonwealth of the Northern Mariana Islands (CNMI), located on and referenced to the Mariana tectonic plate. The adjustment for Alaska was also performed as a separate network, even though it is referenced to the North America plate, because of a lack of reliable ties to the CONUS network.

A3. Compute and publish Federal Geographic Data Committee (FGDC)-compliant network and local accuracies for all marks included in the adjustments (FGDC, 1998).

A4. Adjust and load GNSS projects received before the submittal cutoff date so they may be included in the NA2011 simultaneous adjustment and in completion of the project.

A5. Prepare a formal project report detailing the methods and results of the project.

A6. Develop communication and outreach to the NGS user community during execution of the project, and continue such outreach after completion of the project; include providing digital deliverables.

A7. Incorporate lessons learned from the previous (NSRS2007) nationwide adjustment of passive control.

In addition to the tasks specifically included as part of the NA2011 Project, three related subsequent tasks were identified:

B1. Develop a new hybrid geoid model (now called GEOID12B), using NA2011-derived ellipsoid heights on leveled bench marks, with normal orthometric or Helmert orthometric heights, published in one of the official NSRS vertical datums. GEOID12B has since been replaced by GEOID18, but the new hybrid model is still based on 2011 ellipsoid heights.

B2. Provide results for use in creating additional coordinate transformation grids between this current realization and previous NAD 83 realizations to GEOCON (now NADCON 5.0; see Smith and Bilich, 2017).

B3. Perform a nationwide (specifically CONUS and Alaska) vertical adjustment constrained to North American Vertical Datum of 1988 (NAVD 88) leveled orthometric heights on

benchmarks tied to the NA2011 network to determine GNSS-derived orthometric heights at non-leveled marks (this task was not completed due to lack of resources).

1.2. Evolution of the North American Datum 1983

1.2.1. Overview of NAD 83 history

The North American Datum of 1983 has evolved considerably since its initial completion in 1986 (Schwarz, 1989). An excellent review of its history is provided by Snay (2012), including the roles of Canada and Greenland, in addition to the United States (through NGS). The history of NAD 83 is summarized in Table 1.1.

The original (1986) NAD 83 realization predated the widespread use of GNSS and consisted almost entirely of conventional (classical) horizontal observations, augmented with some Transit Doppler and Very Long Baseline Interferometry (VLBI) observations. Since 1986, NAD 83 has evolved significantly to embrace the growing use of GNSS, as well as to accommodate improvements in the understanding and modeling of crustal motion. The original realization of NAD 83 was essentially a two-dimensional (2D) reference frame; as the usage of GNSS increased, it became three-dimensional (3D). With the advent of NGS' *Horizontal Time Dependent Positioning* (*HTDP*) program in 1992, NAD 83 took its first steps towards becoming a four-dimensional (4D) frame (Snay, 1999; Pearson *et al.*, 2010; Pearson and Snay, 2013; NGS, 2015). *HTDP* served an integral role in the NA2011 Project and is further discussed in this and later chapters. Regarding publication of control, passive marks and CORSs handle time differently. Passive coordinates continue to be published at static epochs, rather than as time-dependent quantities themselves, whereas published velocities are available at CORSs.

The NOAA CORS Network now provide the geometric foundation for NAD 83, and the CORSs have been referenced to various International Terrestrial Reference Frame (ITRF) realizations of the International Terrestrial Reference System (ITRS) since the early 1990s (Soler and Snay, 2004). The ITRF is based on multiple geodetic techniques: GNSS, VLBI, Satellite Laser Ranging (SLR), and Doppler Orbitography and Radiopositioning Integrated by Satellite (DORIS). In contrast, the NGS CORSs are presently a GNSS-only (actually, GPS-only) system. Due to the fact that only GNSS is used for the CORSs, the reference frame based on the CORSs is specified as a realization of the International GNSS Service (IGS). The 2011 NGS CORS realization was referenced to the IGS 2008 (IGS08) realization at epoch 2005.00. CORS NAD 83 coordinates are defined by transformations from IGS08 coordinates. The relationship between IGS08 and NAD 83 is defined more fully in Section 1.3.3 of this report.

1.2.2. Previous national adjustment of GNSS passive control (NSRS2007)

NGS completed the National Spatial Reference System of 2007 (NSRS2007) adjustment of passive control on February 11, 2007. The methods and results of that project are described by Pursell and Potterfield (2008) and Milbert (2009). The 2007 national adjustment was the first nationwide simultaneous adjustment of NAD 83 control since the original adjustment completed in 1986. In contrast to the original adjustment, the 2007 network adjustment consisted only of GNSS observations (vectors) connecting passive marks to one another and to CORSs; no conventional horizontal observations were included.

Table 1.1. Summary of NAD 83 history (modified from Snay, 2012).

Year	Event	Significance
1986	Adopted NAD 83 (1986) coordinates for ~272,000 passive reference marks. Frame orientation, scale, and geocenter location derived from TRANSIT Doppler observations.	Replaced NAD 27 with a geocentric reference system free of meter-level distortions.
1989	First GPS HARN survey (in Tennessee). Subsequently performed HARN surveys through the late 1990s to establish statewide and regional networks spanning the U.S. Used to derive new, more precise NAD 83 coordinates for passive marks on essentially a state-by-state basis. Followed by state and regional FBN surveys from the late 1990s through 2005.	Effected transition from 2D to 3D coordinates. Updated relative horizontal coordinate accuracies from a ~10 ppm to ~1 ppm. Scaled NAD 83 frame by -0.0871 ppm to make consistent with ITRF89 scale (systematically decreased NAD 83 ellipsoid heights by ~0.56 m). The FBN surveys resulted in more accurate ellipsoid heights and helped transition to CORSs as foundational control. A negative impact of HARN and FBN was inconsistency caused by separate statewide and regional adjustments.
1996	Adopted NAD 83 (CORS94) coordinates and velocities for ~60 CORSs.	Related NAD 83 coordinates and velocities for CORSs directly to their ITRF94 coordinates and velocities such that locations in stable North America experience little horizontal motion.
1998	Adopted NAD 83 (CORS96) coordinates and velocities for ~100 CORSs (updated in 2002 for ~350 CORSs).	Related NAD 83 coordinates and velocities for CORSs directly to their ITRF96 coordinates and velocities.
2003	Adopted NAD 83 (PACP00) coordinates for locations on the Pacific tectonic plate and NAD 83 (MARP00) coordinates for locations on the Mariana tectonic plate.	Related NAD 83 coordinates on the Pacific and Mariana plates to their ITRF2000 coordinates such that the NAD 83 coordinates experience little, if any, horizontal motion. Effectively began the era where "NAD 83" meant a set of three independent reference frames.
2007	Adopted NAD 83 (NSRS2007) coordinates for ~70,000 passive marks located in CONUS and Alaska via an adjustment where NAD 83 (CORS96) coordinates for CORSs were held rigidly fixed.	Unified the ~50 statewide/regional HARN and FBN surveys into a single reference frame consistent with NAD 83 (CORS96). Had the negative significance of creating two different realizations for users: NAD 83 (NSRS2007) for passive control and NAD 83 (CORS96) for active control (CORSs).
2011	Initial Multi-Year CORS Solution (MYCS1) completed. Adopted NAD 83 (2011) epoch 2010.00 coordinates and velocities for CORSs located in CONUS, Alaska, and the Caribbean. Adopted NAD 83 (PA11) and NAD 83 (MA11) epoch 2010.00 coordinates and velocities for CORSs located on the Pacific and Mariana plates.	Related NAD 83 coordinates and velocities for CORSs to their IGS08 coordinates and velocities such that locations on the North America, Pacific, or the Mariana plates experience little horizontal motion relative to NAD 83. Greatly improved the accuracy of CORS coordinates and velocities by reducing systematic errors in GPS data.
2012	Adopted NAD 83 (2011/PA11/MA11) epoch 2010.00 coordinates for ~80,000 passive reference marks located in CONUS, Alaska, the Caribbean and the Pacific via adjustments constrained to the CORSs NAD 83 (2011/PA11/MA11) epoch 2010.00 coordinates.	Significantly improved the accuracy of the coordinates of the involved passive reference marks, as well as improved consistency of coordinates with CORS Network. Yielded, for the first time in NSRS history, a consistent reference frame between active and passive coordinates.

Prior to the 2007 adjustment, networks using GNSS observations had essentially been adjusted on a state-by-state basis, beginning in 1989 and continuing through the early 2000s. The names used for these networks have changed over time. Initially they were referred to as "High Precision Geodetic Networks" (HPGN), and later they became known as "High Accuracy Reference Networks" (HARN). Most of the HPGN/HARN networks were completed by the mid-1990s. A second national set of regional/statewide surveys and network adjustments were performed to obtain improved coordinates (particularly ellipsoid heights). The second set of network adjustments were typically called Federal Base Networks (FBNs), as well as Cooperative Base Networks (CBNs) when other organizations participated in the projects. Classical horizontal observations were included in HARN networks, but results were constrained to GNSS-derived coordinates. In this way, NGS updated terrestrial NAD 83 control using the more precise GNSS observations.

The net result of the many individual HPGN/HARN and FBN/CBN adjustments was a system of geodetic control where each adjustment was assigned a datum tag year. The datum tag is typically the year the *initial* adjustment was performed for a network. Adjustments performed in later years could use the tag from an earlier adjustment if the latter adjustment yielded coordinates that did not significantly change from the previous adjustment. For example, results of an FBN survey performed in 1999 in an area where a 1992 HARN existed would be assigned a 1992 datum tag if the FBN adjustment yielded coordinates that agreed with 1992 coordinates at about the 5 cm level horizontally (Vorhouer, 2012). However, the FBN adjustments always yielded new ellipsoid heights, though these generally were not given a datum tag at all.

The NA2011 Project is assigned a datum tag of 2011, even though the adjustment was completed in 2012, because it is constrained to CORSs with NAD 83 coordinates determined in 2011.

Although each HPGN/HARN and FBN/CBN network was tied to neighboring networks, the coordinates were not entirely consistent across the nation due to using somewhat different observations and constraints. Recognizing this deficiency, NGS performed the 2007 national adjustment to obtain a single nationwide network of NAD 83 control in CONUS, Alaska, and the Caribbean. To ensure spatial consistency, the network was constrained only to CORSs, using the most current CORS coordinates available at the time. Unlike the previous HPGN/HARN adjustments, conventional horizontal observations were not included. The result was a system of approximately 70,000 passive NAD 83 marks with a 2007[2] datum tag, consistent with the CORSs. The approximately 200,000 marks based only on conventional observations (even if tied to underlying GNSS control) retained their previously determined HPGN/HARN datum tags, and as such are no longer consistent with the GNSS-derived control.

Comparisons between the 2011 and 2007 national adjustment results are provided in Section 4.4. Among the differences between the projects is that the 2007 adjustment did not include marks in the Pacific, whereas these marks were included in the 2011 adjustment.

[2] Formally, the datum tag is "NSRS2007," however, this broke with previous, and later, choices to use only a four-digit numerical year for the datum tag. So, informally, the datum tag is often shortened simply to "2007."

1.3. The 2011 Multi-Year CORS Solution (MYCS1)

The NOAA CORS Network has become the geometric foundation of the NSRS, and the CORSs were used to constrain the 2011 national adjustment of passive control. In this way, the CORSs effectively define NAD 83 with respect to the ITRS. Because of the importance of the CORSs as foundational geometric control, NGS embarked on a project to determine updated coordinates and velocities by reprocessing all available CORSs data (back to January 1994) using the best available methods and models. This project is the Multi-Year CORS Solution (MYCS). Since additional multi-year CORS solutions will be performed in the future, it is now referred to as MYCS1 (i.e., the first multi-year CORS solution), or as "Repro1," for "Reprocessing 1." A second multi-year solution, MYCS2, was officially released in September 2019 (NGS, 2019a).

MYCS1 was performed for several reasons, as summarized below. A more detailed discussion about MYCS1 is available on the NGS website (NGS, 2013b).

1. **Mixed coordinates**. Previous CORS solutions used coordinates from an earlier solution (1994 to 2002) based on only three to eight ITRF reference frame sites for aligning to the global frame.
2. **Mixed horizontal velocities.** Some horizontal velocities computed from observations were mixed with those modeled using the NGS program *HTDP*.
3. **Lack of vertical velocities.** Previous CORSs with horizontal velocities were assigned a vertical velocity of zero.
4. **Epoch of global reference frame.** The global reference frame used for the previous CORSs was ITRF00 epoch 1997.00; projecting positions to the present was considered unrealistic.
5. **Epoch of plate-fixed reference frames.** The NAD 83 plate-fixed frames for the previous CORSs (CORS96, PACP00, and MARP00 for the North America, Pacific, and Mariana tectonic plates, respectively) were at epoch 2002.00; projecting positions to the present is questionable. In addition, a different epoch was used in Alaska (2003.00), due to a major earthquake in 2002.
6. **Absolute antenna calibration models**. The previous CORS solution was based on relative GNSS antenna calibration models. Reprocessing was necessary to make use of new absolute antenna calibrations as is consistent with the latest global reference frames.
7. **Improved algorithms and models.** In addition to new antenna calibration models, there were other significant changes to existing processing algorithms and models, including compliance with International Earth Rotation and Reference Systems Service (IERS) conventions (e.g., Petit and Luzum, 2010). The changes included improved data discontinuity detection and new models for tropospheric delay, ocean tide loading, and solar radiation pressure on GNSS satellites.
8. **Alignment with most current global reference frame**. To align the CORS Network with the latest state-of-the-art full global reference frame required reprocessing of GPS

data. The reprocessing allowed NGS to make use of the approximately 230 IGS marks that defined the reference frame at that time (IGS08 epoch 2005.00).

1.3.1. Summary of MYCS1 results

Given these major inconsistencies and changes, NGS reprocessed all of its CORSs data collected from January 1, 1994, through April 16, 2011. (January 1994 was used as the beginning date, because precise IGS satellite orbits are not available prior to 1994). NGS' September 2011 release of the resulting NAD 83 coordinates for 2064 NGS CORSs constituted a new realization of the CORS Network. The MYCS1 actually included a total of 2135 marks, but there were 71 marks for which NAD 83 coordinates were not computed (generally outside the NSRS, with the exception of some CORSs in Canada and the Pacific where NAD 83 coordinates were computed). Note that 690 of the CORSs in the MYCS1 were decommissioned or were non-operational as of September 2011. Although other CORSs have been decommissioned, many more have been added since that date, for a net gain of approximately 400 operational CORSs. As of October 2, 2018, there were a total of 2730 CORSs: 1827 operational, 18 preliminary, 87 non-operational, and 798 decommissioned.

NAD 83 CORS coordinates and velocities determined in MYCS1 differed from their previous (CORS96) values. Part of the change was due to differences in processing techniques and models, notably the change from relative to absolute GNSS antenna calibrations (particularly for the ellipsoid height component). The most significant change for horizontal coordinates was due to the change in epoch from 2002.00 to 2010.00 (an epoch of 2003.0 was used for Alaska, due to the November 3, 2002, Denali earthquake). The coordinate differences are summarized in Table 1.2, as well as the NAD 83 velocities and formal MYCS1 accuracy estimates.

Table 1.2. Summary of NAD 83 results for the 2011 Multi-Year CORS Solution (MYCS1).

	ARP coordinate change from CORS96 epoch 2002.0 (2003.0 in AK) to MYCS1 epoch 2010.0 (cm)				NAD 83 MYCS1 velocities, for 1309 computed and 755 modeled CORSs (mm/yr)				Formal accuracy estimates at 95% conf. (cm)	
	North	East	Up	Horiz	North	East	Up	Horiz	Horiz	Vert
Min	-10.63	-28.99	-12.8	0.10	-15.9	-34.4	-21.5	0.1	0.14	0.16
Max	32.15	16.24	16.4	38.48	41.4	19.8	18.4	47.5	31.15	91.99
Median	-0.09	1.40	-0.5	1.94	-0.2	1.8	-1.2	2.1	1.08	3.51
Mean	1.67	0.28	-0.47	3.94	2.2	0.4	-1.6	5.0	1.47	4.85
Std dev	±5.72	±4.94	±2.01	±6.67	±7.4	±6.1	±2.1	±8.5	±1.80	±5.66
Number of CORSs used to compute statistics										
NAD 83 (2011)	2017 (102 in Alaska)				2038 (753 modeled)				1285	
NAD 83 (PA11)	22				22 (1 modeled)				21	
NAD 83 (MA11)	4				4 (1 modeled)				3	
Total	**2043***				**2064**				**1309****	

** Coordinate changes were only computed for CORSs with published NAD 83 coordinates.*
*** Formal accuracies were only determined for CORSs with computed velocities (see text for details).*

Both the 2007 and 2011 national adjustments of passive control were constrained to NAD 83 CORS coordinates. Therefore, the change of CORS coordinates from CORS96 to MYCS1 provides a good estimate of the change in passive marks from the 2007 to the 2011 national adjustments. The change in passive mark coordinates is discussed further in Section 4.4.1.

Changes in CORS antenna reference point (ARP)[3] coordinates shown in Table 1.2 were computed for the 2043 MYCS1 CORSs that also had NAD 83 (CORS96) coordinates. The 21 CORSs without NAD 83 coordinates were IGS marks that were not published by NGS. The sources for the coordinate values were the composite NAD 83 CORSs geodetic coordinate files for MYCS1 (dated September 3, 2011) and CORS96 (dated September 6, 2011). The median and mean horizontal change is about 2 cm and 4 cm, respectively. Both the median and mean changes decrease to about 0.2 cm if an epoch of 2002.00 is used for both the MYCS1 and CORS96 coordinates. This decrease shows that most of the horizontal change is due to eight years (seven years in Alaska) of differential crustal motion and unmodeled tectonic plate rotation, demonstrating that NAD 83 cannot be considered truly "fixed" to the North America plate.

The change in NAD 83 horizontal coordinates and ellipsoid heights for MYCS1 is illustrated in Figure 1.1. The upper map in Figure 1.1 shows that MYCS1 horizontal coordinate changes due to the epoch change were especially large in areas of active crustal deformation, such as western CONUS and Alaska. Systematic horizontal coordinate differences are also evident in Figure 1.1 for the stable part of the North America plate, indicating an apparent clockwise rotation. Ideally, such a rotation should not be present, since the intent is that NAD 83 be fixed to the North America plate. One possible reason for the apparent rotation is that the NUVEL-1A tectonic model (DeMets *et al*., 1994) used to originally define NAD 83 may have had a rotation slightly greater than actual (see Snay, 2012). An alternative (or perhaps additional) possible reason is that there was a small systematic error in the computed rate of change parameters between NAD 83 and ITRF96, rather than a bias in the NUVEL-1A rotation rate. In either case, the net effect is that NAD 83 velocities are non-zero and increase northward from the Euler rotation pole, causing an apparent rotation in the opposite sense of the actual rotation with respect to the global frame.

No clear systematic trend is evident in the change in ellipsoid heights in Figure 1.1, other than a slight overall downward (negative) bias, as indicated by the -0.5 cm median and mean change values in Table 1.2. The overall negative change in ellipsoid height is likely due mainly to the change from relative to absolute antenna calibrations for MYCS1.

[3] The term ARP typically refers to the lowest physical part of the antenna itself. There is a need to instead specify a separate, physically invariant point independent of the antenna for referencing coordinates, even when that point coincides with the ARP. NGS has proposed the term Geometric Reference Point (GRP) for such points (NGS, 2019c). But for consistency with past practice, both at NGS and elsewhere, the term ARP is used in this report.

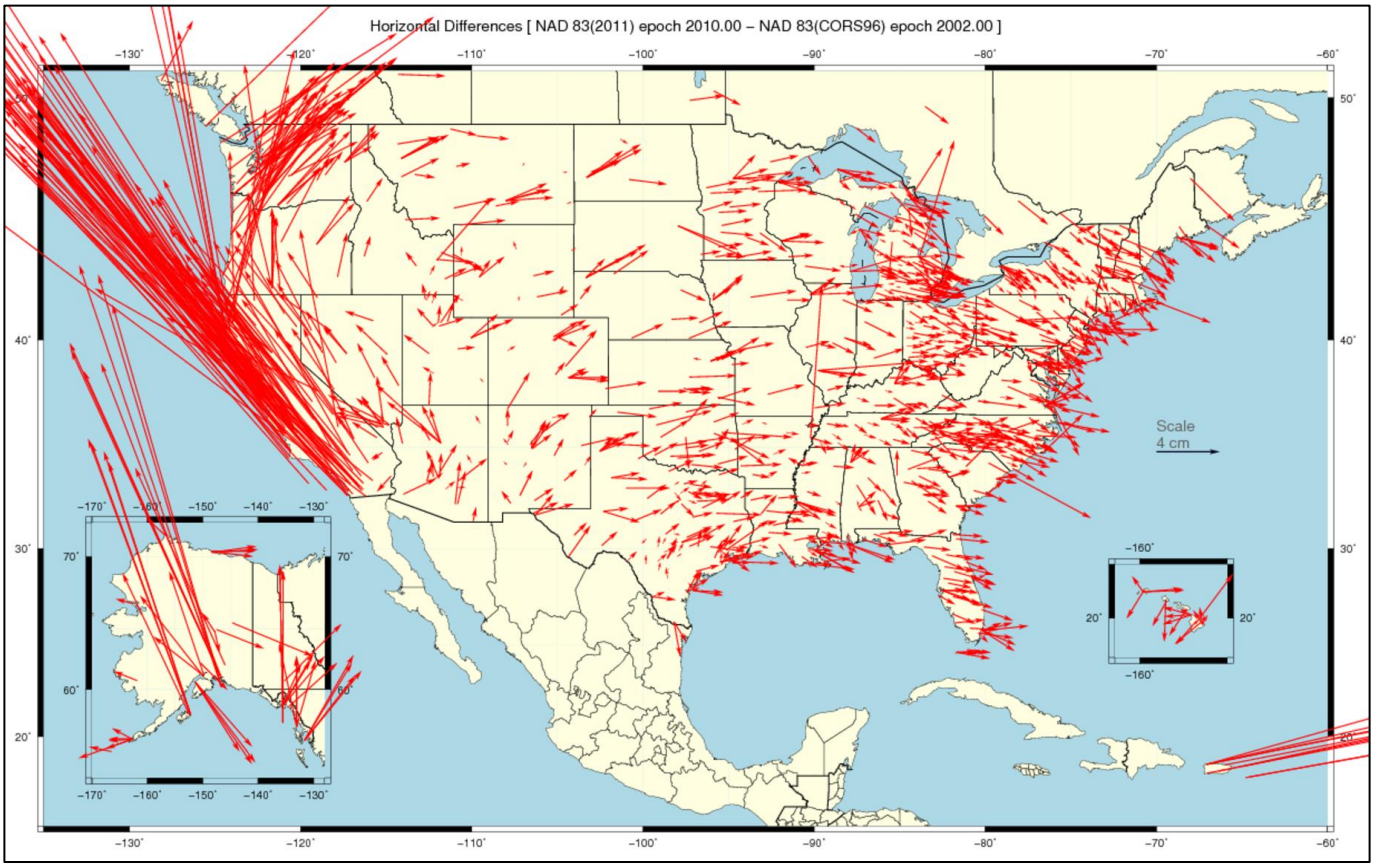

Figure 1.1. NAD 83 CORS coordinate change from CORS96 epoch 2002.0 to MYCS1 epoch 2010.0

The MYCS1 NAD 83 horizontal velocities in Table 1.2 range from essentially zero to 48 mm/yr, with median and mean of 2 and 5 mm/yr, respectively. Most of the large horizontal velocities are associated with crustal deformation along the west coast of CONUS and in Alaska, as clearly shown in Figure 1.1. Such larger NAD 83 velocities, despite NAD 83 being (nominally) plate-fixed, show the importance of accounting for relative movement before performing adjustments at a fixed epoch. *HTDP* was used to transform all GNSS vectors to the 2010.00 epoch prior to performing the 2011 national adjustments. Although an epoch of 2002.00 was previously used for the CORSs (2003.00 in Alaska), for the 2007 national adjustment an epoch of 2007.00 was used instead for western CONUS and Alaska. This discrepancy is further discussed in Sections 3.1.3 and 4.4.1.

1.3.2. "Computed" versus "modeled" MYCS1 coordinates and velocities

The CORSs velocities in Table 1.2 are classified as either "computed" or "modeled." Computed velocities were determined for CORSs in MYCS1 with at least approximately 2.5 years of data available as of April 16, 2011. For these CORSs, enough data were available to reliably compute velocities as part of the solution, along with formal variance-covariance values (i.e., error estimates) for the coordinates and velocities. Reliable velocities made it possible to rigorously determine coordinates at epoch 2010.00, along with formal error estimates. Thus, the coordinates and velocities for these CORSs are referred to as "computed." Of the 2064 CORSs with NAD 83 coordinates in MYCS1, 1309 (63%) are "computed" CORSs.

Reliable velocities could not be determined for CORSs with less than 2.5 years of data in MYCS1. Coordinates for these CORSs were determined at the midpoint time of the data span (as for all other CORSs). However, since velocities were not computed, the only way to determine epoch 2010.00 coordinates was to use estimated velocities. *HTDP* version 3.1.2 velocity models were used for this purpose, so velocities for these CORSs are referred to as "modeled" (unfortunately, with the exception of some parts of Alaska, *HTDP* yields only horizontal velocities, so these CORSs had modeled a vertical velocity of zero). Of the 2064 CORSs with NAD 83 coordinates in MYCS1, 755 (37%) are "modeled" CORSs.

Table 1.2 also includes formal coordinate accuracy estimates from the MYCS1 Solution Independent Exchange (SINEX) file. Because modeled velocities did not include error estimates, formal accuracy estimates were only available for computed CORSs. The computed CORS error estimates were important for the NA2011 Project, because they were the basis for weighting the MYCS1 CORS coordinates used to constrain the adjustments of passive control. The weights were computed as the squared inverse standard deviations of the north, east, and up components. Error estimates of MYCS1 CORSs used for constraining the passive control adjustments are discussed in greater detail in Section 3.1.4. The discussions include comparisons to the error estimates derived from the nationwide adjustments of passive control, and describe how uncertainties (and thus weights) were estimated for modeled MYCS1 CORSs.

Table 1.2 gives the horizontal (circular, per Leenhouts, 1985) and ellipsoid height error (accuracy) estimates, scaled to 95% confidence using standard deviation scalars of 2.4477 horizontally and 1.9600 vertically. These values show a tremendous range in accuracies, from 0.1 to 31 cm horizontally and 0.2 to 92 cm vertically (i.e., ellipsoid height). The standard

deviations (not given in Table 1.2) range from 0.05 to 15 cm horizontally (north and east), and from 0.08 to 47 cm vertically. These values correspond to a variation in constraints weight from 5 to 3,300,000 m^{-2}, a range of over 5 orders of magnitude.

Perhaps more troubling than the range in constraints weight is the magnitude of the error estimates themselves. Of the 1309 NAD 83 MYCS1 CORSs with formal error estimates, more than 100 have errors that exceed 3 cm horizontally and 10 cm vertically (at 95% confidence). Such errors seem excessive for marks intended to serve as the geometric foundation of the NSRS. Note, however, that not all MYCS1 CORSs were used for constraints in the NA2011 adjustments; they could only be used if they had vector connections to marks in GPS projects. Because of this limitation, only 1195 (58%) of the 2064 available CORSs with NAD 83 coordinates could be used as constraints, and of these 973 had formal uncertainties. The maximum standard deviations for the CORSs used as constraints were 12.9 cm horizontally and 32.5 cm vertically (see Table 3.3).

1.3.3. Determining NAD 83 coordinates by transformation from IGS08

For MYCS1, coordinates were determined in the IGS08 reference frame at epoch 2005.00. NAD 83 MYCS1 coordinates were computed from IGS08 using 14-parameter Helmert similarity transformations and (computed or modeled) CORSs velocities. The Helmert transformation relating NAD 83 for the North America tectonic plate to the global frame was originally defined in 1996, as stated on the "1996" row in Table 1.1 and described by others (e.g., Soler and Snay, 2004; Snay 2012). The 1996 NAD 83 transformation was defined with respect to ITRF94 with a reference epoch of t_0 = 1997.0. In 1998, the definition was updated to ITRF96 to create the NAD 83 (CORS96) realization (with ITRF94 = ITRF96). This definition was the basis for the NSRS2007 national adjustment by rigidly constraining the adjustment of passive marks to NAD 83 (CORS96) coordinates of CORSs.

The relationship between NAD 83 and ITRF (at t_0 = 1997.0) remained the same for subsequent CORS-based realizations of NAD 83 for North America. As ITRF changed with time, new transformations relating it to NAD 83 were created as compositions of ITRF94 → NAD 83 and ITRF94 → ITRF*xx* transformations, all with t_0 = 1997.0. For these transformations, IGS*xx* is considered equivalent to ITRF*xx*, and specific realizations of WGS 84 are considered equivalent to specific ITRF*xx* realizations. NGS obtained the transformation parameters between ITRF*xx* realizations from the IERS (e.g., IGN, 2016), and the parameters are recomputed to the desired reference epoch t_0 (such as 1997.0). There was one exception: for transformations involving NAD 83 referenced to the North America plate, NGS (and Canada) elected to adopt the IGS-determined relationship that ITRF96 and ITRF97 are *not* equal, whereas the IERS did consider them equal (Soler and Snay, 2004).

For the composite transformation of ITRF*xx* → NAD 83, the transformation ITRF96 → ITRF*xx* (computed from IERS and IGS parameters) is subtracted from ITRF94 → NAD 83 (determined by NGS and Natural Resources Canada, NRC). In doing so, the ITRF94 terms cancel, and the direction of the "to" ITRF*xx* terms are reversed, resulting in the desired transformation ITRF*xx* → NAD 83. All transformations must be at the same reference epoch t_0 when differencing components. For NAD 83 (2011), this composite transformation is:

(ITRF94 → NAD 83) *minus* (ITRF94 → ITRF2008) = ITRF2008 → NAD 83 (2011)
= IGS08 → NAD 83 (2011)

where IGS08 = ITRF2008 and "(2011)" indicates NAD 83 referenced to the North America plate (but *not* any specific realization of NAD 83). The actual parameters for this composite transformation are given below,

Transformation parameters at t_0 = 1997.00	**ITRF94→NAD 83** (North America) *per NGS and NRC*		**ITRF94→ITRF2008** *IGS: ITRF96→ITRF97 not equal to zero*		**ITRF2008→NAD 83** (North America) *composite*
Translation *X* (m)	0.9910		-0.00243		**0.99343**
Translation *Y* (m)	-1.9072		-0.00389		**-1.90331**
Translation *Z* (m)	-0.5129		0.01365		**-0.52655**
Rotation about *X*-axis (mas)	25.78991		-0.12467		**25.91458**
Rotation about *Y*-axis (mas)	9.65010		0.22355		**9.42655**
Rotation about *Z*-axis (mas)	11.65994		0.06065		**11.59929**
Scale (parts per billion)	0	−	-1.71504	=	**1.71504**
Change in translation *X* (m/yr)	0		-0.00079		**0.00079**
Change in translation *Y* (m/yr)	0		0.00060		**-0.00060**
Change in translation *Z* (m/yr)	0		0.00134		**-0.00134**
Change in rotation about *X* (mas/yr)	0.05322		-0.01347		**0.06669**
Change in rotation about *Y* (mas/yr)	-0.74235		0.01514		**-0.75749**
Change in rotation about *Z* (mas/yr)	-0.03156		0.01973		**-0.05129**
Change in scale (parts per billion/yr)	0		0.10201		**-0.10201**

where *X*, *Y*, and *Z* are Earth-Centered, Earth-Fixed (ECEF) Cartesian coordinates and mas = milliarcseconds. Compare the output values above to IGS08 → NAD 83 (2011) in Table 1.3.

Relationships between NAD 83 and ITRF2000 for the Pacific and Mariana tectonic plates were defined in 2003 as the NAD 83 (PACP00) and NAD 83 (MARP00) frames, respectively (Snay, 2003). These frames were defined such that they were consistent with NAD 83 referenced to North America at epoch 1993.62 (August 14), based on the midpoint time of an extensive GPS survey on islands throughout the Pacific. As with NAD 83 for North America, the transformation parameters were recomputed with respect to ITRF94 at t_0 = 1997.0, and the composite transformations for PA11 and MA11 are constructed in the exactly same manner as done for NAD 83 (2011), although for these the IERS convention ITRF96 and ITRF97 was used:

(ITRF94 → PACP00) *minus* (ITRF94 → ITRF2008) = ITRF2008 → NAD 83 (PA11)
= IGS08 → NAD 83 (PA11)

(ITRF94 → MARP00) *minus* (ITRF94 → ITRF2008) = ITRF2008 → NAD 83 (MA11)
= IGS08 → NAD 83 (MA11)

As with North America, only a single relationship to ITRF is defined for the Pacific and Mariana frames of NAD 83, hence PACP00 = PA11 and MARP00 = MA11.

The transformation parameters from IGS08 to NAD 83 are given in Table 1.3 for the 2011 (North America plate), PA11 (Pacific plate), and MA11 (Mariana plate) frames. Note that these transformations are only valid when the IGS08 and NAD 83 epochs are the same. Because the Earth's crust does not behave as a perfectly rigid body, using these transformations alone will not yield correct results when the epochs differ. This limitation is important, since NGS publishes CORS coordinates at epoch 2005.00 for IGS08 and at epoch 2010.00 for NAD 83— thus they are subject to five years of differential tectonic motion. To obtain more correct[4] results, NGS' *HTDP* program should be used, as it combines the Helmert transformations with crustal motion models. In addition, the Helmert rotation parameters for the North American plate on the NGS web page geodesy.noaa.gov/CORS/MYCS1.shtml#TABLE differ slightly from those in *HTDP* due to rounding. The *HTDP* parameters are given in Table 1.3 are from the source code and should be considered definitive.

Table 1.3. Helmert transformation parameters from IGS08 to NAD 83. Note that transformations using only these parameters will not provide correct results if the IGS08 and NAD 83 epochs differ. In such cases *HTDP* should be used, as it combines these transformations with crustal motion models.

IGS08 to NAD 83 Helmert transformation parameters (from *HTDP*)*			
NAD 83 frame Tectonic plate	**NAD 83 (2011) North America**	**NAD 83 (PA11) Pacific**	**NAD 83 (MA11) Mariana**
Parameters at reference epoch t_0 = 1997.00			
Translation *X* (m)	0.99343	0.9080	0.9080
Translation *Y* (m)	-1.90331	-2.0161	-2.0161
Translation *Z* (m)	-0.52655	-0.5653	-0.5653
Rotation about *X*-axis (mas)	25.91458	27.741	28.971
Rotation about *Y*-axis (mas)	9.42655	13.469	10.420
Rotation about *Z*-axis (mas)	11.59929	2.712	8.928
Scale (parts per billion)	1.71504	1.10	1.10
Rate of change in parameters with time			
Change in translation *X* (m/yr)	0.00079	0.0001	0.0001
Change in translation *Y* (m/yr)	-0.00060	0.0001	0.0001
Change in translation *Z* (m/yr)	-0.00134	-0.0018	-0.0018
Change in rotation about *X* (mas/yr)	0.06669	-0.384	-0.020
Change in rotation about *Y* (mas/yr)	-0.75749	1.007	0.105
Change in rotation about *Z* (mas/yr)	-0.05129	-2.186	-0.347
Change in scale (parts per billion/yr)	-0.10201	0.08	0.08

***NOTE:** The* HTDP *rotation parameters for the North American plate differ slightly from those given on NGS web page https://geodesy.noaa.gov/CORS/MYCS1.shtml#TABLE due to rounding. The* HTDP *source code parameters given here should be considered definitive. Abbreviation "mas" is milliarcseconds.*

[4] For yet more correct results, modeled *vertical* velocities should be used. HTDP only models horizontal crustal deformation, except in central Alaska.

Figure 1.2 illustrates the change in coordinates for the IGS08 epoch 2005.00 to NAD 83 (2011) epoch 2010.00 transformations for most of the region covered by the NSRS, as determined using *HTDP* v3.2.3. The upper map shows the horizontal change, and the lower map shows the ellipsoid height change, both with contours at a 0.1 m interval. Coordinate changes are shown for areas referenced to the North America plate and to the Pacific plate (the Mariana plate is outside the map area). Changes for the NAD 83 (2011) frame (approximately fixed to the North America plate) include the Caribbean plate, as well as the eastern margin of the Pacific plate that is not ocean (western California and the Baja peninsula). The NAD 83 (PA11) frame (fixed to the Pacific plate) includes the Juan de Fuca and Cocos plates. In the upper (horizontal change) map, differential tectonic motion of these smaller plates with respect to the fixed plates is clearly shown by the contours.

Within the North America plate, the irregular shape of the contours illustrates the importance of including differential crustal motion in the transformation, even for a period as short as five years. The contours clearly show major tectonic features, such as the San Andreas Fault system, extending from the Sea of Cortez in Mexico, through San Francisco Bay in California, as well as tectonically active areas in western CONUS and southern Alaska. Had only the 14-parameter transformation in Table 1.3 been used for Figure 1.2 (i.e., differential tectonic motion ignored), the contours would be smooth and regular everywhere within each frame where they are defined, i.e., as they appear in eastern North America and most of the Pacific. They would also be incorrect, however, because the 14-parameter transformation behaves by treating points as if they are on a rigid body, which is clearly inappropriate for tectonically active areas such as western CONUS and Alaska.

Contours showing ellipsoid height change in the lower map of Figure 1.2 are both much smoother and more regular than the upper horizontal change map. The main reason for this is that *HTDP* models horizontal crustal displacements (hence its name); the only exception being vertical displacement modeling in central Alaska. In addition, most steady-state large scale vertical deformation is likely nearly indiscernible over a period of only five years at the resolution displayed on this map. The contours on the lower map are nearly identical to those obtained when using only the 14-parameter transformation for the 2011 and PA11 frames.

The lower map in Figure 1.2 shows an offset of ellipsoid height change contours at the boundary between the regions referenced to the NAD 83 (2011) and (PA11) frames. The offset is mainly a consequence of the transformation parameters for two frames being derived independently, with no marks used to define the PA11 along its eastern boundary. Therefore, the offset is essentially an extrapolation artifact of the PA11 transformation, and its small magnitude (<0.1 m in most areas) shows remarkable consistency between the 2011 and PA11 transformations.

Although these IGS08-to-NAD 83 transformations are not strictly part of the NA2011 adjustments, they are included here for two main reasons. The first is that MYCS1 itself was computed in IGS08, with NAD 83 coordinates computed as a secondary step through these transformations, and therefore, it is an important part of the background information for the NA2011 Project.

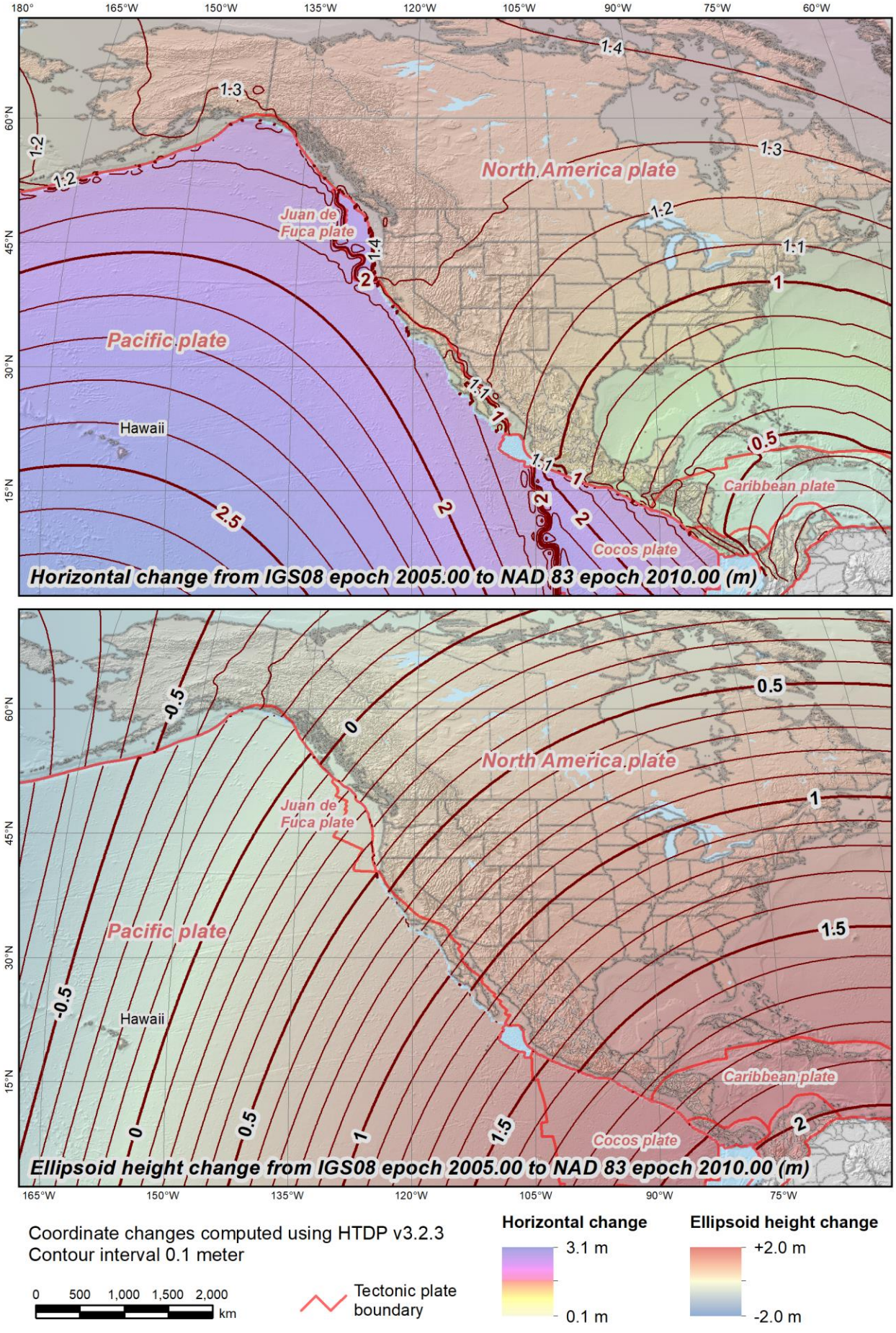

Figure 1.2. IGS08 epoch 2005.00 to NAD 83 (2011 and PA11) epoch 2010.00 per *HTDP* v3.2.3.

The second reason for including the IGS08-to-NAD 83 transformations is that they have been a persistent source of confusion for users of NGS products and services. Over the years, questions and comments have led NGS to recognize that many users (including large government and private organizations) believe the 14-parameter transformations completely define the relationship, and this is incorrect. Thus, this information is provided, in part, as an effort to dispel such misconceptions.

An important final note regarding computation of NAD 83 coordinates by transformation from IGS08 concerns the velocities used to account for crustal motion. Published MYCS1 CORSs velocities were used to transform IGS08 epoch 2005.00 to NAD 83 epoch 2010.00 coordinates. CORS coordinates and velocities are available at geodesy.noaa.gov/CORS/ for specific CORS sites for both NAD 83 epoch 2010.00 and IGS08 epoch 2005.00 (and were updated to ITRF2014 epoch 2010.00 in September 2019). As discussed previously, these velocities were either computed from the MYCS1 solution or modeled using *HTDP*. In either case, the published transformed coordinates will in general not exactly equal those shown in Figure 1.2. For computed CORSs, the difference is due to computed velocities not being exactly equal to modeled velocities. For modeled CORSs, the difference is due to updates of the velocity models. Published modeled velocities were computed using *HTDP* version 3.2.1, whereas Figure 1.2 was created using *HTDP* version 3.2.3. Since velocity models and tectonic plate rotations were updated between these versions, the resulting coordinates may differ, depending on the location. Because the computed MYCS1 velocities themselves were used for the models, these differences for both computed and modeled coordinates are typically small, most likely at the centimeter level or less. However, as new velocity and displacement models are added to future *HTDP* versions, such differences will generally increase. Users performing *HTDP* transformations (in cases where the input and output epochs differ) should be cognizant of possible differences due to computed versus modeled velocities and updates of *HTDP* crustal motion models. Otherwise, if a later version of *HTDP* is used, they may be unable to reproduce previous results.

1.4. Chapter 1 summary

The main purpose of the National Adjustment of 2011 (NA2011) Project was to determine updated NAD 83 coordinates on passive control marks consistent with the latest realization of NAD 83 as determined in the NGS Multi-Year CORS Solution (MYCS1). The results of both MYCS1 and NA2011 were part of ongoing NSRS refinements. Since its initial realization in 1986, NAD 83 has evolved from an essentially 2D frame based almost entirely on conventional horizontal observations to a modern 3D reference frame based on GNSS and explicitly connected to the global frame (IGS08 for the NA2011 Project and ITRF2014 now). MYCS1 was NGS' first complete reprocessing of CORSs data, and it utilized GPS data for the time period when precise orbits were available (from January 1, 1994, through April 16, 2011). The results of MYCS1 represent a significant improvement in consistency and accuracy of the CORS Network, which forms the geometric foundation of the NSRS.

Completion of MYCS1 in September 2011 resulted in three new NAD 83 realizations ostensibly affixed to different tectonic plates, each with its own "datum tag" (in parentheses): NAD 83 (2011) to the North America plate, NAD 83 (PA11) to the Pacific plate, and NAD 83 (MA11) to

the Mariana plate. It is important to recognize that some marks are not referenced to the plates where they are located. The most notable examples are marks in western California (on the Pacific plate) and in the Caribbean (on the Caribbean plate); these are referenced to the North America plate.

MYCS1 results were determined in the IGS08 epoch 2005.00 frame. The MYCS1 NAD 83 epoch 2010.00 coordinates were computed by transformation from the IGS08 epoch 2005.00 values. The transformation consisted of a 14-parameter Helmert transformation (based on a previously defined relationship between NAD 83 and ITRF94 = ITRF96 at epoch 1997.00), plus MYCS1 computed CORSs velocities (or *HTDP*-derived velocities if computed velocities were unavailable). The Helmert transformation determines NAD 83 epoch 2005.00 coordinates, and the (computed or modeled) NAD 83 velocities move the coordinates by five years, from 2005.00 to 2010.00. This time difference of five years is an important component of the relationship between IGS08 epoch 2005.00 and NAD 83 (2011/PA11/MA11) epoch 2010.00. Many users believe that the 14-parameter Helmert transformations alone completely defines these relationships, but they do not. Neglecting the five years of differential crustal motion (velocities) can cause up to 25 cm of error in CONUS (the largest horizontal NAD 83 velocities in CONUS are about 5 cm/yr, in southwestern California).

The NA2011 adjustments were constrained to NAD 83 (2011/MA11/PA11) epoch 2010.00 MYCS1 CORS coordinates, not to IGS08 CORS coordinates. This was accomplished by using *HTDP* to transform all GNSS vectors to the appropriate NAD 83 frame (2011, PA11, or MA11) at epoch 2010.00 epoch prior to performing the NA2011 adjustments. The objective was to make the GNSS observation (vectors) consistent with constrained NAD 83 coordinates, and thus obtain results consistent with the latest published NAD 83 CORS coordinates. Details of the methods and results used for performing the adjustments of passive control are provided in the following chapters.

Chapter 2. Preparing for the National Adjustment

2.1. Input data for the NA2011 Project

Input data for performing the NA2011 Project came from two main sources: the NGS Integrated Data Base (NGSIDB) and the results of the 2011 Multi-Year CORS Solution (MYCS1). The NGSIDB provided all marks and GNSS vectors used to build the networks for the adjustments, including vector ties between marks (i.e., passive-passive, passive-CORS, and CORS-CORS). Results from MYCS1 consisted of CORS coordinates and formal accuracy estimates at 2010.00 for constraining the adjustments.

2.1.1. The NGS Integrated Data Base (NGSIDB)

The NGSIDB is a database of geodetic control data used for defining and providing access to the NSRS (NGS, 2019d). Defined broadly, the NGSIDB contains information concerning a set of unique points (called marks or stations), each with some geodetic information (such as Cartesian coordinates, ellipsoidal coordinates, deflections of the vertical, accelerations of gravity, etc.), as well as the (reduced) observations used for determining these values. The information also includes a large number of associated attributes and metadata, as well as superseded control values. In October 2018, there were 896,419 publishable (i.e., publicly available) geodetic control marks available in the NGSIDB, as summarized in Table 2.1. Non-publishable marks consist mainly of those located outside of the United States and its territories, and those not appropriate for geodetic control (e.g., airport features, temporary bench marks).

The NA2011 Project included only the 81,055 marks with GNSS-derived geometric coordinates (latitude, longitude, and ellipsoid height) available in the NGSIDB as of March 29, 2012, plus their associated observations (GNSS vectors). Not all CORSs were used; only those CORSs that were part of GPS projects could be included in NA2011. Table 2.1 shows a total of 2586 CORSs in the NGSIDB in October 2018, although 842 were decommissioned or non-operational at that time. Every CORSs ID is associated with at least two reference points, the Antenna Reference Point (ARP) and the nominal L1 phase center (phase center coordinates are usually not publicly available from the NGSIDB, although they can be obtained from NGS CORS web pages).

The ARP is typically the lowest physical part of the antenna (i.e., the bottom of the antenna mount). As stated in Footnote 3, there is a need to specify a permanent physical point for referencing coordinates that is not part of the antenna itself, and one that would remain even if the antenna were removed. NGS has proposed the term Geometric Reference Point (GRP) for such points (NGS, 2019c). In most cases, the GRP would coincide in 3D-space with the ARP of an antenna installed at a CORS site. Importantly, a GRP independent of the antenna would allow for situations where there is an offset between the GRP and ARP. Although this change is desirable and would help remove ambiguity as to what is actually being referenced at a CORS, the term ARP will be used throughout this report, to maintain consistency with the naming conventions used at the time this project was performed.

Many CORSs also have a separate external monument that is vertically offset from the ARP. As of October 2018, 513 CORSs had such monuments located up to 1.748 m below the ARP (one is

3.5 mm higher than the ARP). Most of these monuments are on standard mounts 8.3 mm below the ARP, typically designated as "ground reference points" (GRPs) on Plate Boundary Observatory (PBO) CORSs. More details about CORSs are provided Section 2.2.2.

Table 2.1. Summary of publishable geodetic control in the NGSIDB (as of October, 2018).

Mark type	Number	Comments
Marks without leveled heights		
CORSs with ARP only	1904	770 decommissioned or non-operational; 11 with non-publishable orthometric heights
CORSs with ARP and external monument	493	53 decommissioned or non-operational; 4 with non-publishable orthometric heights
GNSS-derived passive	56,254	Horizontal coordinates (and ellipsoid heights) determined using GNSS; 1235 with non-publishable orthometric heights (1388 classified as destroyed)
Conventional horizontal only	220,533	Horizontal coordinates determined using classical (optical) methods; 3753 with non-publishable orthometric heights (13,234 classified as destroyed)
Vertical only, but not leveled	107,862	No horizontal control coordinates, heights not based on leveling; 6571 with non-publishable orthometric heights (19,576 classified as destroyed)
Total without leveled heights	**387,046**	(34,198 classified as destroyed)
Marks with leveled heights		
CORSs with leveled height	189	Leveled height to ARP or external monument; 19 decommissioned or non-operational
GNSS-derived passive plus leveled	31,346	Horizontal coordinates (and ellipsoid heights) determined using GNSS; 281 with non-publishable orthometric heights (1706 classified as destroyed)
Conventional horizontal plus leveled	27,367	Horizontal coordinates determined using classical (optical) methods; 429 orthometric heights not publishable (1992 classified as destroyed)
Vertical only leveled	450,471	Leveled heights with no horizontal control coordinates; 4087 with non-publishable orthometric heights (37,863 classified as destroyed)
Total leveled heights	**509,373**	(41,561 classified as destroyed)
Total all marks	**896,419**	(75,759 classified as destroyed)

Because of the historical distinction between horizontal and (leveled) vertical control, Table 2.1 is split between the 387,046 marks that do not have leveled heights (top), and the 509,373 marks with leveled heights. A small number of CORSs (189) have leveled heights to the ARP and/or

external monument. The 107,862 marks that have no horizontal control coordinates and no leveled heights are mostly marks that have only National Geodetic Vertical Datum of 1929 (NGVD 29) leveled heights that have been converted to NAVD 88 using the NGS *VERTCON* utility (Smith and Bilich, 2019). Note that overall 8.5% of the marks are classified as destroyed. The actual percentage is undoubtedly higher, as destroyed marks must be reported along with supporting evidence.

2.1.2. NGS GPS Projects

Results of NGS-published GPS surveys are loaded into the NGSIDB as GPS projects. The GPS projects were downloaded from the NGSIDB for the NA2011 Project and combined into 58 separate files to create 58 Helmert blocks. Helmert blocking is a method for breaking a large least squares adjustment into smaller components. The blocking method used for the NA2011 Project is discussed more fully in Section 3.3.1.

Three types of GPS project data were downloaded from the NGSIDB as input to the NA2011 Project:

- **Mark coordinates**. Individual mark coordinates in NGS horizontal control "Bluebook" format files ("B-files"). Since a mark can be in multiple GPS projects, there is no one-to-one relationship between projects and marks. Each mark in the B-files has a latitude, longitude, and ellipsoid height, as well as a designation, a unique permanent identifier (PID), and a four-digit mark serial number (SSN) unique within a Helmert block.
- **GNSS vectors**. Mark-to-mark GNSS vector components and variance-covariance information in NGS GPS vector format files ("G-files"). In a G-file, one or more vectors are grouped into processing "sessions." Each session corresponds to a specific GPS project and includes processing start and stop time, baseline processing software used, as well as other information. Within each block, the G-file vector endpoints are related to the marks by the corresponding SSNs in the B-files.
- **GPS project variance factors.** A horizontal and vertical standard deviation ("sigma") scalar value (called "variance factors" in NGS documentation) was computed for each GPS project. The horizontal and vertical components of all vectors in a GPS project were multiplied by their respective variance factors. A detailed discussion of the reasons and process for computing variance factors is provided in Section 3.2.

The B-file and G-file formats are described in detail in the NGS "Bluebook" (NGS, 2019d). "Bluebooking" is the term commonly used for the process of submitting survey results to NGS for publication in the NGSIDB.

A summary of the NGS GPS projects used in the NA2011 Project is given in Table 2.2. A total of 4440 GPS projects were available in the NGSIDB, and of these 4267 were used in the NA2011 Project. This implies 173 projects were skipped, but actually it was 171 projects, because two of the more recent ones, GPS1753 (April 2003) and GPS2650 (April 2008) were replaced by reprocessed versions GPS1753/C and GPS2650/B, respectively. Nearly all of these projects (167) were not used because they were skipped in the 2007 national adjustment and

were not re-evaluated for NA2011. Of the four projects used in 2007 that were skipped in 2011, three— 17298 (Nov 1985), 17396 (April 1989), and GPS349[5] (Aug 1991)—were omitted because they were old projects yielding poor results. One of the four used in the 2007 adjustment (GPS1753) was replaced in NA2011 with a reprocessed version (GPS1753/C). In addition, one project that was skipped in 2007 (GPS266) was included in NA2011. All projects skipped in NA2011 contained observations made prior to April 1997.

The final download of GPS projects from the NGSIDB was completed on March 29, 2012. As shown in Table 2.2, the complete set of GPS observation dates for all projects range from April 12, 1983, to December 21, 2011—a 28.7-year time span. The table shows CONUS split into "Primary" and "Secondary" projects, nominally at the beginning of 1994. However, some older projects were included in the Primary network, and some more recent projects were relegated to the Secondary network (splitting of the networks is more fully described in Section 3.3.2). In addition, the Pacific network was adjusted twice, using two different sets of constraints. The two Pacific networks were defined by exactly the same set of GNSS vectors, but for one the constrained marks were referenced to the Pacific tectonic plate, and for the other to the Mariana tectonic plate. In each Pacific network, marks are given coordinates referenced to one or the other plate, never both plates. Details of defining these networks are provided in Section 3.5.2.

Table 2.2. Summary of NGS GPS projects used in the NA2011 Project.

GPS project type and region	Number projects	Earliest observation	Latest observation	**Num marks	Total number vectors	Number vectors rejected	Percent vectors rejected
Primary (CONUS + Caribbean)	3472	11/12/1987	12/21/2011	86,645	335,530	10,279	3.06%
Secondary (CONUS only)	614	04/12/1983	12/31/2005	25,295	84,493	10,952	12.96%
Alaska	142	08/11/1984	07/31/2011	1342	2846	314	11.03%
Pacific	39	08/10/1993	04/29/2011	690	1852	58	3.13%
Total used	**4267**	**04/12/1983**	**12/21/2011**	**113,972**	**424,721**	**21,603**	**5.09%**
Skipped	171*	02/22/1984	03/19/1997				
Total all	**4440**	**04/12/1983**	**12/21/2011**				

**173 projects were skipped, but two of them were reprocessed, GPS1753 (reprocessed as GPS1753/C) and GPS2650 (reprocessed as GPS2650/B).*
***Greater than overall number of marks because a mark can occur in more than one project.*

Table 2.2 also gives the number of marks and GNSS vectors in the projects, as well as the number and percent of vectors rejected. The number of marks adds up to greater than the total of 81,055, because marks are often occupied in multiple projects. In contrast, the total number of

[5] NGS initially used three digits for projects with a "GPS" prefix, which later changed to four digits. Recently NGS renamed three-digit projects by using zero padding, so that all have four digits (e.g., GPS349 became GPS0349). Zero padding is not used in this report, because many file names and attributes made use of the original names.

vectors equals the total of 424,721 for the entire NA2011 Project, as there is a one-to-one relationship between projects and vectors. Note that the percentage of rejected vectors is significantly greater for Secondary CONUS projects, because they are generally older. GPS projects were processed by a total of 234 organizations (based on the number of unique contributor codes in the NGSIDB). NGS processed slightly more than half (2473, or 55.7%). The remaining 44.3% were processed by a wide variety of federal, state, and local government agencies, as well as private companies, but the results were reviewed and validated by NGS before loading into the NGSIDB.

Figure 2.1 shows the number of NA2011 GNSS marks occupied and vectors processed by NGS and other organizations. The peak number of marks occurred in 1995 (8341 marks), whereas the peak number of vectors processed occurred in 2005 (36,002 vectors). The proportion of GPS marks and vectors processed by NGS has generally decreased over time. Overall, the mean is 35% and 37% for the number of marks and vectors processed by NGS, respectively.

The duration of the GPS projects used in the NA2011 Project varied considerably. Figure 2.2 shows GPS project durations for various time spans, where duration is the time between the first and last GNSS vector observation. For most projects (58%), data collection was completed within one week. An additional 36% took between one week and a year, and 5.6% took over a year. A few projects have even longer time spans; 135 (3.2%) are greater than two years, and the maximum time between the first and last observation for a project is 15.1 years (GPS1808 in North Carolina, starting on February 21, 1990 and ending on March 11, 2005). The variability is indicated by the large difference between the median and mean project durations of 3 and 105 days, respectively. There is no clear trend in the occurrence of short projects and age, with the exception that prior to 1991, only 2 of the 151 projects lasted 24 hours or less. The largest proportion of projects lasting 24 hours or less was 56%, in 1997. Conversely, the largest proportion of projects lasting more than 30 days occurred prior to 1991 (54%). In contrast, from 1991 through 2011, 25% of the projects had durations of more than 30 days, and that proportion was fairly constant over that period.

For projects with unusually long durations (more than several months or a year, for example), it likely would have been more appropriate to group the vectors by time, and compute sigma scalars for each group, rather than compute one scalar for the entire project. This illustrates one of the problems with grouping vectors by project, and it is discussed further in Section 5.2.1.

Maps displaying the spatial distribution of GPS projects for the NA2011 Project are presented in Figure 2.3. The project coordinates were computed as the centroid of the midpoint of every vector in the project. Although projects covering large areas and with a wide range of vector lengths are not well represented by a single point, this approach gives a reasonably good representation of the project location in most cases. The project symbol colors in Figure 2.3 are based on the midpoint year of the project, and the symbol size indicates the number of marks in the project. The maps convey the wide range in distribution, age, and size of GPS projections used for the NA2011 Project, as well as clearly demonstrate the huge disparity in geodetic surveying activity submitted to NGS from state to state. Statistics on the number of marks and vectors for GPS projects are given in Table 2.3.

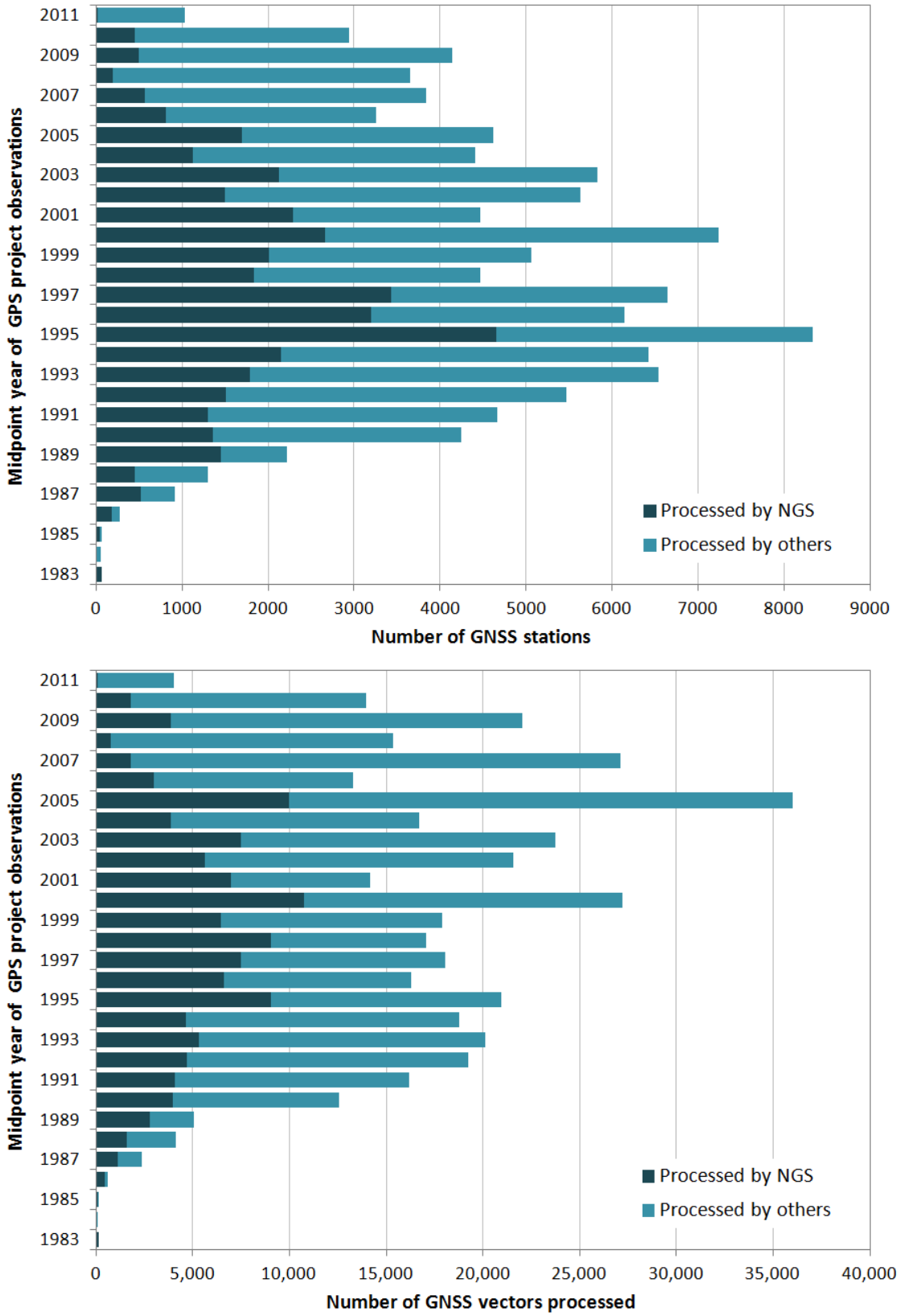

Figure 2.1. Number of NA2011 GPS marks and vectors processed by NGS and other organization.

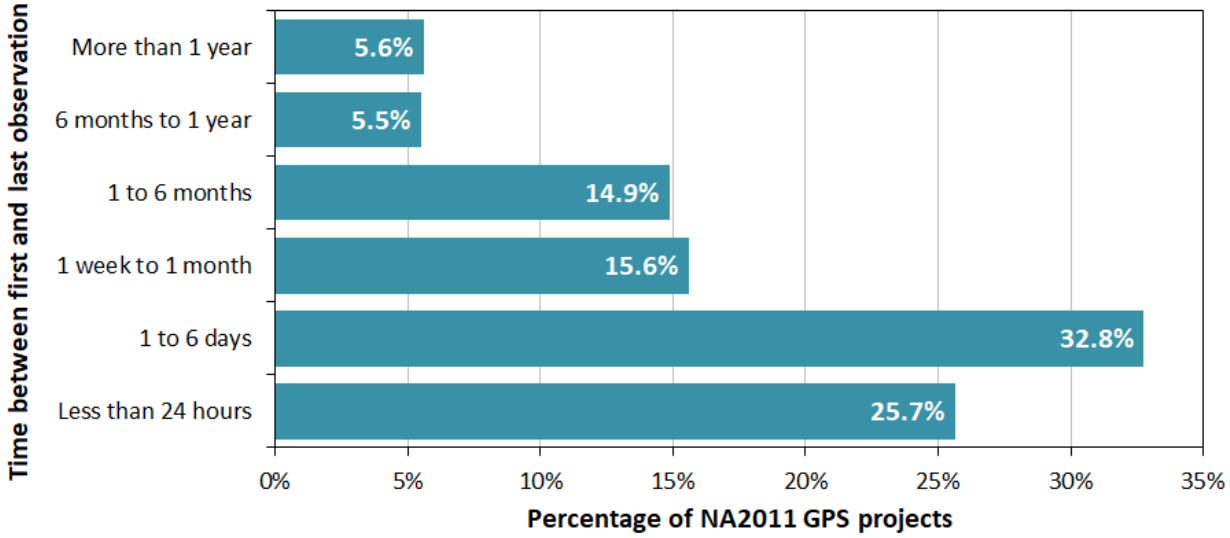

Figure 2.2. Duration of NA2011 GPS projects as time between first and last observation.

There are a couple of unusual entries in Table 2.3 that warrant explanation. One is the minimum vector length of 0.7 mm. Obviously, such a length is not physically possible, and it represents an error in the data. It, along with other data anomalies, is discussed in detail in Chapter 5. The other unusual entry is the maximum of 100% rejection of vectors (in three projects); however, this is not as alarming as it appears. These three projects are very small airport surveys, with a total of five vectors in all three projects combined.

All GPS projects used in the NA2011 Project are included in the electronic files associated with this report (see Appendix D). The GPS project information includes whether they were used in the 2011 or 2007 adjustments, the network they were used in, and the horizontal and vertical scalars applied to the project. Information on the number, date, and duration of occupations was obtained from vector G-file metadata as downloaded from the NGSIDB.

Table 2.3. Statistics on number of marks and vectors for GPS projects used in the NA2011 Project.

	Number marks	Number vectors		Percent rejected	Vector lengths in GPS projects (m)			
		Total	Rejected		Min	Max	Median	Mean
Min	2	1	0	0.0%	0.0007	0.6780	0.6780	0.6780
Max	1051	15,589	754	100.0%	1,896,026	6,147,468	2,102,947	2,064,899
Median	7	16	0	0.0%	515	21,850	3602	6065
Mean	26.7	99.5	5.1	4.5%	8,218	83,554	26,598	31,367
Std dev	±55.6	±374.4	±21.4	±10.8%	±48,148	±274,342	±80,964	±87,460

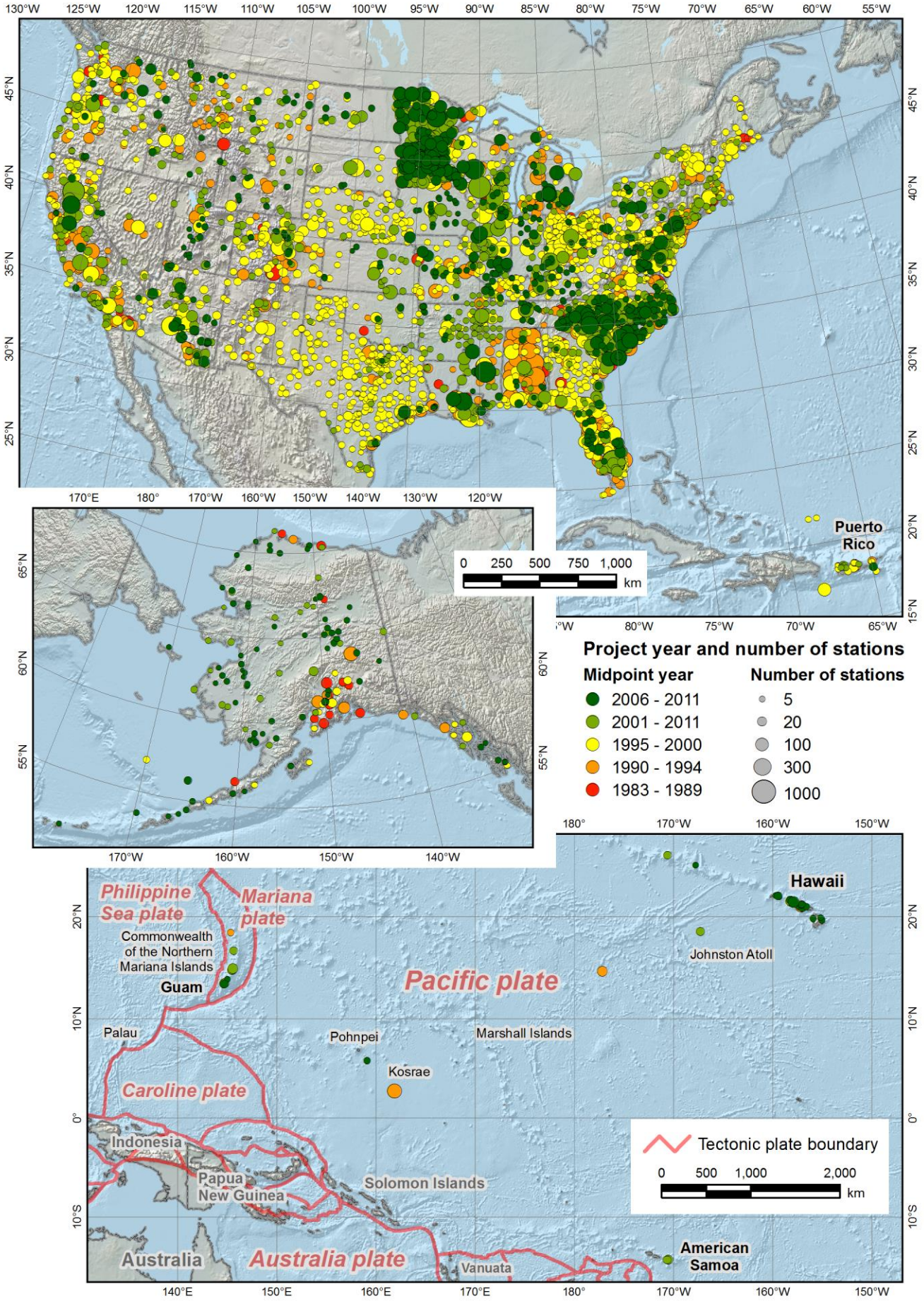

Figure 2.3. Location, year, and number of marks for GPS projects used in the NA2011 Project.

2.2. CORSs and passive control marks

The NA2011 Project was an adjustment of GNSS passive control marks in the NGSIDB constrained to MYCS1 CORS coordinates. For a CORS to be used as a constraint, it must have been part of a GPS project in the NGSIDB. For this reason, not all MYCS1 CORSs were used in the NA2011 Project.

2.2.1. Control marks and the NGS Bluebook file ("B-file")

As stated in the previous section, all marks used in the NA2011 Project were downloaded from the NGSIDB by their association with GPS projects. A total of 81,055 unique marks participated in the adjustment, with 79,860 of these classified as passive marks, and 1195 classified as MYCS1 CORSs. The distinction between "passive" and "MYCS1 CORS" was not always clear. In some cases, a "passive" mark is a continuously operating base that was not part of the NOAA CORS Network. Passive marks were essentially any mark that was not an MYCS1 CORS. The methods used for determining CORSs from the NGSIDB is discussed in Section 2.2.2.

Whether passive marks or constrained CORSs, all marks were downloaded from the NGSIDB in NGS Bluebook file format as "B-files," as described in the Section 2.1.2. All marks were "unique" in the sense each had a unique 6-character PID (**P**ermanent **ID**entifier). The intent is that each PID corresponds to a unique and distinct physical mark, although there are certain instances where a single mark has been accidentally assigned more than one PID. This issue is addressed in greater detail for CORSs in the next section (2.2.2).

Marks used in the NA2011 Project are summarized in Table 2.4, grouped by network and by category. There are CONUS Primary and Secondary, Alaska, and (two) Pacific networks. The table contains six mark categories: MYCS1 CORS, passive, non-MYCS1 CORS, publishable, unpublishable, and excluded. The categories other than MYCS1 CORS are defined briefly below, and all categories are discussed in greater detail in the next section.

1) **Passive control.** Marks with coordinates that were determined in the adjustments. Most are physical marks in the ground, although some are points associated with permanently mounted base stations (usually ARPs) that are not NGS CORSs (consists of 74,850 marks).
2) **Non-MYCS1 CORS.** Stations that are apparently NGS CORSs, but MYCS1 coordinates could either not be determined or could not be unambiguously assigned. These marks were treated as passive and were not constrained (consists of 43 marks, with three of these being outside the United States and three in the "excluded" category below).
3) **Publishable marks.** Marks accessible by the public and published on NGS Datasheets. However, some publishable marks may not always be accessible if other problems exist, for example if they were officially identified as destroyed or lacked a description (consists of 1182 MYCS1 CORSs and 74,893 passive marks, plus 83 "excluded" marks).
4) **Unpublishable marks.** Marks that cannot be accessed by the public for publication on NGS Datasheets. These marks consist mostly of FAA airport marks (such as runway endpoints) that are not considered appropriate for geodetic control, as well as marks

outside the United States and its territories (consists of 15 MYCS1 CORSs and 4884 passive marks, with 4795 of these being FAA marks).

5) **Excluded marks.** Marks with coordinates that could not be determined. This was the situation for 182 marks, because they became disconnected when the CONUS network was split into Primary and Secondary (with 100 of these being unpublishable FAA marks). This disconnection problem is discussed in Section 3.4. One additional mark in Hawaii that was part of an Alaska GPS project also was not computed (discussed in Section 2.4.1).

Table 2.4. Summary of marks in the NA2011 Project.

	All	CONUS all	CONUS Primary	CONUS Secondary	Alaska	Pacific overall	Pacific plate	Mariana plate
CORSs with MYCS1 coordinates constrained in adjustments								
Publishable CORS								
MYCS1 computed	960	898	882	16	39	23	18	5
MYCS1 modeled	220	200	199	1	19	1	0	1
Unpublishable CORSs (located outside U.S.)								
MYCS1 computed	13	13	13	0	0	0	0	0
MYCS1 modeled	2	2	2	0	0	0	0	0
All MYCS1 CORSs	**1,195**	**1,113**	**1,096**	**17**	**58**	**24**	**18**	**6**
Passive marks and non-MYCS1 CORSs determined in the adjustments								
Publishable computed passive control								
Passive marks	74,850	73,470	56,737	16,733	864	516	345	171
Non-MYCS1 CORS	43	42	40	2	1	0	0	0
All publishable	**74,893**	**73,512**	**56,777**	**16,735**	**865**	**516**	**345**	**171**
Unpublishable computed passive control								
Non-MYCS1 CORSs	3	3	2	1	0	0	0	0
Outside U.S. & territories	86	85	68	17	1	0	0	0
FAA airport marks	4,695	4,651	4,081	570	44	0	0	0
All unpublishable	**4,784**	**4,739**	**4,151**	**588**	**45**	**0**	**0**	**0**
Excluded passive control (not computed)								
Excluded FAA marks	100	100	100	0	0	0	0	0
Non-MYCS1 CORSs	3	3	3	0	0	0	0	0
Other excluded	80	79	45	34	1	0	0	0
All excluded control	**183**	**182**	**148**	**34**	**1**	**0**	**0**	**0**
Total all passive	**79,860**	**78,433**	**61,076**	**17,357**	**911**	**516**	**345**	**171**
Total all marks	**81,055**	**79,546**	**62,172**	**17,374**	**969**	**540**	**363**	**177**

An important part of establishing control is to occupy a mark more than once, because multiple occupations help to identify blunders and ensure statistical independence. In the context of the data used for the NA2011 Project, the term "occupation" warrants elaboration.

For most passive marks, an "occupation" is intended to represent a setup of a GNSS antenna over the mark, where each occupation is a different setup of the equipment. Unfortunately, there is no metadata associated with NA2011 input to explicitly indicate an occupation. An occupation is inferred from the processing session start and stop times in the G-file. In most cases, this likely corresponds to the intended meaning of an occupation for passive marks, particularly if there is a significant time gap between sessions.

In any event, an occupation as defined here represents an upper limit: a mark cannot have more occupations than inferred, it can only have less. For example, a mark with two occupations might actually only have one, if for example the receiver was merely turned off and then on (without a new physical setup), or if a single observation file was split into two sessions. One important purpose of estimating occupations is to identify marks with only a single occupation.

For CORSs (and other permanently or semi-permanently mounted GNSS antennas), there cannot actually be multiple independent setups, because the antenna location is essentially fixed in all sessions (although the antenna type and mount can change). A CORS occupation represents its participation in a session (revealing that some CORSs were used many times). This provides an indication as to how often a CORS was used for GPS projects.

Based on this definition of occupations, Figure 2.4 shows most marks were occupied twice (30,166 passive marks and 143 CORSs, for a total of 37.4% of all marks). A total of 3988 marks (4.9%) were occupied more than 10 times, and 562 of these were CORSs. The median number of occupations is 3, and the mean is 4.1.

The maximum number of mark occupations is 468, unsurprisingly for a CORS (LAKE HOUSTON CORS ARP, PID AF9521). For a passive mark that is not a permanent GNSS base, the maximum number of occupations is 151, for mark AVL ARP 2 (PID AC8545) in North Carolina, a topographic survey disk set in concrete. A relatively large number (8182 or 10.1%) of marks were occupied only once. Such single occupations are not considered appropriate for establishing control. Yet this approach was (and still is) part of standard practice for airport control surveys, the rationale being that the single occupations are usually on leveled bench marks, so a check is provided by the sum of the leveled height and hybrid geoid height. Nonetheless, such practice compromises the network, particularly in adjustments such as for the NA2011 Project, which makes no reference to leveled heights. Unfortunately, there is no mechanism for identifying single occupations in existing NGS products (such as Datasheets). However, it is recommend that this information be added (see Section 6.2.2.2), and this information is available in the digital deliverables included with this project (available at ftp://geodesy.noaa.gov/pub/NA2011/).

Also important for ensuring independence is the time interval between multiple occupations. Figure 2.5 shows the time span between the midpoint of the first and last occupations of NA2011 marks occupied multiple times, for enabled observations on passive marks and CORSs (i.e., excluding rejected vectors). The time interval ranges from less than 2 hours for 7901 passive marks (and 4 CORSs) to over 20 years for 268 passive marks (with maximum of 26.7 years for

passive marks and 13.9 years for CORSs). The median time separation between the first and last for all marks is 3.2 days, whereas the mean is 1.5 years, illustrating the great variability.

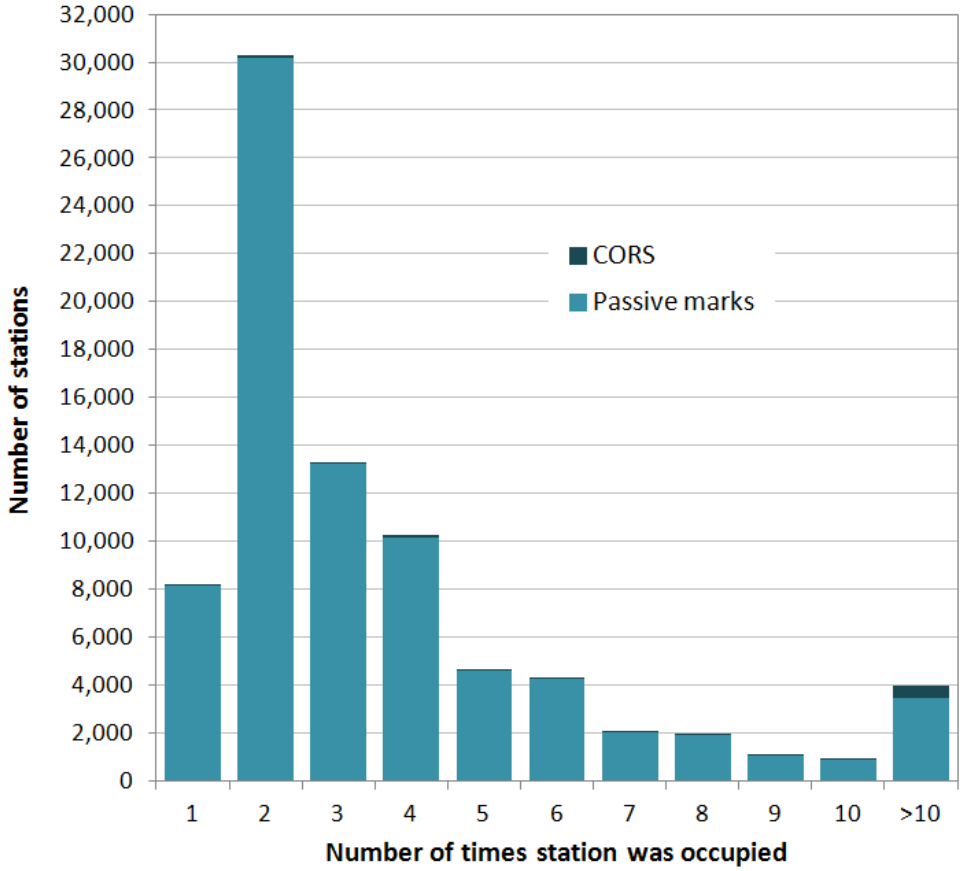

Figure 2.4. Number of times marks were occupied in the NA2011 networks.

2.2.2. Determining CORSs from the NGSIDB

The CORS Network provides the geometric foundation of the NSRS, and coordinates of CORSs from the MYCS1 were used to constrain the NA2011 adjustments. It is important, therefore, that all CORSs in the NA2011 networks be correctly identified and associated with MYCS1 results.

The primary means of identifying CORSs is the unique four-character site ID. In contrast, every mark in the NA2011 networks is identified by its unique PID. MYCS1 results were determined for the antenna reference point (ARP), and every MYCS1 CORS ARP has an associated PID in the NGSIDB. In addition, every CORS has at least one other current PID associated with its L1 antenna phase center (APC). The L1 APC PID is associated with a specific antenna, and its coordinates are generally not available on ***NGS Datasheets*** (NGS, 2019e), although they are available on CORS ***position-velocity sheets***, as mentioned below). Many other CORSs also have an associated external physical monument (denoted as "MON") located some distance below the ARP, also with a PID. Of the 2275 CORSs in the original MYCS1 with NAD 83 coordinates, 476 (20.9%) have an external monument with a distance below the ARP of up to 1.748 m. A

majority of the monuments (371 = 77.9%) are 0.0083 m below the ARP. The 0.0083 m offsets are often used for standard Plate Boundary Observatory (PBO) antenna mounts, usually referred to as ground reference points (GRPs). One MYCS1 CORS monument has a negative offset (-0.0035 m, for CORS CHAB, with monument PID AF9692), indicating it is (slightly) higher than the ARP. Only 26 of the NAD 83 MYCS1 CORSs have external monuments more than 0.1 m below the ARP.

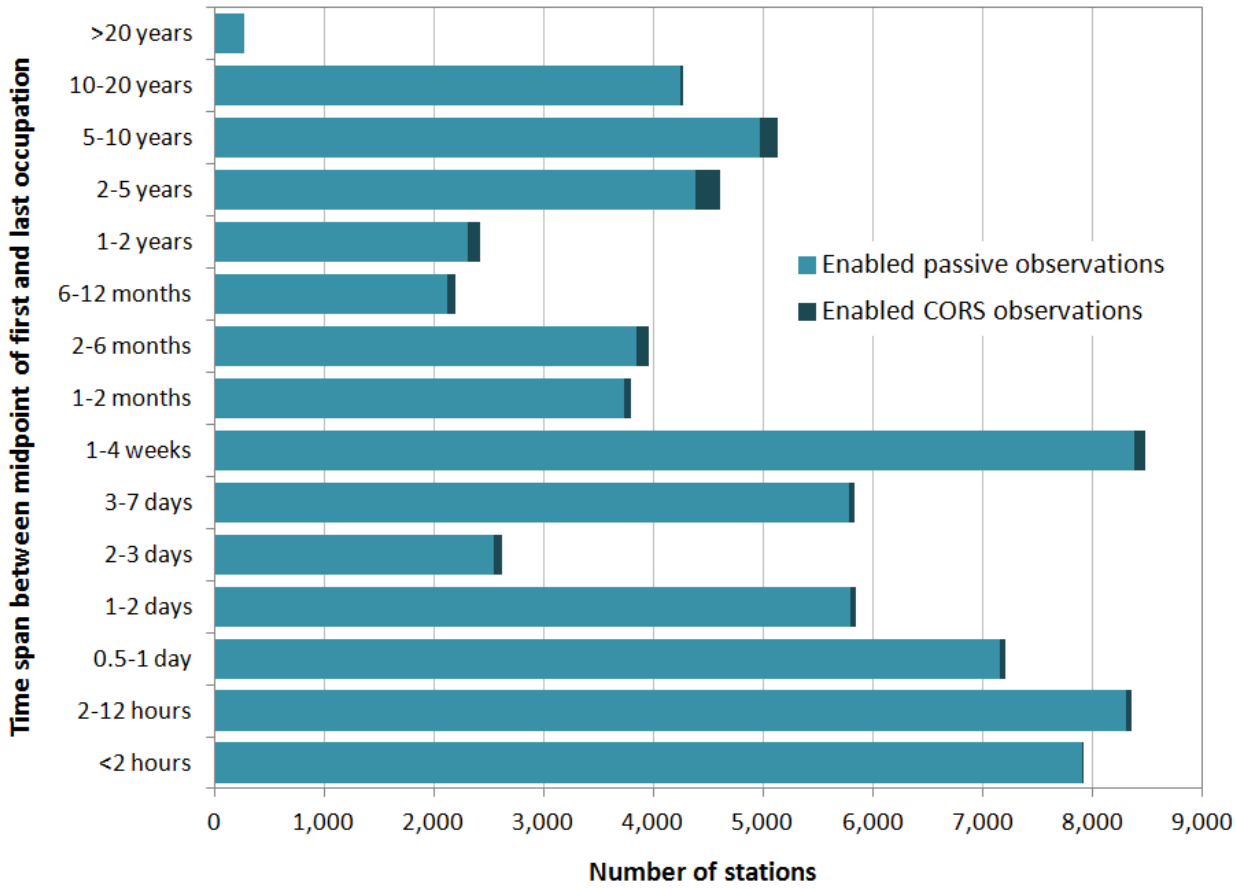

Figure 2.5. Time between midpoint of first and last occupation of marks observed multiple times.

In and of itself, the presence of up to three PIDs per CORS site ID is not a problem. CORS position-velocity sheets are available through the "Position and Velocity" link for each CORS site web page (accessed through https://geodesy.noaa.gov/CORS/). Each CORS position-velocity sheet provides NAD 83 epoch 2010.00 coordinates (and velocities) for the ARP, L1 APC, and external monument (when present). Current sheets also provide MYCS2 ITRF2014 epoch 2010.00 coordinates, and MYCS1 IGS08 epoch 2005.00 values are still available as of this writing (November 2019). Individual position-velocity sheets are also available via anonymous file transfer protocol (FTP) at ftp://geodesy.noaa.gov/cors/coord/coord_08/ (for MYCS1 IGS08) and at ftp://geodesy.noaa.gov/cors/coord/coord_14/ (for MYCS2 ITRF2014). Current CORS NAD 83 coordinates on NGS Datasheets are identical to those derived from ITRF2014 position-velocity sheets. The NAD 83 coordinates derived from MYCS1 IGS08

coordinates were the ones used to obtain the ARP, L1 APC, and external monument (MON) coordinates for all constrained CORSs for the NA2011 Project.

Composite tables of NAD 83 epoch 2010.00 MYCS1 and MYCS2 CORS coordinates are also provided through the same FTP links. The tables provide ARP coordinates and velocities for all CORSs for each frame (2011, PA11, and MA11). However, the tables do not provide L1 APC or monument coordinates. In addition, there are small coordinate discrepancies between the composite tables and the position-velocity sheets, apparently due to rounding. At the time CORS coordinates were last obtained for NA2011 (early 2012), coordinates in the composite table differed from position-velocity sheet values by 0.1 mm in longitude for one, and by 1 mm for 42 others (20 of these were used in NA2011). No discrepancies were found between the CORS position-velocity sheets and the NGS Datasheets. The NGS Datasheet and CORS position-velocity sheet values should be considered definitive and were used for the NA2011 Project.

The existence of a PID for the ARP, L1 APC, and (if applicable) the external monument for all MYCS1 CORSs gives the impression that identifying CORSs in the NGSIDB was a simple matter. However, there were significant difficulties, and most of these fell into one of the four following categories: 1) different information sources for associating PIDs with CORSs; 2) marks in the NA2011 networks that became CORSs during the project; 3) use of the L1 APCs as the monument in GPS projects; and 4) CORSs represented by multiple PIDs. Each of these categories is discussed below.

2.2.2.1. Different information sources for associating PIDs with CORSs

A total of 1244 PIDs (associated with 1008 unique CORS site IDs) were identified as possible CORSs in the NA2011 networks. Of these, 1195 PIDs (associated with 991 CORS site IDs) were used as MYCS1 constraints. The sources for the information on PID associations is the main reason for the difference between the number of CORSs identified versus constrained. The three following sources were used to associate PIDs with CORSs:

1. **MYCS1.** PIDs obtained from MYCS1 results for ARPs, along with associated L1 APC and (if applicable) monument PIDs. All were constrained in the NA2011 Project (consisted of 866 ARPs, 157 L1 APCs, and 172 external monuments, for a total of 1018 in NA2011).
2. **NGSIDB.** Stations classified as CORSs in the NGSIDB (by having a CORS site ID), in addition to the 1018 MYCS1 PIDs (73 classified as CORSs in NA2011, plus 17 classified as passive).
3. **Inferred.** Stations inferred as CORSs from other information, mainly due to their proximity to MYCS1 marks, but also based on a search within mark designations for character strings such as “CORS,” “ARP,” “L1,” “L 1,” “PHASE,” as well as string length, as CORSs usually have longer designations than passive marks (104 classified as CORSs in NA2011, plus 31 classified as passive).

The three CORS PID sources and corresponding monument types are shown in Table 2.5. Out of 1244 possible CORSs, 49 could not be reliably associated with MYCS1 site IDs and consequently were not constrained (i.e., were treated as passive marks). Most of these

unconstrained CORSs (31) are "inferred" from other information (mainly their proximity to marks with MYCS1 coordinates). Monument types for the inferred CORSs were assigned based on the description in the designation. For eight of them the type could not be determined, so they were assigned a monument type of "unknown." In contrast, note that all constrained CORSs had an explicitly identified MYCS1 monument.

Table 2.5. Summary of constrained and unconstrained CORS sources and monument types.

CORSs monument type	All CORSs	Source of PID for CORSs		
		MYCS1	NGSIDB	Inferred
CORSs constrained using MYCS1 coordinates: 991 unique site IDs				
Antenna Reference Point	866	830	1	35
External monument	172	128	0	44
L1 Antenna Phase Center	157	60	72	25
Total constrained CORSs	**1195**	**1018**	**73**	**104**
Unconstrained CORSs (treated as passive) : 44 unique site IDs				
Antenna Reference Point	14	0	11	3
External monument	9	0	0	9
L1 Antenna Phase Center	18	0	7	11
Unknown	8	0	0	8
Total unconstrained CORSs	**49**	**0**	**18**	**31**
Total all CORSs	**1244**	**1018**	**91**	**135**

The 49 apparent CORS PIDs (inferred from the NGSIDB) not constrained in the NA2011 adjustments correspond to 44 CORS site IDs, with 17 of these not represented in the MYCS1. These 49 "passive" CORSs are grouped into one of the following four categories:

- **11 PIDs (10 CORS site IDs not in MYCS1).** No data were available for the MYCS1 (i.e., they are in the list of 68 CORSs from the MYCS1 project with no data, and therefore were not used for MYCS1). A few are also apparently "old" site IDs used in the past but discarded. One site ID, NIST (DN4182 = NIST ANTENNA ARP), is an unpublished IGS mark that does not have MYCS1 coordinates and is also classified as unpublishable by NGS.
- **29 PIDs (4 CORS site IDs not in MYCS1).** Inferred CORSs that were too distant from any mark with MYCS1 coordinates to be considered the same mark (usually more than 10 cm 3D).
- **7 PIDs (1 CORS site ID not in MYCS1).** Rejected as constraints because of poor fit.
- **2 PIDs (2 CORS site IDs not in MYCS1).** Permanent GNSS bases in the NA2011 networks treated as passive but became CORSs in June 2012, too late to be included as constraints in the NA2011 Project. These two CORSs (and other "new" ones) are discussed further in the following section.

2.2.2.2. Stations in the NA2011 networks that became CORSs during the project

New CORSs were added to the CORS Network during the final stages of the NA2011 adjustments. Several of these were already in the NA2011 networks as non-MYCS1 CORS GNSS base stations and so were treated as passive marks in the adjustment (although the adjusted coordinates were superseded by the new CORS coordinates for publication). The last eight CORSs added as MYCS1 constraints (in April 2012) are provided in Table 2.6. The table actually lists nine constrained PIDs, however two (AI4496 and DH9078) are associated with a single CORS external monument (site ID ORVB). As indicated in the table, PID DH9078 was merged with AI4496. However, for the NA2011 adjustment, the two PIDs remained as distinct marks, although both were constrained to the same set of new CORS coordinates. In addition to these eight new CORSs, 12 other new CORSs were added to the NA2011 networks in December 2011 and January 2012 (after completion of MYCS1 but before completion of the NA2011 Project).

As mentioned in the previous section, two marks in the NA2011adjustment were treated as passive control but became CORSs in June 2012, too late to be included as constraints. These two new CORSs are listed in the bottom of Table 2.6, along with the difference in coordinates between the NA2011 adjusted and new CORSs published values.

Table 2.6. NA2011 marks that became CORSs during the last two months of the NA2011 Project.

PID	CORS site ID	CORS designation	Monument type	Coordinate shift from passive to MYCS1 CORS (m)		
				dN	dE	dh
Constrained to new MYCS1 coordinates in NA2011 Project (became CORSs in April 2012)						
DH6764	MASW	MASW_SCGN_CN2001 GRP	Monument	0.009	-0.005	0.004
AI4496	ORVB	OROVILLE DAM GRM	Monument	0.012	-0.010	0.013
DH9078*	ORVB	ORVB OROVILLE DAM CORS POINT	Monument	-0.002	0.002	-0.006
DN4106	P256	FALLMANPRPCN2005 GRP	Monument	-0.014	-0.031	0.010
DL9235	P267	DIXONAVIATCN2005 GRP	Monument	0.000	-0.027	0.056
DK4683	P268	FINCHFARMSCN2005 CORS ARP	ARP	0.007	-0.021	0.025
DL9236	P268	FINCHFARMSCN2005 GRP	Monument	-0.009	-0.024	0.026
DL9240	P345	HOOKERDOMECN2005 GRP	Monument	0.007	-0.004	-0.004
DM3260	SCEB	EDISTO ISLAND CORS ARP	ARP	-0.001	0.005	0.060
Not constrained to MYCS1 coordinates (became CORSs when NA2011 Project completed in June 2012)						
AI4469	AZU1	AZUSA 49911M001	ARP	-0.016	-0.009	-0.021
DN2580	MIMC	MACKINAW CITY CORS ARP	ARP	-0.003	0.002	-0.004

**PID no longer publishable in NGSIDB (merged with AI4496 using same site ID)*

2.2.2.3. Use of CORS L1 antenna phase centers as the monuments in GPS projects

For the 1195 CORSs constrained in the NA2011 networks, 157 (13%) reference the L1 antenna phase center (APC) as the "monument." Using an L1 APC monument is particularly

problematic for older marks, because the antenna type likely changed. Use of the L1 APC as a "monument" was an unfortunate practice in the early years of CORSs, a practice at odds with the implied and practical definition of a survey control monument being a permanent, physically real, perpetually identifiable point, independent of the geodetic equipment. Indeed, 97 (62%) of the 157 constrained L1 APCs have different PIDs from the MYCS1 L1 APC PIDs with the same CORS site ID, because of antenna changes.

The main problem with L1 APC "monuments" is that different antennas use different APC variation models, so changing the antenna will result in an L1 APC at a different location in space. In addition, the L1 APC location varies with changes in satellite positions. The location given for the L1 APC is based on an assigned offset in the antenna model and does not represent the mean position of the L1 APC. These problems are exacerbated by the following additional issues: the L1 APC of CORSs was often used as the "monument" in older GPS projects; NGS does not keep records of previous antenna L1 APC PIDs; and all (or nearly all) L1 APC monuments used in GPS projects were based on relative antenna models (whereas absolute models were used for MYCS1 processing).

Although often used in the past, L1 APC coordinates are now rarely (if ever) used for the control monument of a CORS. For GPS projects in the NA2011 dataset with occupations from 1990 through 1997, 55% of the CORS sessions in the G-files are referenced to the CORS L1 APC. In contrast, only 1.6% referenced the L1 APC from 1998 through 2011 (for current Bluebooking, NGS strongly discourages the use of L1 APC constraints). The sudden decrease in the use of L1 APCs as CORS monuments in 1998 is clearly illustrated in Figure 2.6. The plummet in L1 APC usage is likely correlated with the end of the HARN surveys and the beginning of the FBN surveys (which brought, in general, better GPS surveying methods, such as using GPS for ellipsoid height determination and tying the surveys to the CORS Network, which was much denser in the late 1990s than in the early 1990s). This figure also shows the change in percentage of CORS PIDs identified directly from the MYCS1, versus indirectly from the NGSIDB or inferred. By 2000, at least 90% of the CORS occupations used PIDs that could be associated with the MYCS1 (recall that a CORS "occupation" is its occurrence in a processing session). The large proportion of L1 APC monument usage occurs when direct MYCS1 association is low. This exacerbates the problem, because fewer CORSs were available as constraints for older data, making the network more vulnerable to L1 APC position errors and incorrect association between PIDs and MYCS1 results. Fortunately, L1 APC errors were likely small (as discussed below), and a conservative approach was used for assigning PIDs.

Even though the PID for the L1 APC changes when the antenna changes, NGS does not keep records of superseded antenna PIDs (Cline, 2012). This lack of records required estimating the vertical offset from the ARP to the L1 APC for antennas with different PIDs. As shown in Table 2.5, a total of 97 constrained CORSs had L1 APC PIDs determined from sources other than the MYCS1 results (72 were determined from the NGSIDB and 25 were inferred). Of these "superseded" antennas, the offset could be estimated for the NGISDB CORSs. The relative offsets were estimated by taking the pre-NA2011 ARP and L1 APC ellipsoid heights differences in the NGSIDB and subtracting the MYCS1 ARP and L1 APC ellipsoid height differences for the corresponding CORS site ID. The computed change in L1 APC offsets were checked against

the current antenna types and superseded ellipsoid height values on the NGS Datasheets. The offset corrections from MYCS1 (based on absolute antenna models) to the superseded antennas ranged from zero to 0.019 m, with a mean of 0.017 m. This offset is consistent in direction and magnitude with the change in ellipsoid heights for the overall NA2011 results (mean decrease of 0.020 m). In addition, the change is relatively small, so the effect on the 17 uncorrected superseded antennas is also small. Moreover, the impact of the change is only relevant as a *relative* change between both ends of a GNSS vector. That is, the impact on computed ellipsoid heights is due to the difference in antenna height correction at each end of the vector. As the corrections were nearly all based on consistent antenna models used at the time of processing, the difference between vector endpoints was likely less than a few millimeters.

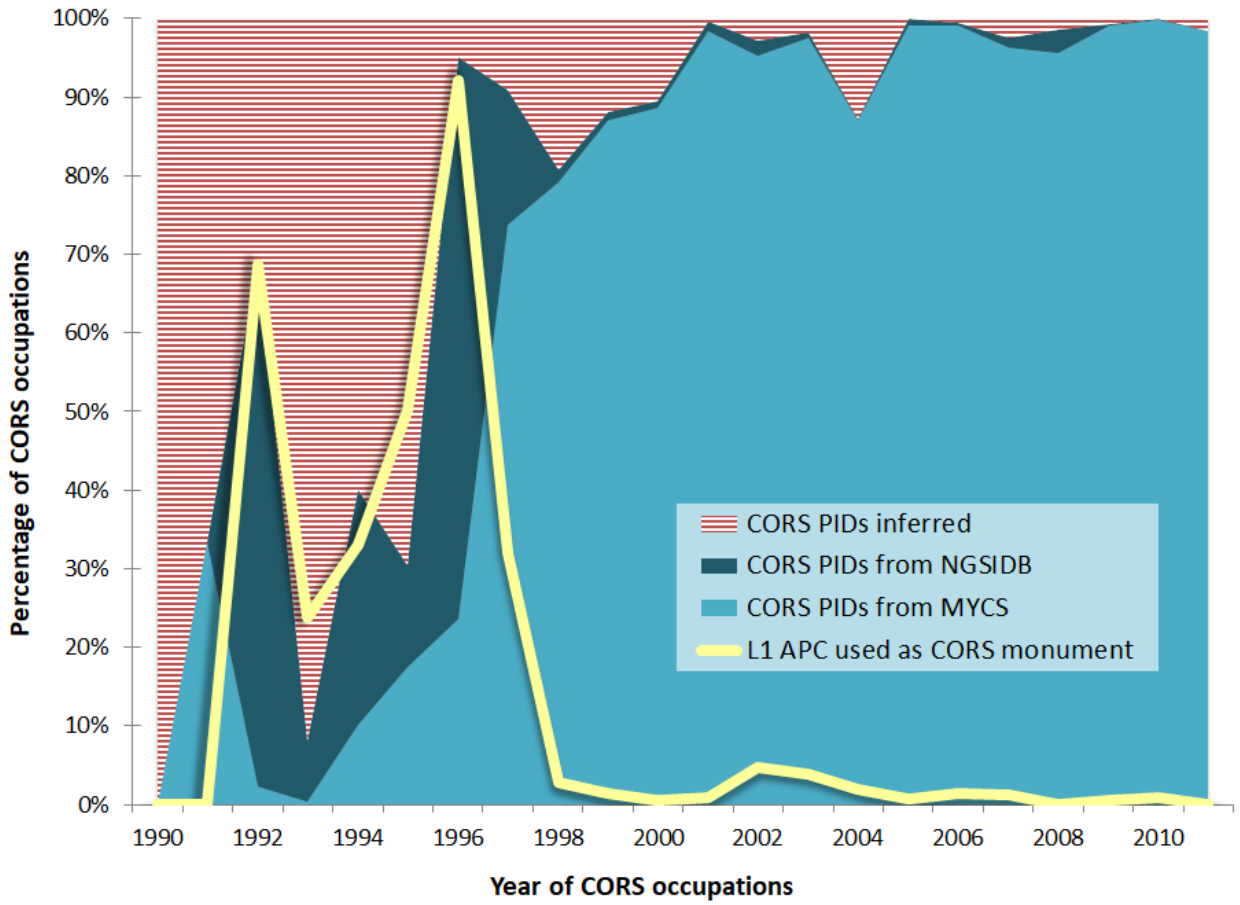

Figure 2.6. Percentage of CORS occupations by year for various categories of CORSs.

Relative difference in antenna offset corrections also applies to another L1 APC monument problem for the NA2011 Project: the change from relative to absolute APC modeling for MYCS1. One of the significant changes in GPS data processing for the MYCS1 was that absolute antenna models were used. In contrast, all the GPS vectors in the NA2011 networks were processed using relative models (or no models at all prior to 1994). But, as pointed out previously for superseded antenna corrections, only the relative difference at the end of the GPS

vectors will impact final computed ellipsoid heights, since the vectors are defined as delta components. It would be problematic if an absolute model were used at one end of a vector and a relative model at the other. However, it is extremely unlikely that this occurred.

2.2.2.4. Individual CORS represented by multiple PIDs

As might be expected by the three different sources for CORS PIDs, some are likely duplicates. "Duplicate" in this context means the same component of a CORS site ID (ARP, monument, or L1 APC) is represented by more than one PID. A proximity analysis revealed that for the 1244 CORS PIDs (both constrained and unconstrained), there are 372 pairs of duplicates within 1 m 3D of one another. Of these 372 pairs, 60 are likely duplicates, because all have the same monument type (although four have "unknown" monuments). Most (47) have the same CORS site ID and are within 0.13 m of one another 3D. For the remaining 312 pairs within 1 m, 44 are too far apart (more than 0.2 m); 208 have a different monument type and so cannot be duplicates (i.e., have different heights); 59 are new Coast Guard beacon CORSs with new site IDs (usually with a different antenna and antenna mount); and one is a permanent GNSS base that had a new mount installed when it became a CORS. A summary of the CORSs evaluated as possible duplicates is given in Table 2.7.

One pair of duplicate base stations is not included in Table 2.7, because it was identified and merged into two CORSs for the NA2011 Project in December 2011. The passive base station DK9969 (BULLHEAD CITY CORS ARP) was merged with CORSs AZBH (DL1709 = BULLHEAD CITY CORS ARP). The process of merging associated the vectors of the passive mark with the CORSs, and the passive mark can no longer be retrieved from the NGSIDB (i.e., the passive marks has essentially been absorbed into the CORS ARP). An attempt was also made to merge two ARP PIDs (AI1946 and AI3680) for the CORS COT1, but a merge was unsuccessful, and the two still exist as duplicates.

Table 2.7. Pairs of possible duplicate CORSs in the NA2011 networks (within 1 m of one another).

Separation between points (m):	**Vertical**		**Horizontal**	**3D**
Number	**Min**	**Max**	**Max**	**Max**
CORS pairs that likely are duplicates in the NGSIDB				
Same monument type	56	-0.054	0.134	0.060	0.134
Unknown monument type	4	-0.004	0.105	0.097	0.105
Total duplicates	**60**	**-0.054**	**0.134**	**0.097**	**0.134**
CORS pairs that likely are NOT duplicates in the NGSIDB				
Too far apart	44	-0.728	0.814	0.645	0.814
Different monument type	208	-0.194	0.194	0.119	0.194
New Coast Guard beacon	59	-0.150	0.243	0.103	0.246
Became CORS with new mount	1	0.179	0.179	0.006	0.179
Total non-duplicates within 1 m	**312**	**-0.728**	**0.814**	**0.645**	**0.814**

Because of the difficulty of merging marks in the NGSIDB, no further attempts were made to merge duplicate marks. This is unfortunate, because correctly and uniquely identifying all CORSs—in particular older ones—was important, since the adjustments were constrained to CORSs, and CORSs were rare in the past. The oldest CORSs occupation in the NA2011 Project was on August 1, 1990. Figure 2.7 shows the percentage of CORSs occupations per year for the NA2011 networks; only 0.04% (10) and 0.02% (6) of the marks are CORSs in 1990 and 1991, respectively. Interestingly, there is not an overall trend of increasing CORSs occupation; the peak year is 1998 with 25.8% CORSs. Between 1992 and 2011, on average 10% of the marks occupied are constrained CORSs in the NA2011 networks.

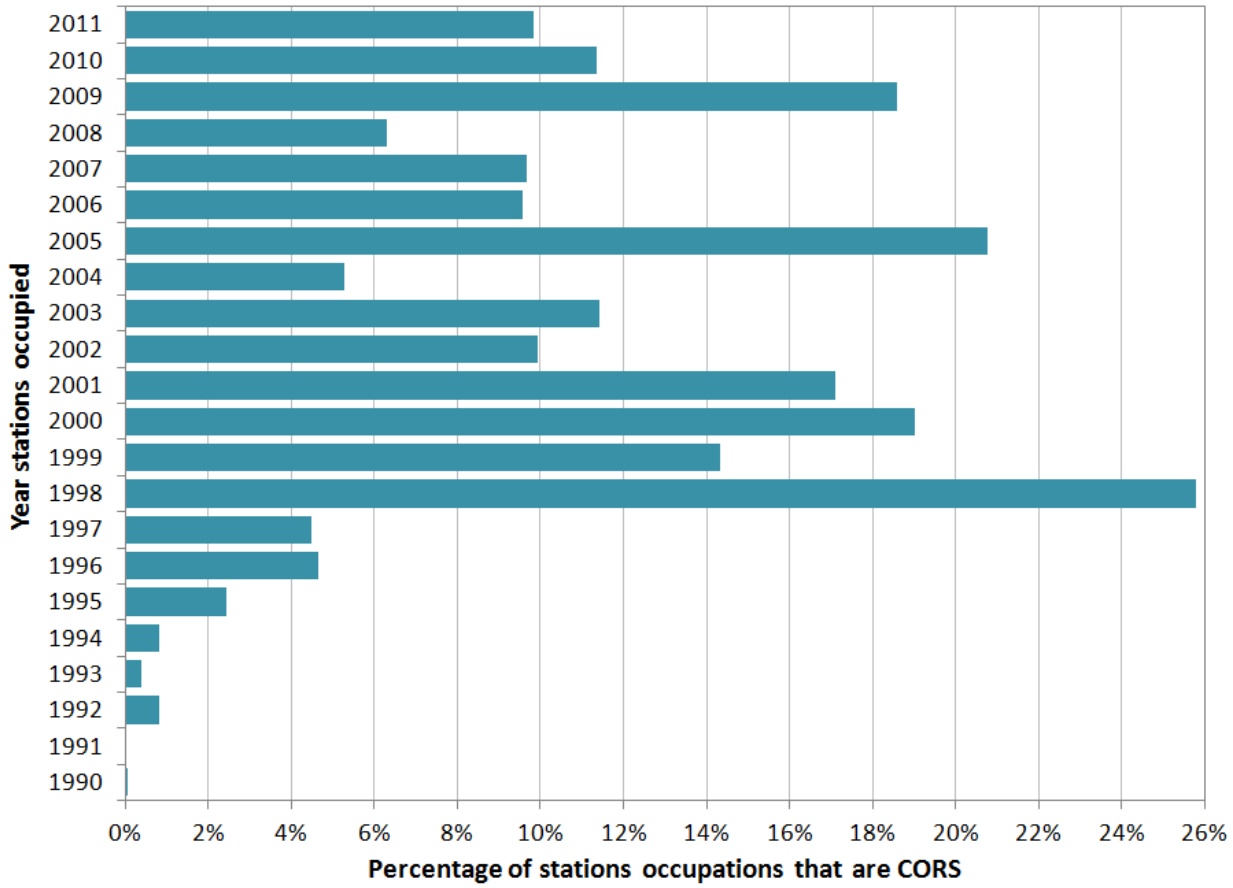

Figure 2.7. Percentage of mark occupations each year that were constrained as MYCS1 CORSs.

So far, the discussion on merging duplicate CORSs has been focused on merging only those with the same monument type (ARP, monument, and L1 APC). However, it would be preferable to merge all components into a single mark so each CORS site ID corresponded to one, and only one, mark in each NA2011 network. To merge different components would require a minor modification to the GNSS vector, analogous to assigning an instrument height. But even the simpler task of merging duplicates with the same monument type could not be done in the time frame of the NA2011 Project. So, there was no possibility of merging all vectors to single points

for each CORS site ID. Such merging would have been a technically more correct way to construct the network. Instead, each PID for a constrained CORS was assigned the corresponding monument of a MYCS1 site ID as a constraint. The number of occurrences of MYCS1 site IDs per constrained CORS (ranging from one to five) is given in Table 2.8, along with the number of occurrences for the three monument types. Since the number of occurrences for all monument types exceeds three, and since the sum for each individual monument type exceeds 991, some constrained CORSs must be duplicates.

Table 2.8. Number of site ID occurrences for constrained CORSs for different monument types.

Number of site ID occurrences	All monument types		ARP only		External monument only		L1 APC only	
1	820	82.7%	833	98.1%	138	89.6%	141	94.6%
2	143	14.4%	15	1.8%	14	9.1%	8	5.4%
3	24	2.4%	1	0.1%	2	1.3%	0	0.0%
4	3	0.3%	0	0.0%	0	0.0%	0	0.0%
5	1	0.1%	0	0.0%	0	0.0%	0	0.0%
Totals	**991**	**100.0%**	**849**	**100.0%**	**154**	**100.0%**	**149**	**100.0%**

The issue of duplicate marks includes passive marks, as well, not only CORSs. In the final adjustment for all networks, 1930 points are within 1 m of one another (965 pairs). Of these, 372 pairs of potential duplicates are constrained marks (CORSs).

Given all the different constraint possibilities for CORSs, it is important to reaffirm that all PIDs associated with CORSs were constrained exclusively to results from the MYCS1. The only exceptions were the 20 new CORSs added to the CORS Network between December 2011 and April 2012 (after completion of the MYCS1, but before the completion of the NA2011 Project). However, the coordinates of these new CORSs are entirely consistent with the MYCS1, i.e., they were determined by the NGS CORS Team as NAD 83 (2011/PA11/MA11) epoch 2010.00 values.

2.3. GNSS observations (vectors)

The "observations"[6] adjusted in the NA2011 Project to determine coordinates are processed GNSS vectors from GPS projects. Each vector is reduced to a mark-to-mark line from one mark to another, represented as delta Earth-Centered, Earth-Fixed (ECEF) Cartesian coordinates. The vectors include standard deviations for each component, as well as off-diagonal correlation or covariance terms. Although the term "GNSS" is typically used in this report, a vast majority of the vectors were derived only from GPS data. Actually, there is no metadata for the vectors to

[6] Quotes acknowledge that processed GNSS vectors are pseudo-observations, often referred to as "reduced" observations. They are derived from the true observations, being the broadcast GNSS signals received at each GNSS receiver in a session. Quotes around the word "observation" will be dropped for the remainder of the report.

indicate if other GNSS constellations were used. Given that receivers and software capable of logging and processing GPS plus GLONASS data were used for GPS projects prior to 2012, it is likely at least some of the vectors were processed using both constellations.

2.3.1. The NGS GPS vector file ("G-file")

GNSS vectors in the NGSIDB are downloaded in "G-file" (GPS file) format, defined in Annex N of the NGS Bluebook (NGS, 2019d). For the NA2011 Project, the G-files were downloaded to serve as Helmert blocks that essentially represented U.S. states and territories. Each G-file block contains vectors from all the GPS projects referenced to that state (i.e., the state that was identified when the project was submitted to NGS). Because GNSS vectors often extend beyond state boundaries, and some projects included marks in multiple states, marks at the vector endpoints could be far outside the state ostensibly represented by a particular G-file block.

A G-file includes the delta ECEF vector components, the standard deviation of each component, and the (upper or lower) off-diagonal correlation (or covariance) values. Vector and standard deviation components are given to the nearest 0.1 mm. The size of the covariance matrix is three times the number of vectors in a processing session. For sequentially processed vectors, there is only one vector in a session, therefore the covariance matrix is 3 × 3 for such sessions. For simultaneous (session or multi-point) baseline processing, the covariance matrix can become quite large. The largest simultaneously processed session in the NA2011 Project consists of 186 vectors, corresponding to a 558 × 558 variance-covariance matrix for that session.

Also included in G-files used for the NA2011 Project is the "from" (standpoint) and "to" (forepoint) mark; session start and stop date and times; the software used for baseline processing; the source and reference frame of the orbits used for processing; the organization that performed the processing; the session GPS day; and the GPS project ID. These G-file metadata were used to characterize the GNSS vectors in this report, although some of the information is ambiguous or incorrect, as discussed below (and in detail in Section 5.1).

Standard G-file format includes text for designating the processing session and codes for the session solution type (e.g., IFDDPF = **I**ono-**F**ree fixed **D**ouble **D**ifference **P**artially **F**ixed solution). However, this information is unfortunately not included in G-files created from the NGSIDB. In addition, all G-files created from the NGSIDB use the long-vector (F) format, normally reserved for vectors where a component is 1,000 km or longer. The F format has slightly less information about each vector than the standard vector (C) format.

2.3.2. GNSS vectors, baselines, and solution types

In this report, the term GNSS "vector" is used to represent a GNSS baseline processing solution. A "baseline" is the idealized line between two points, and there can be only one baseline between a pair of points.[7] A single vector represents one baseline solution (usually at the data-

[7] The baseline is unique, but only if one specifies the exact time. Due to tectonics, the actual length and orientation of a baseline between two points can change with time. Because all vectors were transformed to a common epoch (2010.00), the intent was that all baselines be unique. Strictly speaking, that could not be truly achieved because of the error in the crustal motion models, and the lack of a vertical component for those models in most areas.

weighted mean time of the observations used for baseline processing), so there can be multiple vectors per baseline.

A total of 424,721 vectors were used for the NA2011 Project, separated into three independent networks spanning three regions (CONUS, Alaska, and the Pacific), with CONUS further divided into a Primary and a Secondary network. Table 2.9 lists the count of vectors, sessions, and baselines for the NA2011 Project overall, and by network. Processing session counts are the number of B (session) records in the G-files. Only the number of simultaneously processed sessions are given, because there is one vector per sequentially processed session.

The number of vectors per baseline in Table 2.9 is 1.74 for all networks combined, but such global counts per baseline do not reveal the distribution. A more detailed breakdown of the number of vectors per baseline is given in

Figure **2.8** (a log scale is used to make small percentages more discernible). The figure shows that 43% of all baselines were observed more than once, with 30% observed twice. But only 6.7% were observed three times, 3.9% four times, 0.77% five times, and 0.35% more than ten times. The time between repeat observations of baselines (difference between first vector start and last vector stop times) is highly variable, ranging from 1 minute to 23.9 years, with a median of 3 hours but a mean of 98 days.

Table 2.9. Number of GNSS vectors, sessions, vector rejections, and baselines by NA2011 network.

	All	CONUS	CONUS Primary	CONUS Secondary	Alaska	Pacific
All vectors	**424,721**	**420,023**	**335,530**	**84,493**	**2,846**	**1,852**
Sequential solutions	336,640	333,984	263,601	70,383	1,473	1,183
Percent of total	79.3%	79.5%	78.6%	83.3%	51.8%	63.9%
Simultaneous solutions	88,081	86,039	71,929	14,110	1,373	669
Percent of total	20.7%	20.5%	21.4%	16.7%	48.2%	36.1%
Processing sessions (simultaneously processed means more than one vector per session)						
Simultaneously processed	13,542	12,978	9893	3085	426	138
Total number of sessions	**350,182**	**346,962**	**273,494**	**73,468**	**1899**	**1321**
Rejected vectors in final set of adjustments						
Number	21,603	21,231	10,279	10,952	314	58
Percent of total	5.09%	5.05%	3.06%	12.96%	11.03%	3.13%
Baselines						
Number	244,543	241,911	182,470	59,441	1,687	945
Vectors per baseline	1.74	1.74	1.84	1.42	1.69	1.96

Table 2.9 also gives the number (and percentage) of rejected vectors from the final adjustments for each region. Note the large difference in percentage of rejections between Primary and

Secondary networks (3% versus 13%), as well as the large percentage of rejections in Alaska (11%). Vector rejection criteria and results are discussed in Chapter 3 and Chapter 4, respectively. Table 2.9 includes ten vectors excluded from the project, consisting of vectors connecting Alaska to CONUS and to Hawaii. The reasons for excluding these vectors are given in Section 2.4.1 (see Table 2.16).

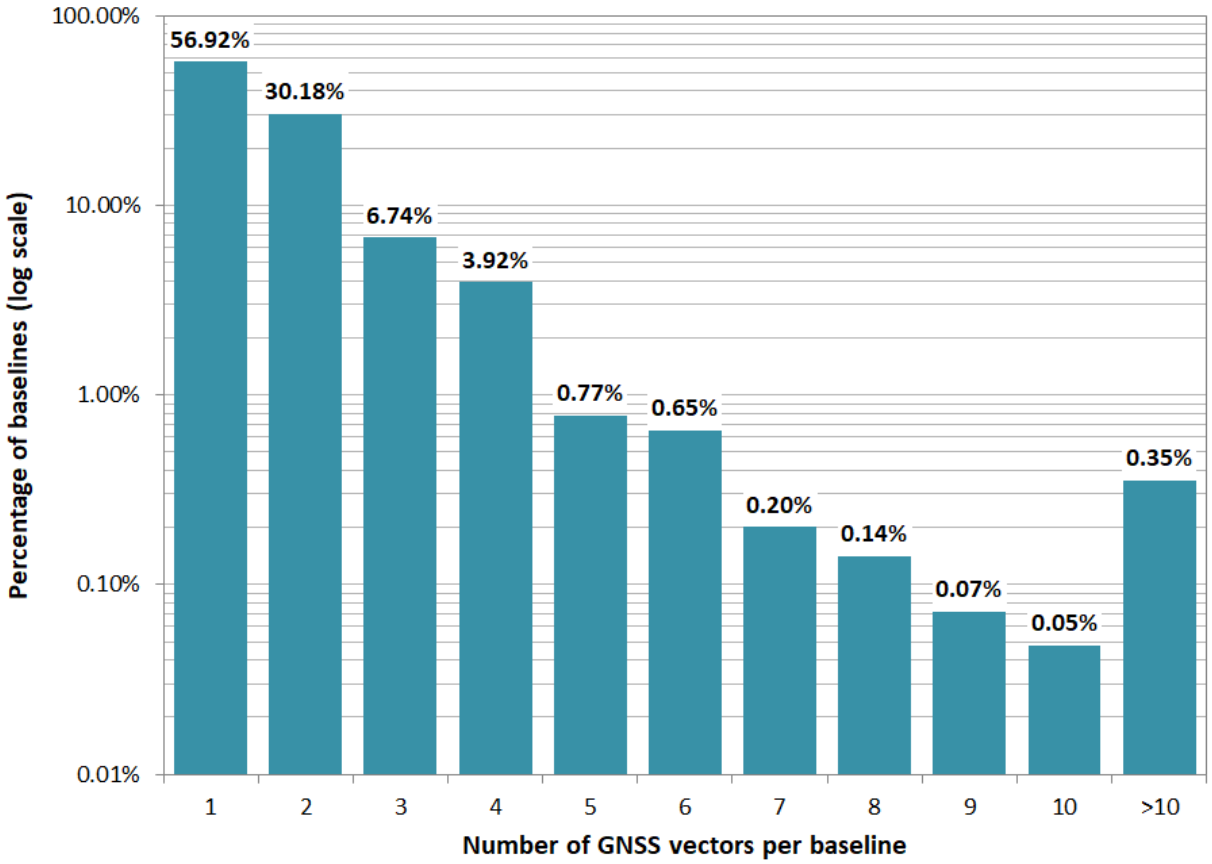

Figure 2.8. Number of GNSS vectors per baseline, as log percentage of all baselines.

In GNSS baseline processing, the term "session" is used for a group of observations overlapping in time. Often the term is used to indicate solutions determined using a "simultaneous" baseline processing technique, where each session includes two or more vectors. As shown in Table 2.9, a large majority (79%) of vectors in the NA2011 Project were not processed simultaneously—regardless of whether they overlapped in time—and instead were processed "sequentially."

Simultaneous processing considers all observables from all satellites at the same time, and since this is the actual physical situation, it can account for correlations between the solved baselines. This is generally considered the most technically correct approach, but it is more complex, and few software packages perform such processing (Hofmann-Wellenhof, 2001, pp. 268-269). NGS' program *PAGES* (and its predecessor *Omni*) can perform simultaneous processing, and together they account for 93% of the simultaneous solutions in the NA2011 Project. Although more "correct," in some circumstances simultaneous processing can be problematic, for example,

with noisy datasets when poor results for a baseline solution degrades other solutions in the session. In such cases, sequential processing can produce more reliable results, and it is part of the reason the NGS *OPUS-Static* service uses sequential processing, even though it relies upon *PAGES* to process each vector independently. In fact, of the 88,756 vectors processed using *PAGES* or *Omni* in the NA2011 Project, 6644 (7.5%) were processed sequentially rather than simultaneously. More details on GNSS processing software are provided in the next section.

For sequential processing, each vector is solved from a single pair of receivers (marks) in isolation, so no correlation is determined with other vectors based on observations at the same time. Most commercial baseline processing software performs sequential processing, as does the NGS *OPUS-Static* service, and it generally works well. However, there is a potential (and common) problem with sequential processing: it can be used to compute every possible vector between all marks observed at the same time. If the number of sequentially processed vectors is equal to, or greater than, the number of receivers in a session, the additional vectors are not independent.[8] This gives rise to the so-called "trivial" (dependent) vector problem. Including trivial vectors in a network adjustment introduces false redundancy and causes overly optimistic estimates of *a posteriori* accuracy and in some cases skews results. The presence and impact of trivial vectors is discussed in detail in Section 5.2.

The number of simultaneous and sequential solutions in the NA2011 Project per year is shown in Figure 2.9. The figure shows that, although the proportion of simultaneous solutions varies, there is no trend, and in any given year there are more sequential than simultaneous solutions. Figure 2.9 also shows the number of sessions per year. The number of sessions is more uniform than the number of vectors, demonstrating that the number of vectors per session must vary (how the number of sessions was determined is described in Section 5.2.1).

Table 2.10 provides statistics for NA2011 Project vector length, processing (session) duration, and *a priori* vector error estimates (as 3D standard deviations or "sigmas"). The table gives minimum, maximum, mean, and standard deviation statistics, as well as percentiles for 1%, 5%, 50% (median), 95% and 99% rankings. The reason for the percentiles is to provide distribution information representing a very small number of instances that would otherwise be masked by more general statistics. For example, the minimum vector length of 0.7 mm is obviously absurd. But the percentiles show that only 1% of the vectors are shorter than 229 m (and only 0.1% are shorter than 31 m). A similar situation exists for vector processing durations—only 1% are less than 10 minutes (0.167 hour) and greater than 25.65 hours. The same is true for 3D sigmas—only 1% are greater than 30 cm. Despite the small percentage of extreme values, they remain a concern and are discussed in depth in Section 5.1.

[8] As mentioned earlier, the only *true* observations are the received signals at each receiver. Thus, the number of independent true observations in a GNSS campaign is equal to the number of receivers. However, if it is assumed that the only "observations" which will be used in an adjustment of GPS data, such as performed in the NA2011 Project, are those *pseudo*-observations which are a combination of data from *two* receivers processed into *one* vector, then the number of independent pseudo- (not true) observations, becomes 1 less than the number of receivers. That is why, as will be shown in Chapter 5, a session with 3 receivers has three true observations, but when combined into vectors for relative positioning, only two vectors are independent pseudo-observations and the third is a "trivial" vector.

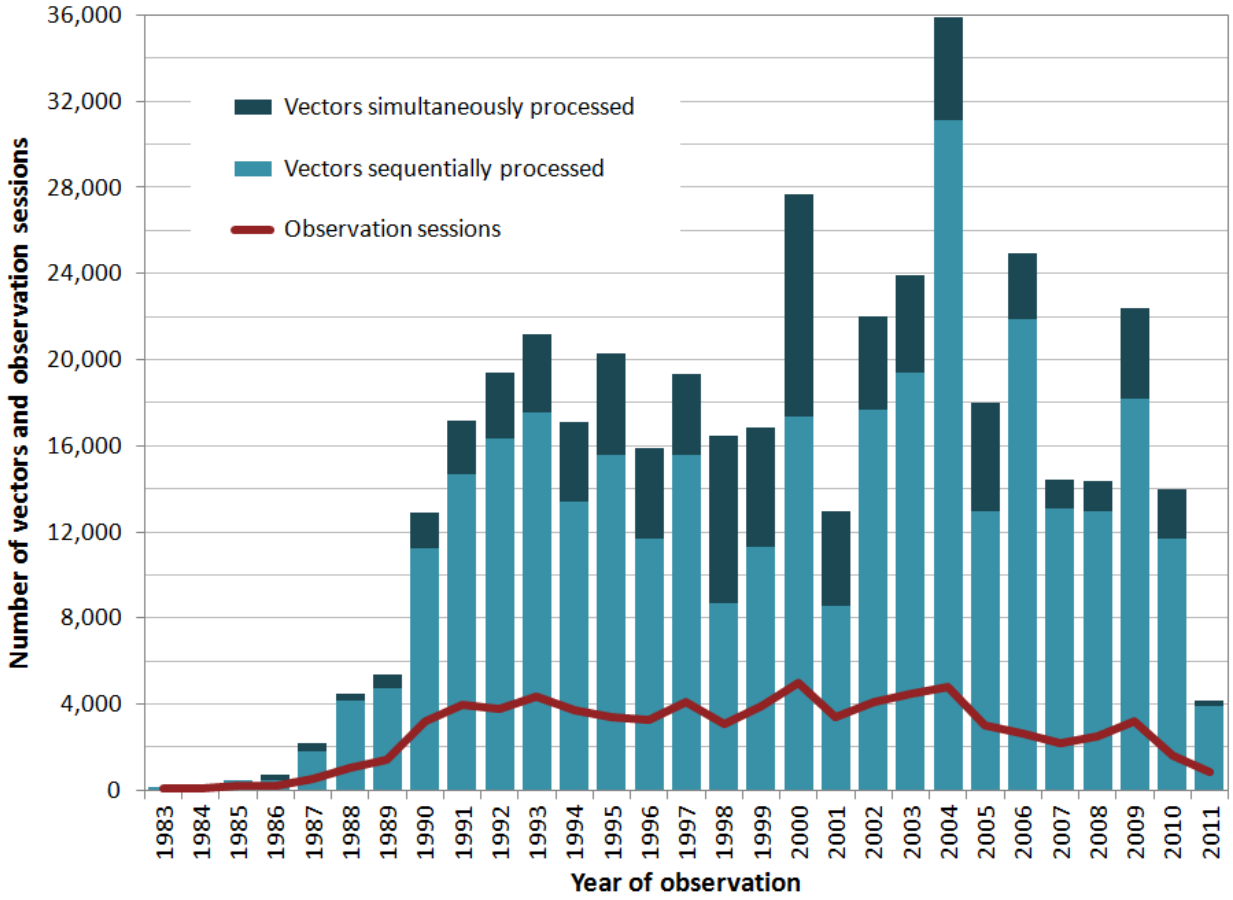

Figure 2.9. Number of sessions and of simultaneously and sequentially processed vectors per year.

Table 2.10. Statistics of GNSS vectors, sessions, and baselines in the NA2011 Project.

	Vector length (m)	Vector processing duration (hours)	Number vectors per baseline	Number vectors simultaneously processed	Vector 3D standard dev (m)
Min	0.0007	0.017	1	2	0.0002
Max	6,147,468	218.067	423	186	17.3203
Mean	33,669	4.545	1.74	6.77	0.0272
Std deviation	±120,504	±8.043	±2.46	±8.41	±0.1549
Percentiles					
1%	229	0.167	1	2	0.0004
5%	589	0.600	1	2	0.0011
50% (median)	7,829	1.517	1	4	0.0085
95%	144,117	23.983	4	21	0.0747
99%	436,477	25.650	6	34	0.3047

Table 2.10 also provides vector length and processing duration, and their mean and median values per observation year are shown in Figure 2.10. For every year, the mean vector length is greater than the median, showing the variability in length (as indicated in Table 2.10). There is only a slight overall increase in mean vector length with time, however median vector length is essentially constant. Mean durations are also greater than median for every year (except 1984), and the mean duration also shows an overall general increase with time, with a peak of 11.2 hours in 1998, corresponding to a local peak median of 3.3 hours. The maximum median of 7.9 hours occurs in 1984, the same year the median duration is greater than the mean (6.8 hours).

Correlation between duration and vector length is visually suggested in Figure 2.10. Linear regression with length as a function of duration does show some positive correlation, although it is fairly weak, yielding a correlation coefficient of +0.35. The coefficient increases to +0.42 when the length is forced to zero at duration zero, but there is an accompanying increase in residuals. In both cases the slope of the regression is approximately 5 to 6 km per hour.

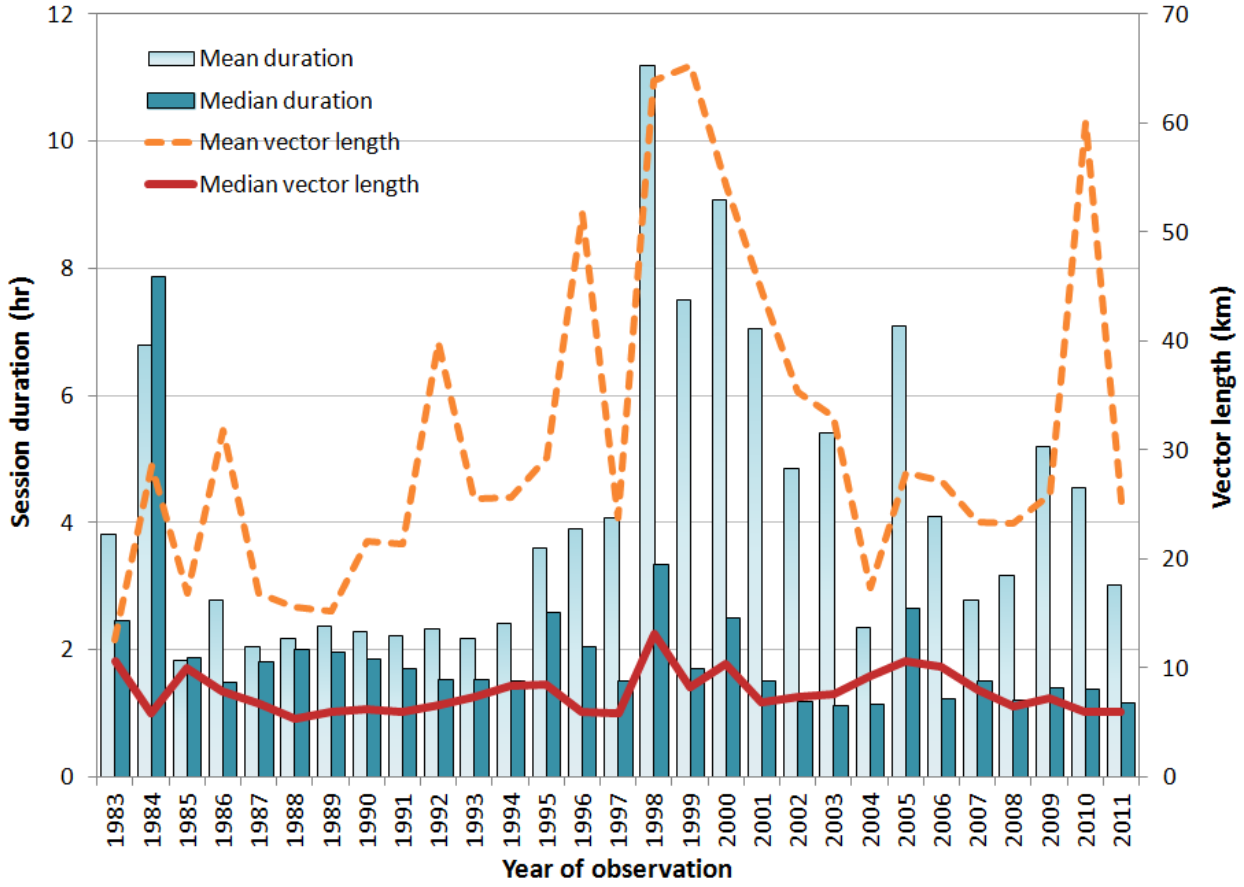

Figure 2.10. Mean and median vector length and duration by year of observation.

One might also expect some correlation between vector 3D standard deviations (sigmas) and vector duration and length. Linear regression showed essentially no correlation, with slope and correlation coefficient near zero for both duration and vector length. Such results are not

surprising, as the processor-derived vector sigmas themselves are often unreliable indicators of solution quality.

2.3.3. GNSS baseline processing software

A wide variety of software was used to process the GNSS vectors in the NGSIDB. Earlier, two NGS baseline programs were mentioned, *PAGES* and *Omni*. However, these two programs were used to process only 21% of the vectors in the NGSIDB. Most vectors were processed using commercial sequential processing software. Based on the information in the G-file metadata (B records), it appears that 34 different types of software were used. It is difficult to be certain of the exact number, because consistent software naming is not used for G-files. Nonetheless, it was possible to determine software with reasonably high confidence, as summarized in Table 2.11. The most commonly used software packages were Trimble products: *GPSurvey* (30%), *Geomatics Office* (20%), and *TRIMVEC* (16%), followed by NGS *PAGES* (15%) and *Omni* (6%).

Although *PAGES* and *Omni* were not used to solve the greatest number of vectors, they strongly dominate simultaneous solutions, accounting for 66% and 27%, respectively (93% total), as shown in Table 2.11. Only nine of the 34 software packages were used for simultaneous processing. Interestingly, all of the widely used commercial programs only perform sequential processing, such as Trimble *GPSurvey, Trimble Geomatics Office, Leica Geomatics Office, Topcon Tools*, and *Ashtech Solutions*. Appendix E provides a more detailed list of software used for processing the GPS vectors in the NGSIDB.

Table 2.11. Summary of software used to process GNSS vectors (from metadata in NA2011 G-files).

GNSS baseline processing software	Years used		All vectors		Simultaneous vectors	
	Earliest	Latest	Number	Percent	Number	Percent
Trimble *GPSurvey*	1990	2011	126,747	29.8%	0	0.0%
Trimble Geomatics Office	2000	2011	84,582	19.9%	0	0.0%
Trimble *TRIMVEC*	1986	1997	69,970	16.5%	2,150	2.4%
PAGES (NGS)	1996	2011	62,289	14.7%	58,234	66.1%
Omni (NGS)	1987	1999	26,467	6.2%	23,878	27.1%
Leica Geomatics Office	2004	2010	13,355	3.1%	0	0.0%
Leica *SKI Pro*	1992	2007	12,044	2.8%	0	0.0%
LINECOMP	1989	1997	8,820	2.1%	0	0.0%
Ashtech Solutions	2002	2010	3,738	0.9%	0	0.0%
Topcon Tools	2003	2009	3,122	0.7%	0	0.0%
GAMIT	1991	2000	2,488	0.6%	2,488	2.8%
PINNACLE	1999	2005	2,409	0.6%	0	0.0%
Other (22 types)	1983	2011	8,690	2.0%	1,331	1.5%

2.3.4. GNSS vector coordinate reference systems and orbit sources

Every session in a G-file includes a solution coordinate reference system code in the B (session) record. The codes are numbered sequentially, and they correspond to the various reference systems of the vectors. These systems nominally correspond to GPS satellite orbits (ephemerides), but that is not always the case. Of the 27 reference systems recognized by NGS that were available through 2011, 25 were used for vectors in the NA2011 Project, as listed in Table 2.12.

Table 2.12. GNSS vector solution coordinate reference systems (from metadata in NA2011 G-files).

Ref sys code	Occurrences		Description of solution coordinate reference system	Observation date range codes should be used	
	Number	Percent		Earliest	Latest
1	1,691	0.3981%	WGS 72 Precise Ephemeris [DMA]	1/6/1980	1/3/1987
2	161,710	38.0744%	WGS 84 Precise Ephemeris [DMA]	1/4/1987	1/1/1994
4	52,002	12.2438%	WGS 84 Broadcast Ephemeris [DOD]	1/23/1987	6/28/1994
5**	1,520	0.3579%	ITRF 89 Epoch 1988.0 (IERS)	?	1/1/1992*
6***	762	0.1794%	NEOS 91.25 Epoch 1988 [NGS]	Spring 1991	10/19/1991
7	661	0.1556%	NEOS 90 Epoch 1988.0 [NGS]	10/20/1991	8/15/1992
8	2,428	0.5717%	ITRF 91 Epoch 1988.0 [NGS]	8/16/1992	12/19/1992
9	1,125	0.2649%	SIO/MIT 1992.57 Epoch 1992.57 [NGS]	12/20/1992	11/30/1993
10	299	0.0704%	ITRF 91 Epoch 1992.6 [NGS]	12/1/1993	1/8/1994
11	3,475	0.8182%	ITRF 92 Epoch 1994.0 [NGS]	1/9/1994	12/31/1995
12	8,236	1.9392%	ITRF 93 Epoch 1995.0 [NGS]	1/1/1995	6/29/1996
13	233	0.0549%	WGS 84 (G730) Epoch 1994.0 [DMA]	1/2/1994	9/28/1996
14	2	0.0005%	WGS 84 (G730) Epoch 1994.0 Broadcast [DOD]	6/29/1994	1/28/1997
15	7,560	1.7800%	ITRF 94 Epoch 1996.0 [NGS]	6/30/1996	2/28/1998
16	2,510	0.5910%	WGS 84 (G873) Epoch 1997.0 [NIMA]	9/29/1996	1/19/2002
17	8,680	2.0437%	WGS 84 (G873) Epoch 1997.0 Broadcast [DOD]	1/29/1997	1/19/2002
18	13,105	3.0856%	ITRF 96 Epoch 1997.0 [NGS]	3/1/1998	7/31/1999
19	12,567	2.9589%	ITRF 97 Epoch 1997.0 [NGS]	8/1/1999	6/3/2000
20	17,825	4.1969%	IGS 97 Epoch 1997.0 [NGS]	6/4/2000	12/1/2001
21	7,698	1.8125%	ITRF 00 Epoch 1997.0	?	1/10/2004*
22	18,310	4.3111%	IGS 00 Epoch 1998.0 [NGS]	12/2/2001	1/10/2004
23	5,850	1.3774%	WGS 84 (G1150) Epoch 2001.0 [NIMA]	1/20/2002	2/1/2012*
24	63,578	14.9694%	IGb 00 Epoch 1998.0 [NGS]	1/11/2004	11/4/2006
26	32,582	7.6714%	IGS 05 Epoch 2000.0 [NGS]	11/5/2006	4/16/2011
27	312	0.0735%	IGS08 Epoch 2005.0 used by NGS	4/17/2011	10/6/2012

**Latest date of intended usage not provided but inferred from usage dates for other reference systems.*
***Not used as a GPS reference frame.*
****Special VLBI coordinate solution; categorized as "provisional" in ADJUST transformations.*

It is interesting to note that some of the purported reference systems are questionable, for example code 5 in Table 2.12. Code 5 is for ITRF89 epoch 1988.0, and it states "not used as a GPS reference frame," yet it was used for 1520 vectors. More interesting is that the most commonly occurring codes correspond to the original realization of WGS 84 (codes 2 and 4), used for 38 + 12 = 50% of the vectors. These two reference frames were supposedly only used from 1987 to 1994, but the last occurrence of these codes was in 2011, the same year as the most recent vectors. In fact, a large majority of instances of these two codes occur after the latest dates in Table 2.12: 54% for code 2 and 94% for code 4, for a total of 32% of all vectors in the NA2011 Project. Code 1 (WGS 72) is the only reference frame older than 2 and 4, and it is assigned to 0.4% of the vectors. Code 1 should have only been used for vectors from January 1980 until January 1987, yet 17.5% were assigned this code after January 1987 (as late as 2006). WGS 72 differs from NAD 83 by much more than WGS 84, but fortunately few vectors in the NA2011 Project appear to have been incorrectly assigned this code. For all vectors, 194,170 (45.7%) use codes after the latest date of usage in Table 2.12.

The significance of coordinate reference system codes is that they are used by the network adjustment software (*NETSTAT* and *ADJUST*) to transform the vectors to the reference frame of the adjustment, in this case NAD 83. A list of parameters for all transformations to NAD 83 defined in the version of *ADJUST* used for this project is provided in Table 2.13 (the ITRF2014/IGS14 transformation has since been added to *ADJUST*). Codes 1 to 17 have no time-dependent parameters; these are given in the lower part of the table for codes 18 to 28 (note that all parameters for codes 27 and 28 are identical). The reference system codes are also used by NGS' *HTDP* program. *HTDP* was used to transform all G-files to the NAD 83 epoch 2010.00 frames, as mentioned in Chapter 1 and discussed in greater detail in Section 3.1.3.

For the commonly used codes 2 and 4 (both original WGS 84)—corresponding to 50% of the vectors—no transformation is performed (i.e., original WGS 84 is taken as equivalent to NAD 83). As stated previously, these codes are incorrectly assigned to most of the vectors where they are used, for an estimated total of 32% of all vectors in the NA2011 Project. Incorrect codes are likely assigned to other vectors, as well. Possible consequences of incorrect reference system codes, and other problems with some of the vector data, are discussed in Section 5.1.7.

Three of the coordinate reference systems used correspond specifically to broadcast orbits: codes 4, 14, and 17. These codes are specified for 14% of the vectors (code 14 was only used for two vectors, processed by NGS using *Omni* in 1994 and 1996). But, the use of reference system codes to indicate broadcast orbits is not typical. Instead, it is indicated under the "orbit source" G-file attribute. If everything was consistent in the G-file metadata, all vectors with codes 4, 14, and 17 would have a broadcast source, however 10% do not. Of the 25 reference system codes, 15 include broadcast orbits as a source. Nearly half of all vectors in the NA2011 Project—201,878 (47.5%) indicate broadcast orbits were used. Although there is some question as to the accuracy of G-file metadata, this is nonetheless a large percentage. The possible impact of broadcast orbits is discussed in Section 5.1.8.

Table 2.13. Transformation parameters to NAD 83 defined in *ADJUST* and *NETSTAT* and software (through *ADJUST* version 6.4.1 and *NETSTAT* version 6.03).

Ref sys code	Transformation to NAD 83 from:	Translation (m)			Rotation (milliarcseconds)			Scale
		T_X (m)	T_Y (m)	T_Z (m)	R_X (mas)	R_Y (mas)	R_Z (mas)	s (ppb)
1 & 3	WGS 72	0	0	4.5	0	0	-554	226.3
2 & 4	WGS 84	0	0	0	0	0	0	0
5, 7-11	ITRF (VLBI) 1989	0.9191	-2.0182	-0.4835	27.5	15.5	10.7	0
6	NEOS 1990	0.8845	-2.0399	-0.4835	22.9	24.9	9.9	0
12-14	ITRF93 epoch 1995.0	0.9769	-1.9392	-0.5461	26.4	10.1	10.3	0
15-17	ITRF94 epoch 1996.0	0.9738	-1.9453	-0.5486	27.5	10.1	11.4	0
18	ITRF96 epoch 1997.0	0.9910	-1.9072	-0.5129	25.79	9.65	11.66	0
19 & 20	ITRF97 epoch 1997.0	0.9889	-1.9074	-0.5030	25.915	9.426	11.599	-0.93
21-24	ITRF00 epoch 1997.0	0.9956	-1.9013	-0.5215	25.915	9.426	11.599	0.62
25	ITRF05 epoch 1997.0	0.9957	-1.9021	-0.5273	25.915	9.426	11.599	1.02
26	IGS05 epoch 1997.0	0.9973	-1.9023	-0.5249	25.904	9.419	11.598	-0.8353
27	IGS08 epoch 2005.0	0.99343	-1.90331	-0.52655	25.91467	9.42645	11.59935	1.71504
28	IGb08 epoch 2005.0	0.99343	-1.90331	-0.52655	25.91467	9.42645	11.59935	1.71504
Time-dependent parameters from time t = 1997.0 (applies only to reference system codes 18-28)								
		dT_X (m/yr)	dT_Y (m/yr)	dT_Z (m/yr)	dR_X (mas/yr)	dR_Y (mas/yr)	dR_Z (mas/yr)	dS (ppb/yr)
18	ITRF96 epoch 1997.0	0	0	0	0.053	-0.742	-0.032	0
19 & 20	ITRF97 epoch 1997.0	0.0007	-0.0001	-0.0019	0.067	-0.757	-0.031	-0.19
21-24	ITRF00 epoch 1997.0	0.0007	-0.0007	0.0005	0.067	-0.757	-0.051	-0.18
25	ITRF05 epoch 1997.0	0.0005	-0.0006	-0.0013	0.067	-0.757	-0.051	-0.10
26	IGS05 epoch 1997.0	0.0005	-0.0006	-0.0013	0.067	-0.757	-0.051	-0.10
27	IGS08 epoch 2005.0	0.00079	-0.0006	-0.00134	0.06667	-0.75744	-0.05133	-0.10201
28	IGb08 epoch 2005.0	0.00079	-0.0006	-0.00134	0.06667	-0.75744	-0.05133	-0.10201

As with G-file metadata for baseline processing software, there is no defined domain for agency orbit sources. In addition to the broadcast categories, there are 14 character strings that represent various agencies. The orbit sources are summarized in Table 2.14, to the extent that they can be determined from G-file header records. For the 222,843 vectors determined using precise orbits, most of the ephemerides were from IGS (61.3%), followed by "precise" with no agency specified (20.0%), and then NGS (16.5%).

Table 2.14. Orbit (ephemeris) sources for vectors in the NA2011 networks.

Orbit source	Number vectors	Percent all vectors	Percent vectors using precise orbits
Broadcast	201,878	47.53%	—
International GNSS Service	136,712	32.19%	61.35%
National Geodetic Survey	36,672	8.63%	16.46%
Defense Mapping Agency	1,441	0.34%	0.65%
Jet Propulsion Laboratory	311	0.07%	0.14%
Other agencies	5,241	1.23%	2.35%
Precise (agency not specified)	42,287	9.96%	18.98%
Blank	179	0.04%	0.08%
Total	**424,721**	**100.00%**	**100.00%**

2.4. Networks of marks and GNSS vectors

Each mark in the NA2011 Project has at least one GNSS vector connection. The redundancy and robustness of a network improves when marks are connected by multiple (enabled and independent) vectors. Also important is that each (passive) mark be physically occupied more than once (see Figure 2.4), although this does not apply to active marks (CORSs), since there is essentially no setup error (however, there are complications in defining and even identifying CORSs that are analogous to setup errors, as discussed earlier in this chapter).

Figure 2.11 shows that 1814 of the marks (2.2%) in the NA2011 Project are connected by only a single vector. The highest frequency is six vectors per mark, for 11,656 marks (14.4%). Unsurprisingly, the marks with the largest number of vector connections are CORSs, which are most prominently displayed in Figure 2.11 for marks connected by more than 100 vectors.

The CORS with the largest number of vector ties is LAKE HOUSTON CORS ARP (CORS ID "LKHU" and PID AF9521), with 5589 vectors (5356 enabled). The passive mark with most vector connections is TEXAS MEDICAL CENTER CORS ARP (PID DI3504) with 372 vectors (370 enabled). Despite "CORS" in its designation, this mark is classified as passive because it is not an NGS CORS, even though it is a continuously operating GNSS receiver. Because GNSS data for this mark were processed as daily 24-hour solutions, the number of occupations is equal to the number of vectors.

The passive mark that is a traditional survey mark with the most vector connections is NBS 5 (PID JV6439), a horizontal control disk with 343 vectors (329 enabled). Mark NBS 5 was occupied 30 times (28 with enabled vector connections). The first occupation was in March 1990 (in June 1992 for enabled vectors), and the last was in June 1998. This mark was occupied as part of a test network for the National Bureau of Standards (NBS) and the Federal Geographic Data Committee (FGDC).

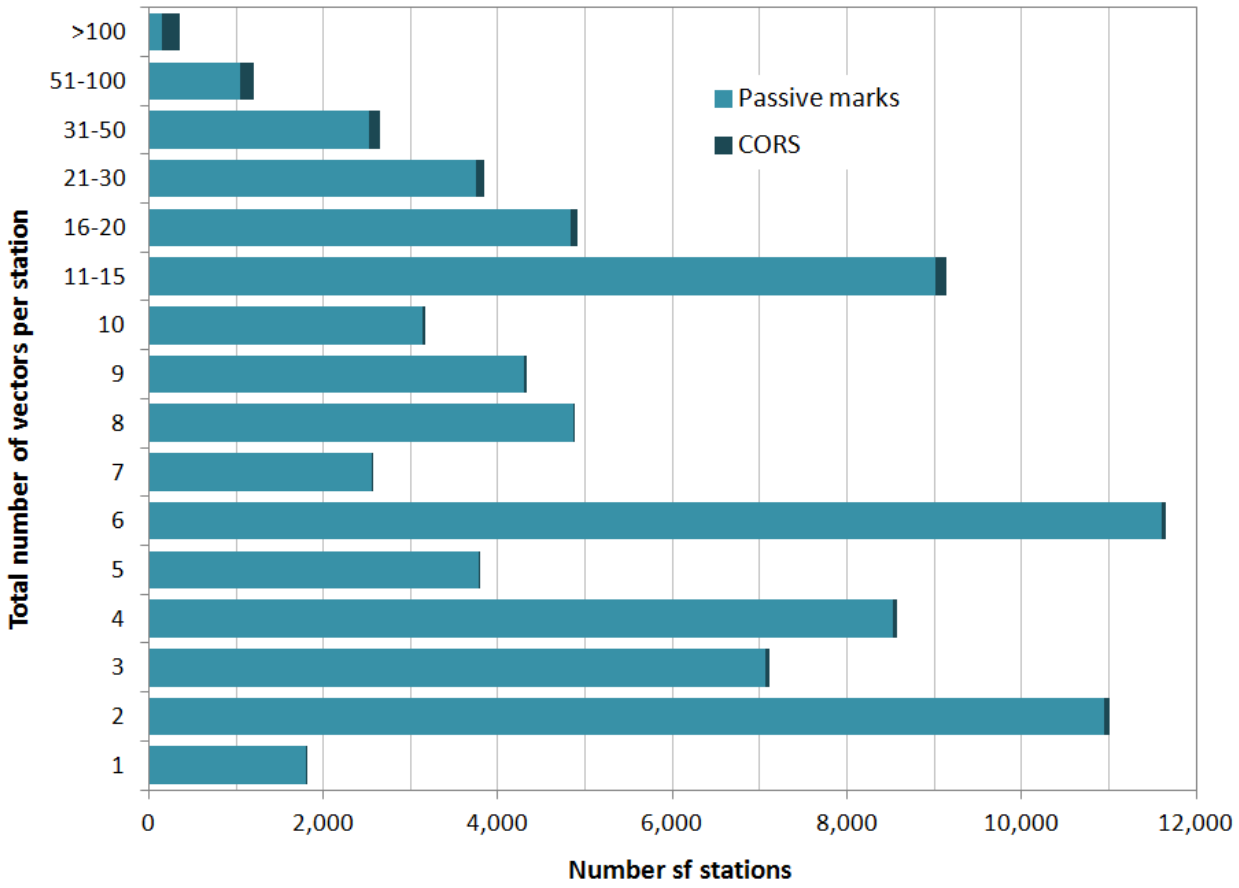

Figure 2.11. Total number of vectors connected to NA2011 marks.

Statistics for vector connections to CORSs and passive marks are summarized in Table 2.15, showing both total and enabled vectors. The number of vector connections to marks is twice the number of vectors, because each vector is connected to two marks. Both CORSs and passive have about 5% of their vectors rejected. As expected, CORSs show a much larger number of enabled vector connections than passive marks (mean and median of 60.5 and 19, versus 9.2 and 6, respectively). The minimum number of vectors is 1 in all cases (13 CORSs have a single vector connection). A total of 1801 passive marks have a single vector connection; these are so called "no-check" marks, because there is no second vector to "check" the computed position (CORSs cannot have a no-check status, because their coordinates were determined in the MYCS1 based on years of data). For passive marks, the number of enabled single vector ties is greater than the total. The reason for this is that 2134 – 1801 = 333 of these marks are tied by at least two vectors, but only one remained enabled in the final adjustment. These 333 marks are referred to as "soft" no-check marks in this report. The 1801 passive marks with a total of one vector connection are "hard" no-check marks. No-check marks are discussed in more detail in Section 3.5.4.

Table 2.15. Statistics of total and enabled vector connections to CORSs and passive marks.

	CORS			Passive		
	Total	**Enabled**	**% enabled**	**Total**	**Enabled**	**% enabled**
Number vector ties	**76,042**	**72,356**	**95.2%**	**773,392**	**733,876**	**94.9%**
Number w/single vector	13	13		1801	2134	
Minimum	1	1		1	1	
Maximum	5589	5356		372	370	
Mean	63.6	60.5		9.7	9.2	
Standard deviation	±199.7	±191.4		±12.0	±11.4	
Percentiles						
5%	2	2		2	2	
25%	8	7		4	3	
50% (median)	20	19		6	6	
75%	65	63		11	10	
95%	231	216		30	28	

2.4.1. Defining the NA2011 networks

The entire set of marks and vectors forming the NA2011 networks is shown in Figure 2.12. The figure shows connections between every mark, and it gives the impression that it is a single network spanning all of CONUS, Alaska, the Pacific, the Caribbean, and extending as far as South America. However, the connections between CONUS and Alaska, and between Alaska and the Pacific (Hawaii) are very tenuous, and there is no connection whatsoever between CONUS and the Pacific. The four think orange baselines represent vector connections radiating from a single mark in Alaska to CONUS and to Hawaii. As discussed later in this section, these vectors were excluded from the network adjustments, and thus CONUS, Alaska, and the Pacific are covered by separate networks.

Figure 2.13 shows the CONUS and Caribbean network, and Figure 2.14 and Figure 2.15 are larger scale maps showing only the CONUS portion of the CONUS and Caribbean network (the GNSS vectors are removed from Figure 2.15 to improve clarity of the mark distribution).

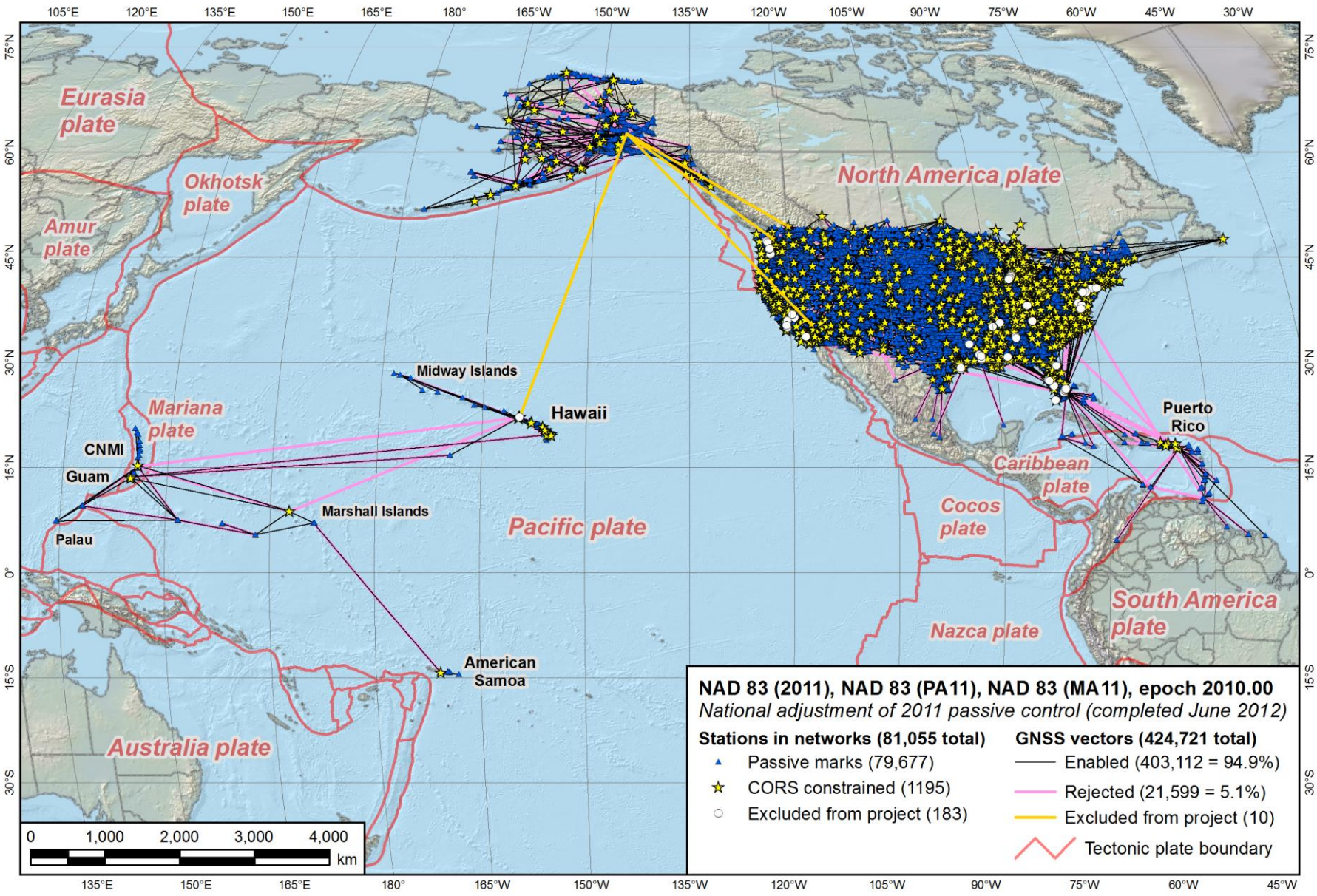

Figure 2.12. Entire extent of the NA2011 networks, showing excluded marks and vector baselines.

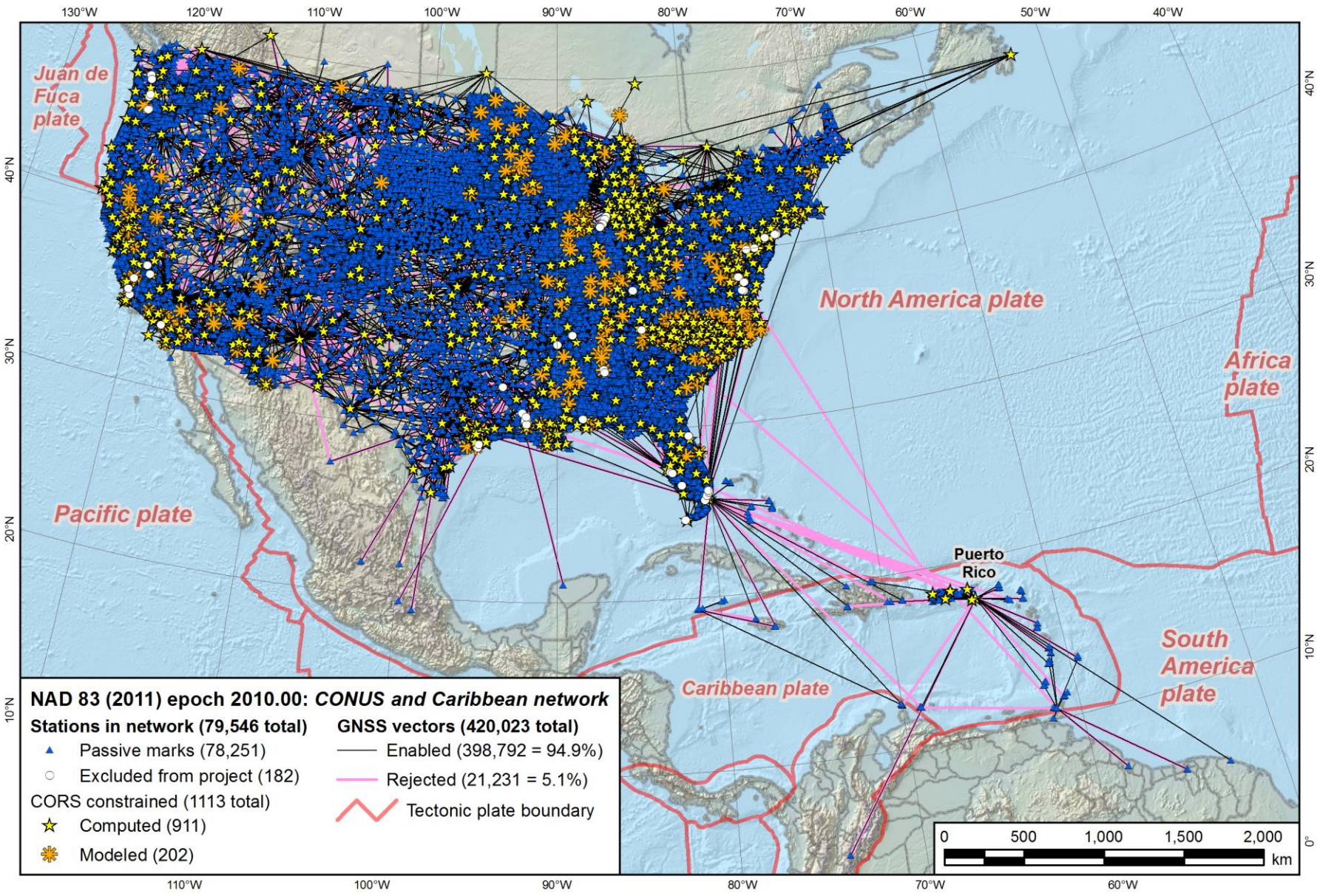

Figure 2.13. NA2011 marks and GNSS vectors in CONUS and Caribbean network.

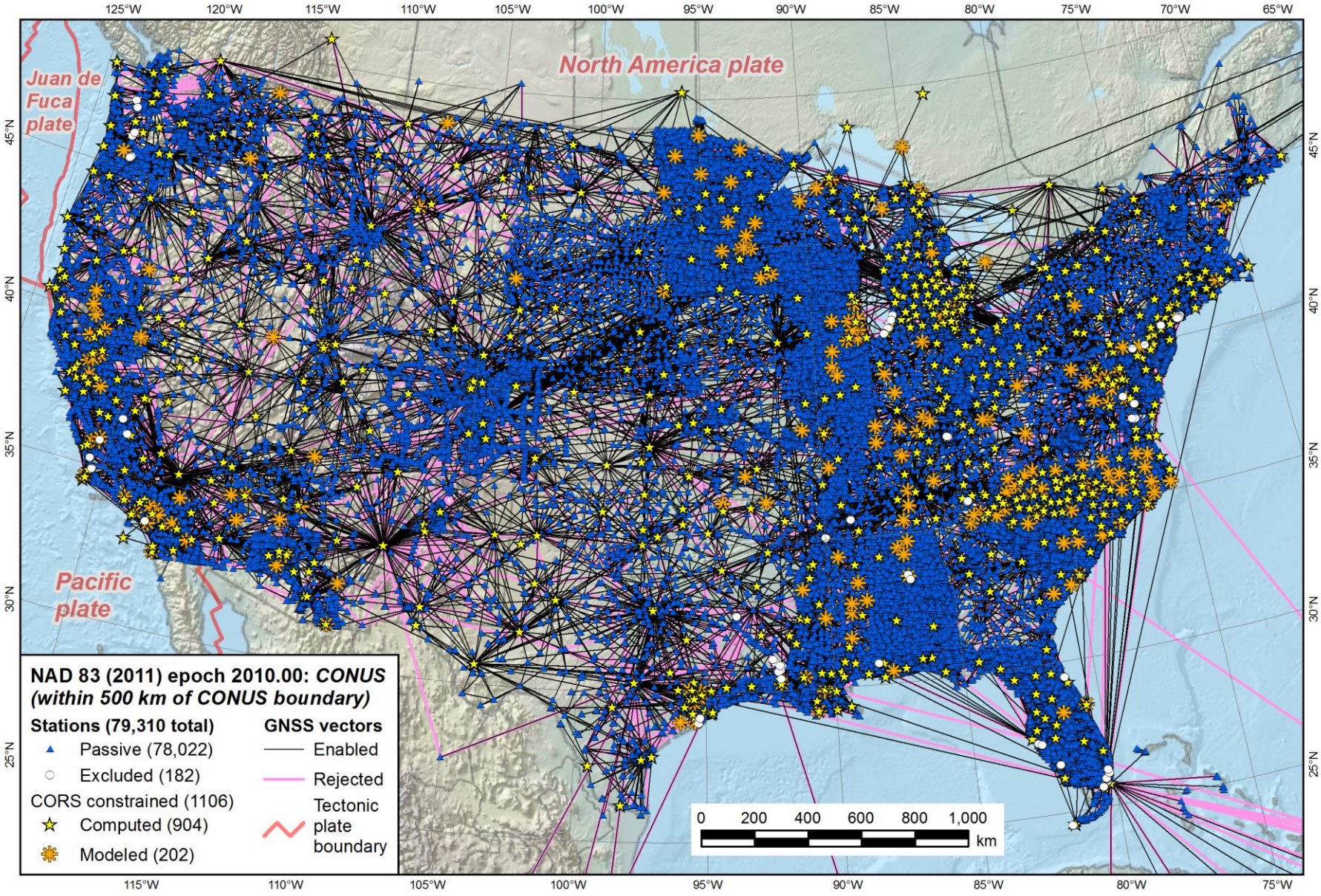

Figure 2.14. NA2011 marks within 500 km of CONUS boundary and associated GNSS vectors.

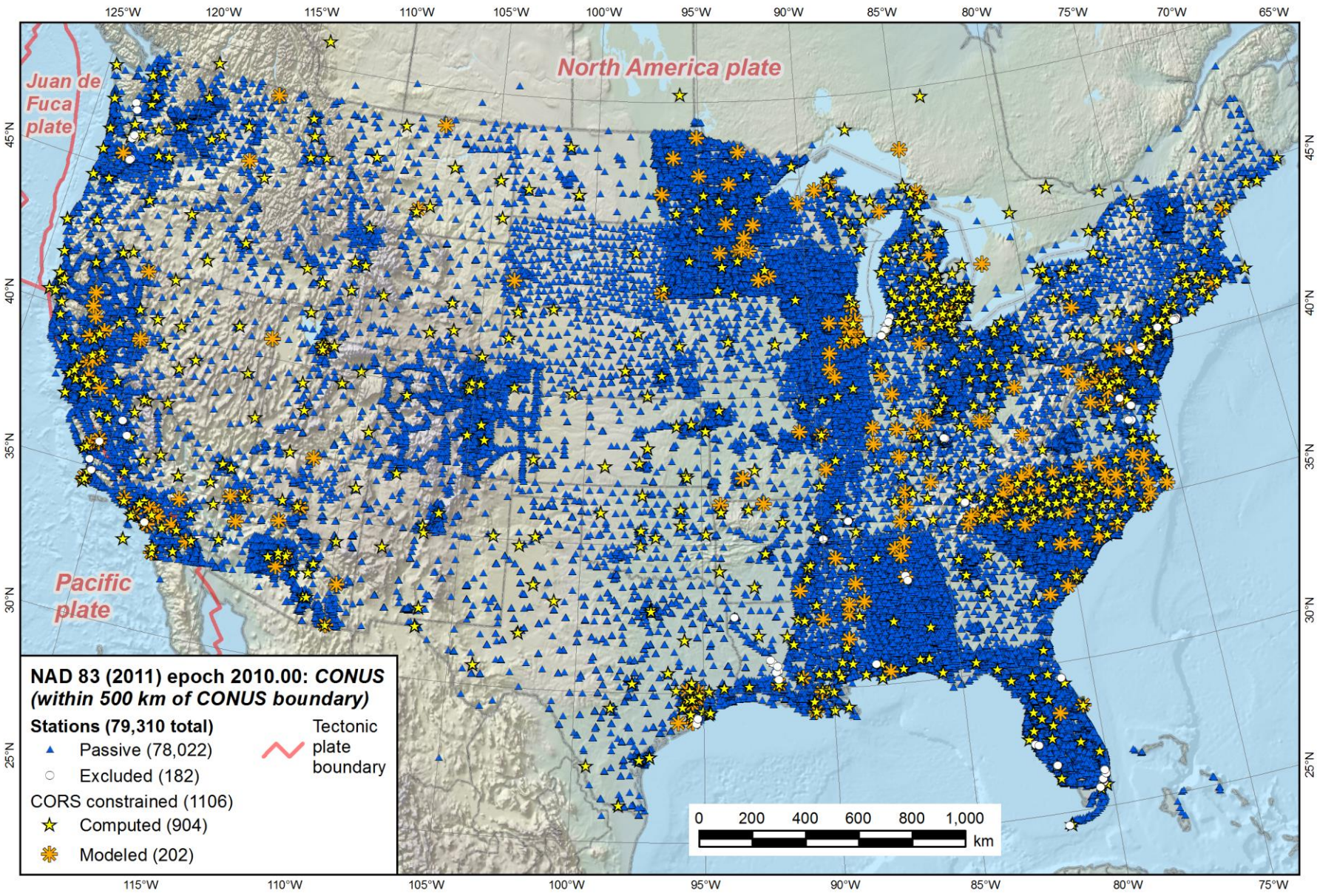

Figure 2.15. NA2011 marks within 500 km of CONUS boundary (GNSS vectors removed).

The Alaska network is shown in Figure 2.16. Although the Alaska network was adjusted separately from CONUS, both are (nominally) affixed to the stable North America tectonic plate, as defined by the NUVEL-1A tectonic model (DeMets *et al.*, 1994). As mentioned earlier, NAD 83 parameters that give its time-dependent relationship to the ITRS were developed (in part) using NUVEL-1A, and those parameters induce residual velocities with respect to the North America plate.

The marks in the Caribbean and South America are affixed to the North America plate in the same way, despite being on different plates. The consequence is that the marks not on the North America plate have relatively large horizontal velocities. For example, marks in Puerto Rico (on the Caribbean plate) have NAD 83 velocities of about 2 cm/year eastward. The same is true of marks in western California, located on the Pacific plate with horizontal NAD 83 velocities of up to 5 cm/year to the north-northwest.

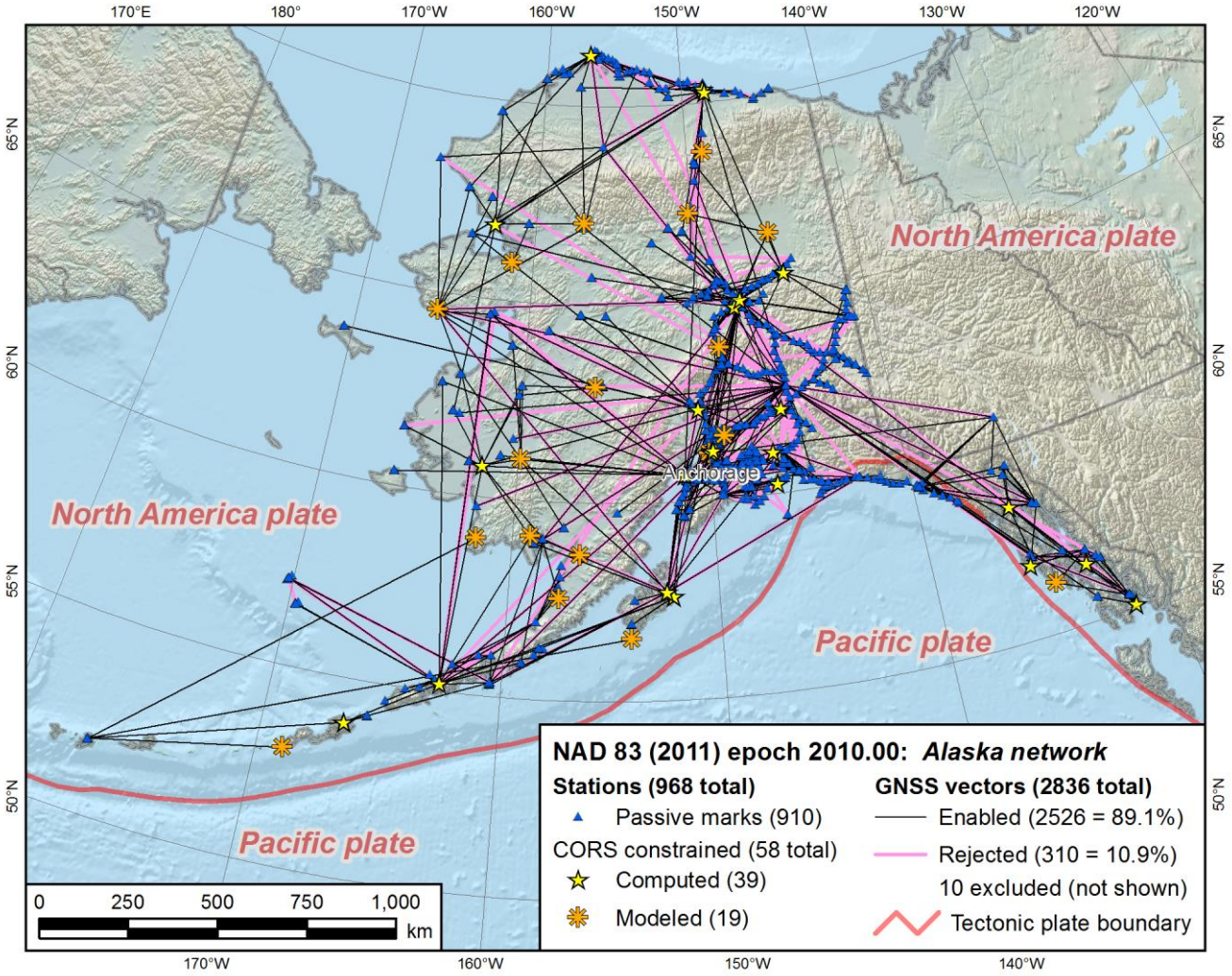

Figure 2.16. NA2011 marks and GNSS vectors in Alaska network.

Most marks in the Pacific network are located on the Pacific tectonic plate. However, as shown in Figure 2.17, a significant number (in Guam and the Commonwealth of Northern Mariana Islands (CNMI) are on the Mariana plate. The western-most marks are on the Philippine Sea plate, near its boundary with the Caroline plate (six marks on Palau and ten on Yap Island). Marks on the Pacific plate are referenced to the Pacific plate, and marks on the Mariana plate are referenced to the Mariana plate. The reason for referencing marks to the Mariana plate, despite its small size, is that the relative horizontal velocities between it and the Pacific plate are quite large, 6 to 7 cm/year. Figure 2.17 uses different symbols for marks referenced to the two plates and shows that the 22 marks on the Philippine Sea plate (on Palau and Yap Island) are referenced to the Mariana plate.

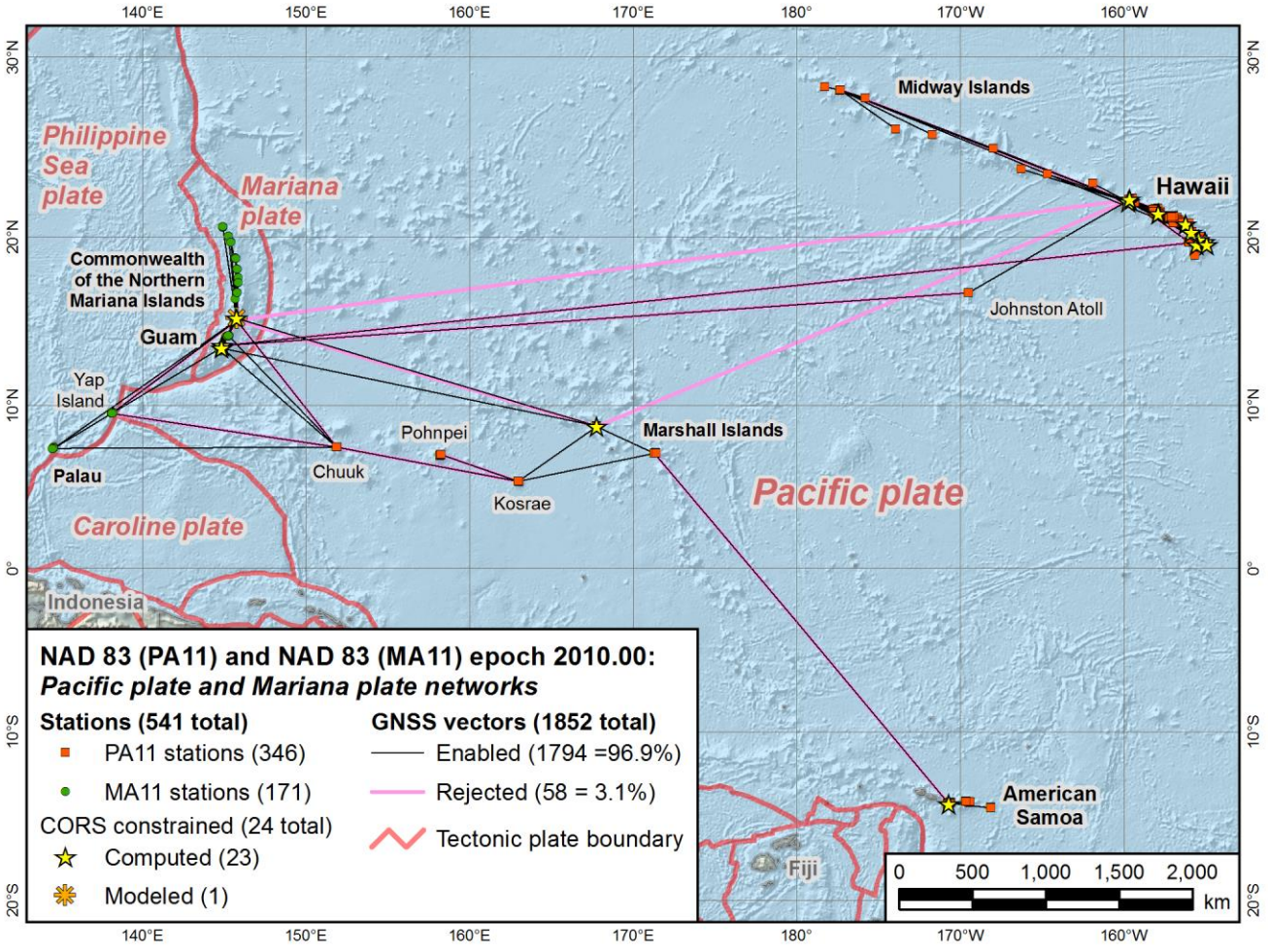

Figure 2.17. NA2011 marks and GNSS vectors in Pacific network.

Although marks in the Pacific are connected in a single network of GNSS vectors, this entire network was adjusted with two different sets of constraints, as mentioned near the beginning of this chapter. For one adjustment, NAD 83 (PA11) coordinates were used for all 24 Pacific

CORSs, and for the other NAD 83 (MA11) coordinates were used. This gave a complete set of marks in both reference frames, however each mark is published with only coordinates from one of the two frames, as shown in Figure 2.17. Additional details about adjusting the Pacific network are provided in Section 3.5.2.

Showing all NA2011 networks together in Figure 2.12 gives the impression the project could have been performed as a single network, because of the four (excluded) baselines from Alaska to CONUS and to Hawaii, but this is not actually the case. The four baselines were observed with ten vectors as part of NGS Alaska project GPS406 in July and August 1990. It consisted of 85 marks and 234 vectors processed using the *Omni* software (34.6% of the vectors were rejected in the NA2011 Project). The ten vectors of these four baselines are listed in Table 2.16.

Table 2.16. The ten vectors of four baselines in GPS406 excluded from the NA2011 Project. All vectors are from Alaska mark SOURDOUGH MON 7281 (PID TT4631). Vectors rejected in the 2007 national adjustment are shaded orange.

Forepoint mark from mark SORDOUGH MON 7281 (PID TT4631)	PID	Vector length (km)	A priori 3D sigma (cm)	Date observed	Session duration (hours)	Rejected status in 2007	State
KOKEE	TU3487	4528.8	0.47	7/20/1990	5.58	Enabled	HI
KOKEE	TU3487	4528.8	0.31	8/4/1990	6.03	Enabled	HI
AVIATION 2	SY1593	2194.1	29.18	8/1/1990	5.87	Rejected	WA
AVIATION 2	SY1593	2194.1	34.85	8/2/1990	5.73	Enabled	WA
AVIATION 2	SY1593	2194.1	29.78	8/3/1990	5.65	Rejected	WA
MOJAVE MINIMAC PHASE CTR	FT1605	3577.8	0.47	7/20/1990	5.58	Enabled	CA
MOJAVE MINIMAC PHASE CTR	FT1605	3577.8	0.31	8/4/1990	6.03	Enabled	CA
PENTICTON 887006	TP1405	2155.7	29.12	8/1/1990	5.87	Rejected	BC*
PENTICTON 887006	TP1405	2155.7	35.87	8/2/1990	5.73	Enabled	BC*
PENTICTON 887006	TP1405	2155.7	29.75	8/3/1990	5.65	Rejected	BC*

**BC is British Columbia, Canada*

All four baselines radiate from Alaska mark SOURDOUGH MON 7281 (PID TT4631). The two vectors of the single baseline to Hawaii are to mark KOKEE (PID TU3487). But KOKEE is not connected to any other mark in the Pacific, so these vectors do not connect the two networks (despite its location in Hawaii, both the KOKEE mark and its vectors are in the Alaska network). In addition, KOKEE was inadvertently included in the 2007 national adjustment, only because it was in Alaska project GPS406 (no other Hawaii marks were included). Since its inclusion was unintentional, its 2007 coordinates were suppressed, and the only published coordinates available are the pre-2007 HARN values (with a datum tag of 1992).

As shown in Table 2.16, the forepoint marks of the three baselines connecting Alaska to CONUS are in California, Washington, and British Columbia. There are a number of problems with the CONUS vectors. They are long (from 2156 to 3578 km), but with fairly short session times (5.6 to 6.0 hours). They were observed in 1990, before the GPS constellation was complete, when there was a lack of precise orbits, and they were processed without antenna models. For the baselines to AVIATION 2 and PENICTION, the 3D *a priori* standard deviations (sigmas) of all six vectors are large (29 to 36 cm). Each of these two baselines has three vectors, and two of three vectors were rejected in the 2007 national adjustment (shaded orange in Table 2.16).

All ten vectors of the four baselines in Table 2.16 were excluded from the NA2011 Project for the reasons given above, as well as because they constituted a very small number of ties from a single mark in Alaska. Although CONUS, Alaska, and the Pacific were treated as three disconnected networks, they were implicitly connected in that all were constrained to MYCS1 coordinates, and the MYCS1 was derived from a single global solution. Note, however, that Alaska and CONUS were adjusted together as a single network in the 2007 national adjustment, using the four enabled vectors in Table 2.16 as the only connections between the networks.

Figure 2.12 through Figure 2.15 show the 183 excluded marks (as white dots), with all but one (KOKEE in Hawaii) located in CONUS. The marks are scattered across CONUS, but with local clusters in western Washington and Oregon, southern California, the southeastern end of Lake Michigan, along the mid-Atlantic coast, and in southern Florida. As Table 2.4 shows, 100 of the 182 excluded CONUS marks are "unpublishable" FAA airport marks (such as runway endpoints). Excluded marks were discussed earlier in this chapter, and in more detail in Section 3.4.

Rejected vectors are shown in all of the preceding network maps as light magenta lines (Figure 2.12 through Figure 2.17). Overall, 5.1% of the vectors were rejected, but the rejections are not uniformly distributed in space, or in time. The percentage of rejected vectors range from 3.1% for the Pacific and CONUS Primary networks to 11.2% for Alaska. Rejection of vectors was done as part of the adjustment analysis process, and details are provided in the following chapters.

As with the vectors, Figure 2.12 through Figure 2.17 show a wide range of control point spacing in the networks. This is particularly true of CONUS in Figure 2.15. A more quantified illustration of the mark density is shown in Figure 2.18, created using a kernel density analysis with a radius of 100 km. The map gives density in units of marks per 100 km^2 (corresponding to a radius of 5.64 km). Note that there are some areas of the country where the density of marks is more than 100 per 100 km^2. In contrast, there are other areas, particularly in the interior west, where there is less than 1 mark per 100 km^2.

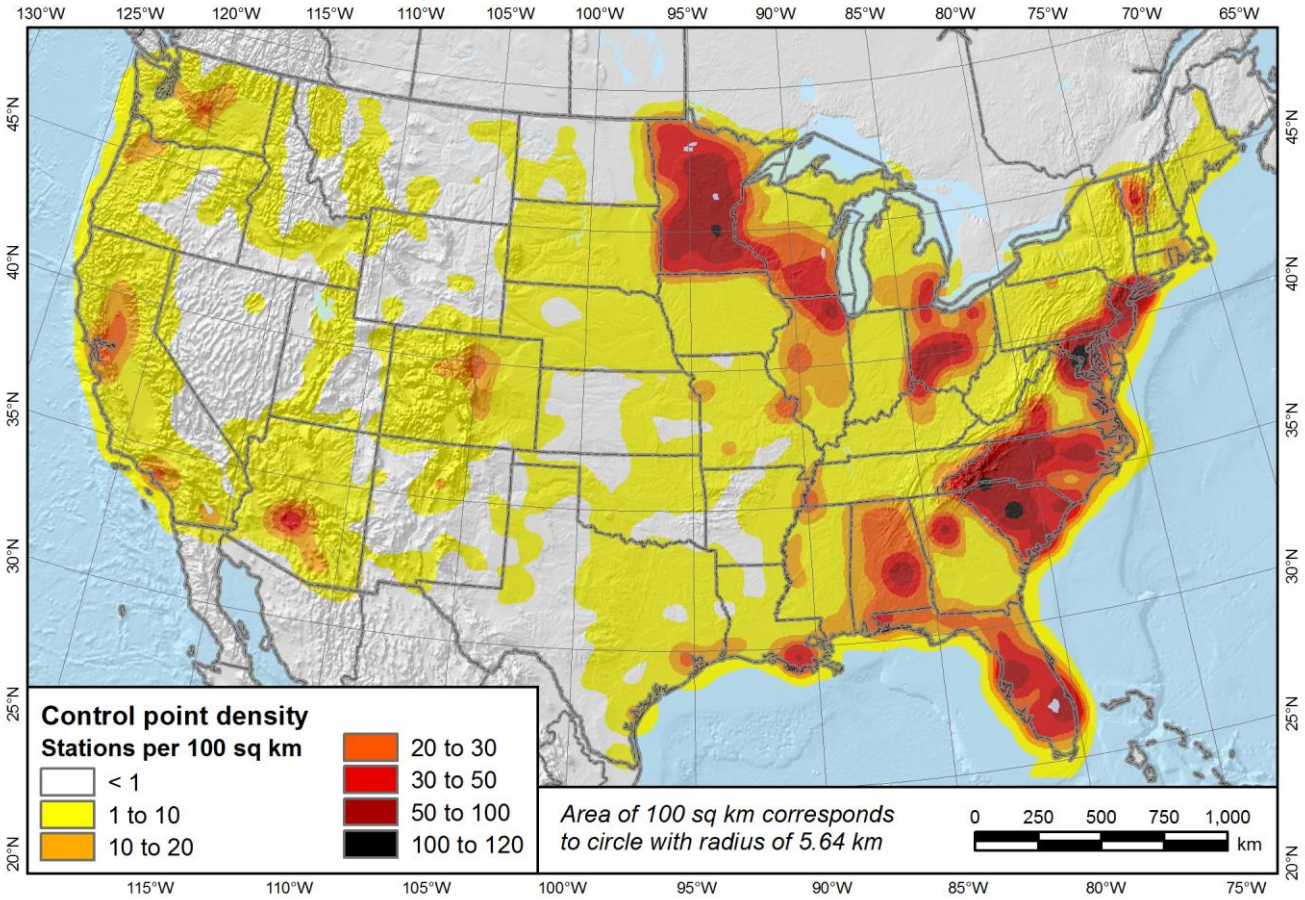

Figure 2.18. Kernel density plot of CONUS passive control marks for search radius of 100 km.

Time evolution of the CONUS and Alaska GNSS vector networks is shown Figure 2.19 and Figure 2.20 (both the CONUS and Alaska maps are at the same scale). Change is shown in six time blocks, three in each of the figures. The CONUS and Alaska networks have a total of 422,869 vectors. Some context as to the history of represented by these figures can be gained by referring to Chapter 1, especially Table 1.1.

Figure 2.19:

- **1983 through 1989 (7 years).** *13,478 GNSS vectors (3.19% of total).* The early days of GPS; first observation on April 12, 1983, in Ohio (project GPS010). First HARN in Tennessee, and first statewide HARN in Florida, both in 1989. Alaska surveys associated with Prudhoe Bay oil fields and Alaska Pipeline. Most surveys over small areas, with networks typically composed of triangles made from short vectors (mean length 17 km). Main exception is in New Mexico with long vectors radiating from single mark, and some long vectors in Alaska.
- **1990 through 1993 (4 years).** *70,352 GNSS vectors (16.64% of total; cumulative 19.83%).* Began to see very long vectors spanning entire continent (mean vector length

increased to 26 km), including ties from Alaska to CONUS and to Hawaii, and ties to marks in Mexico. But, long vectors are problematic because of incomplete constellation, lack of precise orbits, and single-frequency receivers. Many large state-specific HARN surveys performed.

- **1994 through 1997 (4 years).** *72,535 GNSS vectors (17.15% of total; cumulative 36.98%).* Initial operational capability (IOC) achieved for GPS in June 1993 (24 operating satellites); full operational capability (FOC) declared in July 1995 after DoD testing completed. Most HARN surveys completed. Starting to see hub-style survey networks (session processing). Vector connections were made from CONUS to Caribbean and South America.

Figure 2.20:

- **1998 through 2001 (4 years).** *73,832 GNSS vectors (17.46% of total; cumulative 54.44%).* Transition from HARN to Federal Base Network/Cooperative Base Network (FBN/CBN) surveys. Most surveys networks are "starburst" pattern hub-style surveys. Beginning of Height Modernization ("Height Mod") Program surveys. Increasing number of ties to CORSs due to rapid growth of CORS Network during this period.
- **2002 through 2005 (4 years).** *99,327 GNSS vectors (23.49% of total; cumulative 77.93%).* Surveys becoming more concentrated in specific states as local partners do fieldwork, especially Height Mod surveys. Latest observation for vectors in 2007 national adjustment was October 13, 2005.
- **2006 through 2011 (6 years).** *93,345 GNSS vectors (22.07% of total; cumulative 100.00%).* Trend of most surveys being done in only a few states continues. More use of long vector ties in processing (to better model tropospheric errors). Hub and multi-hub network designs dominate, but "triangulated" networks still used (e.g., statewide survey in Mississippi). This period includes essentially all vectors added since the 2007 national adjustment. Last four observations were on December 21, 2011, in Illinois (project GPS2864).

The time evolution of the Pacific network is shown in Figure 2.21, in four time blocks. The first observations were in August 1993 in project GPS667.[9] This project included the long vector ties connecting Hawaii, CNMI, Guam, American Samoa, and several other Pacific islands. The only other project with vectors spanning such distances (such as connecting Hawaii and Guam) was GPS2388, with occupations done from 2000 through 2002.

[9] After completion of the NA2011 adjustments, it was discovered that an older GPS project, GPS415, was inadvertently not included. This issue is addressed in Section 6.2.1.1.

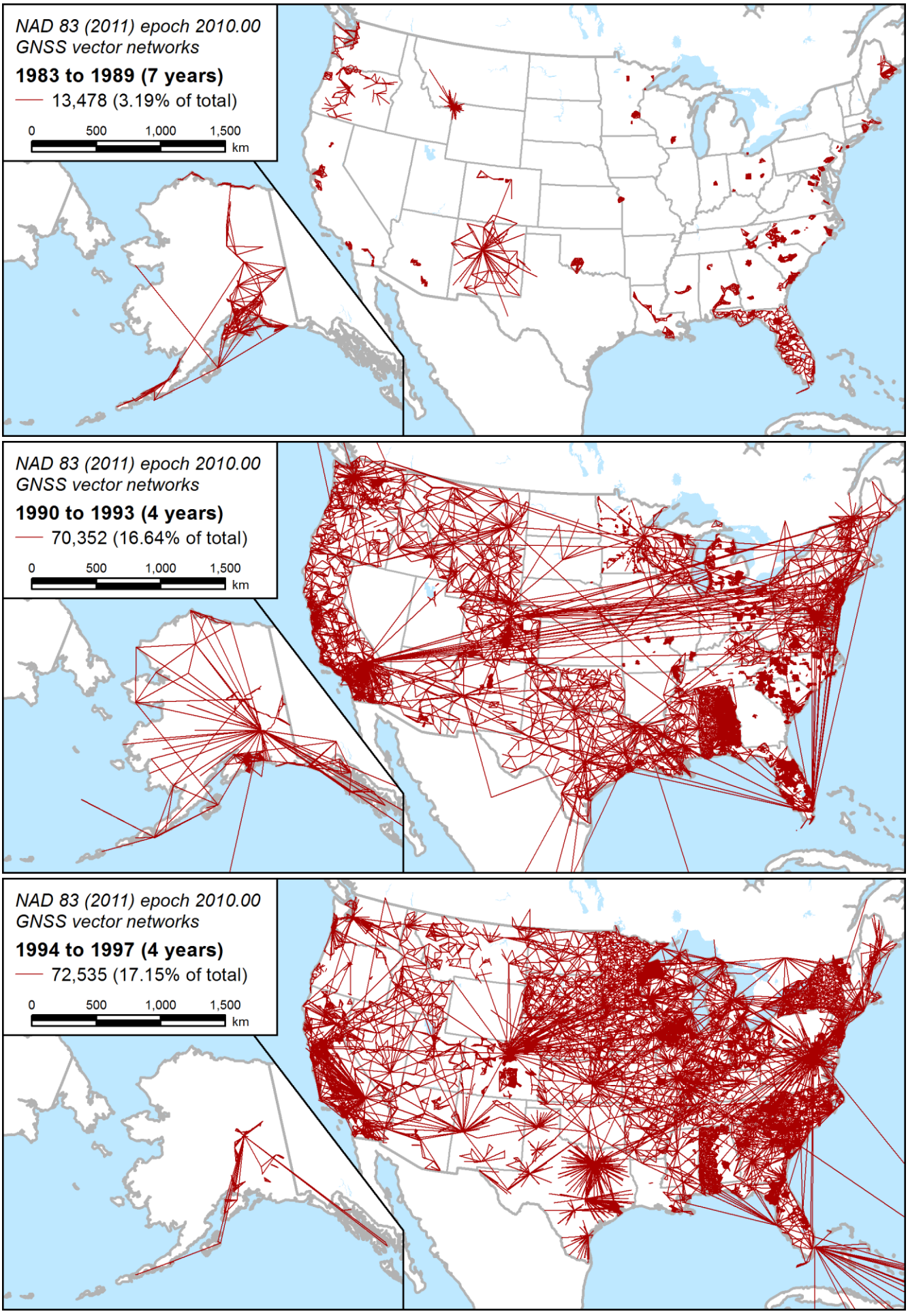

Figure 2.19. Evolution of CONUS and Alaska networks (1983-1989, 1990-1993, and 1994-1997).

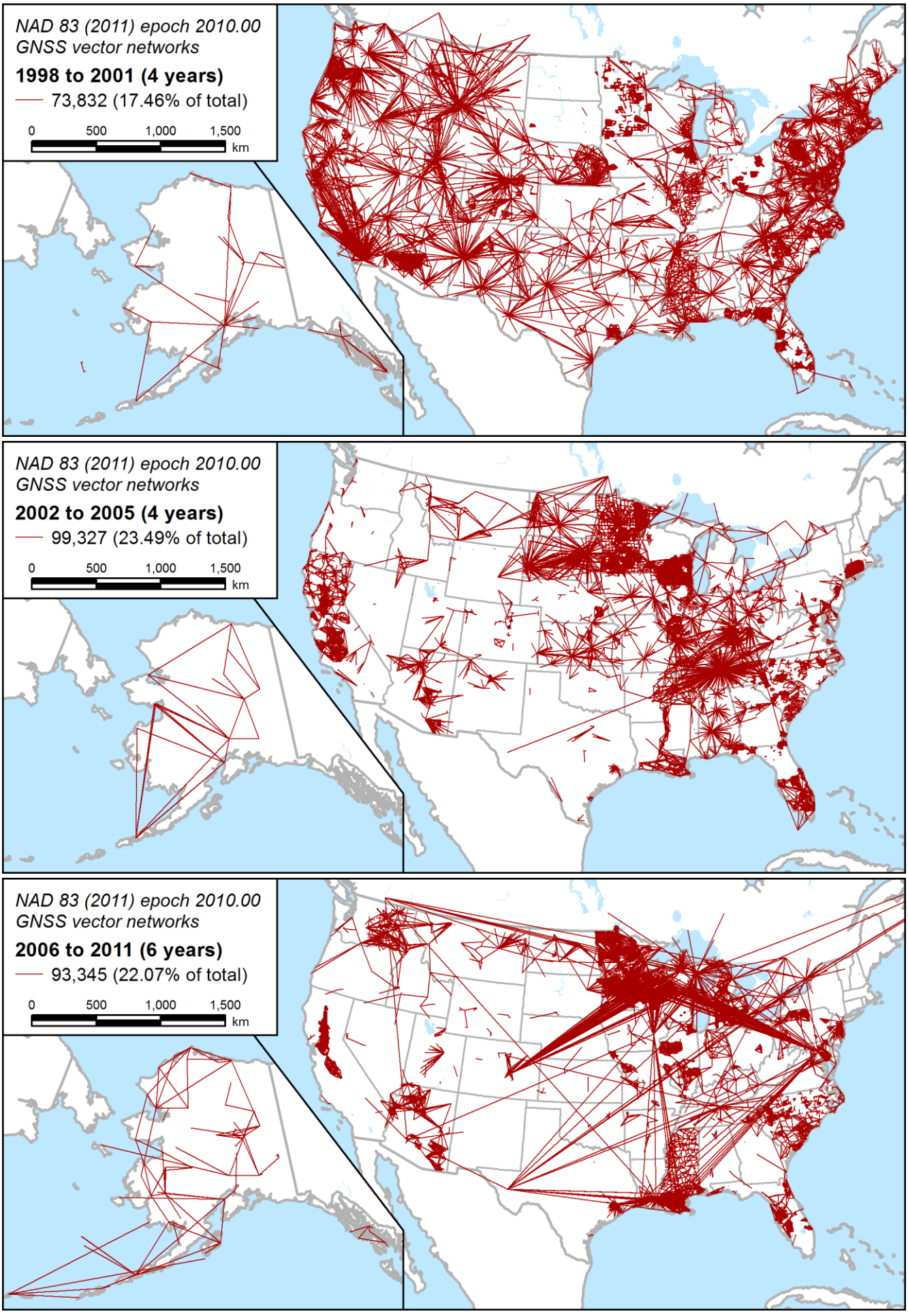

Figure 2.20. Evolution of CONUS and Alaska networks (1998-2001, 2002-2005, and 2006-2011).

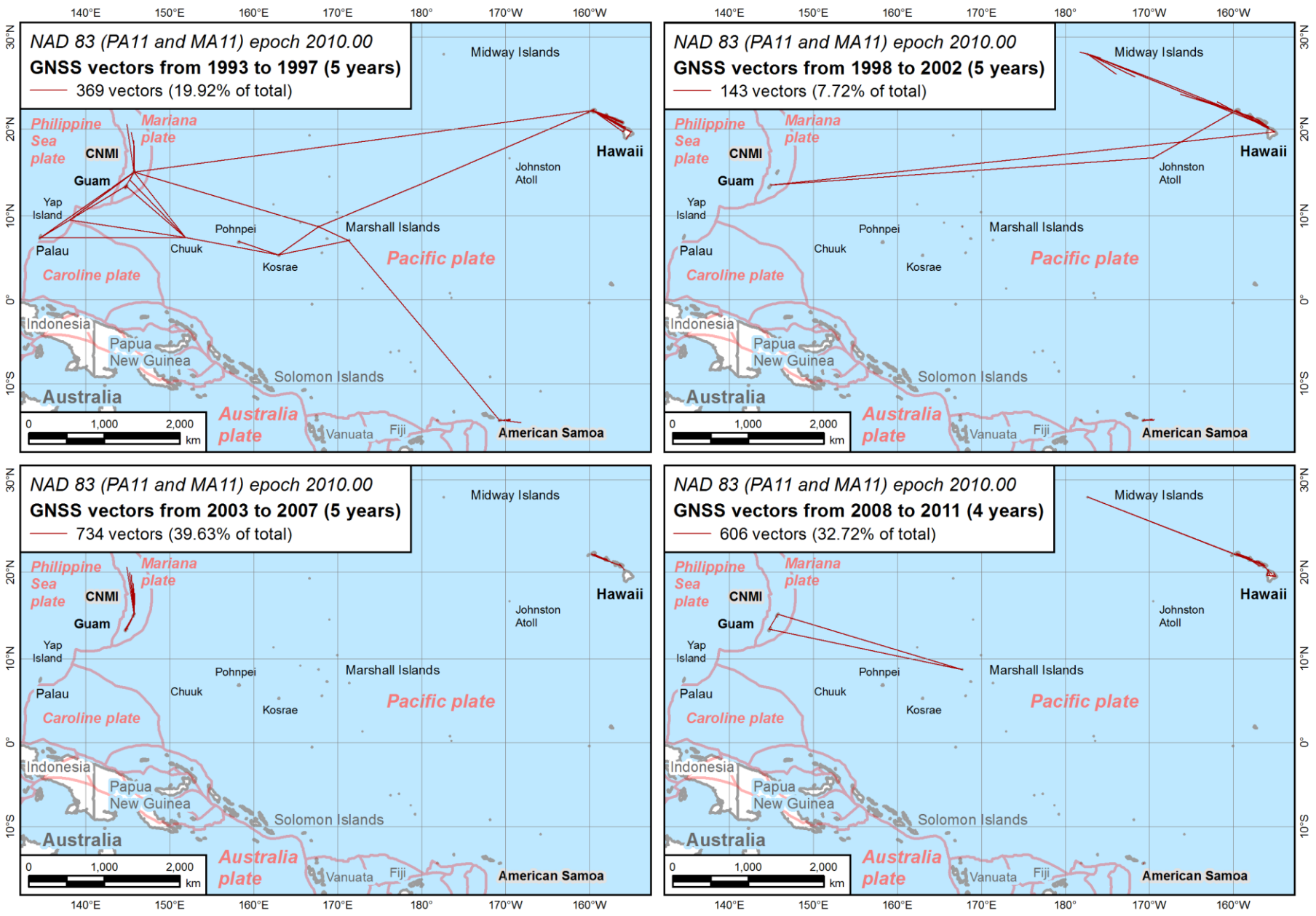

Figure 2.21. Evolution of the Pacific network (1993-1997, 1998-2002, 2003-2007, and 2008-2011).

2.5. Chapter 2 summary

The purpose of this chapter was to provide a comprehensive description of the data used in the NA2011 Project, including assessments of data quality, identification of issues affecting results, and an explanation of how certain issues were addressed. Input data for building the NA2011 networks was derived from 4267 GPS projects in the NGSIDB and consisted of:

- 81,055 existing mark *a priori* coordinates
- 424,721 GNSS vectors (and their covariances) connecting the marks as (reduced) observations
- 1195 MYCS1 CORS coordinates (and their uncertainties) as mark constraints.

Certain difficulties were encountered in correctly identifying MYCS1 CORSs for some marks in the NGSIDB. These problems mainly fell into one of the following four categories:

- Different information sources for associating PIDs with CORSs
- Stations in the NA2011 networks that became CORSs during the NA2011 Project
- Use of L1 APCs as the monument in GPS projects for antennas that have been replaced
- CORSs represented by multiple PIDs.

GNSS vectors used in the adjustment varied greatly in length, occupation duration, age, *a priori* error estimates, baseline processing software used, coordinate reference system, and sources for orbits. Some of the vector characteristics were potentially problematic for the adjustments, and their impact is explored in greater depth in Chapter 5.

The vector connections between marks created the networks adjusted in the NA2011 Project. Although it appears all marks can be connected in a single network, there is actually no vector connection between the North America and Pacific networks (the single mark in Hawaii is connected to Alaska by two vectors, but it is not connected to any other Pacific mark). In addition, CONUS and Alaska are connected by eight vectors to the same mark in Alaska. All eight vector connections between CONUS and Alaska are to one mark in Alaska, and they were observed in 1990 with relatively short occupations and were therefore excluded from the adjustments. For these reasons, the NA2011 adjustment consisted of three networks: 1) CONUS and the Caribbean; 2) Alaska, and 3) the Pacific. The CONUS network was later split into a Primary and Secondary network, and the Pacific network was adjusted with two separate sets of constraints, one based on NAD 83 (PA11) and the other based on NAD 83 (MA11) coordinates. The reasons for using these approaches for the CONUS and Pacific networks are discussed in the next chapter, along with other methods for performing the NA2011 adjustments.

Chapter 3. Methods Used for the 2011 National Adjustments

3.1. Adjustment approach

The overall approach used for performing the network adjustments of the National Adjustment of 2011 (NA2011) Project had broad similarities to the 2007 national adjustment (Pursell and Potterfield, 2008; Milbert, 2009). As with the 2007 project, only vectors from GPS projects obtained from the NGS Integrated Database (NGSIDB) were adjusted in the NA2011 Project—no conventional horizontal observations were included—and the adjustments were constrained only to CORSs. Both the 2011 and 2007 projects used the same "variance factor" technique for scaling the vector standard deviations of individual GPS projects, as described in Section 3.2.

The NGS program *NETSTAT* was used for the 2011 and 2007 projects to perform the least squares network adjustments. In both cases, the main reason for using *NETSTAT* was that it could perform Helmert blocking, essential because of the large number of observations and unknowns. The Helmert blocking scheme used for NA2011 was similar to that used for the 2007 project and is described in Section 3.3.1.

Despite the overall similarity between the 2011 and 2007 national adjustments, there were significant differences, and these differences are summarized in Table 3.1. The first two characteristics of the projects listed in the table were covered in Chapter 2; additional details for the subsequent characteristics are provided in this chapter.

3.1.1. On the use of GIS

Geographic Information System (GIS) software was an integral part of performing the NA2011 Project. It was of such significance that it is listed in Table 3.1 as one of the notable differences with the 2007 national adjustment. Previous projects made little use of graphical methods for analysis, and, as far as can be discerned, none had ever made use of GIS. The importance of GIS to this project cannot be overstated; it scarcely could have been completed without it.

The GIS platform used for NA2011 is Esri's *ArcGIS*. Early in the project, the Python 2 computer language was used to develop scripts that created GIS features from the input and output files for *NETSTAT* and *ADJUST*. Two feature types were created, point features for the adjusted marks, and line features of the GNSS vectors, both in Esri "shapefile" format (now an open industry standard). These features are available as part of NA2011 Project deliverables.

Importantly, the features include many attribute fields. For the mark feature, these include adjusted coordinates; estimated accuracies; sigmas used for constraints; coordinate shifts; number of vector ties; and date and time when the mark was first and last occupied (both for all vectors and for enabled vectors). The vector shapefile fields include the "from" (standpoint) and "to" (forepoint) marks; vector components, sigmas, length and variance factors; session information, including number of trivial vectors and false redundancy scalar; session start and stop times and duration; post-adjustment residuals as north, east, up, horizontal, and 3D values; GPS project ID; software used; and the agency that processed the vector.

Table 3.1. Summary of differences between the 2011 and 2007 national adjustments.

Characteristic	2011 national adjustment	2007 national adjustment
1. Marks and observations used	4267 projects; 81,055 marks, and 424,721 vectors from April 1983 through Dec 2011 (includes 541 marks and 1852 vectors in Pacific Ocean)	3418 projects; 67,693 marks; and 283,691 vectors from April 1983 through Oct 2005.
2. CORS coordinates	CORS NAD 83 coordinates from initial Multi-Year CORS Solution (MYCS1) at epoch 2010.00; coordinates were consistent, current, and based on the best available data and processing methods.	CORS NAD 83 coordinates stored in the NGSIDB used for most of CONUS (and Caribbean) at epoch 2002.00; for AK epoch of 2003.00 used. Epoch 2007.00 (derived from models) used for five west CONUS states AZ, CA, NV, OR, and WA.
3. CORS constraints	Weighted (stochastic) constraints were used for the CORSs, generally based on formal standard deviations from MYCS1.	Adjustment rigidly constrained to nearly all CORSs (using constant standard deviation of 0.001 cm). 5 CORSs with a 2D 10 cm sigma, 7 CORSs with a 3D 10 cm sigma, 3 CORS Not weighted at all)
4. Differential crustal motion modeling	*HTDP* applied to all GPS vectors to account for differential crustal motion and residual rotation of tectonic plates between date of observations and 2010.00.	Tectonic modeling only applied to six western states AZ, CA, NV, OR, WA, and AK. *HTDP* was used for all except CA, where the program *SECTOR* was used.
5. Network configuration	CONUS split into Primary and Secondary network; most of the Secondary network observations prior to 1994.	Adjusted all observations in a single network.
6. Alaska	Adjusted separately from CONUS.	Included with CONUS in single network.
7. Pacific Ocean	Included a (separate) network for islands in the Pacific Ocean.	Did not include observations from the Pacific Ocean.
8. Use of *ADJUST* and *NETSTAT*	*ADJUST* used to perform Alaska and Pacific adjustments; *NETSTAT* used for CONUS.	*NETSTAT* used for entire single network.
9. Gulf Coast subsidence region	Downweighting of observations done to account for effects of subsidence along the northern coast of Gulf of Mexico.	No special approach was used for Gulf Coast region or any other subsidence areas.
10. GIS	Heavily used for analysis and visualization.	Not used.

The lists of attribute fields in the previous paragraph is incomplete for the mark or vector feature. A complete list with descriptions for each field is provided in the appendices, along with two other GIS features created for the project: a point feature of the MYCS1 CORSs used as constraints, and a point feature of the NA2011 GPS projects. As with the adjusted mark and vector features, both are attribute-rich. The attributes are defined in the appendices for each of the four GIS feature types (as listed below), and all are available for download as electronic deliverables at ftp://geodesy.noaa.gov/pub/NA2011/.

- **Appendix A.** Properties of NA2011 Adjusted Mark GIS Feature Classes
- **Appendix B.** Properties of NA2011 GNSS Vector GIS Feature Classes

- **Appendix C.** Properties of the NA2011 Constrained MYCS1 CORSs GIS Feature Class
- **Appendix D.** Properties of the NA2011 GPS Project GIS Feature Class

All the GIS features are provided both in shapefile and Esri file geodatabases (version 10.7) formats. File geodatabases have more advanced functionality, including support for NULL fields, creating relationship classes, and topology; however, a disadvantage of file geodatabases is that they require specialized software (although it need not necessarily be Esri software), and the software must be the same, or a higher version, as the geodatabases. Shapefiles do not have these limitations, but they are an older format with less functionality. For those interested only in the attribute fields, all of the features are also provided in Microsoft *Excel* format.

As stated above, GIS proved not only useful but essential for the NA2011 Project. It is important to stress that GIS is not only for making "pretty" maps. GIS consists of spatially enabled databases and the software tools necessary for analysis and visualization. Nearly all of the figures in this report—not just the numerous maps, but also the charts—were created from GIS datasets. Most of the analyses, performed both during the project and after it was completed, were done with the GIS data and various tools that leveraged those data. The variety of analyses performed are too lengthy to list here, but an indication of the capabilities can be inferred from the content of this report.

3.1.2. Least squares adjustment programs *ADJUST* and *NETSTAT*

The NGS program *ADJUST* was initially developed in the late 1980s as a general-purpose geodetic least squares adjustment program intended to handle any type of geodetic observation (Milbert and Kass, 1987). *ADJUST* accomplishes this by transforming all observations to a common local geodetic horizon (LGH) north-east-up coordinate system. In doing so, a wide variety of geodetic observations can be combined and adjusted simultaneously in LGH space. The adjustment results are transformed from LGH to the desired output coordinates, usually geodetic latitude, longitude, and (optionally) height. According to NGS policy (NGS, 2012), all geodetic observations (with the exception of leveling) adjusted for loading into the NGSIDB must be adjusted using *ADJUST*. Leveling is also limited to a specific process and computer program (called *ASTA*).

ADJUST has been updated over the years, with functionality added and refined, although its basic structure has remained the same. For the 2007 national adjustment, it was realized that *ADJUST* could not readily perform the adjustments, because it was unable to handle the large number of marks and observations. To accommodate such large networks required the development of a Helmert blocking program,[10] so the network of observations could be broken into manageable sizes ("blocks"). The blocks are adjusted separately and then combined as if the entire network were adjusted simultaneously. Rather than modify *ADJUST*, NGS decided to create a program specifically to perform Helmert block adjustments of GNSS vectors. The

[10] For the creation of the original NAD 83, NGS had already developed (in house) Helmert blocking software capable of solving over 900,000 equations (Bossler, 1987). By 2007, that software had been lost and NGS hired a consultant to develop *NETSTAT* as its replacement, so that the 2007 national adjustment could be performed. This demonstrates the importance of proper archiving and storage of historic computer files and programs.

resulting program was *NETSTAT* (so named because originally it was intended to compute ***NET***work ***STAT***istics). As *NETSTAT* used only GNSS vectors, it could perform the adjustment in the Earth-Centered, Earth-Fixed (ECEF) Cartesian coordinate system of the vectors. The advantage of an adjustment of ECEF vectors is that it is already linear, therefore no iteration is required—the solution is obtained in a single step. In contrast, an LGH coordinate system requires iteration, because the observation equations are not linear and so linearized approximations must be used. A non-iterative approach is a significant advantage for large networks, when a single iteration may take several days to complete.

When properly implemented, an adjustment in ECEF coordinates will yield the same results as one using LGH coordinates. Since NGS policy required that *ADJUST* be used for adjustments of all data loaded into the NGSIDB, it was critically important to demonstrate that both programs gave the same results, and this was done for the 2007 adjustment and again for the 2011 adjustment. For NA2011, an adjustment of the Alaska network was done in both programs, and the coordinates and network accuracies obtained were identical (to the displayed precision).

Although *ADJUST* was not used to perform the network adjustments for the 2007 national adjustment, it was used in NA2011 for the adjustments of the Alaska and Pacific networks. *ADJUST* also played an important role in both national adjustments: it was used to compute the GPS project "variance factors" (the topic of Section 3.2).

3.1.3. Modeling velocities with *Horizontal Time Dependent Positioning* (*HTDP*)

GNSS vectors computed from observations spanning nearly 30 years (from April 1983 through December 2011) were combined in the NA2011 network adjustments. The endpoints of some of the vectors are located in areas of known significant horizontal differential crustal movement, such as the west coast of CONUS and south-central Alaska. This relative motion is not captured by the Eulerian North America tectonic plate rotation included in the Helmert transformation parameters in *NETSTAT* and *ADJUST* (see Table 2.13). Horizontal velocities in these regions can exceed 5 cm/year with respect to the North American frame. In 30 years, such velocities can cause the vector endpoints to move more than 1.5 m with respect to one another, particularly for long vectors with one end in a tectonically active area. Moreover, it appears the Helmert parameters for the North America frame overestimate the Eulerian rotation for its tectonic plate, as discussed previously, and later in this section. In addition, Helmert parameters for the Pacific and Mariana frames are not included at all in *NETSTAT* or *ADJUST*. The resulting relative motion from these various sources cause the vectors to rotate and change in length, and the magnitude is often too large to ignore.

NGS created a program, *Horizontal Time Dependent Positioning* (*HTDP*), to address such relative motion issues (Pearson and Snay, 2013). *HTDP* includes velocity and earthquake displacement models for the entire NSRS, allowing it to estimate coordinates at different times. *HTDP* also includes 14-parameter Helmert transformations between NAD 83 and various global reference frames, such as ITRF, IGS, and WGS 84. Combining the velocity and displacement models with reference frame transformations allows *HTDP* to transform positions between frames at different epochs. With the exception of central Alaska, *HTDP* velocity and displacement modeling is horizontal only, hence the program's name.

HTDP has long been used for modeling tectonic changes to GNSS and classical horizontal control survey data prior to adjustment of those data. Version 2.7 of the program was used for GNSS vectors in the 2007 national adjustment for the western U.S. states of Arizona, Nevada, Oregon, Washington, and Alaska. However, *HTDP* was not used for California. At the time of the 2007 adjustment, it was believed another non-NGS program called *Scripps Epoch Coordinate Tool and Online Resource* (*SECTOR*) would provide more reliable results in California (Pursell and Potterfield, 2008). *SECTOR* is an online utility created and maintained by the Scripps Orbit and Permanent Array Center (SOPAC, 2017). Unlike *HTDP*, which computes coordinates and velocities at all locations within its modeled region, *SECTOR* only performs computations at permanent GNSS antennas in the SOPAC array.

Version 3.1.2 of *HTDP* was used for the NA2011 Projects because it was current at the time of the project, and it is the same version used for estimating "modeled" MYCS1 CORS velocities and coordinates (as discussed in Chapter 1). However, that version of *HTDP* did not include a model for the Philippine Sea tectonic plate, and some marks are located on that plate (on Yap Island and Palau). To address this problem, the Philippine Sea plate was added to create *HTDP* version 3.2.2, an otherwise identical version to version 3.1.2. *HTDP* v3.2.2 was used to transform GNSS vectors for the NA2011 Pacific network.

For the NA2011 Project, *HTDP* was used to transform all GNSS vectors from their global reference frames at the date of the observation to the NAD 83 2011, PA11, and MA11 frames at epoch 2010.00 (the vector reference frame and date is stored in the G-file, as described in Section 2.3). One reason for this is consistency: it makes sense to apply the same transformations to all observations within a frame, especially since many vectors have endpoints inside and outside areas of active crustal motion (and even on different tectonic plates). Transforming all G-files to the appropriate NAD 83 frame with *HTDP* also means no transformation is performed by *NETSTAT* or *ADJUST*. This is particularly important for marks referenced to the Pacific and Mariana tectonic plates, because the Helmert transformations between those frames and the global frames are not defined in *NETSTAT* or *ADJUST*.

Another compelling reason to transform all vectors with *HTDP* is that nearly all locations in the NSRS have non-negligible horizontal NAD 83 velocities. The original intent was that the NAD 83 frame be affixed to the North America tectonic plate, so that most locations in North America would have NAD 83 horizontal velocities near zero. However, as mentioned in Section 1.3.1, the Helmert parameters for the North America frame appear to induce an apparent greater-than-actual plate rotation rate. The higher rotation rate created NAD 83 velocities that are in the opposite sense of those with respect to the global frame (e.g., IGS08). A similar thing occurred for the Pacific and Mariana plates, although the effect is smaller, possibly because the rotations used for these frames were derived more recently (Snay, 2003).

NAD 83 velocities are given in Table 3.2 for various locations in the NA2011 networks, as shown in Figure 3.1. Although *HTDP* versions 3.1.2 and 3.2.2 were used for the NA2011 Project, current *HTDP* version 3.2.5 was used for Table 3.2 because it incorporates more recent information from the CORSs, and so it provides a more accurate representation of velocities. In

addition, NGS products and services use the latest available version of *HTDP* (e.g., for *OPUS* solutions and Bluebooking).

Table 3.2. NAD 83 and IGS08 horizontal velocities at various locations in the NSRS (from *HTDP* v3.2.5). The feature locations are shown in Figure 3.1.

Feature location	Tectonic plate	NAD 83 frame	NAD 83 velocities (cm/yr)			IGS08 velocities (cm/yr)		
			North	East	Horiz	North	East	Horiz
East CONUS								
Augusta, Maine	North America	2011	-0.18	0.21	**0.28**	0.59	-1.54	**1.64**
Washington, D.C.	North America	2011	-0.09	0.18	**0.20**	0.39	-1.46	**1.51**
Miami, Florida	North America	2011	-0.09	0.17	**0.19**	0.26	-1.05	**1.08**
Central CONUS								
Bismarck, North Dakota	North America	2011	0.06	0.23	**0.24**	-0.46	-1.61	**1.67**
Kansas City, Missouri	North America	2011	0.04	0.21	**0.21**	-0.22	-1.45	**1.47**
Corpus Christi, Texas	North America	2011	0.03	0.00	**0.03**	-0.33	-1.29	**1.33**
West CONUS								
Denver, Colorado	North America	2011	0.06	0.18	**0.19**	-0.62	-1.43	**1.56**
Phoenix, Arizona	North America	2011	0.18	0.08	**0.20**	-0.76	-1.30	**1.51**
Portland, Oregon	North America	2011	0.73	0.47	**0.87**	-0.61	-1.06	**1.22**
California								
Sacramento, California	North America	2011	0.93	-0.87	**1.28**	-0.35	-2.26	**2.29**
Monterey, California	Pacific	2011	3.83	-2.67	**4.67**	2.53	-4.01	**4.74**
San Diego, California	Pacific	2011	3.02	-2.63	**4.00**	1.89	-3.93	**4.36**
Caribbean								
San Juan, Puerto Rico	Caribbean	2011	0.35	1.91	**1.94**	1.27	1.01	**1.62**
Alaska								
Fairbanks, Alaska	North America	2011	-0.10	0.16	**0.19**	-2.16	-0.98	**2.37**
Anchorage, Alaska	North America	2011	0.20	-0.49	**0.53**	-1.90	-1.53	**2.43**
Seward, Alaska	North America	2011	2.78	-0.82	**2.89**	0.69	-1.86	**1.99**
Pacific plate								
Honolulu, Hawaii	Pacific	PA11	0.01	0.03	**0.03**	3.50	-6.24	**7.15**
Pago Pago, American Samoa	Pacific	PA11	-0.02	0.02	**0.03**	3.42	-6.69	**7.51**
Wake Island	Pacific	PA11	-0.05	-0.02	**0.05**	2.87	-7.00	**7.57**
Mariana and Philippine Sea plate								
Hagåtña, Guam	Mariana	MA11	0.00	0.00	**0.00**	0.40	-1.09	**1.16**
Saipan, CNMI	Mariana	MA11	0.00	0.00	**0.00**	0.41	-1.08	**1.16**
Koror, Palau	Philippine Sea	MA11	1.08	-5.96	**6.06**	1.44	-7.05	**7.19**

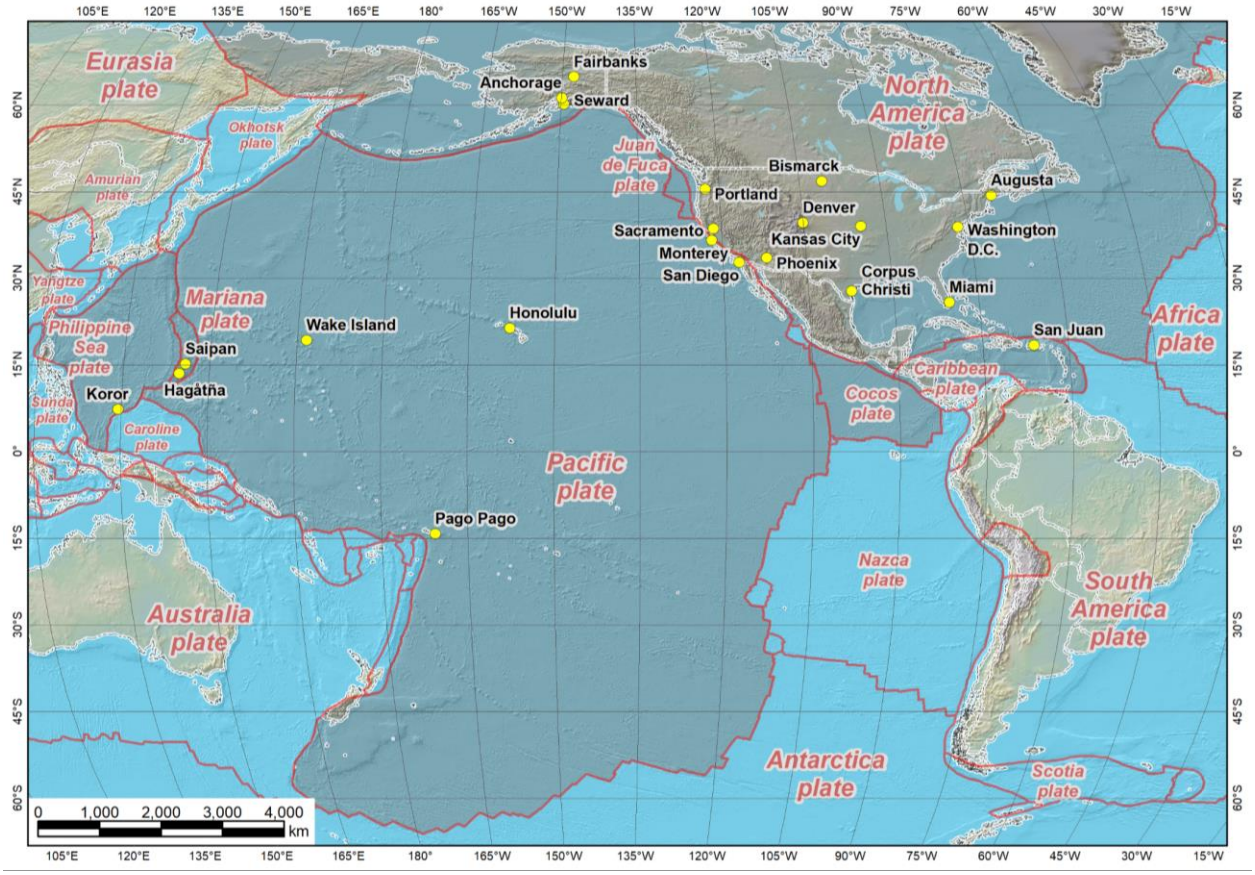

Figure 3.1. Tectonic plates modeled in HTDP (shaded) indicating where velocity can be calculated. The 22 labeled points are the locations listed Table 3.2 with horizontal NAD 83 and IGS08 velocities.

Figure 3.1 shows the seven tectonic plates (shaded) modeled in *HTDP* for version 3.2.2 and later. The labeled point features are 22 locations (mainly cities) distributed throughout the NSRS. These feature locations are listed in Table 3.2, along with their modeled NAD 83 and IGS08 horizontal velocities. The intent is to show the general distribution and variation of NAD 83 velocities throughout the NSRS. IGS08 velocities are given to provide a comparison to the no-net-rotation velocities for the global frame on which NAD 83 (**11) was based. Note that some of the NAD 83 velocities are on par with the IGS08 velocities in locations such as Alaska, California, San Juan (Puerto Rico), and Koror (Palau).

The feature locations in Figure 3.1 were selected to provide good representative examples for discussion. In Table 3.2, they are grouped in one of the following regions: east CONUS, central CONUS, west CONUS, California, the Caribbean, Alaska, the Pacific plate, and the Mariana and Philippine Sea plate. The tectonic plate of the location is given, along with the NAD 83 frame the location references (as 2011, PA11, or MA11).

The NAD 83 velocities for the point features in Table 3.2 correspond to the plates referenced at those locations. However, the plate referenced may not be the same as the plate where a feature resides, and such features have the highest NAD 83 velocities. For example, San Juan is on the

Caribbean plate, but it is referenced to the North America plate, and its velocity is fairly high, 1.9 cm/yr (higher than its IGS08 velocity of 1.6 cm/yr). More dramatic are Monterey and San Diego in California, with the highest NAD 83 velocities in the table, 4.7 and 4.0 cm/yr respectively. These velocities occur because they are also referenced to the North America plate, but they are west of the San Andreas Fault system and thus are on the Pacific plate (their IGS08 velocity magnitudes are similar but not quite in the same direction). Compare these to Sacramento, located east of the San Andreas Fault system, on the North America plate. The velocity is much lower (1.28 cm/yr), but still high for a North America plate location.

As mentioned previously, locations on the stable part of the North America plate generally exhibit non-negligible velocities, because the plate rotation model used for NAD 83 is not quite correct. The locations in east and central CONUS have approximately the same velocity distribution, generally increasing from south to north, from near zero in Corpus Christi, to almost 0.3 cm/yr in Maine. West CONUS is more or less similar, but there is an increase in velocity in the Pacific Northwest, as shown by the 0.9 cm/yr rate in Portland. IGS08 CONUS velocities are larger (from 1.1 to 1.7 cm/yr), but show a trend consistent with a rotation in the opposite direction. This shows why using *HTDP* for all GNSS vectors in CONUS is important. Likewise, for Alaska, which shows the small NAD 83 velocity of 0.2 cm/yr in Fairbanks, increasing south to 2.9 cm/yr in Seward near the subduction zone between the North American and Pacific plates.

The islands on the Pacific plates all have NAD 83 velocities of 0.05 cm/yr or less. These velocities are in stark contrast to their IGS08 velocities of over 7 cm/yr, the highest in Table 3.2, demonstrating that the plate rotation model used for the Pacific plate is actually quite good; it nearly cancels the large IGS08 velocities. But *HTDP* was still required for the Pacific, because its Helmert transformation is not included in *ADJUST* or *NETSTAT*, and because it has vector endpoints on the Mariana and Philippine Sea plate.

The lowest NAD 83 velocities are in Hagåtña (Guam) and Saipan, of 0.00 cm/yr. At first glance, this might be interpreted as meaning this plate rotation model seems to perform very well indeed. However, the actual rotation for the Mariana plate was not well-defined (at the time of the NA2011 adjustment), because it lacked data points north of Saipan. The disappointing location in this region is Koror (Palau). Koror is located on the Philippine Sea plate but is referenced to the Mariana plate, and it has the highest NAD 83 velocity in the Table 3.2 list, 6.1 cm/yr. The decision to reference Palau (and nearby Yap Island) to the Mariana plate was made near the end of the NA2011 Project. Unfortunately, it has since been realized that these areas would have much lower velocities if they were instead referenced to the Pacific plate; the velocity of Koror would have decreased from 6.06 to 0.08 cm/yr.

Maps of the NAD 83 velocity distribution for CONUS are shown in Figure 3.2, and for Alaska in Figure 3.3. These maps provide a more detailed illustration of the velocity distribution and variability than the list in Table 3.2. In particular, they show the concentration of high velocities near plate boundaries. Particularly noticeable is the strike-slip motion along the San Andreas Fault in California, and subduction zone compression along the north Gulf of Alaska coast (and to a lesser extent along the Pacific Northwest coast).

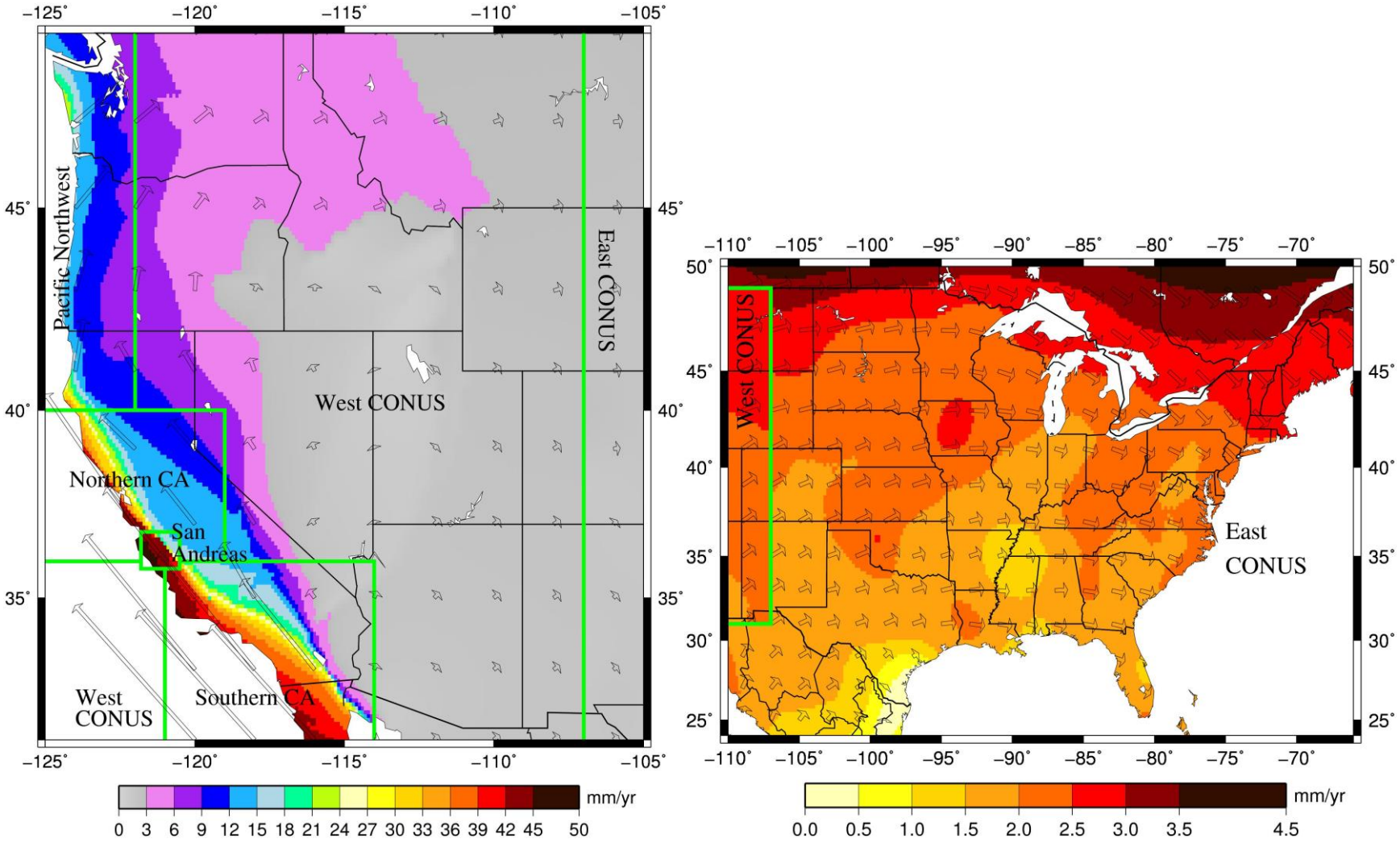

Figure 3.2. NAD 83 horizontal velocities in west and east CONUS from *HTDP* v3.2.5.

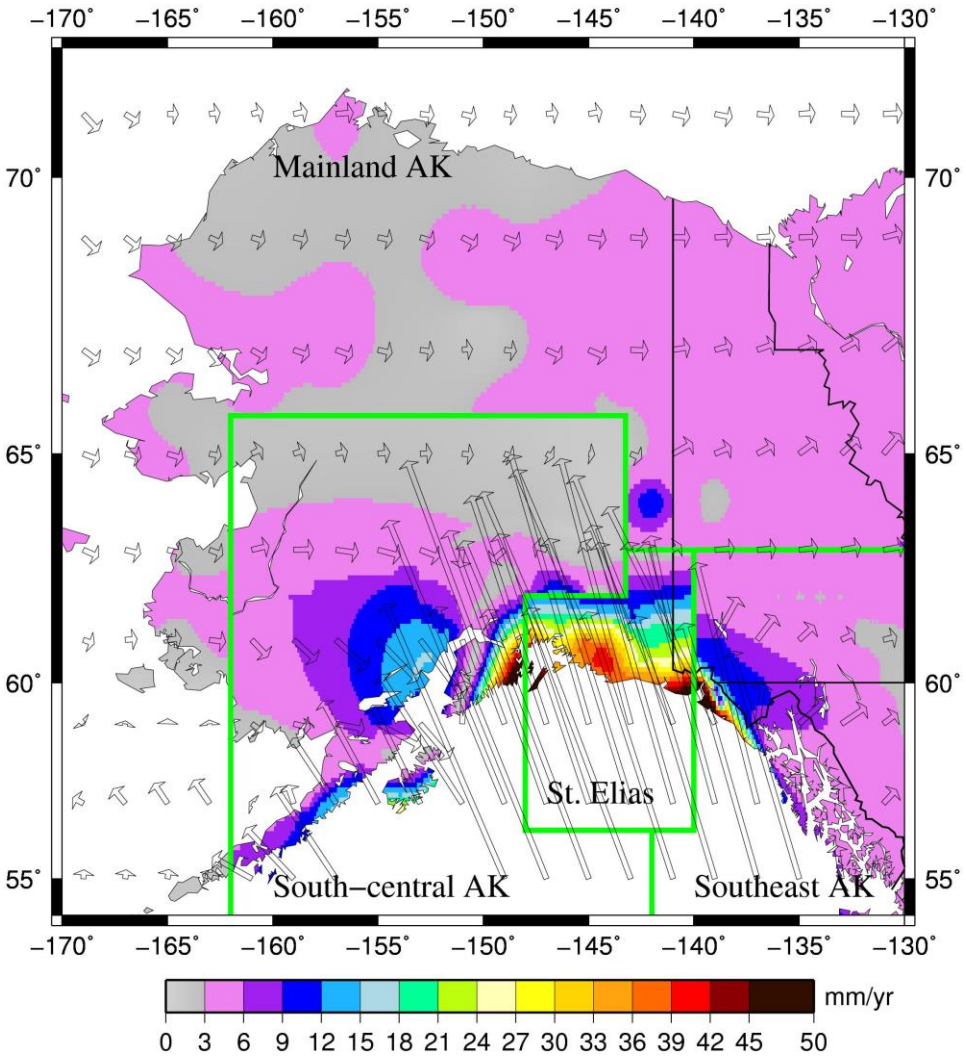

Figure 3.3. NAD 83 horizontal velocities in Alaska from *HTDP* v3.2.5.

3.1.4. Weighting of CORS constraints

As with the 2007 national adjustment, the NA2011 adjustment was constrained only to CORSs. In both cases, this decision was based on the role of the CORSs as providing the geometric foundation of the NSRS. Moreover, in both cases, the adjustments were constrained to the NAD 83 coordinates of the CORSs, not their global coordinates (IGS08, in the case of MYCS1). This point is important, because, as discussed in Section 1.3, the MYCS1 coordinates were computed as IGS08 epoch 2005.00. The NAD 83 MYCS1 coordinates were computed by Helmert transformation to obtain NAD 83 epoch 2005.00 values. CORS velocities were then applied to move the NAD 83 coordinates to epoch 2010.00. The velocities were either computed from the data as part of MYCS1, or they were modeled using HTDP (v3.1.2). The decision to use epoch 2010.00 (rather than 2005.00) was driven by a desire to provide NGS customers with more up-to-date coordinates. The down side of using epoch 2010.00 is that it created a complex

relationship between the IGS08 and NAD 83 frames, one that depended on using crustal motion models in addition to a 14-parameter Helmert transformation.

The major difference in the CORSs between the 2007 and 2011 national adjustments is MYCS1: it resulted in a consistent set of rigorously determined coordinates for all CORSs at a common epoch. MYCS1 also provided formal uncertainties, at least for all CORSs with "computed" velocities (those with more than 2.5 years of data). In contrast, the CORS coordinates used for the 2007 adjustment were not part of a single unified solution, were at different epochs (2002.00, 2003.00, and 2007.00), and had no formal uncertainty estimates.

Having formal uncertainties for the CORSs opened a new possibility—the use of weighted (stochastic) constraints. The 2007 adjustment used rigid constraints based on a standard deviation ("sigma") of 0.001 cm for all components on 673 (98%) of the 685 available CORSs. Of the remaining 12, five used 10 cm sigmas for the height component (with the horizontal components unconstrained), and seven used 10 cm sigmas for all three components. In this case, a sigma of 10 cm is essentially unconstrained; the corresponding weight is $(10 \text{ cm} / 0.001 \text{ cm})^2 = 100{,}000{,}000$ times less than the rigidly constrained marks. Since formal uncertainties were available for computed MYCS1 CORSs, it seemed worthwhile to pursue the idea of weighted constraints for the NA2011 Project.

Table 1.2 summarizes the formal uncertainties for all NAD 83 MYCS1 CORSs (given at the 95% confidence level). Of the 2064 MYCS1 CORSs with NAD 83 coordinates, 1195 were connected to passive marks with vectors in the NA2011 network and were used as constraints. However (as shown in Table 2.4), only 973 of the 1195 connected CORSs had formal uncertainties; the other 222 were "modeled" CORSs with no uncertainty estimate (as discussed in Section 1.3.2).

Statistics of the formal standard deviations ("sigmas") of the 973 "computed" CORSs are summarized in Table 3.3, along with the corresponding weights used for constraints. Note the large range in formal uncertainties, from 0.05 to 12.92 cm horizontal and 0.08 to 32.52 cm vertical. Because the weights are the squared inverse sigmas, their ranges are, of course, larger: approximately 4 orders of magnitude horizontal and 5 orders vertical. These are surprisingly large ranges, particularly considering MYCS1 represents the results of a single solution for all the CORSs (the variance-covariance values were obtained from the MYCS1 SINEX solution file). Table 3.3 also includes the percentiles, providing more details on the distribution and showing the median (50^{th} percentile) is somewhat smaller than the mean, which is more influenced by the large sigmas. It shows that 90% have horizontal and vertical sigmas of less than about 1 and 4 cm, respectively. However, it also shows that a few CORSs had large sigmas at the decimeter level.

Of the 973 computed CORSs used for the NA2011 Project, eight had 3D MYCS1 formal sigmas of greater than 10 cm, and these eight CORSs are listed in Table 3.4. The one with the largest sigmas is located in California; however, there is no geographic correlation; all eight are located in different states distributed throughout CONUS.

Table 3.3. Formal sigmas and corresponding constraint weights for "computed" MYCS1 CORSs ("sigmas" are the formal uncertainties represented as SINEX standard deviations).

Statistic for the 973 "computed" MYCS1 CORSs	Standard deviation (cm)			Weight (m^{-2}) corresponding to sigma		
	North	East	Up	North	East	Up
Minimum	0.06	0.05	0.08	3,188,776	3,335,849	1,562,500
Maximum	8.64	12.92	32.52	134	60	9
Mean	0.52	0.45	2.02	36,742	49,748	2,452
Standard deviation	±0.56	±0.60	±2.28	±31,899	±27,915	±1,922
Percentiles						
1%	0.07	0.07	0.17	1,907,651	2,100,399	367,309
5%	0.12	0.10	0.35	756,144	1,039,111	82,764
10%	0.14	0.12	0.50	500,151	683,013	40,603
50% (median)	**0.39**	**0.32**	**1.48**	**66,769**	**97,049**	**4,596**
90%	1.01	0.82	3.88	9,877	14,872	665
95%	1.44	1.21	5.79	4,797	6,836	298
99%	2.14	2.02	9.79	2,179	2,448	104

Table 3.4. Computed MYCS1 CORSs constrained with 3D formal sigmas greater than 10 cm.

CORSs ID	Designation	PID	State	MYCS1 formal sigmas (cm)			
				North	East	Up	3D
P304	MENDOTA__CN2004 GRP	DG8531	CA	8.64	6.93	32.52	34.36
RCM5	RICHMOND 5 CORS L1 PHASE CENTER	AA5492	FL	6.44	12.92	29.12	32.50
FMC2	FORT MACON 2 CORS L1 PHASE CENTER	AB6286	NC	5.75	4.76	22.32	23.54
WNFL	WINNFIELD CORS ARP	AF9639	LA	2.94	2.95	16.22	16.75
MNP1	MONTAUK POINT 1 CORS L1 PHASE CENTE	AB6303	NY	4.40	3.45	15.71	16.68
AL90	ALDOT 9 DIV OFF CORS ARP	DI3826	AL	2.72	2.57	11.79	12.37
BACO	BALTIMORE COUNTY GPS BASE	AJ8029	MD	2.56	2.31	11.17	11.69
PASO	EL PASO RRP CORS L1 PHASE CENTER	AB6383	TX	2.09	2.02	9.79	10.21

There was some debate as how best to weight constraints to the 222 modeled CORSs. One suggestion from the NGS CORS Team was to assign a sigma of 5 cm to each component; however, this seemed too "loose" for CORSs. Moreover, it was not appropriate to assign the same value to all three components, since the height sigmas for MYCS1 CORSs are typically about 3 to 4 times greater than the horizontal. In addition, test adjustments yielded post-adjustment sigmas of less than 5 cm for the modeled CORSs when the computed CORSs were

constrained. Their sigmas were roughly 0.5 to 2 cm horizontal and 2 to 5 cm vertical. There was also a desire to have the modeled sigmas generally larger than the computed sigmas, to reflect the use of modeled velocities in determining their coordinates. Table 3.3 shows that the mean sigmas for computed CORSs were about 0.5 cm horizontal and 2 cm up. It also shows that 90% of the modeled CORSs had sigmas of less than about 1 cm horizontal and 4 cm up. Based on these considerations, it was decided to assign north and east sigmas of 1 cm and height sigmas of 3 cm for all modeled CORSs. The weights based on these assumed sigmas for the modeled CORSs are 10,000 m^{-2} horizontal and 1111 m^{-2} vertical, which roughly corresponds to the 90th percentile for the computed CORSs weights. A summary of statistics on the constraint sigmas used for computed-only and all constrained CORSs (i.e., both computed and modeled) is given in Table 3.5.

Table 3.5. Summary statistics on sigmas used for weighting constrained CORSs (for the 973 computed and all 1195 computed and modeled CORSs; for all modeled CORSs, $\sigma_n = \sigma_e = 1$ cm and $\sigma_u = 3$ cm).

Statistic for constrained CORSs	Computed CORSs only (973)				All constrained CORSs (1195)			
	North	East	Up	3D	North	East	Up	3D
Median	0.39	0.32	1.48	1.56	0.47	0.40	1.83	1.93
Mean	0.52	0.45	2.02	2.14	0.61	0.55	2.20	2.35
Standard deviation	±0.56	±0.60	±2.28	±2.42	±0.54	±0.58	±2.09	±2.23

Analyses were performed to compare the difference in adjustment results between rigid and weighted constraints. The earliest of analyses were done in September and October 2011 as adjustments of the entire combined CONUS and Alaska network at that time. The standard deviation of unit weight (σ_0) of the minimally constrained ("free") adjustment was $\sigma_0 = 1.24$. With rigid constraints (0.001 cm on each component) on 640 CORS ARPs, this increased to $\sigma_0 = 1.39$. Using the MYCS1 sigmas for weighting the CORS constraints yielded $\sigma_0 = 1.25$ (nearly the same as the free adjustment). For all 83,779 marks in the adjustment (both unconstrained passive and constrained CORSs), the maximum difference in adjusted coordinates when weighted constraints were used was 7 cm horizontal and 5 cm vertical, but the mean difference was zero, with a standard deviation of about 1 cm in all components. A total of 185 marks had a component that shifted by more than 3 cm, and half of those marks were in California.

Several adjustments were performed to compare the difference between rigid and weighted constraints. The last adjustment was done for CONUS-only in January 2012 (excluding Alaska), and it yielded the following results:

1. Minimally constrained: σ_0 = **1.37**
2. Weighted constraints (using actual MYCS1 sigmas only): σ_0 = **1.38**
3. Rigid constraints (sigma = 0.001 cm): σ_0 = **2.20**

The σ_0 was substantially larger for the rigidly constrained adjustment (by a factor of 2.20/1.38 = 1.59), implying constraint sigmas of 0.001 cm on all components are too small (i.e., too optimistic). The mean MYCS1 sigma of all components for the constrained CONUS CORSs is 1.12 cm, which is 1120 times larger than 0.001 cm. This result may seem to suggest a discrepancy, since σ_0 increased by a factor of only 1.59, even though the rigid constraint sigmas are about 1000 times smaller. Moreover, the rigid constraints are the same for all components, whereas the weighted constraint up-components for all constrained CORSs are on average 3.8 times greater than the horizontal components (although this does not alter the overall observation regarding the difference in ratios).

However, the ratio of σ_0 does not translate directly to the ratio in constraint sigmas, because the relationship between them is strongly nonlinear. The value of σ_0 is the square root of the sum of the weighted squared residuals divided by the network degrees of freedom, which is only partially affected by constraint sigmas. While changing the constraint sigmas does affect σ_0, it can only go so far, since σ_0 will become constant as the constraint sigmas increase or decrease. For large constraint sigmas, σ_0 will decrease, but it will not become much less than its minimally constrained value. For small constraint sigmas, σ_0 will increase, but it will level off to a maximum value as the constraints become "rigid" with respect to the sigmas of the observations.

A series of constrained adjustments can be performed to show the variation in σ_0 as the constraint sigmas change. This is inconvenient to do for the CONUS network, because each adjustment takes many hours. The Alaska network can be used for the purpose of this discussion (complete results are given in Chapter 4). The final minimally constrained adjustment for Alaska gave σ_0 = 1.822. A series of adjustments was performed with constraint sigmas equal on all components, starting with the "rigid" value of 0.001 cm, and increasing to 10 cm. The σ_0 values for each of these adjustments is plotted in Figure 3.4, with the constraint sigma values plotted on a log scale. As the constraint sigmas increase, σ_0 levels off to a constant value of about 1.8 for constraint sigmas > 3 cm. Constrain sigmas < 0.01 cm can be considered "rigid," since that is where σ_0 approaches a nearly constant value of about 3.3. As with the CONUS network, the range from 0.001 to 1 cm is a factor of 1000 (three orders of magnitude), yet the change in σ_0 is a factor of only 3.26/1.91 = 1.71. Other constrained GPS network adjustments behave in the same way, with σ_0 bound asymptotically between maximum and minimum values varying much less than the constraint sigmas, and in a strongly nonlinear way.

A decision was made by the NA2011 Project team to use weighted constraints for all subsequent adjustments. Admittedly, the decision on whether to use rigid or weighted constraints is not completely clear. Part of the reason for deciding to use weighted constraints was that it was considered more realistic. Statistics from the MYCS1 showed uncertainty estimates varying by 2 to 3 orders of magnitude; weighting them all equally does not seem appropriate. Likewise, weighting the modeled CORSs the same as computed CORSs also did not seem appropriate. Assigning very tight "rigid" constraints (e.g., based on sigmas of 0.01 cm) obviously cannot reflect this variation, nor can it adequately capture the actual observed random noise behavior seen at all, even the best behaved, CORSs. It also treats the CORSs as essentially errorless. That was the intent in the 2007 national adjustment, and has, in fact, been the general approach to how

NGS (and its predecessor agencies) have historically adjusted and provided geodetic control. That is, it has been common practice to take the most accurate data possible, perform an adjustment to determine coordinates, and then *hold those coordinates fixed* (either as the way to provide access to the NSRS for the public or as the foundation for layered adjustments of less accurate observational data to further propagate the network.) That is not to say this approach is without its disadvantages. Both the "fixed geodetic control" and the "weighted geodetic control" camps have had their champions throughout the history of the NSRS.

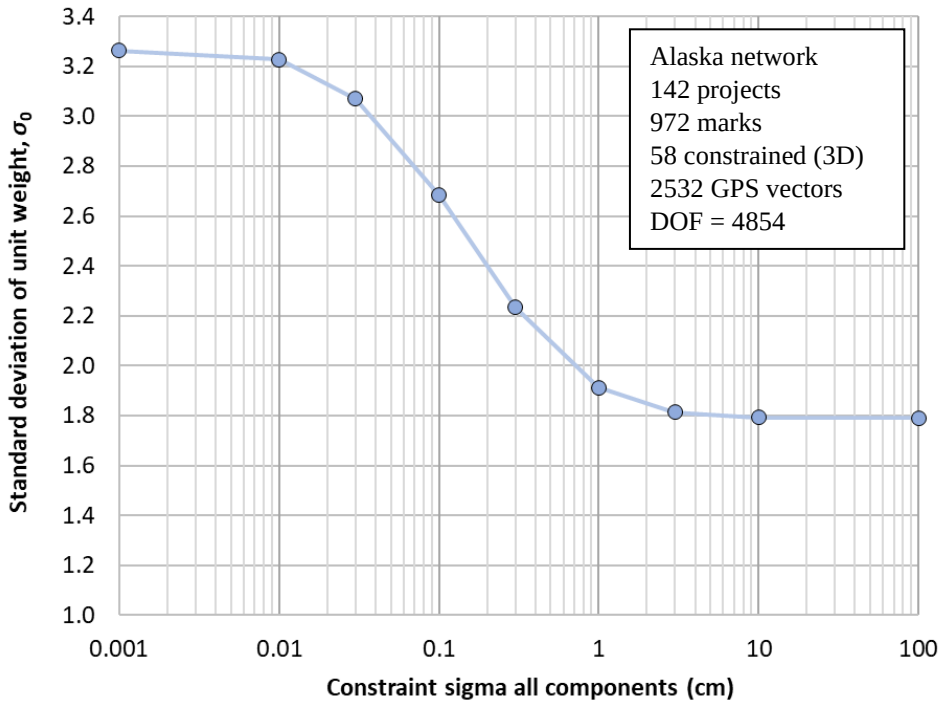

Figure 3.4. Change in σ_0 as a function of constant constraint sigmas for the Alaska network.

While the "fixed geodetic control" approach could to some degree be justified by a lack of reliable uncertainty estimates in the 2007 adjustment, such an approach did not seem appropriate given the availability of formal uncertainty estimates on (most) CORSs as of 2011. And finally, rigid constraints that do not reflect the actual uncertainties tend to distort network adjustments, affecting statistics, such as the post-adjustment uncertainties on the unconstrained marks. Since those uncertainties should be used to publish accuracy estimates, it was deemed more appropriate to have them based on the best available uncertainties for the constrained CORSs.

3.2. GPS project variance factors

3.2.1. Scaling GNSS vector standard deviations in GPS projects

One of the important innovations of the 2007 national adjustment was scaling of the vector uncertainties (standard deviations or "sigmas") for individual GPS projects. The necessity of performing the scaling and some details about the process are discussed by Pursell and Potterfield (2008) and by Milbert (2009). These two reports, as well as the Bluebook (NGS 2019d), and supplemental *ADJUST* documentation (NGS, 2018a), often refer to these scalars as

variance factors, even though the values are applied to the GPS standard deviations, not their variances (i.e., standard deviation squared). To maintain consistency with existing documentation, the term "variance factor" is also used in this report, particularly in the following section describing how the factors are computed. But they are also referred to as *sigma (or standard deviation) scalars*, especially in this section, to make clear what exactly is being scaled. But the terms are synonymous.

The same rationale and approach for scaling GPS vector sigmas in the 2007 adjustment was used for the NA2011 Project. Factors previously computed for 3423 GPS projects as part of the 2007 adjustment were used in NA2011. For the NA2011 Project, factors were computed for an additional 868 GPS projects, with 844 of those used, giving a final total of 4267 GPS projects in NA2011. The procedure was the same for both the 2007 and 2011 projects: variance factors were computed on a project-by-project basis by using *ADJUST* to perform a minimally constrained adjustment for projects in the NGSIDB (details of the computation process are described in the next section). The computed factors were then loaded into the NGSIDB, so they would be included with each project when it was downloaded. For new GPS projects submitted to NGS, the variance factors are now computed and stored as part of loading the project results into the NGSIDB.

A summary of the 4267 GPS project sigma scalars (variance factors) used for NA2011 is given in Table 3.6. This table shows a very large range, from 0.05 to 58.43 for horizontal scalars and 0.02 to 69.97 for vertical scalars. The mean values are much lower, 4.02 and 2.16, respectively. The table also gives percentiles, where the 50^{th} percentile (median) is 1.16 and 0.98, respectively. Having the median so much lower than the mean indicates there is not a large number of extreme values, and this is also reflected in the 95^{th} and 99^{th} percentiles. Interestingly, the 50^{th} and 10^{th} percentiles are close to 1. This implies a large number of projects have variance factors close to 1, which is counter to expectation for GPS projects, since it is typical for their solution uncertainties to be optimistic, meaning the variance factors would be greater than 1.

The GPS project variance factors (sigma scalars) are for the entire nearly 30-year set of projects. To illustrate how they vary with time, the mean and median variance factors for each year are plotted in Figure 3.5. The plot shows that the median values were very close to 1 for projects in 2004 and prior. The mean values, however, begin to increase much earlier, around 1992. After 2004, both the median and the mean values are significantly greater than 1.

To show the actual variation (masked by the mean, and in particular, the median), Figure 3.6 is a plot of all 3D variance factors (square root of the squared sum of the horizontal and vertical factors) as a function of time. The scatter in values becomes significant in the early 1990s, with the greatest range in values occurring in 1995 and 2008. The most striking feature of the distribution as the prominent horizontal band near the bottom that consists of a large number of projects with a variance factor (standard deviation scalar) of about 1. That corresponds to the median vector sigma scalar near 1 in Figure 3.5, but in Figure 3.6 the band extends further right, to about 2008. Both figures demonstrate that a significant number of projects had variance factors of near 1, and over a long span of time.

Table 3.6. Summary of NA2011 GPS project sigma scalars and vector sigmas (unscaled and scaled).

Statistic	GPS project vector sigma scalars		Unscaled GPS vector 3D sigmas as stored in NGSIDB (cm)		Scaled GPS vector 3D sigmas (cm)	
	Horiz	Vert	All vectors	Enabled only	All vectors	Enabled only
Number	*4267*		*424,721*	*403,112*	*424,721*	*403,112*
Minimum	0.05	0.02	0.02	0.02	0.02	0.02
Maximum	58.43	69.97	1732.03	1732.03	8298.33	8298.33
Mean	4.02	2.16	2.72	2.25	4.57	3.85
Std deviation	±5.86	±3.27	±15.49	±0.81	±24.16	±17.64
Percentiles						
1%	0.42	0.16	0.04	0.04	0.34	0.34
5%	0.79	0.33	0.11	0.10	0.61	0.60
10%	0.93	0.43	0.15	0.14	0.85	0.83
50% (median)	**1.16**	**0.98**	**0.85**	**0.81**	**2.21**	**2.11**
90%	11.35	4.96	4.07	3.38	7.57	6.27
95%	15.35	6.96	7.47	5.55	12.19	9.43
99%	27.91	15.33	30.48	19.36	44.91	31.19

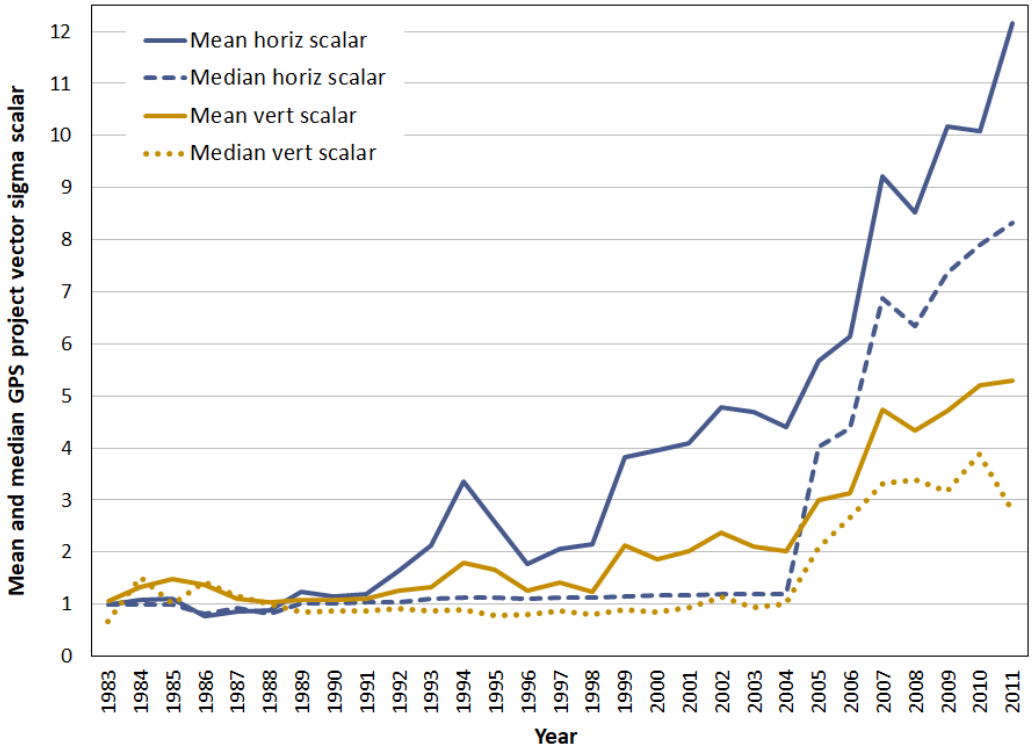

Figure 3.5. Mean and median GPS project vector sigma scalars (variance factors) by year.

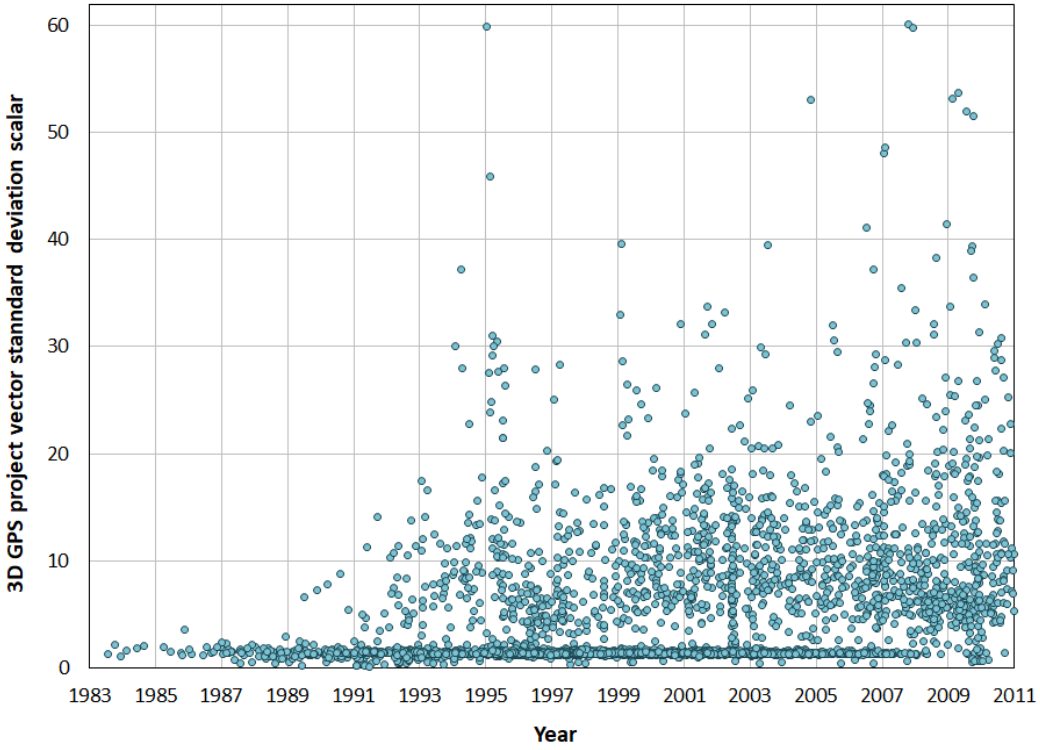

Figure 3.6. Scatter plot of 3D standard deviation scalars (variance factors) as function of time.

The reason for the puzzling unity variance factors is that the vector sigmas for many projects were scaled, and the scaled values were stored in the NGSIDB (rather than the original values). This will be discussed in greater detail shortly. But first, it is worthwhile to consider the vector sigmas themselves, and these are given in Table 3.6 as the original values (i.e., as stored in the NGSIDB) and after scaling with the variance factors. Statistics are given both for all NA2011 vectors, and for the final set of enabled vectors only.

The most striking thing concerning the vector 3D sigmas in Table 3.6 is the extremely large range, from 0.02 to 1732 cm, with the maximum increasing to 8298 cm for scaled sigmas—even for the enabled vectors. It is somewhat alarming to see vectors with such large sigmas being used in a network of geodetic control. On the other hand, the large sigmas also mean they have very low weight, and so they are effectively "rejected," in the sense they contribute almost nothing to the final coordinates. They also constitute a very small number of vectors; the sigma of the 99th percentile of enabled vectors is 31 cm.

Figure 3.7 is a plot of the median 3D vector sigmas by year, as original and scaled values, for both all and enabled-only vectors. The most prominent characteristic of the plot is the exponential-like decrease in median sigmas with time. The median of the original sigmas decrease from a high of approximately 8 cm in 1983 to a nearly constant 0.3 to 0.2 cm from 2006 to 2011. The reason for the larger sigmas prior to 2006 is a combination of data quality and storing scaled vector sigmas mentioned previously (and further discussed below). Interestingly,

the scaled median sigmas are at a constant value of roughly 2 cm between 1992 and 2011, and this shows the variance factors achieved some consistency in that time period, with a slight decrease over time. Prior to 1993, the scaled sigmas are much greater, which presumably reflects the greater error in the data during the early years of GPS (affected by an incomplete constellation, inaccurate orbits, no antenna modeling, early-generation single-frequency receivers, etc.).

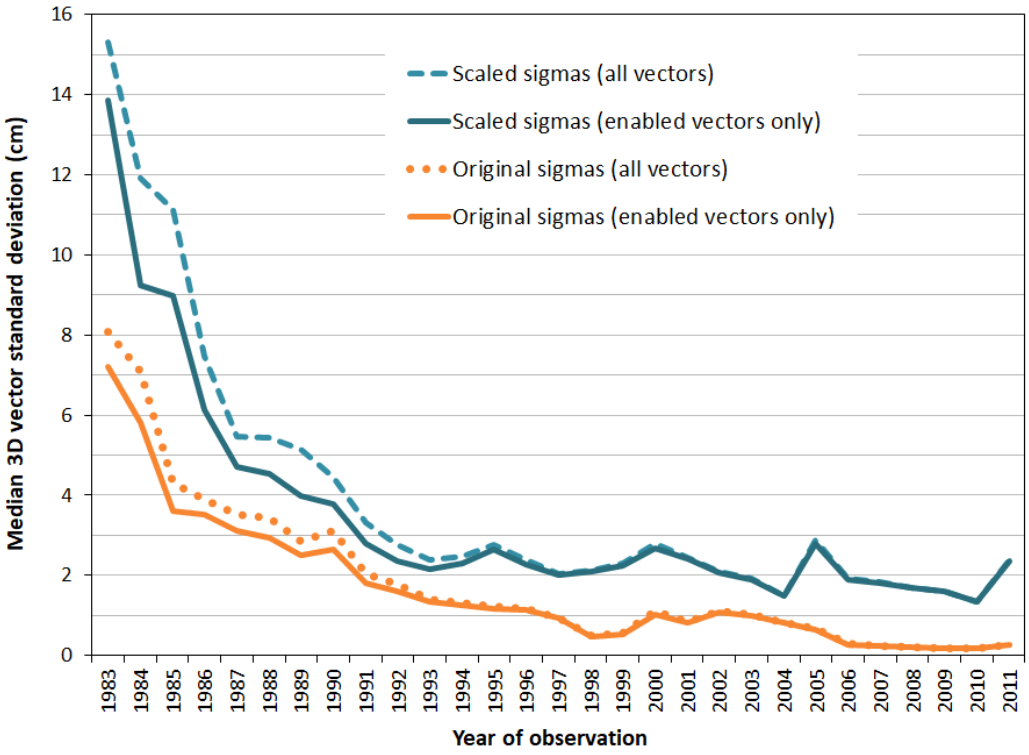

Figure 3.7. Median of scaled and unscaled vector 3D standard deviations by year.

3.2.2. Variance factors determined for GPS projects in the NGSIDB

Scaling of vector uncertainties was essential to ensure consistent weighting of observations when the 4267 GPS projects were combined into four separate network adjustments (CONUS Primary and Secondary, Alaska, and Pacific). The GPS projects spanned nearly 30 years and the data quality varied greatly. In addition, the data were processed using wide range of software and methods, resulting in vastly different estimates of vector uncertainties. These characteristics are exhibited by the statistics in Table 3.6 and the plots in Figure 3.7, although both are also affected by scaling of vector sigmas and by loading those scaled values into the NGSIDB.

Based on the variance factors computed by *ADJUST*, vector uncertainties currently produced by the NGS baseline processing program *PAGES* are typically optimistic by a factor of about 20 horizontally and 10 vertically (although it can vary, due to such things as network size, redundancy, and solution quality). Large factors are not uncommon for other popular baseline processing software used by scientists and engineers. For example, Kashani *et al.* (2004)

estimated the vector sigmas computed from baseline processing in *Bernese GNSS Software* were optimistic by a factor of 23. In contrast, commercial processing engines (both post-processed and real-time) use other (often proprietary) methods and can yield much different (often lower) variance factors. In certain cases, these processors can give variance factors of nearly 1, which likely occurs because the sigmas are scaled by the processing software prior to export, so they are less optimistic.

One method for addressing optimistic uncertainties is to scale them based on the results of a minimally constrained least squares network adjustment of the observations. Assuming all outliers and systematic errors have been removed and all the observations are similarly "optimistic," the uncertainties (standard deviations) of the observations can be scaled by the same amount. Usually the scale factor is taken as the *a posteriori* standard deviation of unit weight, σ_0, from the adjustment. After the adjustment, the observation standard deviations are multiplied by σ_0, the adjustment is performed again, and the process is repeated until $\sigma_0 = 1$. This type of approach is implemented in many commercial software packages and was formerly employed by NGS in many Bluebooking projects using their *MODGEE* program. *MODGEE* scales the sigmas of the GNSS vectors in the G-file based on a scale factor (σ_0) entered by the user (FAA, 2007). NGS no longer uses *MODGEE* for Bluebooking (NGS, 2012b).

The problem with the *MODGEE* approach is that it applies the same scalar to all three components of the uncertainty. Yet, vertical GNSS uncertainties are often too small by a different amount than the horizontal GNSS uncertainties, so applying a single scale to both will not yield the best solution. In addition, it is well known that vertical GNSS uncertainties are greater than the horizontal uncertainties, often by a factor of 2-3 (Eckl *et al.*, 2001; Gillins and Eddy, 2016). This realization led NGS to implement a scaling procedure in the *ADJUST* program that separately scales the horizontal and vertical uncertainties. Such an approach is possible with *ADJUST*, because it transforms observations to the LGH[11] (Milbert and Kass, 1987).

Not only was the type of scaling performed by *MODGEE* a problem, but so was the practice of storing the scaled vector sigmas in the NGSIDB rather than the original sigmas. The name itself betrays its purpose—it is intended to ***MOD***ify a ***GEE***-file. This modification is the reason for median variance scalars that are nearly equal to 1 in Table 3.6 and Figure 3.5, and for the prominent horizontal band of points with variance factors of approximately 1 in Figure 3.6. It is also likely the main reason vector sigmas were larger in the past (although it is not clear when the practice of storing vectors modified with uniform scale factors began). In hindsight, it would have been better to store the original sigmas along with the scale factors, as is the practice today. But it turns out not to be of much consequence, because the procedure used to determine variance factors with *ADJUST* can, to a significant degree, assign sigma scalars that are

[11] Note that a vector, unlike a point, does not have a unique LGH. That is, north, east, and up generally point in different directions at the vector end points. Therefore some approximation occurs when computing LGH uncertainty components for a vector (and thus "local accuracies" derived from adjusted vector uncertainties). The error in this approximation grows as the vector length grows. However, this error has no effect on the adjustment itself, since the vectors are transformed at the standpoint (origin), rather than at the midpoint.

appropriate for a project modified by *MODGEE*. Details on the method used by *ADJUST* to determine variance factors are given in the next section.

3.2.3. GNSS variance factor computation using *ADJUST*

The process for horizontal and vertical uncertainty scaling in *ADJUST* is discussed to some extent in two NGS reports (Pursell and Potterfield, 2008; Milbert, 2009), the Bluebook (NGS 2019d), as well as supplemental *ADJUST* documentation (NGS, 2018a). However, the process is not covered in much depth in any of these documents, and apparently NGS has not documented it elsewhere. To provide some insight into the process, it is described in greater detail below.

The method used by *ADJUST* is an unbiased estimate of the variance component that allows separate horizontal and vertical sigma scalars to be determined. It follows a method developed by Lucas (1985), although that particular approach required that the observations be uncorrelated, and obviously, the horizontal and vertical components of GPS vectors *are* correlated. The approach used by *ADJUST* to handle the correlated observations is one of the reasons the method is being documented in this report.

Within *ADJUST*, uncertainty scaling is performed using the "VV" (Variance Factor Indicator and Constraint) command to estimate the variance component of a group of observations. For GNSS observations, it can be appended with an "HU" command to create a "VVHU" option that solves for uncertainty scale factors for the horizontal and vertical (up) components (see also the NGS *Constrained Adjustment Guidelines* [NGS, 2018b] for further detail on how these options are implemented in the execution of *ADJUST*).

ADJUST transforms observations to the LGH and performs the adjustment in LGH space to compute differential north, east, up (Δn, Δe, Δu) shifts for each component of the marks. For the VVHU option, the horizontal and up components are determined in separate minimally constrained adjustments. The general (nonlinear) observation equation for all cases (whether 3, 2, or 1D) is

$$\mathbf{Jx} = \mathbf{k} + \mathbf{v} \tag{3.1}$$

where **x** is the vector of differential corrections to the unknown parameters to be determined, **J** is the Jacobian matrix (partial derivatives of the observation equations evaluated at the computed values of the parameters), **k** is the vector of observations minus their computed values, and **v** is the vector of residuals. The specific mathematical models and observation equations used in *ADJUST* for LGH systems are given by Milbert and Kass (1987, pp. 36-40). The well-known least squares solution of Equation (3.1) is

$$\mathbf{x} = (\mathbf{J}^T\mathbf{P}\mathbf{J})^{-1} (\mathbf{J}^T\mathbf{P}\mathbf{k}) \tag{3.2}$$

where **P** is the weight matrix, typically estimated by taking the inverse of the variance-covariance (VCV) matrix, $\mathbf{\Sigma}$, of the unadjusted observations. Because the adjustment is performed in an LGH system, the VCV sub-matrix for each set of observations within $\mathbf{\Sigma}$ is first rotated from ΔX, ΔY, ΔZ ECEF coordinates to north-east-up (Δn, Δe, Δu) LGH coordinates as

$$\boldsymbol{\Sigma}_{\Delta n \Delta e \Delta u} = \mathbf{R}\, \boldsymbol{\Sigma}_{\Delta X \Delta Y \Delta Z}\, \mathbf{R}^{\mathrm{T}}. \tag{3.3}$$

R is the familiar geocentric ECEF to LGH rotation matrix,

$$\mathbf{R} = \begin{bmatrix} -\sin\varphi\cos\lambda & -\sin\varphi\sin\lambda & \cos\varphi \\ -\sin\lambda & \cos\lambda & 0 \\ \cos\varphi\cos\lambda & \cos\varphi\sin\lambda & \sin\varphi \end{bmatrix}, \tag{3.4}$$

where φ is geodetic latitude and λ is geodetic longitude of the observation in the VCV sub-matrix at the standpoint (vector origin). The resulting horizontal and up observations are correlated; i.e., the off-diagonal terms are non-zero (for both *XYZ* and *neu* VCV matrices).

For a 3D GNSS network, the dimensions of the (square) weight and VCV matrices equal the number of observations, n, which is 3 times the number of vectors, $n = 3v$. For a minimally constrained adjustment, the number of unknowns, u, is the number of marks, m, minus 1, which is multiplied by 3 for a 3D observation to get $u = 3\,(m - 1)$. The degrees of freedom (redundancy number) is the number of observations minus the number of marks, $r = n - u = 3\,(v - m + 1)$. When the network is split into horizontal and up components, the redundancy is split proportionally between components, i.e., $r_H = 2\,(v - m + 1)$ and $r_U = v - m + 1$, where the *H* and *U* subscripts denote horizontal and up.

The observation residuals of a least squares adjustment are given by rearranging Equation (3.1) as $\mathbf{v} = \mathbf{J}\mathbf{x} - \mathbf{k}$. When the VVHU adjustments are performed in *ADJUST*, the weighted sum of squared residuals (variance sum, $\mathbf{v}^{\mathrm{T}}\mathbf{P}\mathbf{v}$) is computed for the entire network of 3D observations, and individually for the horizontal and up components of the observations, $(\mathbf{v}^{\mathrm{T}}\mathbf{P}\mathbf{v})_H$ and $(\mathbf{v}^{\mathrm{T}}\mathbf{P}\mathbf{v})_U$. Because the horizontal and up observations are correlated, the sum $(\mathbf{v}^{\mathrm{T}}\mathbf{P}\mathbf{v})_H + (\mathbf{v}^{\mathrm{T}}\mathbf{P}\mathbf{v})_U$ will not equal the total $\mathbf{v}^{\mathrm{T}}\mathbf{P}\mathbf{v}$ for the network. The remainder is the variance sum of the correlated observations, $(\mathbf{v}^{\mathrm{T}}\mathbf{P}\mathbf{v})_{cor} = \mathbf{v}^{\mathrm{T}}\mathbf{P}\mathbf{v} - (\mathbf{v}^{\mathrm{T}}\mathbf{P}\mathbf{v})_H - (\mathbf{v}^{\mathrm{T}}\mathbf{P}\mathbf{v})_U$. The value of $(\mathbf{v}^{\mathrm{T}}\mathbf{P}\mathbf{v})_{cor}$ can be positive or negative and is typically less than about 10% of the total $\mathbf{v}^{\mathrm{T}}\mathbf{P}\mathbf{v}$.

Although $(\mathbf{v}^{\mathrm{T}}\mathbf{P}\mathbf{v})_{cor}$ is a relatively small proportion of the total $\mathbf{v}^{\mathrm{T}}\mathbf{P}\mathbf{v}$, it must be accounted for since the objective of VVHU is to determine scale factors yielding $\sigma_0 = 1$ for the overall adjustment. The approximate method *ADJUST* uses is to add two-thirds of $(\mathbf{v}^{\mathrm{T}}\mathbf{P}\mathbf{v})_{cor}$ to $(\mathbf{v}^{\mathrm{T}}\mathbf{P}\mathbf{v})_H$ and one-third to $(\mathbf{v}^{\mathrm{T}}\mathbf{P}\mathbf{v})_U$ to compute "corrected" horizontal and up variance sums for the two components. Using this approach, the standard deviation of unit weight for each component is computed using its respective redundancy number,

$$(\sigma_0)_H = \sqrt{(\sigma_0)^2_{\Delta n} + (\sigma_0)^2_{\Delta e} + 2(\sigma_0)_{\Delta n \Delta e}} = \sqrt{\frac{(\mathbf{v}^{\mathrm{T}}\mathbf{P}\mathbf{v})_H + \frac{2}{3}(\mathbf{v}^{\mathrm{T}}\mathbf{P}\mathbf{v})_{cor}}{r_H}} \tag{3.5a}$$

$$(\sigma_0)_U = (\sigma_0)_{\Delta u} = \sqrt{\frac{(\mathbf{v}^{\mathrm{T}}\mathbf{P}\mathbf{v})_U + \frac{1}{3}(\mathbf{v}^{\mathrm{T}}\mathbf{P}\mathbf{v})_{cor}}{r_U}} \tag{3.5b}$$

The (unitless) magnitudes of $(\sigma_0)_H$ and $(\sigma_0)_U$ are the initial estimates of the horizontal and up variance factors, V_H and V_U, respectively, and $(\sigma_0)_{\Delta n \Delta e}$ is the initial horizontal covariance.

The horizontal and up sigmas of the observations are multiplied by the initial V_H and V_U values, and a minimally constrained adjustment is automatically performed again. The resulting $(\sigma_0)_H$ and $(\sigma_0)_U$ from this new adjustment are multiplied by the previous V_H and V_U to obtain updated V_H and V_U values. The original observation standard deviations are multiplied by the updated V_H and V_U values, and the process is repeated until Equations (3.5a) and (3.5b) both equal 1 (i.e., the corrected variance sum equals *r* for each component), or until the maximum allowed number of iterations is reached. The V_H and V_U values from the final iteration are written to the output B-file. There, they can be used for subsequent constrained adjustments or, in the case of the 2007 and 2011 national adjustments, they can be used to combine GPS projects, where each project has its own pair of V_H and V_U values.

Usually, VVHU convergence is achieved in less than five iterations. In rare instances, the process does not converge or it fails, due to a negative corrected variance sum. Such failures sometimes occur for certain types of networks, such as those with few observations and little redundancy. It would be fairly simple to modify *ADJUST* to handle such situations gracefully, although that has not yet been done. A likely better solution would be to solve the Variance Component Model (VCM) rigorously (Schaffrin and Snow, 2017). The VVHU process fails entirely if there is no redundancy in the network, because both the variance sum and degrees of freedom are zero, though this is also true when solving for a single variance of unit weight in a least squares solution.

In general, $V_H \neq V_U$, and for *PAGES*-derived vectors, V_H is typically 2-3 times greater than V_U. The mean ratio $V_H / V_U = 2.3$ for all 4267 GPS projects, and increases to 3.0 for the 557 projects from 2007 through 2011 (when the use of *MODGEE* to scale vector sigmas was essentially discontinued). Despite the "typical" V_H and V_U values obtained from *PAGES*, it is difficult to make general statements concerning the expected values of V_H and V_U (both absolute and relative), even for *PAGES* itself. The reason is that the actual V_H and V_U values for a network are dependent on the observation residuals, redundancy, baseline processor used, and whether the vector sigmas were modified before being used in an adjustment (e.g., by using *MODGEE*). The advantage of the VVHU variance scaling method used in *ADJUST* is that it makes no assumptions concerning the horizontal and up distribution of uncertainties. Rather, it determines both the absolute and relative magnitude of the variance factors from the residuals of the minimally constrained adjustment for each component and its corresponding redundancy. Changing the residuals or redundancy (for example by rejecting or enabling observations) will change the variance factors. In addition, as discussed previously, different baseline processing can yield uncertainties differing by well over an order of magnitude for the same GNSS dataset (Gillins *et al.*, 2016; Kashani *et al.*, 2004; Øvstedal, 2000). Since VVHU uses the actual residuals, redundancy, and vector sigmas, it can be used to determine the correct weights of observations for heterogeneous GNSS networks (although there is some approximation due to how the horizontal and vertical correlations are handled). VVHU also makes it possible to combine different groups of GNSS vectors into a single network (for example from different

times, areas, or baseline processors), because the observation from each group can be scaled separately to obtain appropriate weights.

One of the central ideas of using VVHU is to apply it to a set of stochastically consistent observations. For example, it would be best to use VVHU for networks processed using the same baseline processor with observations of comparable duration and not spanning an excessively long period of time. It is not obvious how long a duration is too long, and this likely depends on other factors. The longest-duration GPS project in the NA2011 Project is 15 years (see Section 2.1.2). That time span is certainly excessively long for a single variance factor, yet that is how it was handled. There are 241 projects with a duration of one year or more, suggesting it might be better to use criteria other than GPS project (such as time, region, and baseline processor) to group vectors for VVHU calculations.

Another situation where VVHU may not be able to correctly determine variance factors is for GNSS networks including so-called "trivial" (dependent) vectors. As discussed briefly in Section 2.3.2 (and in greater detail in Section 5.2), these can occur in sequential (single) baseline processing. The presence of trivial vectors tends to reduce V_H and V_U, because it increases the (apparent) degrees of freedom by introducing false redundancy. In cases where there are many trivial vectors, V_H and V_U can even be less than 1. That is, the false redundancy makes the network appear more precise than indicated by the baseline processor uncertainty estimates. In such cases, VVHU can be used as a tool to detect the possible presence of trivial vectors.

Ideally, variance factors would be recomputed based on changes in vector rejections during analysis, so that the change in residuals and degrees of freedom would be accounted for in subsequent (and final) adjustments. This was not done for the NA2011 Project (nor the 2007 national adjustment), because the VVHU computation procedures were manual and much too time-consuming, as were the adjustments themselves (particularly for the CONUS networks). An automated method would be necessary to make this practical, and it should be pursued in any future national or regional readjustments.

3.3. Network adjustment methods

The NA2011 Project consisted of 81,055 marks connected by 424,721 observations (GNSS vectors) spanning nearly 30 years (from April 1983 to December 2011). In a minimally constrained least squares adjustment, that represents $u = 3 \times 81{,}054 = 243{,}162$ unknown parameters determined by $n = 3 \times 424{,}721 = 1{,}274{,}163$ observations. The resulting system of equations has redundancy (degrees of freedom) of $r = 1{,}274{,}163 - 243{,}162 = 1{,}031{,}001$.

A complete least squares solution of this large system of equations requires a staggeringly large number of mathematical operations, mostly matrix multiplications and inversions. A "complete" solution means not only the unknown parameters (adjusted mark coordinates) and their uncertainties (used for computing "network accuracies"), but also the network statistics, observation residuals, and the uncertainty of the adjusted observations (used for computing "local accuracies").

3.3.1. Helmert blocking strategy for CONUS

Despite using sparse matrix methods and Cholesky decomposition, the national adjustments for CONUS were still too large to perform as single simultaneous adjustments. Helmert blocking was used to break the large network into smaller subnetworks or "blocks." The blocks were partially solved independent of one another and then reassembled into a single solution. Pursell and Potterfield (2008) give an excellent and detailed description of Helmert blocking, as well as how it was developed and implemented in the *NETSTAT* software for the 2007 national adjustment.

The NA2011 Project used the same Helmert blocking strategy as was used in 2007. As with the 2007 adjustment, there are seven levels, with the lowest level consisting of blocks corresponding to a state or part of a state (i.e., some states were split into two blocks, and Minnesota was split into four). Here "state" refers to the state where the GPS project was nominally performed, although often these networks consisted of connections to marks in other states.

The CONUS Helmert blocking diagram used in NA2011 is shown in Figure 3.8. Level 1 consists of 58 blocks with the block name corresponding to the two-letter state abbreviation. Due to a large number of marks and observations, four states are split into a north-south or east-west blocks: California (CA), Florida (FL), North Carolina (NC), and South Carolina (SC), and their abbreviations are appended as N, S, E, W. Minnesota (MN) is the only state split into four blocks, north-north (NN), north-south (NS), south-north (SN), and south-south (SS), as shown in Level 1. In contrast, the 2007 blocking strategy for Level 1 consisted of 48 blocks, with Minnesota as a single block (see Figure 15.1 in Pursell and Potterfield, 2008). Unlike all other blocks in Level 1, it was split into two (N and S) blocks that were separately adjusted before Level 1 was computed and then combined into a single Minnesota block in level 1. Minnesota was also handled in a special way in NA2011. Its four blocks were computed in Level 1, and, as shown in Figure 3.8, they were combined into a N and S block, and then into a single block. This combination of Minnesota into a single block was done with intermediate computations performed between levels 1 and 2.

Level 2 of the NA2011 Helmert blocking scheme consists of 24 blocks, with four being single state blocks created from combining the California, Florida, North Carolina, and South Carolina blocks, and the remainder are combined states and are simply designated as B *xx*, where "B" is "Block" and *xx* is its sequential number, with B 1 corresponding to the single highest (Level 7) block through B 51 in Level 2. The 2007 blocking scheme had 32 blocks in Level 2. A significant difference for Level 2 of the 2007 network is the inclusion of an Alaska block, whereas Alaska is not included at all in the 2011 CONUS network.

Levels 3 to 7 have the same number of blocks in both the 2007 and 2011 adjustments. All told, there are 116 blocks in seven levels (including the three Minnesota blocks between levels 1 and 2) for NA2011. In the 2007 adjustment there were a total of 113 blocks. Despite the difference in the number of blocks in levels 1 and 2, the overall number of blocks is essentially the same. They differ only because in NA2011 four blocks were added for Minnesota, and one was removed for Alaska, for a net difference of three. The block distributions are otherwise the same.

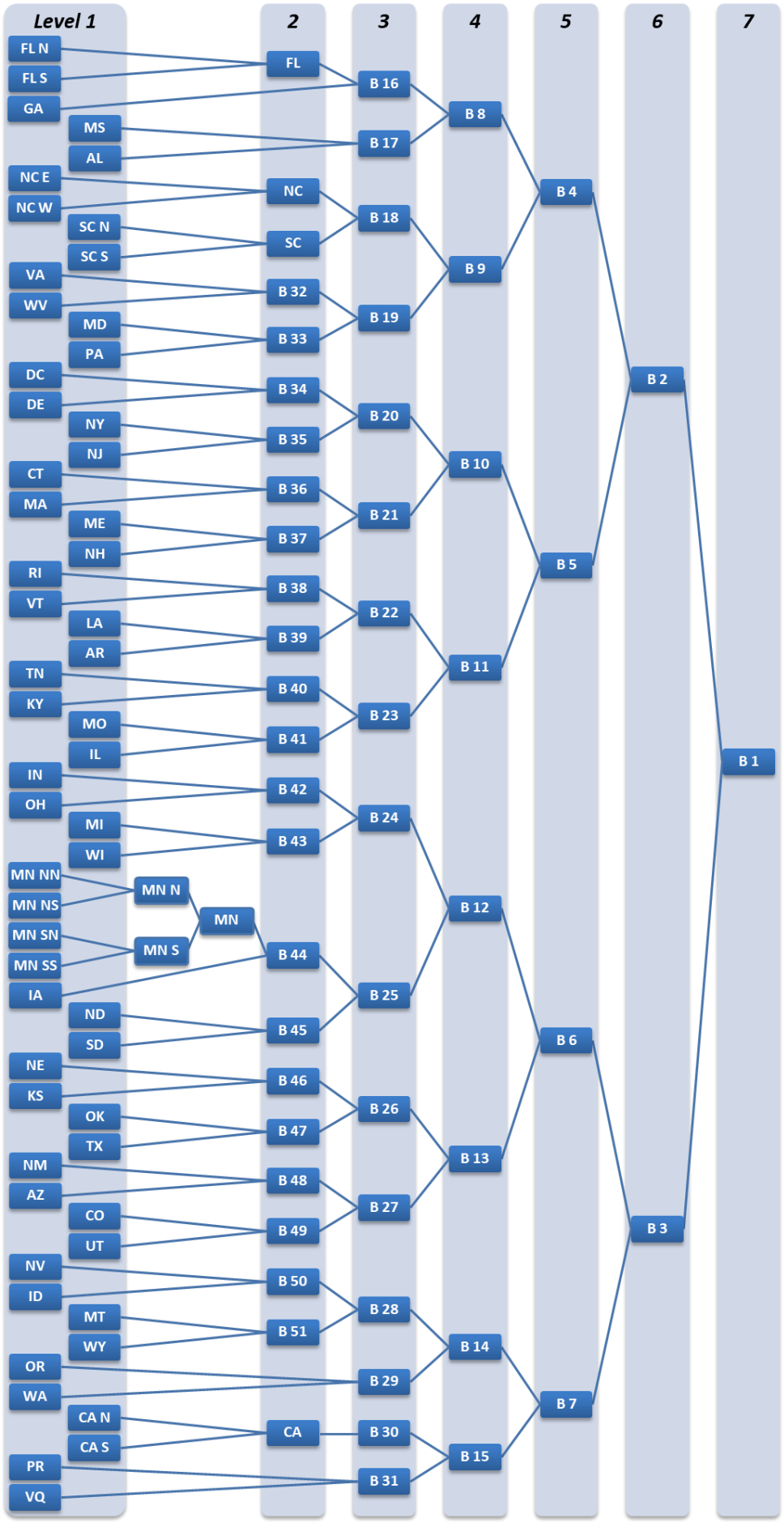

Figure 3.8. Helmert blocking diagram for CONUS overall and Primary networks.

3.3.2. Dividing CONUS into Primary and Secondary networks

The CONUS network for NA2011 consisted of 79,546 marks and 420,023 GNSS vectors, split among the 116 blocks shown in Figure 3.8. CONUS was split into a Primary and Secondary network, based primarily on the age of the observations. Details of the split and the reasons for it are given later in this section, as well as a discussion of how constraints were handled.

The CONUS Primary network consisted of 62,172 marks and 335,530 vectors, but it used exactly the same Helmert blocking strategy as the overall CONUS network. The CONUS Secondary network consisted of 17,374 marks and the remaining 84,493 CONUS vectors. This was a large enough network that Helmert blocking was still necessary, and its blocking scheme is shown in Figure 3.9.

To simplify creation of the CONUS Secondary blocks, the blocking strategy adhered to the overall CONUS scheme to the extent possible. Similar to the CONUS scheme, it consisted of seven levels with 15 blocks in levels 4 to 7. Level 1 consists of 43 state blocks, none of which are split. The eight CONUS states and territories not included are Arkansas (AR), Connecticut (CT), Iowa (IA), North Dakota (ND), New Hampshire (NH), Nevada (NV), Puerto Rico (PR), and the U.S. Virgin Islands (VQ). In other words, these blocks only occur in the Primary network. Note that for NA2011, "CONUS" include all 48 states in the conterminous United States, plus the District of Columbia (DC), Puerto Rico (PR), and the U.S. Virgin Islands (VQ), for a total of 51 states and territories.

There are 5321 CONUS marks both in the Primary and Secondary networks. The network they are assigned to is based on the source of final coordinates. In most cases (5129 marks), the coordinates were derived from vectors in the Primary network. But 192 marks in both networks had coordinates derived from the Secondary network vectors due to problems with the Primary network vectors. These were mostly Primary vectors that were in a disconnected component or that were single (no-check) vectors; however, 13 were excluded because of large error estimates and a larger number of ties in the Primary network. The issue with disconnected components is discussed in Section 3.4.

Table 3.7 and Table 3.8 list the 58 and 43 Helmert blocks of the CONUS Primary and Secondary networks, respectively. These tables give the number of marks and vectors for each block (the total number of marks is greater than the actual number of marks due to junction marks that occur in more than one block). For both networks, the majority of marks and vectors are in only a few of the blocks. The six Primary blocks making up Minnesota (4 blocks) and North Carolina (2 blocks) account for about 29% of the marks and vectors. Likewise, the three largest Secondary blocks (Florida, Alabama, and South Carolina) account for about 30% of the marks and vectors. The number of vectors does not necessarily indicate the computational burden, because sequentially processed vectors have only a 3×3 variance-covariance matrix. In contrast, simultaneously processed vectors can have a very large session variance-covariance matrix (up to 558×558 for the largest session in the network) and thus require more time to invert.

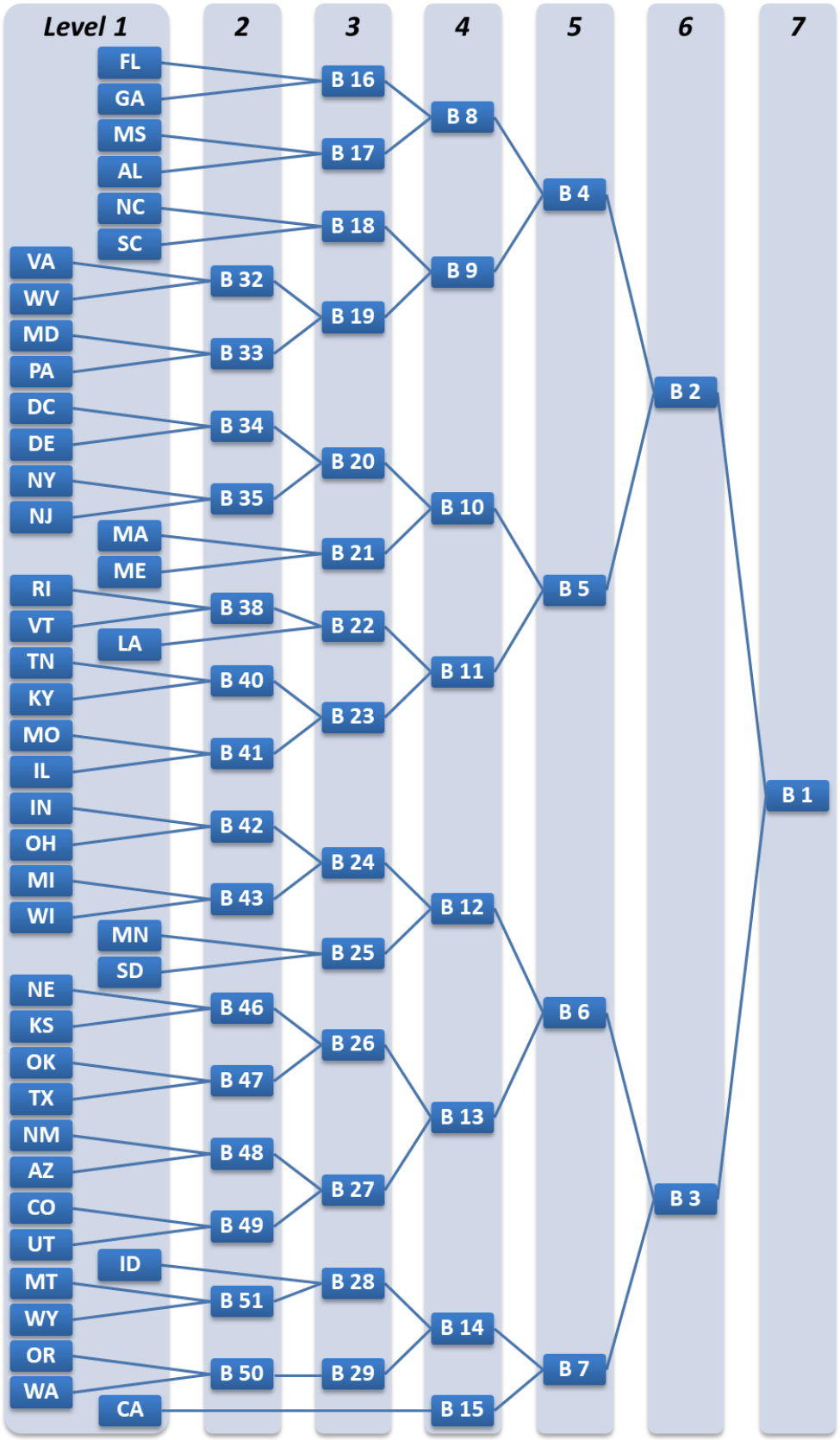

Figure 3.9. Helmert blocking diagram for CONUS Secondary network.

Table 3.7. Marks, vectors, and calculations for 58 Helmert blocks of CONUS Primary network.

Block	Marks	Vectors	Block	Marks	Vectors	Block	Marks	Vectors
AL	1591	5219	**MD**	1598	8182	**OK**	117	512
AR	429	1602	**ME**	297	1054	**OR**	784	3182
AZ	1570	7808	**MI**	1272	10,844	**PA**	716	3344
CA (N)	1670	12,787	**MN (NN)**	2859	15,224	**PR**	117	355
CA (S)	1521	11,875	**MN (NS)**	2621	11,618	**RI**	159	584
CO	1606	7234	**MN (SN)**	3578	20,507	**SC (N)**	2447	7948
CT	103	971	**MN (SS)**	3476	19,131	**SC (S)**	2709	8928
DC	22	127	**MO**	775	3119	**SD**	486	1275
DE	116	1594	**MS**	1194	4827	**TN**	686	2701
FL (N)	2148	11,004	**MT**	332	1073	**TX**	1586	6469
FL (S)	2552	10,656	**NC (E)**	3352	12,585	**UT**	345	1372
GA	1326	3773	**NC (W)**	3642	13,989	**VA**	1282	4581
IA	372	1049	**ND**	206	906	**VQ**	140	383
ID	262	1068	**NE**	600	2074	**VT**	728	2146
IL	2928	14384	**NH**	63	110	**WA**	892	3248
IN	318	843	**NJ**	799	4965	**WI**	2685	41,241
KS	409	1369	**NM**	398	1301	**WV**	249	696
KY	953	4207	**NV**	253	1068	**WY**	253	1020
LA	536	3426	**NY**	586	3027			
MA	270	503	**OH**	2479	8442	**Total**	**67,463**	**335,530**

Helmert blocking requires an overall larger number of individual adjustments than would be needed simply for splitting the network into the separate 58 Primary and 43 Secondary blocks. Additional adjustments are required for all the blocks at the six additional levels for both networks (each containing junction marks and their associated observations). Once the highest level (7) is reached, constraints are applied to obtain a solution for that block. This solution and matrix inverse are back-substituted and propagated to the blocks on the next level down, and is repeated until the Level 1 is reached. At that level the final solution and covariances are obtained (see Pursell and Potterfield, 2008, for a detailed description of the process). As the diagrams in Figure 3.8 and Figure 3.9 indicate, Helmert blocking is a significantly more complex process than a single simultaneous adjustment; however, the computational cost is lower, since each individual adjustment is small compared to the entire network. The result is a significant reduction in computation time, and this is why Helmert blocking was necessary for the 2007 and 2011 national adjustments.

Table 3.8. Marks, vectors, and calculations for 43 Helmert blocks of CONUS Secondary network.

Block	Marks	Vectors	Block	Marks	Vectors	Block	Marks	Vectors
AL	2273	9186	**MD**	123	3314	**PA**	239	643
AZ	231	902	**ME**	168	343	**RI**	83	159
CA	1187	4662	**MI**	578	1984	**SC**	1733	6548
CO	269	1671	**MN**	1163	4662	**SD**	11	38
DC	11	33	**MO**	355	1377	**TN**	134	297
DE	32	126	**MS**	139	42	**TX**	118	8322
FL	2914	9688	**MT**	2	422	**UT**	36	84
GA	234	800	**NC**	1152	415	**VA**	1422	2969
ID	99	218	**NE**	16	27	**VT**	27	43
IL	82	490	**NJ**	147	7983	**WA**	634	1369
IN	14	36	**NM**	185	82	**WI**	37	1195
KS	73	256	**NY**	649	1269	**WV**	27	61
KY	258	578	**OH**	1438	456	**WY**	111	26
LA	945	2188	**OK**	29	94			
MA	26	36	**OR**	129	255	**Total**	**22,764**	**84,493**

The time to perform adjustments increases when additional parameters are included, for example by adding constraints to the adjustments. In the case of 3D coordinate adjustments, constraint equations increase the size of the design matrix by adding three rows (one for each coordinate constrained). If the constraint is applied to a new point, three new parameters are introduced, and so three columns to the design matrix are also added. Using a large number of constraints on new parameters can therefore substantially increase computation time. That, in fact, is what occurred in the constrained adjustment of the CONUS Secondary network (as discussed later in this section), to increase its total computation time from a few hours to approximately a week.

Initially there was no plan to split the CONUS network, and this was not done for the 2007 adjustment. At first it was assumed unnecessary, because the older observations generally had larger sigmas (as shown in Figure 3.7), so they would get lower weights in the adjustment and thus have less influence on the final coordinates. In addition, the computed variance factors for each GPS project were intended to help correctly weight all projects, including old ones. But there was some difficulty with preliminary results based on the older observations, including large numbers of rejections, large residuals, and large error estimates for the adjusted marks. Such issues led to the concern that the old observations were having a deleterious impact on the overall results.

There were also other known deficiencies for GPS observations older than around 1994 that contributed to the decision to split the CONUS network:

- Early generation GPS receivers and antennas (often single frequency)
- No antenna phase center variation models
- Incomplete GPS constellation; completed in June 1993 (24 satellites)
- Accurate satellite orbits not available
- No processing models or poor processing models (e.g., troposphere, ocean loading)
- MYCS1 positions based on data to January 1, 1994
- Virtually no CORSs to use as constraints

In discussions over how to handle the problem with old data, there were those who advocated doing nothing other than relying on the project variance factors and treating all observations the same, regardless of age. Others advocated discarding all observations older than the oldest data used for MYCS1 (i.e., all vectors prior to 1994). But that latter decision would have removed 84,180 (19.8%) of the vectors, as well as 17,524 (21.6%) of the marks last occupied before 1994. There was also the option of scaling the older projects to reduce their weight in the adjustment, but no convincing method was proposed for determining an appropriate downweighting mechanic.

A compromise was made, to split CONUS into a "Primary" network consisting of observations after about 1993, with a "Secondary" network of all earlier observations. The Primary network would be adjusted independently. The adjusted Primary marks in common with the Secondary network would be used as its (stochastic) constraints, and this would help with the very small number of CORSs prior to 1994.

Splitting CONUS based on observation dates was complicated by the fact that the vectors were organized by GPS projects, and some GPS projects span several years. This problem was handled by removing CONUS GPS projects from the Primary network with the *first* observation before epoch 1994.00, **and** the *last* observation before epoch 1995.00. This solution removed 513 projects (78,010 vectors) from the overall CONUS network to create the Primary network. However, it was decided that 16 "important" major HARN projects in the Secondary network should be moved to the Primary network. It was also decided to move 117 Primary projects in two known major subsidence regions that were observed prior to 2006 to the Secondary network. Most of these projects (112) were in the northern Gulf Coast region (in southern Louisiana, Mississippi, and Alabama, and southeast Texas), from 1995 to 2005 (7671 vectors). The remaining five projects were in the northern Central Valley of California, from 1999 to 2005 (1493 vectors). Additional efforts to better account for the effects of subsidence on adjustment results in the Gulf Coast region are discussed in Section 3.5.1.

For the final network configuration, there were 3472 projects in the Primary network and 614 projects in the Secondary network, with the number of marks and observations given previously.

A summary of the number of Helmert blocks, projects, marks, vectors, and overall time spans are shown in Table 3.9. The table separates CORSs from passive marks and also lists the Alaska and Pacific networks. The Primary and Secondary networks include a total of 5321 marks in both networks, as mentioned previously, with the coordinates of most (5129) determined by vectors in the Primary network.

Table 3.9. Summary of NA2011 network blocks, projects, vectors, marks, and observation dates.

Overall network	Helmert blocks	Projects	Vectors	Network that marks are referenced to	Number marks	First observation	Last observation
CONUS Primary	58	3472	335,530	***Primary CORS***			
				Primary only	1068	9/2/1993	12/21/2011
				Both Primary & Secondary	28	8/1/1990	4/7/2011
				Primary passive			
				Primary only	55,827	11/12/1987	12/21/2011
				Both (ref'd to Primary)	5101	4/13/1983	10/19/2011
				Primary disconnected	148	4/14/1994	1/22/2003
				Primary total*	**62,172**	**11/12/1987**	**12/21/2011**
CONUS Secondary	43	614	84,493	***Secondary CORS***			
				Secondary only	16	3/16/1992	9/29/2005
				Both Primary & Secondary	1	11/13/1992	7/22/1995
				Secondary passive			
				Secondary only	17,132	4/12/1983	12/31/2005
				Both (ref'd to Secondary)	191	4/4/1985	9/17/2010
				Secondary disconnected	34	5/23/1984	2/22/1993
				Secondary total**	**17,374**	**4/12/1983**	**9/17/2010**
CONUS total	**101**	**4086**	**420,023**	**CONUS total**	**79,546**	**4/12/1983**	**12/21/2011**
Alaska***	1	142	2,846	Alaska CORS	58	4/23/1996	7/28/2011
				Alaska passive	911	8/11/1984	7/31/2011
				Alaska total	**969**	**8/11/1984**	**7/31/2011**
Pacific***	1	39	1,852	Pacific (PA11) CORS	18	8/10/1993	4/18/2011
				Pacific (PA11) passive	345	8/10/1993	4/29/2011
				Pacific (MA11) CORS	6	8/25/1993	8/10/2008
				Pacific (MA11) passive	171	8/12/1993	8/10/2008
				Pacific total	**540**	**8/10/1993**	**4/29/2011**
NA2011 total	**103**	**4267**	**424,721**	**NA2011 total**	**81,055**	**4/12/1983**	**12/21/2011**

** Total number Primary marks includes the Secondary ones in both networks = 62,172 + 191 + 1 = 62,364*
*** Total number Secondary marks includes the Primary ones in both networks = 17,374 + 5101 + 28 = 22,503*
**** Single network; Helmert blocking not used.*

As Table 3.9 shows, there is a much smaller number of CORSs available to use as constraints for the Secondary network. Actually, Table 3.9 is a bit misleading, because the total number of CORSs available for constraints in the Secondary network is more than the 16 + 1 = 17 listed under Secondary. It also includes the 28 listed under Primary that are in both networks, for a total of 28 + 16 + 1 = 45 CORSs for the Secondary network. But this is far less than the 1068 + 28 + 1 = 1097 CORSs available as constraints for the Primary network.

More details about Secondary network constraints are given in Table 3.10, which shows statistics for all 5262 constraints, as well as the 45 CORS-only and the 5217 passive-only stochastic constraints. All passive marks in common between the Primary and Secondary networks were stochastically constrained. This was done to maintain consistency with the Primary network and compensated for the lack of CORSs in the Secondary network.

Table 3.10. Sigmas used for constraint weights in the CONUS Secondary network (sigmas for passive marks are *a posteriori* values from final constrained CONUS Primary network adjustment, scaled by the standard deviation of unit weight).

Sigmas used for constraint weights in Secondary network (cm)	All constrained marks			CORSs only			Passive marks only		
	North	East	Up	North	East	Up	North	East	Up
Number	**5262**			**45**			**5217**		
Minimum	0.04	0.04	0.12	0.07	0.07	0.15	0.04	0.04	0.12
Maximum	10.88	31.74	25.31	1.09	1.05	4.82	10.88	31.74	25.31
Mean	0.40	0.35	0.98	0.40	0.38	1.56	0.40	0.35	0.98
Standard deviation	±0.43	±0.58	±1.38	±0.32	±0.31	±1.30	±0.43	±0.58	±1.38
Percentiles									
1%	0.08	0.07	0.17	—	—	—	0.08	0.07	0.17
5%	0.09	0.08	0.19	—	—	—	0.09	0.08	0.19
10%	0.14	0.11	0.28	0.09	0.08	0.22	0.14	0.11	0.28
50% (median)	**0.29**	**0.25**	**0.64**	**0.31**	**0.26**	**1.11**	**0.29**	**0.25**	**0.64**
90%	0.72	0.61	1.79	1.00	1.00	3.25	0.72	0.60	1.78
95%	0.99	0.86	2.79	1.09	1.05	4.82	0.98	0.86	2.71
99%	1.78	1.75	6.37	—	—	—	1.79	1.76	6.39

Table 3.10 also includes statistics of the sigmas for the constrained Secondary network marks. The passive marks sigmas are the *a posteriori* values from the Primary network adjustment (scaled by the standard deviation of unit weight from the Primary network). The CORS sigmas are from the MYCS1 formal uncertainties (three of the CORSs are modeled, and they use the 1 cm horizontal and 3 cm up values used in the other networks). The mean and median sigmas of the CORSs and passive marks are fairly similar, although the largest sigmas occur for the passive marks. Compare to Table 3.3, which gives statistics for formal sigmas (and weights) of

all the modeled CORSs used as constraints for the NA2011 networks. As with the CORS constraints in the Primary network, the published coordinates of constrained marks in the Secondary network (both CORSs and passive) equaled their input values, *not* their adjusted values, to maintain coordinate consistency.

Figure 3.10 shows the distribution of all Primary and Secondary vectors by year. Most of the vectors prior to 1994 are in the Secondary network; the Primary vectors prior to 1994 are those from early major HARN surveys. All of the Secondary vectors later than 1994 are for the projects located in subsidence regions that were moved from the Primary to the Secondary network. No Secondary network marks occur after 2005.

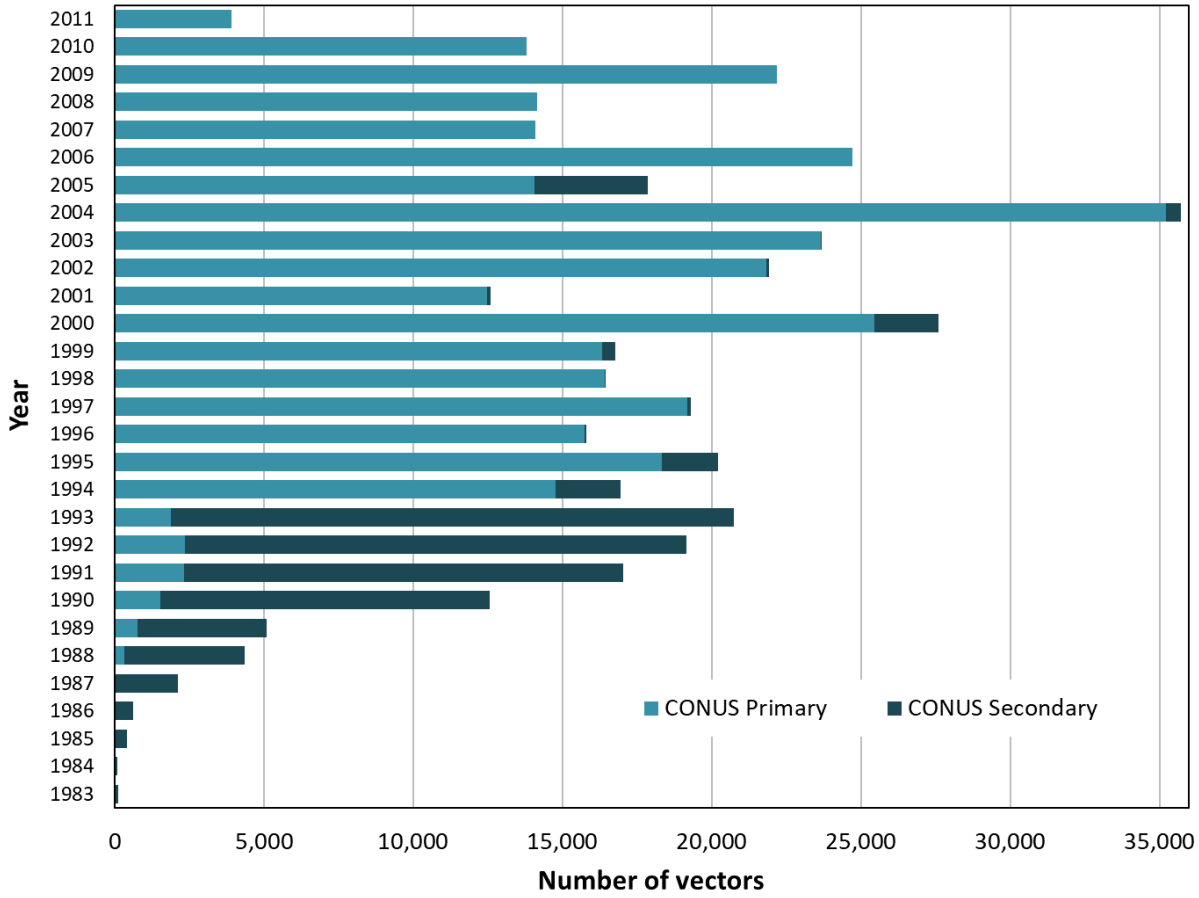

Figure 3.10. NA2011 CONUS vectors in the Primary and Secondary networks, grouped by year.

The geographic distribution of CONUS Primary and Secondary network vectors is shown in Figure 3.11, with the Primary vectors in the top map and the secondary vectors in the bottom. The top map shows that coverage of CONUS was fairly complete in the Primary network, which included ties to the Caribbean. However, the coverage is not uniform; some states have many more vectors than others. But the Primary network coverage is much more uniform than that of the Secondary network, where about 15 states have few or no vector ties (unsurprisingly, the bottom map of Figure 3.11 is similar to the upper two maps in Figure 2.19, which together show

the NA2011 network through 1993). Most of the Secondary network vectors are short and form networks of triangles. Note there are also many very long vectors spanning the entire east-west and north-south width of the United States. Such vectors are possibly problematic, because of the previously mentioned limitations prior to 1994, such as lack of accurate orbits, absence of antenna models, and less sophisticated atmospheric and ocean loading models.

The maps in Figure 3.12 show the geographic distribution of the 57,043 CONUS Primary-only (top) and 17,182 Secondary-only (bottom) marks. These maps more clearly show the uneven distribution of marks, particularly the Secondary marks. CORSs used as constraints for these networks are not shown for clarity; Figure 2.14 and Figure 2.15 show the constrained CORSs for the CONUS network.

The map in Figure 3.13 shows both the Primary-only and Secondary-only marks, as well as the 5321 marks in both networks. Of these marks, 75 could not be constrained, because they were unintentionally disconnected from the Primary marks in the process of splitting the network (as described in the next section). Thus, there were 5321 – 75 = 5246 constrained marks in common between the two networks, with 29 of these being CORSs and 5217 passive marks (with coordinates and sigmas determined in the Primary network). An additional 16 CORSs were only in the Secondary network, for a total of 5217 passive marks + (29 + 16) CORSs = 5262 constrained marks in the Secondary network. The total of 45 CORSs used as constraints in the Secondary network are also shown in Figure 3.13. Most of the 16 CORSs that were only in the Secondary network were put in that network because they are in subsidence regions: 11 in the north Gulf Coast region and two in the California Central Valley region.

3.4. CONUS subnetworks and excluded marks

Splitting the CONUS network into Primary and Secondary networks created multiple disconnected (independent) subnetworks (i.e., partial networks not connected to other partial networks by any enabled vectors). Minimally constrained adjustments of the subnetworks required a single constrained mark, to avoid singularities (when no vector connections existed), or "undetermined" marks (when only rejected vector connections existed). Whenever possible, a single CORS was used as constraints for each subnetwork. As so few CORSs were available for the Secondary network, using a Primary mark for minimum constraints was required for most subnetworks.

After splitting the CONUS network, the Primary network consisted of 36 subnetworks (62,364 marks total), and the Secondary network consisted of 222 subnetworks (22,503 marks total). Nearly all marks (over 99%) were in a single, very large subnetwork of the Primary network, and a majority (58%) were in one large subnetwork of the Secondary network. The number and percent of marks in the ten largest subnetworks of the two networks are listed in Table 3.11 (the subnetwork number is the sequential number assigned to identify subnetworks). The 26 Primary subnetworks not listed in Table 3.11 each contain less than ten marks, and the smallest three each contain three marks. There are 134 Secondary subnetworks containing less than ten marks, and the smallest 43 each contain two marks (i.e., one vector).

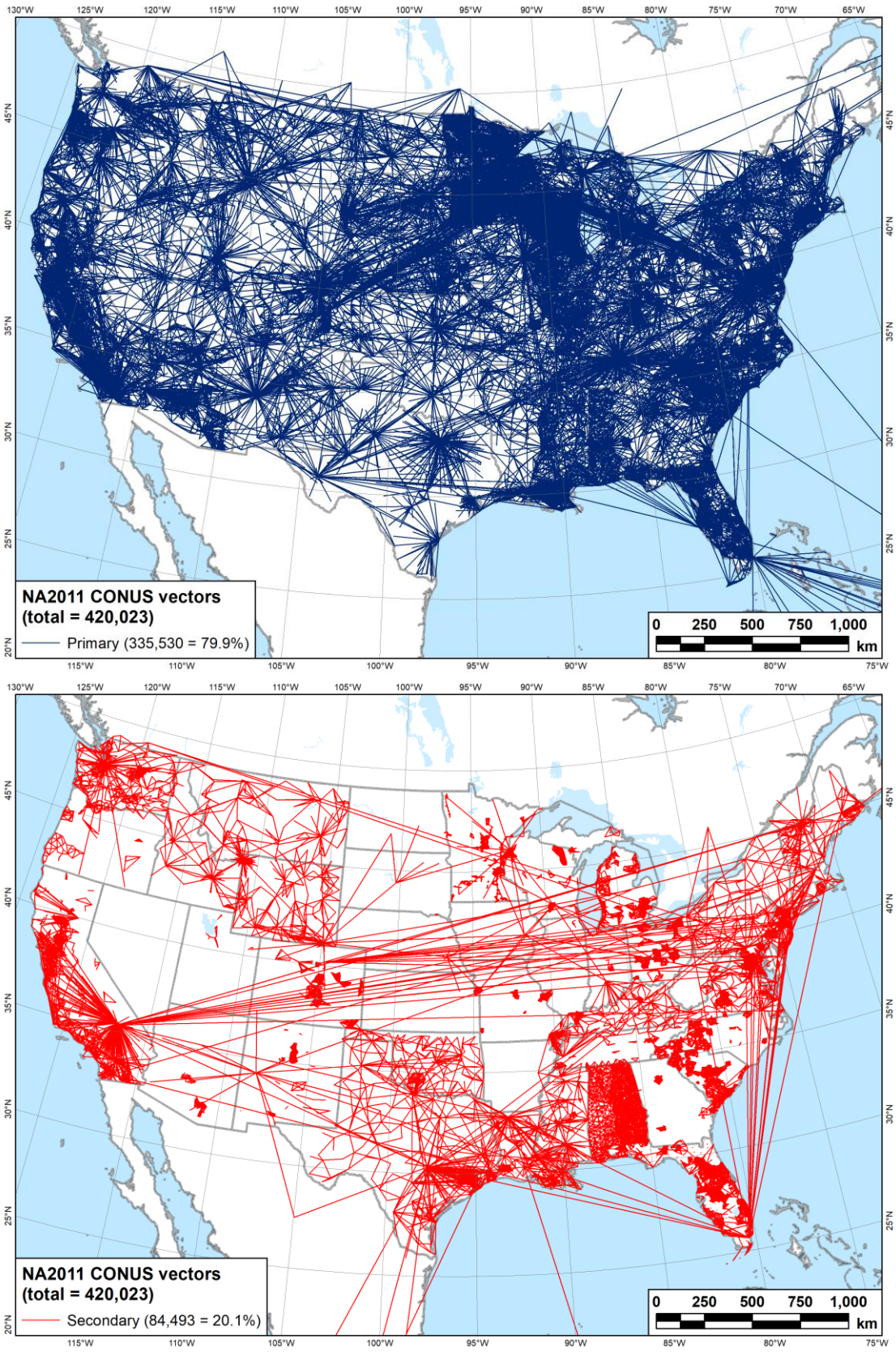

Figure 3.11. Primary (top) and Secondary (bottom) networks of GNSS vectors in NA2011 Project.

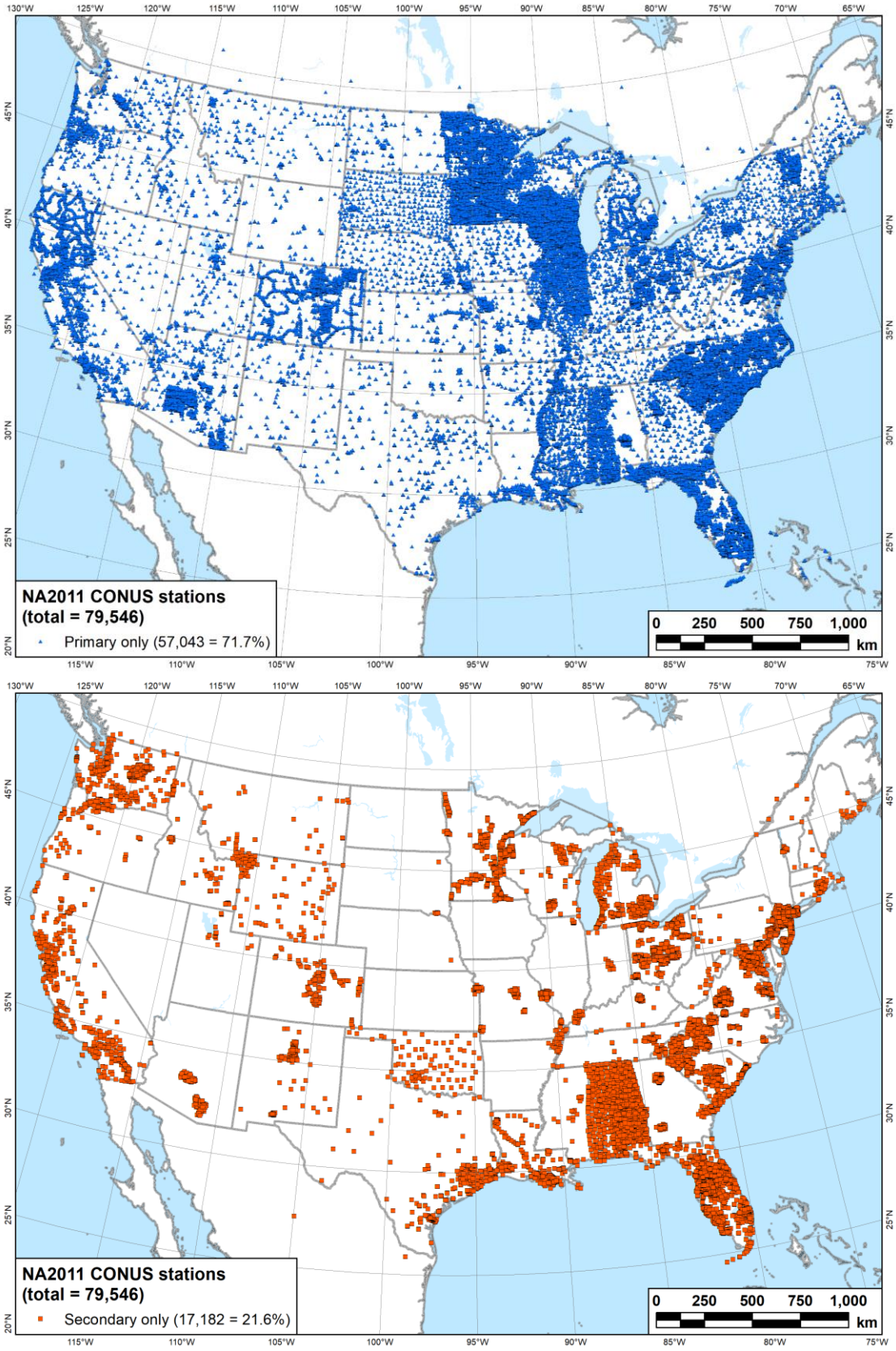

Figure 3.12. Primary only (top) and Secondary only (bottom) marks in the NA2011 networks.

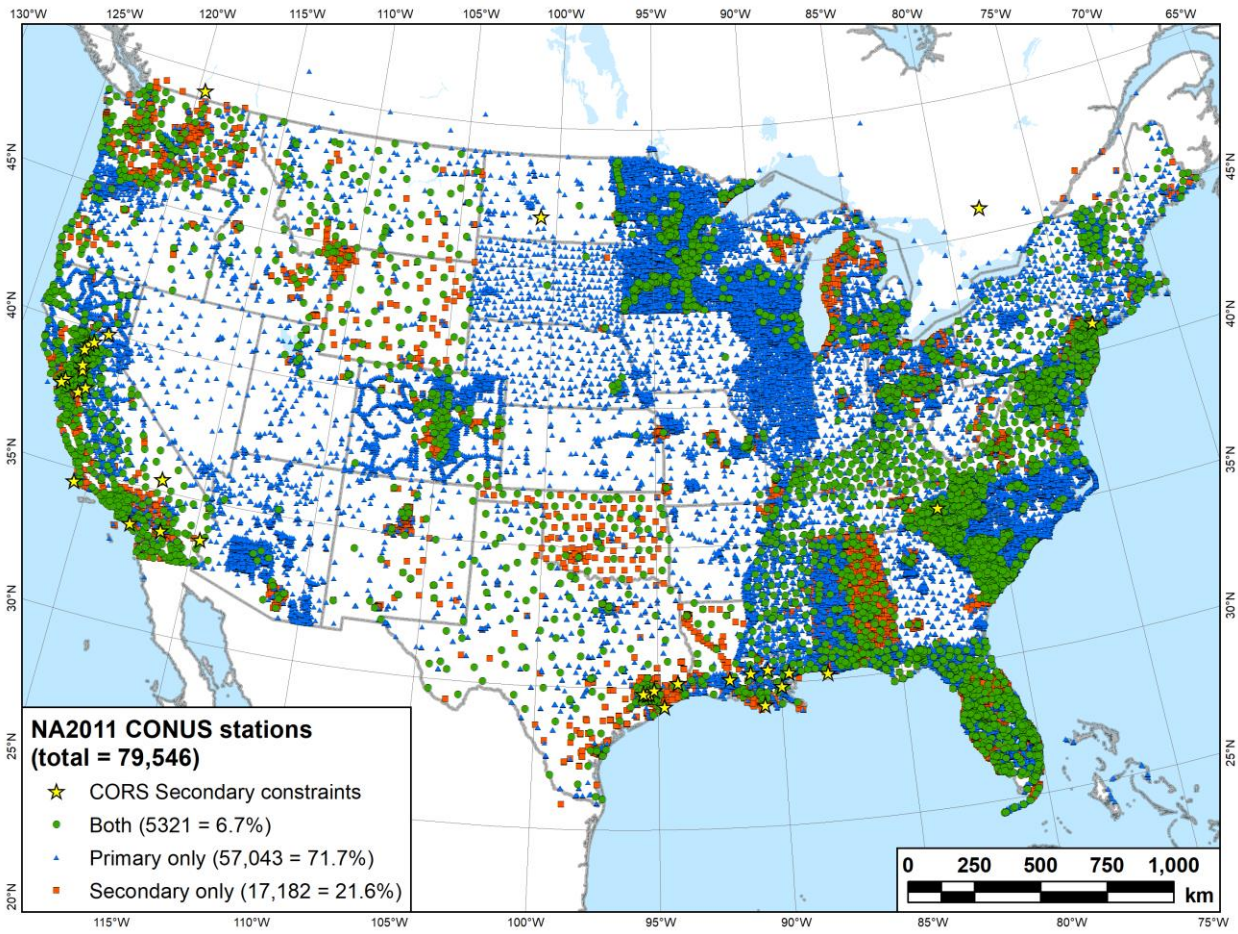

Figure 3.13. Marks in the Primary, Secondary, and both the Primary and Secondary networks.

An unintended consequence of splitting CONUS into Primary and Secondary networks is that 182 marks became disconnected from their respective network and so were inadvertently excluded from the adjustments. That is, a mark in the Primary network connected only to marks in the Secondary network was not included in the adjustment of either network. Likewise, the same is true for Secondary marks connected only to Primary marks, and this occurred for 148 Primary marks and for 34 Secondary marks.

Excluded marks were also mentioned in Section 2.4.1, and their locations are shown in Figure 2.12 through Figure 2.14. The latest occupation dates range from March 1987 through January 2003. Most of the marks (100) are unpublishable Federal Aviation Administration (FAA) airport points, such as runway endpoints, and are unsuitable for geodetic control (i.e., NGS Datasheets are not publicly available). Ten of the remaining 82 are Secondary Airport Control Stations (SACS), and since they were (unintentionally) excluded from the adjustment, their published coordinates are still referenced to the 2007 realization of NAD 83. To determine NAD 83 (2011) coordinates requires that the (excluded) vectors connecting to NA2011 marks be used in adjustments constrained to the NA2011 published coordinate values. The 148 Primary marks occur in 27 subnetworks, so 27 small network adjustments would be needed to restore

these marks. Similarly, the 34 Secondary marks occur in 8 subnetworks, thus 8 adjustments would be needed. These readjustments had not yet been performed at the time of this writing (July 2020). Table 3.12 lists the 82 publishable marks excluded from the NA2011 adjustment, and the ten SACS are denoted by "(SACS)" following their designation.

Table 3.11. Independent subnetworks of the CONUS Primary and Secondary networks.

Primary network subnetworks				Secondary network subnetworks			
Subnetwork number	Mark count	Percent marks		Subnetwork number	Mark count	Percent marks	
		Increment	Cumul.			Increment	Cumul.
1	61,898	99.253%	99.253%	1	13,054	58.010%	58.010%
15	210	0.337%	99.590%	32	1463	6.501%	64.511%
35	15	0.024%	99.614%	8	1075	4.777%	69.289%
17	12	0.019%	99.633%	171	645	2.866%	72.155%
24	12	0.019%	99.652%	72	476	2.115%	74.270%
31	12	0.019%	99.671%	175	409	1.818%	76.088%
33	12	0.019%	99.691%	31	340	1.511%	77.599%
28	10	0.016%	99.707%	173	298	1.324%	78.923%
29	10	0.016%	99.723%	180	288	1.280%	80.203%
32	10	0.016%	99.739%	118	248	1.102%	81.305%
Multiple (26)	163	0.261%	100.000%	Multiple (212)	4207	18.695%	100.000%
Total	**62,364**	**100.000%**		**Total**	**22,503**	**100.000%**	

Another consequence of splitting the network into Primary and Secondary is that 14 of the 36 Primary subnetworks had no CORSs to use as constraints. Each of these subnetworks was constrained to a single arbitrarily chosen passive mark (using sigmas of 1 cm horizontal, 3 cm up for constraint weights). A total of 111 marks occur in these 14 Primary subnetworks, and 70 of them are in disconnected subnetworks (i.e., coordinates were not determined). Of these 70 disconnected marks, 45 are unpublishable FAA marks. The 41 publishable marks in subnetworks with no CORSs constraints are listed in Table 3.13, along with the state where each occur and the last date each was occupied. The marks include 7 primary airport and 13 secondary airport control marks (indicated by "PACS" and "SACS" in parentheses after the designation). All 41 mark coordinates were derived from vectors in the Secondary network.

3.5. Special methods used for the NA2011 Project

Performing the National Adjustment of 2011 necessitated certain special methods be employed to deal with unusual or difficult situations. Such situations and methods include subsidence along the northern Gulf of Mexico coast, separate adjustments of the Alaska and Pacific networks, appropriate handling of vectors crossing tectonic plate boundaries in the Pacific, no-check marks (i.e., those determined by a single vector), and iterative adjustments for rapid vector residual evaluations. These and other issues are discussed in this section.

Table 3.12. The 82 publishable marks excluded due to disconnected subnetworks.

PID	Designation	State	Last occupied	PID	Designation	State	Last occupied
AA8035	5001	FL	11/10/1994	ME3331	NEW BUFF 1	MI	5/14/1991
AA8036	5002	FL	11/10/1994	ME3332	NEW BUFF 4	MI	5/15/1991
AA8037	5003	FL	11/11/1994	ME3333	NEW BUFF 6	MI	5/15/1991
AA8038	5004	FL	11/10/1994	ME3334	NEW BUFF 9	MI	5/15/1991
AA8039	5005	FL	11/11/1994	AA9590	NEWTAM AZ MK	FL	5/11/1996
AA8040	5006	FL	11/11/1994	ME3335	NORTH BEND	MI	5/15/1991
AM7043	11E 02N RESET	NY	8/7/2001	ME3336	NUKE	MI	5/16/1991
AA5245	12 T 3	NJ	4/15/1994	AE7138	OPF C (SACS)	FL	5/25/1996
AA8183	59 35	AL	3/13/1995	ME3337	PANEL 10	MI	5/16/1991
AA8184	59 36	AL	3/13/1995	NG0801	PANEL 11	MI	5/16/1991
BK2024	A 840 RESET	LA	3/8/1989	GV6163	PANEL 11	VA	4/11/1991
NG0796	BLUE	MI	5/17/1991	SY5739	PHOTO PANEL NO 10	WA	7/9/1991
AW7103	BRAZ	TX	2/22/1993	SY5740	PHOTO PANEL NO 14	WA	7/10/1991
ME3328	BUFF	MI	5/15/1991	AA5246	REMOTE	NJ	4/15/1994
NG0797	CAP	MI	5/16/1991	AM7044	S 377 TBM	NY	8/10/2001
AB5072	CARR PARKFIELD MON	CA	7/26/1995	DF4280	SBP D (SACS)	CA	1/22/2003
BK0126	CARRON	LA	3/10/1989	DF4281	SBP E (SACS)	CA	1/22/2003
ME3329	CON	MI	5/15/1991	AE7704	SMC 128	MD	7/10/1997
RD1617	EPF 10	OR	1/14/1988	AE7705	SMC 129	MD	7/10/1997
RD1618	EPF 16	OR	1/15/1988	AE7724	SMC 148	MD	5/19/1997
AA0042	EYW AP STA A	FL	5/11/1996	AE7729	SMC 153	MD	7/10/1997
KU1516	F 19 A NC	NY	8/10/2001	AE7742	SMC 166	MD	5/19/1997
AA9751	FLL K	FL	5/23/1996	AE7820	SMC 244	MD	7/10/1997
AM7045	GUARD TBM	NY	8/10/2001	AE7825	SMC 250	MD	7/10/1997
BK3340	HAAS	LA	3/8/1989	AI9436	SMX A (SACS)	CA	12/12/2000
GV3682	HARMONY	VA	4/13/1991	AI9438	SMX CL END RWY 12	CA	12/12/2000
JU1728	HIGHLAND AZ MK	PA	3/23/1987	AI9437	SMX CL END RWY 2	CA	12/12/2000
AW0063	HOSKINS RESET	TX	2/22/1993	AI9439	SMX CL END RWY 20	CA	12/12/2000
GV6162	HUMMEL	VA	4/11/1991	AI9440	SMX CL END RWY 30	CA	12/12/2000
NG0800	JACOB	MI	5/16/1991	BK2684	SUNSET 2	LA	3/10/1989
AA5221	LFUCG GPS STA 0007 A	KY	9/21/1994	AA8185	TARRANT 0	AL	2/16/1995
AA5222	LFUCG GPS STA 0016 A	KY	9/21/1994	AA8186	TARRANT 1030	AL	2/16/1995
AI9435	M 739 RESET (SACS)	CA	12/12/2000	AB5035	TRAK BOMMER CANYON L 1	CA	7/22/1995
BK3343	MACLAND	LA	3/10/1989	AB5034	TRAK BOMMER CANYON MON	CA	7/24/1995
BX2609	MEEKER	LA	3/8/1989	AI3517	VIS C (SACS)	CA	1/25/2000
AB9812	MEM C (SACS)	TN	4/12/2000	AD1509	W 247 (SACS)	FL	5/18/1996
AB9819	MEM N (SACS)	TN	4/13/2000	RD1624	WATERTANK NAVAID	OR	1/14/1988
SC1322	MERIDIAN RESET	WA	5/21/1987	AM0095	WELL USE 1912 1931 1933	TX	2/22/1993
AI5173	MSCAA CONTROL PT 58	TN	4/15/2000	JU0843	WESTGATE	PA	3/23/1987
SC1378	MT PLEASANT	WA	5/21/1987	AG5052	X 252	FL	5/29/1996
KU1563	NC	NY	8/10/2001	AE9113	X47 A (SACS)	FL	3/23/1996

Table 3.13. The 41 publishable marks in subnetworks constrained by a single passive mark.

PID	Designation	State	Last occupied	PID	Designation	State	Last occupied
DH2737	37 20	AL	3/13/1995	FE2887	MEM F (PACS)	TN	4/15/2000
DH2742	37 25	AL	2/16/1995	AA1810	MIA AP 1961 STA B2 (PACS)	FL	6/1/1996
DH2780	37 27	AL	3/13/1995	AA1811	MIA AP 1965 STA A3 (SACS)	FL	6/1/1996
DH2743	37 3	AL	2/16/1995	AA1812	MIA C 1993 (SACS)	FL	6/1/1996
CQ3507	ARP 2 DTN (PACS)	LA	6/9/2001	FE2879	MKL AP STA A (SACS)	TN	8/12/1999
FV1315	CAR	CA	7/26/1995	FE2880	MKL AP STA B (PACS)	TN	8/12/1999
CQ3508	DTN AP STA A (SACS)	LA	6/9/2001	AA3880	MKL C (SACS)	TN	8/10/1999
AA4530	FAT MON 1 (SACS)	CA	1/11/2000	BH2018	MOB AIRPORT (PACS)	AL	3/22/1999
AA4529	FAT MON 10 (PACS)	CA	1/11/2000	AA8546	MOB AP STA A1 (SACS)	AL	3/22/1999
AA4531	FAT MON 2 (SACS)	CA	1/11/2000	AA8547	MOB ARP (SACS)	AL	3/17/1999
AA4532	FAT MON 9 (SACS)	CA	1/11/2000	DX5266	NIGUEL A	CA	7/24/1995
FV1445	GREEN	CA	3/19/1994	CQ2126	PORT (SACS)	LA	3/12/2001
DX5294	HPGN CA 12 02	CA	7/24/1995	HV9753	SMC 003	MD	7/10/1997
AG8297	I75 83 A52	FL	11/11/1994	HV9764	SMC 004	MD	7/10/1997
AG8303	I75 83 A53	FL	11/11/1994	HV9786	SMC 006	MD	5/23/1997
AG8309	I75 83 A54	FL	11/10/1994	HV9806	SMC 078	MD	5/19/1997
AG8327	I75 83 A57	FL	11/10/1994	HV9814	SMC 085	MD	5/19/1997
HZ2580	LFUCG GPS STA 0003	KY	9/21/1994	AA3723	TYS B (SACS)	TN	11/25/2002
HZ2592	LFUCG GPS STA 0015	KY	9/21/1994	AA3724	TYS D (SACS)	TN	11/25/2002
HZ2644	LFUCG GPS STA 0084	KY	9/21/1994	AA3725	TYS E (PACS)	TN	11/25/2002
HZ2646	LFUCG GPS STA 0086	KY	9/21/1994				

3.5.1. Subsidence along northern Gulf of Mexico coast

Land subsidence is a known issue affecting the northern coast of the Gulf of Mexico (Holdahl *et al.*, 1989; Dixon *et al.*, 2006). For the NA2011 Project, this region consisted of southeast Texas; southern Louisiana, Mississippi, and Alabama; and the western Florida panhandle. NGS has endeavored to provide reliable heights in this region, although it is difficult task due to the age of observations on passive marks and the expense of performing new surveys. NGS and others have attempted to estimate subsidence rates from repeat leveling (Zilkoski and Reese, 1986; Shinkle and Dokka, 2004) and repeat GNSS observations using CORSs on specially designed, very deep "extensometer" mounts (Zilkoski *et al.*, 2003; Zilkoski and Middleton, 2011) and satellite-based radar interferometry (Dixon *et al.*, 2006). NGS has also participated in repeated GNSS and leveling projects in the region. The most recent large campaign-style surveys (for data in the NA2011 Project) were in Louisiana (Project GPS2772, September 2009 to January 2011, with 179 marks and 627 vectors) and Mississippi (Project GPS2827, November 2008 to March 2010, with 658 marks and 2581 vectors). There was also continuous GNSS data collection in the Harris-Galveston Subsidence District (HGSD) used in project GPS2797. Data from this project were adjusted and loaded into the NGSIDB with observations as recent as

December 2009 (recall that the latest NA2011 observations are from December 2011). In addition, extensive geodetic leveling was performed from west Florida to the Louisiana border between May and December 2009 in leveling project L27115 (although it cannot be used directly for NA2011 ellipsoid heights, the leveling helped in determining subsidence rates). Subsidence rates in the region are difficult to estimate reliably from the available data. Rates appear to range from about 1 to 5 mm/year.

The purpose of the NA2011 Project was to produce the best estimate of 3D NAD 83 coordinates at epoch 2010.00, and their associated uncertainties. The observation dates for vectors in the region span from June 1985 to January 2011 (a range of 25.6 years). This is obviously problematic in a subsidence region; at a rate of 5 mm/yr, the heights of the vector endpoints in the region could decrease by 13 cm over the time span of the observations.

One strategy for dealing with the subsidence was to move older vectors to the Secondary network, to thus eliminate their impact on the results of the Primary network. This strategy was done for observations older than 2006, both in the subsidence regions along the Gulf Coast and in the California Central Valley. However, given the known issues and the large amount of data over the 25.6-year time span for the Gulf Coast, it was decided more should be done to address subsidence.

The approach adopted—in addition to moving older data to the Secondary network—was to assign additional error to the height component of the vectors based on age and estimated subsidence rates. The purpose of doing this was twofold:

- To decrease the influence of older observations by assigning the greater error to the height component, and thus downweight that component.
- To increase the height uncertainties proportional to their age and subsidence rate so the estimated height accuracies would be more conservative (and thus more realistic).

Importantly, this additional error was explicitly limited to the height component, rather than downweighting of the entire observation. The intent was for this approach to have little or no impact on the horizontal coordinates or their accuracy estimates. The following general approach was used to modify the height component error of the vectors (G-file) affected by subsidence:

- Rotate the vectors—and their associated variance-covariance (VCV) values—from Earth-Centered, Earth-Fixed (ECEF) coordinates to local geodetic horizon (LGH) coordinates.
- Increase the variance (standard deviation squared) of the height component by adding the squared product of the subsidence rate and the difference between the date of the observation and 2010.00.[12]

[12] Admittedly, this approach treats an unknown systematic error (subsidence) as a random error. With additional time and resources, a more robust solution could have been attempted but was not possible within the constraints of this project.

- Rotate the vector and VCV values (with the modified height variance) back to ECEF coordinates.
- For vectors that were part of a multi-vector session solution, additional computations were required to correctly compute the modified off-diagonal (cross-vector) covariances.

A more detailed description of the process follows. The GNSS vector VCV matrix, $\mathbf{\Sigma}$, from the G-file was rotated from ΔX, ΔY, ΔZ ECEF coordinates (at the latitude and longitude of the vector midpoint) to the delta north-east-up (Δn, Δe, Δu) LGH. This was done using Equation (3.3), which gave the following expanded LGH VCV matrix (with the Δ symbols removed for clarity in subsequent equations):

$$\mathbf{\Sigma}_{neu} = \mathbf{R}\,\mathbf{\Sigma}_{XYZ}\,\mathbf{R}^{\mathrm{T}} = \begin{bmatrix} \sigma_n^2 & \sigma_{ne} & \sigma_{nu} \\ \sigma_{ne} & \sigma_e^2 & \sigma_{eu} \\ \sigma_{nu} & \sigma_{eu} & \sigma_u^2 \end{bmatrix} \tag{3.6}$$

where $\mathbf{R}$ is the rotation matrix in Equation (3.4), and the σ^2 values are the squared vector sigmas rotated to the LGH. After the rotation, the vector up-variance was increased by the product of the subsidence rate, s, and the time difference with respect to the NA2011 epoch, $\Delta t = t$ – 2010.00, at the midpoint time t of the observation:

$$\overline{\sigma}_u^2 = \sigma_u^2 + (s\,\Delta t / V_U)^2 \tag{3.7}$$

where V_U is the variance factor up-component computed for each GPS project, as described earlier in Section 3.2.3. It was necessary to divide by V_U, because the sigmas from the G-file were scaled by the variance factors before performing adjustments. Otherwise the additional error due to subsidence would be scaled by an amount that depended on the individual GPS projects, which obviously cannot affect subsidence. The V_U scalars ranged from 0.036 to 31.717 for the Gulf Coast vectors identified as affected by subsidence (identification of these vectors is described below).

The increased up-variance, $\overline{\sigma}_u^2$, was substituted back in the *neu* VCV matrix resulting in a new *neu* VCV matrix, $\overline{\mathbf{\Sigma}}_{neu}$, with a single element modified. This new VCV matrix was then rotated back to the *XYZ* system to give the modified *XYZ* VCV matrix (in which all elements were modified):

$$\overline{\mathbf{\Sigma}}_{XYZ} = \mathbf{R^{-1}}\,\overline{\mathbf{\Sigma}}_{neu}\,(\mathbf{R^{-1}})^{\mathrm{T}} = \begin{bmatrix} \overline{\sigma}_X^2 & \overline{\sigma}_{XY} & \overline{\sigma}_{XZ} \\ \overline{\sigma}_{XY} & \overline{\sigma}_Y^2 & \overline{\sigma}_{YZ} \\ \overline{\sigma}_{XZ} & \overline{\sigma}_{YZ} & \overline{\sigma}_Z^2 \end{bmatrix} \quad . \tag{3.8}$$

The procedure described above is for a single sequential vector with a 3×3 VCV matrix. But if the vector was part of a group of vectors processed simultaneously in a session, the transformation becomes more complicated. Consider the case where the downweighted vector is

vector number 1 in a session of three vectors. The original *XYZ* VCV matrix of the session can be expanded as

$$\boldsymbol{\Sigma}_{XYZ} = \begin{bmatrix} \boldsymbol{\Sigma}_{XYZ_1} & \boldsymbol{\Sigma}_{XYZ_1,\,XYZ_2} & \boldsymbol{\Sigma}_{XYZ_1,\,XYZ_3} \\ \boldsymbol{\Sigma}_{XYZ_1,\,XYZ_2} & \boldsymbol{\Sigma}_{XYZ_2} & \boldsymbol{\Sigma}_{XYZ_2,\,XYZ_3} \\ \boldsymbol{\Sigma}_{XYZ_1,\,XYZ_3} & \boldsymbol{\Sigma}_{XYZ_2,\,XYZ_3} & \boldsymbol{\Sigma}_{XYZ_3} \end{bmatrix} \tag{3.9}$$

where each of the nine elements of the $\boldsymbol{\Sigma}_{XYZ}$ matrix in Equation (3.9) is a 3×3 matrix. The diagonal elements of $\boldsymbol{\Sigma}_{XYZ}$ are the VCV matrices of the vectors, and the off-diagonal elements are the off-diagonal covariances between the vectors in the session. In this case, $\boldsymbol{\Sigma}_{XYZ_1}$ in Equation (3.9) is replaced by $\overline{\boldsymbol{\Sigma}}_{XYZ}$ computed in Equation (3.8). But only performing that replacement could make $\boldsymbol{\Sigma}_{XYZ}$ in Equation (3.9) become non-positive definite, and thus cause singularities in an adjustment. To prevent this from occurring, the terms $\boldsymbol{\Sigma}_{XYZ_1,\,XYZ_2}$ and $\boldsymbol{\Sigma}_{XYZ_1,\,XYZ_3}$ in Equation (3.9) must also be modified. For example, consider the expansion of the $\boldsymbol{\Sigma}_{XYZ_1,\,XYZ_2}$ term:

$$\boldsymbol{\Sigma}_{XYZ_1-XYZ_2} = \begin{bmatrix} \sigma_{X_1X_2} & \sigma_{X_1Y_2} & \sigma_{X_1Z_2} \\ \sigma_{Y_1X_2} & \sigma_{Y_1Y_2} & \sigma_{Y_1Z_2} \\ \sigma_{Z_1X_2} & \sigma_{Z_1Y_2} & \sigma_{Z_1Z_2} \end{bmatrix} \tag{3.10}$$

The original elements can be computed using the standard deviations, σ, and correlations, ρ, from the original unmodified G-file (recall that the G-files used in NA2011 give correlations rather than covariances). The first term in Equation (3.10) is:

$$\sigma_{X_1X_2} = \rho_{X_1X_2}\,\sigma_{X_1}\,\sigma_{X_2} \tag{3.11}$$

Where σ_{X_1} and σ_{X_2} are the *X*-component sigmas of vectors 1 and 2, and $\rho_{X_1X_2}$ is the correlation between those sigmas. Equation (3.8) changes σ_{X_1} but does not change $\sigma_{X_1X_2}$ or σ_{X_2}. Therefore $\rho_{X_1X_2}$ must also change, and it by definition must satisfy the relationship

$$\sigma_{X_1X_2} = \overline{\rho}_{X_1X_2}\,\overline{\sigma}_{X_1}\,\sigma_{X_2} \tag{3.12}$$

where $\overline{\sigma}_{X_1}$ is obtained from Equation (3.8). The new correlation is computed by dividing Equation (3.11) by (3.12), to give the modified correlation for the first term:

$$\overline{\rho}_{X_1X_2} = \rho_{X_1X_2}\,\frac{\sigma_{X_1}}{\overline{\sigma}_{X_1}} \tag{3.13}$$

The other modified correlations were computed in a similar manner, until all affected elements in the G-file session correlation matrix were modified, such that only the standard deviation of the height component was affected, and the VCV matrices remained positive definite. These G-files with modified sigmas and correlations were used in the NA2011 adjustments in place of the original vectors.

Subsidence rates for the region were estimated based on information from various sources, such as from the previously cited references, long-term GNSS data analysis results for the HGSD, and

internal NGS analysis of recently completed GPS and leveling projects in Louisiana and Mississippi. The subsidence region and rates resulting from this effort are shown in Figure 3.14. A subsidence rate of 2 mm/yr was assigned to the overall region, as defined by the outer envelope. Internal to this were higher and lower rates. The highest (and best-known) rate of 5 mm/yr was assigned to the Houston region. A rate of 3 mm/yr was used for the Mississippi delta region. A lower rate of 1 mm/yr was assigned to the Mobile, Alabama area. A GNSS vector was affected by the estimated subsidence if one of its end points fell within a subsidence region, and this impacted 16,118 vectors (7213 Primary and 8905 Secondary), observed from June 1985 through January 2011.

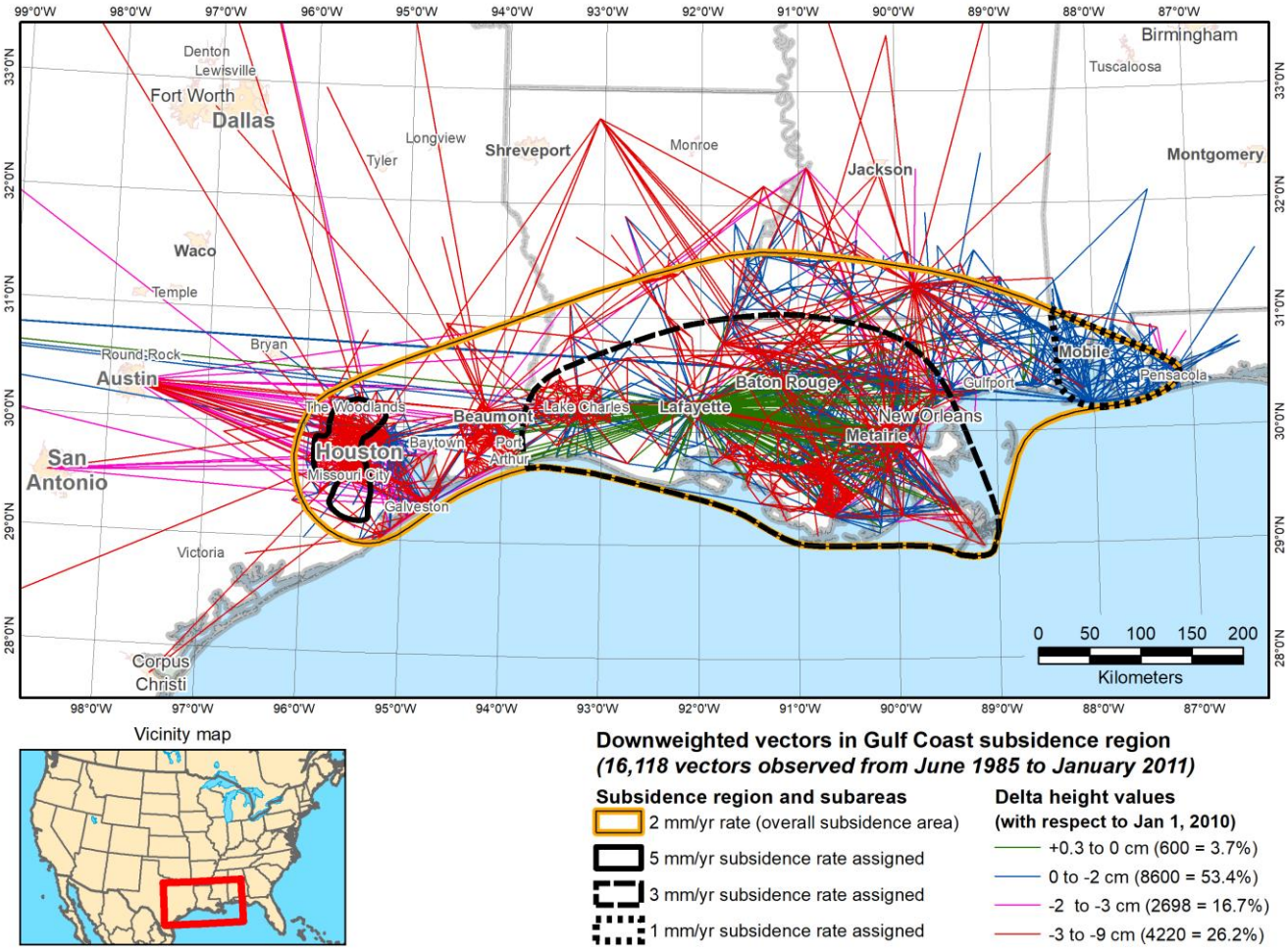

Figure 3.14. Gulf Coast subsidence region showing estimated subsidence rates and affected vectors.

Table 3.14 summarizes the subsidence rates, midpoint age of the observations, and resulting change in ellipsoid height for the affected GNSS vectors in the Gulf Coast subsidence region. The age is with respect to epoch 2010.00 (a negative age means the observation occurred after 2010.00). The change in ellipsoid height was squared and added to the GNSS up-variance, and the square root of that sum was assigned as the estimated height component of the GNSS error. Changes in ellipsoid heights were not otherwise used to calculate the final ellipsoid heights of

marks. The maximum estimated error due to subsidence was large, 7 cm for the Primary and 9 cm for the Secondary network. But the median error values are more modest, 0.4 cm for the Primary network, which is almost an order of magnitude less than the median of 2.9 cm for the Secondary network.

Table 3.14. Summary of estimated subsidence values for the Gulf Coast subsidence region (age of observation is with respect to epoch 2010.00; absolute value of delta height is the additional error due to subsidence assigned to observations).

	All GNSS observations			Primary network only			Secondary network only		
	Rate (mm/yr)	Age (years)	Delta height (m)	Rate (mm/yr)	Age (years)	Delta height (m)	Rate (mm/yr)	Age (years)	Delta height (m)
Number		**16,118**			**7213**			**8905**	
Minimum	1	-1.052	-0.0896	1	-1.052	-0.0733	1	4.001	-0.0896
Maximum	5	24.570	0.0032	5	20.798	0.0032	5	24.570	-0.0080
Mean	3.0	7.256	-0.0213	2.7	3.514	-0.0079	3.3	10.288	-0.0322
Standard dev	±1.3	6.002	0.0189	±1.0	4.418	0.0093	±1.4	5.372	0.0177
Percentiles									
1%	1	-0.735	-0.0733	1	-0.741	-0.0356	1	4.026	-0.0733
5%	1	0.070	-0.0570	1	-0.722	-0.0216	2	4.247	-0.0710
10%	2	0.156	-0.0461	2	0.061	-0.0193	2	4.389	-0.0569
50% (median)	**3**	**5.056**	**-0.0181**	**3**	**2.075**	**-0.0041**	**3**	**9.220**	**-0.0292**
90%	5	15.828	-0.0004	5	11.754	-0.0001	5	18.528	-0.0093
95%	5	18.981	-0.0002	5	12.687	0.0022	5	19.867	-0.0088
99%	5	19.886	0.0022	5	15.831	0.0022	5	23.039	-0.0081

It is important to reiterate that the subsidence regions and their rates are approximate. There was not enough time or resources available to perform an in-depth study to obtain "better" subsidence estimates. Even if more accurate rates could have been determined from the data available at that time, the effort to perform the analysis—*and* to demonstrate that the resulting rates were indeed more accurate—was far beyond what was possible for the NA2011 Project. Moreover, it is entirely possible such additional effort would not have yielded demonstrably better rates. Nonetheless, the magnitude of actual subsidence was likely large enough to warrant this approximate approach.

The approximate nature of the subsidence rates is why they were *not* intended to provide accurate ellipsoid heights on marks not recently observed. Rather, they were intended to reduce the influence of the older observations *and* to increase the uncertainty of heights based on the older observations. These are crucial distinctions.

The maps in Figure 3.15 (Primary network) and Figure 3.16 (Secondary network) show post-adjustment ellipsoid height error (at 95% confidence) of marks in the Gulf Coast region without

and with downweighting of vector up-component error, based on subsidence rate and age of the observation. The top map shows results when no downweighting was applied, and the bottom map shows when downweighting was applied. Note that the error bars are at different scales in the two figures, because the error estimates are significantly greater for the Secondary network, due mainly to the greater age of the observations.

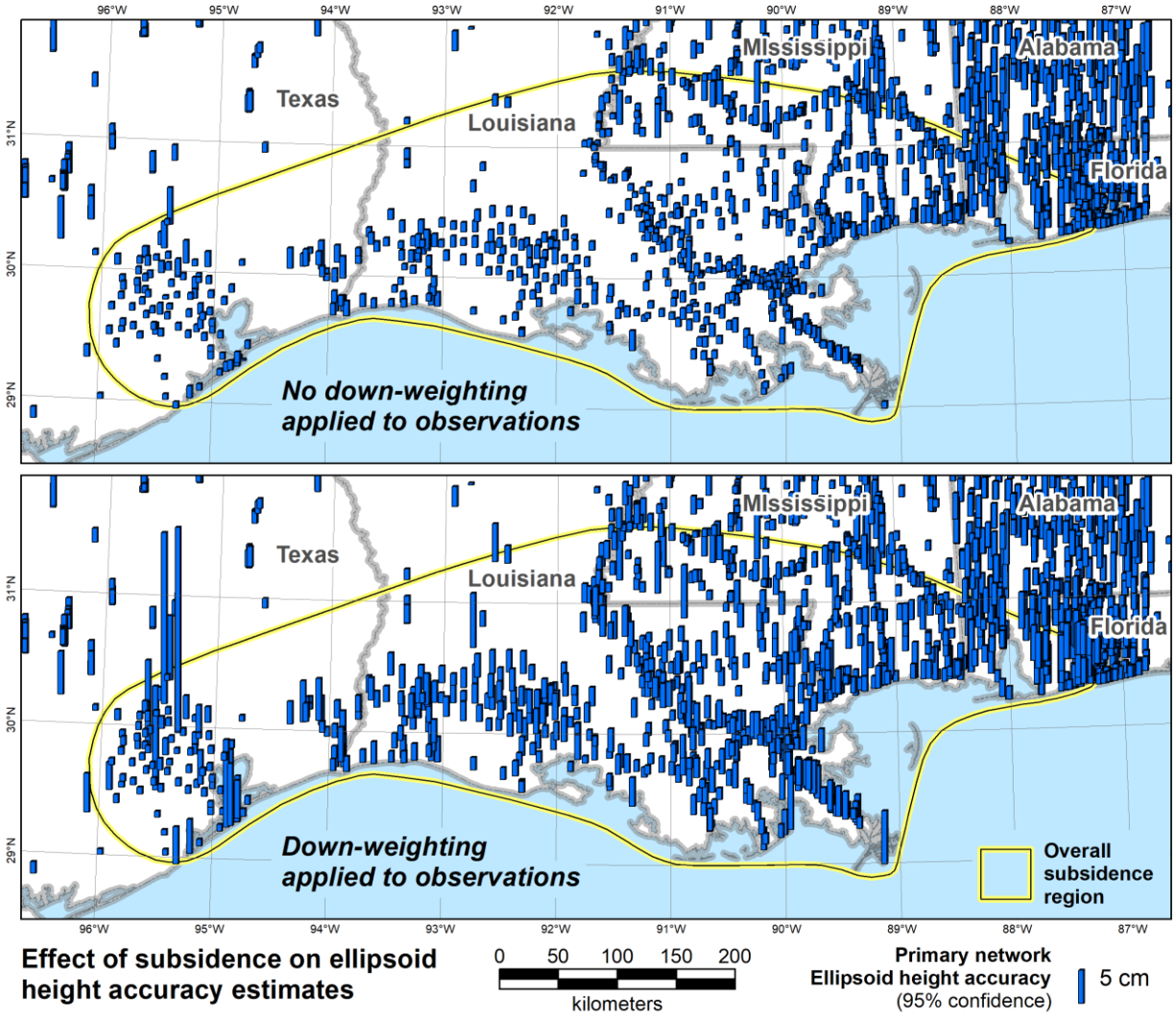

Figure 3.15. Effect of subsidence downweighting on the Gulf Coast region Primary network. Ellipsoid height errors are at 95% confidence (top map with no downweighting, bottom with downweighting).

The height errors shown in Figure 3.15 and Figure 3.16 with no downweighting are from preliminary constrained adjustments performed in April 2012. The errors with downweighting applied are from the final constrained adjustments of NA2011 performed in June 2012. So, there is not a perfect one-to-one relationship between the top and bottom maps, as there were some changes to the networks, although the changes were relatively minor. Nonetheless the change in height errors shown provides a reasonably good indication of the effects of downweighting on the adjustment results.

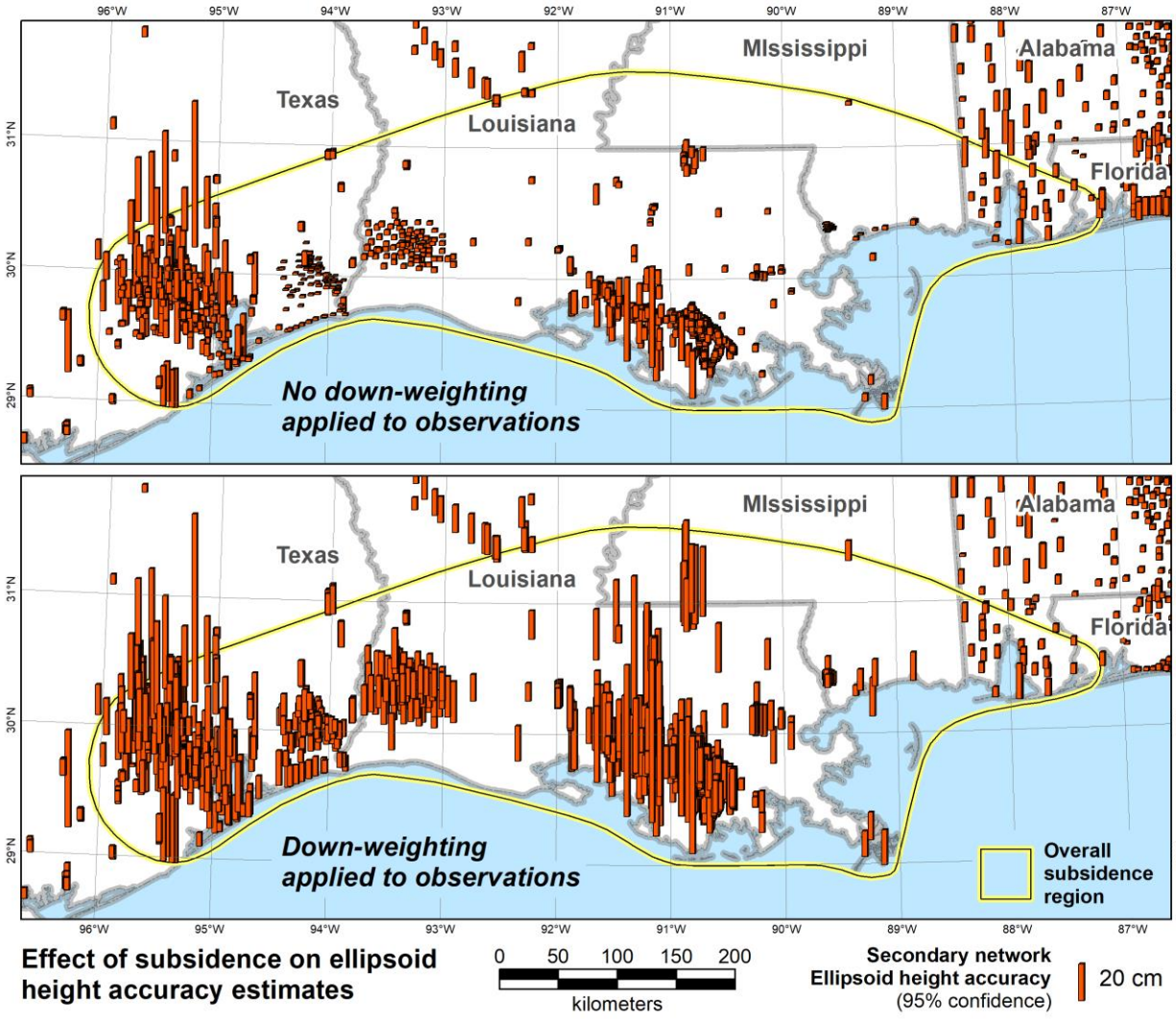

Figure 3.16. Effect of subsidence downweighting on the Gulf Coast region's Secondary network. Ellipsoid height errors are at 95% confidence (top map with no downweighting, bottom map with downweighting).

For the Primary network, the most significant increase in height error occurs for a few marks in the Houston area (at the west end of the subsidence region in Figure 3.15). This occurred because some of the marks in that area were tied to older observations included in the Primary network (as indicated by the maximum age of 20.8 years for the Primary network observations in Table 3.14). These older observations consist of 21 vectors observed from 1995 to 1998, with estimated subsidence errors of 11.7 to 14.7 cm, connected to five marks with final error estimates of about 14 to 30 cm (95% confidence). They probably should have been moved to the Secondary network, but the impact is minor, as they were significantly downweighted.

The increase in ellipsoid height error is more striking for the Secondary network (Figure 3.16), most notably in Louisiana. Note in particular the two groups of closely spaced marks on either side of the Texas-Louisiana border. Without downweighting, the estimated errors on this group of marks is small, ranging from 0.6 to 5.2 cm (95% confidence), even though they are based on

old observations in a known subsidence area (last observed mostly in 1990 and 1991, but with a few as late as 1997). Downweighting increased the error estimates to a factor of 5 to 6, resulting in a range of 4 to 24 cm.

3.5.2. Alaska and Pacific networks

As mentioned previously, the Alaska and Pacific networks were adjusted separately from CONUS. In the 2007 national adjustment, Alaska was included as part of the overall Helmert block, but it was adjusted separately in NA2011 because of the weak ties to CONUS (see Section 2.4.1 and Table 2.16). The 2007 adjustment did not include the Pacific network at all.

Although the CONUS Primary, CONUS Secondary, Alaska, and Pacific networks were adjusted separately, they were all referenced to the consistent set of CORS coordinates from the MYCS1. Since the MYCS1 was a single global solution, the four NA2011 networks were constrained to a consistent set of control coordinates at epoch 2010.00. A similar statement can be made concerning the 2007 adjustment: even though the ties between CONUS and Alaska were weak, it likely had negligible impact on coordinates, since both CONUS and Alaska were constrained to their own sets of CORSs.

Both the Alaska and Pacific networks were small enough that Helmert blocking was not needed. The Alaska network consisted of 969 marks and 2846 vectors, and the Pacific network 540 marks and 1852 vectors. These networks could still be adjusted in *NETSTAT*, but a problem was discovered—it did not produce correct results if only a single block was used. Thus, to use *NETSTAT*, it would be necessary to split each into at least two blocks. In addition, *NETSTAT* was being intensively used to perform the constrained CONUS Secondary adjustments at the time the Alaska and Pacific adjustments were undertaken. Because of the large number of CONUS Secondary constraints, each constrained adjustment required about a week to complete. For these reasons, it was instead decided to perform the Alaska and Pacific adjustments using the program *ADJUST*. It had already been shown that *NETSTAT* and *ADJUST* produce identical results.

Alaska was adjusted in the same manner as the CONUS Primary network, using the same approach to constraining CORSs. But unlike CONUS, at the time of the MYCS1, most CORSs in Alaska were relatively new, so most had less than 2.5 years of data available for MYCS1 processing. Thus, Alaska had a larger (nearly twice) the proportion of "modeled" CORSs (i.e., without formal uncertainty estimates). Of the 58 CORSs in Alaska, 19 (33%) were modeled, as compared to 202 of 1113 for CONUS (18%); see Table 2.4. The formal sigmas of the "computed" CORSs used as constraints for each network are summarized in Table 3.15 for each of the four NA2011 networks (compare to Table 3.3 for all NA2011 CORSs used as constraints). The median and mean sigmas for all computed CONUS and Alaska CORSs are approximately the same in all four networks, although Primary CONUS has by far the largest maximum sigmas. The largest sigmas for any MYCS1 mark with NAD 83 coordinates actually occurs in Alaska (CORS CHI6; see Table 1.2), with sigmas of σ_N = 15.16 cm, σ_E = 8.16 cm, and σ_U = 46.93 cm. But that CORS was not used for NA2011 constraints (i.e., it was not tied to any surveys loaded into NGSIDB), and the four CORSs with the largest sigmas in Alaska were not used as NA2011 constraints for the same reason.

Table 3.15. Formal sigmas and number of CORSs for the four NA2011 networks ("sigmas" are the formal uncertainties represented as SINEX standard deviations).

Network	CONUS Primary			CONUS Secondary			Alaska			Pacific		
Computed CORS sigmas (cm)	North	East	Up	North	East	Up	North	East	Up	North	East	Up
Minimum	0.06	0.06	0.08	0.12	0.11	0.41	0.12	0.09	0.30	0.07	0.05	0.08
Maximum	8.64	12.92	32.52	1.09	1.05	4.82	1.30	0.86	4.50	0.99	1.13	4.35
Median	0.39	0.32	1.48	0.38	0.36	1.59	0.56	0.37	1.90	0.13	0.13	0.50
Mean	0.53	0.45	2.04	0.43	0.40	1.80	0.59	0.39	1.99	0.29	0.31	1.26
Standard dev	±0.57	±0.62	±2.34	±0.31	±0.31	±1.44	±0.39	±0.26	±1.42	±0.29	±0.33	±1.37
Number (and percent) of CORS types												
Computed	895 (82%)			16 (94%)			39 (67%)			23 (96%)		
Modeled	201 (18%)			1 (6%)			19 (33%)			1 (4%)		
Totals	**1096**			**17**			**58**			**24**		

For the CORSs used in the Pacific network, only one of the 24 Pacific CORSs was modeled, and the sigmas for the computed CORSs were generally smaller than those of CONUS and Alaska CORSs (see Table 3.15). The biggest difference with the Pacific network, however, is how plate tectonic motion was handled.

Referring to Figure 2.17, it can be seen that many vectors have endpoints on both the Pacific and Mariana plates, and the vectors are referenced to CORSs on both those plates (18 on the Pacific plate, 6 on the Mariana plate). The CORSs on these plates are referenced to the NAD 83 coordinates corresponding to the plate where they are located. As shown in Table 3.2, the NAD 83 horizontal velocities for both plates are nearly zero, but their IGS08 velocities are not small and are dissimilar. Differencing the mean velocities for points on these plates shows they are moving relative to one another at about 6 cm/yr, and this is significant. Such large relative velocities present a problem for attempting to adjust the Pacific as a single network. Marks on Palau and Yap Island compounded the velocity problem, because they are located on the (edge of) the Philippine Sea Plate (see Figure 2.17), adjacent to the Caroline plate.

An approach initially attempted for dealing with marks referenced to different tectonic plates was to adjust the Pacific network in the IGS08 frame, rather than the NAD 83 PA11 and MA11 frames. All the vectors were brought to the IGS08 2005.00 epoch using *HTDP*. The published IGS08 epoch 2005.00 CORS coordinates were used as constraints (weighted by their formal MYCS1 sigmas). The resulting IGS08 coordinates on passive marks could then be transformed to NAD 83 (PA11) or (MA11) at epoch 2010.00 using *HTDP*.

The problem with using the IGS08 frame for the adjustment is that there are no velocities on the passive marks. Thus *HTDP*-modeled velocities would have to be used for all passive marks. That means all the error in the modeled velocities would propagate directly into the final (transformed) coordinates. Given the small number of computed CORSs (23) over a vast area (larger than CONUS), it was deemed more appropriate to adjust in the NAD 83 frame. The advantage is that the transformation errors become part of the observation error budget, which is propagated through the network based in geometric closure, and the errors manifest themselves in the final post-adjustment errors. In addition, adjusting in the NAD 83 frame allows the network to be constrained to the same reference frame in which the coordinates are published. Such an approach attempts to remove systematic observation errors prior to performing the adjustment, the preferred approach. It is analogous to modeling refraction and deflection of the vertical for optical geodetic observations before adjusting those observations.

To adjust the Pacific in NAD 83 required the entire network be adjusted in both the PA11 and MA11 frames. This was possible, since CORS coordinates were in IGS08 and could be transformed to any of the three NAD 83 frames (by using the same transformations used to compute the published NAD 83 coordinates). The two Pacific network adjustments were performed and analyzed separately, although they behaved very similarly, because the PA11 and MA11 epoch 2010.00 coordinates were consistent. For the final adjusted coordinates, marks on the Mariana and Philippine Sea plate were assigned MA11 coordinates; all others were assigned PA11 coordinates. The results are discussed further in Chapter 4.

3.5.3. Iterative adjustments for automated rejection and enabling of observations

GPS projects loaded into the NGSIDB include the rejection status of the vectors, so the rejections are also included in the NA2011 networks. Over 42,000 (more than 10%) of the vectors downloaded from the NGSIDB were rejected, and this seemed an unusually large proportion. It was found that many were rejected as part of the 2007 national adjustment. With new connections between marks created by combining projects into new networks, it was necessary to assess both the enabled and rejected vectors.

In *NETSTAT* and *ADJUST*, vector rejection is done by downweighting (rather than by removal). The advantage of downweighting is that the rejected vectors have residuals that can still be evaluated to determine whether they can be re-enabled. But this method of rejection has two potential pitfalls: it can mask situations where all vectors connecting a mark are rejected, and it can also cause incorrect adjustment statistics (e.g., if rejected vectors are counted for the degrees of freedom). Fortunately, neither of these problems occurred, because unconstrained marks connected by only rejected vectors are identified as "undetermined," rejected vectors are not counted for degrees of freedom, and their residuals do not contribute to the variance sum.

When previously rejected vectors are re-enabled, another minimally constrained adjustment is performed, and that of course changes their residuals, as well as the residuals of other vectors. This change can result in excessively large residuals on previously enabled vectors, which must then be rejected and the adjustment must be run again, resulting in a new set of residuals. This process can be repeated multiple times to ensure all rejected vectors should, in fact, be rejected. But, with a starting set of over 40,000 rejected vectors, and about 25 hours required to run a

single minimally constrained adjustment, it was not feasible to manually analyze, reject, and re-enable vectors.

To address the problem with residuals analysis, an automated iterative adjustment approach was implemented. The method was performed as minimally constrained adjustments of the entire CONUS network (before splitting into Primary and Secondary). Initially, a rejection criterion of 5 cm was used. That is, enabled vectors with residuals greater than 5 cm were rejected, and rejected vectors with residuals less than 5 cm were enabled (this was the same rejection criterion used in the 2007 adjustment). However, this criterion was changed to the following for performing the iterative adjustments:

1. Reject vectors with horizontal residuals > 4 cm and vertical (up) residuals > 5 cm
2. Enable vectors with horizontal residuals <= 4 cm and vertical (up) residuals <= 5 cm

After an adjustment was completed, rejected vectors with residuals meeting the above criteria were automatically enabled, and another adjustment was performed. Then, for the new adjustment, enabled vector with residuals exceeding the criteria were automatically rejected, and another adjustment was again performed. The procedure was repeated until no further rejections or re-enabling occurred.

3.5.4. No-check marks

As stated in Section 2.4, there are two types of "no-check" marks:

1. "Hard" no-check: Marks tied by one, and only one, vector (i.e., no rejected vector ties)
2. "Soft" no-check: Marks tied by one enabled, plus one or more rejected vectors

No-check marks are a problem, because they have no redundancy, so there is no "check" on the computed position. This situation is also problematic for determining reliable post-adjustment accuracy estimates, since the vector residuals are zero (actually, no-check marks in simultaneous solutions can have non-zero residuals due to inter-vector correlations, but they are small and there is still no occupational redundancy). Most no-check marks occur in FAA airport surveys, because of the unfortunate practice of making only single ties to some marks, mainly leveled bench marks used for vertical (orthometric height) control. Ending the practice of single ties in control surveys is one of the recommendations in Section 6.2.2.1.

Nothing can be done to add an observation to a hard no-check mark, other than adding vectors to the network from some other source (such as from new fieldwork). Soft no-check marks, on the other hand, can have redundancy introduced by enabling one or more of the rejected vectors connected to it.

To reduce the number of no-checks, once the automated iterative adjustments were completed, the rejected vectors tied to soft no-checks with residuals of less than 10 cm were enabled. Some iteration was necessary to accomplish this, since changing rejection status affects other vectors. Once completed, this approach reduced the number of no-check marks by approximately 700, for a total of 2134 no-check marks (1801 hard and 333 soft) in all four of the final NA2011

networks. The no-check marks for each NA2011 network are provided in Table 3.16, including 365 unpublishable no-check marks (343 FAA marks, five located outside the United States, and 17 disconnected marks).

Table 3.16. No-check marks in the four NA2011 networks ("hard" no-checks have no rejected vector ties; "soft" no-checks have one or more rejected vector ties; "unpublishable" marks are mostly FAA marks, but included are a few located outside of the United States and disconnected marks).

Type of no-check	All	CONUS overall	CONUS Primary	CONUS Secondary	Alaska	Pacific overall	Pacific plate	Mariana plate
Hard publishable	1,454	1,190	871	319	129	135	81	54
Hard unpublishable	347	337	18	319	10			
Hard total	**1,801**	**1,527**	**889**	**638**	**139**	**135**	**81**	**54**
Soft publishable	315	300	60	240	15			
Soft unpublishable	18	18	1	17				
Soft total	**333**	**318**	**61**	**257**	**15**			
Total all	**2,134**	**1,845**	**950**	**895**	**154**	**135**	**81**	**54**
Percent passive marks	**2.7%**	**2.4%**	**1.6%**	**5.2%**	**16.9%**	**26.2%**	**23.5%**	**31.6%**

There are also 13 CORSs connected by a single vector in the NA2011, but they are not considered no-check, because they were realized in a global solution in MYCS1 and were used as constraints. As a result of this, the percentages of no-check marks in Table 3.16 are with respect to passive marks (it includes 17 of the 183 disconnected "excluded" marks designated as no-check). Overall, 2.7% of NA2011 marks are no-check. However, much larger percentages are no-check in the Alaska and Pacific networks, due to the relatively large proportion of airport surveys in those projects. In Alaska, 17% of the NA2011 are no-check. For the Pacific networks, over a quarter (26%) of the marks are no-check. Such large numbers of no checks reduce the redundancy and thus affect network statistics for these networks, as discussed in Section 4.3.2.

3.6. Chapter 3 summary

This chapter described the methods used to prepare for and perform the various NA2011 Project network adjustments. The chapter began with a comparison of the differences between the NA2011 Project and the 2007 national adjustment, and these were summarized in a list of ten characteristics. Expanding upon those differences formed the bulk of the chapter's content.

Many different software packages were used for the NA2011 Project, and custom programs and scripts were written to perform specific tasks. The most significant program was, of course, *NETSTAT*, which was used to perform most of the network adjustments. *ADJUST* was used to adjust the Alaska and Pacific networks and to compute GPS project variance factors for projects loaded into the NGSIDB after November 2005. *HTDP* was used to transform all G-files to NAD 83 at epoch 2010.00, rather than just those located in tectonically active areas. To allow transformation of the Pacific network, the Philippine Sea tectonic plate was added to *HTDP* for

this project. GIS software—specifically Esri's *ArcGIS*—played a crucial role in visualization and analysis. The project could not have been completed in such a short time without GIS.

For the 2007 adjustment, nearly all CORSs were rigidly constrained by assigning a standard deviation ("sigma") of 0.01 mm to each component of the CORS coordinates. In contrast, weighted (stochastic) constraints were used for NA2011. This approach was possible because formal sigmas were available from the MYCS1 for most of the CORSs. Stochastic constraints seemed a more appropriate approach, given the great variation in MYCS1 sigmas (from 0.05 to 32.5 cm). In such a situation, stochastic constraints would not warp the network as much as rigid constraints, and it would likely result in more realistic sigmas on the adjusted (unconstrained) marks.

So-called GPS project "variance factors" were used to scale GNSS vector sigmas to provide consistent weighting of the combined observations and to appropriately scale the horizontal and vertical components. The same approach was used for the 2007 adjustment, but little specific documentation could be found anywhere at NGS concerning the computation process, so details were provided in this chapter.

CONUS was divided into a Primary and Secondary network, primarily on the basis of age, with observations older than 1994 relegated to the Secondary network (in general; exceptions were made to use some older projects in the Primary, and some younger observations in the Secondary network). Because of the large size of the two CONUS networks, Helmert blocking was used to perform the adjustments (62,364 marks and 335,530 vectors in the Primary network, and 22,503 marks and 84,493 vectors in the Secondary).

The following special methods used to perform the adjustments were discussed:

- Downweighting the up-component of the 16,118 vectors affected by subsidence in the northern Gulf Coast region, based on vector age and estimated subsidence rates.
- Separately adjusting the Alaska and Pacific networks using *ADJUST*. The entire Pacific network was adjusted using two separate sets of CORS constraints, one referenced to the Pacific plate (PA11 coordinates) and one to the Mariana plate (MA11 coordinates).
- Performing a series of iterative adjustments of the entire CONUS network to automatically reject and enable vectors. Doing so reduced the number of rejected vectors by nearly half, from about 43,000 to about 22,000.
- Reducing the number of no-check marks by approximately 700. This was accomplished by enabling rejected vectors (through relaxing the allowable size of residuals) connected to marks with only a single enabled vector tie.

The various methods employed to complete the NA2011 Project resulted in a final set of coordinates (and estimated network and local accuracies) for the marks in each of the four networks. These results are discussed in the next chapter.

Chapter 4. Analysis and Discussion of Adjustment Results

Final adjustments for the four NA2011 networks were completed in June 2012. Statistics from the final minimally constrained and fully constrained adjustments are summarized in Table 4.1 for each of the networks. Two final adjustments were performed for the Pacific network, one with the vectors referenced to the Pacific tectonic plate (designated PA11) and the other to the Mariana tectonic plate (designated MA11). The overall statistics for the two adjustments, however, are the same, although there were very slight differences in vector components and residuals due to the transformation to their respective frames. Note that the degrees of freedom (DOF) do not include the vectors rejected by downweighting.

Table 4.1. Summary of final adjustment statistics for the NA2011 Project. Statistics are identical for the Pacific network referenced to the Pacific and Mariana tectonic plates (PA11 and MA11, respectively).

	CONUS Primary	CONUS Secondary	Alaska**	Pacific (PA11 and MA11)
Number marks	62,364*	22,503*	972	540
Total number vectors	335,530	84,493	2846	1852
Number enabled vectors	325,251	73,541	2532	1794
Number rejected vectors	10,279	10,952	314	58
Percent vectors rejected	3.06%	12.96%	11.03%	3.13%
Number of subnetworks	36	222	2	3
Minimally constrained adjustments				
Degrees of freedom (DOF)	788,769	153,780	4686	3771
Standard deviation of unit weight	1.298	1.059	1.822	1.164
Fully constrained adjustments				
Number constrained marks	1125	5262	58	24
Degrees of freedom (DOF)	792,036	168,900	4854	3834
Standard deviation of unit weight	1.315	1.575	2.124	1.255

* *Includes 5321 marks in both the CONUS Primary and Secondary networks; network assigned based on source of final coordinates (5129 to the Primary and 192 to the Secondary network).*

** *Includes ties to three marks in CONUS and one in Hawaii, but results for those marks were not loaded into the NGSIDB.*

The total number of marks in the CONUS Primary and Secondary networks in Table 4.1 are greater than assigned to those networks, because 5321 are in both networks, as discussed in Section 3.3.2. There are three additional marks in the Alaska network that are in CONUS and were excluded from the Alaska network, as discussed in Section 2.4.1 and shown in Table 2.16 (although the marks are included in the CONUS network based on vector ties to them within CONUS).

Results of the final CONUS Primary and Secondary network adjustments were loaded into the NGS test database on June 13, 2012. By June 20, results from the Alaska and Pacific networks were also loaded into the test (development) database. Testing was conducted to ensure the correct mark information was being published on test NGS Datasheets (and that disconnected marks excluded). Once correct output was confirmed, the results from all five sets of adjustments were loaded into the production database on June 27, 2012.

4.1. Preliminary results and adjustment sequence

A large number of network adjustments were performed prior to final adjustments in June 2012. A year earlier, the first adjustment of the entire (minimally constrained) CONUS-plus-Alaska network was run to completion on June 21, 2011. It took 26 hours to complete and consisted of 59 Level 1 Helmert blocks (the 58 shown in Figure 3.8 plus an Alaska block). Many adjustments followed, in part due to additional data being pulled from the NGSIDB several times, until the final database pull on March 29, 2012. Although an adjustment ran to completion in June 2011, the results were preliminary and not entirely correct. Many challenges were encountered in performing adjustments. Most of these challenges were associated with correctly identifying Helmert block junction marks, as new data were added and any existing blocks were redefined (e.g., splitting the Minnesota from its initial two blocks to four blocks to speed up Level 1 computations). Other challenges in successfully performing adjustments were also encountered, and most have been previously discussed. These include:

- Identifying CORSs to use as constraints
- Evaluating rigid versus weighted (stochastic) constraints
- Identifying incorrect or missing GPS Project variance factors
- Removing GPS projects that should have been skipped and restoring accidentally skipped projects
- Finding duplicated marks
- Removing Alaska from the CONUS network
- Downweighting the up-component of vectors in northern Gulf Coast subsidence region
- Determining velocities of marks on the unmodeled Philippine Sea tectonic plate
- Identifying constraints for subnetworks created by splitting CONUS into Primary and Secondary networks
- Recognizing singularities created by disconnected marks
- Correcting input formatting errors

Another reason for such a large number of adjustments was the series of iterative minimally constrained adjustments done to automatically reject and enable vectors based on their residuals, as discussed in Section 3.5.3. The first set of these adjustments were performed in early January 2012 as complete CONUS adjustments (with Alaska removed, but before separating the vectors into Primary and Secondary networks). Results of the first six (and the final) iterations of this initial effort are listed below, each with its standard deviation of unit weight (σ_0):

Iteration 1: **Initial →** 384,305 vectors enabled (42,672 rejected = 9.99%), σ_0 = **1.329**
Iteration 2: **Enable 20,985 →** 405,290 vectors enabled (21,687 rejected = 5.08%), σ_0 = **1.405**
Iteration 3: **Reject 2046 →** 403,244 vectors enabled (23,733 rejected = 5.56%), σ_0 = **1.364**
Iteration 4: **Enable 1136 →** 404,380 vectors enabled (22,597 rejected = 5.29%), σ_0 = **1.368**
Iteration 5: **Reject 99 →** 404,281 vectors enabled (22,696 rejected = 5.32%), σ_0 = **1.368**
Iteration 6: **Enable 51 →** 404,332 vectors enabled (22,645 rejected = 5.30%), σ_0 = **1.367**
…
Last iteration: **Final →** 404,516 vectors enabled (22,461 rejected = 5.26%), σ_0 = **1.427**

The iterative adjustments were expedited by performing adjustments for each of the 58 Level 1 Helmert blocks simultaneously on separate computer central processing units. Using this quasi-parallel-processing approach, the time to perform a single minimally constrained adjustment decreased from about 25 hours to about 10 hours. Approximately ten iterations were required for the iterative adjustments to stabilize (i.e., for no change in the vectors identified for enabling or rejecting).

As can be seen by the above iteration results, the number of rejected vectors in the network was reduced by nearly half. Note this process occurred while the CONUS network underwent several changes over the course of the project. The changes included splitting CONUS into Primary and Secondary networks and downweighting the up component of vectors in the northern Gulf of Mexico subsidence region. In addition, data were added to the networks several times during the project, and these changes required the iterations be repeated. The final iterative adjustments were performed on the Primary network in March 21, 2102 and on the Secondary network on April 22, 2012. A single series of iterative reject/enable minimally constrained adjustments were also performed for both the Alaska and Pacific networks, although these were done manually in *ADJUST* (rather than the automated used for *NETSTAT*). Once the final iterative adjustments were completed, all subsequent edits to rejection status were done manually, based on analysis and refinements of later adjustments, including reducing the number of no-check marks (as described in Section 3.5.4).

Such a large number of adjustments were performed for the NA2011 Project that a complete tally was not maintained (particularly for the iterative reject/enable adjustments). Table 4.2 lists the main adjustments performed for the project, divided into the different types of networks. The table also shows the first (May 20, 2011) and last (March 29, 2012) downloads from the NGSIDB (a total of at least ten database downloads were performed for the project). The networks adjusted consisted of CONUS plus Alaska, CONUS only (with Alaska excluded), the CONUS Primary and Secondary networks, Alaska, and two versions of the Pacific (referenced to the Pacific and Mariana tectonic plates as PA11 and MA11, respectively). Although a complete transcript was not maintained of all adjustments performed, records from the project show at least 168 network adjustments were performed (97 using *NETSTAT* and 71 using *ADJUST*). Blank numeric entries in the table means the missing value was not available.

Table 4.2. Summary of database downloads and adjustments performed for the NA2011 Project.

	Date	Number projects	Number marks	GNSS vectors Total	Enabled	% reject	Std dev unit wt	Comment
Downloads from NGS Integrated Data Base							**Total of at least 10 database downloads**	
First	5/20/2011	4127	77,694	398,588				
Last	3/29/2012	4267	81,055	424,721				
CONUS + Alaska adjustments							**Total of at least 23 adjustments**	
First (free)	6/21/2011	4127	77,694	398,588			?	First run, but with errors
Second (free)	6/30/2011	4139	78,155	404,768	364,509	9.95%	1.62	First successful run
First rigid constrained	8/24/2011	4127	77,726	395,836	353,548	10.68%	1.37	Previous failed
First weighted constrained	10/4/2011				367,256		1.25	
Last weighted constrained	11/17/2011		79,107	414,455	371,962	10.25%	1.27	
Last rigid constrained	11/17/2011		79,107	414,455	371,962	10.25%	1.52	
Last adjustment (free)	12/21/2012		80,245		386,223		1.356	
CONUS only adjustments							**Total of at least 13 adjustments**	
First iterative (free)	1/1/2012	4067	79,304	426,977	384,305	9.99%	1.329	First in series of ~10
Last iterative (free)	1/4/2012	4067	79,304	426,977	404,516	5.26%	1.427	Last in series of ~10
Last weighted constrained	1/18/2012	4067	79,304	426,977	404,631	5.23%	1.38	
Last rigid constrained	1/24/2012	4067	79,304	426,977	404,631	5.23%	2.20	Last rigid adjustment
CONUS Primary adjustments							**Total of at least 30 adjustments**	
First free	2/21/2012	3556	63,005	351,083	334,272	4.79%	2.67	Missing variance factors
Second free	2/28/2012	3568	63,207	353,327	330,545	6.45%	1.384	
First constrained	3/16/2012	3571	63,253	353,821	340,962	3.63%	1.335	
Final constrained	**6/4/2012**	**3472**	**62,364**	**335,530**	**325,251**	**3.06%**	**1.315**	**Loaded in NGSIDB**
Final free	6/7/2012	3472	62,364	335,530	325,251	3.06%	1.298	
CONUS Secondary adjustments							**Total of at least 15 adjustments**	
First free	4/18/2012	614	22,503	84,493	70,251	16.86%	1.120	
First constrained	5/15/2012	614	22,503	84,493	73,461	13.06%	1.575	Not all constraints used
Final free	6/4/2012	614	22,503	84,493	73,541	12.96%	1.059	
Final constrained	**6/9/2012**	**614**	**22,503**	**84,493**	**73,541**	**12.96%**	**1.575**	**Loaded in NGSIDB**
Alaska adjustments							**Total of at least 10 NETSTAT and 43 ADJUST adjustments**	
First free (NETSTAT)	4/26/2012	142	969	2,846			1.833	
First free (ADJUST)	5/29/2012	142	972	2,846	2,458	13.63%	1.847	
First iterative (free)	6/3/2012	142	972	2,846	2,458	13.63%	1.847	First in series of 23
Last iterative (free)	6/10/2012	142	972	2,846	2,532	11.03%	1.822	Last in series of 23
Final free	6/10/2012	142	972	2,846	2,532	11.03%	1.822	
Final constrained	**6/13/2012**	**142**	**972**	**2,846**	**2,532**	**11.03%**	**2.124**	**Loaded in NGSIDB**
Pacific adjustments (PA11 and MA11)							**Total of at least 6 NETSTAT and 28 ADJUST adjustments**	
First free (ADJUST), PA11	5/30/2012	39	540	1,852	1,740	6.05%	1.159	
First iterative (free), MA11	6/13/2012	39	540	1,852	1,741	5.99%	1.159	First in series of 11
Last iterative (free), MA11	6/15/2012	39	540	1,852	1,792	3.24%	1.161	Last in series of 11
Final free (both)	6/15/2012	39	540	1,852	1,794	3.13%	1.164	
Final constrained (both)	**6/15/2012**	**39**	**540**	**1,852**	**1,794**	**3.13%**	**1.255**	**Loaded in NGSIDB**
All network adjustments							**Total of at least 168 network adjustments performed for project**	

4.2. Analysis of GNSS network vectors

An analysis of the enabled vector residuals for each of these networks is given in the following three sections: 4.2.1 (CONUS Primary and Secondary) , 4.2.2 (Alaska), and 4.2.3 (Pacific). Rejected vectors are discussed in Section 4.2.4, the effect of vector lengths is explored in Section 4.2.5, and a loop analysis of vector misclosures is covered in Section 4.2.6.

Earlier in this report, two tables (Table 2.10 and Table 3.9) and three figures (Figure 2.9, Figure 2.10, and Figure 3.10) provide information on the number of vectors and observation durations, including distributions by time. Those tables and figures, however, did not provide much detail concerning the numbers of vectors and duration by year for each of the four networks. Figure 4.1, Figure 4.2, and Figure 4.3 provide additional details for the individual networks.

Figure 4.1 shows the number of enabled vectors by year. The top chart is of the CONUS Primary and Secondary networks. A log scale is used for the vertical axis (number of vectors) because of the extreme variation in the number of vectors, from a minimum of eight in 1987 for the Primary network, to a maximum of 34,611 in 2004, also for the Primary network. The bottom chart is of the Alaska and Pacific networks. An arithmetic scale is used for the number of vectors, because the variation is not nearly so great as for the CONUS networks. The minimum and maximum number of vectors both occur in the Pacific network, in 1997 and 1993, respectively.

Figure 4.2 and Figure 4.3 show the mean- and median-enabled vector observation durations, respectively, for the four networks. The durations exceed the maximum value on the horizontal axis for the Pacific network in three years (2000, 2009, and 2010) for the mean durations, and in two years (2000 and 2010) for the median durations. These off-the-chart mean and median values are given in the figure captions. Figure 4.2 and Figure 4.3 do not show observations from all four networks for most years, and this can make these figures somewhat difficult to read because of the resulting unequal number of duration bars per year. Observations are represented for all networks in only six years (1993, 1995, 1997, 2000, 2001, and 2004).

The longest durations in Figure 4.2 and Figure 4.3 correspond to the Pacific network, and this makes sense, as long occupation times were required due to the great distances between islands. The next longest durations are associated with Alaska, as Alaska similarly often involves long distances. Together, those account for all of the mean and median observations exceeding 13 hours, with the exception of a conspicuously large duration in the last year of the Secondary network in 2005. This large duration is also odd because the median (23.9 hours) is longer than the mean (20.3 hours). The reason for these odd statistics is the unusual distribution of durations: 16% of the observations are less than 6 hours, and 82% are almost exactly 24 hours (the remaining 2% are 12 to 22 hours). There are only two Secondary projects in 2005, and both were put into the Secondary network because they are in subsidence regions. One is GPS2422 in the Central Valley of California and its observations are less than six hours. The other is GPS2305 in the Harris-Galveston Subsidence District region, and all of its observations are greater than 12 hours.

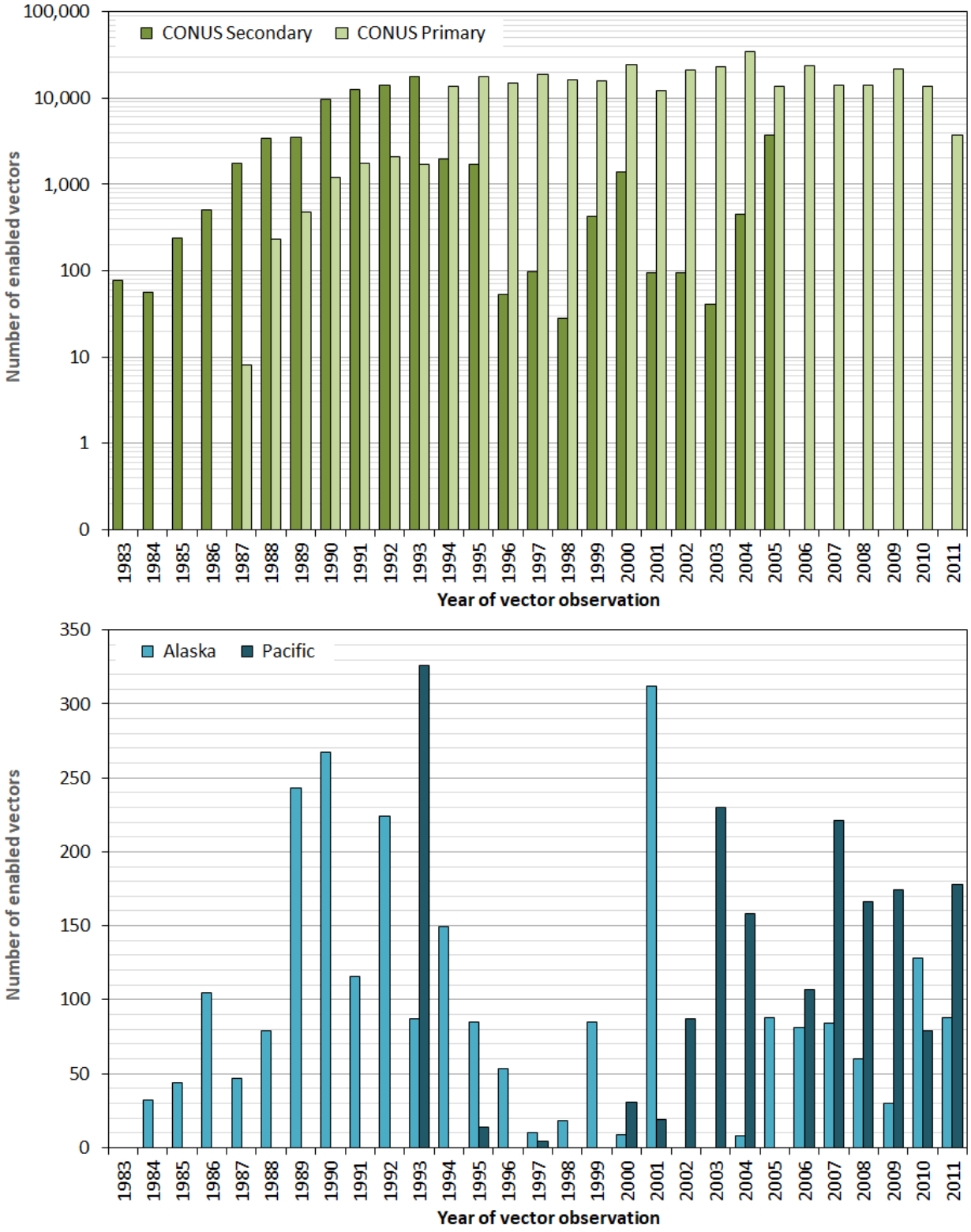

Figure 4.1. Number of enabled vectors by year for the four NA2011 networks. The Primary and Secondary networks (top) use a log scale for vertical axis because of the large range in number of vectors; the Alaska and Pacific networks (bottom) use an arithmetic scale.

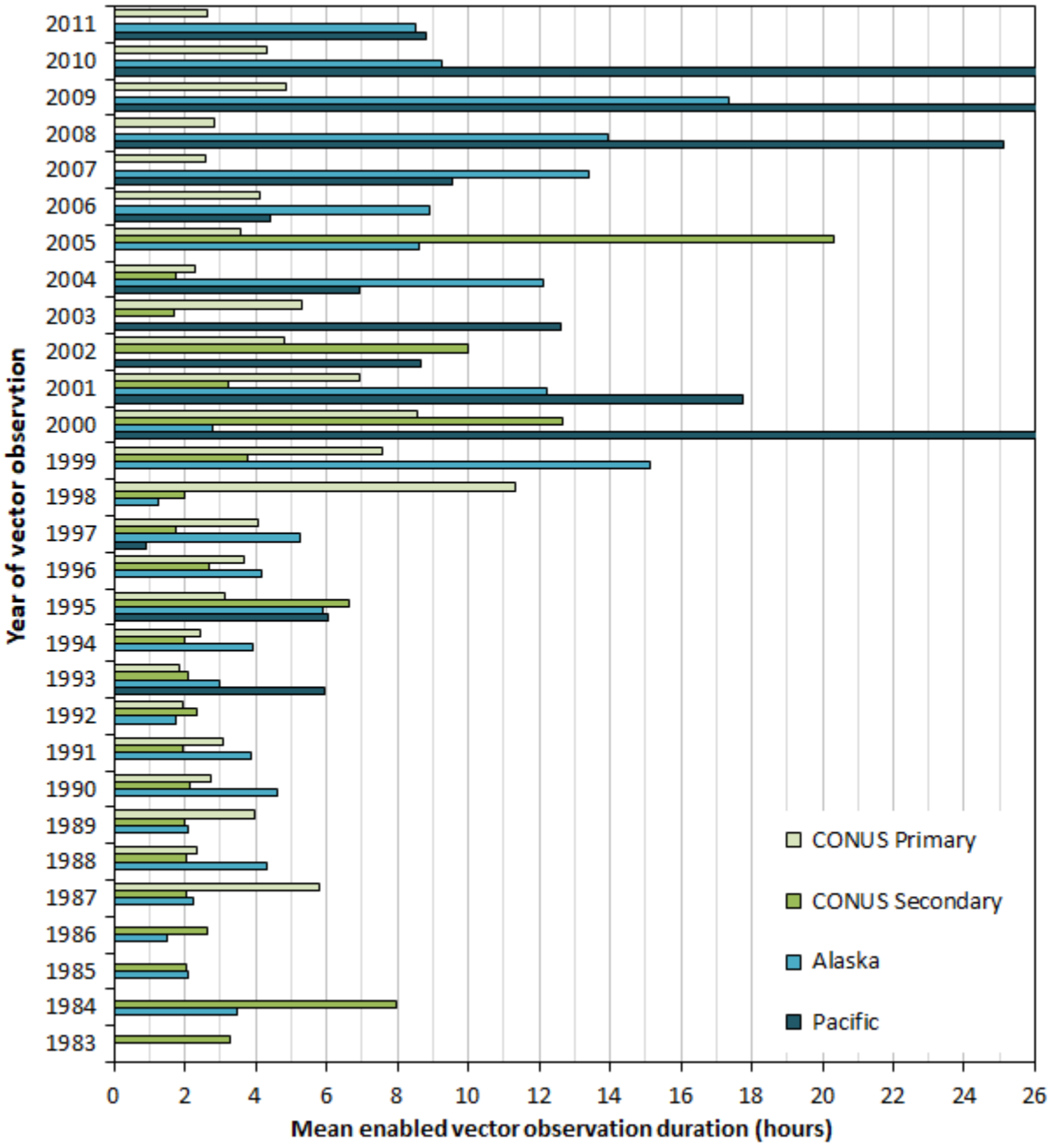

Figure 4.2. Mean vector observation duration by year for the four NA2011 networks. The three Pacific network values exceeding the duration scale are 37.9 hr in 2010, 44.4 hr in 2009, and 36.0 hr in 2000.

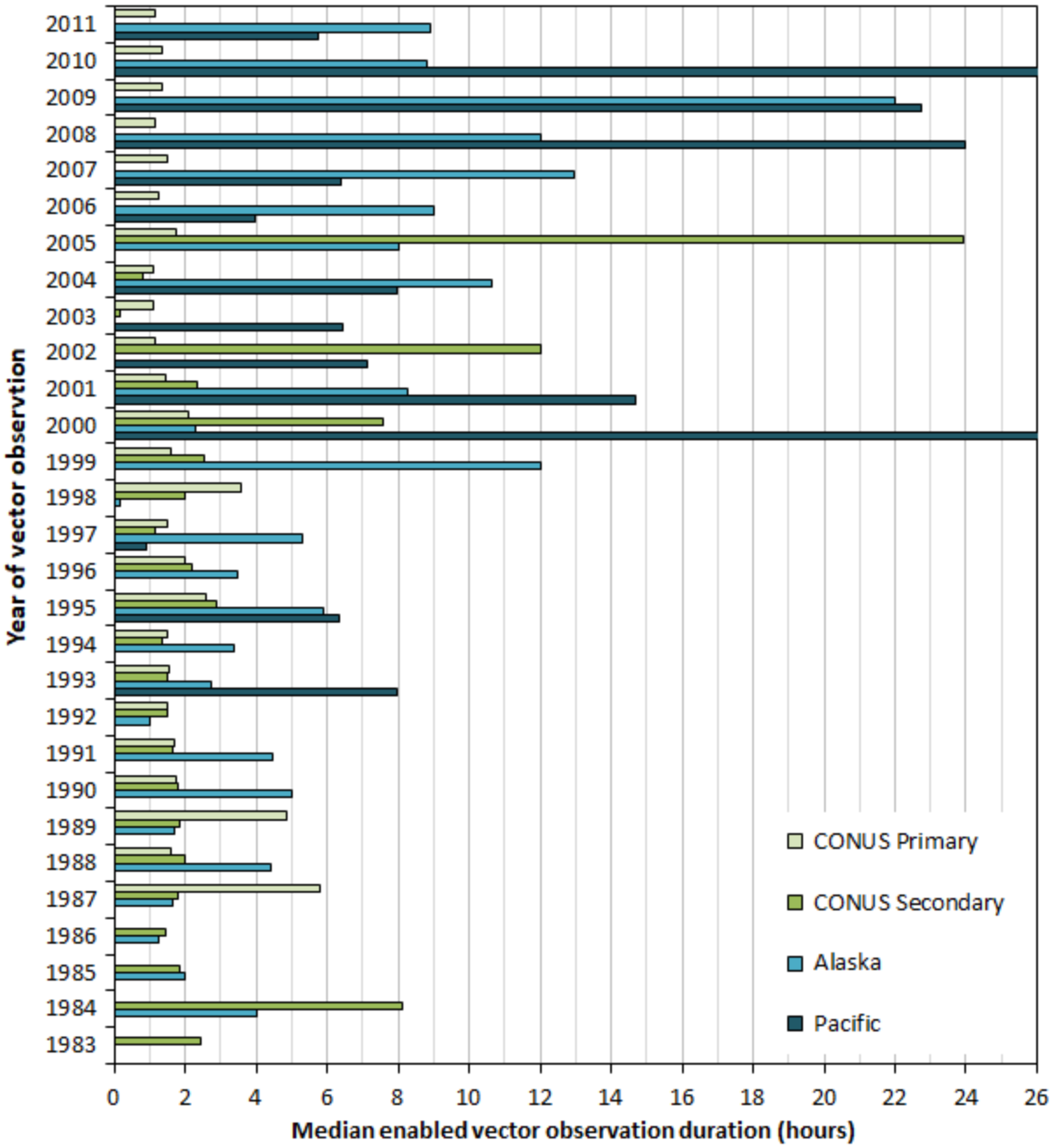

Figure 4.3. Median vector observation duration by year for the four NA2011 networks. The two Pacific network median values exceeding the duration scale are 44.4 hours for 2010 and 47.8 hours for 2000.

4.2.1. CONUS Primary and Secondary network vectors

Statistics of the enabled GNSS vector residuals for the final minimally constrained adjustments of the CONUS Primary and Secondary networks are provided in Table 4.3. Histograms of the residuals (over a range of ±3 cm) for both networks are given in Figure 4.4. Table 4.3 shows that 95% of the centered residuals (from percentiles 2.5% to 97.5%) are within about ±1.2 and

±2.5 cm (horizontal and up) for the Primary network, and are within about ±1.5 and ±2.9 cm (horizontal and up) for the Secondary network. Both histograms in Figure 4.4 show more than 95% of the residuals for all components of both networks.

Table 4.3. Enabled vector residual statistics for the CONUS Primary and Secondary networks.

	Minimum constraint enabled vector residuals (cm)					Date observed (decimal year)	Duration (hours)
	North	East	Up	Horz	3D		
CONUS Primary network							
Number	**325,251** (10,279 rejected vectors not included)						
Minimum	-8.61	-8.85	-9.82	0.00	0.00	1987.86	0.02
Maximum	5.25	7.22	10.19	8.87	10.23	2011.97	218.07
Mean	-0.004	-0.005	-0.010	0.607	1.077	2002.54	4.74
RMSE	±0.57	±0.58	±1.14	±0.81	±1.40	±2002.54	±9.64
Percentiles							
0.5%	-2.00	-2.11	-3.91	0.01	0.04	1990.68	0.08
2.5%	-1.21	-1.22	-2.54	0.05	0.11	1994.11	0.48
5.0%	-0.90	-0.90	-1.87	0.08	0.17	1994.71	0.57
50.0% (median)	**0.00**	**0.00**	**0.00**	**0.46**	**0.82**	**2003.02**	**1.40**
95.0%	0.89	0.88	1.85	1.66	2.93	2010.07	23.98
97.5%	1.20	1.20	2.54	2.08	3.55	2010.45	24.00
99.5%	2.01	2.05	3.93	3.10	4.65	2011.30	47.75
CONUS Secondary network							
Number	**73,541** (10,952 rejected vectors not included)						
Minimum	-12.11	-17.46	-21.11	0.00	0.00	1983.47	0.02
Maximum	10.84	18.73	16.92	20.86	21.82	2006.00	194.38
Mean	0.004	-0.015	-0.015	0.719	1.263	1992.86	3.38
RMSE	±0.71	±0.73	±1.32	±1.01	±1.67	±1992.87	±6.63
Percentiles							
0.5%	-2.60	-2.67	-4.22	0.00	0.00	1985.92	0.20
2.5%	-1.52	-1.56	-2.89	0.01	0.03	1987.43	0.58
5.0%	-1.09	-1.10	-2.22	0.05	0.12	1988.38	0.77
50.0% (median)	**0.00**	**0.00**	**0.00**	**0.51**	**0.96**	**1992.44**	**1.68**
95.0%	1.10	1.07	2.21	2.14	3.43	2005.02	23.93
97.5%	1.50	1.50	2.91	2.67	4.06	2005.51	23.93
99.5%	2.55	2.66	4.19	3.70	5.23	2005.77	23.98

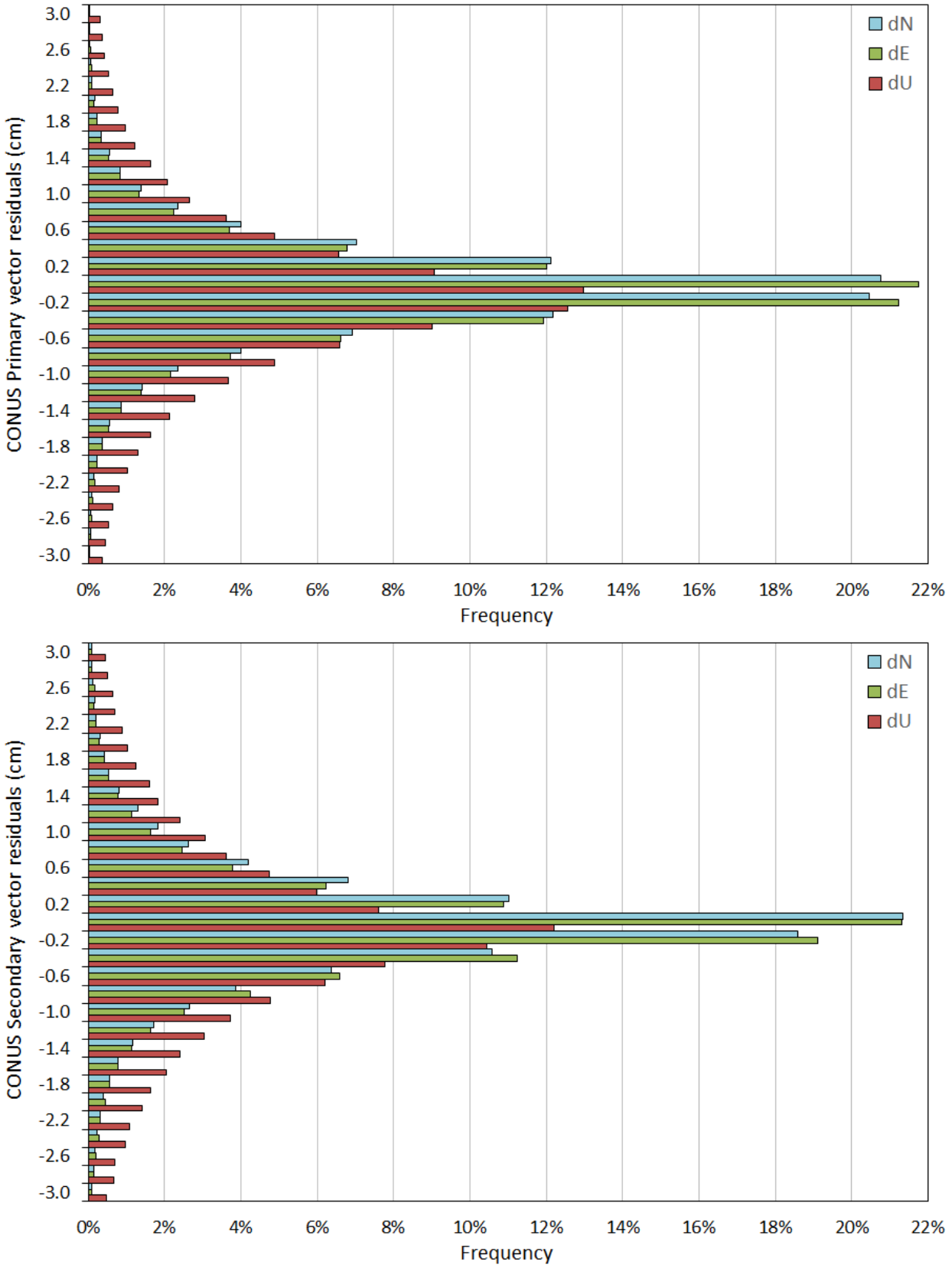

Figure 4.4. Histograms of CONUS networks vector residuals, Primary (top) and Secondary (bottom).

As both Table 4.3 and Figure 4.4 show, the residuals for both networks are centered on zero, the distributions are not discernably skewed, and the Primary network residuals exhibit considerably less dispersion. Despite the presence of some large outliers (discussed below), the mean is near zero and the median is zero by vector component. The difference in precision of residuals between the two networks is reflected by their ranges, root mean square error (RMSE), and the peakedness of their histograms. RMSE values for the Primary network are ±0.6 and ±1.1 cm (horizontal and up) and ±0.7 and ±1.3 cm (horizontal and up) for the Secondary network.

Vector observation date and duration for both CONUS networks are also given in Table 4.3. As expected and intended, the Primary network observations generally occur later (from 1987.86 to 2011.97, with a median of 2003.02) than the Secondary observations (from 1983.47 to 2006.00, with a median of 1992.44). The observation durations do not vary substantially between the two networks. For both, 95% of the durations are between about 0.5 and 24 hours. The median and mean values are 1.4 and 4.7 hours for Primary and 1.7 and 3.4 hours for Secondary.

Figure 4.5 shows the median and mean minimally constrained 3D residuals grouped by year for the Primary and Secondary networks. The median and mean values are similar, despite the presence of outliers, due to the small number of outliers (discussed below). For the Primary network, the residual magnitudes show an overall decrease with time, particularly from 1988 to 1993. After 1996, the residuals are fairly constant, with a median and mean over that period of roughly 0.8 and 1.1 cm, respectively. The marked increase in residual magnitudes in 2011 was due to a relatively high number of large residuals in several projects. Of 3771 enabled vectors, 110 (2.9%) had enabled 3D residual of 4 cm or greater. These large residuals occurred in nine projects, with most in three large projects, each with more than 1000 vectors: GPS2835 (California), GPS2829 (Wisconsin), and GPS2842 (South Carolina). Notably, two of the projects (GPS2842 and GPS2852) were the only two in NA2011 with erroneous covariances from *Trimble Business Center*, which is discussed in Section 5.1.3. In contrast, the year prior (2010) has the smallest residual magnitudes: of 13,699 enabled vectors, 97 (0.7%) had 3D residuals of 4 cm or greater. For comparison, 1.4% of all enabled Primary vectors have residual magnitudes of 4 cm or greater.

For the Secondary network, the trend is not as clear. There is an overall decrease in the mean residual magnitude from 1983 to 1995. This trend is exhibited by the median from 1988 to 1995, however it is much more irregular prior to 1988. The large increase in residual magnitude from 1997 to 2000 peak, followed by a decrease to 2003, then another increase to 2006. These large residuals, and the somewhat erratic behavior, is due to downweighting of the up-component of the vector uncertainties in the northern Gulf Coast region. Recall from Section 3.5.1 that most of the Secondary network vectors after 1994 were put into the network, because they had one end in the Gulf Coast subsidence region. Of the 8156 Secondary vectors from 1995 to 2005, 6403 (78.5%) are downweighted, and 191 (2.3%) have a 3D residual of 4 cm or greater. For the peak residual magnitude in 2000, there are 1401 Secondary vectors, with all but four downweighted, and 126 (9.0%) have a 3D residual of 4 cm or greater. This percentage is substantially larger than the 2.7% of all enabled Secondary vectors with residual magnitudes of 4 cm or greater.

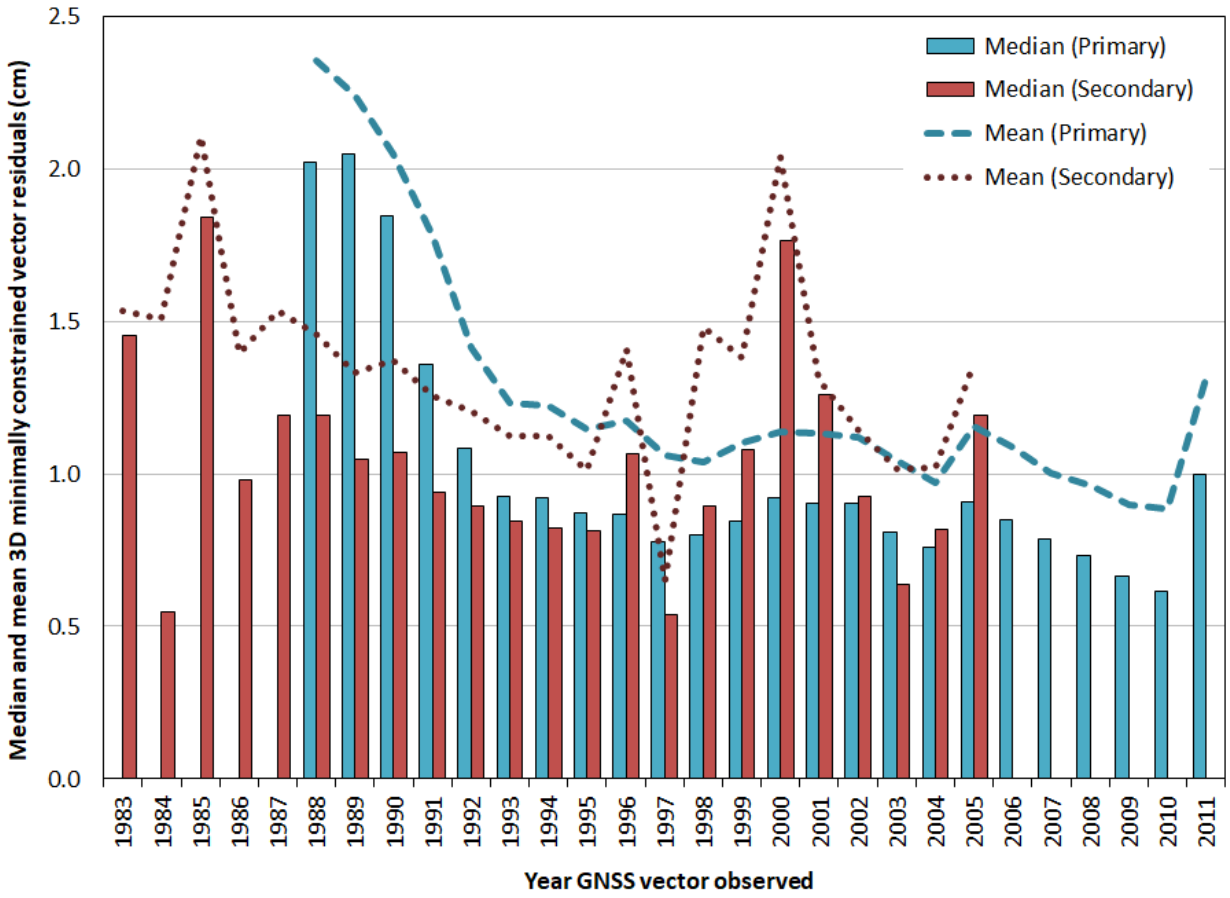

Figure 4.5. Median and mean CONUS Primary and Secondary 3D vector residuals by year observed.

Figure 4.6 shows the enabled minimally constrained residual magnitudes by observation duration for the Primary and Secondary networks (omitting the four Secondary residuals greater than 20 cm). The top chart shows durations from 1 minute to 100 hours (Table 4.3 shows a maximum duration of 218 hours for Primary and 194 hours for Secondary, but this only applies to a total of 70 of 398,792 vectors). To provide more detail for the much more common shorter durations, the bottom chart only shows those of 10 hours or less (accounting for 90.5% of observations).

Visually, overall Figure 4.6 suggests a decrease in residuals with increasing observation duration, particularly for the Secondary vectors and for the top chart (up to 100 hours). The trend is not as clear for the bottom chart (10 hours and less), particularly for the Primary vectors. For both cases, an envelope based on the larger residuals would reflect this trend. However, there is a great deal of scatter and variability, so it is not quite clear how much duration affects residuals, although it does seem to reduce the number of large residuals.

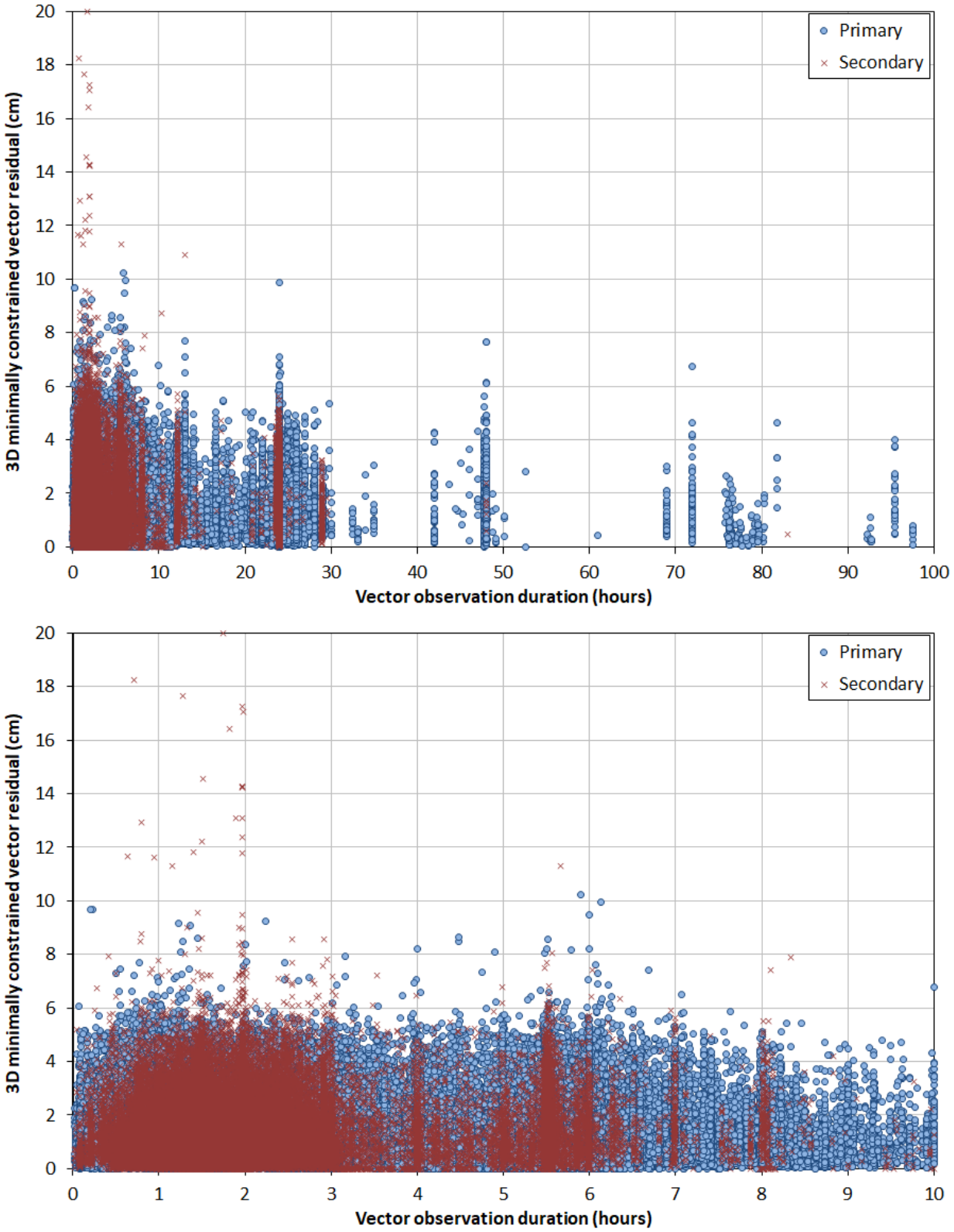

Figure 4.6. CONUS Primary and Secondary 3D vector residuals by observation duration. The upper plot is for durations from 1 minute to 100 hours. The bottom plot is from 1 minute to 10 hours.

The number of 3D residuals grouped in bins by magnitude are shown in Figure 4.7 for both networks, and for both minimally constrained or "free" (top) and fully constrained (bottom) cases. A log scale is used for the number of residuals to emphasize the residual tails that have large magnitudes but are few in number (to allow counting the number of residuals directly from the chart). The value on the horizontal axis is the upper end of the residual magnitude for its bin. The tail is much longer for constrained residuals, to the degree it requires a large range in magnitude to display all vector residuals (maximum of 155 cm). Consequently, the bins for constrained residuals are not all of equal size. The value on the horizontal axis is the upper end of the residual magnitude for its bin.

Free residuals for the Secondary network in Figure 4.7 exhibit a substantially longer tail than Primary residuals. Of the ten vectors in the 16 to 22 cm bins, eight are from a single 1991 Alabama project, GPS306. In fact, 16 of the 26 vectors with residuals greater than 10 cm are from that project. Although fairly large, this is an extremely small number of residuals, less than 0.04% of the Secondary network.

Constrained residuals in Figure 4.7 for the Primary vectors do not differ much from the free residuals; the constrained 10 to 15 cm bin contains two vectors (versus one vector in the 10 to 11 cm bin for free). This indicates the constraints were consistent with the vector geometry and weights, and it is also reflected by the small increase in the standard deviation of unit weight in Table 4.1, from 1.298 (free) to 1.315 (constrained), an increase of only 1.3%.

Secondary network constrained residuals show a much longer tail, with four vectors in the 130 to 160 cm bins (all from 1991 South Carolina project GPS335). In addition, there is a large gap in the Secondary residual tail; the next largest bin is 60 to 70 cm and contains five vectors. As expected in such a case, Table 4.1 shows a substantial increase in the standard deviation of unit weight, from 1.059 (free) to 1.575 (constrained), an increase of 49%. Clearly the long constrained residual tail is a manifestation of inconsistency between the weighted constraints used for the Secondary network and the geometry of the vectors (and their uncertainties).

Of the 5262 constrained marks in the Secondary network, 5217 (99.1%) were passive marks common to both networks with coordinates (and uncertainties) determined in the Primary network. From Table 3.10, the sigmas (determined in the Primary adjustment) used for weighting the constraints had median values of 0.29, 0.25, and 0.64 cm for the north, east, and up components, respectively. Based on the large increase in standard deviation of unit weight in the Secondary network constrained adjustment, it appears that at least some of these sigmas were too small. Increasing constrained coordinate sigmas would have likely improved the adjustment statistics (and reduced the long residuals tail).

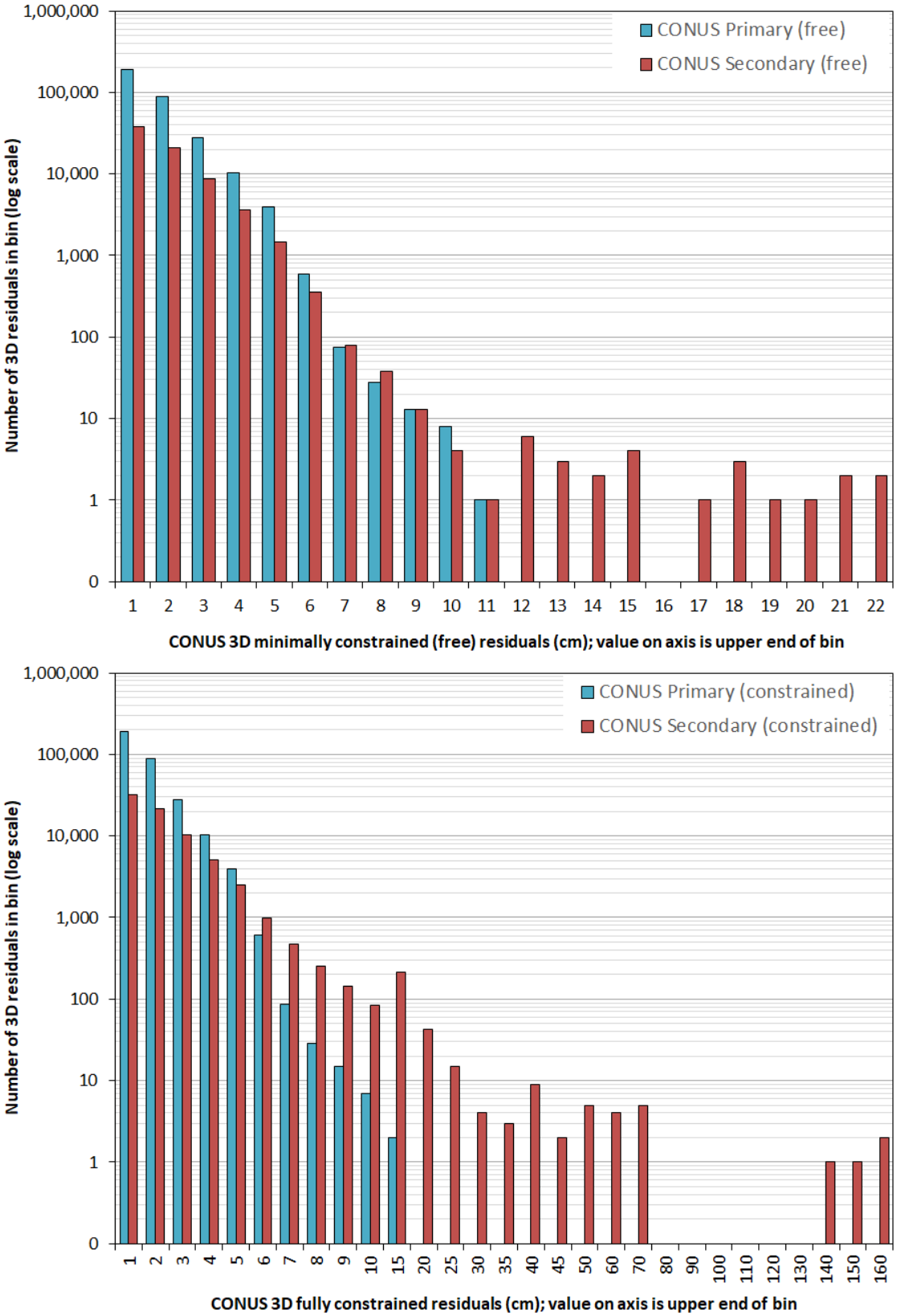

Figure 4.7. CONUS free (top) and constrained (bottom) 3D vector residuals grouped by magnitude (log scale on vertical axis). Note the much larger range of the horizontal axis for constrained residuals.

The sigmas from the Primary network marks used as constraints for the Secondary network were not modified. To do so would first require determining an appropriate approach (for example, by comparing the constrained mark shifts to their sigmas). An obstacle in performing such analyses was that a single fully constrained adjustment took about a week to compute. Only two constrained adjustments of the Secondary network were performed for the NA2011 Project. The first constrained only 3002 (57%) of the 5262 available marks, and took less than a week. The one constrained adjustment using all 5262 available constrained marks was completed on June 9, 2012 (see Table 4.2). At that time, the Alaska and Pacific network adjustments had not yet been completed. With a June 30 deadline for loading results into NGSIDB, there was not time to perform additional analyses and adjustments for the constrained Secondary network.

The presence of long residuals tails was also reported for the 2007 national adjustment by Milbert (2009). The tails were overall reduced somewhat for NA2011, particularly in the Primary network. The 95th percentile free horizontal and absolute value up residuals for the combined NA2011 Primary, Secondary, and Alaska networks were 1.77 and 2.64 cm, respectively, versus 2.02 and 2.73 cm for the 2007 network (which included CONUS and Alaska).

Maps showing the distribution of minimally constrained 3D vector residuals for the Primary and Secondary networks are in Figure 4.8 and Figure 4.9 for CONUS, and for the Primary network in the Caribbean in Figure 4.10 (there were no Secondary vectors in the Caribbean). For all three figures, the upper map shows enabled vectors only and the lower map shows rejected vectors only (recall from Section 3.5.3 that vectors were rejected by downweighting, so they still have residuals, even though the rejected vectors did not contribute to determining adjusted coordinates are network statistics). The maps were prepared such that the largest residuals are on top, to make them more readily visible. For both networks, the distribution of residuals is not uniform, with most apparently concentrated in specific states. However, this is not necessarily the case, since a state with more vectors will appear to have a larger proportion of rejections, even if the percent rejected is the same as another state with less vectors. The distribution of vector rejections is discussed in more detail in Section 4.2.4.

4.2.2. Alaska network vectors

Statistics of the enabled GNSS vector residuals for the final minimally constrained adjustment of the Alaska networks are given in Table 4.4. A histogram of the residuals is shown in Figure 4.11, over a range of ±9 cm. The full range of residuals in Table 4.4 is much larger (maximum magnitudes of 22 cm horizontal and 38 cm up), but it also shows 95% of the centered residuals (from percentiles 2.5% to 97.5%) have maximum magnitudes of 6.4 cm horizontal and 8.7 cm up. So, the histogram shows more than 95% of the residuals for all components (including the full range of residuals would conceal details of the vast majority of data).

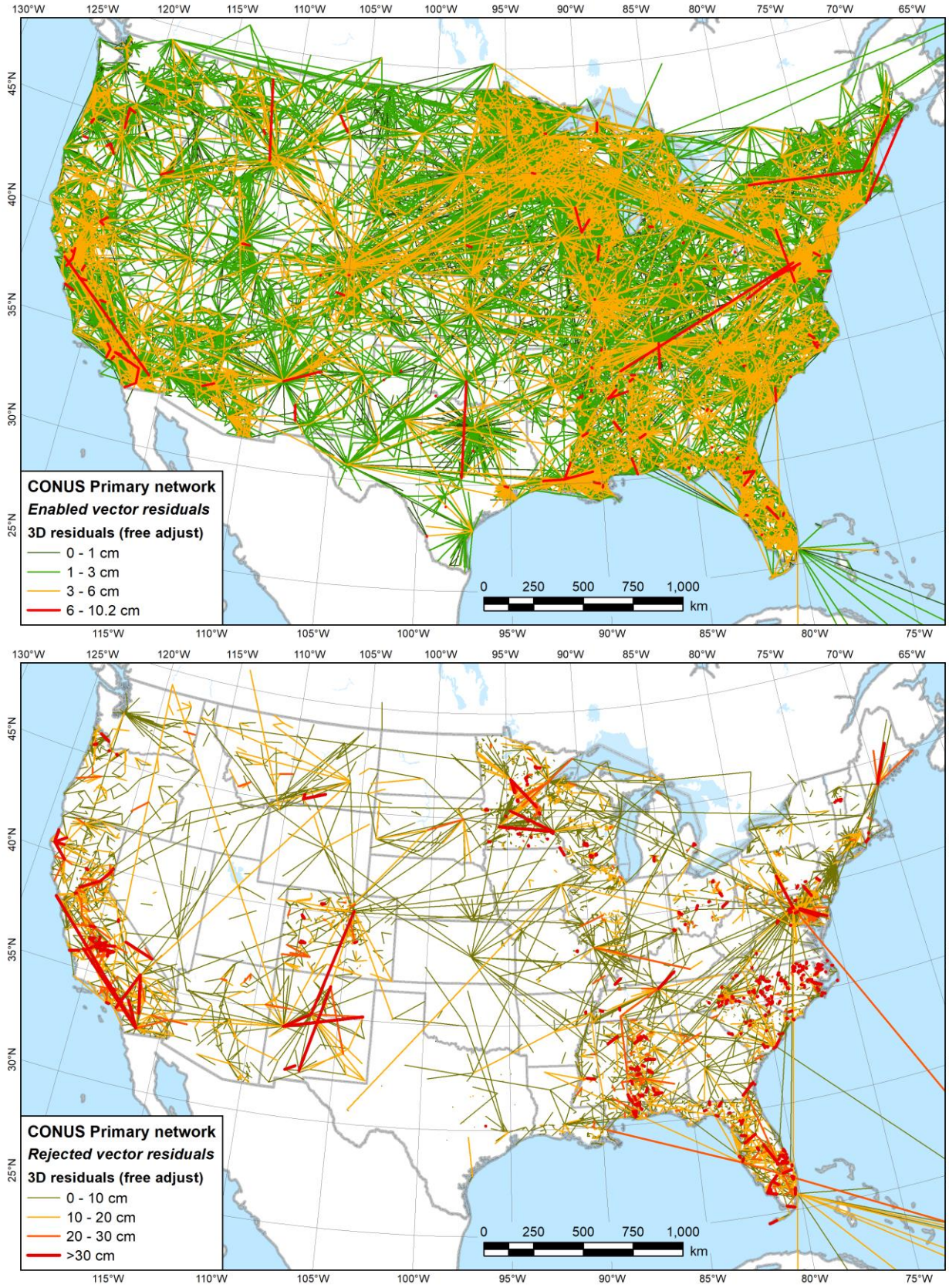

Figure 4.8. Map of CONUS Primary network vector residuals, enabled (top) and rejected (bottom).

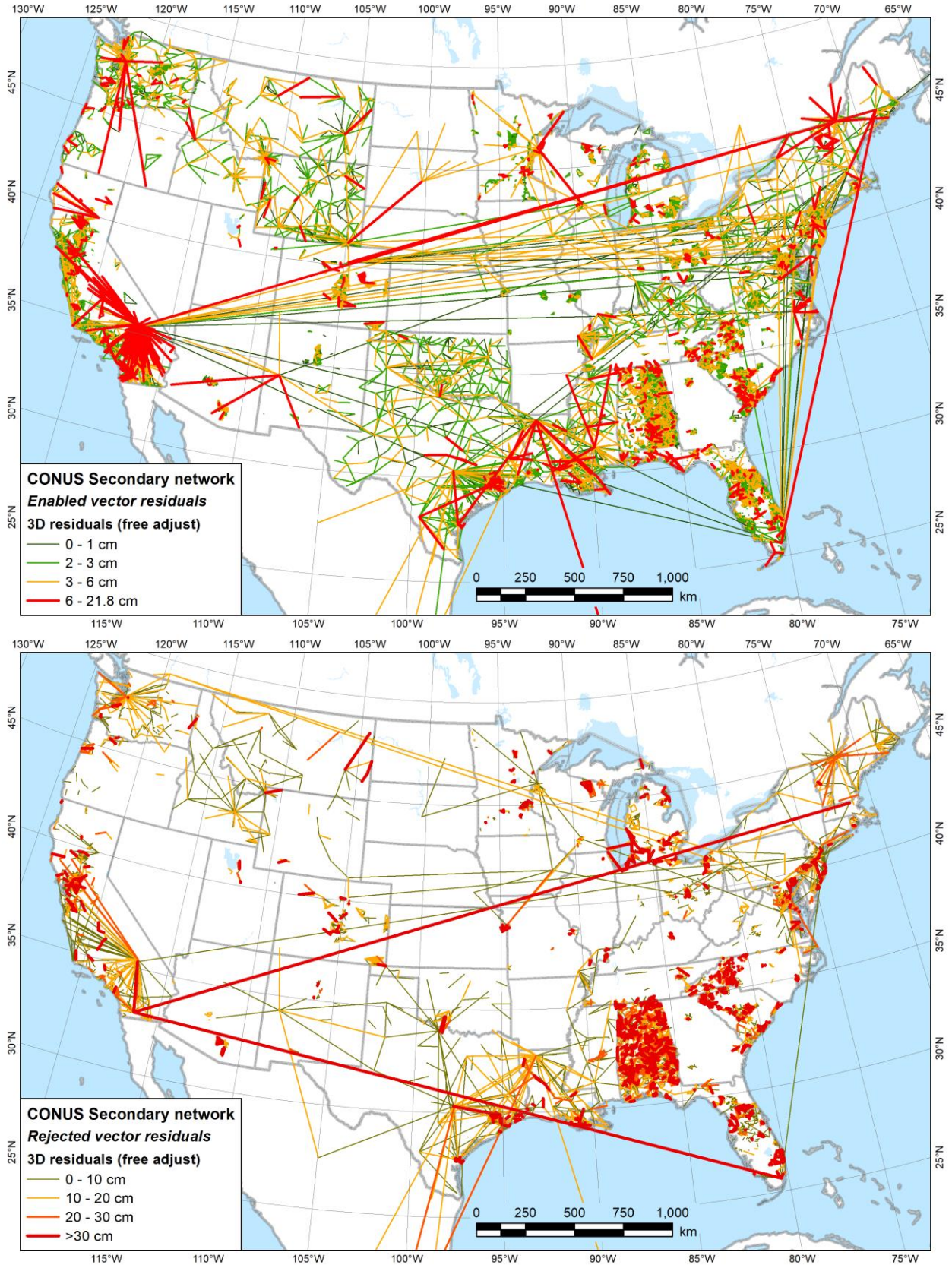

Figure 4.9. Map of CONUS Secondary network vector residuals, enabled (top) and rejected (bottom).

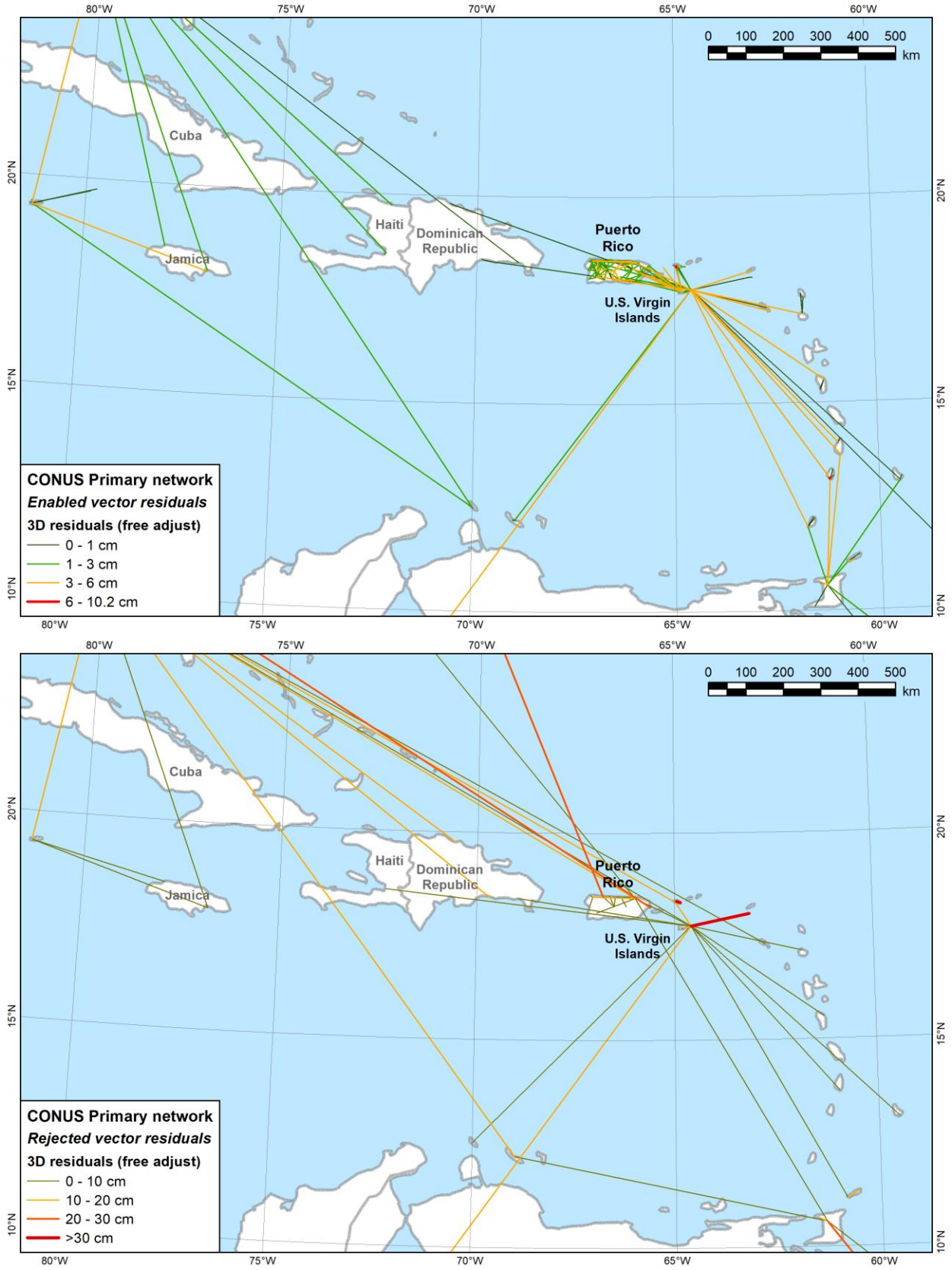

Figure 4.10. Network vector residuals in the Caribbean, enabled (top) and rejected (bottom).

Table 4.4. Enabled vector residual statistics for the Alaska network.

	Minimally constrained enabled vector residuals (cm)					Observation date (decimal year)	Duration (hours)
	North	East	Up	Horz	3D		
Number	**2532** (314 rejected vectors not included)						
Minimum	-17.11	-22.10	-38.23	0.00	0.00	1984.61	0.03
Maximum	15.33	17.70	18.65	22.47	38.32	2011.58	30.63
Mean	0.086	0.050	-0.217	1.858	2.903	1996.68	6.38
RMSE	±2.24	±2.56	±3.49	±3.40	±4.88	±1996.69	±9.12
Percentiles							
0.5%	-9.27	-10.98	-17.57	0.00	0.00	1984.63	0.08
2.5%	-4.76	-5.80	-8.69	0.00	0.00	1985.70	0.17
5.0%	-2.95	-3.47	-5.40	0.00	0.01	1986.51	0.97
50.0% (median)	**0.00**	**0.00**	**0.00**	**0.68**	**1.37**	**1994.48**	**4.42**
95.0%	3.18	3.65	4.40	8.30	11.21	2010.60	24.00
97.5%	5.29	6.38	6.84	10.93	14.01	2011.50	24.00
99.5%	10.44	11.91	11.37	14.99	20.29	2011.57	24.00

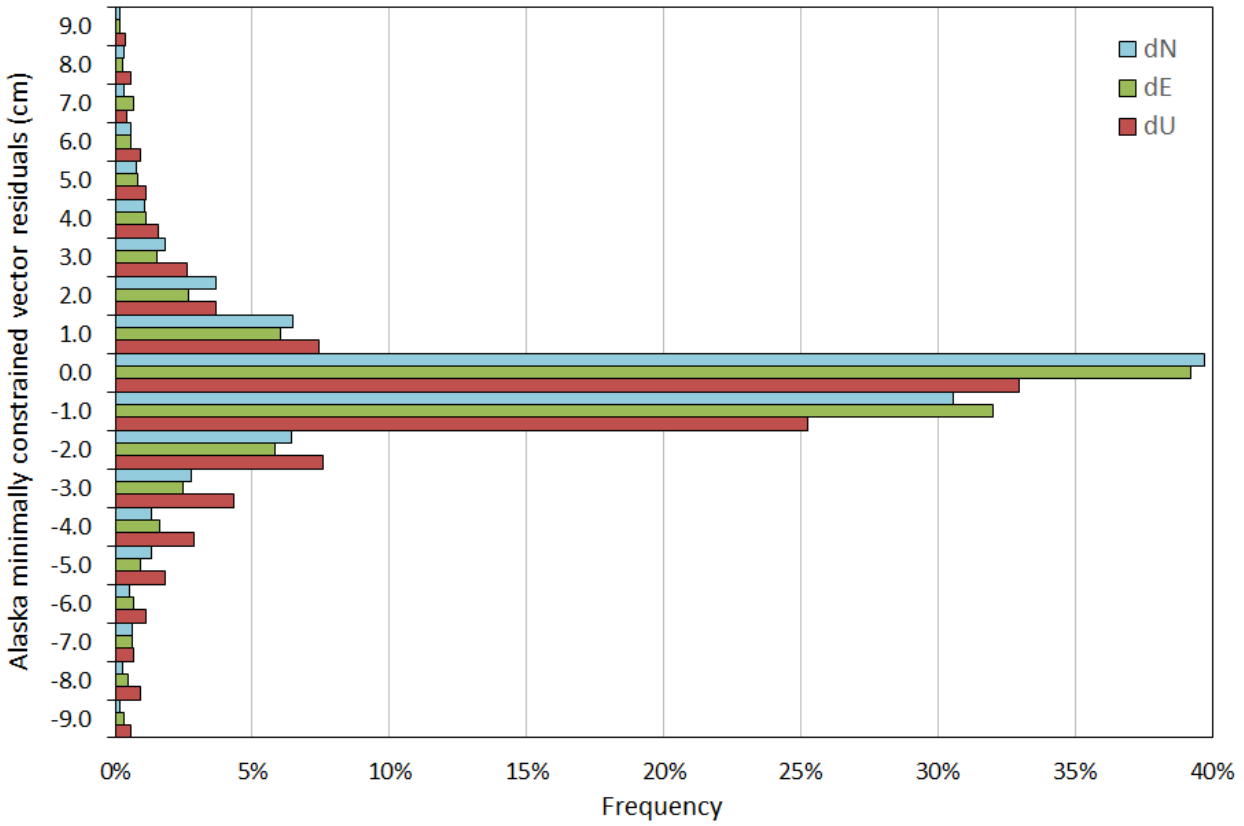

Figure 4.11. Histogram of enabled minimally constrained vector residuals for Alaska network.

As Figure 4.11 shows, the residuals for both networks are centered near zero and the distributions are not discernably skewed. Despite the presence of some large outliers (discussed below), for all components the median is zero, and the mean is close to zero, although the mean of the up residuals is biased slightly negative (-0.2 cm). RMSE values are ±2.24 cm north, ±2.56 east, and ±3.5 cm up. The pronounced peakedness of the histogram is due to the large proportion of no-check marks (16.9%; see Table 3.16). No-check marks have residuals of zero (or very close to zero for correlated simultaneously processed solutions), causing a large peak in the zero (±1.0 cm) histogram bin. A total of 5.0% of the Alaska 3D residuals are exactly zero, compared with 0.2% for the Primary and 1.6% for the Secondary networks.

Figure 4.12 shows the median and mean minimally constrained 3D residuals grouped by year for the Alaska network (vector observation dates and duration are given in Table 4.4). Most of the observations in Alaska are fairly old (see Figure 4.1); the mean and median dates are 1996.7 and 1994.5. Durations range from 2 minutes to 30.6 hours, with a mean and median of 6.4 and 4.4 hours, respectively.

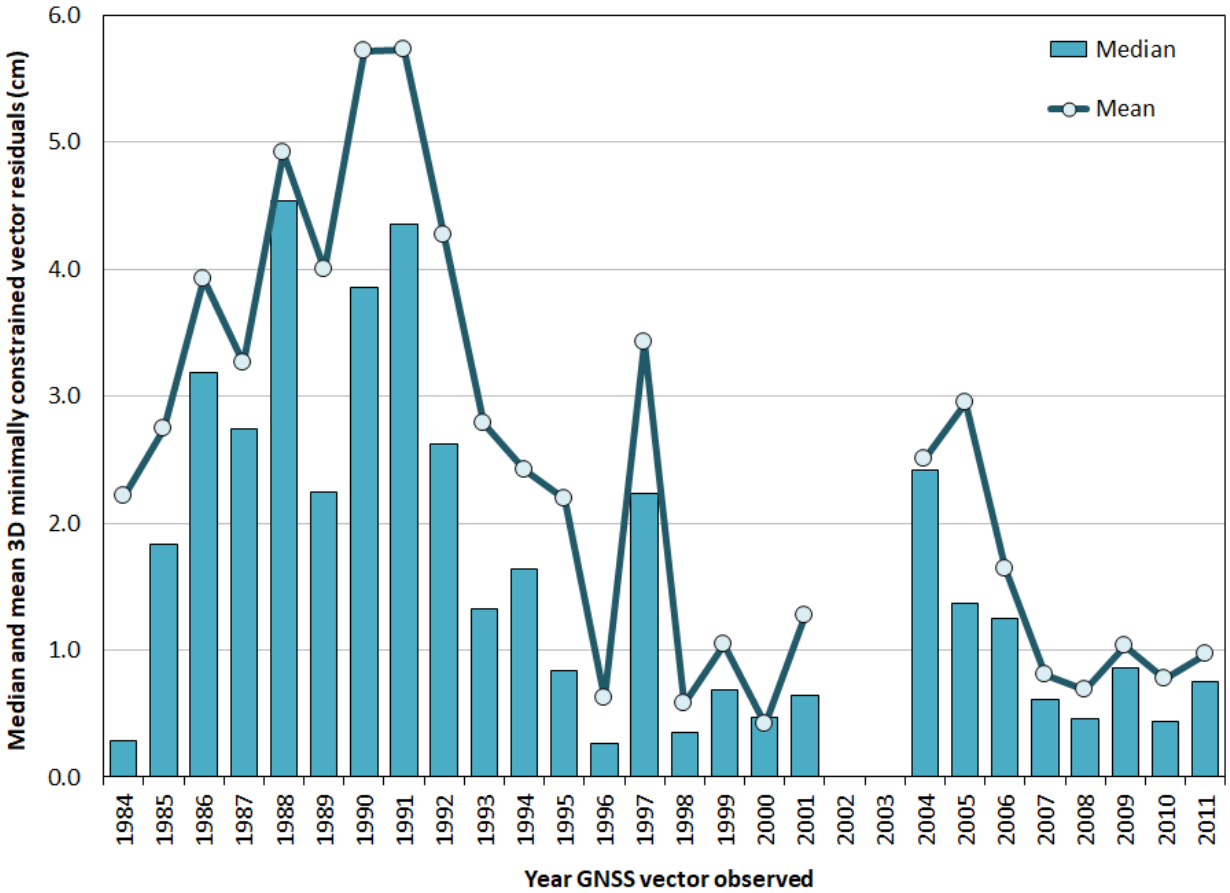

Figure 4.12. Median and mean Alaska network vector residuals grouped by year observed.

As with the CONUS networks, the residual magnitudes in Figure 4.12 show an overall decrease with time, particularly after 1988 to 1990. Prior to that, the residuals are generally lower, likely in part an artifact of the small sample size; there are only 228 enabled vectors from 1984 through 1987 (9.0% of the total). After 1990, two local maximums occur in the mean and median residuals, in 1997 and 2004. As shown in Figure 4.1, there is a very small number of Alaska network vectors in 1997 and 2004. There are only ten vectors in 1997, all in a single project, GPS1292. In 2004, there are only eight vectors, also in a single project (with two parts), GPS2111 and GPS2111/B.

Enabled minimally constrained residual magnitudes by observation duration for Alaska are shown in Figure 4.13, from the minimum duration of 2 minutes to the maximum of 30.6 hours given in Table 4.4. As for the CONUS networks shown in Figure 4.6, the scatter of points suggests a decrease in maximum residuals with increasing observation duration, particularly for durations greater than 6 hours in the Alaska network. A spike in residuals occurs at a duration of about 5.7 hours, but it corresponds to only three vectors (in project GPS406 observed in July/August 1990). It appears there is no change in residuals for durations of less than 6 hours, although the relationship between duration and magnitude of residuals is not clear due to scatter.

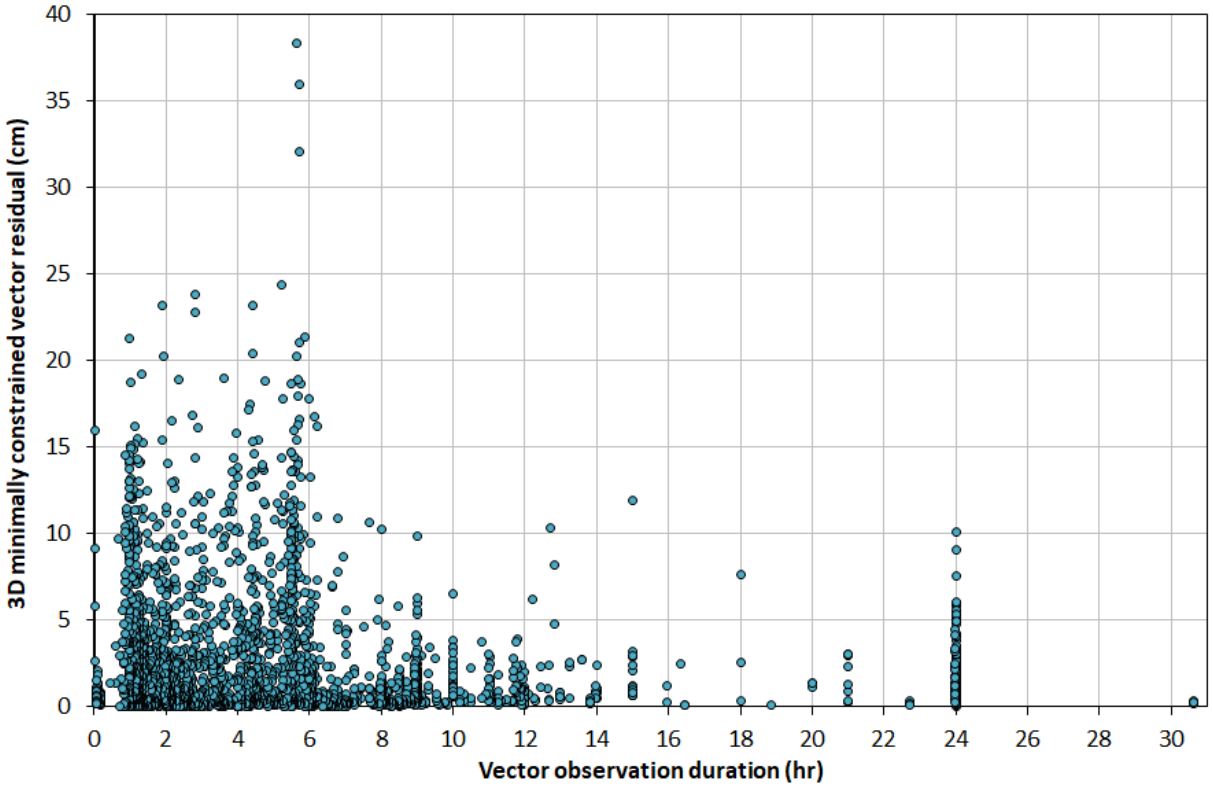

Figure 4.13. Alaska network vector residuals by observation duration (from 2 minutes to 30.6 hours).

Figure 4.14 shows the number of 3D residuals grouped in bins by magnitude, for both minimally constrained ("free") and fully constrained cases. As for the similar plot in Figure 4.7, a log scale is used for the number of residuals. Again, because of a fairly long tail, the bins for residuals are not all of equal size. The value on the horizontal axis is the upper end of the residual magnitude for its bin.

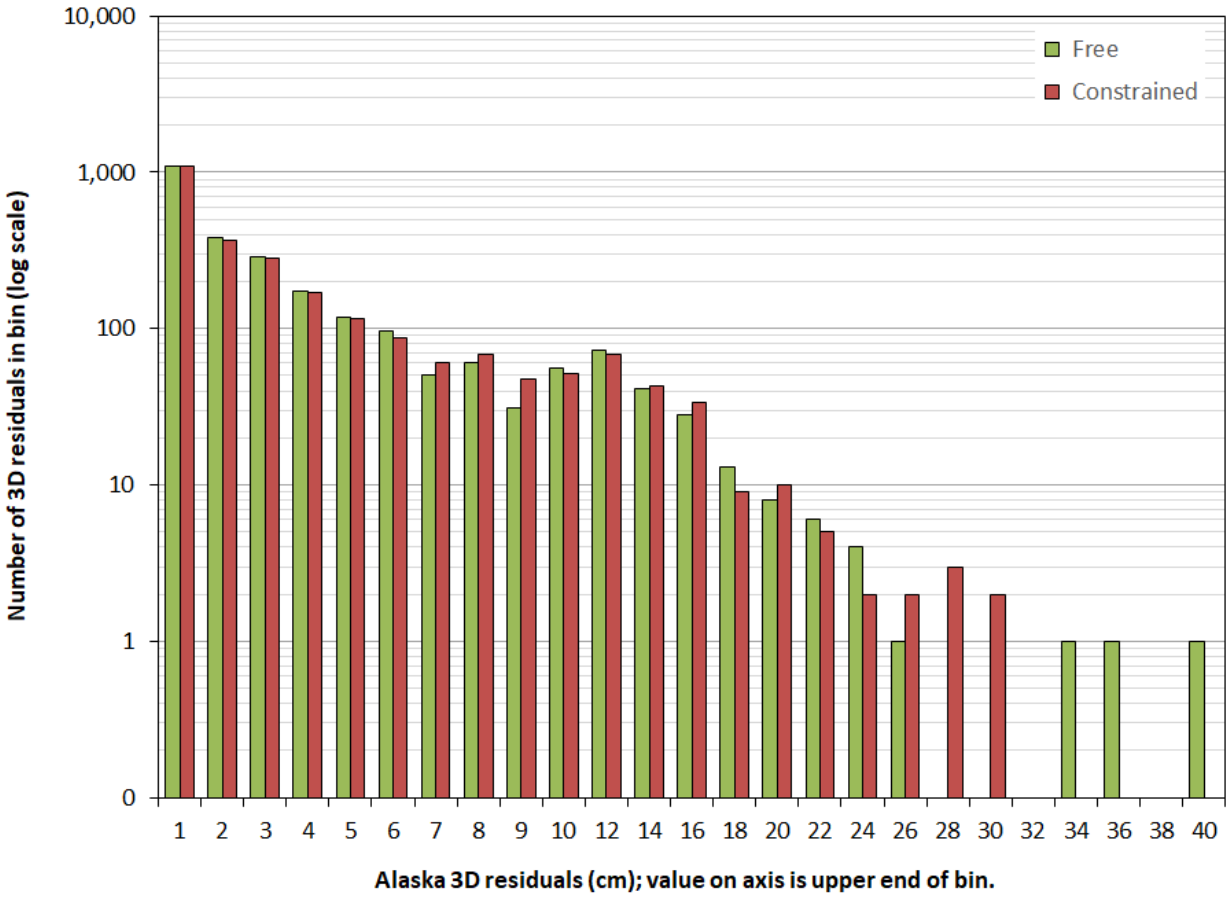

Figure 4.14. Alaska minimally and fully constrained vector residuals grouped by magnitude (log scale on vertical axis to emphasize bins with a small number of residuals).

The curious thing to note in Figure 4.14 is that the largest residuals occur for the minimally constrained, rather than the fully constrained adjustment. There are three residuals in the 32 to 40 cm bins for the free adjustment (mostly in the height component), with a large gap to the next largest single residual in the 24 to 26 cm bin. For the constrained adjustment, the largest two residuals are in the 28 to 30 cm bin. Despite the larger maximum free residuals, the residual statistics show overall less dispersion. Table 4.4 gives RMSE values of ±2.24, ±2.56, and ±3.49 cm for the north, east, and up components of the free residuals. The corresponding RMSE values of the constrained residuals (not tabulated) are slightly greater: ±2.27, ±2.61, and ±3.52 cm. In addition, the standard deviation of unit weight of the adjustments (Table 4.1) go from 1.910 for the free adjustment to 2.124 for the constrained adjustment, an increase of 11.2%. This substantial increase implies the residuals should also increase overall in the constrained

adjustment. And in general they do increase, despite the presence of the anomalous three, very large, free residuals.

These three large residuals in the free adjustment were mentioned previously in reference to the largest residual magnitudes in Figure 4.13, where it was stated they are in project GPS406. Of the 159 enabled vectors in that project, the constrained residuals decreased for 59. It appears this occurred at least in part because of the large vector sigmas. The 3D vector sigmas, after scaling with the variance factor, were greater than a decimeter for 100 of the vectors. The marks that the three vectors with very large sigmas are connected to are determined by other vectors with much lower sigmas, and thus even greater weight. Although it could be argued that these three vectors should have been rejected, their impact on the adjusted coordinates is small, since they have such low weight. Because of this, it appears there is little negative consequence to having these vectors in the network. A brief inspection shows these vectors may have been retained for connectivity between the Alaska mainland and the panhandle.

Project GPS406 was also mentioned in Section 2.4.1 (see Table 2.16). It is the unusual project with a single mark in Alaska connected to CONUS by eight vectors Hawaii by two vectors. All ten vectors are classified as excluded (but they remained in the network since they were in correlated sessions with many other vectors). Although these six (enabled) long vectors are not the ones with unusually large residuals, it seems worth noting the commonality.

Maps showing the distribution of minimally constrained 3D vector residuals for the Alaska network are in Figure 4.15. The upper map shows enabled vectors only, and the lower map shows rejected vectors only.

4.2.3. Pacific network vectors

Final minimally constrained adjustment statistics of the enabled GNSS vector residuals for the PA11 and MA11 networks are given in Table 4.5. Results of the two network adjustments are nearly identical, as expected, since the only difference is due to slight changes in orientation and length of the vectors resulting from their PA11 and MA11 transformations. To better show their similarity, the shaded values in Table 4.5 are ones that differ between the two networks at the significance shown—all differ by a single digit in the last decimal place, except for the 95.5 percentile up residual, and it differs by only two digits.

Histograms of the residuals for both networks are shown in Figure 4.16, and they, too, are nearly identical. Residuals are plotted over a range of ±9 cm, even though the full range of residuals in Table 4.5 is larger (maximum magnitudes of 13 cm horizontal and 22 cm up). However, 95% of the centered residuals (from percentiles 2.5% to 97.5%) have maximum magnitudes of 4.5 cm horizontal and 11.2 cm up. So, the histogram shows more than 95% of the horizontal residuals and nearly 95% of the up residuals (only 21 up vectors that fall between -9.00 and -11.2 cm are excluded).

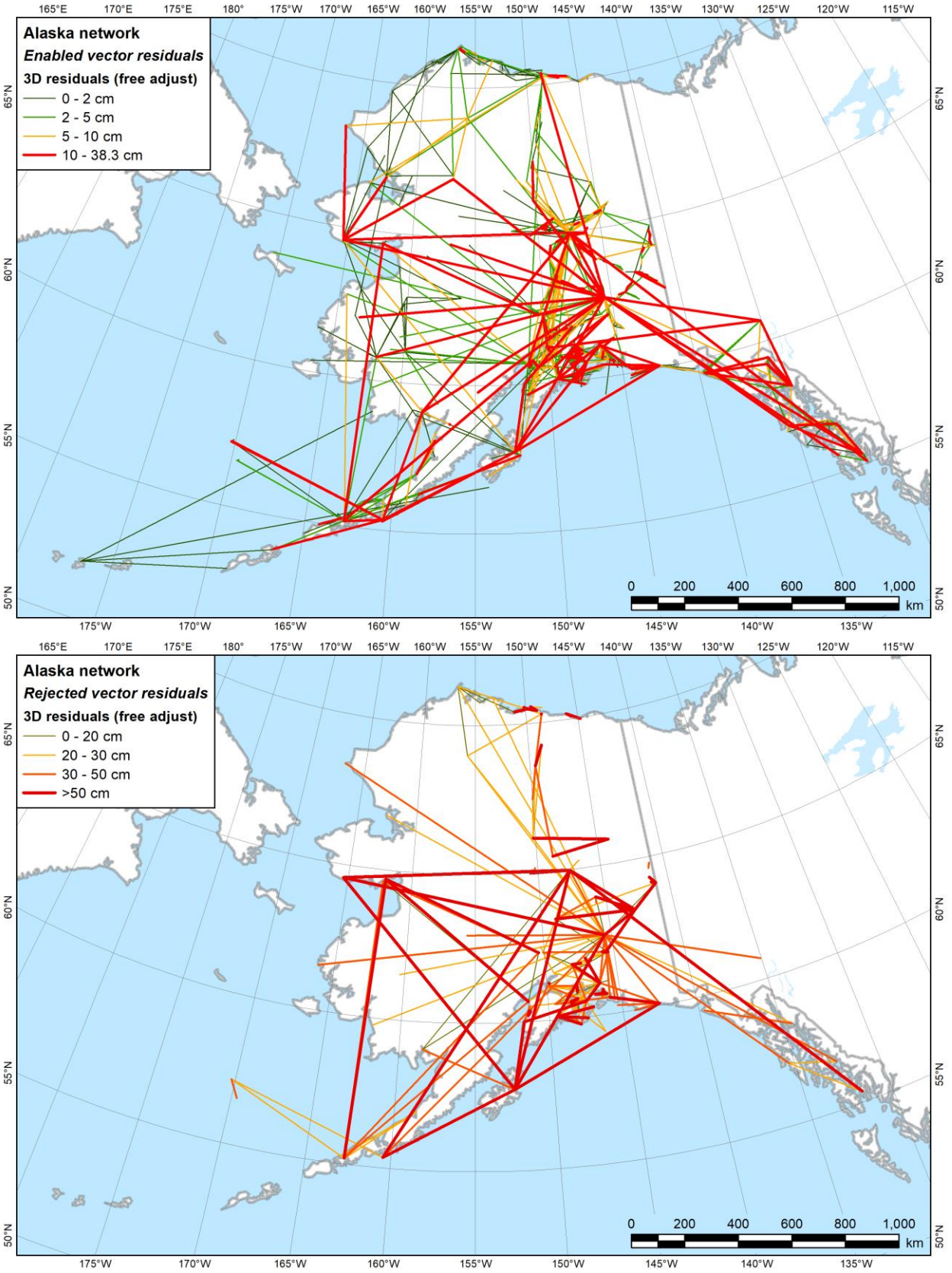

Figure 4.15. Map of Alaska network vector residuals, enabled (top) and rejected (bottom).

Table 4.5. Enabled vector residual statistics for the Pacific PA11 and MA11 networks. Values are shaded that differ between the two networks at the significance shown. The observation dates and durations are identical for both networks, but are included for ease of reference.

	Minimally constrained enabled vector residuals (cm)					Observation date (decimal year)	Duration (hours)
	North	East	Up	Horz	3D		
Pacific PA11 network (referenced to Pacific tectonic plate)							
Number	**1794** (58 rejected vectors not included)						
Minimum	-10.14	-11.90	-22.18	0.00	0.00	1993.61	0.20
Maximum	8.86	13.34	17.91	13.78	22.41	2011.33	100.80
Mean	-0.052	0.174	-0.243	1.171	2.658	2004.43	15.20
RMSE	±1.05	±1.72	±3.74	±2.02	±4.25	±2004.44	±26.14
Percentiles							
0.5%	-4.56	-6.04	-15.63	0.00	0.00	1993.61	0.27
2.5%	-2.23	-2.64	-11.16	0.00	0.00	1993.61	0.87
5.0%	-1.49	-1.74	-6.87	0.00	0.00	1993.62	1.28
50.0% (median)	**0.00**	**0.00**	**0.00**	**0.62**	**1.53**	**2006.42**	**6.61**
95.0%	1.45	3.15	4.85	4.36	10.46	2011.30	70.72
97.5%	2.09	4.46	7.32	5.77	13.55	2011.30	100.27
99.5%	3.70	9.09	13.49	11.35	18.16	2011.32	100.80
Pacific MA11 network (referenced to Mariana tectonic plate)							
Number	**1794** (58 rejected vectors not included)						
Minimum	-10.13	-11.90	-22.18	0.00	0.00	1993.61	0.20
Maximum	8.86	13.33	17.91	13.78	22.41	2011.33	100.80
Mean	-0.052	0.174	-0.243	1.171	2.657	2004.43	15.20
RMSE	±1.05	±1.72	±3.74	±2.02	±4.25	±2004.44	±26.14
Percentiles							
0.5%	-4.57	-6.03	-15.63	0.00	0.00	1993.61	0.27
2.5%	-2.23	-2.65	-11.16	0.00	0.00	1993.61	0.87
5.0%	-1.49	-1.75	-6.87	0.00	0.00	1993.62	1.28
50.0% (median)	**0.00**	**0.00**	**0.00**	**0.62**	**1.53**	**2006.42**	**6.61**
95.0%	1.45	3.16	4.85	4.37	10.46	2011.30	70.72
97.5%	2.09	4.45	7.32	5.77	13.55	2011.30	100.27
99.5%	3.70	9.08	13.47	11.35	18.15	2011.32	100.80

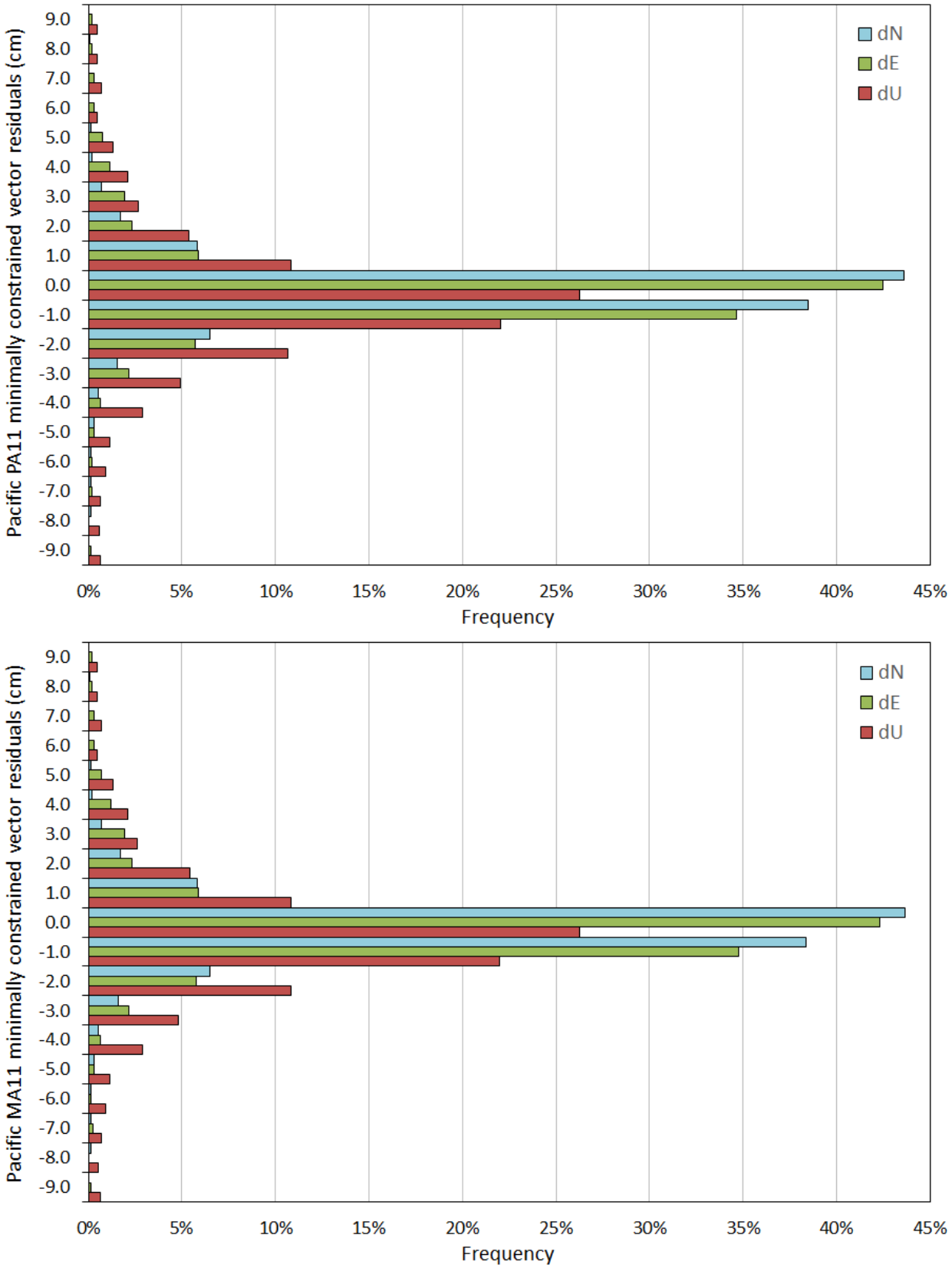

Figure 4.16. Histograms of vector residuals for Pacific networks, PA11 (top) and MA11 (bottom).

As with the other free adjustment residual histograms, these are centered near zero, and the distributions are not discernably skewed. Despite the presence of some large outliers (discussed below), for all components the median is zero, and the mean is close to zero, although the mean up residual is biased slightly negative (-0.2 cm). RMSE values are ±1.05 cm north, ±1.72 east, and ±3.74 cm up.

The Pacific residuals in Table 4.5 and Figure 4.16 show a greater difference between horizontal and vertical than do the CONUS and Alaska networks. For the Pacific, the ratio of up to horizontal RMSE is 3.6 (north) and 2.2 (east). In contrast, the ratio for CONUS Primary is 2.0 (north and east), for CONUS Secondary is 1.9 (north) and 1.8 (east), and for Alaska it is 1.6 (north) and 1.4 (east). The significantly larger ratio for the north than the east Pacific components is due to the presence of ten vectors with unusually large east residuals (magnitudes of 10.4 to 13.3 cm). Half of these are in the 1993 project GPS667/D, but the others are in four different projects at quite different times (from 2000 to 2011).

The Pacific histograms are more markedly peaked than Alaska due to an even larger proportion of no-check marks than Alaska, 26.2% (see Table 3.16). Since the no-check residuals are zero (or very near zero), they cause a large peak in the zero (±1.0 cm) histogram bin. A total of 7.2% of the Pacific 3D residuals are exactly zero, compared with 0.2% for the Primary, 1.6% for the Secondary, and 5.0% for the Alaska networks.

Median and mean minimally constrained 3D residuals of both Pacific networks are shown in Figure 4.17, grouped by year (vector observation dates and duration are given in Table 4.5). As expected, the residuals are nearly identical for the two networks. There is no clear trend in residual magnitudes with time. The median and mean differ significantly in 1993 and 2000, due to the high variability of residuals in those years. The year with the most Pacific vectors (326) is 1993 (see Figure 4.1), and the 3D residuals that year range from 0.0 to 12.5 cm, with a large standard deviation (±5.6 cm). In contrast, there were only 31 vectors in 2000, but also with a large range in residual magnitudes (0.2 to 22.4 cm) and standard deviation (±4.6 cm). For comparison, the standard deviation for all 3D residuals in the Pacific network is ±3.3 cm (differing from the RMSE of 4.25 cm in Table 4.5, because RMSE was taken about zero, whereas standard deviation is dispersion about the mean).

Figure 4.18 shows enabled minimally constrained residual magnitudes by observation duration, from the minimum of 12 minutes to the maximum of 100.8 hours in Table 4.5. As for the CONUS and Alaska networks (Figure 4.6 and Figure 4.13), the scatter of points suggests a decrease in maximum residuals with increasing observation duration. A spike in residuals occurs at 48 and 53 hours, but it corresponds to only three vectors. The lower plot is a detail for durations of 10 hours and less; it suggests a slight increase in residuals with increasing duration. Once again, the trend is not clear, as was the case for the other networks.

Figure 4.19 shows the number of 3D minimally constrained (free) and fully constrained residuals grouped in bins by magnitude for the PA11 network (essentially identical to the MA11 network). As with similar plots in Figure 4.7 and Figure 4.14, a log scale is used for the number of

residuals to emphasize the large magnitude tail, since they are few in number. The value on the horizontal axis is the upper end of the residual magnitude for its bin.

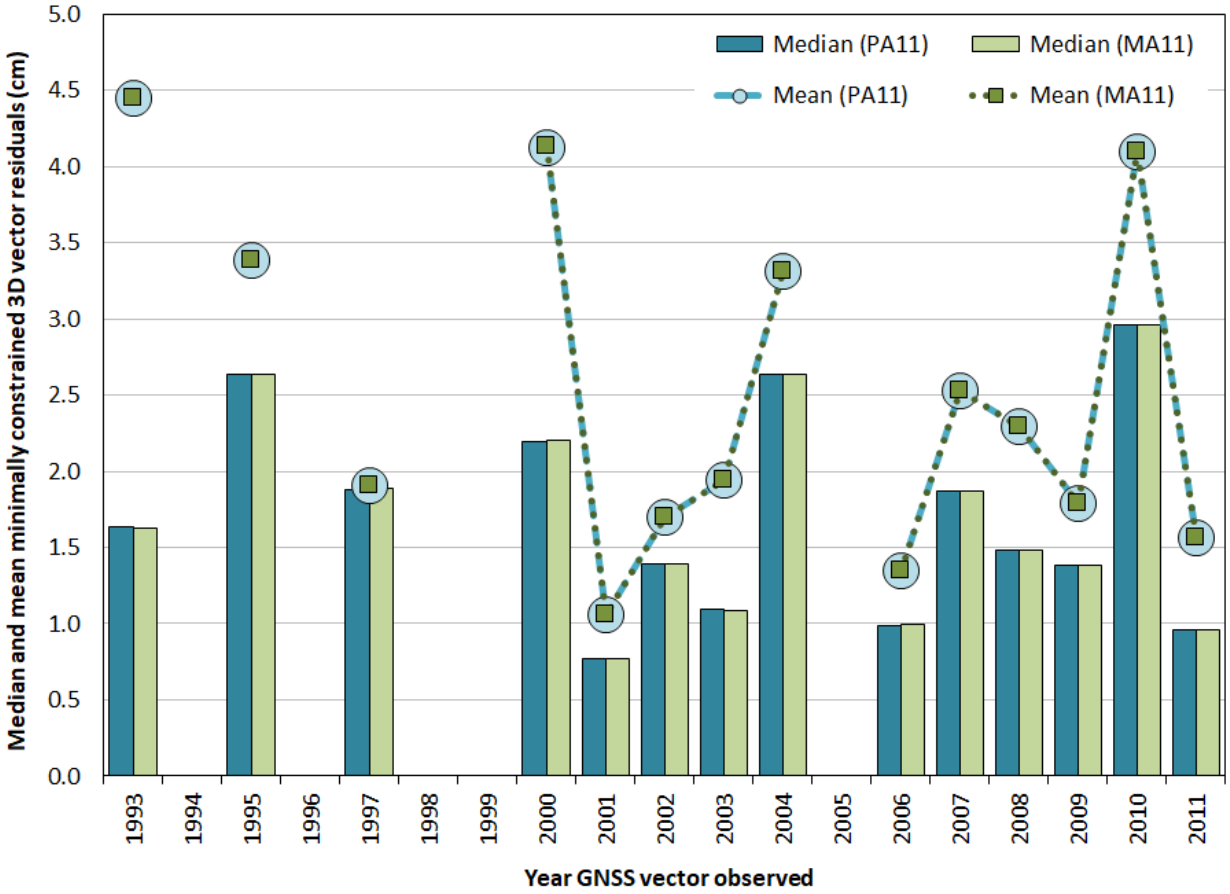

Figure 4.17. Median and mean PA11 and MA11 3D vector residuals grouped by year observed.

The constrained residual tail in Figure 4.19 is somewhat longer that the free residual tail and includes four vectors with residuals in 24 to 29 cm bins, whereas the maximum free residual is a single vector in the 22 to 23 cm bin. In addition, the other high residual bins (16 to 22 cm) contain a larger number of constrained than free residuals. The presence of larger constrained residuals is consistent with the adjustment statistics in Table 4.1, which show an increase in standard deviation of unit weight from 1.164 (free) to 1.255 (constrained), an increase of 7.8%.

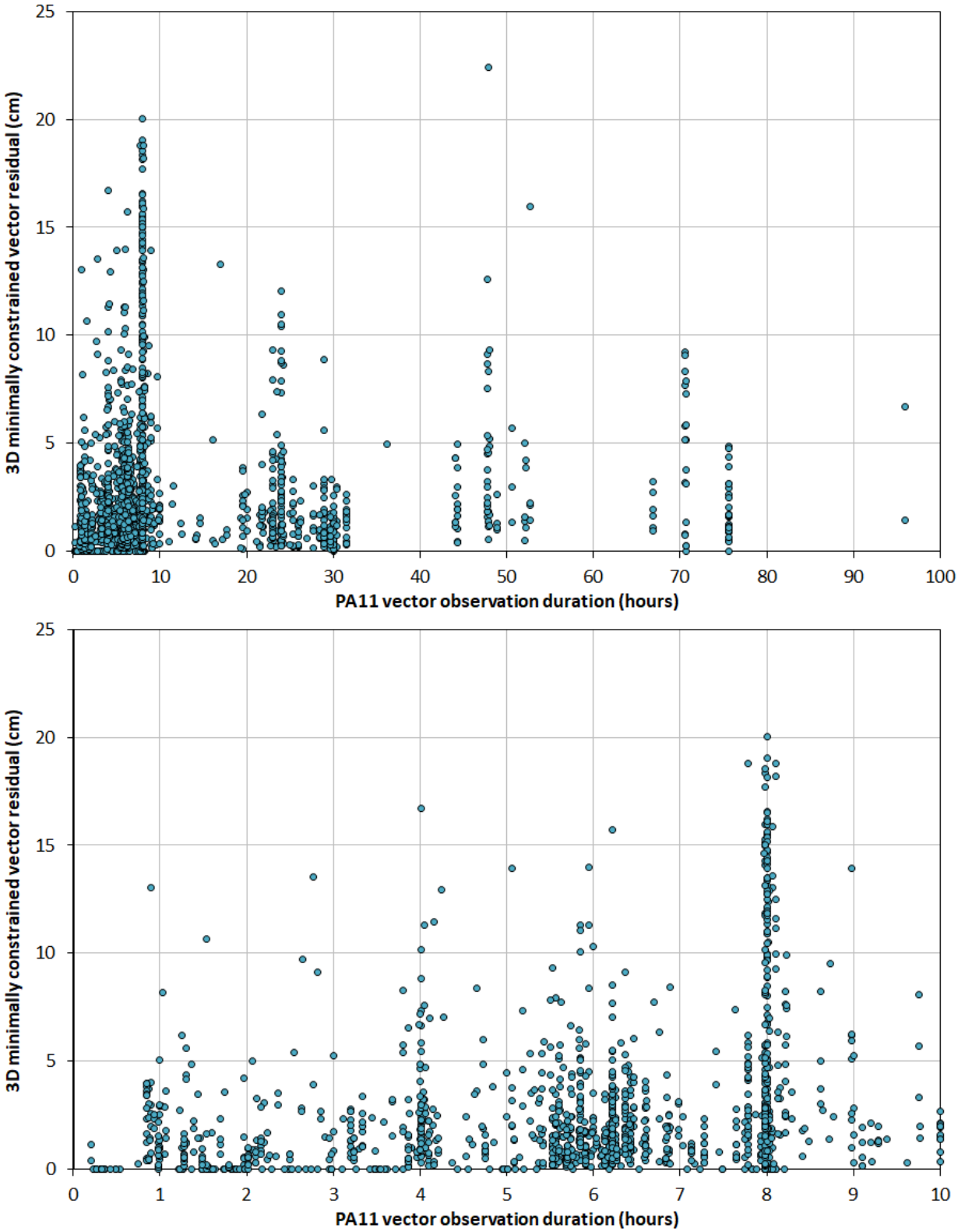

Figure 4.18. Pacific PA11 vector residuals by observation duration. The upper plot is for durations from 12 minutes to 100 hours. The bottom plot is a detail from 12 minutes to 10 hours.

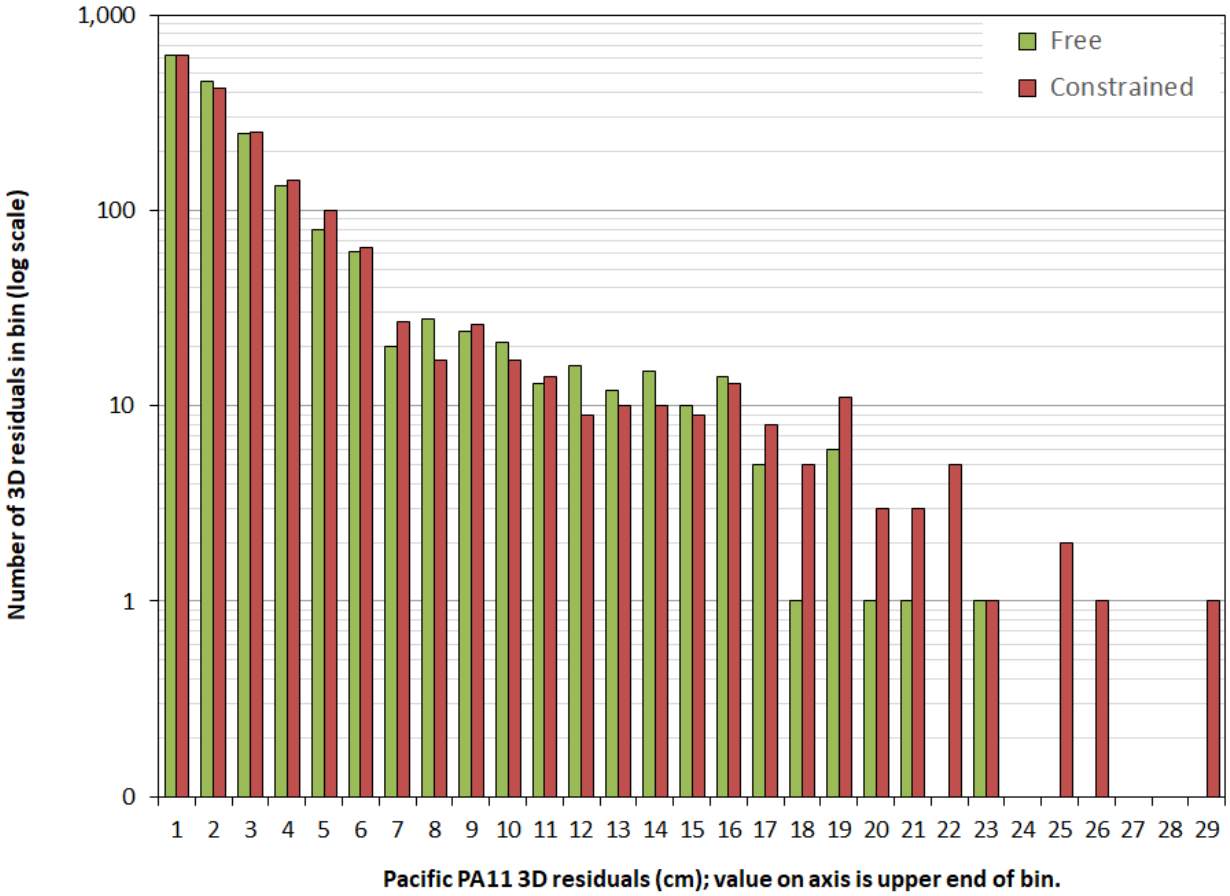

Figure 4.19. Pacific PA11 and MA11 3D vector residuals grouped by magnitude (log scale on vertical axis to emphasize bins with a small number of residuals).

The four largest constrained residuals are in the previously mentioned 1993 project GPS667/D. They all have observation durations of about 8 hours, so they correspond to the peak at 8 hours in Figure 4.18. Two of the vectors connect the Marshall Islands to American Samoa and are therefore very long—3061 km—particularly for observations of only 8 hours made in 1993, before the GPS constellation was complete and using older processing methods and models. One of the other two is also quite long, connecting the Marshall Islands to Kosrae Island (939 km), and the shortest is 318 km, connecting the Hawaiian Islands of Kaua'i and Lana'i. The great length of many of the vectors in the Pacific—together with the relative sparseness of the network, age of many of the observations, and unmodeled earthquakes on various islands—are among the reasons for the presence of vectors with such large residuals.

Maps showing the distribution of minimally constrained 3D vector residuals for the Pacific PA11 network are in Figure 4.20. The upper map shows enabled vectors only and the lower map shows rejected vectors. The MA11 vectors are not shown, because they are essentially identical.

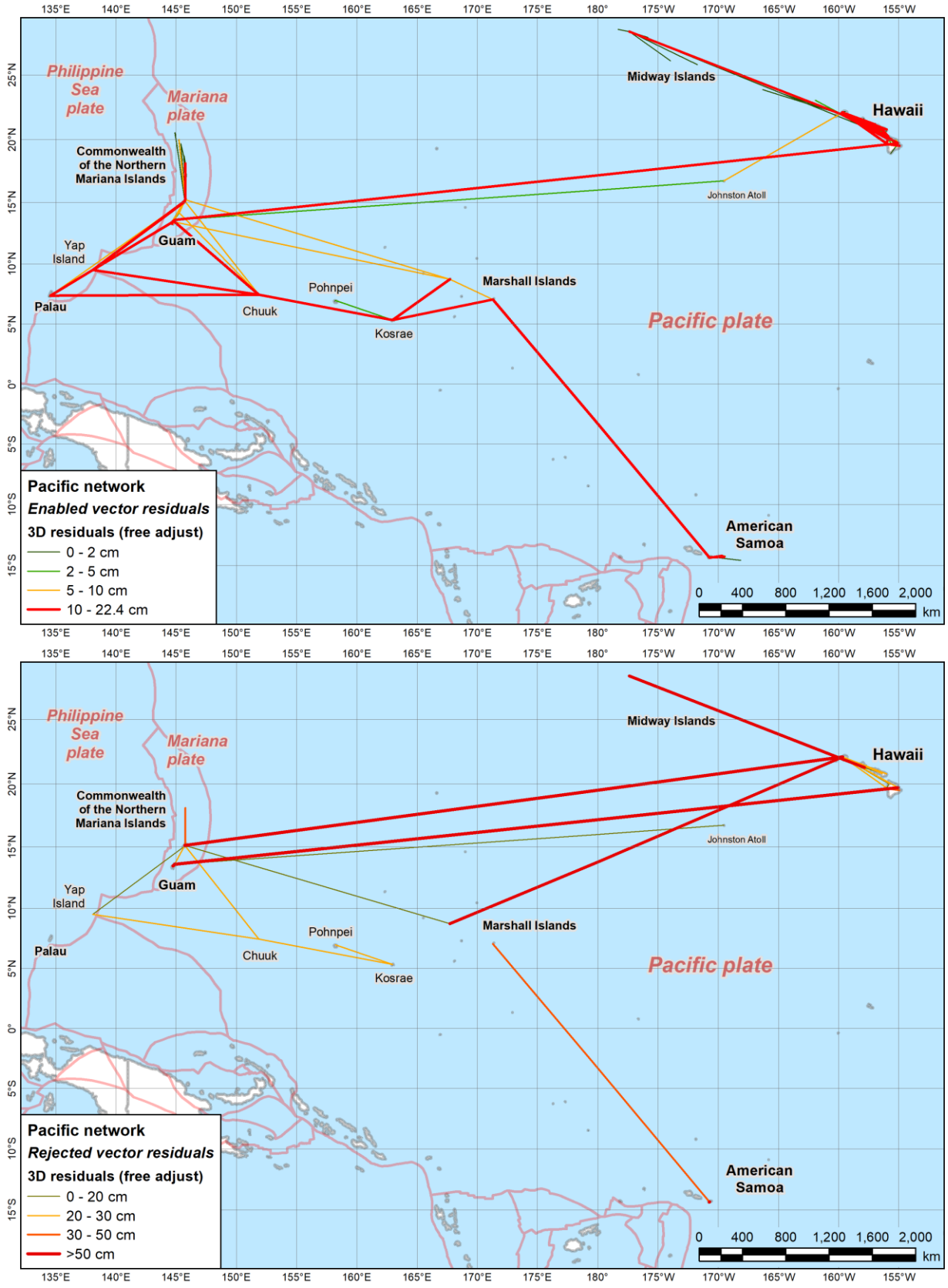

Figure 4.20. Map of Pacific PA11 network vector residuals, enabled (top) and rejected vectors (bottom).

4.2.4. Rejected GNSS vectors

A significant number of vectors were rejected in the final NA2011 networks—21,603 (5.1%) of 424,721 vectors in all four networks. Rejected vectors were not actually removed from the networks, rather they were rejected by downweighting. To reject a vector, each Earth-Centered, Earth-Fixed (ECEF) ΔX, ΔY, ΔZ component was assigned a standard deviation (sigma) of 100 m. Since the weight is the inverse squared sigma, such large sigmas gave the rejected vectors extremely low weight, so low they made no contribution to the adjusted coordinates. The number of rejected vector components was subtracted from the input number of observations, so the value for the network degrees of freedom (DOF) was the same as if the vectors had been removed. However, the DOF would not be exactly the same in cases where true removal of rejected vectors created disconnected subnetworks, because additional constraints would be needed for each component in a minimally constrained (free) adjustment. These required constraints would not be available for increasing the DOF if the rejected vectors were removed, but they would be available if the rejected vectors were retained (through downweighting).

Part of the reason for rejection by downweighting rather than removing vectors is to prevent accidentally creating disconnected subnetworks. Unconstrained subnetworks cause a rank defect in the normal matrix, resulting in adjustment failure due to numerical singularity. This problem is not mathematical, as disconnected subnetworks can each be constrained, and singularities thus avoided. Rather, it is a problem of convenience, bookkeeping, and determining appropriate constraints for subnetworks. In contrast, downweighting provides a simple method to perform a single adjustment, rather than needing to set up separate adjustments for each independent subnetwork.

Another advantage of rejection by downweighting is for simultaneously processed sessions. In these sessions, removing a vector requires reconstructing or re-indexing the variance-covariance matrix, whereas no change to the matrix is required when vectors are downweighted. Although this problem is mainly one of bookkeeping, it nonetheless would require new coding for both *ADJUST* and *NETSTAT*.

For the NA2011 Project, an important advantage of rejection by downweighting is that it allowed analysis and possible re-enabling of previously rejected vectors. Such an analysis was performed in several series of iterative adjustments, as described in Section 3.5.3, and it resulted in reducing the number of rejected vectors by nearly half. These iterative adjustments were so useful it was decided to continue using rejection by downweighting, despite its liabilities as described by Milbert (2009). However, rejection by removal would overall be preferred if rank-defect problems could be resolved (say by the use of additional constraints) and analysis of rejected vectors could be performed. To test the impact on the NA2011 Project, an early version of the CONUS network was adjusted, both by removal and by downweighting of rejected vectors. The resulting coordinates and network accuracies were the same in both cases, to the output numerical precision of the *NETSTAT* software.

As shown in the vector residual maps in the previous section (Figure 4.8, Figure 4.9, Figure 4.15, and Figure 4.20), vector rejections were not uniform in space, and they varied by networks. Vector rejections were also not uniformly distributed in time.

Table 4.6 provides the residual statistics for all enabled and rejected minimally constrained vectors in the NA2011 Project. A histogram of the residuals for each type is shown in Figure 4.21. Although both histograms have the same frequency scale, the enabled residual histogram has a bin size of 0.5 cm, versus 5 cm for the rejected residuals (an order of magnitude larger). This result is hardly surprising, considering the rejected vectors are downweighted and were initially rejected because of poor fit from the start. Still, it is interesting to see the rejected residuals also follow a more-or-less normal distribution. Approximately 35% of the horizontal residuals are within ±5 cm for the rejected residuals and ±0.5 cm for the enabled residuals. Up residual distributions are more disparate however, with approximately 13% of the rejected up residuals being within ±5 cm, and about 25% of the enabled up residuals being within ±0.5 cm.

Table 4.6. Unrejected and rejected minimally constrained GNSS vectors for all four NA2011 networks.

	Enabled vectors					Rejected vectors				
Number	**403,118**					**21,603**				
Residuals (cm)	**North**	**East**	**Up**	**Horz**	**3D**	**North**	**East**	**Up**	**Horz**	**3D**
Minimum	-17.11	-22.10	-38.23	0.00	0.00	-413.98	-981.81	-967.16	0.00	0.00
Maximum	15.33	18.73	18.65	22.47	38.32	9174.27	9928.24	7596.88	8341.73	11,344.60
Mean	-0.002	-0.006	-0.013	0.638	1.129	11.600	5.820	0.487	22.587	32.294
RMSE	±0.63	±0.65	±1.22	±0.90	±1.52	±271.42	±187.20	±72.53	±281.40	±337.60
Percentiles										
0.5%	-2.20	-2.33	-4.08	0.00	0.00	-45.26	-94.19	-89.89	0.13	1.88
2.5%	-1.28	-1.30	-2.66	0.04	0.10	-16.29	-30.75	-28.70	0.30	4.18
5.0%	-0.94	-0.94	-1.96	0.07	0.16	-9.64	-17.12	-19.43	0.46	4.81
50.0% (median)	**0.00**	**0.00**	**0.00**	**0.47**	**0.85**	**0.03**	**-0.01**	**-0.49**	**4.25**	**9.14**
95.0%	0.94	0.92	1.94	1.78	3.08	9.86	16.37	18.18	36.14	47.97
97.5%	1.28	1.27	2.65	2.26	3.74	17.56	29.51	27.39	59.08	77.21
99.5%	2.19	2.28	4.08	3.42	4.98	73.11	116.72	90.84	206.64	295.99

The number of all NA2011 enabled and rejected vectors grouped by minimally constrained residual magnitude is shown in Figure 4.22. Unlike previous similar plots in Figure 4.7, Figure 4.14, and Figure 4.19, the residuals are in meters rather than centimeters, due to the large size of the rejected vector residuals. These large residuals also required unequal bin sizes. The residual value on the horizontal axis corresponds to the upper end of the bin.

Figure 4.22 shows the number of enabled vectors exceeds rejected vectors for residuals of less than 6 cm. The figure also shows that nearly 4000 rejected residuals have magnitudes of 6 cm or less. These rejected vectors could be possible candidates for re-enabling, if additional time had been available for further analysis and iterative adjustments. Actually, with additional time, normalized residuals would have been evaluated, as well, rather than only the residual magnitudes, since it also accounts for redundancy and precision (repeatability).

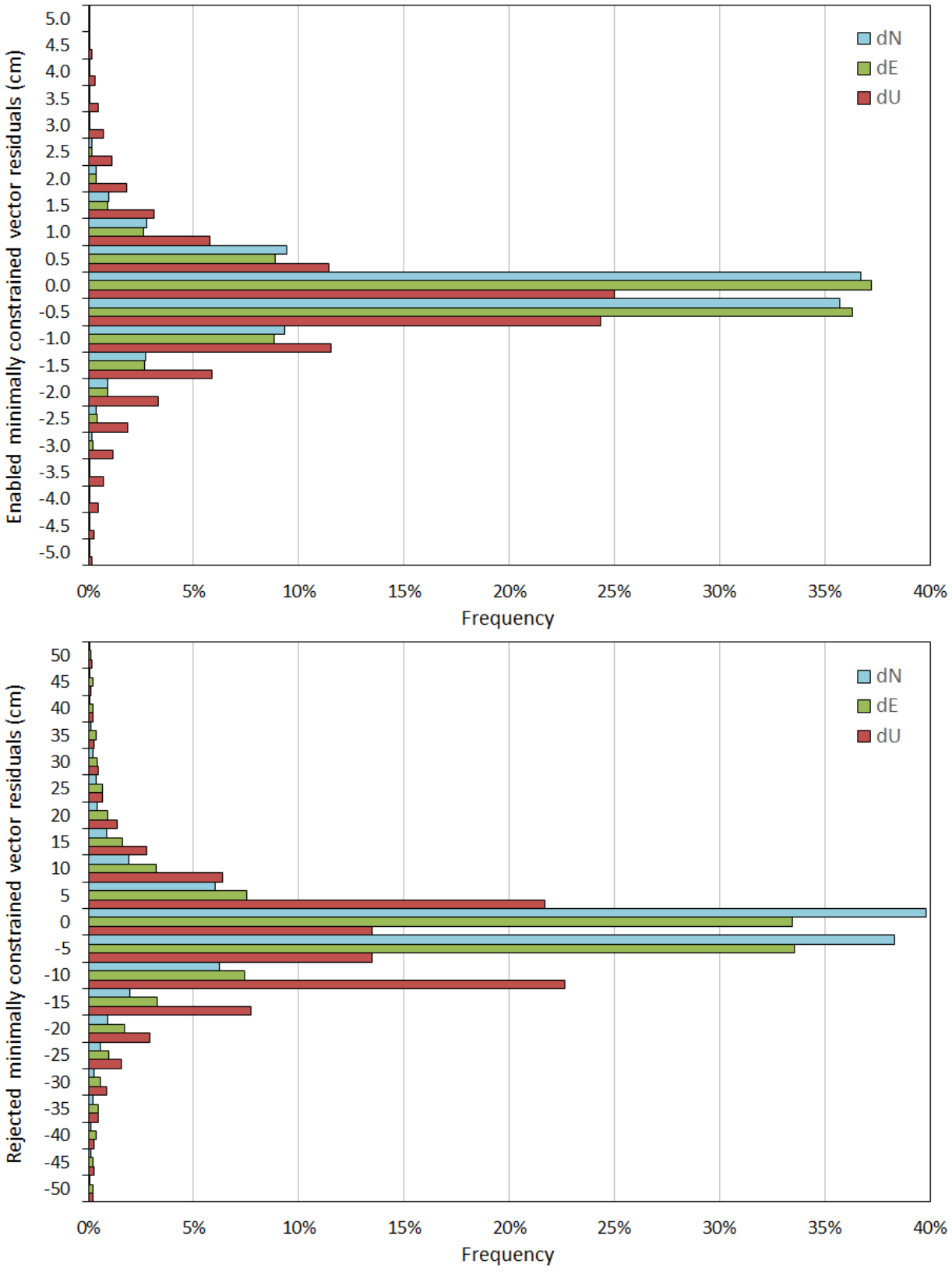

Figure 4.21. Histograms of vector residuals in all four networks, enabled (top) and rejected (bottom). Note that bin size for enabled vectors is 0.5 cm, and for rejected vectors is 5 cm.

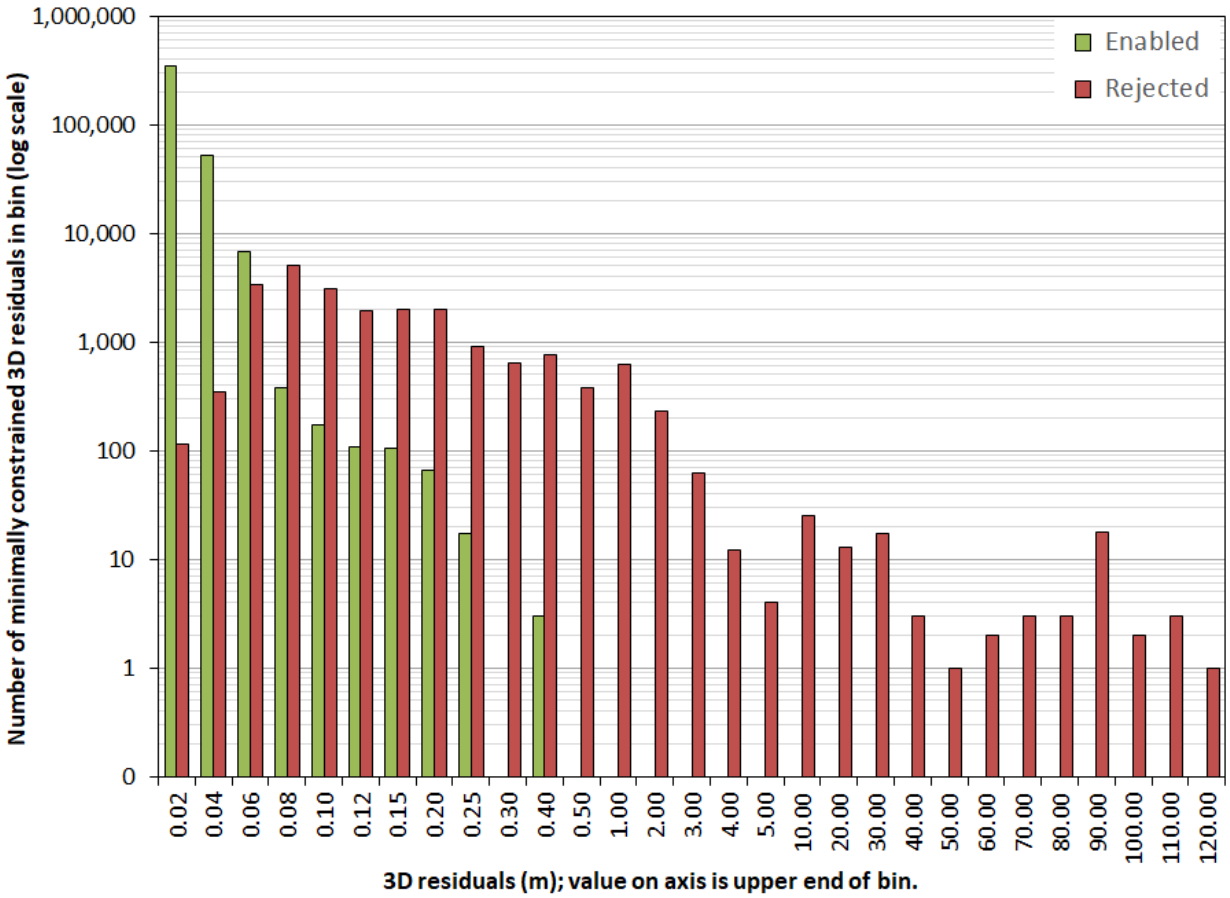

Figure 4.22. Enabled and rejected 3D vector residuals for all networks grouped by magnitude (log scale on vertical axis to emphasize bins with a small number of residuals; note that residuals are in ***meters***).

Large residuals are expected for rejected vectors, although some (in Figure 4.22) seem excessively large. Note that four rejected residuals are greater than 100 m, which is the sigma assigned to each ECEF vector component when rejected by downweighting. These vectors, and perhaps some of the other 62 that are greater than 10 m, may actually be referenced to incorrect marks. This possible problem is discussed in Section 5.1.2, but it affects only a very small number of vectors.

The percentage of vectors rejected is shown in the two plots in Figure 4.23. Both plots show the percent rejected for all four NA2011 networks. Superimposed on that are the percent rejections for the two CONUS networks in the upper plot, and the Alaska and Pacific network in the lower plot. For the combined rejections of all four networks, there is a clear, nearly exponential decrease in the percent of rejected vectors, from about 37% in 1983 and 1984 to about 15% by 1990. After 1990, the decrease continues to about 3% in the early 2000s. Throughout the 2000s it remains fairly constant, although there are local peaks in that time frame, as well as earlier. The reason for the peaks becomes clearer when the individual networks are considered.

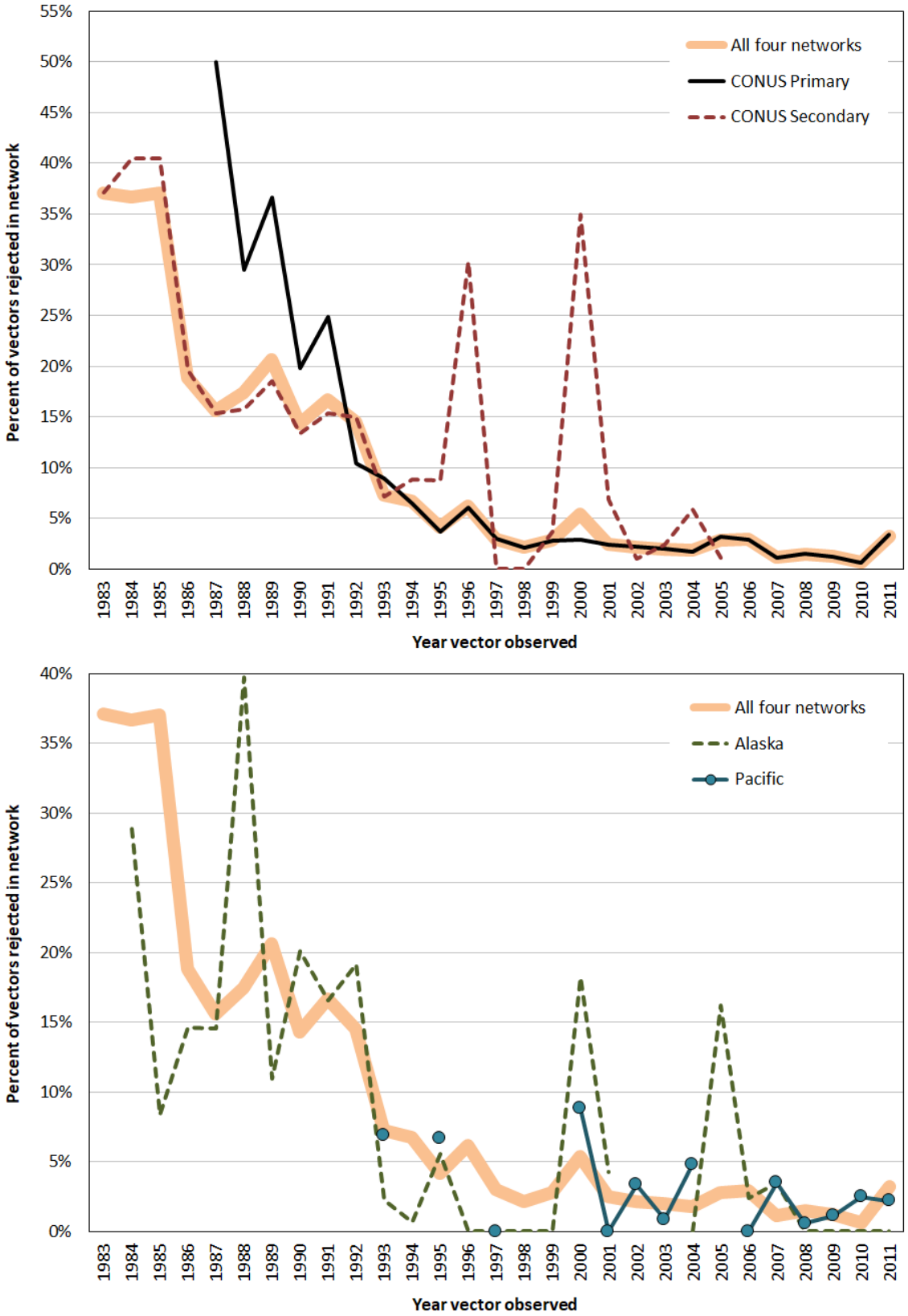

Figure 4.23. Percent rejected vectors for all networks and for individual networks. CONUS rejections are shown in top chart, and Alaska and Pacific rejections are shown in bottom chart.

The upper plot of Figure 4.23 shows that older CONUS Primary projects have high rejection rates, with a maximum of 50% in 1987 (although there is only one project in that year, GPS419/C in Colorado, contained only 16 vectors). The rejection rate for the Primary vectors remains higher than 10% in 1992 and prior, and during most of that time the rejection rate exceeds that of the Secondary network. Recall from Section 3.3.2, all the GPS projects prior to 1993 were initially assigned to the Secondary network. Because of the presence of some "important" pre-1993 projects (most notably large HARN surveys), some of these projects were reassigned to the Primary network. Upon inspection of results, it seems some or most of these projects should have remained in the Secondary network.

For the Secondary network in the upper plot of Figure 4.23, two prominent percent rejection peaks occur in 1996 (30% rejected) and 2000 (35% rejected). Just as some Secondary vectors were reassigned to the Primary network, some Primary vectors after 1994 were assigned to the Secondary network, and as discussed in Section 3.5.1, this was done for projects in subsidence areas with observations prior to 2006. The 1996 rejection peak is for 76 vectors from six projects in southern Louisiana and Texas. The 2000 rejection peak is for 2152 vectors in the same states, plus Mississippi. All of these vectors had their up-component downweighted due to subsidence. Most of the year 2000 vectors were rejected due to large negative up-component residuals (mean and median of about -9 cm for the minimally constrained rejected vectors).

The lower plot in Figure 4.23 superimposes the Alaska and Pacific rejections on the combined NA2011 network. Rejections for the Pacific never exceed the high of about 9% in 2000. Alaska, on the other hand, shows a large percentage of rejections. For 1992 and earlier, rejections always exceed 10%, with a maximum of 40% in 1988. After 1992, the percentage of rejections decreases substantially, although there are two peaks, one of 18% in 2000 (from a total of only 11 vectors in one project, GPS1475), and one of 16% in 2005 (from a total of 105 vectors in four projects).

The maps of rejected vectors in the previous section suggest the rejection rate generally increases with vector length. To evaluate this possibility, the vectors were binned by vector length, and the rejection rate for each bin was computed. Because there are far more short than long vectors (see Table 2.10), the size of the length bins increase with increasing vector length, to prevent an excessively large number of short vectors in a single bin (since more than half of all vectors are less than 8 km). The goal was to provide a statistically valid sample size for each bin by attempting to make the number of vectors per bin more-or-less constant (to the extent possible). The resulting vector length bins, corresponding number of vectors, and percent rejected vectors are listed in Table 4.7. Bin sizes were selected such that the log of the length increment was approximately constant. Note the large number (and percent) of vectors in three bins from 0 to 8 km. Together these account for 50.7% of all vectors, and 17.7% are less than 2 km.

Figure 4.24 is a plot of percent rejection versus vector length (log scale), where the length is at the midpoint of each bin in Table 4.7. The plot clearly shows a general increase in rejection with vector length. A logarithmic regression curve is provided, plotted as a line, since the length axis is on a log scale. Although the coefficient of determination is fairly good ($R^2 = 0.62$), it is not

suggested that such a regression equation be used for prediction. In this case, the curve is considered merely descriptive.

Table 4.7. Percent rejected vectors by vector length (the maximum vector length is 6147.5 km).

Vector length bins (km)			Total vectors per bin		Number of vectors:		Percent rejected
Lower end	Upper end	Midpoint	Number	Percent	Enabled	Rejected	
>= 0	< 2	1	75,120	17.69%	74,150	970	**1.29%**
>= 2	< 4	3	48,377	11.39%	47,435	942	**1.95%**
>= 4	< 8	6	91,884	21.63%	89,476	2408	**2.62%**
>= 8	< 16	12	88,910	20.93%	84,375	4535	**5.10%**
>= 16	< 24	20	29,979	7.06%	26,899	3080	**10.27%**
>= 24	< 40	32	25,856	6.09%	22,208	3648	**14.11%**
>= 40	< 60	50	17,643	4.15%	15,735	1908	**10.81%**
>= 60	< 90	75	13,813	3.25%	12,505	1308	**9.47%**
>= 90	< 130	110	9613	2.26%	8739	874	**9.09%**
>= 130	< 200	165	9310	2.19%	8672	638	**6.85%**
>= 200	< 300	250	6049	1.42%	5623	426	**7.04%**
>= 300	< 500	400	4696	1.11%	4299	397	**8.45%**
>= 500	< 800	650	2010	0.47%	1778	232	**11.54%**
>= 800	< 1200	1000	554	0.13%	439	115	**20.76%**
>= 1200	< 2800	2000	796	0.19%	695	101	**12.69%**
>= 2800	< 6200	4500	111	0.03%	90	21	**18.92%**
		Totals	**424,721**	**100.00%**	**403,118**	**21,603**	**5.09%**

4.2.5. Effect of GNSS vector length on sigmas and residuals

Given the correlation between vector length and percent rejection shown in the previous section, a question naturally arises as to whether vector age also has an effect on vector residuals and sigmas (standard deviations). Table 4.8 provides statistics on the vector lengths, sigmas, and residuals for the 403,118 enabled vectors in all four NA2011 networks. The sigmas are scaled by the computed GPS project variance factors, and the up residual is taken as an absolute value to make it more directly comparable to the horizontal and 3D residuals. Despite a maximum vector length of 6147.5 km, the mean and median are 32.0 and 7.5 km, respectively. These values are similar to those reported in Table 2.10 (33.7 and 7.8 km), but they are slightly smaller here, because Table 4.8 considers only the 403,118 enabled vectors (out of 424,721 total). The decrease in mean and median vector length is due to a greater rejection rate for longer vectors, as shown in the previous section.

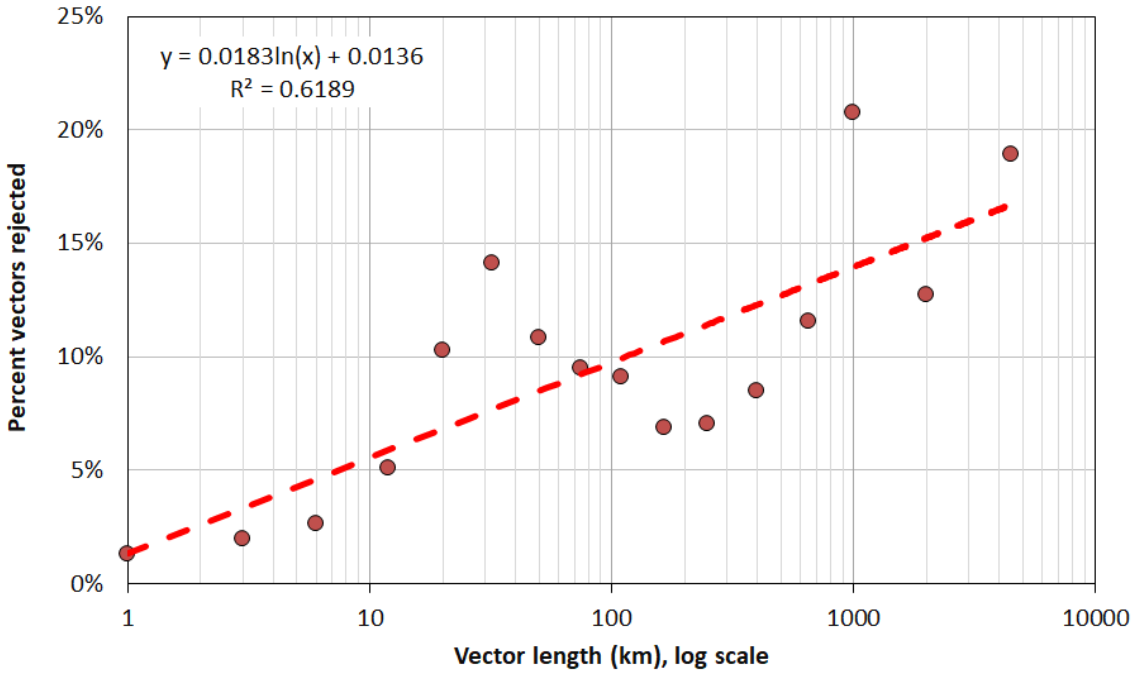

Figure 4.24. Percent rejected vectors for all networks as function of vector length (log scale on horizontal vector length axis)

Table 4.8. Statistics of enabled vector lengths, sigmas, and residuals for all four NA2011 networks (the 3D vector sigmas have been scaled by the project variance factors).

	Vector length (km)	Scaled 3D sigma (cm)	Minimally constrained residuals (cm)		
			Up (ABS)	Horizontal	3D
Number = 403,118					
Minimum	0.0	0.02	0.00	0.00	0.00
Maximum	6147.5	8298.33	38.23	22.47	38.32
Mean	32.0	3.85	0.81	0.64	1.13
Std deviation	±114.5	±17.64	±0.92	±0.64	±1.02
Percentiles					
1%	0.2	0.34	0.00	0.02	0.04
5%	0.6	0.60	0.03	0.07	0.16
10%	0.9	0.83	0.07	0.12	0.25
50% (median)	**7.5**	**2.11**	**0.51**	**0.47**	**0.85**
90%	65.3	6.28	1.95	1.34	2.38
95%	139.7	9.43	2.65	1.78	3.08
99%	407.4	31.21	4.08	2.93	4.50

All 3D sigmas are plotted with respect to vector length in Figure 4.25, with a log scale on both axes to mitigate the extreme ranges in both values. Despite the high density of plotted points and the scatter, the "cloud" of point shows a vaguely discernible trend of sigmas increasing with vector length. The trend is indicated by the red logarithmic regression curve. The curve is for illustration only; there is far too much dispersion for a reliable regression.

Although Figure 4.26 does (weakly) suggest a correlation between vector sigmas and length, the main reason for providing it is to point out the features indicated by the two arrows. The upper arrow is for a series of sigmas versus vector length following a diagonal line (in log-log space). The lower arrow is for a series of sigmas constant with respect to length. Both arrows represent problems with the GNSS vector data.

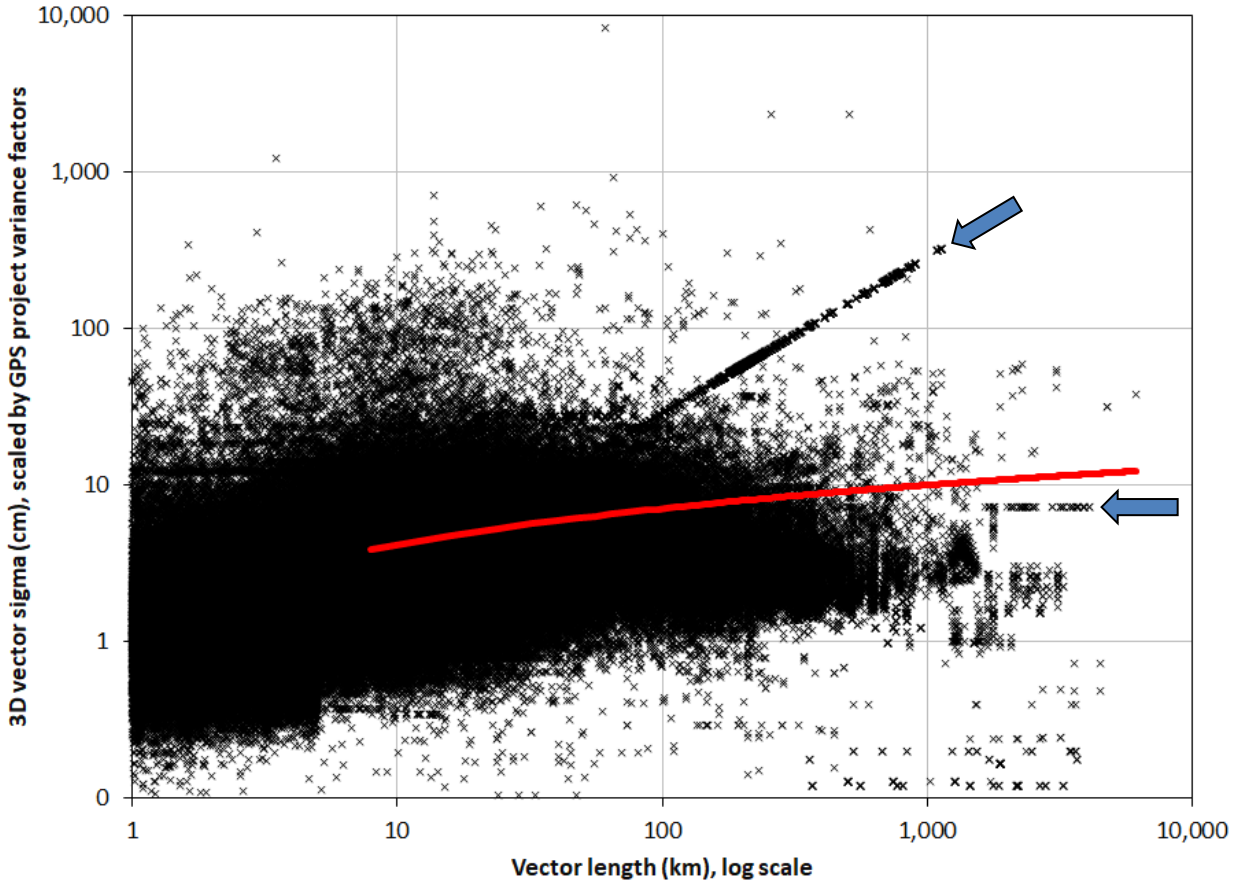

Figure 4.25. Enabled 3D vector sigmas as a function of vector length (log scale on both axes; red curve is logarithmic regression for entire dataset).

The diagonal line of vector points is from the 2000 project GPS1460 (California). The project consists of 2108 vectors total (35 rejected). Every vector sigma is the same linear function of its vector length. The average is 0.286 cm/km, but the range is extremely small (0.285 to 0.300 cm/k), so it is effectively identical for all vectors. This behavior is simply not realistic, particularly in view of the known weak correlation between error and distance in GNSS solutions. This relationship leads to very large sigmas on long vectors. For this project, vector

lengths range from 26 to 1126 km. The corresponding 3D sigmas range from 7.5 cm to 3.2 ***meters***. Clearly this is not correct, and it means most of the vectors for this large project were improperly weighted. According to the NGSIDB metadata, NGS processed this project using the scientific session baseline processing software *GAMIT-GLOBK* from Massachusetts Institute of Technology.

The horizontal line of vector points is from the 1992 project GPS394 (New Jersey). The project consisted of 300 vectors total, and 91 enabled (plus 13 rejected) vectors were assigned identical sigmas of exactly 1 cm on all three components (the values in Figure 4.25 are 3D sigmas of 7.138 cm, after scaling by the project variance factor). This behavior also is not even remotely realistic. G-file metadata indicates that NGS processed this project using *Omni* software (the predecessor of NGS *PAGES* software).

It probably is not possible to satisfactorily correct the sigma errors in projects GPS1460 and GPS394. An empirical approach could be attempted using the VVHU functionality of *ADJUST*, but it would not yield reliable results, since it would simply apply two constant variance factors (one horizontal, one vertical) to all of the sigmas on these straight lines, yielding two different, but still straight lines. This is a rather disturbing discovery, and not just because of the possible impact of these two projects (their vectors make up only 0.5% of the total in the NA2011 Project). The troublesome part is the question as to whether other such problematic vectors are hidden in the dense cloud of points in Figure 4.25. These two projects were only found because their lengths and sigmas were large enough that they were not obscured by other points. To find others would require additional analysis of all NA2011 vectors.

The same analysis technique used for the percent of rejections versus baseline length was also used to further investigate the impact of vector length on vector sigmas and residuals. Vector lengths were pooled into the same bins as defined in Table 4.7, and the mean and median 3D sigma and residuals (absolute value up, horizontal, and 3D) were computed for each bin.

Plots of mean and median enabled 3D vector sigmas versus (log) vector length are shown in Figure 4.26. The plots include a logarithmic regression curve (with equation and R^2 value), although these are for illustration rather than prediction. A log regression was used rather than power regression, even though the latter actually fits the data better (particularly the plot of mean values). But a log regression is considered more realistic, as its rate of increase decreases with increasing vector length, the expected behavior for GNSS solutions. This behavior will be shown in the loop analysis in the next section.

In both Figure 4.26 plots, the data exhibit an increase in vector sigmas with vector length. However, note the vertical sigma scale of the mean plot is an order of magnitude greater than the median plot, so its rate of increase is much greater. For example, at 1000 km the mean regression predicts a sigma of 16 cm (large for GNSS), versus 4.6 cm for the median regression (a more realistic value). This figure is a manifestation of the sensitivity of the mean to extreme values. In such cases, the median provides a more appropriate measure of center, which is certainly the case here, since this dataset includes a very wide range of values.

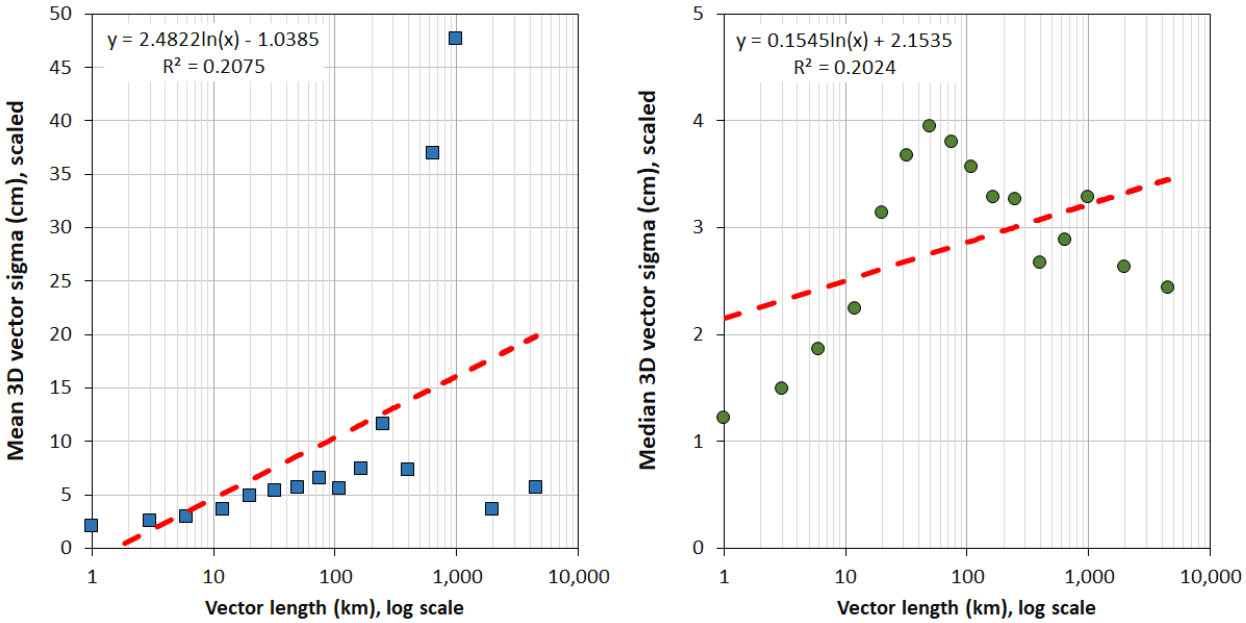

Figure 4.26. Mean and median enabled 3D vector sigmas as a function of vector length (log scale on horizontal vector length axis).

Figure 4.27 is similar to Figure 4.26, but it instead shows the enabled minimally constrained 3D vector residuals as a function of (log) vector length. In this case, the vertical axes of both plots are the same. The plot based on mean values also has a greater rate of increase, due again to the sensitivity of the mean to extremes (note the residual outlier of 3 cm at 1,000 km for the mean plot). The R^2 value for residuals indicate stronger correlation (about 0.6, versus 0.2 for sigmas in Figure 4.26).

Based on analysis of the vector sigmas and residuals for the NA2011 Project dataset, it is evident that both increase as vector length increases, although it appears the increase is generally not large. This is consistent with the finding that rejections also increase with vector length.

4.2.6. GNSS vector loop closure analysis

Analysis of the geometric closure of loops made by vectors provides insight into NA2011 network accuracy. Rather than consider all possible loops, graph theory was used to define all independent loops (called "fundamental circuits" in graph theory). The first step in this process is to build an adjacency matrix for the network, a square matrix used to represent a finite graph. The elements of the matrix indicate whether pairs of vertices are adjacent or not in the graph. Using the adjacency matrix, the spanning tree of the network forming the minimum number of vector connections between marks is found. While the spanning tree is being built, fundamental circuits (i.e., loops) are made by examining connected vertices. Vectors not used to form the spanning tree itself—but connect to vertices on the spanning tree—are added to the loops. See Deo (1974) for a description (Chapter 3) and algorithms (Chapter 11).

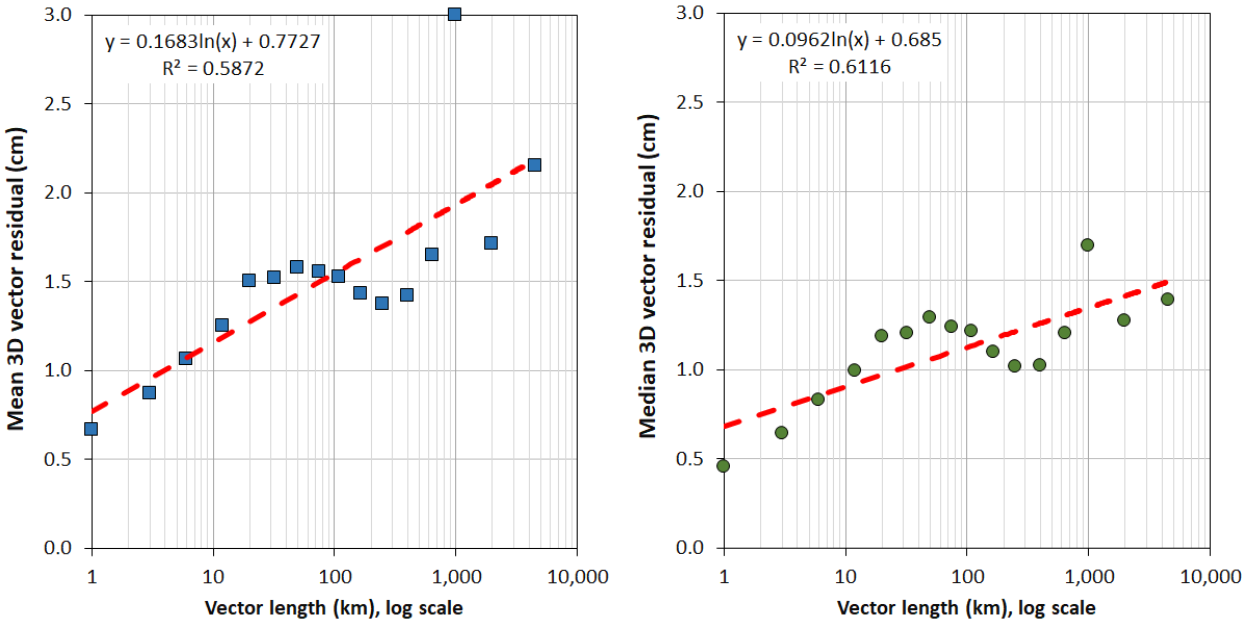

Figure 4.27. Mean and median 3D vector residuals as a function of vector length (log scale on horizontal vector length axis).

A loop closure analysis was performed in February 2012, using all enabled GNSS vectors in the CONUS network at that time (excluding Alaska, but before it was split into Primary and Secondary). The network consisted of 404,631 enabled vectors forming 70,226 independent loops with a total length of 925,019 km.

Statistics of the loop analysis are given in Table 4.9. The number of legs (GNSS vectors) in the loops ranged from 3 to 407, with a mean of 13.2 and median of 4. Loop lengths ranged from 0.04 to 7017 km, with a mean of 128 km and a median of 37 km. The maximum horizontal and 3D misclosures are nearly the same, 20.7 and 20.9 cm, respectively. The maximum relative 3D closure (with respect to loop length) is 70 parts per million (ppm), with a mean and median of 0.4 and 0.2 ppm, respectively.

Misclosures for the north, east, and up components are shown in Figure 4.28, with respect to total loop distance. There is no obvious increase in misclosures with distance (although this is investigated further below). The misclosures are well-centered on zero, as indicated by the zero mean and median values in Table 4.9. The ranges for north and east misclosures are greater than those for the up misclosures (as expected for GNSS data), and there is more dispersion in the up misclosures. The dispersion is exhibited in the greater scatter of the up misclosures in Figure 4.28, as well as the standard deviations and percentiles in Table 4.9. The east standard deviation of both the north and east components is 0.7 cm and 1.1 cm for the up component. The percentiles show 99% (between 0.5% and 99.5%) of the misclosures are within about ±2.3 cm horizontally and ±3.7 cm in height.

Table 4.9. Enabled GNSS vector loop analysis statistics for February 2017 CONUS network (70,226 independent loops with total length of 925,019 km).

	Number legs	Length (km)	GNSS vector loop misclosures (cm and parts per million)					
			North (cm)	East (cm)	Up (cm)	Horz (cm)	3D (cm)	3D (ppm)
Minimum	3	0.04	-8.3	-11.4	-9.3	0.0	0.0	0.000
Maximum	407	7017.0	17.4	15.5	8.0	20.7	20.9	79.057
Mean	13.2	128.2	0.0	0.0	0.0	0.7	1.1	0.376
Std deviation	±28.6	±344.6	±0.7	±0.7	±1.1	±0.6	±0.9	±0.800
Percentiles								
0.5%	3	2.5	-2.2	-2.2	-3.7	0.0	0.0	0.000
2.5%	3	5.0	-1.3	-1.3	-2.5	0.0	0.1	0.005
5%	3	6.9	-1.0	-1.0	-1.9	0.1	0.1	0.015
50% (median)	**4**	**36.9**	**0.0**	**0.0**	**0.0**	**0.5**	**0.9**	**0.196**
95%	59	536.0	1.1	1.1	1.9	1.9	2.9	1.233
97.5%	101	1027.2	1.4	1.5	2.4	2.3	3.4	1.777
99.5%	195	2396.0	2.3	2.4	3.6	3.3	4.7	3.736

Although the loop closure indicates little distance dependence on the misclosures, it was evaluated more directly by performing an analysis similar to that done for sigmas and residuals in the previous two sections. As with those analyses, the loops were grouped by length to create bins with a similar number of loops. The results of this analysis for the median 3D loop misclosures in each bin is shown in Figure 4.29, and it exhibits very similar behavior to the median curves for vector sigmas and residuals. Based on a mean of the regression equation coefficients and constants, the 3D values for vector sigmas, residuals, and loop misclosures in centimeters are all roughly $0.1 \times \ln(L) + 1$, where L is length in kilometers. This is an interesting finding, and it reflects an expected consistency between these quantities. Granted, loops and vectors cannot be directly related, since a loop is a collection of vectors that will not all be of the same length. For this case, most loops consist of four or less vectors; however, some loops have many more vectors (up to 407). However, in the aggregate—as done here with length bins—it is not unreasonable to treat loop and vector lengths as approximately equivalent.

Figure 4.29 also shows relative 3D loop misclosure, in parts per million (ppm), with respect to loop length. This plot exhibits a rapid decrease in relative loop misclosure, from 2.7 ppm at 1 km, to 0.5 ppm at 10 km, to 0.1 ppm at 100 km, and to 0.01 ppm at 1000 km. This, of course, is the great strength of GNSS: it gives incredibly precise results over very long distances. The plot also shows that the rate of increase in error decreases with distance, as mentioned earlier (whether represented by sigmas, residuals, or loop misclosures).

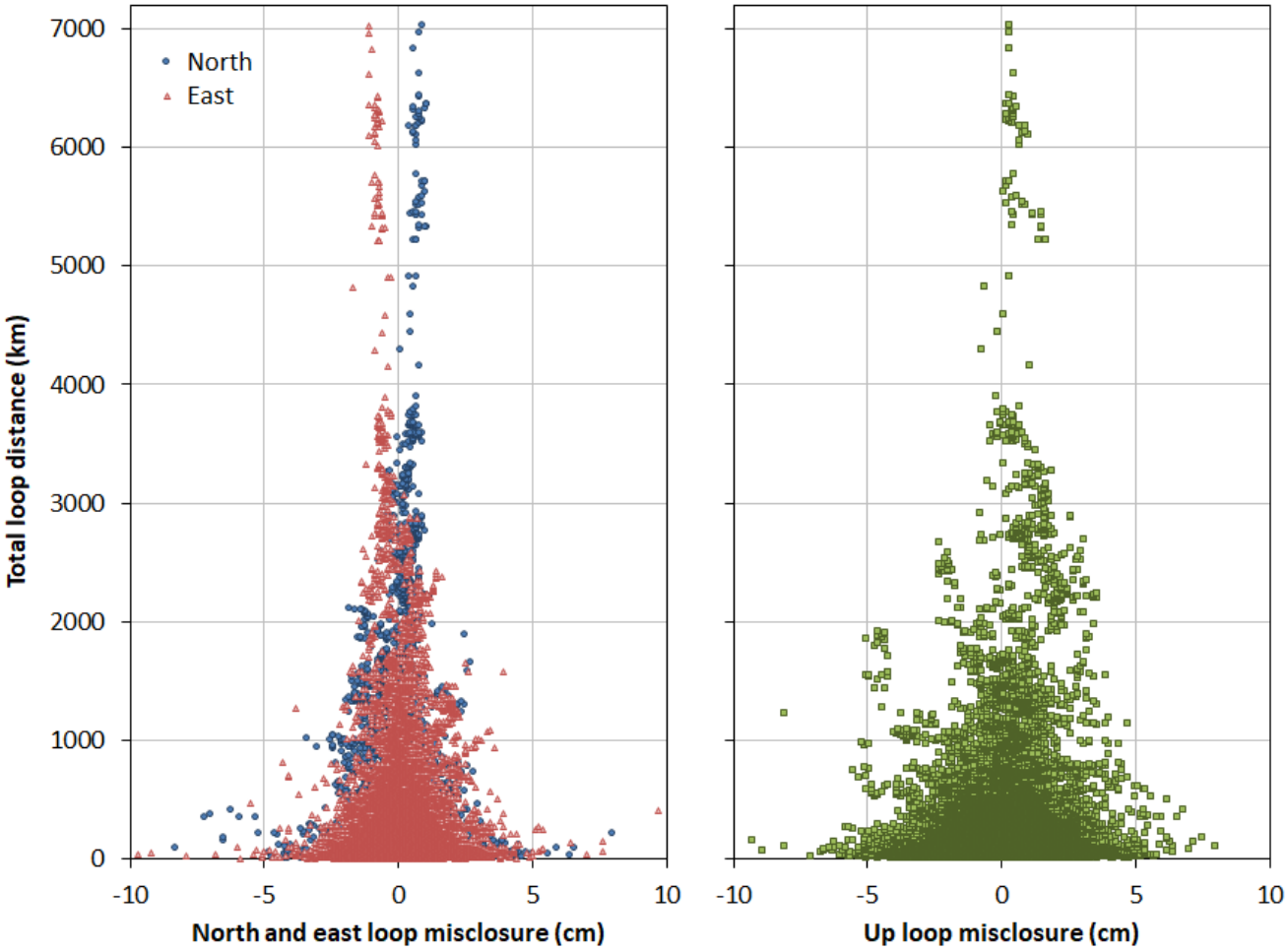

Figure 4.28. North, east, and up misclosures for independent enabled GNSS vector loops.

The misclosure analysis yielded remarkably good results. It demonstrates, through geometry alone, that the NA2011 CONUS network is quite precise (and thus accurate, if no bias is present). But a question arises as to whether the loop analysis is somewhat optimistic due to the presence of "trivial" (statistically dependent) vectors in the NA2011 networks (as discussed later in Section 5.2). Any loop created from a single GNSS processing session that contains one or more trivial vectors would be expected to show an artificially small misclosure. But it is not clear such a problem had much impact on the analysis done here, for two reasons. One is that the degree of "trivialness" (i.e., statistical dependence) is not uniform in a session, due both to the highly variable total number of vectors in sessions, and also because not all possible trivial vectors were used in the sessions containing trivial vectors. The other is that loops are constructed without regard to whether vectors participated in a session, and so some number of trivial vectors would be excluded through the loops-building process alone. Considerable analysis would be required to determine the effect of trivial vector false redundancy on the loop closure analysis. Although not done for the loop analysis, the impact of trivial vectors on NA2011 results is explored more fully in Sections 5.2.3 and 5.2.4.

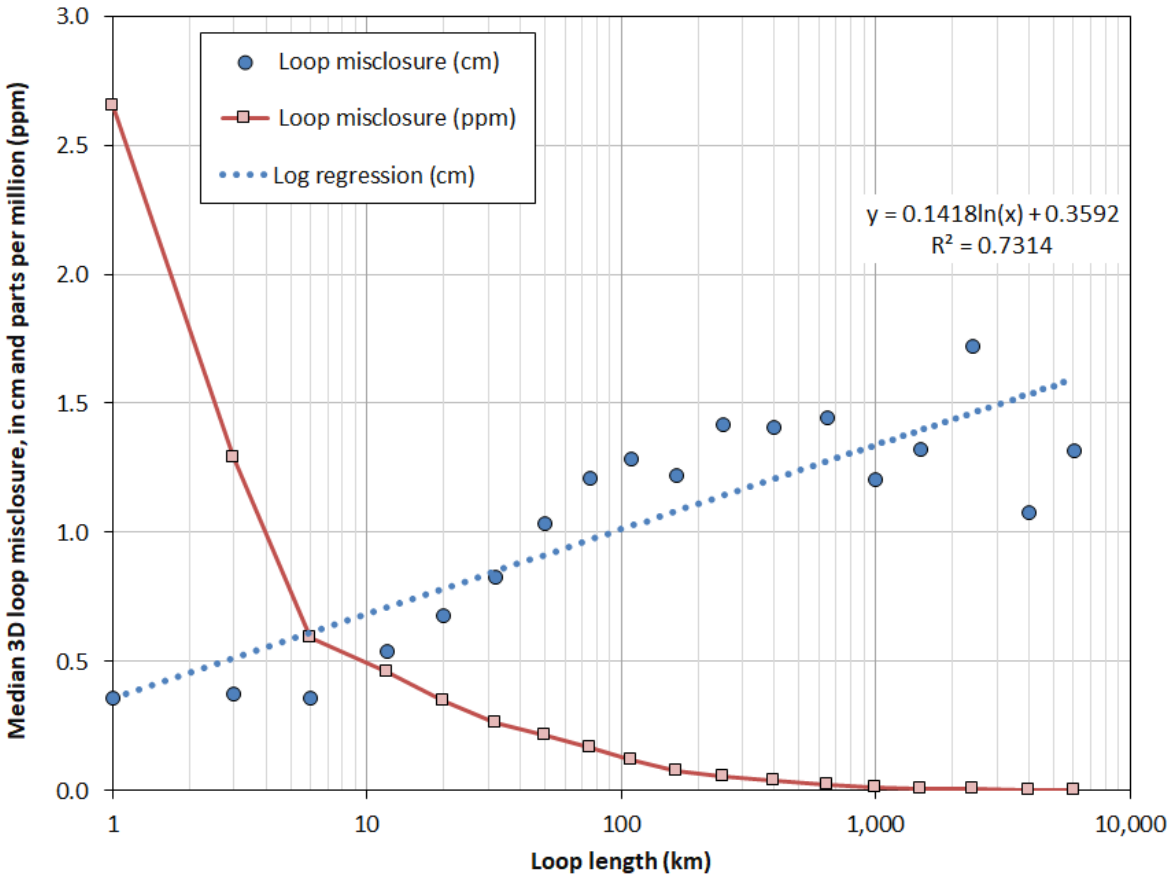

Figure 4.29. Median 3D loop misclosures in cm and parts per million as function of vector length (log scale on horizontal vector length axis).

After splitting the CONUS network into Primary and Secondary, no further loop closure analyses were performed. In the future, such analyses could be done by combining all vectors and considering the length of the vectors composing the loops to address the previously raised issue of equating loop and vector lengths. Such analyses could possibly also take into account the presence of trivial vectors.

4.3. Mark coordinate accuracy estimates

The main output of the NA2011 Project were the mark coordinates from the final constrained adjustments of the five networks—CONUS Primary, CONUS Secondary, Alaska, and the two versions of the Pacific network (PA11 and MA11). Along with those coordinates are accuracy estimates based on the formal uncertainties derived from the network solution covariance matrices of propagated observation and constraint standard deviations. Two types of accuracies are published for the marks, network and local. NGS has published the basis for the geodetic control accuracies in *Geospatial Positioning Accuracy Standards* (FGDC, 1998), Parts 1 and 2. However, NGS departed slightly from the FGDC standards, and the standards have not yet been updated to reflect this change. These departures are listed below (the first three were

implemented as part of the 2007 national adjustment, and the fourth was adopted in the NA2011 Project);

1. The actual computed accuracy estimates are given, rather than assigning them to categories (e.g., 1-mm, 2-mm, 5-mm, 1-cm, 2-cm, 5-cm, etc.).
2. The local accuracy value given for a mark is based on the median for all adjusted observations connected to that mark, rather than the arithmetic mean.
3. A distance is provided along with the local accuracy. It is the median distance from the mark to all marks it is connected to by direct or correlated observations (no distance is specified in the standards).
4. The CORSs are not assumed errorless, as they were for the 2007 adjustment. Instead the formal uncertainties of the initial Multi-Year CORS Solution (MYCS1) were assigned to the constrained CORS coordinates, and thus were propagated into the network.

The FDGC standards require accuracies be published at 95% confidence, but it does not specify how horizontal accuracies are represented. NGS uses the method by Leenhouts (1985) to compute the 95% confidence radius of an accuracy circle, based on the error ellipse dimensions (Milbert, 2009). The Leenhouts method is used for both network and local horizontal accuracies. Unless otherwise stated, all horizontal accuracies given at 95% confidence in this report are based on the Leenhouts method.

Network and local accuracies are defined in Part 1 of the 1998 FGDC standard, but some confusion still exists as to their meaning, in particular local accuracies. Both network and local accuracies are given at 95% confidence. Network accuracy represents the uncertainty of a point with respect to the geodetic network, and it is associated exclusively with the single control mark. Network accuracy is computed from the post-adjustment covariance matrix for that mark, scaled by the adjustment standard deviation of unit weight.

Local accuracy is the uncertainty of the adjusted observations connecting two points, and thus it is shared by a pair of points. Local accuracy represents the uncertainty of the mark with respect to another mark it is connected to by an observation (the observation can be a direct vector tie or a correlated observation from simultaneous baseline processing). Every passive mark has at least one local accuracy, but most have many local accuracies, representing all the adjusted observations used to position that mark. Local accuracies are computed from the post-adjustment covariance matrix of the adjusted observations. Because local accuracies are determined for all adjusted observations, they may not be spatially "local" at all; the distance is simply the length of the connecting vector (or distance between correlated observations for marks not directly connected). Thus a "local" accuracy may have a distance of thousands of kilometers. The published local horizontal accuracy, ellipsoid height accuracy, and distance of a mark is the median, computed for each value individually. The median is used, rather than the mean, because the median is much less sensitive to extreme values, and so it is a better measure of central tendency in the presence of large outliers.

4.3.1. Passive mark accuracies

Both CORS and passive mark coordinates and accuracies were determined in the NA2011 adjustments. As the CORSs were constrained using weighted (stochastic) constraints, the final adjusted coordinates and uncertainties differed from the *a priori* values. The difference depended both upon the standard deviations (sigmas) used for the constraints, as well as how well they fit in the adjusted network. These adjusted CORS coordinates and accuracies were *not* published; only the values from MYCS1 were published for CORSs. The difference in MYCS1 and NA2011 CORS coordinates and uncertainties are discussed in the next section. Only passive mark coordinates and accuracies from the NA2011 adjustments were published. Likewise, the constraint sigmas of Primary network mark used as constraints in the Secondary network were used for the published accuracies, not the adjusted sigmas. There were two exceptions where the *a posteriori* sigmas from the Secondary network adjustment were used for the published accuracies (rather than from the Primary network). One exception was for 103 constrained Primary no-check marks that had more than one enabled vector tie in the Secondary network (i.e., were not no-check in that network). The other exception was for 13 Primary control marks that had large constraint sigmas (greater than 8 cm in any component). All but one of these also had more vector ties in the Secondary than the Primary network.

Table 4.10 summarizes the NA2011 horizontal and ellipsoid height network accuracies for passive control, based on the final constrained adjustments. The table provides results for all combined marks, as well as for each of the individual networks. For the Pacific, there were 264 marks with PA11 coordinates and 117 marks with MA11 coordinates. The table does not include the 2,134 no-check marks (Section 4.3.2), the 1195 MYCS1 CORSs used as constraints (Section 4.3.3), nor the 183 disconnected marks (Section 3.4).

Table 4.10 also shows statistics on the number of enabled vector ties and occupations with enabled vector ties (note the minimum number of vector ties is two, because no-check marks are excluded). The maximum number of vectors and occupations for the Primary network (and overall) is 370, because it is a single occupation. The mark is an antenna mount for a continuously operating GNSS receiver classified as passive, because it is not an NGS CORS (TEXAS MEDICAL CENTER CORS ARP, PID DI3504). Other non-CORS "permanent" antennas were handled in the same manner, as discussed in Section 2.2.2.

Much of the information in Table 4.10 is shown graphically in the following four figures. Figure 4.30 shows the percentage of network horizontal and ellipsoid height accuracies in 1-cm increments, from zero to 10 cm for each of the four networks. The proportion of horizontal accuracies decreases rapidly as the accuracy worsens (i.e., as the numeric accuracy values increase). For horizontal accuracy, the maximum percentage occurs in the 0 to 1 cm bin for the CONUS Primary network (67%). For the other networks, the maximum occurs in the 1 to 2 cm bin: 45% for CONUS Secondary; 24% for Alaska; and 36% for the Pacific. Alaska has the largest horizontal errors of the networks. It is the only network with more than 1% of marks with horizontal accuracies larger than 10 cm, also reflected by the statistics in Table 4.10. The median accuracy of the Alaska marks is 3.7 cm; the next largest is less than half that value, 1.6 cm for the Pacific marks. The large errors in Alaska are due, at least in part, to the state's

tectonic activity. The *HTDP* crustal deformation models have improved since the NA2011 Project's completion. The improvements include addition of new grids that model vertical displacements in central Alaska. The impact of these improvements is discussed in Section 6.2.1.3, including an example readjustment of the Alaska network using G-files transformed using the latest version of *HTDP* (see Table 6.2).

Table 4.10. Network accuracies, vector ties, and occupations for NA2011 passive marks. Does not include the 1195 constrained MYCS1 CORSs, 2134 no-check, or 183 disconnected marks. Pacific consists of 264 PA11 and 117 MA11 marks. Accuracies are at 95% confidence.

	All passive marks		CONUS Primary		CONUS Secondary		Alaska		Pacific	
Number	**77,560**		**59,979**		**16,444**		**756**		**381**	
Accuracies (cm)	**Horz**	**Eht**	**Horz**	**Eht**	**Horz**	**Eht**	**Horz**	**Eht**	**Horz**	**Eht**
Minimum	0.09	0.16	0.09	0.16	0.17	0.22	0.57	1.22	0.46	0.92
Maximum	626.74	317.46	150.33	150.76	626.74	111.49	296.51	317.46	26.96	16.99
Mean	1.523	2.641	0.964	1.649	2.570	5.387	22.660	20.723	2.405	4.434
Std deviation	±5.871	±5.558	±1.174	±1.850	±6.848	±6.743	±43.714	±36.549	±2.393	±2.838
Percentiles										
1.0%	0.21	0.31	0.20	0.31	0.41	0.59	0.77	1.58	0.54	1.15
5.0%	0.30	0.41	0.28	0.39	0.57	0.90	0.96	1.88	0.63	1.53
10.0%	0.36	0.51	0.33	0.47	0.74	1.31	1.08	2.17	0.73	1.76
50.0% (median)	**0.88**	**1.49**	**0.74**	**1.23**	**1.63**	**3.45**	**3.67**	**6.19**	**1.58**	**3.47**
90.0%	2.32	4.80	1.77	3.12	4.15	11.29	73.99	54.23	4.87	9.54
95.0%	3.23	7.11	2.26	4.12	6.70	17.46	132.02	89.39	7.07	9.87
99.0%	10.58	20.72	3.92	7.43	19.76	35.93	191.46	196.49	10.24	12.99
Enabled vectors and occupations	**Num vecs**	**Num occup**	**Num vecs**	**Num occup**	**Num vecs**	**Num occup**	**Num vecs**	**Num occup**	**Num vecs**	**Num occup**
Minimum	2	1	2	1	2	1	2	1	2	1
Maximum	370	370	370	370	127	99	72	42	78	15
Mean	9.429	3.791	10.363	4.123	6.246	2.633	5.534	2.993	7.428	3.018
Std deviation	±11.431	±4.204	±12.530	±4.611	±5.141	±1.868	±6.233	±3.025	±7.674	±2.195
Percentiles										
1.0%	2	1	2	1	2	1	2	1	2	1
5.0%	2	1	2	1	2	1	2	1	2	1
10.0%	2	2	2	2	2	1	2	1	2	1
50.0% (median)	**6**	**3**	**6**	**3**	**5**	**2**	**4**	**2**	**6**	**2**
90.0%	19	7	22	8	11	4	11	5	14	6
95.0%	29	10	32	11	15	5	16	7	17	7
99.0%	54	19	58	20	26	9	29	15	51	12

As with the horizontal accuracies, the ellipsoid height accuracies in Figure 4.30 show a decrease in number as the accuracy worsens, although the decrease is not as rapid or as uniform as for horizontal accuracies. For the CONUS Primary network, the maximum percentage again occurs in the 0 to 1 cm bin, but at a much lower percentage of 38% (versus 67% for horizontal). That is nearly equal to the 37% of Primary marks in the 1 to 2 cm bin, for a total of 75% of marks within 0 to 2 cm for ellipsoid height accuracy. The peak values occur on the 2 to 3 cm bin for CONUS Secondary (19%) and the Pacific (22%), and it occurs in the 3 to 4 cm bin for Alaska (14%). Pacific marks are also the only ones showing a large increase in the proportion of marks at worse accuracies—the 2.4% of marks in the 8 to 9 cm bin increases to 8.1% in the 9 to 10 cm bin. It then decreases to 1.8% in the 10 to 11 cm bin (not shown in Figure 4.30). This peak is somewhat surprising, since the Pacific median ellipsoid height accuracies are almost identical to the CONUS Secondary mark median accuracies and are much less than the Alaska median accuracies (see Table 4.10). Part of this may simply be due to the small and variable sample size of large accuracies in the Pacific network; there are only 9 marks in the 8 to 9 cm bin and 31 marks in the 9 to 10 cm bin.

Figure 4.31 is similar to Figure 4.30, but it shows the percentage of horizontal and ellipsoid height network accuracies together in each of its two charts with respect to all 77,560 passive marks (omitting no-check and disconnected marks). The upper chart gives accuracies in 1-cm bins from 0 to 20 cm, and it includes about 99% of the marks. However, above about 10 cm the bars are too short to see clearly. To make bins with a small number of marks more visible—and to capture the remaining 1% of marks—the lower chart uses a vertical log scale for the number of marks and has a maximum accuracy bin of 500 to 1000 cm (5 to 10 m). Accommodating such large accuracy values required using irregularly sized bins, as shown in the figure. The small number of large values creates a long accuracy "tail," similar to the residual tails discussed earlier in this chapter. Such long tails are undesirable, particularly for accuracies, since it means some marks have large accuracy values. Granted, it is a small number, but it is nonetheless questionable to publish marks with such large error estimates as geodetic "control," even if only on a small number of marks.

The largest accuracies in Figure 4.31 (and Table 4.10) are indeed large, with a maximum of 6.27 and 3.17 ***meters***, horizontally and vertically, respectively. Oddly, the maximum error is horizontal, and it is twice as large as the maximum vertical error (usually the opposite is true). Figure 4.31 shows only a single mark with values this large, but it is not the same mark for horizontal and height accuracies. The maximum horizontal error occurs in the Secondary network for mark J 24 (PID QM0023), occupied once in 1992 in project GPS698 (Wisconsin). It had been a no-check mark, but one vector was re-enabled to remove the no-check. The resulting residuals were not particularly large (maximum 3D of 7.3 cm). The reason the error estimate on the mark is so large is because the 3D errors (sigmas) on the two enabled GNSS vectors are very large—2.6 and 3.8 ***meters*** (note the two marks connected to J 24 do not have unusually large error estimates, but they are also connected to other vectors with small sigmas). Such large vector sigmas cannot be correct, and this may be another case similar to GPS1460 discussed previously, where the vector uncertainties were incorrectly populated.

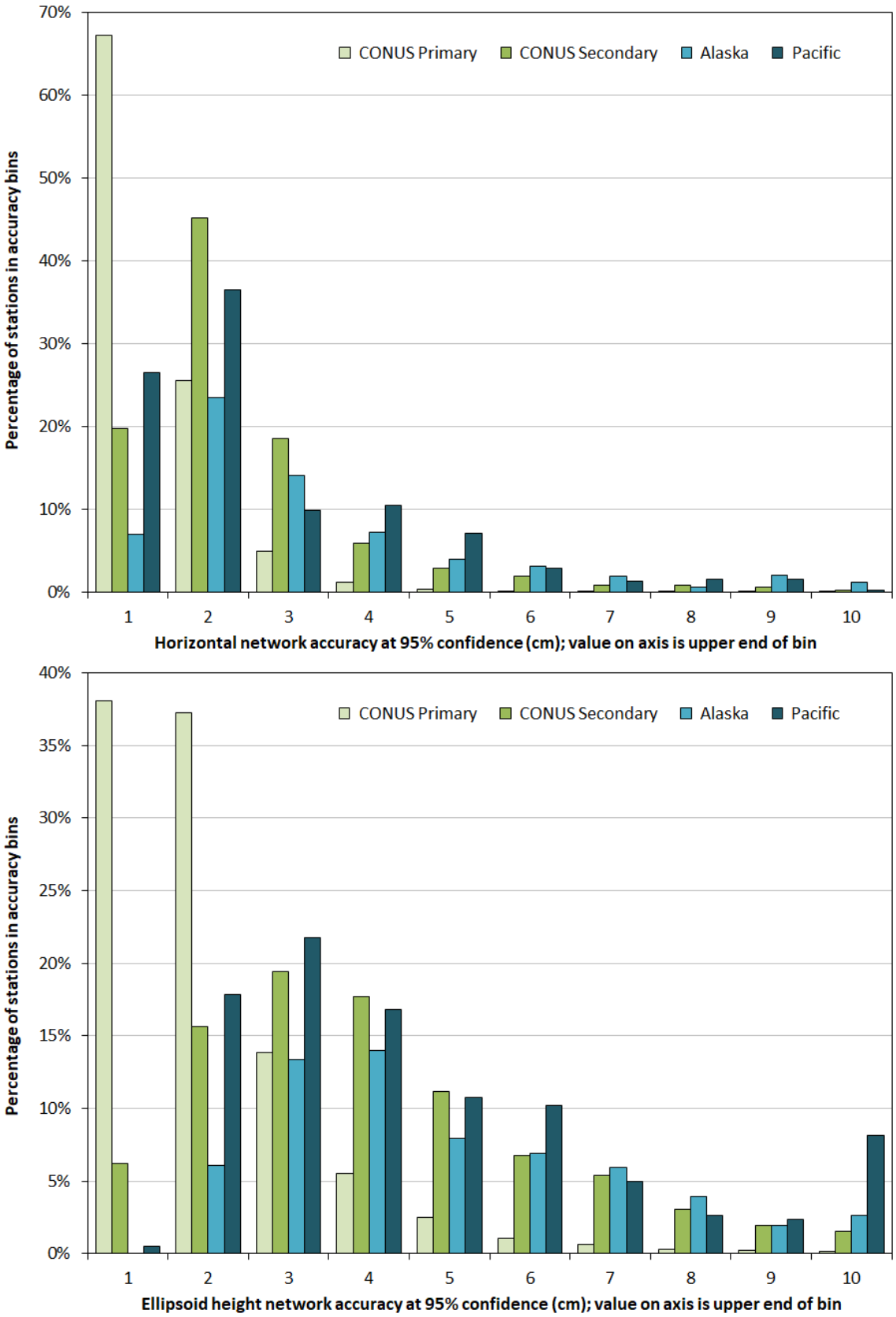

Figure 4.30. Distribution of horizontal (top) and vertical (bottom) accuracies by network.

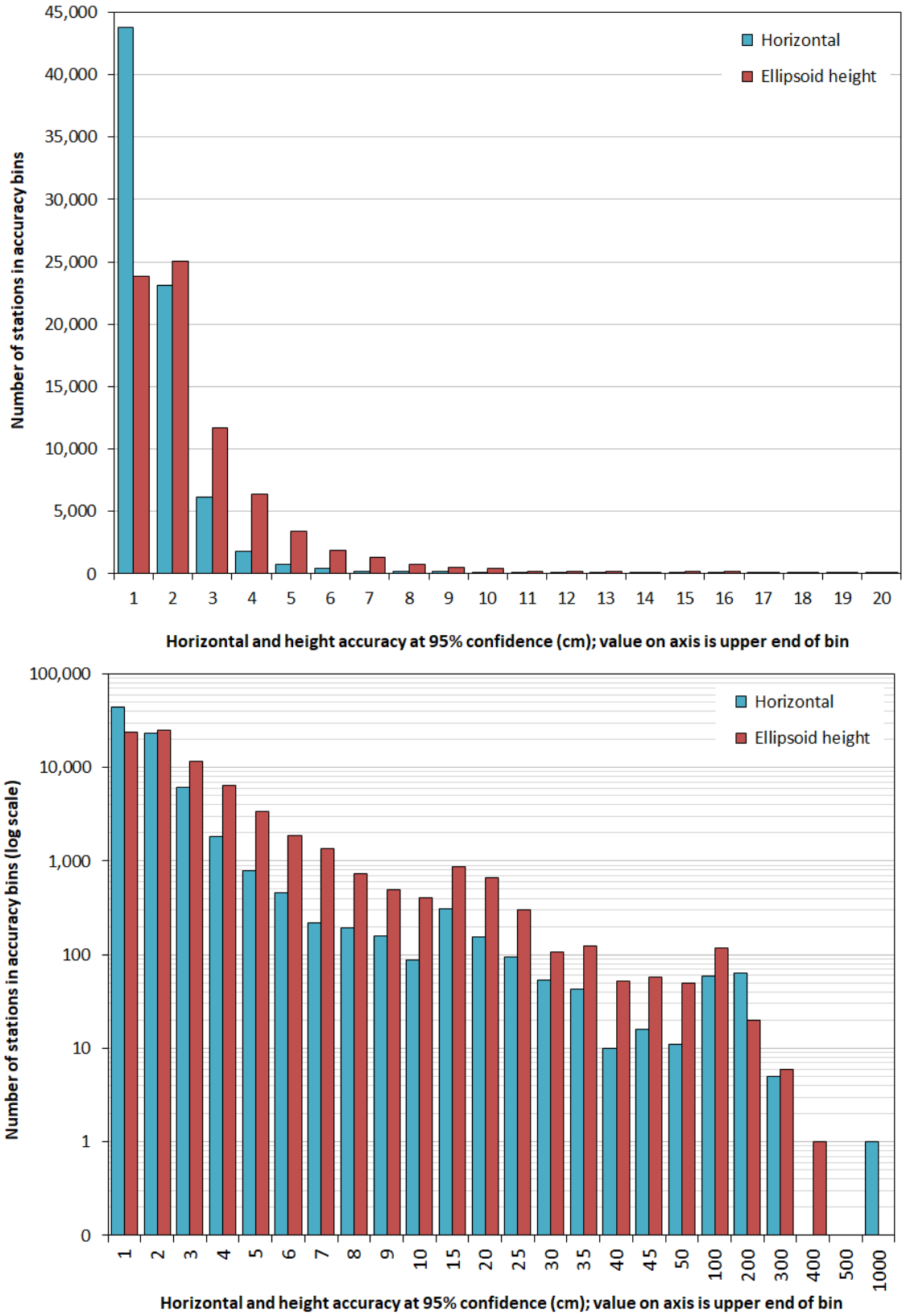

Figure 4.31. Distribution of network accuracies for all networks. Top chart is for accuracies of 0 to 20 cm, bottom is for all accuracies (log scale on vertical axis emphasizes accuracy bins with few marks).

The mark with the maximum ellipsoid height error (3.17 m) in Figure 4.31 is AKDOTPF GPS 14 (PID DH4688) in Alaska. It, too, is determined by two vectors in a single occupation, and one was re-enabled to remove a no-check status. The occupation was done in 1989 in project GPS137/4. Similar to the previously discussed Wisconsin mark, the two vectors both have very large 3D sigmas, 1.7 and 3.0 ***meters***. This also cannot be correct. Vectors with such erroneous sigmas should have been corrected or removed prior to finalizing this adjustment.

In Figure 4.31, there are an additional 68 and 26 marks with horizontal and height errors, respectively, in the 100 to 300 cm range. Again, it is both interesting and odd to find there are more marks with large horizontal errors. Without investigating these marks for this report, it is likely at least some also have inflated errors due to erroneously large vector sigmas. Certainly, it is questionable to consider marks with such errors as geodetic control; however, it is also difficult to determine what to do about them. Removing these marks from the NA2011 Project would not remove them from the NGSIDB; under current NGS policy they would still be published with whatever coordinates and accuracies were determined from a previous adjustment (although they could in principle be classified "unpublishable" or otherwise be flagged). A better method is needed to deal with such marks, and the same could be said for other marks with large errors. There has been no agreement as to what accuracy should be the cutoff for geodetic control. In the NA2011 Project, there are 821 marks with horizontal accuracies greater than 10 cm, and 836 with ellipsoid height errors greater than 20 cm. Most of these marks are the same, but many are not. The techniques and tools developed during the NA2011 Project (and mostly after the adjustments were completed) will make it easier to identify such marks in future large adjustments.

Figure 4.32 shows the median and mean horizontal and ellipsoid height accuracies grouped by the last year a mark was occupied with connections to enabled vectors. The figure shows a dramatic exponential-like improvement in accuracy with time, and it is strikingly similar to GNSS vector sigmas plotted by year in Figure 3.7. Both the median and mean show a steep spike in 1984 for large horizontal error. This spike is due to a project in Pennsylvania (GPS029) where the marks that were not occupied again after 1984 have a median horizontal accuracy of about 24 cm—the same as the peak in Figure 4.32. Apart from that peak, and another fairly large horizontal and height spike in 1989, the median and mean accuracies decrease steadily with time, flattening out around 2007. There is a minor increase in 2011, as was observed for the residuals (see Figure 4.5 and the associated discussion for an explanation on what occurred).

Figure 4.33 shows median and mean horizontal and ellipsoid height accuracies of marks by the number of connected vectors (top) and occupations (bottom), in both cases considering only enabled vectors. For both plots there is a clear improvement in accuracy with increasing vector ties and occupations, as expected. Increasing the number of vectors from 2 to 6 improves the accuracies for all cases by approximately 50%. Adding additional vectors further improves accuracies but at a diminishing rate; an additional 12 vectors (total of 18 vectors) improves by another 50%. Beyond around 30 vectors, there is essentially no improvement in accuracy.

In an analysis where all the vectors are evaluated collectively, as shown in the top plot of Figure 4.33, there is not really any way to ensure that the vectors represent independent observations.

Many of the marks with a large number of vectors are likely baseline processing hubs with perhaps very few (even only one) independent occupations. The bottom plot in Figure 4.33 attempts to address this deficiency by considering the number of occupations as a proxy for observation independence. The results are similar to the number of vectors (but smoother); increasing the number of occupations from 2 to 6 improves the accuracy by about 50%, with diminishing improvement for additional occupations.

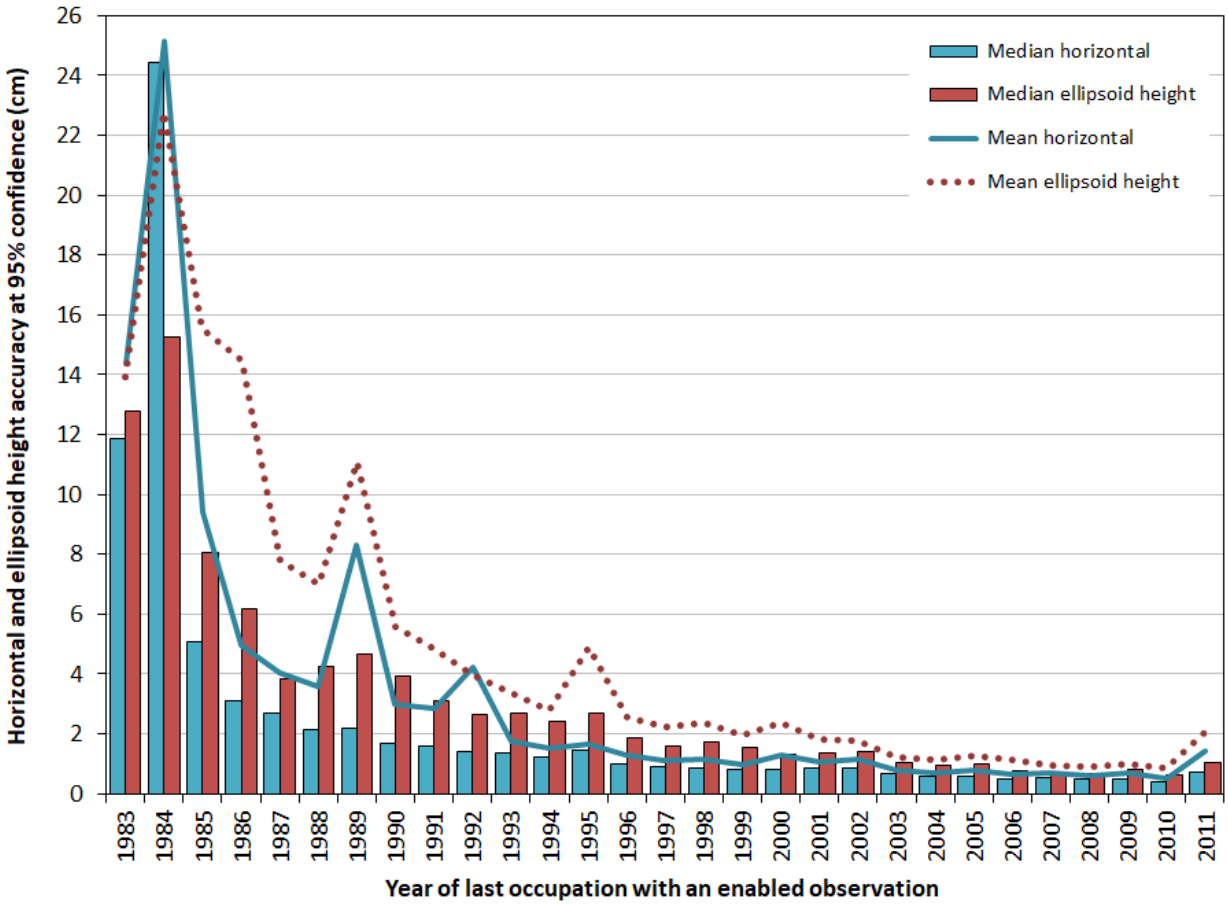

Figure 4.32. Median and mean accuracies by year of last occupation with an enabled observation.

Like the vectors, the independence of occupations is unknown, since they are inferred from the processing session start and stop times in the vector G-file (as discussed in Section 2.2.1). The actual number of occupations can be determined from other data, such as field logs or the original B-files loaded into the NGSIDB (which include occupation information). However, that would require monumental effort for the NA2011 Project, and it still would not guarantee complete and correct information. Despite the limitations in determining independent occupations, they are likely overall quite reliable, and they provide an estimate as to the amount of independent data needed to significantly improve accuracies.

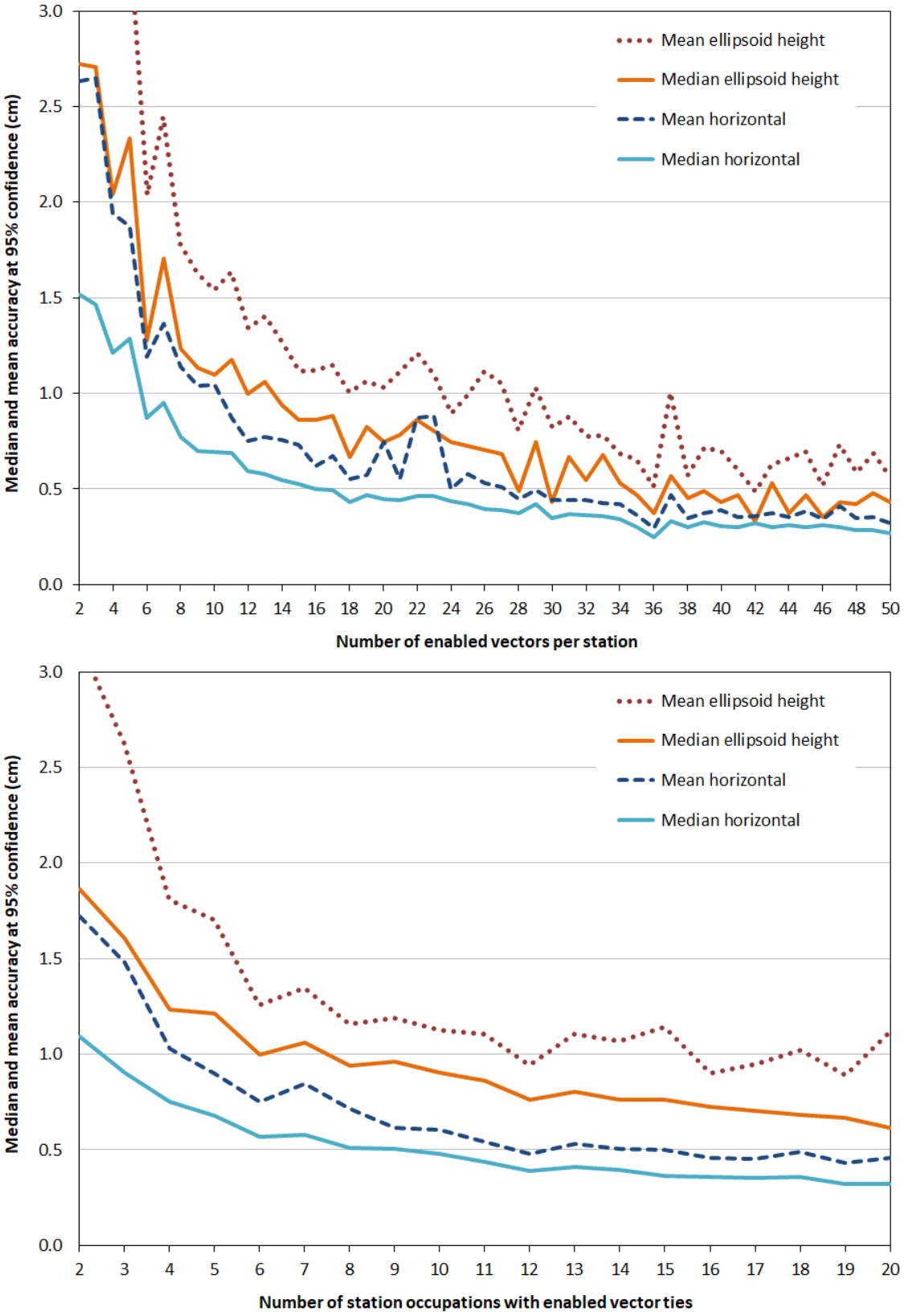

Figure 4.33. Median and mean accuracies by number of vectors (top) and occupations (bottom). Only enabled vectors are counted in both charts.

Accuracy estimates for the adjusted coordinates and observations were computed from the *a posteriori* standard deviations (sigmas) determined in the network adjustments, scaled by the network adjustment standard deviation of unit weight. These north, east, and up standard deviations are in the adjustment output coordinate files (the B-files described in Section 2.1.2). These values are stored for individual marks to use for network accuracies, and they are stored for point pairs of adjusted observations for computing local accuracies.

For ellipsoid height accuracies, the up sigma is multiplied by the univariate scalar of 1.9600 to scale it to 95% confidence. For the horizontal accuracies, the bivariate scalar of 2.4477 is used with the method of Leenhouts (1985). Since this method requires using the horizontal error ellipse axes, the horizontal (north-east) correlation coefficient for each point (and adjusted observation point pair) is also stored in the output B-files. With the north and east sigmas and the north-east correlations, the horizontal error ellipse axes can be computed. For the 2007 national adjustment, NGS chose to store only the horizontal correlation coefficient, to compute the horizontal accuracy. Unfortunately, the other two correlations (north-up and east-up) were not stored, and the same is true for the NA2011 Project. Omitting the other two correlations means the complete error distribution is not stored, so error ellipsoids cannot be computed, nor can the errors be correctly rotated into ECEF coordinates.

Since enough information is stored to compute horizontal error ellipses, their shape and orientation can be used to analyze anisotropy of the accuracy estimates. Figure 4.34 shows the distribution of error ellipse azimuth and elongation for the 77,560 passive marks (excluding no-check and undetermined marks). The azimuths are shown as vertical bars from 0° to 180° and centered on bins 5° wide (the axis labels are at the lower end of each bin). Elongation is displayed as the mean and median ratio of semi-major and semi-minor axes (a/b) within each of the 5° bins.

Figure 4.34 shows most of the error ellipses have a north-south orientation. The ellipse major axis is within ±10° of north for 48% of the marks, versus 3% within ±10° of east, consistent with expectation for GNSS, since the GPS satellite orbits in particular do not provide overhead coverage to the north.

Also note the presence of two small 45° and 135° azimuth peaks, corresponding to local minimums in the median and mean elongation ratios. These are artifacts resulting from the fixed format of the sigma values (to two decimal places). When the north and east sigma values are identical (artificially common, due to the fixed format), the ellipse orientation is exactly 45° or 135° (depending on the sign of the correlation). This occurs for 1891 (2.4%) of the marks.

Overall the error ellipses are not very elongated. The mean and median elongation ratios for all marks are nearly the same, 1.33 and 1.28, respectively. But much larger differences occur when the mean and median are computed for the 5° bins. Maximum elongations of 1.96 (mean) and 1.51 (median) occur at an approximate 90° azimuth. This is somewhat counter to expectation, since the maximum elongations are perpendicular to the most common orientations. In addition, the mean is substantially greater than the median, indicating the presence of very elongated ellipses at that azimuth, and, indeed, that is the case.

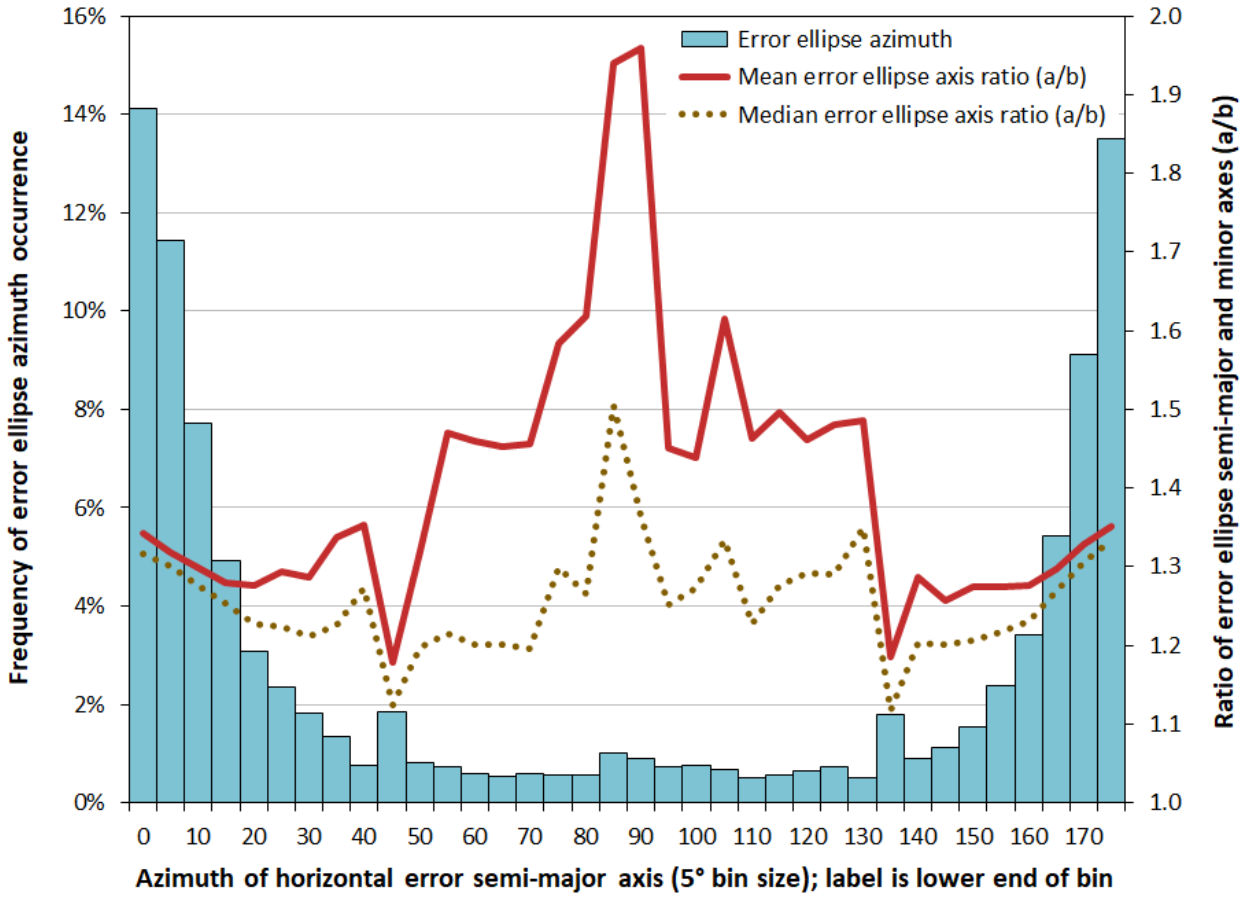

Figure 4.34. Horizontal error ellipse orientation and elongation.

Two ellipses have much greater elongation than all others—ratios of 50.4 and 39.2. These occur for marks ASH (PID HD1334) and GR 10 (PID AC7131), respectively. Both have azimuths close to zero, contrary to what is implied by Figure 4.34. These two marks are in project GPS1158 (Missouri) where *LINECOMP* and *TRIMVEC* software were used to process 567 vectors observed from 1991 through 1996. The project is unusual in several respects. Of 120 marks, only these two have an elongation ratio greater than 2. These two marks are on the edge of the network and are connected to each other, and the vector between them is nearly north-south (although they are also connected to other marks). There is tremendous variation in the vector sigmas. The 378 scaled 3D vector sigmas from *LINECOMP* range from 0.0049 to 1.68 ***meters*** (mean of 0.63 m). The 189 *TRIMVEC* vectors range from 0.004 to 1.34 ***meters*** (mean is 0.042 m), but only four *TRIMVEC* vectors have sigmas of 1.34 m; all others are less than 0.05 m. The network contains a large number of trivial vectors, nearly all that are possible for each session (see Section 5.2 for an explanation of how the presence of trivial vectors was determined), and all the vectors are short (1.3 to 19.8 km). There are no connections to CORSs in the project, and only two marks in this project were *ever* tied to CORSs (these CORS connections occur in three later projects in 1996, 1999, and 2003). The following network accuracy information is published for these marks:

PID	Designation	95% confidence accuracy (cm)		Standard deviations (cm)		
		Horizontal	Ellipsoid height	North	East	Up
HD1334	ASH	34.57	20.74	17.63	0.35	10.58
AC7131	GR 10	34.55	20.76	17.62	0.45	10.59

Note the horizontal accuracy does not reveal the great elongation. The elongation can be discerned from the north and east standard deviations, but that too would be unclear if the ellipses were oriented near ±45°. Without further analysis it is not completely clear why these two marks alone have extremely elongated error ellipses. But the project does have several issues that were discussed previously, such as unrealistically large and highly variable vector sigmas, large mark error estimates, and trivial vectors. This represents the type of project that should have been corrected or omitted from the NA2011 Project and any future adjustments.

Returning to the entire NA2011 dataset, the next largest error ellipse elongation ratio (excluding no-check marks) is 14.7 (mark T 44, PID RJ0241), and there are 93 others with ratios greater than 5. A total of 1678 marks (2.2%) have an elongation ratio of 2 or greater, with a mean and median orientation of 92° and 90°, respectively. The marks are distributed throughout all four networks, in nearly every state and territory, and are not concentrated in any particular areas. Most of the marks with elongated error ellipses are fairly old; the median enabled occupation date is 1992. Yet 31 of the marks were observed as recently as 2011, in project GPS2852. This project had erroneous covariances exported from *Trimble Business Center* (*TBC*) software (discussed in Section 5.1.3), which is likely the reason for the elongated ellipses. However, the next most recent marks with elongated ellipses were observed in 2010 and were processed using *PAGES*. Without a deeper analysis, it is not known why most of these highly elongated ellipses occur, but for now they are attributed to the distribution of covariances and constraints associated with the network geometry.

Maps showing the distribution of marks with symbol size proportional to accuracy are in Figure 4.35 through Figure 4.38 for CONUS Primary and Secondary horizontal and ellipsoid height accuracies. Figure 4.35 and Figure 4.36 show the CONUS horizontal accuracy estimates for the Primary and Secondary marks, respectively. Accuracies of greater than 10 cm have been filtered from the maps to prevent obscuring with large symbols. Yet even with the filter, both maps show an uneven distribution, not only of marks (already known), but also of accuracy magnitudes, with marks of similar accuracies tending to cluster in specific states. The accuracies are generally worse (larger) for the Secondary marks. But large errors also occur in the Primary network, and they can be quite variable. Compare, for example, the accuracies in Wisconsin to the adjacent state of Illinois. The Wisconsin errors are generally smaller, and they may be artificially low due to the presence of trivial vectors (see Section 5.2.3 for a more detailed discussion, with particular emphasis on Wisconsin).

The ellipsoid height accuracies are shown in Figure 4.37 and Figure 4.38 for CONUS Primary Secondary marks, respectively. The distribution is similar to the horizontal accuracies, with large (and small) values occurring at essentially the same marks. Again, the errors in Wisconsin are very small, apparently for the same reasons. Marks along the Gulf Coast have small

horizontal accuracies, but large ellipsoid height accuracy values. Ellipsoid height accuracies for Secondary marks are missing from parts of southern Louisiana, because they were filtered from the map (greater than 10 cm for Primary and greater than 20 cm for Secondary).

Similar horizontal and ellipsoid height network accuracy map pairs are also provided for the Caribbean (Figure 4.39), Alaska (Figure 4.40), and the Pacific (Figure 4.41).

4.3.2. Accuracy estimates for no-check marks

Accuracy estimates were not reported for no-check marks in the previous section. There is no redundancy, therefore the estimates are of questionable reliability, hence the reason for omitting them. In such a situation, the uncertainty computed for the mark is a combination of the uncertainty of its single enabled vector, and the uncertainty propagated from the mark to which it is connected. As has already been shown, accuracies of some vectors are unrealistically high (and also for some marks), and these would propagate directly to the no-check mark.

Despite the problem with no-check marks, their accuracies are published on NGS Datasheets, (although they are tagged with position source "NO CHECK" rather than "ADJUSTED"). Because they were omitted from the accuracy discussions in the previous section, they are summarized in Table 4.11 and can be compared to the accuracies of redundant marks in Table 4.10 (the number of vectors and occupations are not shown in Table 4.11, because there is only one for each mark).

Table 4.11. Network accuracies for NA2011 passive no-check marks. Does not include 17 of the 183 disconnected marks that are no-check. Accuracies are at 95% confidence. Compare to Table 4.10.

No-check:	All passive marks		CONUS Primary		CONUS Secondary		Alaska		Pacific	
Number total	**79,677**		**60,928**		**17,323**		**910**		**516**	
Number no-check	**2,117 (2.7%)**		**949 (1.6%)**		**879 (5.1%)**		**154 (16.9%)**		**135 (26.2%)**	
Accuracies (cm)	**Horz**	**Eht**	**Horz**	**Eht**	**Horz**	**Eht**	**Horz**	**Eht**	**Horz**	**Eht**
Minimum	0.16	0.25	0.16	0.25	0.37	1.14	0.92	1.84	1.22	3.12
Maximum	2076.46	678.65	327.55	467.97	181.07	156.00	2076.46	678.65	234.72	466.32
Mean	10.96	12.01	4.09	6.15	8.73	13.31	68.00	35.16	8.67	18.26
Std deviation	±63.77	±27.84	±16.62	±18.30	±15.05	±16.02	±221.80	±68.57	±22.32	±43.72
Percentiles										
1.0%	0.38	0.61	0.25	0.44	0.62	1.64	1.13	1.84	1.27	3.36
5.0%	0.68	1.27	0.49	0.88	1.34	2.55	2.05	1.96	1.58	5.06
10.0%	0.97	1.82	0.68	1.22	1.76	2.82	2.16	2.90	2.02	5.51
50.0% (median)	**2.69**	**5.86**	**1.65**	**3.41**	**3.64**	**8.29**	**11.15**	**15.57**	**4.22**	**11.03**
90.0%	15.73	22.50	6.26	10.84	23.60	29.81	107.60	85.49	10.63	21.19
95.0%	30.39	41.00	9.47	16.06	31.81	44.79	473.08	110.17	29.27	35.10
99.0%	119.10	97.35	50.49	47.05	74.76	90.94	1504.93	497.77	175.83	370.63

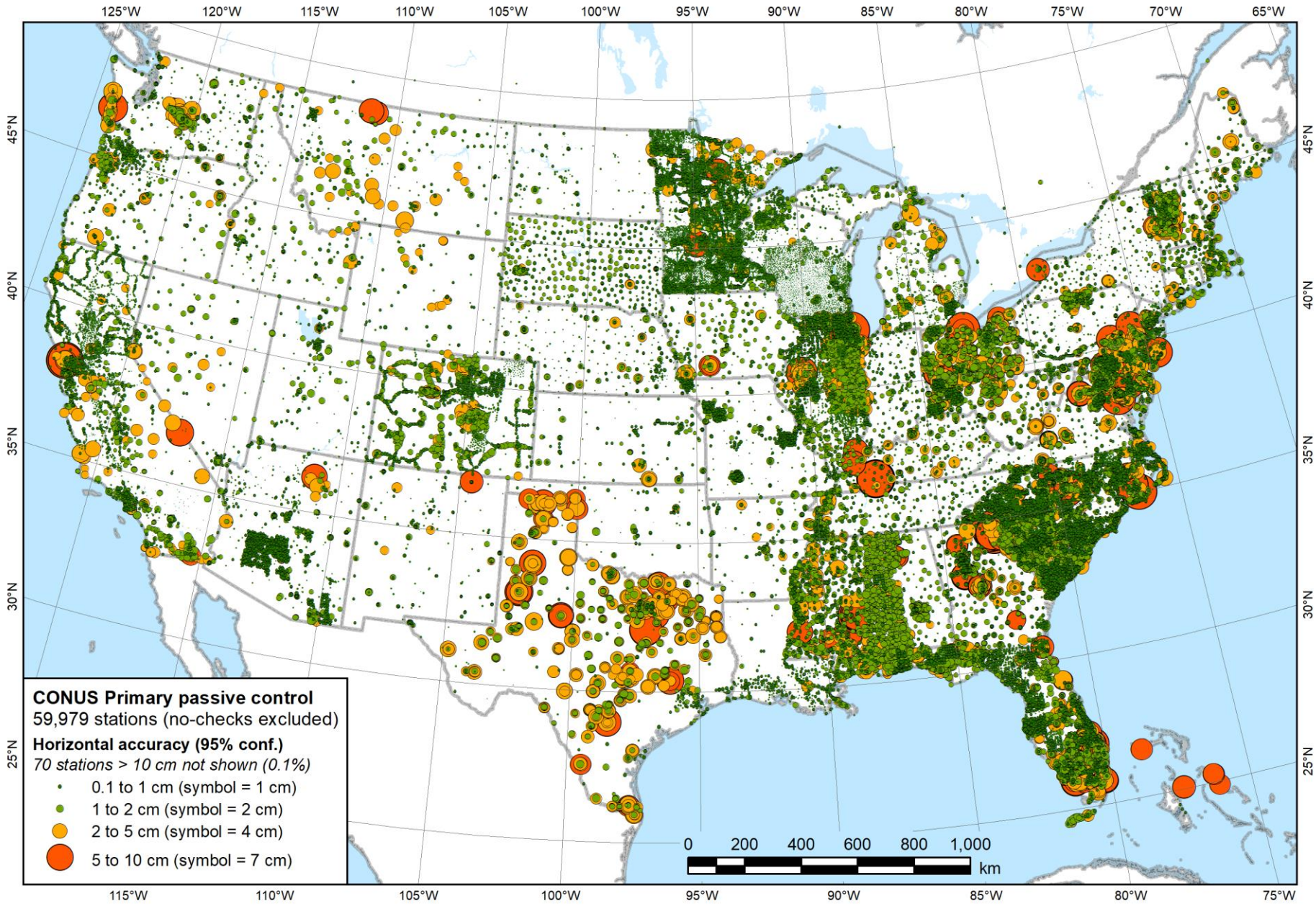

Figure 4.35. Map of horizontal network accuracy estimates for CONUS Primary passive control.

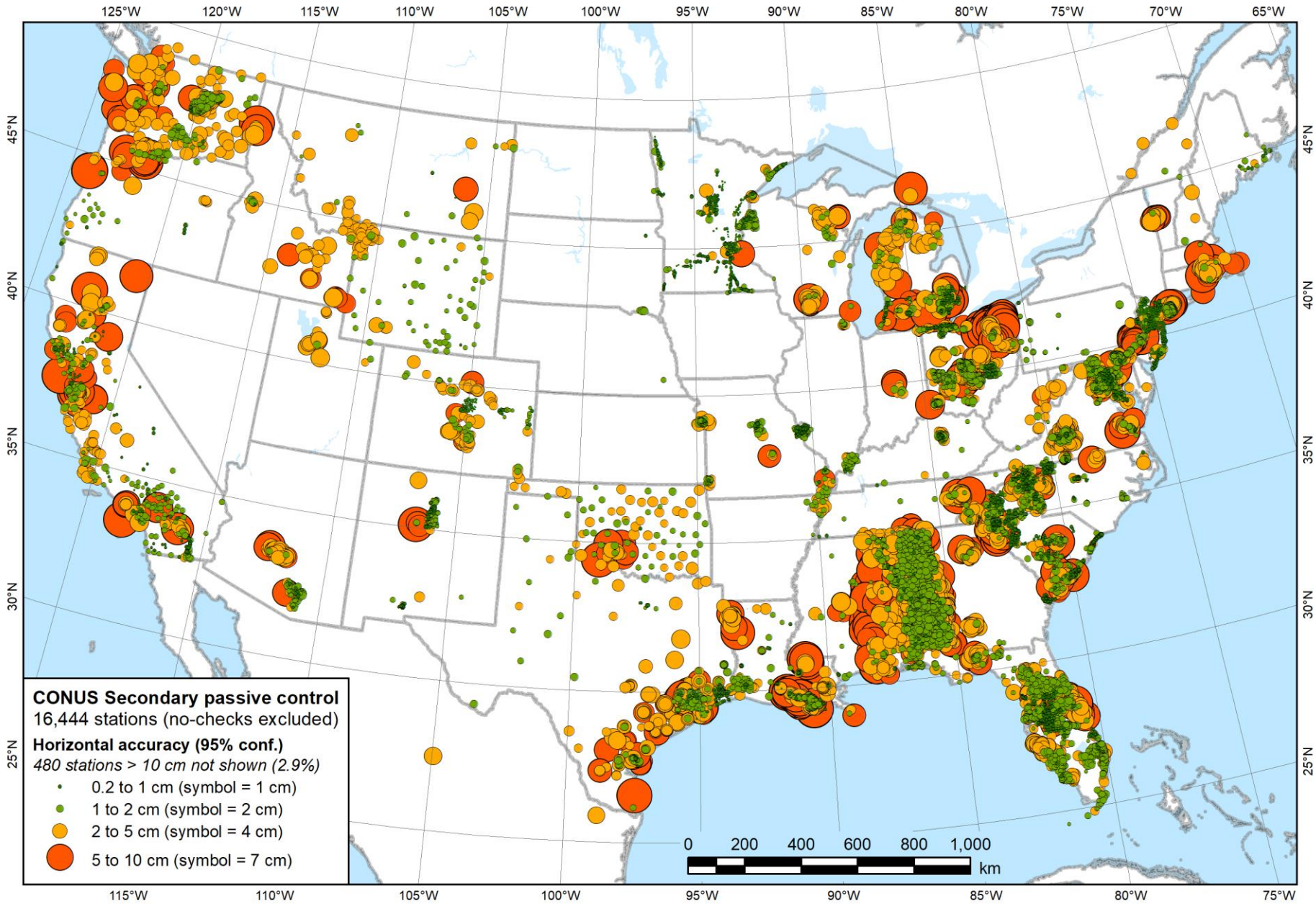

Figure 4.36. Map of horizontal network accuracy estimates for CONUS Secondary passive control.

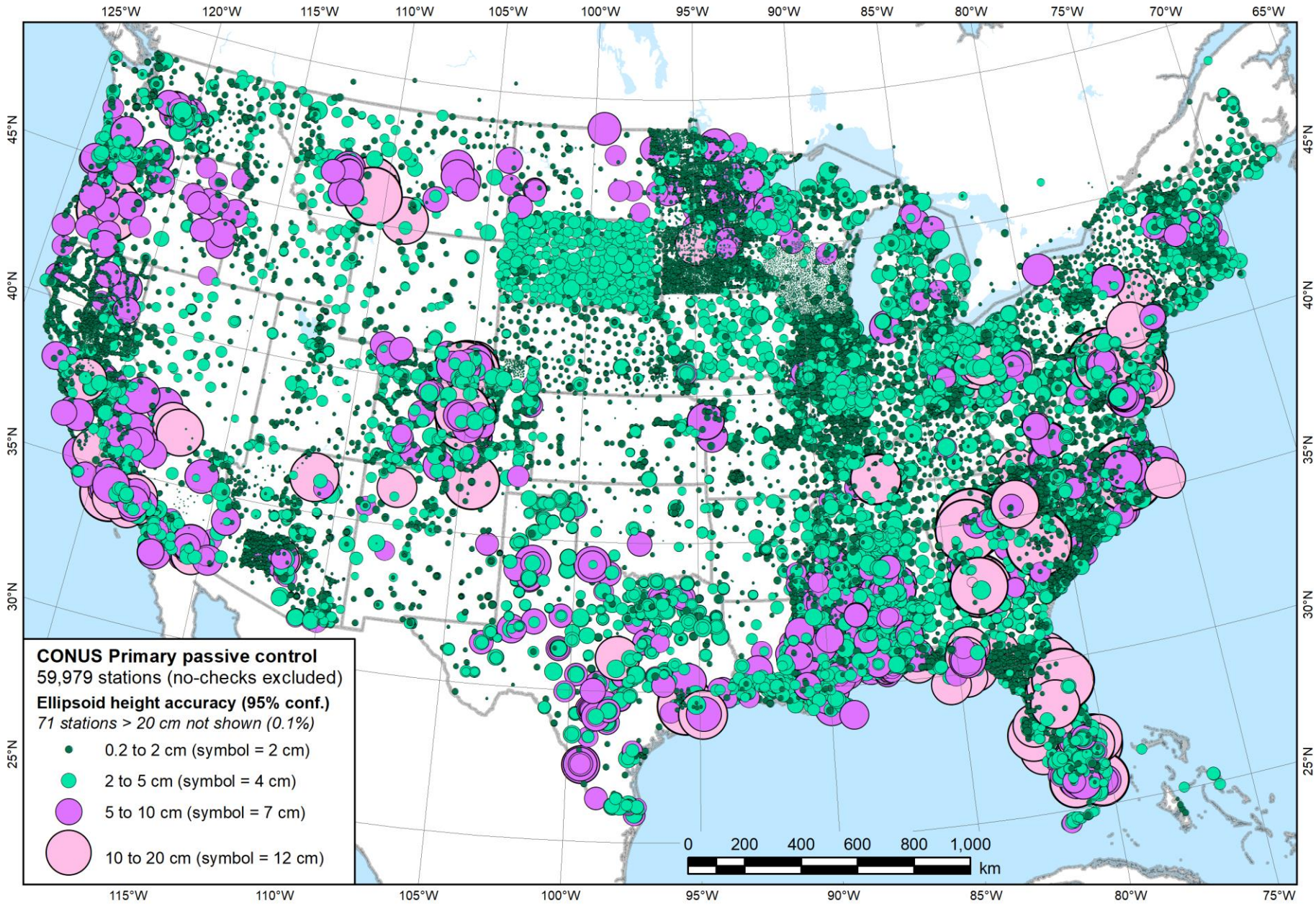

Figure 4.37. Map of ellipsoid height network accuracy estimates for CONUS Primary passive control.

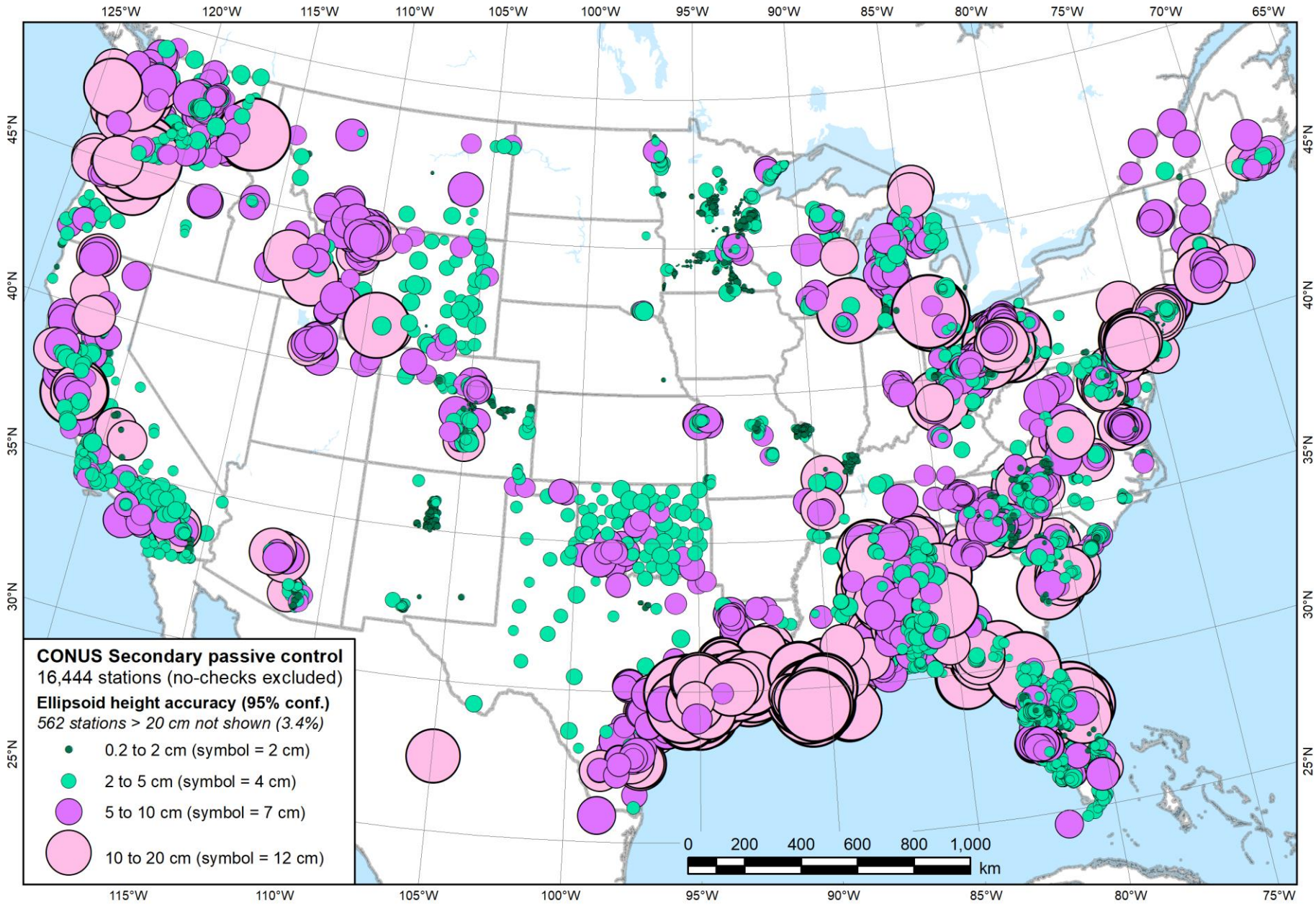

Figure 4.38. Map of ellipsoid height network accuracies for CONUS Secondary passive control.

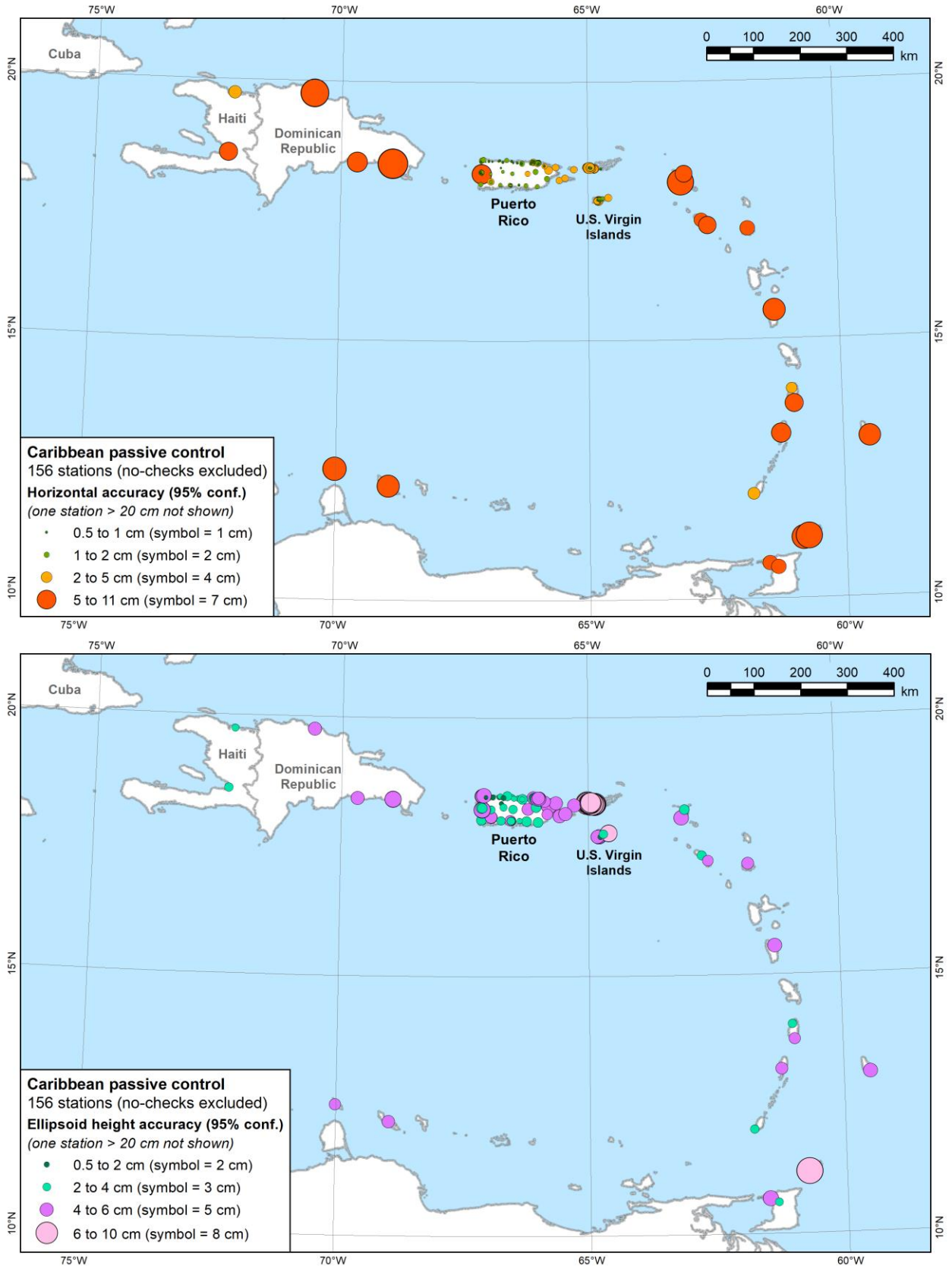

Figure 4.39. Maps of Caribbean accuracy estimates, horizontal (top) and ellipsoid height (bottom).

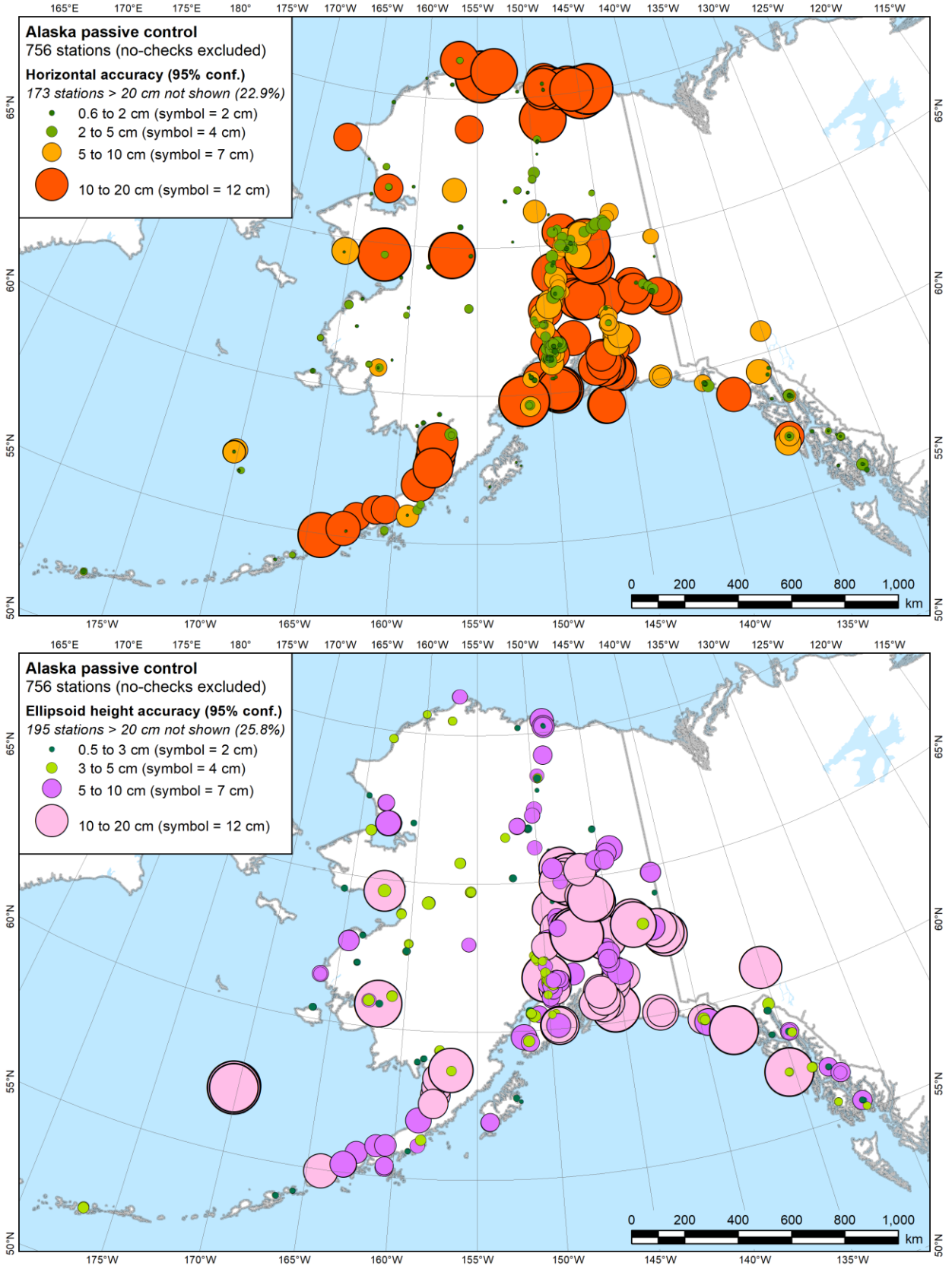

Figure 4.40. Maps of Alaska network accuracy estimates, horizontal (top) and ellipsoid height (bottom).

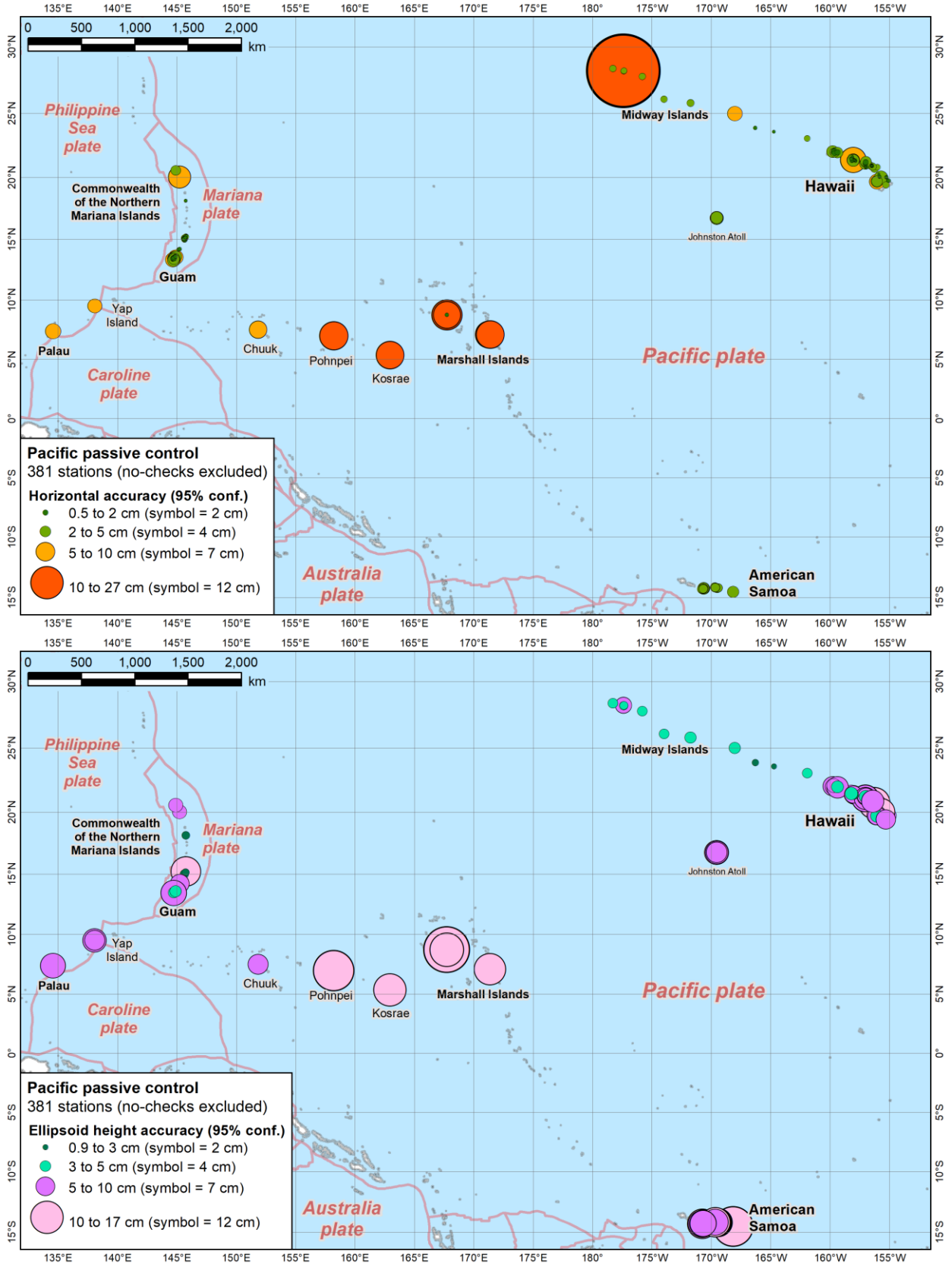

Figure 4.41. Maps of Pacific network accuracy estimates, horizontal (top) and ellipsoid height (bottom).

Table 4.11 also gives the number and percentage of no-check marks in each network, based on the total number of passive marks, but not including the 183 disconnected "excluded" marks (with 17 of these marks being no-check). The numbers (and percentages) of no-check marks differ somewhat from the values in Table 3.16, because that table includes the 17 disconnected no-check marks.

Every accuracy value in Table 4.11 is greater than its corresponding value in Table 4.10, except for the maximum horizontal accuracy value of the CONUS Secondary network. The median accuracy values of no-check marks are consistently 2 to 4 times greater than for the redundant marks. Since there is no redundancy in the derived coordinates, there is no "check" on its values, and because of that, the estimated accuracies cannot be considered reliable. Although some may be trustworthy, there is no way to be certain, so it is recommended their accuracies not be used. Their coordinate should also not be used in most circumstances.

4.3.3. Comparison of NA2011 and MYCS1 CORS accuracy estimates

Published MYCS1 CORSs were used to constrain the NA2011 adjustments, and their formal uncertainties were used to weight the constrained coordinates. As discussed in Chapter 3, formal accuracies were only available for "computed" MYCS1 CORSs. For "modeled" MYCS1 CORSs, a standard deviation (sigma) of 1 cm was assigned to each horizontal component and 3 cm to the up component. Of the 1,195 MYCS1 CORSs used as constraints, 973 (81.4%) were computed and 222 (18.6%) were modeled.

Because the CORS coordinates were assigned stochastic weights, new CORS coordinates and uncertainties for those new CORS coordinates were also determined as part of the NA2011 adjustments. As mentioned in Chapter 1, some of the original CORS coordinate uncertainties were very large. The largest for MYCS1 NAD 83 coordinates were 31.1 cm horizontal and 92.0 cm ellipsoid height at 95% confidence (see Table 1.2) for CORS CHI6 (an Alaska U.S. Coast Guard CORS, now decommissioned). The largest north, east, and up formal sigmas for CORS coordinates used as constraints were 8.64, 6.93, and 32.52 cm for P304 (see Table 3.3), followed by 6.44, 12.92, and 29.12 cm for RCM5 (decommissioned USCG CORS). At 95% confidence these are 19.28 and 26.32 cm horizontal and 63.76 and 57.09 cm ellipsoid height, respectively. In contrast, the smallest sigmas on MYCS1 CORS coordinates used as constraints were 0.06, 0.05, and 0.08 cm north, east, and up; 36 CORSs used as constraints have 3D sigmas of less than 0.3 cm. This is a tremendous range, as shown in Table 4.12.

The median sigmas in Table 4.12 for the 973 computed MYCS1 CORSs used as constraints were 0.39, 0.32, and 1.48 cm north, east, and up. In addition, the table also gives statistics of the sigmas determined from the constrained NA2011 adjustments for these CORSs. The medians are 0.12, 0.11, and 0.33 cm north, east, and up. Table 4.12 also gives the ratio of formal MYCS1 to NA2011 sigmas. Based on the median ratios, the MYCS1 sigmas are typically about 3.0 times larger horizontally and 4.5 times larger vertically than those determined from the NA2011 adjustments; however, there is a large range in the ratios as well. About 10% of the ratios are less than 1 (the minimum is 0.5), and about 10% are greater than about 9 horizontally and 14

vertically (with a maximum of about 113 horizontally and 175 vertically). These are extremely large ratios.

Part of the reason for significantly smaller sigmas in the NA2011 adjustment is likely due to the large number of enabled vectors connected to many of the CORSs. As shown in Table 4.13, the number of vector ties range from 1 (for eight CORSs) to 5356. This large number of ties is for CORS LKHU in Texas, as mentioned near the beginning of Section 2.4. It is part of the Harris-Galveston Subsidence District (HGSD), where these vector ties occur in 465 "occupations" (in this case, since the mark is a CORS, each occupations is actually a 24-hour processing session). The sessions are from 2000 through 2009, corresponding to a mean of 11.5 vectors per session, not a large number. The mean and median number of CORS vector ties are 69 and 24, respectively, not excessively large numbers (the mean and median vector ties for passive marks are 9.2 and 6, respectively; see Table 2.15). The statistics on the number of vector ties to CORSs differ somewhat from Table 2.15, because only computed CORSs are considered in Table 4.13. For the 3D sigmas, the statistics for the ratio of computed MYCS1 to NA2011 adjusted are consistent with Table 4.12.

Table 4.12. Comparison of formal sigmas from MYCS1 and the constrained NA2011 adjustments. MYCS1 sigmas are for the 973 "computed" CORSs used as constraints for the NA2011 adjustments.

	Sigmas from MYCS1 SINEX file (cm)			**Sigmas from constrained NA2011 adjustments (cm)**			***Ratio MYCS1 sigma to NA2011 sigma***		
Number = 973	**North**	**East**	**Up**	**North**	**East**	**Up**	***North***	***East***	***Up***
Minimum	0.06	0.05	0.08	0.02	0.02	0.04	*0.5*	*0.5*	*0.5*
Maximum	8.64	12.92	32.52	1.20	1.38	4.79	*109.9*	*115.5*	*174.6*
Mean	0.52	0.45	2.02	0.17	0.15	0.48	*4.5*	*4.3*	*6.8*
Std deviation	±0.56	±0.60	±2.28	±0.15	±0.14	±0.49	*±6.7*	*±6.2*	*±9.7*
Percentiles									
1.0%	0.07	0.07	0.17	0.03	0.03	0.05	*0.7*	*0.7*	*0.7*
5.0%	0.12	0.10	0.35	0.04	0.04	0.09	*0.8*	*0.8*	*0.8*
10.0%	0.14	0.12	0.50	0.05	0.04	0.11	*0.9*	*0.9*	*1.0*
50.0% (median)	**0.39**	**0.32**	**1.48**	**0.12**	**0.11**	**0.33**	***3.1***	***3.0***	***4.5***
90.0%	1.01	0.82	3.88	0.34	0.30	1.00	*9.1*	*8.3*	*14.1*
95.0%	1.44	1.21	5.79	0.44	0.39	1.35	*11.5*	*11.3*	*18.4*
99.0%	2.14	2.02	9.79	0.82	0.73	2.59	*25.6*	*22.1*	*39.7*

It is possible that part of the reason for the smaller sigmas on adjusted NA2011 CORSs is due to the large number of vector ties to many of the CORSs. To evaluate whether there is a correlation between MYCS1 to NA2011 sigma ratios and the number of vectors, the 3D sigma ratios and number of enabled vector ties are plotted in Figure 4.42. Because of the large range in values, a log scale is used for both axes. Despite the scatter, an upward trend is visually apparent, as also

suggested by the plotted power regression curve (although R^2 = 0.20 is fairly low). In addition, the correlation coefficient for the dataset is positive, but low, at only +0.069. Nonetheless, there is at least a weak trend. To address its effect, the ratios were recomputed with the trend removed and are provided in Table 4.13. Doing so decreased the mean ratio from 6.2 to 3.0, and the median from 4.1 to 2.5, and it decreased the variability, as well. Yet even when detrended, the MYCS1 sigmas are still greater than the NA2011 sigmas by a factor of about 3 overall.

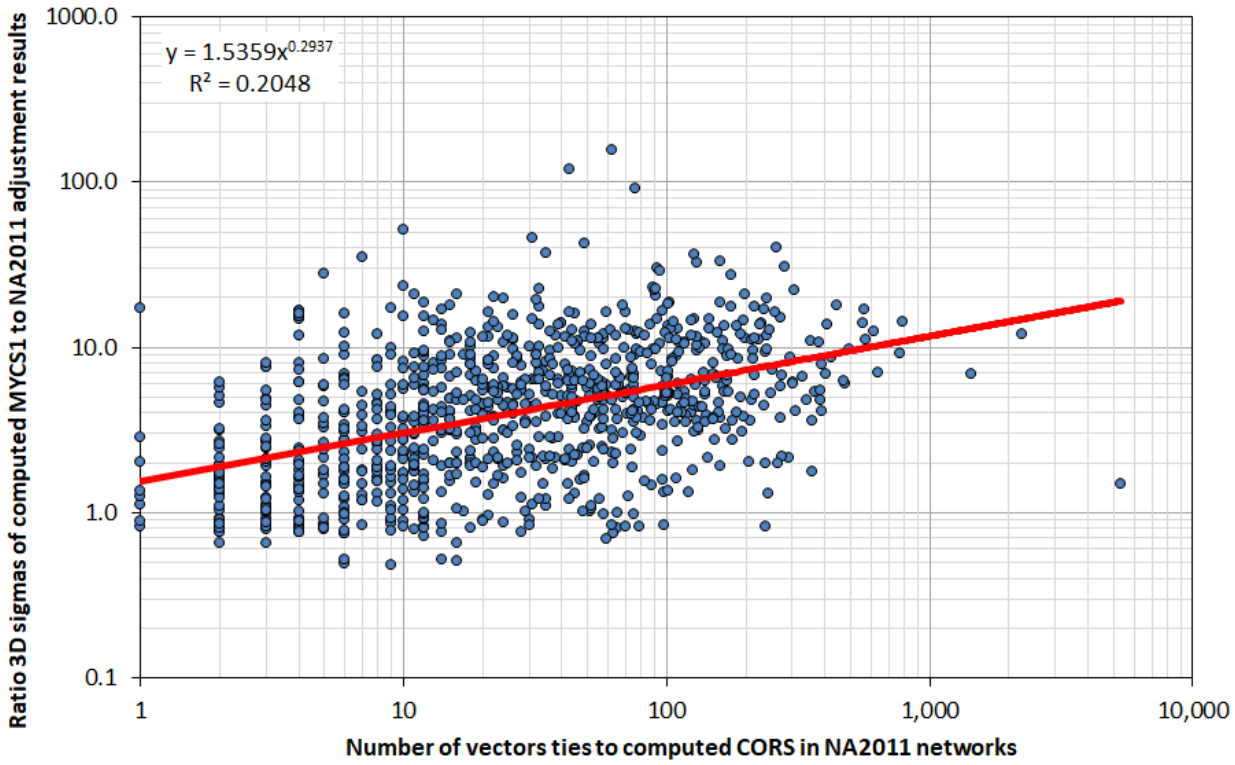

Figure 4.42. Ratio of 3D sigmas for computed MYCS1 CORSs to NA2011 versus number of vector ties (log scale both axes). NA2011 3D sigmas are from final constrained adjustments.

According to the NGS CORS Team, the MYCS1 variances were scaled by a factor of 50 (Griffiths, 2012). This corresponds to a sigma scalar of $\sqrt{50} \approx 7$, and it was applied to account for overly optimistic uncertainty estimates from the solution, in conformance with IGS practice. It is possible scaling the sigmas by 7 was overly aggressive, particularly since some of the MYCS1 sigmas are so large (up values exceed 10 cm for 18 NAD 83 CORSs in the MYCS1 solution). However, it is also possible some uncertainty estimates from the NA2011 adjustment are optimistic, even though the standard deviation of unit weight for the adjustments suggest otherwise (see Table 4.1). At this point it is unknown which scenario is correct, but review of the datasets suggests the formal MYCS1 uncertainties are overall somewhat pessimistic, and the NA2011 uncertainties are generally optimistic (likely due at least in part to the presence of trivial vectors). In consideration of future CORS reprocessing, it would be appropriate to carefully consider how CORS uncertainty scaling is performed. Likewise, any future national or large

regional adjustments would benefit from a more in-depth evaluation of the estimated errors, including a more rigorous approach to identifying and removing outlier observations.

Table 4.13. Number of CORSs vector ties, MYCS1 and NA2011 3D sigmas, and sigma ratios. Only enabled vectors are considered for ties to "computed" CORSs. Sigmas are for "computed" MYCS1 and constrained NA2011 adjustments. Detrended ratio is based on power regression in Figure 4.42.

Number = 973	Number enabled vector ties	3D sigmas (cm)		*Ratio MYCS1 to NA2011 3D sigmas*	
		MYCS1	NA2011	*Actual*	*Detrended*
Minimum	1	0.12	0.05	*0.5*	*1.6*
Maximum	5356	34.36	5.13	*156.9*	*31.9*
Mean	69	2.14	0.53	*6.2*	*3.0*
Std deviation	±210	±2.42	±0.52	*±8.8*	*±2.0*
Percentiles					
1.0%	2	0.19	0.08	*0.7*	*1.7*
5.0%	2	0.38	0.11	*0.8*	*1.8*
10.0%	4	0.53	0.13	*1.0*	*1.9*
50.0% (median)	**24**	**1.56**	**0.37**	***4.1***	***2.5***
90.0%	161	4.07	1.10	*12.8*	*4.4*
95.0%	241	6.13	1.50	*16.5*	*5.5*
99.0%	562	10.21	2.73	*35.6*	*10.1*

Of the 1195 constrained CORSs, 222 were "modeled," so formal uncertainties were not available for the constraints. As discussed in Section 3.1.4, these CORSs were assigned sigmas of 1 cm for the north and east components, and 3 cm for the up component. To see how those values compare to the sigmas from the NA2011 adjustment, a comparison of values is given in Table 4.14. The statistics show the assumed sigmas used for modeled CORSs were likely too optimistic. The median sigmas from the NA2011 adjustments were 5.00, 5.88, and 6.67 cm north, east, and up.

As shown by the MYCS1 to NA2011 ratios in Table 4.14, the median of the assumed MYCS1 sigmas are about 20% of the horizontal and 45% of the computed up sigma from NA2011. It appears, then, that larger sigmas for the modeled CORSs would likely have been appropriate, although there was some unease about making them too "loose." Note that median NA2011 sigmas are 5 to 7 cm for all components, and the up component is not much larger than the horizontal components. Recall that the NGS CORS Team had initially suggested using sigmas of 5 cm for all three components of modeled CORSs (Section 3.1.4). It is very interesting to see how well that matches actual results from the NA2011 adjustment.

Table 4.14. Comparison of sigmas for "modeled" MYCS1 and the constrained NA2011 adjustments. MYCS1 sigmas are for the 222 "modeled" CORSs used as constraints for the NA2011 adjustments.

Number = 222	Assumed sigmas used for "modeled" CORSs (cm)			Sigmas from constrained NA2011 adjustments (cm)			*Ratio MYCS1 sigma to NA2011 sigma*		
	North	East	Up	North	East	Up	*North*	*East*	*Up*
Minimum	1.00	1.00	3.00	0.74	0.75	0.78	*0.04*	*0.04*	*0.09*
Maximum	1.00	1.00	3.00	25.00	25.00	33.33	*1.36*	*1.34*	*3.83*
Mean	1.00	1.00	3.00	6.39	7.37	7.87	*0.30*	*0.27*	*0.73*
Std deviation	±0.00	±0.00	±0.00	±0.28	±0.27	±0.75	*±4.81*	*±5.67*	*±5.93*
Percentiles									
1.0%	1.00	1.00	3.00	0.76	0.77	0.80	*0.05*	*0.04*	*0.10*
5.0%	1.00	1.00	3.00	0.99	1.19	1.19	*0.06*	*0.05*	*0.15*
10.0%	1.00	1.00	3.00	1.50	1.60	1.77	*0.08*	*0.06*	*0.18*
50.0% (median)	**1.00**	**1.00**	**3.00**	**5.00**	**5.88**	**6.67**	***0.20***	***0.17***	***0.45***
90.0%	1.00	1.00	3.00	12.50	16.67	16.67	*0.67*	*0.62*	*1.69*
95.0%	1.00	1.00	3.00	16.67	19.50	20.00	*1.01*	*0.84*	*2.52*
99.0%	1.00	1.00	3.00	20.00	25.00	30.00	*1.31*	*1.30*	*3.76*

4.4. Adjusted and constrained coordinate shifts

The final adjusted coordinates of the NA2011 Project differed from the previously published values, mainly for the following reasons:

1. Computed for a different epoch (2010.00 versus 2002.00 and 2007.00 for the 2007 national adjustment)
2. Constrained to a set of newly computed and consistent MYCS1 CORS coordinates
3. Weighted (stochastic), rather than rigid constraints, were used for the CORSs
4. Included new observations
5. CONUS was split into a Primary and Secondary network based mainly on age (nominally split at beginning of 1994)
6. The up-component of observations in the Gulf Coast subsidence region were downweighted
7. The Pacific was not previously adjusted as a single network

All passive mark coordinates from the NA2011 adjustment were updated in the NGSIDB, as were their published accuracies (with the exception of the 183 disconnected marks). Because weighted constraints were used, the adjustment also resulted in a change in coordinates for the CORSs (and accuracies, as discussed in the previous section). However, the CORS coordinates and accuracies in the NGSIDB were *not* updated with the values from the NA2011 adjustment.

The published CORS coordinates are values exclusively determined in MYCS1, and from later processing for those CORSs added after MYCS1. This decision was made at the project's outset, governed by the idea that CORSs are computed separately from the passive mark coordinates and uncertainties to serve as the independent geometric foundation of the NSRS. Moreover, the MYCS1 reprocessing was executed in a highly consistent manner, and thus it was considered inappropriate to allow the much more heterogeneous methods and results from passive marks to influence the MYCS1. For consistency, the same approach was used for Primary control stochastic constraints of the Secondary network adjustment.

4.4.1. Passive mark coordinate shifts from previously published values

The shifts in passive mark coordinates from their previous published values are summarized in the following four tables: Table 4.15 (all passive control), Table 4.16 (CONUS Primary and Secondary),

Table **4.17** (Alaska), and Table 4.18 (Pacific PA11 and MA11). No-check marks are included, but the 183 disconnected marks are not (note that all but one are in the two CONUS networks; the remaining one is in the Alaska network but is located in Hawaii; see Section 2.4.1 and Table 2.16). The coordinate differences are given as NA2011 values minus previously published values. Each table gives the shift in latitude, longitude, and ellipsoid height (as delta north, east, and up), as well as the horizontal shift and its azimuth. Because most of the marks (98%) are in CONUS, their shifts dominate the statistics in Table 4.15. Nonetheless, the statistics are useful to show the overall change of the NA2011 Project. The range in shifts are large, exceeding a meter horizontally (the maximum is 2.8 m) and ±60 cm in height. But these large changes are unusual. The median shifts are -0.1, +1.8, and -2.0 cm north, east, and up. The median horizontal shift is 1.9 cm at a 96° azimuth, due mainly to a slightly incorrect rotation rate for the North America plate being used as part of the NAD 83 datum definition (discussed in more detail later in this section). Note that 99% of the horizontal shifts are within 13.8 cm, and 98% of the height shifts are between -7.1 and +4.4 cm.

Coordinate shifts for CONUS Primary and Secondary are shown in Table 4.16. They make up the majority of marks by far, so consequently the statistics are very similar to Table 4.15. The main difference is that the maximum shifts are much smaller, particularly for Primary marks. The maximum horizontal shift is 33.6 cm, with 99% less than 10.6 cm, and 98% of the height shifts are between -5.4 and +4.4 cm. The Secondary marks show larger shifts, especially in height. The maximum horizontal shift is 92.5 cm, with 99% less than 12.8 cm, and 98% of the height shifts are between -9.7 and +7.8 cm. The CONUS ellipsoid height shifts show an overall negative bias of about 2 cm. This same bias was also observed for the MYCS1 results in CONUS compared to previously published CORS heights.

Coordinate shifts for Alaska are shown in

Table **4.17**. These shifts differ considerably from those for CONUS. This network exhibits the largest horizontal shifts, a maximum of 2.84 m and a median of 6.6 cm. It is also at a much different azimuth than CONUS; the median of 267° is opposite that of CONUS. The horizontal shifts are highly variable, with standard deviations of ±20 to 22 cm in the horizontal components,

about an order of magnitude greater than CONUS. Some of these horizontal shifts are due to differences in how the adjustments were performed and constrained, as well as the use of additional data, but some shifts are also due to tectonic deformation. This will be more evident in a map of displacement vectors, discussed below.

The Alaska ellipsoid height shifts do not exhibit the negative 2 cm bias seen in CONUS. The median shift is +1 cm, but that cannot be interpreted as a systematic effect due to high dispersion in heights (standard deviation of ±8.0 cm, versus ±1.55 cm for Primary and ±2.78 cm for Secondary).

Unlike CONUS and Alaska, the Pacific was not included in the 2007 national adjustment, so there was no consistent set of *a priori* coordinates. The previously published coordinates were based mostly on individual local surveys, with some referenced to CORSs and others to local passive control. Although there were some surveys with observations spanning the Pacific, most of those were done in the early 1990s (the year with the most observations was 1993; see Figure 4.1). In addition, the marks are on two separate tectonic plates, and that was probably not taken into account in adjusting previous surveys (in part because *ADJUST* does not include transformations for the Pacific and Mariana tectonic plates, only the North America plate). All of this contributed to results that were likely consistent locally, but not necessarily regionally.

Table 4.15. Coordinate shifts for all NA2011 passive marks from previously published values (excluding 183 disconnected marks).

	All Passive Marks (num = 79,677*)				
Shifts	**North (cm)**	**East (cm)**	**Up (cm)**	**Horiz (cm)**	**Azimuth (deg)**
Minimum	-140.7	-159.3	-67.2	0.0	0°
Maximum	89.6	247.1	62.8	284.4	360°
Mean	0.22	1.55	-1.98	2.58	107.6°
Std deviation	±3.00	±3.94	±2.68	±4.51	±58.8°
Percentiles					
1.0%	-2.8	-6.9	-7.1	0.7	21°
5.0%	-1.2	-1.1	-4.0	1.1	52°
10.0%	-0.9	0.7	-3.5	1.4	67°
50.0% (median)	**-0.1**	**1.8**	**-2.0**	**1.9**	**96°**
90.0%	1.4	2.6	-0.2	3.4	134°
95.0%	2.7	3.2	0.9	5.3	294°
99.0%	8.6	6.4	4.4	13.8	341°

** There is one less height difference, because one CONUS Secondary mark had no previously published ellipsoid height, mark HEAVEN (PID FO1140).*

Table 4.16. Coordinate shifts for CONUS Primary and Secondary marks (excluding 182 disconnected marks).

	CONUS Primary (num = 60,928)					CONUS Secondary (num = 17,323*)				
Shifts	**North (cm)**	**East (cm)**	**Up (cm)**	**Horiz (cm)**	**Azimuth (deg)**	**North (cm)**	**East (cm)**	**Up (cm)**	**Horiz (cm)**	**Azimuth (deg)**
Minimum	-10.0	-22.4	-41.1	0.0	0°	-25.0	-58.3	-55.1	0.2	0°
Maximum	25.0	26.6	17.6	33.6	360°	71.8	78.3	62.8	92.5	360°
Mean	0.19	1.61	-1.96	2.27	106.0°	0.10	1.80	-1.89	2.54	104.9°
Std deviation	±1.48	±1.71	±1.55	±1.61	±57.5°	±2.03	±2.37	±2.78	±2.56	±50.7°
Percentiles										
1.0%	-1.9	-5.8	-5.4	0.7	21°	-3.1	-6.1	-9.7	0.8	19°
5.0%	-1.1	-0.7	-3.8	1.1	53°	-1.4	0.2	-4.8	1.1	50°
10.0%	-0.8	0.7	-3.4	1.3	68°	-1.1	0.9	-3.8	1.4	63°
50.0% (median)	**-0.1**	**1.8**	**-2.1**	**1.9**	**95°**	**-0.2**	**1.8**	**-1.8**	**2.0**	**99°**
90.0%	1.2	2.5	-0.4	3.0	128°	1.4	2.8	-0.3	3.9	134°
95.0%	2.4	2.9	0.7	4.5	291°	2.6	3.9	0.7	5.8	170°
99.0%	7.8	5.4	3.0	10.6	340°	8.8	7.9	7.8	12.8	336°

** There is one less height difference, because one CONUS Secondary mark had no previously published ellipsoid height, mark HEAVEN (PID FO1140).*

Table 4.17. Coordinate shifts for Alaska marks (excluding one disconnected mark in Hawaii).

	Alaska (num = 910)				
Shifts	**North (cm)**	**East (cm)**	**Up (cm)**	**Horiz (cm)**	**Azimuth (deg)**
Minimum	-140.7	-54.8	-63.8	0.5	1°
Maximum	89.6	247.1	25.8	284.4	360°
Mean	7.08	-0.70	-0.63	17.76	230.2°
Std deviation	±21.93	±19.83	±8.02	±24.68	±104.6°
Percentiles					
1.0%	-33.8	-34.0	-26.6	0.9	4°
5.0%	-13.4	-23.8	-13.9	1.7	48°
10.0%	-8.5	-18.0	-11.3	2.4	74°
50.0% (median)	**1.8**	**-1.7**	**1.0**	**6.6**	**267°**
90.0%	44.4	8.9	5.6	55.1	342°
95.0%	57.1	23.3	8.3	66.2	347°
99.0%	77.9	67.2	22.8	89.9	356°

The lack of region-wide consistency for previously published Pacific marks is reflected in the mark shift statistics in Table 4.18, as it gives results for the PA11 and MA11 separately. Standard deviations of the horizontal shifts are large, but more importantly, the components are very unequal. For PA11, the north and east shift standard deviations are ±5.86 and ±11.92 cm, and for MA11 they ±8.78 and ±47.99 cm. These represent unusually large differences for the components, whereas for the other three networks they are nearly equal. The level of inconsistency is clearly exhibited by the vector displacement maps later in this section.

The ellipsoid height shift also has the largest height standard deviations of the networks, ±13.9 cm for PA11 and ±27.8 cm for MA11. The median height changes of the two networks are opposite, -1.5 cm for PA11 and +2.1 cm for MA11, but, given the high dispersion, this apparent difference in bias is negligible. Again, the large differences are likely due to the local character of the individual GPS projects.

Table 4.18. Coordinate shifts for Pacific PA11 and MA11 marks.

	Pacific PA11 (num = 345)					Pacific MA11 (num = 171)				
Shifts	**North (cm)**	**East (cm)**	**Up (cm)**	**Horiz (cm)**	**Azimuth (deg)**	**North (cm)**	**East (cm)**	**Up (cm)**	**Horiz (cm)**	**Azimuth (deg)**
Minimum	-39.1	-48.7	-58.3	0.4	26°	-24.5	-159.3	-67.2	0.6	1°
Maximum	3.2	90.1	37.1	98.2	245°	6.2	7.8	7.3	159.9	356°
Mean	-2.84	-1.44	-6.02	5.54	149.1°	-4.25	-28.48	-14.73	30.67	220.4°
Std deviation	±5.86	±11.92	±13.87	±12.48	±50.2°	±8.78	±47.99	±27.84	±47.62	±107.9°
Percentiles										
1.0%	-26.4	-48.7	-54.4	0.4	28°	-24.4	-159.3	-67.2	0.6	4°
5.0%	-21.4	-36.7	-52.0	0.6	81°	-23.3	-157.5	-66.1	0.9	9°
10.0%	-3.0	-1.2	-16.1	0.8	93°	-19.2	-63.6	-63.6	2.0	26°
50.0% (median)	**-1.2**	**0.7**	**-1.5**	**2.3**	**144°**	**0.8**	**-1.9**	**2.1**	**2.6**	**258°**
90.0%	-0.1	3.5	2.3	5.6	216°	2.4	1.4	7.1	64.6	316°
95.0%	0.4	4.2	4.8	45.8	241°	5.7	2.4	7.2	157.7	319°
99.0%	1.6	6.7	12.2	55.4	242°	6.1	4.9	7.3	159.9	350°

Maps of the NA2011 shifts from previously published coordinates are shown in Figure 4.43 through Figure 4.51. Figure 4.43 displays two rasterized maps of the CONUS shifts, horizontal magnitude (top) and ellipsoid height change (bottom). The maps were created from the CONUS Primary and Secondary marks shifts by interpolated inverse distance weighting (with a power of 2 using the 12 nearest marks). Most of the horizontal mark shifts (56.2%) are 0 to 2 cm. The largest shifts overall occur in California, west of the San Andreas Fault system, and to a lesser

extent, along the Pacific Northwest coast. Horizontal mark shifts in these areas are often in the 6 to 10 cm range, and in some places in the 10 to 20 cm range. These shifts are mostly associated with plate boundary tectonic motion. In fact, most of the horizontal shifts in the CONUS NA2011 adjustment are due to tectonic motion (more evident in Figure 4.44 through Figure 4.46, as will be discussed below). The map also shows some localized large horizontal shifts, mostly associated with specific GPS projects. All of those visible in Figure 4.43 are projects in the Secondary network.

The ellipsoid height shifts in the lower map of Figure 4.43 show the overall negative bias of the ellipsoid height shifts for CONUS. Mainly, this has been attributed to change from relative to absolute antenna models for MYCS1 processing, although it is only clearly exhibited for CONUS passive marks. There are no other systematic biases or trends in the height changes, apart from local effects most likely due to the change in the coordinates of individual CORSs and the split between Primary and Secondary networks.

Figure 4.44 through Figure 4.51 are displacement maps that use vectors to show the horizontal and ellipsoid height shifts of individual marks. Because of the large number of marks in CONUS—and the especially high concentration in some states—displacement vectors could not be shown for all marks in CONUS. To reduce clutter, the vectors in Figure 4.44 through Figure 4.46 were thinned using a 50-km filter; this decreased the number of CONUS marks by 93%, from 79,677 to 5414; however, even with the filtering, the vector density and variability are too great to use for ellipsoid height change. Consequently, a map with height displacements is not presented for CONUS; instead refer to the lower map displayed in Figure 4.43.

Figure 4.44 through Figure 4.46 show horizontal displacement vectors for (filtered) CONUS Primary and Secondary marks. Figure 4.44 essentially shows both networks in their entirety, including the Caribbean; Figure 4.45 shows CONUS only, to provide greater detail; and Figure 4.46 shows only the western part of CONUS, to better illustrate the large displacements associated with the North American and Pacific plate boundary. Although there is variability in orientation, the vectors in these two figures clearly exhibit consistent patterns. The patterns represent the change in position due to tectonic motion, since the epoch of NA2011 (2010.00) is more recent than the epochs used for the 2007 adjustment. The use of epochs for 2007 was not entirely consistent. For most of CONUS (as well as the Caribbean), the epoch was nominally 2002.00, because that was the epoch of the constrained CORS coordinates. Although *HTDP* was not used to transform these G-files, they were transformed using a 14-parameter transformation (per Table 2.13), and this transformation aligned the GNSS vectors with NAD 83 reasonably well for most of CONUS (although it does not work as well for the Caribbean). In five western CONUS states (Arizona, California, Nevada, Oregon, and Washington), plus Alaska, an epoch of 2007.00 was used (and at the time Alaska CORSs were referenced to epoch 2003.00, rather than 2002.00). Vectors for projects in those states (with the exception of California) were transformed to NAD 83 epoch 2007.00 using *HTDP*. The California Spatial Reference System *SECTOR* utility (SOPAC, 2017) was used for California (but it only performs the transformation at continuously operating marks, such as CORSs).

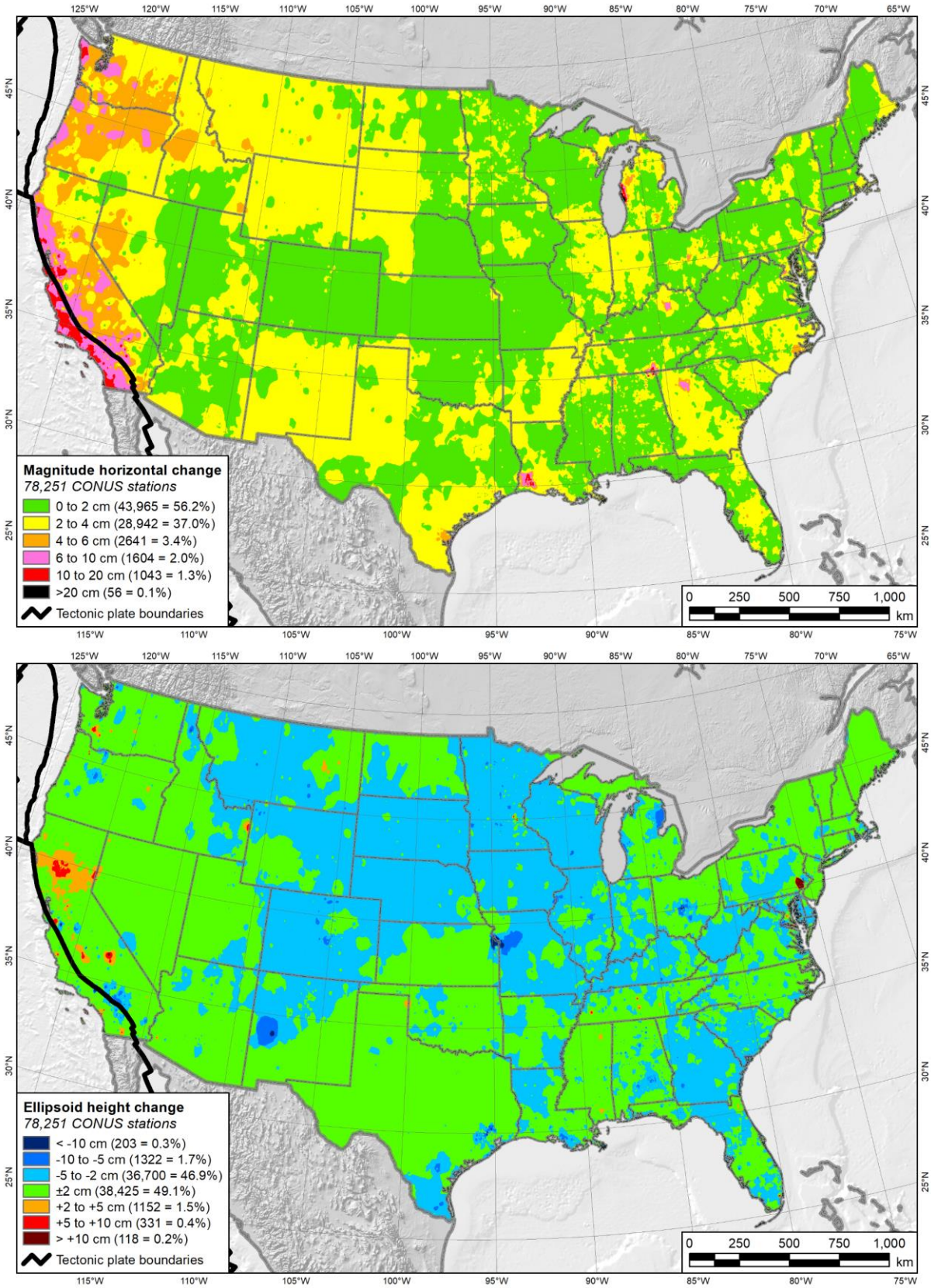

Figure 4.43. Maps of horizontal shift magnitude and ellipsoid height change for CONUS passive marks.

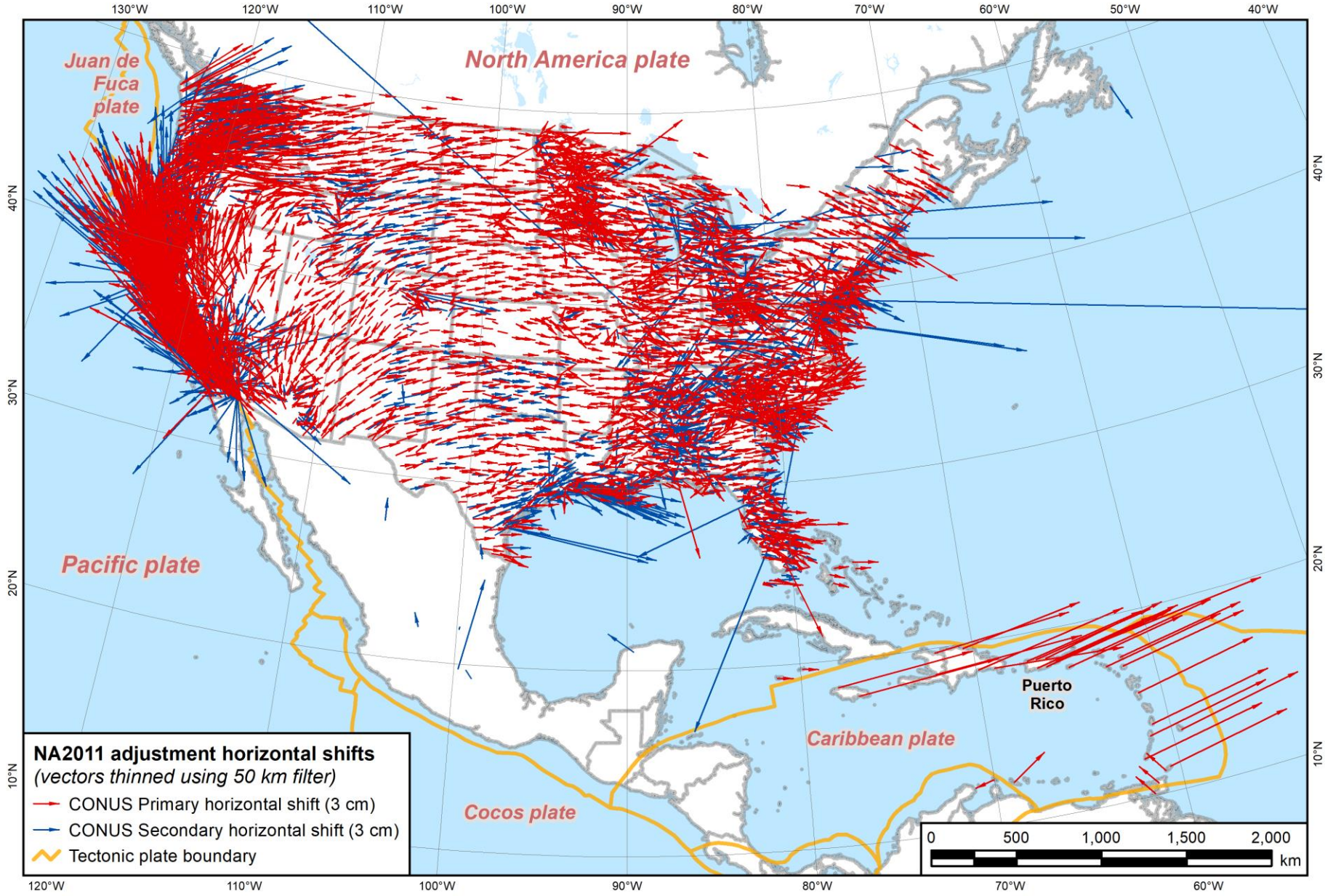

Figure 4.44. Map of horizontal NA2011 passive mark shifts for CONUS and the Caribbean (vectors thinned using 50 km filter).

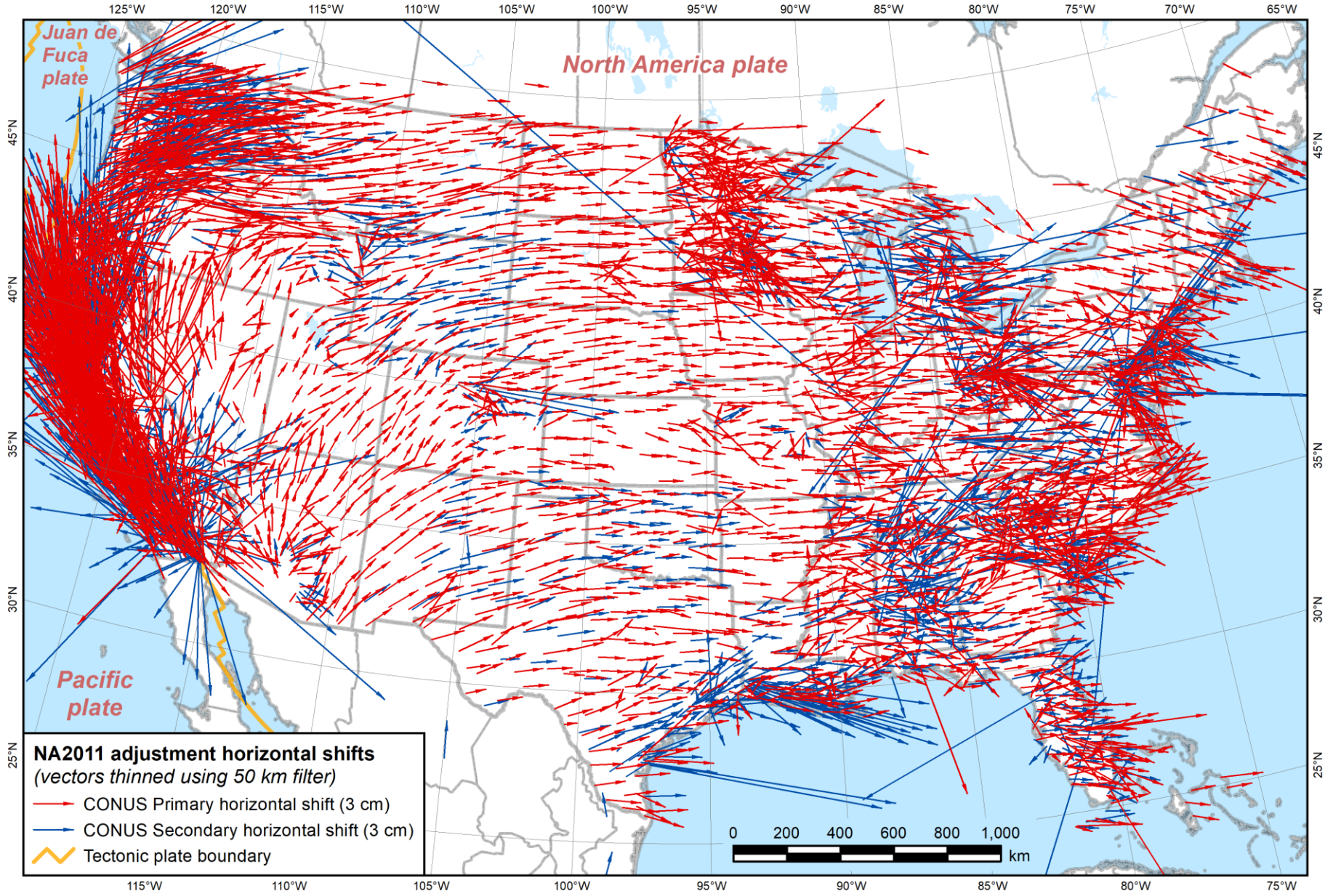

Figure 4.45. Map of NA2011 horizontal passive marks shifts for CONUS only (vectors thinned using 50 km filter).

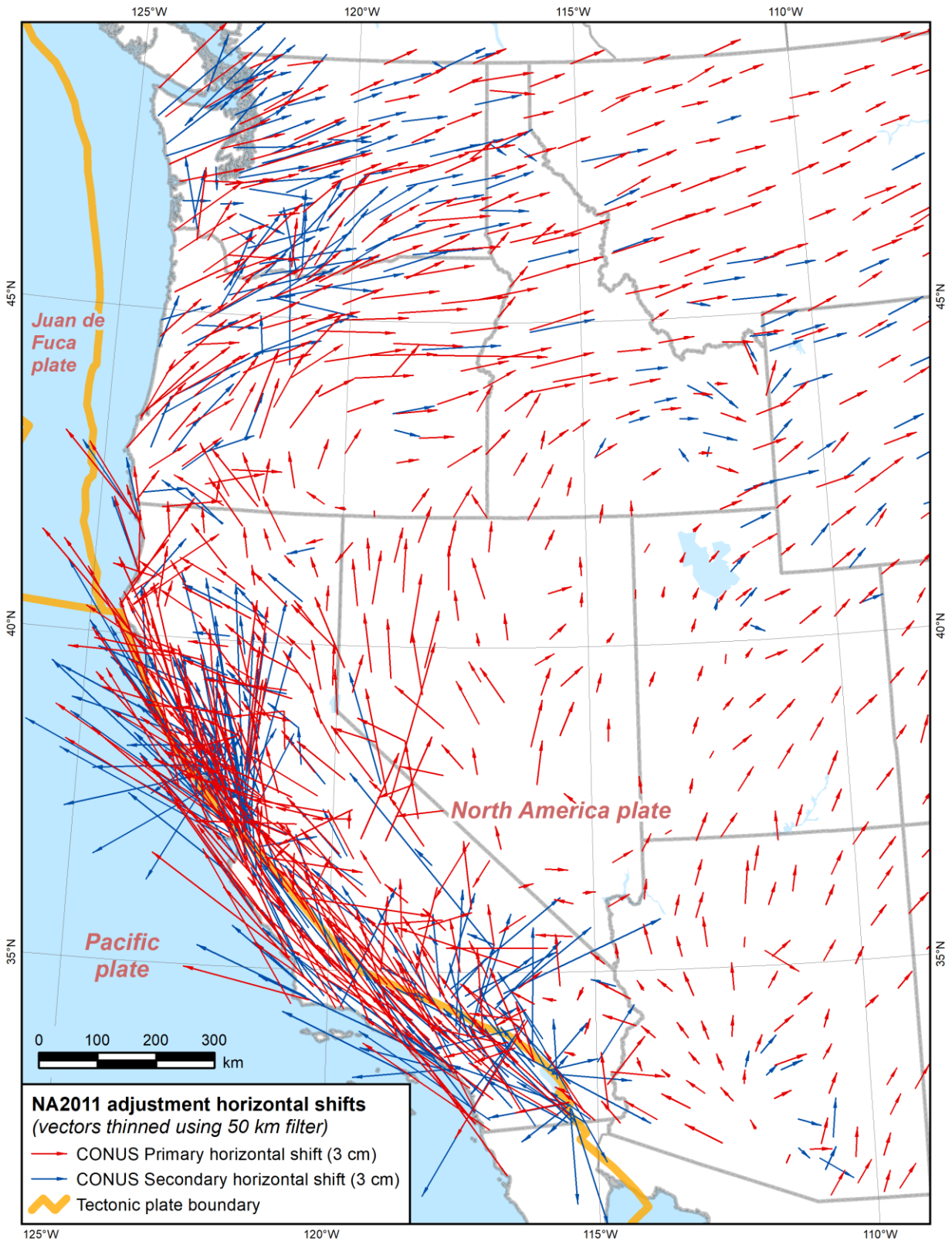

Figure 4.46. Map of NA2011 horizontal passive marks shifts for western CONUS (vectors thinned using 50 km filter).

These varied approaches to dealing with time dependence in the 2007 adjustment created some inconsistencies, for example by equating epochs 2002.00 and 2007.00. Referring to Table 3.2, even the "stable" parts of central CONUS have velocities around 0.2 cm/yr, so that alone would create a systematic 1 cm discrepancy for the five-year time difference between epochs. The problem is, of course, more severe in areas such as the Caribbean, as they are on a different plate, but the G-files were not transformed with *HTDP* in the 2007 national adjustment. For example, the NAD 83 velocity for Puerto Rico is about 2 cm/yr (see Table 3.2). In 2007, this systematic discrepancy was masked by constraining to epoch 2002.00 CORS coordinates.

Despite inconsistencies in handling epoch for the 2007 adjustment, the displacement vectors from that adjustment to NA2011 clearly show a pattern consistent with the known frame rotation rates. Displacements in most of CONUS are consistent in magnitude and direction with the eight-year time difference between epochs 2002.00 and 2010.00, about 1.5 to 2 cm. The horizontal displacement vectors in the Caribbean (Figure 4.44) are very consistent, approximately 16 cm, the value expected for the eight-year time difference. Displacement vectors in western California (Figure 4.46) show the expected north-northwest orientation for their location on the Pacific plate margin. The magnitudes of approximately 10 to 15 cm are consistent with the 3 to 5 cm/yr NAD 83 velocities and the three-year time difference (2007.00 to 2010.00). The expected displacement pattern is also seen in western Oregon and Washington. Note the similarity of the CONUS displacement vectors to the modeled *HTDP* velocity vectors in Figure 3.2 and the MYCS1 CORS coordinate shifts in Figure 1.1. That the NA2011 adjustments of CONUS were able to detect such small velocities is evidence of its overall fidelity and accuracy.

Substantial outliers also exist among the displacement vectors in Figure 4.44 through Figure 4.46. There are those that appear as the "noise" one might expect when performing an adjustment with new observations, constraints, and network design. Others are unusually large, particularly for Secondary marks, with some so large the vector endpoint is entirely off the map. The largest of these is a 92-cm shift, for a no-check mark in South Carolina (DYAR, PID ED3698), which extends off the map northwest towards Alaska. It is unclear what should be done about such marks, as it is not obvious whether the new position is more accurate than its previous one. To make such determinations would require considerable analysis and could still prove inconclusive. However, it would be appropriate to identify such behavior and provide that information to NGS customers.

Ellipsoid height shifts for the Caribbean are shown in Figure 4.47. The striking issue here is that all the shifts on and near Puerto Rico are positive, whereas all others in the Caribbean are negative. One possible reason for this anomaly is that all the CORSs used as constraints in the Caribbean were located on Puerto Rico and the Virgin Islands; the next closest ones are in southern Florida, 1500 km from Puerto Rico (see Figure 2.13). Another possible reason is that all of the other marks in the Caribbean were occupied in April 1996.

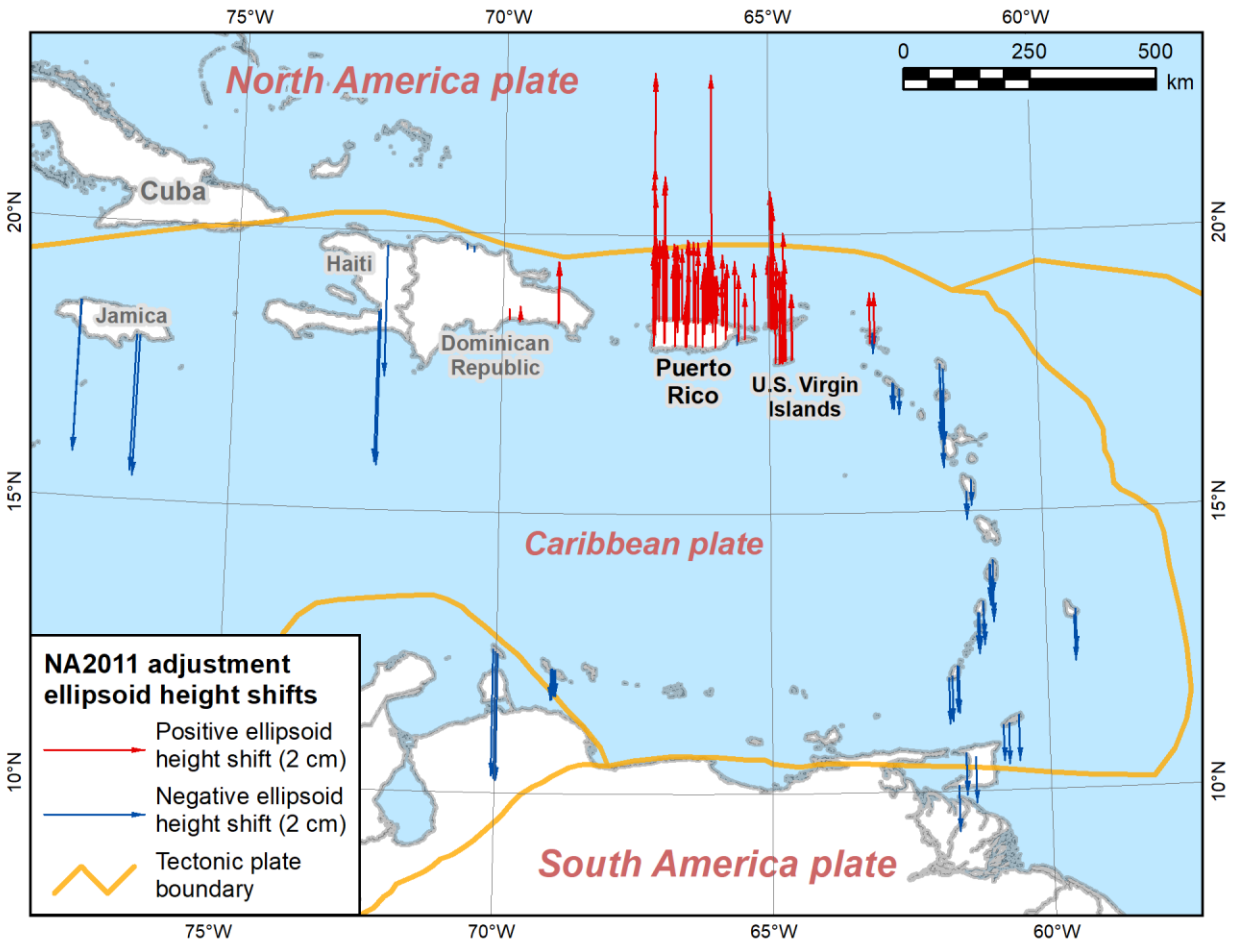

Figure 4.47. Map of NA2011 ellipsoid height shifts of Caribbean passive marks.

Figure 4.48 shows NA2011 horizontal displacement vectors for Alaska. The variability in orientation and magnitude explains why the standard deviations were so high in

Table **4.17**. However, many of the vectors are consistent with expectation for NAD 83 velocities, especially in south central and southwest Alaska along the Gulf of Alaska coast, as can be seen by comparing to the *HTDP* modeled velocities for Alaska in Figure 3.3. However, many of the vectors with correct orientation are too long for the three-year time span between 2007.00 and 2010.00. Many are too long even for the seven-year time span from 2003.00 to 2010.00 (if the epoch 2003.00 CORS coordinates had been used for constraints in the 2007 national adjustment). Similar observations could be made regarding vectors along the Alaska-Canada border and along the north coast; they have the correct orientation, but some are much too long. Part of the reason for this may be because *HTDP* modeling has improved significantly in Alaska since the version used for the 2007 adjustment (similar is true for California). Another significant improvement occurred in *HTDP* for Alaska shortly after completion of the NA2011 Project, including the first use of vertical velocities. Better results may have been achieved in Alaska had the more updated version of *HTDP* been used (as recommended in Section 6.2.1.3). There were also new GPS projects tied to new CORSs in the NA2011 adjustment.

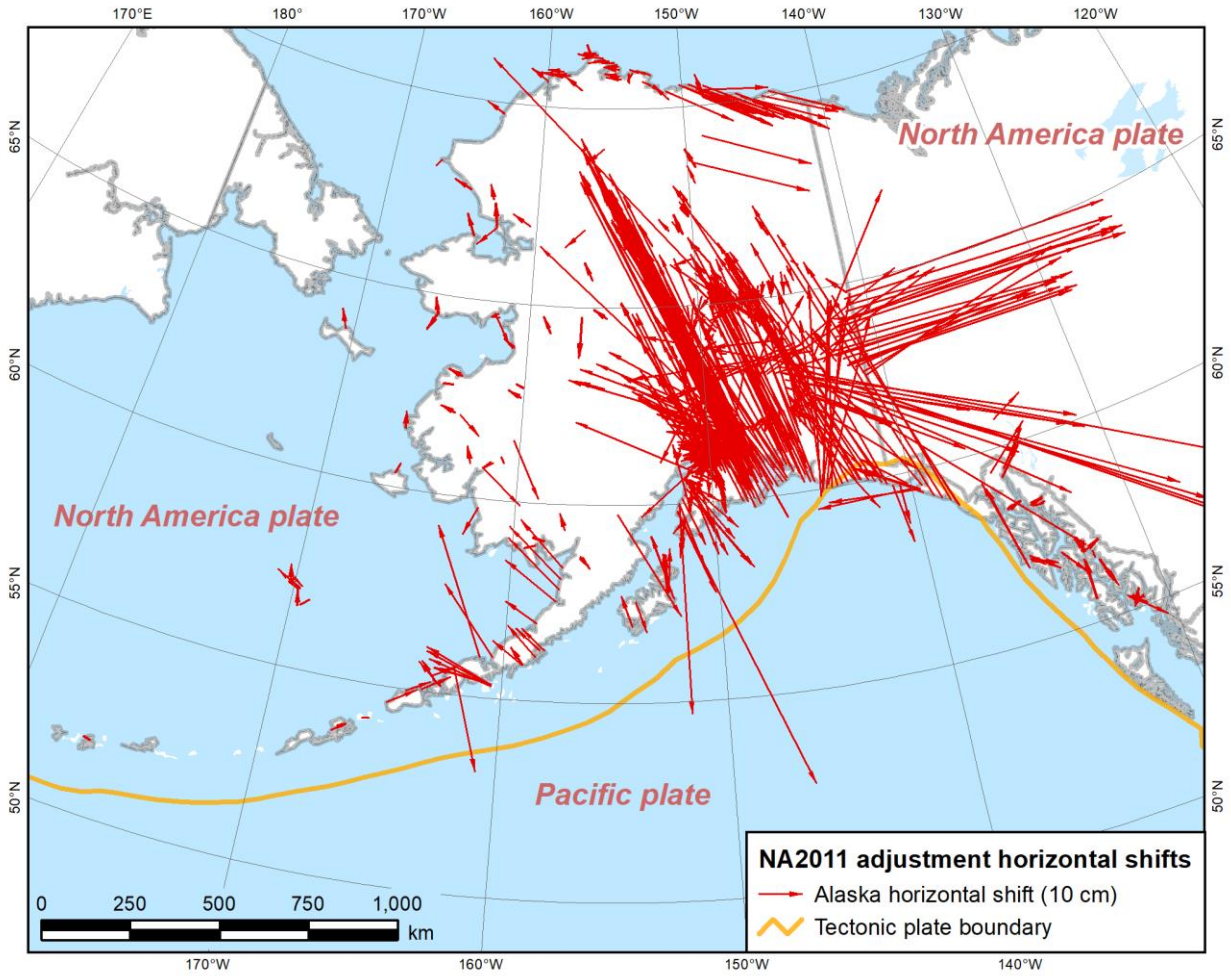

Figure 4.48. Map of NA2011 horizontal shifts of Alaska passive marks.

Ellipsoid height displacements for Alaska are shown in Figure 4.49. For most vectors, there is a clustering of similar sign and magnitude. Some seem reasonable for the setting, e.g., downward shifts along the north coast where oil is being extracted, as well as upward shifts along the southwest peninsula where subduction uplift could be occurring. But, clearly there are anomalies, such as the group of marks on one of the Pribilof Islands in the Bering Sea. One part of the group is up by 6 cm, but the other adjacent part is down by 40 cm. Upon inspection, it was found that the two vectors establishing the entire group in the 2007 adjustment were rejected in NA2011 in favor of six newer observations that were not available for the 2007 adjustment. The newer observations resulted in new coordinates on some of the marks after the 2007 adjustment (not all marks were observed). These new coordinates shifted up in NA2011, but those based only on the old observations shifted down by 40 cm. The net effect is that the entire group of marks on the island are now consistent. So, what first appeared as a problematic discrepancy is actually an improvement.

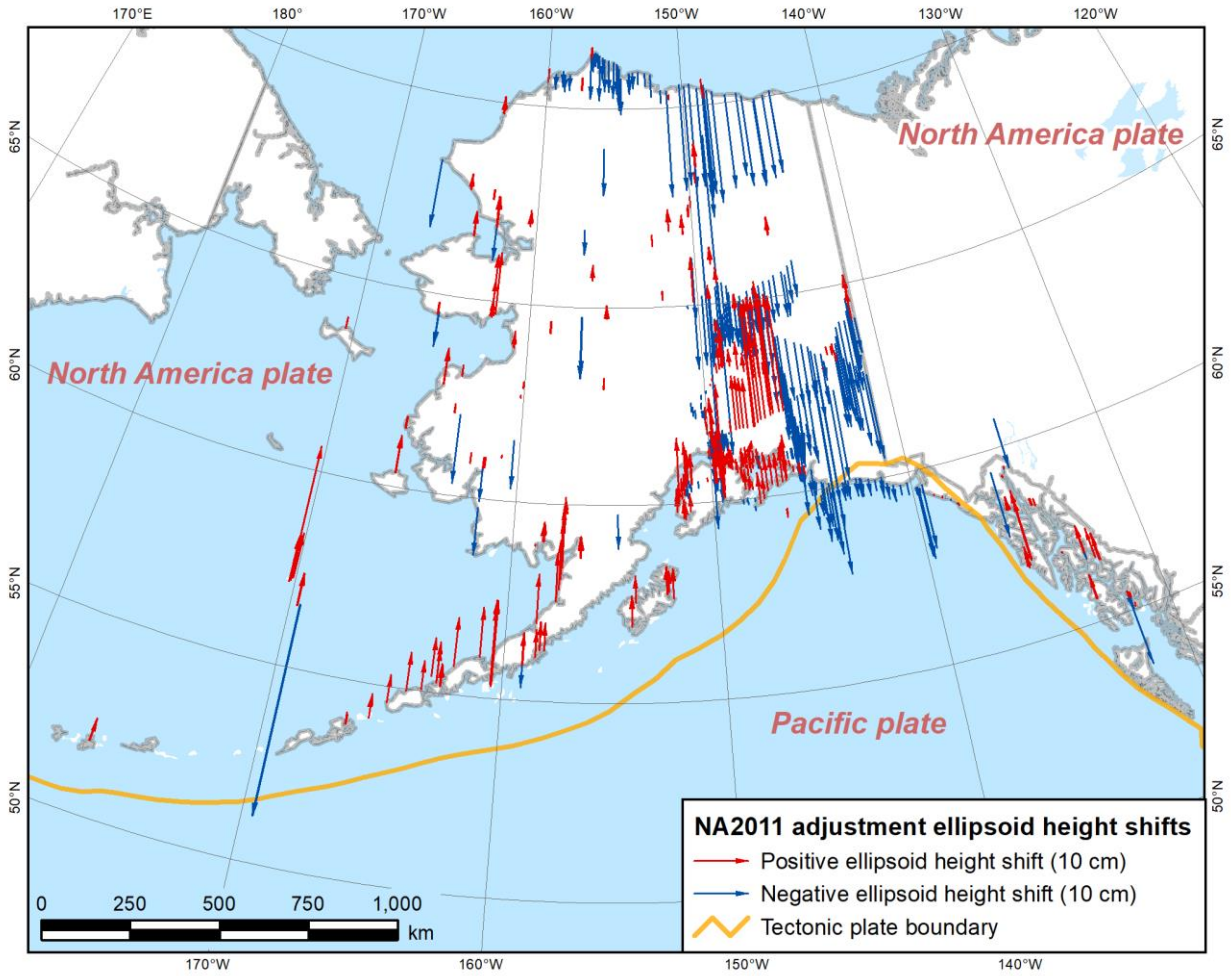

Figure 4.49. Map of NA2011 ellipsoid height shifts of Alaska passive marks.

Horizontal displacement vectors for the Pacific PA11 and MA11 networks are shown in Figure 4.50. Because of the wide variation in orientation and length of the shifts, they are displayed in two maps. The top map shows the extent of the vectors for the PA11 network, although it also shows some of the MA11 vectors. The bottom, slightly larger scale map, shows displacements for the MA11 network. These maps show why the horizontal standard deviations are so large in Table 4.18. Coordinate changes in different parts of the Pacific plate vary greatly. The shifts are relatively small and variable (approximately 0 to 8 cm) in Hawaii, mostly southward (approximately 8 cm) in the Midway Islands, small (approximately 3 cm) to the southeast in American Samoa, large (approximately 50 to 160 cm) and to the west-southwest for most islands on the southwestern part of the Pacific plate, and large (approximately 50 cm) to the west-southwest for many marks on the Mariana and Philippine Sea plates. But the most conspicuous characteristic of the shifts are very large differences at some adjacent marks.

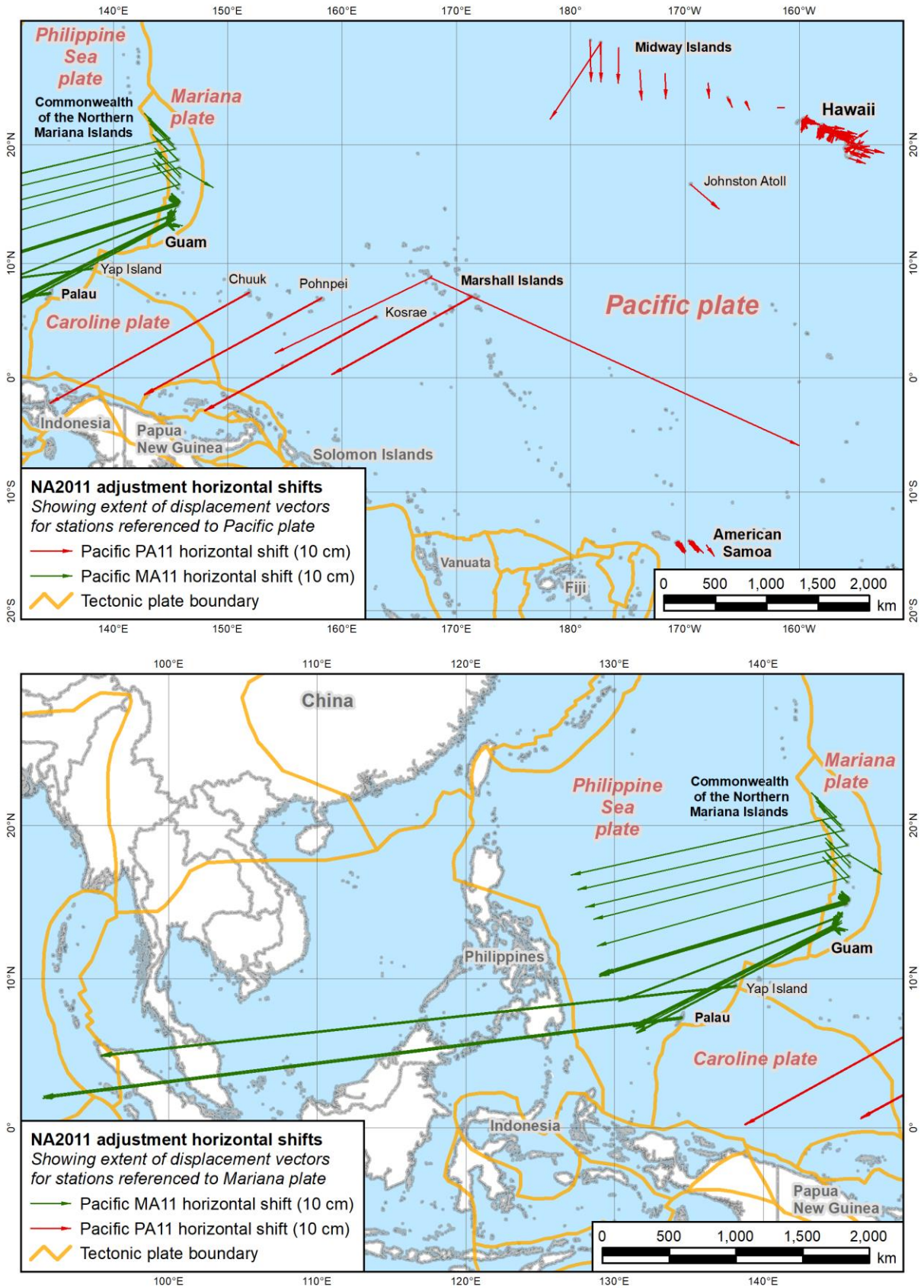

Figure 4.50. Maps of horizontal shifts for Pacific PA11 (top) and MA11 (bottom) passive marks.

In the upper map of Figure 4.50, on Kwajalein Island in the Marshall Islands, there are large displacements in completely different directions. One is 42 cm to the west-southwest (consistent with other islands in the region) for mark KWAJELINE (PID AA5108), set by National Ocean Service (but unpublishable because it lacks descriptive text), observed with 12 enabled vector ties in August 1993 (the same time other islands in that region show the same shifts). The other mark, 182 0000 TIDAL 8 (PID DK7537), is 1.34 km away with a shift of 98 cm to the east-southeast (far different from all other shifts in the Pacific), and was observed in August 2008 with four enabled vectors. There are two other marks on the islands, both with shifts of only 0.5 cm. One is the MYCS1 computed CORS KWJI (used as a constraint), and the other is 182 0000 TIDAL 12 (PID DK3433) tied to KWJI in September 2000 with 8 vectors, only 1.18 km away, with the same near zero shift as KWJI. So, there are three passive marks on this tiny island, all with completely different horizontal shifts. The mark with a 98 cm shift (182 0000 TIDAL 8) was not connected to nearby KWJI, because it was decommissioned in 2002. Instead, it is connected to a CORS on Guam (GUUG) and on Saipan (CNMR), both about 2500 km distant. These two tidal marks are only 250 m apart, yet one shows a shift of 0.5 cm, the other 98 cm. Since the newer mark (TIDAL 8) was observed with CORSs on the Mariana plate—and as discussed previously, it is unlikely the relative tectonic motion was correctly taken into account—the NA2011 adjustment probably resolved the approximately 1 m discrepancy between these marks. Unfortunately, there is no tie between the marks and, therefore, no way to confirm without new observations connecting them. These two tidal marks also show height shift differences of 10 cm, the new one -12 cm, the previous one -2 cm, and this is important, as these are used as the basis of local tidal elevations on the island.

Both maps in Figure 4.50 show that large discrepancies—and the largest of all horizontal shifts—occur for MA11 marks. Significant discrepancies in shifts occur for many adjacent marks of the 151 on the Mariana plate. These can be classified into five groups, where the shifts are associated with different observation times (and thus several different and separate adjustments prior to NA2011), as listed below.

1. Forty marks on nearly all the Mariana plate islands have horizontal shifts of 54 to 65 cm to the west-southwest, all observed in August 1993 (although one was again observed in February 1997). All of these are in the 1993 GPS project GPS667 (which has four parts, one with no suffix, as well as parts B, C, and D). It has many GPS vector ties across the Pacific, including Hawaii, American Samoa, the Marshall Islands, Guam, and CNMI).

2. Ten marks on the Northern Mariana Islands show consistent shifts of 8 cm to the northwest, observed in August and September of 2003.

3. One mark, with a shift of 9 cm to the southeast (observed in both in 1993 and 2003).

4. Forty-seven marks on Saipan and Tinian show shifts of 2 cm to the northwest, consistent with Saipan CORS CNMR and CNMI shifts. All marks were observed in May and June 2003 (and a few also in 1993, and one also in 2007).

5. Fifty-seven marks on Guam and Rota have variable shifts, but most are fairly small, all are less than 4 cm, and they are largely consistent with the 1.3 to 2.7 cm CORS shifts (GUUG and GUAM). The marks were last observed in 2008 (one mark), 2007, 2004, and 2003. Nine were also first observed in August 1993.

The consequence of these many different shifts is that there are marks within a few hundred meters of one another (or less) with horizontal shifts that can differ by more than half a meter. But again, as discussed for the situation on Kwajalein Island, it is likely these shifts from the NA2011 adjustments actually resolved positional discrepancies between these marks. As also occurred on Kwajalein Island, many marks that are close together are not tied by observations, which is unfortunate.

The 16 marks on Palau and Yap Island show consistent shifts of 160 and 158 cm, respectively, nearly due west. All were observed in August 1993, along with many other marks across the Pacific in project GPS667. As mentioned previously, these marks are on the Philippine Sea plate but are referenced to the Mariana plate (MA11). Had they instead been referenced to the Pacific plate (PA11), their shifts would have been about 69 and 66 cm. Although those shifts are still large, they are less than half the MA11 values. More importantly, they also would have near-zero velocities, as mentioned in Section 3.1.3. Their MA11 velocities are about 6.06 cm to the west-northwest.

Ellipsoid height shifts for both PA11 and MA11 marks are shown in Figure 4.51 (the two can be distinguished by location). The largest for both networks are -40 to -67 cm for 78 marks, all only observed in the 1993 project GPS667 (except for one mark in Guam also observed in 1997). All of the positive shifts in the western Pacific occur for 110 marks on the Mariana plate, and they are all associated with their last observations that took place in 2003 or later (with the exception of one in 1997). In American Samoa, all shifts are -1.6 to -5.3 cm, including those observed in 1993. The Midway Islands all show positive shifts (of +2 to +37 cm), with every one observed in 2001, except for one in 2011 with the largest shift. Hawaii marks show both positive and negative shifts, although the largest number and magnitude are negative: 158 marks from approximately 0 to -28 cm, versus 91 from approximately 0 to 14 cm, and it appears there is no correlation between shifts and the age of observations (from 1993 through 2011) as there is in most other parts of the Pacific. As with the horizontal shifts, it appears the height shift discrepancies represent improvements in the consistency of coordinates for the Pacific, as they were determined from a "single" simultaneous adjustment (actually two adjustments, but the same network in both cases, simply with respect to different geodetic frames).

4.4.2. Shifts of constrained CORS coordinates

CORS coordinates determined from the MYCS1 reprocessing project were the constraints for the NA2011 constrained adjustments. But because weighted (stochastic) constraints were used, their coordinates were able to shift in the adjustment. The amount they shifted depended both on the weights used and how well the network geometry fit with the MYCS1 coordinates. One concern for the NA2011 Project was that the CORSs would shift too much, thus resulting in passive mark coordinates not sufficiently consistent with MYCS1.

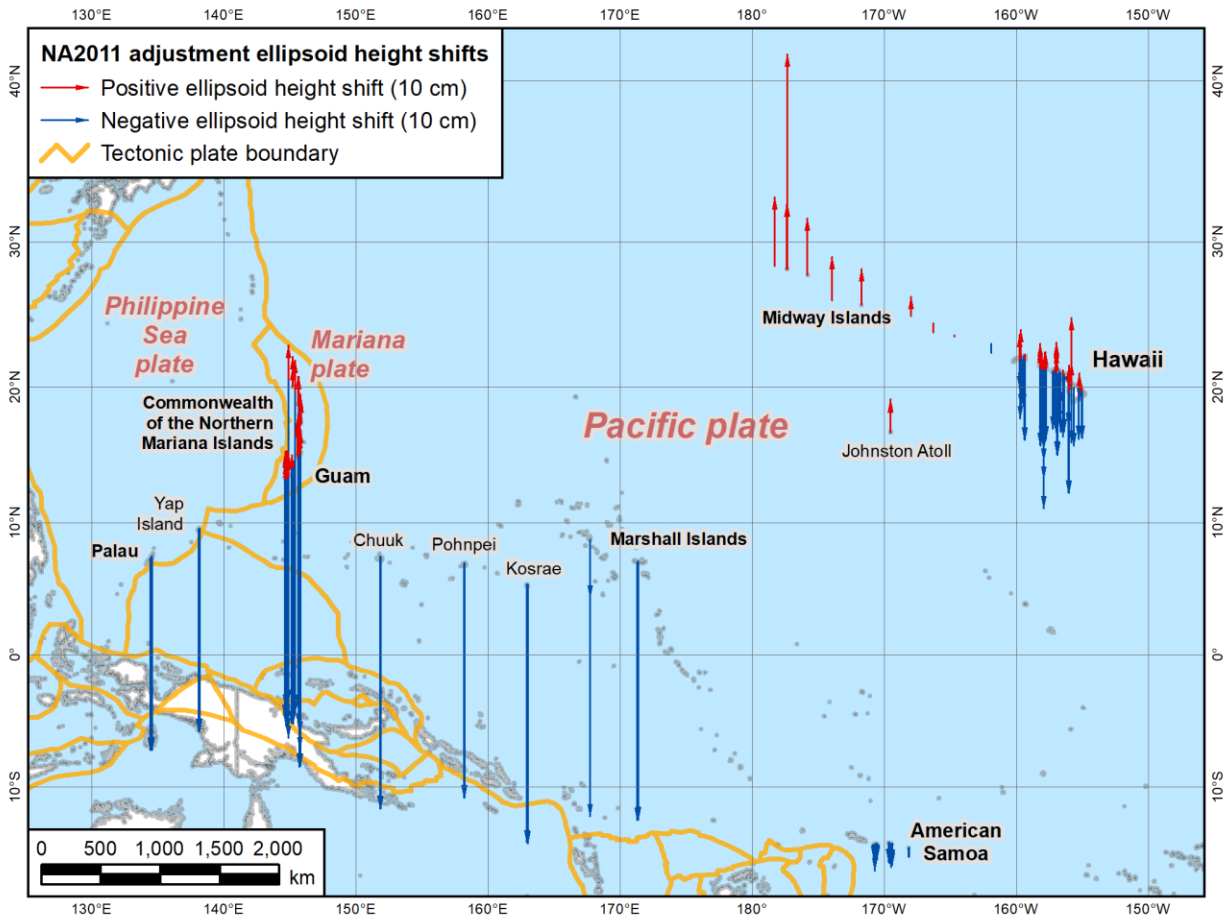

Figure 4.51. Map of NA2011 ellipsoid height shifts of Pacific PA11 and MA11 passive marks.

Table 4.19 provides statistics for the shifts in constrained CORS coordinates, separated into "computed" and "modeled" MYCS1 CORSs. The maximum magnitude of horizontal and up shifts for the computed CORSs are fairly large and are about the same, 13 to 14 cm. The maximum shifts for the modeled CORSs are significantly less, and also nearly the same horizontally and up, about 7 to 8 cm. However, the median shift magnitudes for the computed CORSs are somewhat lower than for the modeled CORSs, 0.9 cm horizontally and 0.6 cm up, versus 1.2 cm horizontally and 0.7 cm up for the modeled CORSs. For both types of CORSs, roughly 95% of the horizontal shifts are less than 4 cm horizontal and 3 cm up. Considering the signed shifts, 98% of both types of CORSs are within approximately ±4 cm north and east, and within about ±6 cm up.

As covered in Chapter 3, it is known that the formal sigmas used for computed CORS weights vary greatly, from 0.05 to 32.5 cm, with the largest sigmas on the height component (see Table 3.3). The modeled CORSs have constant sigmas of 1 cm north and east and 3 cm up, and these may be too small, based on comparison to their *a posteriori* sigmas from the NA2011 adjustments (see Table 4.14).

Table 4.19. Shift in constrained "computed" and "modeled" CORSs.

	Computed CORSs (num = 973)					Modeled CORSs (num = 222)				
Shifts (cm)	**North**	**East**	**Up**	**ABS Up**	**Horiz**	**North**	**East**	**Up**	**ABS Up**	**Horiz**
Minimum	-11.50	-8.07	-12.90	0.00	0.00	-3.59	-3.02	0.00	0.00	0.00
Maximum	9.88	8.03	9.80	12.90	14.02	4.50	6.78	8.50	8.50	6.82
Mean	0.08	0.05	0.37	1.33	0.91	0.17	-0.05	0.51	1.56	0.89
Std deviation	±1.15	±1.03	±1.93	±1.45	±1.25	±0.86	±0.94	±2.01	±1.37	±0.92
Percentiles										
1.0%	-3.56	-3.73	-4.45	0.00	0.00	-3.37	-2.60	-4.58	0.00	0.04
5.0%	-1.24	-1.13	-2.60	0.10	0.10	-0.82	-1.20	-2.60	0.10	0.16
10.0%	-0.62	-0.78	-1.60	0.10	0.16	-0.55	-0.78	-1.80	0.30	0.25
50.0% (median)	**0.06**	**0.03**	**0.30**	**0.90**	**0.56**	**0.17**	**-0.09**	**0.40**	**1.20**	**0.66**
90.0%	0.89	0.82	2.40	3.00	1.80	0.99	0.70	3.30	3.50	1.77
95.0%	1.33	1.32	3.40	3.90	3.18	1.45	1.16	3.89	4.29	2.59
99.0%	3.64	3.57	6.73	7.23	6.92	2.94	4.49	6.02	6.13	5.87

With such a great range in formal sigmas used for computed CORS constraints, it is natural to consider their effect on the coordinate shifts. One way of evaluating the effect is through a ***constraint ratio*** (Gillins and Eddy, 2016). The constraint ration (CR) is the unitless ratio of the absolute value of the coordinate shift to the sigma assigned to the constrained component. Constraint ratios for computed and modeled CORSs are given in **Error! Not a valid bookmark self-reference.** for the north, east, and up components. The purpose of the CR is to provide an assessment as to whether a constrained mark should in fact be constrained. The metric is that the shift should not exceed the sigma for a component, corresponding to the confidence level of that component. Thus, if the CR is greater than 2, it exceeds the constrained sigma at about the 95% confidence level. A CR of 3 corresponds to approximately 99.7% confidence on a component.

The median CRs in **Error! Not a valid bookmark self-reference.** are fairly low, about 0.9 horizontal and 0.6 up for computed CORSs, and 0.4 for all components of modeled CORSs. However, the maximum CRs are large, in particular for the horizontal components of the computed CORSs (maximum CR of 58). About 10% of the computed CORS have CRs greater than 3; by comparison only about 1% of the modeled CORS have CRs that are greater than 3.

When using weighted constraints, the expectation may be that larger shifts will be correlated with larger sigmas (i.e., smaller weights); however, the shifts are also a function of how well the observations fit the constrained coordinates. For the NA2011 adjustments, the correlation between shifts and sigmas is fairly weak. The correlation coefficients between the sigmas and absolute value of shifts are +0.107 north, +0.020 east, and +0.201 up. These values are positive, however not strongly positive. The lack of significant correlation is presented visually in Figure 4.52, as a scatter plot of the constrained coordinate shifts versus the sigmas used to weight each component. A log scale is used for the sigmas, since they range over nearly three orders of

magnitude. For clarity, the vertical shift axis only extends to 5 cm, therefore the 46 individual components with shifts greater than 5 cm are not shown (41 of these are computed CORSs). Logarithmic regression curves are plotted as a visual guide. Although each shows some positive correlation, they have essentially no predictive value ($R^2 < 0.03$ for all). Overall, the data do not provide much support for the supposition that large coordinate shifts accompany small constraint sigmas.

Table 4.20. Constraint ratios for "computed" and "modeled" CORSs.

	Computed CORSs (num = 973)			Modeled CORSs (num = 222)		
Constraint ratios	**North**	**East**	**Up**	**North**	**East**	**Up**
Minimum	0.00	0.00	0.00	0.00	0.00	0.00
Maximum	43.89	58.47	16.67	4.50	6.78	2.83
Mean	1.72	2.16	1.16	0.58	0.56	0.52
Std deviation	±3.13	±4.21	±1.68	±0.65	±0.75	±0.46
Percentiles						
1.0%	0.00	0.00	0.00	0.00	0.00	0.00
5.0%	0.04	0.06	0.02	0.03	0.03	0.03
10.0%	0.11	0.12	0.08	0.06	0.07	0.10
50.0% (median)	**0.80**	**0.91**	**0.57**	**0.40**	**0.36**	**0.40**
90.0%	4.01	4.95	3.02	1.29	1.16	1.17
95.0%	6.25	7.81	4.42	2.01	1.93	1.43
99.0%	16.57	21.97	8.35	3.56	4.49	2.04

The large size of some of the constrained coordinate shifts is a concern. In the following paragraphs, discrepancies are explored in greater depth for those CORSs with the largest shifts in constrained coordinates: CARR and HDF1 (horizontal) and GUS1/GUS2 and STP6 (vertical). The situation for each CORS is unique, requiring substantial effort to determine the reason for the shifts. Such analyses can be extremely labor-intensive, representing a challenge for such large networks. Also note that the CORSs discussed below are decommissioned: CARR in 2003; HDF1, GUS1/GUS2 in 2008; and STP6 in 2017. All but CARR were U.S. Coast Guard CORSs, with antennas installed in pairs less than about 30 m apart, usually mounted on the same structure.

All 18 CORSs with horizontal constraint shifts of more than 5 cm have north and east constraint sigmas of significantly less than 5 cm (they range from 0.1 to 1.0 cm). Only three are modeled CORSs. The three constrained CORSs with the largest horizontal shifts (10 to 14 cm) are the two reference points of CARR (California) and the ARP of HDF1 (New York).

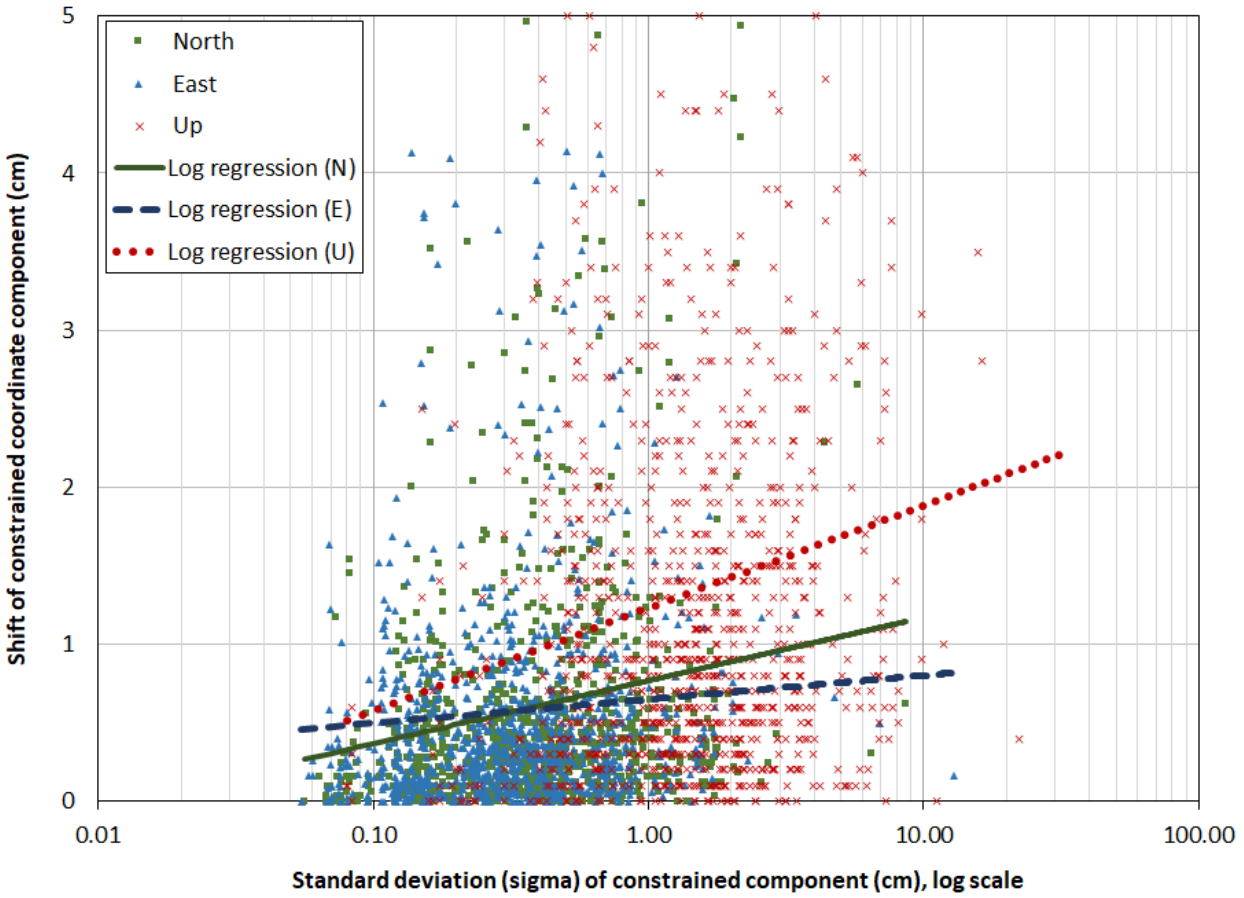

Figure 4.52. Plot of constrained coordinate shifts versus component sigma for computed CORSs.

The adjusted coordinates of the two CARR points shifted by -11 cm north and 8 cm east (but only a +0.9 cm up) from their constrained MYCS1 values. CARR was among the problematic CORSs discussed in Section 2.2.2, in that it was difficult to unambiguously identify. Of the three different marks identified as the CARR CORS in the NGSIDB, two were constrained. One was clearly part of MYCS1 as an external monument (designation LEXI 1989; PID AF9689), but another was inferred based on its location and designation as an L1 phase center (designation CARR PARKFIELD L 1 PHS CTR; PID AB5073). The third (designation CARR PARKFIELD MONUMENT; PID AB5072) was not constrained as a CORS because of its 6-cm positional discrepancy, and because its NGSIDB description implied it was an eccentric survey mark for the CARR CORS site. As additional evidence of problems with this CORS, note that no component of CARR was constrained in the 2007 national adjustment, including LEXI 1989 (PID AF9689) used in MYCS1. It appears, then, that this CORS was a problem for the 2007 adjustment as well.

Given that the shift of CARR was almost entirely horizontal, and its location in California, the large shifts may have been due to problems with the computed velocity (it was decommissioned in 2003), inappropriately modeled crustal motion in the region, erroneous coordinates at connected marks, or some combination of these effects.

A total of 182 enabled vectors are tied to the two CARR marks constrained as CORSs in the NA2011 network. Fortunately, the enabled vectors were connected directly to seven other CORSs (COSO, HARV, MHCB, MONP, MUSB, PAR1, VNDP), mitigating the impact of CARR. The seven connected CORSs have a mean horizontal constraint shift of only 0.2 cm north and -1.1 cm east, indicating they were negligibly influenced by the large shift of CARR. CARR was also directly connected to 16 passive marks, all of which were connected to many other marks. All 16 connected passive marks shifted fairly consistently, with a mean shift of 6.3 cm north and -4.5 cm east. These shifts are with respect to their published NAD 83 epoch 2007.00 coordinates. Applying the MYCS1-computed NAD 83 velocities of CARR (3.01 cm/yr north and -2.08 cm/yr east) to these marks for 2010 – 2007 = 3 years reduces and reverses the shift to -2.7 cm north and 1.7 cm east. This mean shift is much different than the -11 cm north and 8 cm east shifts of the two CARR points, indicating that the CARR shift had little impact on the 16 directly connected passive marks. This result also shows the importance of having multiple ties from different control marks.

HDF1 (designation HUDSON FALLS 1 CORS ARP; PID AI8826) shifted 9.9 cm north and 0.6 cm east from its constrained MYCS1 coordinates. It had 90 enabled vector ties, and, as with CARR, these were connected to other marks with multiple vector ties. However, there are three marks tied only to HDF1. Two of these marks are nearby CORSs reference marks HUD1A (PID AI9622) and HUD1B (PID AI9623), both within about 300 to 400 m of HDF1. The third is D 233 (PID OE0128), 55 km from HDF1. Although HDF1 constrained coordinates shifted 9.9 cm horizontally (and 0.8 cm up), these three marks connected only to HDF1 shifted less than 2 cm horizontally (as did all other marks connected to HDF1). Moreover, the magnitude and eastward direction of the passive mark shifts are consistent with the general apparent horizontal rotation of the NAD 83 frame, whereas HDF1 shifted 9.9 cm to the north. Thus, there is about a 10-cm horizontal inconsistency between the MYCS1 and the adjusted coordinates. The interesting thing here is that both results may be correct.

It appears HDF1 is moving south (at 1.3 cm/year, based on its MYCS1 computed NAD 83 velocity). This is in contrast to the other CORSs in the region, which are generally moving to the east-southeast, and at a much slower rate (generally about 0.2 to 0.3 cm/year). For the 8 years from 2002.0 to 2010.0, the HDF1 velocity would move it 10.4 cm south, similar to the series of published HDF1 coordinates from March 2002 to August 2007 that show a southward change of 10.3 cm. It appears, then, that HDF1 was moving differently than the general region. Given this is not a tectonically active area (central New York state), it seems likely the movement was of the supporting structure, rather than local crustal deformation. Because it is tied to one CORS and 23 passive marks, which are in turn tied to other CORSs and passive marks, the vectors had enough rigidity to force HDF1 into a location consistent with the other CORSs in the region—even though HDF1 had small constraint sigmas (0.23, 0.18, 0.80 cm N, E, U). So, it is entirely possible, and perhaps even likely, that HDF1 moved 10 cm south while the other marks in its region moved about 1 to 2 cm east-southeast. Both are captured by the NA2011 Project, because the adjusted coordinates of passive marks and the MYCS1 coordinates of CORSs are published. That is what appears most likely from the available evidence, and if so, it shows how a network

of vectors tied to passive marks and (most importantly) multiple CORSs can mitigate anomalous behavior at a single CORS.

For shifts in constrained ellipsoid heights, a total of 32 CORSs have shifts of 5 cm or greater. All but three have constraint sigmas of less than 5 cm, but they vary considerably, from 0.5 cm (JPLM) to 32.5 cm (P304), and only four are modeled CORSs. The three constrained CORSs with the largest height shift magnitudes (10 to 13 cm) are GUS1 and GUS2 (Alaska) and STP6 (Wisconsin), and all of these are decommissioned USCG CORSs.

CORSs GUS1 and GUS2 have 34 enabled vector ties, connected to one CORS and 12 passive marks with ties from other marks, with the exception of one, the CORS reference mark GUST USCG B (PID AD9355), connected only to GUS1. Rather than shifting the -12.5 cm of GUS1, the ellipsoid height of this mark shifted +2.3 cm, and in fact all of the other passive marks also shifted in height between +2.3 and -0.3 cm. The situation here appears similar to HDF1, because the surrounding CORSs (one directly connected and others indirectly through shared passive marks) show constraint shifts within ±3 cm. And so again, similar to HDF1, the network ties to other CORSs forced this constrained mark to shift. Here, however, the situation could be different, because change in height can be highly localized and variable. GUS1 and GUS2 have computed MYCS1 up velocities of +1.8 cm/year, which would result in a +12.6 cm of height change in the 7 years from 2003.0 to 2010.0 (all the surrounding CORSs have up velocities of less the 0.5 cm/year). It is possible the local area around GUS1 and GUS2 uplifted by about 12 cm, including the eight nearby passive marks (all within about 2 km). If so, then the adjusted heights of those passive marks are too low by about 12 cm, but there is no way to tell without additional observations.

HDF1 and GUS1/GUS2 are examples of a how the vector network can "force" the constrained CORS coordinates to shift based on the coordinates of the surrounding constrained CORSs, and in the case of HDF1, this appears to have been beneficial, but in the case of GUS1/GUS2 it may have been deleterious. In either case, it is impossible to know for certain without additional observations or other information. These examples illustrate the complexities and possible pitfalls of combining datasets that span long time intervals.

The next largest ellipsoid height shift (+9.8 cm) occurred at STP6. STP6 has 11 vector ties, including one CORS and 10 passive marks. However, the other CORS in its pair, STP5, shifted -0.2 cm; the two antennas are only 28.8 m apart and are likely mounted on the same structure. In addition, STP6 has a (computed) up velocity of -0.08 cm/yr; whereas STP5 has an up velocity of -0.62 cm/yr (the same as STP1, the one STP5 replaced). This is a large velocity difference for two antennas so close together, and it may indicate a problem in the MYCS1 results for STP6. From the 2002.00 epoch of the previous coordinates, the height change due to the velocity difference is 0.54 cm/yr × 8 years = 4.3 cm, accounting for nearly half of the up shift. The 10 passive marks tied to STP6 have vector ties to many other passive marks, including several other CORSs. The up shifts on these passive marks are small and consistent (from -1.6 to -3.4 cm), and the five other CORSs these passive marks are connected to have shifts within ±1.2 cm. Thus, it appears the impact of the +9.8 cm shift of STP6 was mitigated by other vector connections.

Although only a small number of CORSs had significant shifts, it would obviously be preferable to have smaller shifts, but it is unclear what could have been done. Unconstraining them was an unacceptable option, because it would have made the shifts even larger. Tighter constraints may have helped, but most likely not by much unless they were made very small. The three CORSs with the largest horizontal shifts had constraint sigmas of 0.2 to 0.5 cm horizontally, and the three with the largest height shifts had up sigmas of 1.0 to 2.2 cm. Much smaller sigmas would have forced the observations to fit the coordinates, but that would have pushed the discrepancy (and errors) elsewhere. Considering the limited time for analysis—and the project requirement that CORSs be constrained—not much else could have been done, and the results are overall quite satisfactory. During the course of the project, discrepancies with CORSs were communicated to the CORS Team (in particular for HDF1). No action was taken to modify the MYCS1 coordinates of any CORSs, based mainly on the idea it was a single, consistent solution (in particular for the computed CORSs).

4.5. Chapter 4 summary

This chapter presents results of the final five constrained NA2011 adjustments and the associated minimally constrained adjustments, as well as pertinent preliminary and intermediate NA2011 results. The work performed for the project spanned one year, beginning with the first successful adjustment of the combined CONUS and Alaska networks in June 2011, to the final adjustments of five networks in June 2012. At least 168 separate adjustments were performed, 97 using *NETSTAT*, and 71 using *ADJUST*. Many of those adjustments were completed in a series of several iterations so as to reject and re-enable vectors, based on their residuals. As a result of this approach, the number of rejected vectors was reduced by nearly half.

Final coordinates were determined in three main regions and were completed on the dates below using the software listed. After loading and checking results in a test database, all results were loaded into the NGSIDB on June 27, 2012.

1. **CONUS.** Adjusted using *NETSAT* with Helmert blocking
    a. **Primary**. Completed on June 4, 2012
    b. **Secondary**. Completed on June 9, 2012
2. **Alaska.** Adjusted using *ADJUST*. Completed on June 13, 2012
3. **Pacific.** Adjusted using *ADJUST*. Both PA11 and MA11 completed on June 15, 2012
    a. **Pacific PA11**. Vectors and marks referenced to Pacific plate.
    b. **Pacific MA11**. Vectors and marks referenced to Mariana plate

Analysis of results in this chapter were performed in three main categories, grouped by chapter section:

1. GNSS vector residuals, vector component errors, and geometric closure (Section 4.2)
2. Adjusted mark accuracy estimates and comparison to MYCS1 accuracies (Section 4.3)

3. Shifts of adjusted coordinates from their previously published values and of their constrained coordinates (Section 4.4)

Despite the large dataset sizes, considerable effort went into providing detailed information concerning problems and discrepancies, including examples using specific marks and vectors. Some problems were identical to those found in the 2007 national adjustment, such as long "tails" in vector residual and coordinate error distributions (i.e., consisting of a small number of large values). A significant number of marks shifted by a large amount from their previously published values, particularly in Alaska and the Pacific, but rather than presenting problems, most of these are believed to represent improvements in coordinate consistency. Some CORSs used as constraints shifted by substantial amounts, potentially affecting a few directly connected passive marks. For the most part, however, it appears the large shifts at constrained CORSs were absorbed at connected marks by additional vector ties from other CORSs and passive marks.

Splitting CONUS into Primary and Secondary networks brought about the unintended consequence of creating disconnected subnetworks, causing 182 marks to be excluded from the results (an additional mark in Hawaii connected only to a mark in Alaska was also excluded, for a total of 183). This situation occurred due to these marks only being connected by rejected vectors. The 182 disconnected marks could be restored by identifying their enabled vector connections and performing adjustments to determine their coordinates, either individually or as part of a larger regional or national adjustment.

Providing examples of problematic results may give the impression the adjustments were compromised, but such occurrences were the exception; a vast majority of the results indicate high accuracy and reliability. Consider the following summary statistics:

1. **GNSS vector residuals.** 95% of the minimally constrained vector residuals are within ±1.3 cm horizontal and ±2.7 cm up for the 403,118 enabled vectors of the entire NA2011 Project.
2. **GNSS vector loop closures.** 95% of CONUS network misclosures are within ±1.5 cm horizontally and ±2.5 cm in height for 70,226 independent loops, with a total length of 925,019 km. 95% of the 3D relative loop misclosures are 2.9 parts per million or less.
3. **Mark accuracies.** Median network accuracy estimates (at the 95% confidence level) for all 77,560 passive marks with redundant observations are 0.9 cm horizontal and 1.5 cm in ellipsoid height. For 95% of these marks, the accuracy values are 3.2 cm or less horizontal and 7.1 cm or less in ellipsoid height. Compare this to the 95% confidence formal accuracies of the entire set of 1,309 "computed" NAD 83 MYCS1 CORSs (see Table 1.2): median of 1.1 cm horizontal and 3.5 cm ellipsoid height. For 95% of the MYCS1 stations, accuracy values are 3.8 cm or less horizontal and 13.1 cm or less in ellipsoid height (a disturbingly large value).
4. **Detection of tectonic motion.** The adjustment results for CONUS and the Caribbean were of sufficient accuracy and consistency to clearly resolve relative tectonic plate velocities of the NAD 83 (2011) frame (approximately 0.2 cm/year for central CONUS and 2 cm/year for Puerto Rico).

These statistics demonstrate the overall excellent results achieved for the NA2011 Project. Whereas it is true that somewhat better results could have been realized through more detailed and robust analyses, any such improvements would have been at the margins, affecting only a few percent of the marks. While better methods would have certainly been desirable, not all options could be pursued with the available resources and time constraints. Considering the magnitude of work performed over such a short time period of time, and with so few personnel, the NA2011 Project results are quite exceptional.

Chapter 5. Problems Found After Completion of Adjustments

A number of issues with the GNSS vector data were discovered after completion of the NA2011 adjustments and publication of results. While it is unfortunate that these issues were not found before completing the adjustments, most had a very small impact, either in magnitude or number of vectors affected, or both. Fortunately, nearly all of the issues can be corrected, and even though they were identified after completion, they can be resolved for any future adjustments.

The following section of this chapter described each type of issue found, along with its impact and how it can be corrected. The last issue discussed concerns so-called "trivial" (or "dependent") vectors. Because if is a fairly complex and subtle issue, an entire section of the chapter is devoted to a discussion of how trivial vectors were found, their likely impact, and how they can be handled in future adjustments.

5.1. Issues with GNSS vectors in the NA2011 networks

Issues found with GNSS vectors are in the data as stored in the NGS Integrated Data Base (IDB). All of the issues represent potential problems and are grouped into the nine categories listed in Table 5.1. Most of these affect an extremely small percentage of vectors, although a few affect a large proportion.

Table 5.1. Issues identified with vectors in the NA2011 networks.

	Issue	Affected vectors	
		Number	Percentage
1	Vectors with length less than 20 cm	49	0.01%
2	Baselines with vectors differing in length by more than 10 cm	~2300*	~0.5%
3	Erroneous vector covariances	145	0.03%
4	Duplicate vectors	553	0.13%
5	Erroneous or suspect session start and stop times (not edited)	528	0.12%
	Erroneous or suspect session start and stop dates and times (edited)	269	0.06%
6	Session duration of 5 minutes or less	2846	0.67%
	Session duration greater than 5 days	129	0.03%
7	Incorrect reference system codes with ~3 ppm max error	296	0.07%
	Incorrect reference system codes with ~0.15 ppm max error	140,674	33.15%
8	Broadcast orbits used while SA active (on or before May 1, 2000)	133,547	31.44%
	Broadcast orbits used while SA inactive (after May 1, 2000)	68,331	16.09%
9	Vectors repeated on a baseline within a session	4,452	1.05%
	"Trivial" (dependent) vectors	137,449	32.36%

*Approximately half the total of 4613 vectors in the baselines.

Most of the issues identified were determined from information in the G-files and therefore depend on the accuracy of that information, with the exception of the first three items in Table 5.1. These items are based directly on the vector components or covariances. Item 4 (duplicate vectors) is also determined from vector components, along with consideration of identical start and stop times (if duplicates are identified by components alone, the number increases from 553 to 854). Using identical time as a criterion assumes the time metadata in the G-file B (session) record is correct. It is known that in some cases the times in the B records are not correct, and this is the issue addressed in item 5. Items 6 to 9 in Table 5.1 are based, at least in part, on session times, as well as reference system codes (item 7) and orbit source (item 8), and both of these are in the G-file B record.

Despite the known errors in session times, it is assumed that the vast majority of time entries are correct. That assumption is made because session times in G-files should be automatically populated by the baseline processor, and time is part of the GNSS data. Nonetheless, in some cases the times may have been populated by other means (particularly in the case of older processing software). It is also possible session times could be in local, rather than GPS time, and in such cases the time offset ranges from 5 to 8 hours for CONUS and may be as many as 12 hours in the Pacific.

The issues in Table 5.1 are discussed in the following nine sections, each numbered the same as in the table. Various types of baseline processing software are mentioned in the discussion; refer to Section 2.3.3 and Appendix E for more information about such software.

5.1.1. Unrealistically short vectors

The NA2011 Project included 53 vectors (0.012%) that are less than 1 m long, as described below. All, with the exception of three, likely do not represent actual processing solutions (i.e., they cannot be "real" vectors).

1) **Vector lengths from 0.0007 to 0.0240 m:** 38 vectors for the same impossible "baseline" from a CORS to itself (GOLDSTONE CORS TOWER), but the two CORSs have different PIDs (AI2694 and AF9649). The vectors were processed in 1998, apparently using a test version of *PAGES* for project GPS1288 (consisting of a total of 3768 vectors). All of these vectors should be rejected or excluded from future adjustments (none are rejected in the NA2011 Project).
2) **Vector lengths from 0.064 to 0.171 m:** 11 vectors, all for various CORSs between their monument and L1 APC (0.064 to 0.171 m), an obvious absurdity. All were processed using *MPGS* software in 1995 in project GPS994 (consisting of a total of 144 vectors). This project also includes a CORS monument-L1 APC pair with a 0.588-m vector. All of these vectors should be rejected or excluded from future adjustments (one is rejected).
3) **Vector length of 0.445 m:** Duplicate pair from an airport runway centerline end point to an adjacent point on the runway. This vector is at least physically possible, and it is assumed to be the shortest "real" vector in the NGSIDB (although it is duplicated). The vector was observed in the 2005 airport control project GPS1761/37 and was processed using Trimble

GPSurvey. One of the duplicates should be rejected or excluded from future adjustments (both are enabled).

4) **Vector length of 0.678 m:** One vector between a boundary monument and an adjacent punch mark, observed in 1993 and processed using Trimble *TRIMVEC* software in project GPS703/B. Although less than 1 m long, this vector appears legitimate.

5.1.2. Baselines with large differences in vector lengths

The NA2011 network consists of 244,543 baselines measured by 424,721 GNSS vectors. A vast majority (99.4%) of baselines determined by two or more vectors consist of vectors with lengths differing from one another by 10 cm or less (after transformation to a common epoch of 2010.00). The 0.6% of baselines with vectors differing in length by more than 10 cm are summarized in Table 5.2. These 1460 baselines are represented by 4613 vectors. Of these, 141 baselines (consisting of 485 vectors) differ by more than 1 m, and two (consisting of six vectors) differ by more than an astonishing 1 km. Such extreme differences are certainly due to the misidentification of vector endpoint marks (i.e., the vectors are not actually on the same baseline), and these vectors should either be assigned to the correct baseline or removed. As might be expected, large differences in vectors for the same baseline results in the non-fitting vectors being rejected. This behavior is shown in Table 5.2 by the high percentage of vectors rejected in baselines that include vectors with large differences in length.

Table 5.2. Baselines with large differences in vector lengths.

Maximum difference in vector lengths	Number of baselines	Percent of baselines	Number of vectors in baselines	Percent of rejected vectors in baselines
> 0.1 m	1460	0.5970%	4613	51.27%
> 1 m	141	0.0577%	485	52.58%
> 10 m	36	0.0147%	139	48.20%
> 100 m	20	0.0082%	59	42.37%
> 1000 m	2	0.0008%	6	33.33%

Since the largest vector length differences in Table 5.2 are likely due to vectors being associated with the wrong baselines, some of the vectors could possibly be restored to the network by identifying the correct baselines. However, the percentage of affected vectors is small, amounting to approximately half of the 4613 vectors in Table 5.2, or about 2300 (0.5%) of the vectors in the NA2011 networks.

5.1.3. Erroneous vector covariances from *Trimble Business Center* software

Trimble Business Center (*TBC*) software was used to process 145 vectors (0.034% of total) in the NA2011 networks. These vectors have erroneous covariances due to a "bug" in the *TBC* G-file exporter for *TBC* versions prior to 2.80 (and prior to version 16.0 of the *TBC* baseline processing

module, which is sometimes the software name given in the G-file B record). The negative sign was stripped from the vector covariance values, so the exported G-file contained all positive covariances, and this is essentially impossible. However, the actual vector covariances in the *TBC* database were correct; the negative signs were lost only in the exported G-file. In September 2012, NGS identified the G-file covariance problem in *TBC* and it was corrected by Trimble on October 9, 2012. The problem no longer occurs for *TBC* version 2.80 (version 16.0 of the baseline processor) or for later versions.

The 145 *TBC* vectors with erroneous covariances were connected to 86 marks in the following two NA2011 GPS projects:

1. **GPS2842 (Spartanburg, South Carolina).** 49 marks connected by 65 TBC vectors observed September to October 2011 and processed by the South Carolina Geodetic Survey. This project included an additional 973 vectors processed by *Trimble Geomatics Office* (which does not have the covariance problem). All of the 49 marks connected to *TBC* vectors were also connected to at least four other non-*TBC* vectors, so the impact on the results for these marks is most likely fairly small. Nonetheless, all *TBC* vectors should be removed or rejected or replaced by vectors with corrected covariances.

2. **GPS2852 (Falls Church, Virginia).** 37 marks connected by 80 *TBC* vectors observed October to November 2011 and processed by KCI Technologies. Four of the marks connected by *TBC* vectors are CORSs, and two marks are connected by other non-*TBC* vectors. Unfortunately, 31 marks are connected only to erroneous *TBC* vectors. As with project GPS2842, all *TBC* vectors should be removed or rejected, but in this case it would cause the 31 *TBC* vector-only marks to become undetermined (i.e., they would have no coordinates). The only option for correcting these 31 marks is to replace the vectors with those that have corrected covariances. The 31 marks connected only by erroneous *TBC* vectors are listed in

3. Table **5.3**. Note the unusually large accuracy values on these marks. It is not known whether these large values are due to the erroneous covariances, but regardless, the vectors should at a minimum be removed or replaced with corrected ones.

In addition to the two projects listed above, the following GPS project with erroneous TBC vectors was loaded in the NGSIDB after the cutoff for the NA2011 Project:

> **GPS2881 (King George County, Virginia).** 38 TBC vectors observed in May 2012 and processed by Geometronics GPS, Inc. Loaded into the NGSIDB in July 2012, constrained to NSRS2007 (not included in the NA2011 Project).

Although not part of the NA2011 networks, GPS2881 is included here for the sake of completeness. As with the other projects, the vectors should either be removed or replaced.

Table 5.3. NA2011 marks in project GPS2852 determined only by erroneous *TBC* vectors.

PID	Desig-nation	Accuracy 95% conf. (cm)		PID	Desig-nation	Accuracy 95% conf. (cm)	
		Horizontal	Ellipsoid ht			Horizontal	Ellipsoid ht
DN5786	FC01	12.04	17.68	DN5802	FC17	32.04	50.27
DN5787	FC02	10.54	16.19	DN5803	FC18	31.39	51.08
DN5788	FC03	12.69	17.25	DN5804	FC19	32.96	51.76
DN5789	FC04	14.04	18.50	DN5805	FC20	33.20	51.72
DN5790	FC05	17.48	20.76	DN5806	FC21	26.36	35.20
DN5791	FC06	33.08	47.12	DN5807	FC22	20.07	25.34
DN5792	FC07	16.38	20.60	DN5808	FC23	21.67	26.60
DN5793	FC08	15.34	19.60	DN5809	FC24	18.49	23.30
DN5794	FC09	16.04	20.03	DN5810	FC25	17.85	21.46
DN5795	FC10	20.71	23.19	DN5811	FC26	15.81	20.05
DN5796	FC11	15.19	19.84	DN5812	FC27	16.08	21.38
DN5797	FC12	15.66	19.80	DN5813	FC28	17.70	22.70
DN5798	FC13	15.90	20.27	DN5814	FC29	15.93	21.93
DN5799	FC14	22.24	31.48	DN5815	FC30	13.98	16.76
DN5800	FC15	34.73	53.63	HV9517	V 1766	17.28	21.27
DN5801	FC16	34.01	52.61				

5.1.4. Duplicate vectors

Duplicate vectors are vectors that are represented more than once in the NA2011 networks. Duplicates were initially identified as vectors with identical components and identical standard deviations (sigmas). Identical components include those of equal but opposite sign (i.e., reversed vectors); five pairs are identical but reversed.

Based on the criterion of identical components and sigmas, there are 854 duplicate vectors in 321 sets ranging from 2 to 21 vectors per set, as shown in Table 5.4. Note that 14.3% of the duplicate vectors were rejected in the final adjustments. All duplicates are in the same G-file as one another.

Even with identical components, a vector cannot truly be a duplicate unless it was based on the same observables (i.e., it has the same start and stop time with the same satellites observed). To account for the common observables requirement, Table 5.4 also shows duplicates based on identical components (and sigmas), as well as identical start and stop times. Based on these more stringent criteria, there are 553 duplicate vectors in 210 sets, and 15.7% of these are rejected.

Table 5.4. Summary of duplicate vectors in the NA2011 networks. Duplicates are identified based on identical components (and sigmas) only on the left half of the table, and by both identical components and start/stop times on the right.

Number duplicate vectors per set	Identical components only				Identical components and start/stop time			
	Number duplicate sets	Number duplicate vectors	Percent duplicate vectors	Percent rejected	Number duplicate sets	Number duplicate vectors	Percent duplicate vectors	Percent rejected
2	257	514	60.2%	13.6%	188	376	67.9%	13.3%
3	22	66	7.7%	9.1%	3	9	1.6%	0.0%
4	21	84	9.8%	4.8%	6	24	4.4%	16.7%
5	4	20	2.3%	25.0%	1	5	0.9%	0.0%
6	4	24	2.8%	0.0%	0	0	0.0%	—
7	6	42	4.9%	66.7%	5	35	6.4%	80.0%
13	1	13	1.5%	100.0%	1	13	2.4%	100.0%
14	5	70	8.2%	20.0%	5	70	12.7%	20.0%
21	1	21	2.5%	100.0%	1	21	3.8%	100.0%
Totals	**321**	**854**	**100.0%**	**14.3%**	**210**	**553**	**100.0%**	**15.7%**

Since vector components and sigmas are stored to the nearest 0.1 mm, it is unlikely they all could be the same for non-duplicate vectors. Nevertheless, it is possible, particularly since the apparent duplicates are measurements of the same baseline. Some of the apparent duplicates that do not have exactly the same start and stop times overlap significantly in time. Such vectors are "partially" duplicated, since they utilize some of the same observations during processing. These partial duplicates (and all true duplicates) are discussed in the trivial (dependent) vector assessment in Section 5.2.

Whether fully or partially duplicate, such vectors introduce false redundancy to the networks—just like trivial vectors. Complete duplicates should be removed, and partial duplicates should either be removed or their false redundancy accounted for (as discussed in Section 5.2). Even if duplicates are identified by identical components only, they amount to only 0.2% of the vectors in the network, so this can hardly be considered a major problem. But trivial vectors (including duplicates overlapping in time) are a different matter; they account for about one third of all vectors in the NA2011 networks, as shown in Table 5.1.

5.1.5. Erroneous or suspect session start and stop date and time

There are 797 vectors in the NA2011 networks with erroneous or suspect date and time information. As Table 5.1 shows, 528 of these have unedited suspect times, and 269 have dates and times that were edited. A more detailed list of the edited values is provided in Table 5.5, along with the years when the problem occurs. Overall, 25% of the problematic values occur for observations before 1990, and 93% are for observations before 2000.

Table 5.5. Erroneous and suspect dates and times in G-file session records

Comment date and time	Number	Before 1990		Before 2000		Earliest year	Latest year
		Number	Percent	Number	Percent		
Edited start date	9	9	100%	9	100%	1986	1986
Edited end date	139	11	8%	82	59%	1989	2009
Edited start and end date	34	1	3%	34	100%	1989	1997
Edited start time	18	15	83%	18	100%	1984	1990
Edited end time	1	1	100%	1	100%	1989	1989
Edited start and end time	68	68	100%	68	100%	1983	1986
Total edited	**269**	**105**	**39%**	**212**	79%		
Time value suspect (not edited)	528	91	17%	527	100%	1983	2000
Total all	**797**	**196**	**25%**	**739**	93%		

Suspect time values are those where the start or end hour was 24 or greater, and/or the start or end minute was 60 or greater. These values were not edited, because they represented times that appeared to be reasonable. For example, a session start date and time of 12/14/1986 57:43 was taken as 57+ hours (2.4 days) later than the midnight which began 12/14/1986, or 12/16/1986 9:43. Likewise, an end date and time of 12/14/1986 67:24 was taken as 12/16/1986 19:24.

Editing of dates and times was kept to a minimum, but it was necessary for some vectors. The reasons for the edits are summarized in Table 5.6. In all cases the edits were done in consideration of the date and times for other adjacent sessions in the G-files.

Table 5.6. Reasons for editing dates and times in G-file session records, and number edited.

Reason for editing vector date and time data	Number edited
Start date and time after end date and time	29
Start date and time same as end date and time	59
End date three weeks to more than one year after start date	128
Hour >= 24 and/or minute >= 60 and mismatch with adjacent G-file records	19
Start and/or end date on day zero of month	34
Total	**269**

5.1.6. Unusually short and long session durations

In addition to the suspect and erroneous session dates and times discussed previously, the NA2011 network includes vectors with questionable durations, both those that appear unusually short or long. Although these unusual durations could have been included in the previous item, they are considered separately, because they are at least technically possible.

Figure 5.1 shows both unusually short and long vector processing session durations on a single plot. The upper horizontal axis is in minutes, and the lower horizontal axis is in days. The vertical axis is the number of vectors in log scale to make both large and small values discernible. The short duration observations range from 1 to 15 minutes, with peaks of 2,449 vectors at 5 minutes and 1182 vectors at 10 minutes. There are 210 vectors with durations between 1 and 3 minutes (note that time is given to the nearest minute in G-files). Although not shown in Figure 5.1, there are an additional 6,688 vectors with durations from 16 to 30 minutes.

For long durations, Figure 5.1 shows vectors with sessions greater than 48 hours. The bar for a duration of 2 days includes vectors with sessions greater than 48 hours and less than or equal to 72 hours; 3 days is for greater than 72 hours and less than or equal to 96 hours, and so on. The number of vectors generally decreases as the session duration increases, with no vectors whatsoever for five- and seven-day durations. There is an increase from 3 vectors for an 8-day duration to 58 vectors for a duration of 9 days. All 58 of these vectors are in a single project (GPS1883) processed using Trimble *GPSurvey*. Sessions of a 9-day duration seem unlikely, but may be possible using that software. The next longest (apparent) session is 26 days, which was classified as erroneous and edited to a more realistic value, as discussed previously.

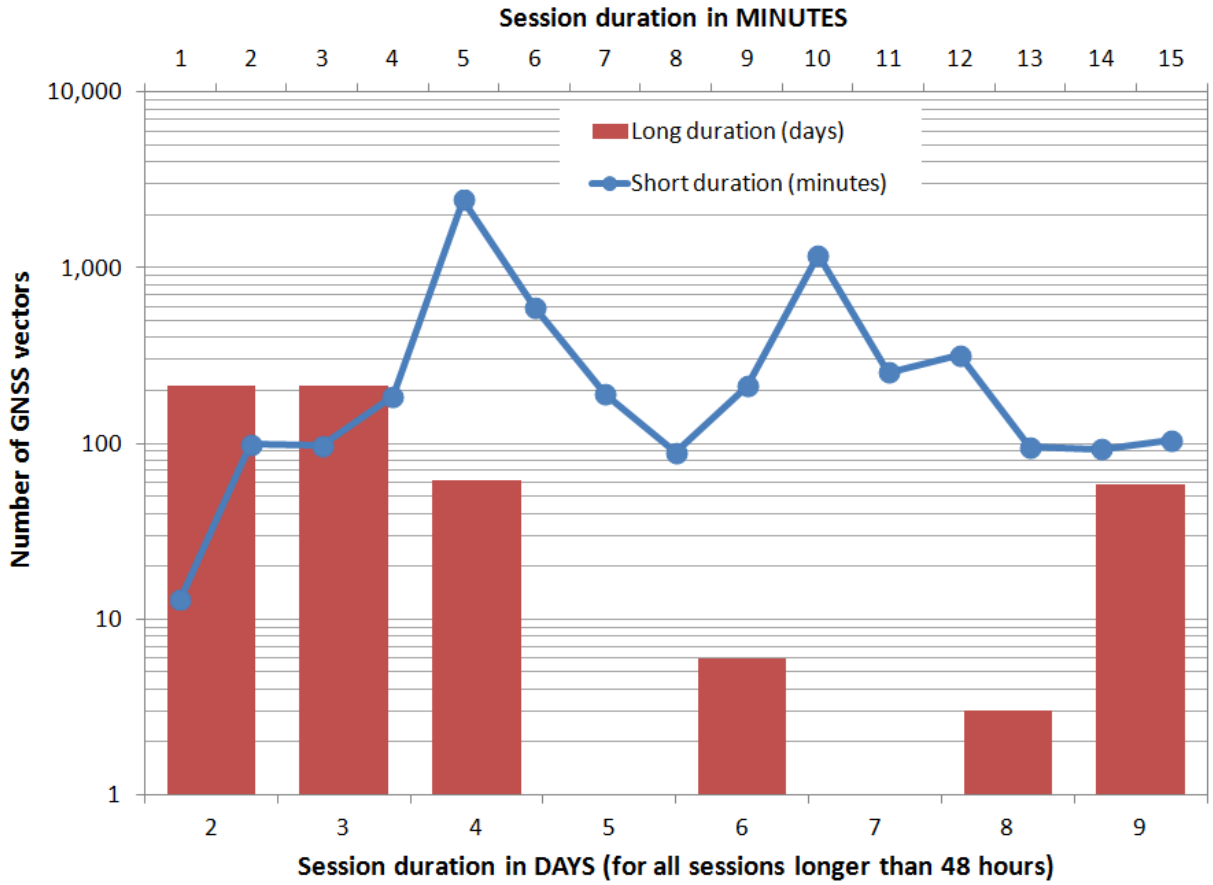

Figure 5.1. Number of GNSS vectors for short and long session durations.

A question arises as to whether the very short durations (15-minute and less) are, in fact, correct, given that errors in dates and times are known to exist in the G-files. While some may well be erroneous, it is unlikely all are incorrect. A one-minute fixed-integer static solution is possible for short baselines, even if not advisable. It is worth noting that test projects were loaded into the NGSIDB, and that some of the projects with very short duration observations may have been experiments rather than efforts to establish geodetic control. Such projects should probably not have been included in NA2011.

Of the 5983 vectors with 15-minute or less sessions, 5975 (99.9%) were processed with commercial software optimized for short-duration occupations (the other 8 vectors were of 14- and 15-minute duration processed with *Omni* software). These 8 vectors are also short, with a median length of 0.9 km, a mean of 1.6 km, and a max of 74.4 km (for a 5-minute session). In contrast, the long-duration (greater than 48-hour) vectors are substantially longer, with a median of 7.3 km, a mean of 80.7 km, and a max of 1771.5 km (for a 69-hour session).

Given the presence of very short session durations, the possibility also exists that some are post-processed (or even real-time) kinematic ("stop-and-go") solutions. There is nothing in the format of G-files used for NA2011 to identify vectors as kinematic, or even to indicate whether processing occurred in real time. Although kinematic solutions are not necessarily problematic, it would be preferable to have such metadata.

5.1.7. Incorrect reference system codes

G-file B (session) records include a code that specifies the reference system of the vector components. Table 2.12 lists the codes, as well as the number of NA2011 network vectors that use each code, and the applicable date range. The codes are intended to provide the reference system of the orbits (ephemerides) used for the baseline processing, and this gives the orientation and scale of the vectors determined in the solutions. However, as discussed in Section 0, a total of 194,170 (45.7%) NA2011 vectors used codes for observations taken later than the code end date, based on the date given in the G-file B record.

Table 5.7 summarizes information in Table 2.12 by grouping reference system codes into five categories. The categories are based on the approximate maximum magnitude of change from the latest reference systems, code 27 and 28 (IGS08 and IGb08, which have identical transformation parameters). The latest used for vectors in NA2011 is code 27. The maximum magnitude of change was computed using the difference in rotation and scale parameters from reference systems 27 and 28, as given in Table 2.13. The resulting parts per million (ppm) differences in Table 5.7 are approximate maximum values, because the full magnitude of the rotation component was used, but the actual magnitude depends in location and will usually be smaller. The scale component is a relatively constant value of about 0.001 to 0.003 ppm for all cases except reference system 1 (WGS 72), which is about 0.2 ppm.

Table 5.7. Reference systems in G-files and approximate maximum difference with IGS08.

Ref sys code	Representative reference system name	Codes used in original G-files		Code used after final date for use of code		Approximate max difference with IGS08
		Number	Percent	Number	Percent	
1	WGS 72	1691	0.40%	296	0.07%	**3 ppm**
2 & 4	WGS 84 (original)	213,712	50.32%	136,580	32.16%	**0.15 ppm**
5 - 11	ITRF 89, ITRF 91, ITRF 92	10,270	2.42%	4,094	0.96%	**0.1 ppm**
12 - 17	ITRF 93, ITRF 94	27,221	6.41%	8,798	2.07%	**0.01 ppm**
18 - 26	ITRF 96, IGS 97, IGS 00, IGS 05	171,515	40.38%	44,402	10.45%	**0.003 ppm**
	Totals	**424,409**	**99.93%**	**194,170**	**45.72%**	

The issue at hand is to determine the magnitude of rotation and the scale errors for vectors that used the incorrect reference system code (as indicated by using it after its final date in Table 2.16). Incorrectly using code 1 (WGS 72) produces the largest error, about 3 ppm (e.g., up to 3 cm error in a 10-km vector). Fortunately, only 296 vectors (0.07%) are incorrectly assigned this code, and 82 (28%) of those are rejected. Of the enabled vectors, 41 are longer than 10 km, and the maximum length is 53.7 km (corresponding to about 16 cm error). The median and mean enabled vector lengths are 6.3 and 8.4 km, respectively.

Of greater concern is the large number of vectors incorrectly assigned reference system codes 2 and 4, corresponding to maximum differences of about 0.15 ppm with respect to IGS08, and Table 5.7 shows that 136,580 vectors (32.2%) fall in that category. An additional 4094 incorrectly assigned codes 5 to 11 have a similar maximum difference with IGS08 of 0.1 ppm, for a total of 140,674 vectors (33.1%) with potential errors of up to 0.15 ppm. This corresponds to a (worst-case) 1.5 cm error for a 100-km vector. The actual rotation error depends not only on location, but on the reference system that should have been used, and in most cases it should not have been IGS08. However, all later reference systems differ from IGS08 by a maximum of 0.01 ppm or less, which is more than an order of magnitude less than that of systems 2 and 4. As a result, and because these calculations are approximate worst-case, it is reasonable to consider the errors with respect IGS08. Moreover, the maximum difference between IGS08 and reference systems 12 through 26 is 0.01 ppm, corresponding to 1 cm for a 1000-km vector. This difference is about an order of magnitude greater than the error due to using a broadcast orbit of 2 m accuracy. Broadcast orbits are discussed in the following section.

In summary, it appears that one third of the NA2011 vectors have reference systems that differ from the correct reference system by up to about 0.15 ppm. The difference is a systematic error of the orientation and scale of the vector components used in the adjustments. Both *ADJUST* and *NETSTAT* programs use the reference system codes in the G-files to transform the vectors to

the NAD 83 frame, and the transformations will be in error by the same amount. For the NA2011 Project, all vectors were transformed using *HTDP* to NAD 83 (2011) epoch 2010.00 before adjustment. The same systematic errors occur with the *HTDP* transformations, as it uses the G-file reference system codes and the same (or very similar) transformation parameters as *ADJUST* and *NETSTAT*.

The simplest solution for this problem in future adjustments would be to correct the G-file reference system codes based on the dates in the G-files and the known (or assumed) orbit reference system used. Such an approach is not a perfect solution, however, due to the uncertainty of the actual reference systems used, but this would likely reduce the errors for a large majority of incorrect G-file codes by an order of magnitude or more.

5.1.8. Broadcast orbits

In addition to reference system codes, G-files also have a B (session) record field that gives the orbit (ephemeris) source. As stated in Section 0, the G-file records indicate broadcast orbits were used for nearly half of all vectors in the NA2011 Project—201,878 (46.5%). Although there is some question as to the accuracy of G-file metadata, this is nonetheless a large percentage.

The distribution by year of vectors with broadcast orbits is shown in Figure 5.2. The peak percentage (93%) of vectors with broadcast orbits was in 1988, and the proportion of vectors with broadcast orbits has more-or-less steadily declined since then. Also plotted in Figure 5.2 is the mean and median length of vectors with broadcast orbits. The mean for all broadcast is 7.2 km, substantially lower than the mean of 33.7 km for all vectors (Table 2.10 and Figure 2.10). The median vector length is 4.8 km, also significantly lower than the median of 7.8 km for all vectors. The smaller difference between mean and median lengths indicates less variability in length for broadcast orbits than for all vectors.

Are broadcast orbits a problem? A conservative "rule of thumb" for the impact on baseline solution accuracy is about 50 parts per billion (ppb) of the ephemeris error (Leick *et al.*, 2015, p. 312). When GPS selective availability (SA) was turned off by order of President Clinton at midnight UTC on May 1, 2000 (epoch 2000.3333), broadcast orbit accuracy improved from about 100 m to about 5 m. For a 10 km baseline, an error of 100 m in the ephemeris causes about $100 \times 50 \times 10^{-9} \times 10{,}000 = 0.05$ m error in the computed vector, decreasing to about 0.0025 m when SA was turned off. Broadcast orbit accuracy has been improving ever since, and the orbits now typically have a weighted RMS of about 1 m (IGS, 2019). A 1-m orbit error contributes about 0.005 m error to a 100-km vector.

As shown in Figure 5.2, the median and mean vector lengths associated with broadcast orbits are less than 10 km for every year after 1986. Moreover, prior to turning off SA, only 1% of the vectors are longer than 38 km, and 0.1% are longer than 84 km. Thus, only a small percentage of vectors are long enough to be significantly impacted by ephemeris errors due to using broadcast orbits when SA was on (assuming the broadcast orbit metadata are correct). It should also be noted that other processing techniques (such as orbital relaxation) were used in the early

years of GPS baseline processing, so the errors may be considerably less than implied by broadcast orbits accuracies when SA was on.

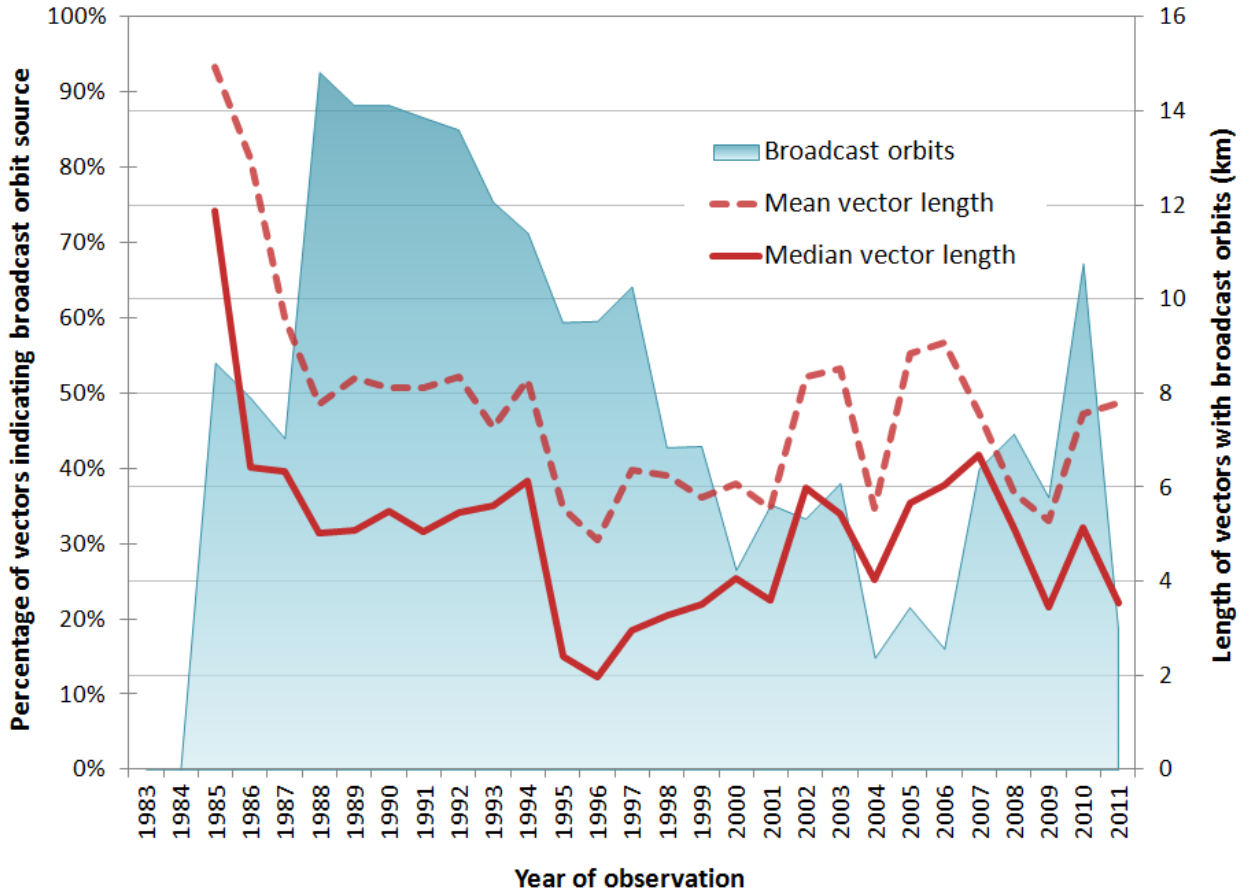

Figure 5.2. Percentage and mean length of vectors with broadcast orbit by year of observation.

Table 5.8 summarizes the estimated error of broadcast orbits both before and after SA was turned off. The maximum vector length is 244 km for SA on and 241 km for SA off. The estimated error of the vectors was computed using 0.05 ppm of ephemeris error, where ephemeris error of 100 m was used with SA on and 3 m with SA off. Although 31.4% of vectors are (apparently) based on broadcast orbits when SA was on, only 2.1% of those are longer than 20 km. And of those longer than 20 km, 41% were rejected in the NA2011 networks, and 14% of vectors 10 to 20 km long were rejected. For vectors based on broadcast orbits after SA was turned off, the vector error due to ephemeris error is more than 3 cm for only 5 vectors (0.001%).

Table 5.8. Estimated vector error due to use of broadcast orbits, with SA on and off (based on assumed orbit uncertainty of 100 m with SA on and 3 m with SA off)

Vector length range (km)	SA on (observed before May 2, 2000, 0:00 UTC)				SA off (observed after May 2, 2000, 0:00 UTC)			
	Number vectors	Percent of all 424,721 vectors	Apprx vector error due to 100 m orbit error (m)	Percent rejected	Number vectors	Percent of all 424,721 vectors	Apprx vector error due to 3 m orbit error (m)	Percent rejected
0 - 5	70,166	16.520%	0.000 - 0.025	2.1%	34,098	8.028%	0.000 - 0.001	0.7%
5 - 10	31,436	7.402%	0.025 - 0.05	6.1%	19,859	4.676%	0.001 - 0.002	1.5%
10 - 20	23,233	5.470%	0.05 - 0.10	14.5%	11,065	2.605%	0.002 - 0.003	2.7%
20 - 50	8,240	1.940%	0.10 - 0.25	40.7%	2,912	0.686%	0.003 - 0.008	6.0%
50 - 100	392	0.092%	0.25 - 0.50	49.0%	267	0.063%	0.008 - 0.015	22.5%
100 - 200	69	0.016%	0.50 - 1.00	36.2%	125	0.029%	0.015 - 0.030	43.2%
200 - 250	11	0.003%	1.00 - 1.25	36.4%	5	0.001%	0.030 - 0.038	0.0%
Total	**133,547**	**31.443%**			**68,331**	**16.088%**		

Unlike correcting reference system codes as discussed in the previous item, there is no way to correct for low-accuracy orbits in processed vectors. The only way to reduce the error is to reprocess the GNSS observables with more accurate orbits. If reprocessing cannot be done, another alternative is to downweight vectors derived from broadcast orbits. This could be done by applying the rule of thumb of 0.05 ppm of the ephemeris error to the vector uncertainties.

5.1.9. Trivial (dependent) and repeated vectors

Trivial (dependent) vectors introduce false redundancy to GNSS networks. Although this problem is well-known and has been extensively documented (e.g., Craymer and Beck, 1992; Han and Rizos, 1995; Øvstedal, 2000), trivial vectors often exist in control networks, including the NA2011 networks. In sequential (one-vector-at-a-time) GNSS baseline processing of data from three or more simultaneously occupied marks, it is possible for the number of solved vectors to equal or exceed the number of marks. Specifically, if there are n marks (GNSS receivers) in a session, then a total of $n(n-1)/2$ vectors are possible. However, only $n-1$ of these vectors are truly independent, and the remainder are to some extent linear combinations of the independent vectors. These additional dependent vectors are termed "trivial," because they are based on (nearly) the same GNSS observables as the independent vectors, therefore their presence essentially means the same data are used more than once. The reason for differences in observations is that each receiver is at a different location and is subject to different environmental factors, such as multipath, obstructions, and atmospheric conditions, as well as a somewhat different view of the satellite constellation. In addition, the receivers usually have different start and stop times (unless the data files are trimmed to exactly match). Despite these variations, there is significant redundancy in the observations, and to treat them as if they are independent causes overly-optimistic accuracy estimates, among other potential problems.

Despite the false redundancy problem with trivial vectors, they do contain useful information about the correlation between vectors. Simultaneous baseline processing can account for the intervector correlations and does not create trivial vectors. But, as shown in Table 2.9, only 20.7% of the vectors in the NA2011 networks were processed simultaneously; the other 79.3% were processed sequentially. In sequential baseline processing, each vector is processed in isolation, and if a session is limited to the independent vectors, then all of the intervector information is lost. If all possible vectors are included, then the intervector correlations are captured. With this point of view, using all possible sequentially processed vectors is desirable—if the false redundancy can be appropriately accounted for.

The method used to identify trivial vectors, and a discussion of their impact on the NA2011 networks, is discussed in the next section.

5.2. Determining the presence and impact of trivial vectors

5.2.1. Defining GNSS processing sessions

The goal of the following discussion is to identify the presence of trivial vectors in the NA2011 networks. Identifying trivial vectors first requires identifying GNSS observation sessions**. For that purpose, a session is defined as a group of one or more vectors with observations that are temporally and spatially correlated**—that is, they overlap in time and space. Here a "group" of one vector constitutes a session only if it was indeed observed by itself. This definition applies whether the vectors were processed simultaneously or sequentially. Indeed, it will be shown that a large majority of multi-vector sessions consist entirely or partially of sequentially processed vectors. Note that a "session" as defined here can span multiple GPS projects. If two GNSS receivers are in the field during times that overlap with one another, and each receiving signals from at least one common satellite, the observations at those two receivers *are* correlated, even if they were participating in separate GPS projects.

In a G-file, a session is a group of one or more vectors associated with a session (B) record. By this definition, the number of sessions equals the number of B-records, and this indicates there are 350,182 "sessions" in the NA2011 networks (see Table 2.9). The simultaneously processed sessions (with two or more vectors) account for only 13,542 sessions (3.9% of total). The vast majority—336,640 (96.1%)—consist of a single sequentially processed vector. And each of these is considered a "session" with no regard as to whether any were observed at the same time and in the same area as others.

A reasonable initial assumption is that all sessions exist within individual GPS projects, since projects nominally represent a single field campaign. However, it is known that sessions get split across GPS projects, because many GPS projects have multiple "parts." Each of these part was treated as an individual GPS project for the NA2011 Project (as it was for the 2007 national adjustment). GPS project parts have the same project base number (and are usually in the same geographic areas and performed at roughly the same time), but have an additional part number as a project ID suffix. In many cases the project parts also overlap in time. For example, project GPS1526 has 23 parts (GPS1526/1, GPS1526/2, GPS1526/3, etc.) in four separate state block G-files (one in Wisconsin and three in Minnesota). Of the 23 parts, 12 have observations in all four

G-files that overlap in time by 94% to 100%, and their project part centroids are 18 to 136 km apart. These 12 project parts form six session pairs (i.e., they overlap in time by a significant amount), of which four are split across different G-files. In such cases it makes sense to consider the time overlaps as common sessions. A total of 296 project base numbers are split into 2779 parts in the NA2011 networks. The number of parts per project base number range from 2 to 448, with a median of 2 and a mean of 9.4.

Because a single session can span multiple GPS projects, determining the presence of trivial vectors requires evaluating all GNSS vectors, regardless of the GPS project in which they occur. That task is not simple, and to accomplish requires various approximations and somewhat arbitrary decisions, as described over the next several pages. The intent is to show that the criteria established for determining sessions is nonetheless reasonable, within the context of the data used for the NA2011 Project. Later refinements are certainly possible, but that is beyond the scope of this report, and it depends on whether and how trivial vectors will be handled by NGS in the future.

Given that time overlap is required for vectors to be in a common session, a logical criterion could be based on how much the observations overlap in time. A time overlap of only 1% seems much too short, but requiring 100% overlaps seems excessive. Fortunately, the time overlap assessment is simplified for the NA2011 networks because of the vectors observations that overlap at all, a large majority overlap by more than 90%. The time overlap for all observations (regardless of spatial separation) is shown in Table 5.9 for various minimum overlap criteria. When no minimum overlap is specified, the minimum is only 0.06% overlap—very little overlap indeed. However, even for this case the mean overlap is 93.98%, and the median is 100.00% for all cases.

Table 5.9. Time overlap of all GNSS vector observations for various minimum overlap criteria.

Minimum time overlap criterion	0%	25%	50%	75%	100%
Minimum	0.06%	25.00%	50.00%	75.00%	100.00%
Maximum	100.00%	100.00%	100.00%	100.00%	100.00%
Median	100.00%	100.00%	100.00%	100.00%	100.00%
Mean	93.98%	95.88%	97.45%	98.66%	100.00%
Standard deviation	±17.30%	±12.15%	±7.56%	±3.77%	±0.00%
Resulting number of sessions	**25,961**	**35,082**	**45,340**	**58,248**	**144,750**
Percent of all vectors grouped in sessions	93.89%	91.74%	89.32%	86.29%	65.92%

Table 5.9 also gives the number of sessions generated with each minimum time overlap criterion, ranging from 25,961 to 144,750 sessions for 0% to 100% minimum overlap. A lower minimum overlap decreases the number of sessions, because it allows the grouping of more vectors into separate sessions. For a minimum required overlap of zero (i.e., end time greater than or equal to start time of vector pairs), 93.89% of all vectors are grouped into multi-vector sessions, versus 65.92% of vectors when 100% overlap is required to create a session. Compare this to the G-file

definition of a session, where there are a total of 350,182 "sessions," and only 20.7% of the vectors are grouped into multi-vector sessions (see Table 2.9).

A minimum time overlap of 50% was selected as the time criterion for determining whether vectors could be grouped into a common session, corresponding to 45,340 sessions in Table 5.9. This criterion means that the baseline solution for a vector is taken as correlated with at least one other vector if they "share" observables during at least half of the processing duration between receiver pairs forming the baselines. Likewise, they are considered uncorrelated if they share observables for less than half the processing duration. This binary criterion is admittedly arbitrary, but it is reasonable in this context because a large majority of time overlap exceeds 90%. A more refined approach could be pursued, for example by applying the percent of overlap to the correlation, rather than simply having it be "on" or "off." Such a consideration is left for later work and is outside the scope of this report. In addition, the question of spatial correlation must also be addressed.

Although a time criterion alone is likely appropriate for determining vector sessions within individual GPS projects, it is not sufficient by itself for vectors in separate projects. In such cases an additional criterion is needed to takes into account the spatial separation of vectors. For example, Washington D.C. project GPS1865 has a session that overlaps in time by 99.5% with a session in Saipan project GPS1837/A. The median vector length is 24 km for GPS1865 and 6 km for GPS1837/A. But the project centroids are about 12,600 km apart. In such cases, the vectors are processed using observables from almost entirely different parts of the satellite constellation, so the observations will be essentially uncorrelated, and therefore it is not reasonable to combine these vectors into a single common session. Similar inappropriate session groupings occur for projects in the Alaska and CONUS networks, the Alaska and Pacific networks, and widely separated projects in the CONUS networks (both within and between the CONUS Primary and Secondary networks). However, "nearby" projects can and do occur, and if they are observing the same GNSS satellites (likely if they are "near" one another), then they should be grouped into a common session, if some chosen "distance criterion" is met.

Using a distance criterion for evaluating session groupings across projects can be difficult, because individual projects vary widely in spatial extent, number of vectors, and vector length. Of the 4267 GPS projects used, 1698 (39.8%) consist entirely of vectors less than 10 km in length, whereas 712 (16.7%) include vectors that differ in lengths by more than 100 km. In addition, as shown in Table 2.3, the number of vectors in GPS projects range from 1 to 15,589.

To account for the variation in distance between GPS projects, a spatial separation metric was computed as the ratio of the length of vectors in a project pair to the distance between the projects. The mean of the GPS project median vector lengths was used as a representative vector length for a project pair (the median was used because it is less sensitive to extreme values). Distance between projects was taken as the distance between project centroids (determined previously for the map of project locations in Figure 2.3). Plots of the number of sessions as a function of minimum time overlap are shown in Figure 5.3, as a family of six curves for various length-to-distance ratios. The top curve is for the case where the ratio is 100%, i.e., the median vector length of the project pair being evaluated is equal to or greater than the distance between

project centroids. The next curve below that is for a median vector length of at least one-quarter (25%) of the distance between projects, and so on. The bottom curve is for the case where all vectors are considered based on time overlap, regardless of distance (note that this curve corresponds to 58,248 sessions for a time overlap of 75%, as shown in Table 5.9). For a distance ratio greater than 5%, the number of sessions is not strongly correlated with time overlap for a minimum time overlap criterion of less than about 70%. However, the number of sessions rapidly increases when the minimum required time overlap exceeds about 80% for all length-to-distance ratios.

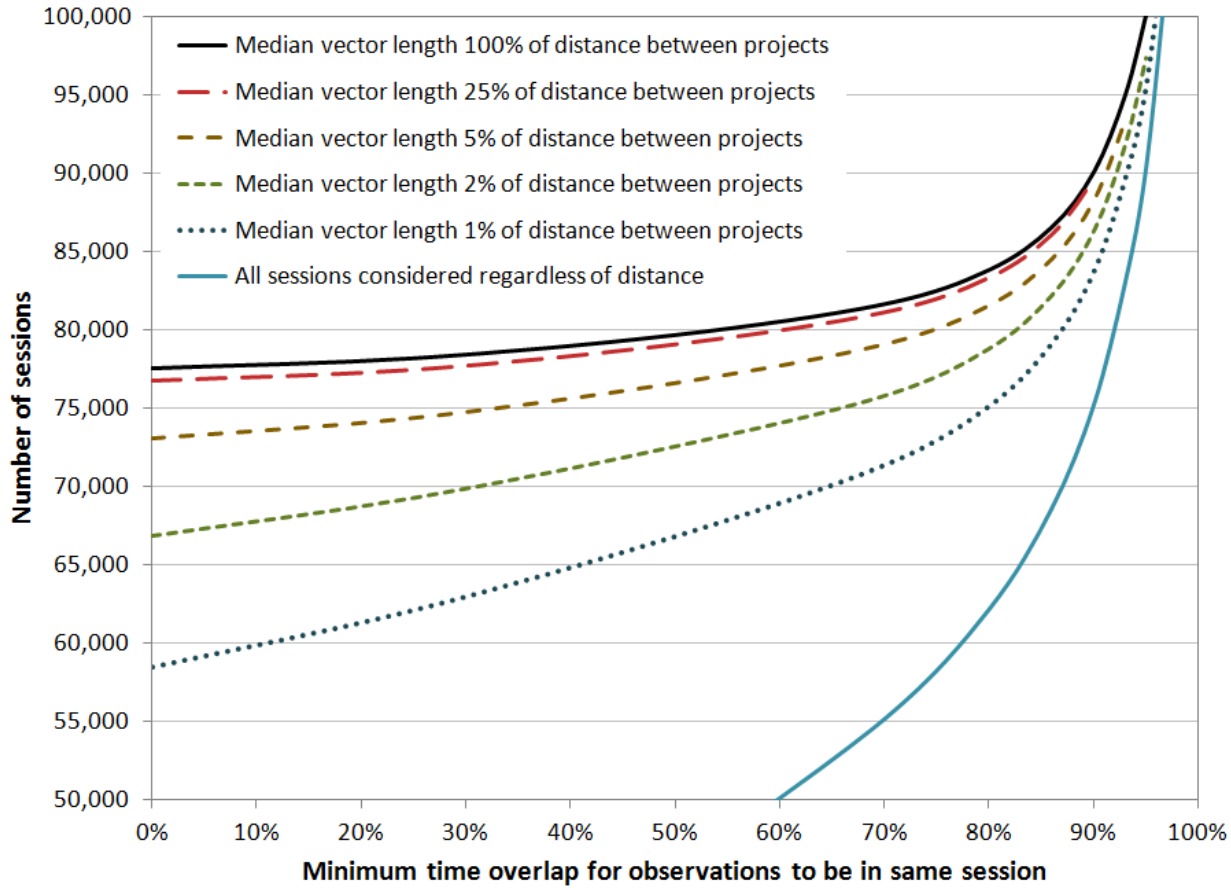

Figure 5.3. Number of sessions based on time overlap and distance between GPS projects.

Figure 5.3 also shows that the spacing between curves becomes closer as the length-to-distance ratio approaches 100%. This means the number of sessions becomes insensitive to distance as the median vector length approaches the distance between projects. Still, it is not entirely clear what length-to-distance ratio should be used as a criterion for defining sessions. The main

objective is to group as many vectors as possible into sessions that overlap in time, while avoiding inappropriate groupings of widely separated vectors.

To arrive at an estimate of a spatial separation criterion, the spatial separation between GPS projects in the four separate networks was evaluated (CONUS Primary, CONUS Secondary, Alaska, and Pacific). A plot for this evaluation is shown in Figure 5.4 for a minimum time overlap of 50%, as the number of vector pairs from separate projects assigned to common sessions for various vector length-to-project-distance ratios. The plot is divided into a portion showing groupings of project sessions within the same network; grouping between CONUS Primary and Secondary networks; and groupings between CONUS, Alaska, and Pacific projects. One reason for splitting by network is that they were adjusted separately. Another reason is that the CONUS, Alaska, and Pacific networks are widely separated in space and therefore could provide a reasonable threshold for a spatial separation criterion, at least initially.

The three combined categories in the upper plot of Figure 5.4 shows the cumulative number of vectors from all separate GPS projects grouped into sessions, regardless of location. The lower plot is a detail of the upper plot to more clearly show session pairs from different networks that are grouped into common sessions.

For a length-to-distance ratio of 5%, a total of 3,683 vector pairs from different projects are grouped into common session (beyond the maximum of 3000 vector pairs on the vertical axis). The number of vector pairs decreases to 1201 at a distance ratio of 25%. A distance ratio of 23% is the smallest that prevents forming sessions between vector pairs in the CONUS, Alaska, and Pacific networks. Also at the 23% to 25% distance ratio, groupings occur for 61 vector pairs for projects in the CONUS Primary and Secondary networks.

Based on this assessment of grouping vector pairs by projects, a vector length-to-project-distance ratio of 25% was selected (along with a minimum 50% time overlap). That is, vector pairs in separate GPS projects will be grouped into a common session if the distance between two projects is no more than 4 times their median vector length. Like the 50% time overlap criterion, the 25% distance ratio is binary and somewhat arbitrary. But also like the time overlap criterion, the 25% distance ratio criterion captures a vast majority of the possible vector pairs (as will be will be discussed below). Together, the time and distance criteria correspond to 79,076 sessions, as shown by the curve in Figure 5.3 for a 25% length-to-distance ratio at 50% time overlap.

A problem with using the length-to-distance ratio described above is that it can exclude sessions with very short vectors in separate projects when the projects (and hence the vectors) are still fairly close together (as mentioned previously, about 40% of the GPS projects consist entirely of vectors less than 10 km in length). To reduce the problem of excluding nearby vectors, any sessions in projects less than 100 km apart were grouped into common sessions if they met the time overlap criterion, regardless of the distance ratio. For a 50% time overlap, applying this 100-km inclusion buffer reduced the number of sessions by 891 (from 79,076 to 78,185).

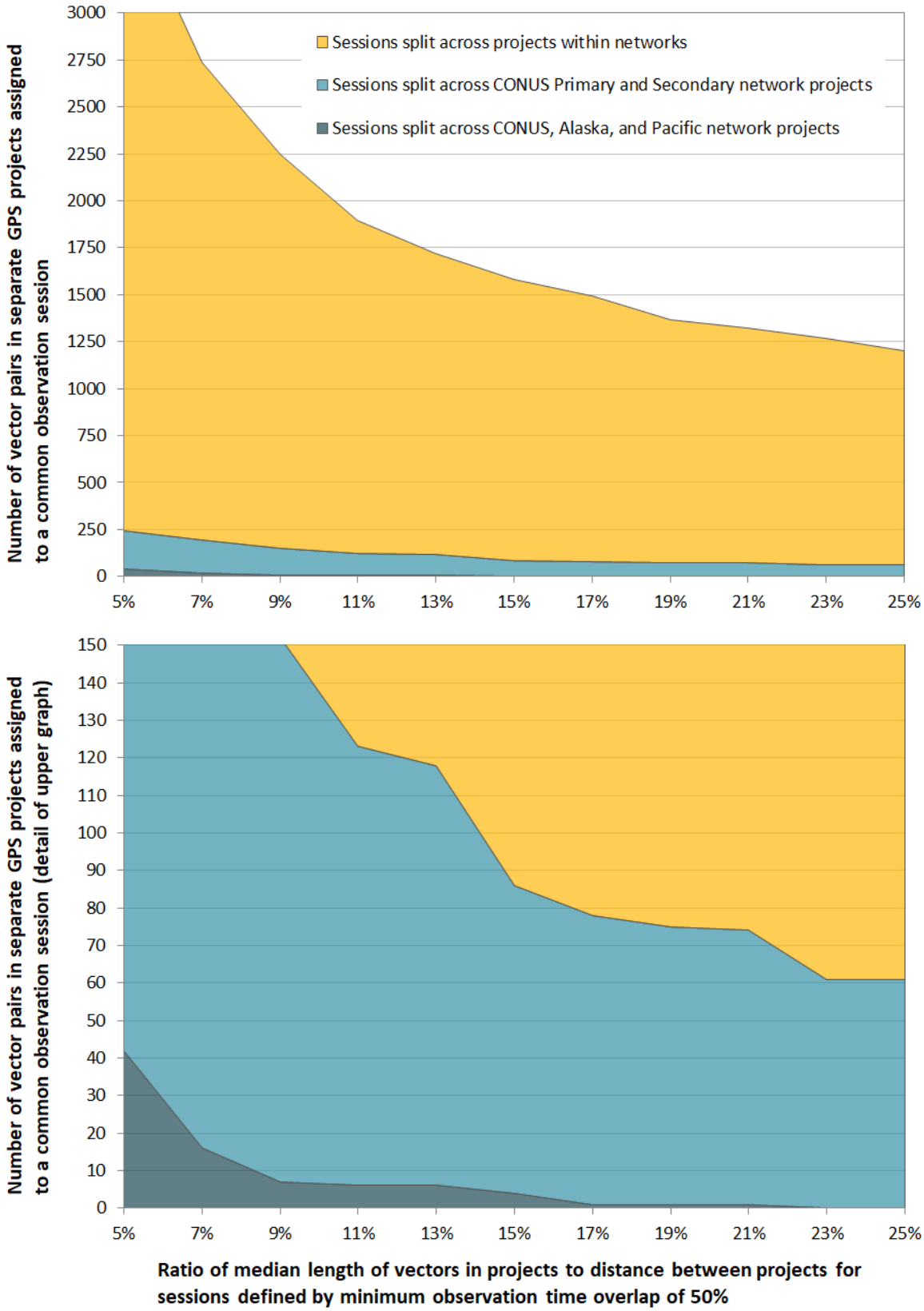

Figure 5.4. Number of vector pairs in separate GPS projects assigned to common observation sessions (lower graph is a detail of upper graph showing pairs in different networks assigned to common sessions).

A summary of the final set of observation sessions is provided in Table 5.10 and is based on a minimum 50% time overlap and 25% vector length-to-project distance ratio. In addition, any sessions in separate projects less than 100 km apart are grouped into sessions with other vectors, if they meet the minimum overlap time criterion of 50%. This approach resulted in a total of 78,185 sessions, with 18,108 being single-vector and 60,077 being multi-vector sessions. The difference with a G-file-based definition of sessions is striking. As shown in Table 2.9, the G-file B records indicate there are 350,182 sessions, with 336,640 being single- and 13,542 being multi-vector. The B record count gives 2.42 times as many sessions than even the most conservative estimate: 144,750 sessions corresponding to 100% time overlap with spatial separation ignored (see Table 5.9). The number of sessions decreases to 45,340 for 50% time overlap, and increases to 78,185 when the spatial separation criteria described above are applied. Although the method used here for defining correlated sessions is by no means perfect, it is unquestionably more realistic than counting G-file B records. The number of sessions *must* fall between 25,961 and 144,750 for a time overlap range of 0% to 100%. Estimating where within that range was the goal of the approach used here. Refinements are certainly possible, for example by using the maximum of 144,750 sessions and scaling the correlation by percent of time separation and distance. Such work is left for future investigations.

Table 5.10. Number of derived GNSS observation sessions by network in the NA2011 Project (based on 50% time overlap and 25% vector length-to-project distance ratio criteria, plus grouping of inter-project vectors with project centroids less than 100 km apart).

	All	CONUS All	CONUS Primary only	CONUS Secondary only	CONUS Primary & Secondary	Alaska	Pacific
Number of sessions							
Single-vector	18,108	17,624	14,662	2,962	0	307	177
Multi-vector	60,077	59,220	44,258	14,887	75	593	264
Total	**78,185**	**76,844**	**58,920**	**17,849**	**75**	**900**	**441**
Number of vectors							
Sequential	336,640	333,984	263,462	70,104	418	1,473	1,183
Simultaneous	88,081	86,039	71,757	13,890	392	1,373	669
Total	**424,721**	**420,023**	**335,219**	**83,994**	**810**	**2,846**	**1,852**
Vectors per session	5.43	5.47	5.69	4.71	10.80	3.16	4.20

Note that the CONUS network in Table 5.10 includes a session category for both Primary and Secondary. The 75 sessions in this category consist of 810 vectors, with 311 of those in the Primary network and 499 in the Secondary network. These occurred because of temporal and spatial overlap in the two networks.

Earlier in this section it was stated that a reasonable initial assumption for determining sessions is that all their vectors would occur within individual projects. Table 5.11 shows this assumption is largely correct: 98.0% of sessions (consisting of 96.3% of all vectors) do *not* span multiple GPS projects. Considerable effort was expended in determining the remaining 2.0% of sessions. However, such analysis was unavoidable since the number of sessions spanning multiple projects was not known in advance. Although 2.0% is a small percentage, it corresponds to 1560 sessions, consisting of 15,817 vectors (3.7% of all vectors).

Table 5.11. Distribution of sessions and vectors by the number of GPS projects per session.

Number GPS projects per session	Sessions		Vectors	
	Number	Percent	Number	Percent
1	76,625	98.005%	408,904	96.276%
2	1,413	1.807%	13,851	3.261%
3	88	0.113%	1,176	0.277%
4	24	0.031%	319	0.075%
5	13	0.017%	145	0.034%
6	15	0.019%	218	0.051%
7	7	0.009%	108	0.025%
Total	**78,185**	**100.000%**	**424,721**	**100.000%**

The small percentage of sessions spanning multiple GPS projects demonstrates that a more refined method than used here for determining such sessions may be difficult to justify. However, a more refined approach might be warranted if NGS elects to account for the presence of trivial vectors in the future. That would be even more important if NGS abandons grouping vectors by GPS project in the future, which is a possibility.

The distribution of vector processing within the 78,185 sessions is provided in Table 5.12, showing both the number (and percentage) of sessions and vectors. Multi-vector sequentially processed sessions constitute 62% of sessions (and 74% of vectors), and such sessions may include trivial vectors. Also, sessions do not necessarily consist of one type of processing; 2.8% of sessions include both sequentially and simultaneously processed vectors, and 1.0% include more than one set of simultaneously processed vectors.

The number of sessions per day is provided in Table 5.13, along with the number of vectors per session (as total, sequential, and simultaneous per session). The maximum number of vectors per session is 230. Interestingly, this number corresponds to sequential rather than simultaneous processing. There are two sequentially processed sessions consisting of 230 vectors, and later it will be shown that nearly all possible vectors were processed in these two (and many other) sessions. As mentioned previously, such processing creates statistically dependent ("trivial") vectors that introduce false redundancy, and this can cause unrealistically optimistic uncertainty

estimates and can affect computed coordinate. For these two sessions, there are 22 simultaneously occupied marks, and 209 of the 230 vectors are trivial.

Table 5.12. Number and percentage of GNSS sessions and vectors for different processing types.

Vectors per session	Processing solution type in session	Sessions		Vectors	
		Number	Percent	Number	Percent
One	Sequential	18,108	23.2%	18,108	4.3%
Multiple	All sequential	48,518	62.1%	313,129	73.7%
Multiple	All simultaneous	8,529	10.9%	59,359	14.0%
Multiple	Both sequential and simultaneous	2,217	2.8%	19,722	4.6%
Multiple	Two or more simultaneous sets	813	1.0%	14,403	3.4%
	Totals	**78,185**	**100.0%**	**424,721**	**100.0%**

Table 5.13. Statistics of GNSS vectors, sessions, and baselines in the NA2011 Project.

	Number sessions per day	Total number vectors per session	Sequential vectors per session	Simultaneous vectors per session	Number vectors simultaneously processed
Min	1	1	1	2	2
Max	74	230	230	193	186
Mean	10.11	5.43	4.89	7.62	6.77
Std dev	±8.91	±7.37	±6.41	±10.75	±8.41
Percentiles					
1%	1	1	1	2	2
5%	1	1	1	2	2
50%	8	3	3	4	4
95%	28	15	15	24	21
99%	41	36	36	42.42	34
Number of sessions		78,185	68,843	11,559	
Number of vectors		424,721	336,640	88,081	

Table 5.13 shows there are a maximum of 193 vectors in simultaneously processed sessions, but it also shows there is a maximum of 186 vectors that were simultaneously processed in a session. The reason for the difference is that some sessions consisted of two or more sets of simultaneously processed vectors (813 sessions are of this type, as shown in Table 5.12). In other words, in these cases all vectors were processed simultaneously, but not all were processed together in a single processing session. For the maximum of 193 vectors in simultaneously processed sessions, the vectors were processed in two separate simultaneous sessions, one

consisting of seven vectors and the other of 186 vectors (where the 186-vector session is the largest simultaneous session in the NA2011 project, as mentioned previously).

Statistics for the number of marks per session are shown in Table 5.14 for the various GNSS processing types. Although overall there is a large range in the number of marks per session (from 2 to 194), the mean and median number of marks per session are only 4.7 and 4, respectively. Sessions with only a single vector are obviously limited to two marks, and there can be no trivial vectors. Similarly, sessions where all vectors are processed simultaneously cannot include trivial vectors. However, a majority of sessions (48,518 or 62% of all sessions) include multiple vectors that were processed sequentially, and the number of marks in these sessions range from 3 to 80. Such sessions are the ones most likely to include trivial vectors. That determination is the topic of the next section.

Table 5.14. Statistics for number of marks per session for different GNSS processing session types.

	Number marks per session for all processing types	Single vector per session (sequential)	All vectors processed sequentially	All vectors processed simultaneously	Both sequential and simultaneous	Two or more simultaneous sets
Min	2	2	3	3	3	3
Max	194	2	80	180	121	194
Mean	4.67	2.00	4.68	7.96	8.99	16.92
Std dev	±4.81	±0.00	±2.23	±7.76	±8.01	±25.53
Percentiles						
1%	2	2	3	3	4	4
5%	2	2	3	3	4	5
50%	4	2	4	5	6	9
95%	10	2	9	23	23	77
99%	22	2	13	34.7	42.8	164.5
Total sessions	**78,185**	**18,108**	**48,518**	**8,529**	**2,217**	**813**

5.2.2. Identifying trivial and repeat vectors in GNSS sessions

Trivial vectors occur in sequentially processed sessions with three or more marks when the number of vectors is equal to or greater than the number of marks (receivers). In addition to trivial vectors, false redundancy can also be introduced to a session in baselines represented by more than one vector overlapping in time (including duplicate vectors discussed previously, if they also overlap in time). As with defining sessions, defining a repeated baseline within a session is to some degree arbitrary. In this report, a vector is repeated if data for a single baseline are processed to yield more than one vector solution for that session and the data overlaps in time by at least 50%. The 50% time overlap criterion is consistent with that used for defining sessions.

The 78,185 sessions determined for the NA2011 Project were evaluated for the presence of trivial and repeated vectors, and the results are summarized in Table 5.15 (by sessions) and Table 5.16 (by vectors). Both tables show the repeated baseline and trivial vector counts, as well as their sum, which is categorized as the total count of redundant vectors. Both tables also categorize the number of sessions and vectors by the session processing type. The 18,108 sessions consisting of a single vector obviously cannot have redundant vectors. In addition, the 8529 sessions where all vectors were processed simultaneously as a single set (consisting of 59,359 vectors) also cannot include redundant vectors. Table 5.16 shows that most vector redundancy is due to trivial, rather than repeated, vectors: 137,449 of the 141,901 redundant vectors (96.8%) are trivial vectors. This is particularly the case for the 48,518 sessions (consisting of 313,129 vectors) processed entirely sequentially. For that processing type, of the 137,787 redundant vectors in 28,136 sessions, 134,968 (98.0%) are trivial vectors.

Table 5.15. Sessions with repeat baselines and trivial (dependent) vectors by session processing type.

Session processing type	Total number of sessions	With repeat vectors		With trivial vectors		With redundant vectors (both repeat and trivial)	
		Number	Percent	Number	Percent	Number	Percent
Single vector (sequential)	18,108	0	0.00%	0	0.00%	0	0.00%
All simultaneous	8,529	0	0.00%	0	0.00%	0	0.00%
All sequential	48,518	785	1.62%	27,560	56.80%	28,136	57.99%
Sequential and simultaneous	2,217	251	11.32%	370	16.69%	568	25.62%
Two or more simultaneous sets	813	123	15.13%	223	27.43%	310	38.13%
Total sessions	**78,185**	**1,159**	**1.48%**	**28,153**	**36.01%**	**29,014**	**37.11%**

Table 5.16. Vectors with repeat baselines and trivial (dependent) vectors by session processing type.

Session processing type	Total number of vectors	Repeat vectors		Trivial vectors		Redundant vectors (sum of repeat and trivial)	
		Number	Percent	Number	Percent	Number	Percent
Single vector (sequential)	18,108	0	0.00%	0	0.00%	0	0.00%
All simultaneous	59,359	0	0.00%	0	0.00%	0	0.00%
All sequential	313,129	2,819	0.90%	134,968	43.10%	137,787	44.00%
Sequential and simultaneous	19,722	724	3.67%	1,683	8.53%	2,407	12.20%
Two or more simultaneous sets	14,403	909	6.31%	798	5.54%	1,707	11.85%
Total vectors	**424,721**	**4,452**	**1.05%**	**137,449**	**32.36%**	**141,901**	**33.41%**

Table 5.17 provides statistics for the 29,014 sessions containing redundant (both repeat and trivial) vectors (i.e., it excludes the 49,171 sessions containing no redundant vectors). Of these sessions, 1,175 include up to 69 repeated baselines per session, with a median and mean of 2 and 3.25 per session, respectively. The maximum of 69 repeated baselines occurs once, in 48-hour session 2003-086-01 (on March 27 and 28, 2003) consisting of 70 marks and 138 vectors in Tennessee NGS project GPS1753/C. This is an interesting example, because it was reprocessed in an early version of the online NGS software *OPUS-Projects* (*OP*) to replace a previous version of the project. *OP* is part of the NGS suite of *OPUS* products. Rather than sequentially processing a single GPS occupation as done in *OPUS-Static*, *OP* performs simultaneous baseline processing of multiple campaign-style GPS occupations (Armstrong *et al.*, 2015; Mader *et al.*, 2012; Weston *et al.*, 2007). The problem described here with *OP* results has since been fixed.

Tennessee session 2003-086-01 processed in *OP* consists of 138 vectors radiating from a single CORS hub to 69 marks. Each baseline is represented by two vectors in the session, because *OP* automatically used 48-hour CORS datasets when a mark occupation crosses GPS midnight. This created false redundancy, because the entire 48-hour CORS dataset was used in both sessions, so a significant portion of the processing results was represented twice in the network. Note this type of false redundancy can also be generated with 24-hour sessions when the passive mark occupations cross GPS midnight.

Table 5.17. Statistics for the 29,014 sessions that contain repeated and trivial vectors.

29,014 sessions with redundant vectors	Marks	Baselines	Vectors	Repeated baselines	Max repeat vectors per baseline	Trivial vectors	Total redundant vectors
Minimum	2	1	2	1	1	1	1
Maximum	108	230	230	69	20	209	209
Median	4	6	6	2	1	3	3
Mean	5.10	8.83	8.99	3.25	1.18	4.88	4.89
Std deviation	±3.75	±8.60	±8.90	±4.45	±1.03	±6.63	±6.78
Number sessions	**29,014**	**29,014**	**29,014**	**1,175**	**1,175**	**28,153**	**29,014**

The three sessions with the next largest numbers of repeated baselines per session (68, 35, and 33) also occur for Tennessee project GPS1753/C, and for the same reason (two vectors per baseline from processing in *OP*). Although no other sessions in the NA2011 Project were processed using *OP*, a similar thing occurred in other sessions, where two short occupations were included in the same session as a single long occupation spanning both. This is indicated in Table 5.17 by the maximum repeated vectors per baseline. Although the maximum is 20 vectors per baseline, the median and mean are 1 and 1.18, indicating that in most cases the repeated baseline in a session is represented by a single pair of vectors (i.e., one repeated vector).

The distribution of repeated vectors per baseline within a session is provided in Table 5.18, including the number of duplicate vectors as defined previously (i.e., with identical components and sigmas). This also shows that a large majority of repeated vectors are pairs, 3206 of 3905 vectors (82%). The maximum of 20 repeated vectors in a baseline occurs in session 2000-263-02, with all of them being duplicates, corresponding with the maximum of 21 duplicate vectors in Table 5.4. Although having a baseline within a session represented by 21 vectors is extreme false redundancy, in this particular instance all vectors are rejected. The 21 duplicates occur in a 24-hr session of 8 marks and 68 vectors in NGS Texas project GPS1538 for the Harris-Galveston Subsidence District (HGSD). NGS processed the vectors sequentially using *PAGES*; it is not known why or how the duplicate vectors were created.

Table 5.18. Distribution of repeated vectors per baselines within a session.

Number of repeated vectors per baseline in a session	Number sessions	Number baselines	Number vectors	Number duplicate vectors	Percent duplicate vectors
1	1,057	3,206	3,206	143	4.5%
2	94	132	264	20	7.6%
3	14	39	117	21	17.9%
4	4	3	12	0	0.0%
6	0	5	30	30	100.0%
7	0	1	7	0	0.0%
8	0	2	16	0	0.0%
9	0	3	27	0	0.0%
11	0	1	11	0	0.0%
12	2	1	12	0	0.0%
13	2	6	78	65	83.3%
15	1	7	105	0	0.0%
20	1	1	20	20	100.0%
Total	**1,175**	**3,407**	**3,905**	**299**	

The next largest number of repeated vectors per baseline for a session is 15, and this occurs on seven baselines in sessions 1992-161-20, and none of them are duplicates. The session is in Maryland project GPS432 consisting of 177 vectors, but only 14 marks. This project has two other similar sessions that also include a large number of non-duplicate repeated vectors per baseline (maximums each of 13 and 12 vectors per baseline). Together, these three sessions consist of 437 vectors, with 375 (86%) repeated and only four rejected. For the total 38 baselines, half (19) are not repeated, and the other half are repeated within a session from 1 to 15 times. For the highly repeated vectors per baseline, this represents a large degree of false

redundancy in the NA2011 network. In future adjustments, such repeat baselines should be downweighted or removed. These three sessions also include some trivial vectors, ranging from 8 to 24% of the total number of trivial vectors possible (based on the number of marks).

Although repeated vectors within a session create false redundancy, a relatively small number of sessions and baselines are affected. Table 5.17 shows that of the 29,014 redundant sessions, 28,153 (97.0%) are due to the presence of trivial vectors rather than repeated vectors. The number of trivial vectors per session ranges from 1 to 209, with a median and mean of 3 and 4.9 per session, respectively.

The number of sessions with trivial vectors can be misleading, because even if only one trivial vector exists in a session it is counted. The number of trivial vectors per session also does not completely define the degree of redundancy or "trivialness" of the session. More important is the number of trivial vectors with respect to the maximum possible. This is shown in Table 5.19 as the number and percent of sessions for different ratios of the actual number of trivial vectors to the maximum possible. In most sessions with trivial vectors—77.6%—all possible trivial vectors are present. An additional 0.6% of sessions have more than 90% of possible trivial vectors present. A fairly large percentage of sessions (19.3%) are "partially" trivial, with 10% to 90% of possible trivial vectors. And 2.6% have less than 10% of possible trivial vectors, which likely represents a negligible contribution to false redundancy.

Table 5.19. Distribution of trivial vectors in sessions by ratio of actual number to maximum possible.

Ratio actual trivial to max possible	Sessions	
	Number	Percent
1	21,834	77.55%
>= 0.9 and < 1	174	0.62%
>= 0.5 and < 0.9	2,186	7.76%
>= 0.1 and < 0.5	3,241	11.51%
> 0 and < 0.1	718	2.55%
Total	**28,153**	**100.00%**

5.2.3. Accounting for false redundancy due to trivial vectors

The false redundancy introduced by repeated and trivial vectors was not considered in the NA2011 adjustments, because it was not known that so many such vectors were present. Although the NA2011 adjustments are complete and results published, it is still important to estimate the impact of redundant vectors. Doing so provides a means for NGS to account for such effects in future adjustments of existing GNSS vectors.

In the case where all possible (sequentially processed) trivial vectors are used in a session, the false redundancy can be accounted for by multiplying each vector variance-covariance matrix by $n / 2$, where n is the number of marks (receivers) in the session. This has been shown (Craymer and Beck, 1992 and Han and Rizos, 1995) to yield results equivalent to simultaneous processing,

if the trivial vectors are exact linear combinations of the independent vectors. But, as mentioned earlier, in actual sequential baseline processing, the trivial vectors are rarely (if ever) perfect linear combinations. However, they are nonetheless significantly redundant and the $n / 2$ variance factor offers a rational, simple (and conservative) means for estimating the impact of trivial vectors on uncertainty estimates.

As shown in Table 5.19, a large proportion (78%) of the sessions in the NA2011 networks include at least 90% of all possible trivial vectors. For these sessions, the vector standard deviations can be scaled by the square root of the trivial variance factor, using the following redundancy scalar (i.e., multiplier) to account for false redundancy:

$$R = \sqrt{n/2} \tag{5.1}$$

However, a significant proportion of sessions (22%) have less than 90% of the maximum possible trivial vectors, and 14% have less than half the maximum number. Moreover, the number of marks per session is highly variable, and the proportion of possible trivial vectors in these sessions also varies significantly both within and between the session groups.

Since a significant number of sessions with trivial vectors include less than the maximum possible, a method is needed to account for "partially" trivial sessions. It is thus desirable to recast Equation (5.1) so that it can account such sessions.

Recall from the beginning of Section 5.1.9 that the total number of possible vectors in a session is $v = n\,(n - 1) / 2$, and the number of independent vectors is $v_I = n - 1$. Let the actual number of trivial vectors be v_T. For the case where all possible trivial vectors are in a session, the total possible number of trivial vectors is $v_{Tmax} = v - v_I = n\,(n - 1) / 2 - (n - 1) = (n - 1)(n - 2) / 2$. This relationship can be used to modify Equation (5.1) to obtain R in terms of the actual number of trivial vectors (v_T) and the total number or mark in a session:

$$R = \sqrt{1 + \frac{v_T}{n - 1}} \tag{5.2}$$

Note that for the case where $v_T = (n - 1)(n - 2) / 2$ (i.e., the number of all possible trivial vectors, v_{Tmax}), Equation (5.2) reduces to Equation (5.1). For no trivial vectors, $v_T = 0$ and $R = 1$, as expected. For "partially" trivial sessions, R varies between 1 and $\sqrt{n/2}$.

For large network adjustments (such as done for the NA2011 Project), it is useful to consider the aggregate contribution of all sessions with the same number n of marks to the overall network adjustment results. The mean redundancy factor, $\bar{R}$, for all sessions with n marks can be estimated by summing the total number of trivial vectors in all sessions divided by the number of sessions containing trivial vectors, s_T:

$$\bar{R} = \sqrt{1 + \frac{\left(\frac{\sum_{i=1}^{s_T} v_T}{s_T}\right)}{n - 1}} \tag{5.3}$$

Figure 5.5 uses equations (5.1), (5.2), and (5.3) to represent the potential and actual estimated impact of trivial vectors on the NA2011 networks. Figure 5.5 is admittedly complex, but it summarizes a great deal of useful information about the impact of false redundancy on the NA2011 networks. The following discussion serves as a guide for navigating the content of that figure.

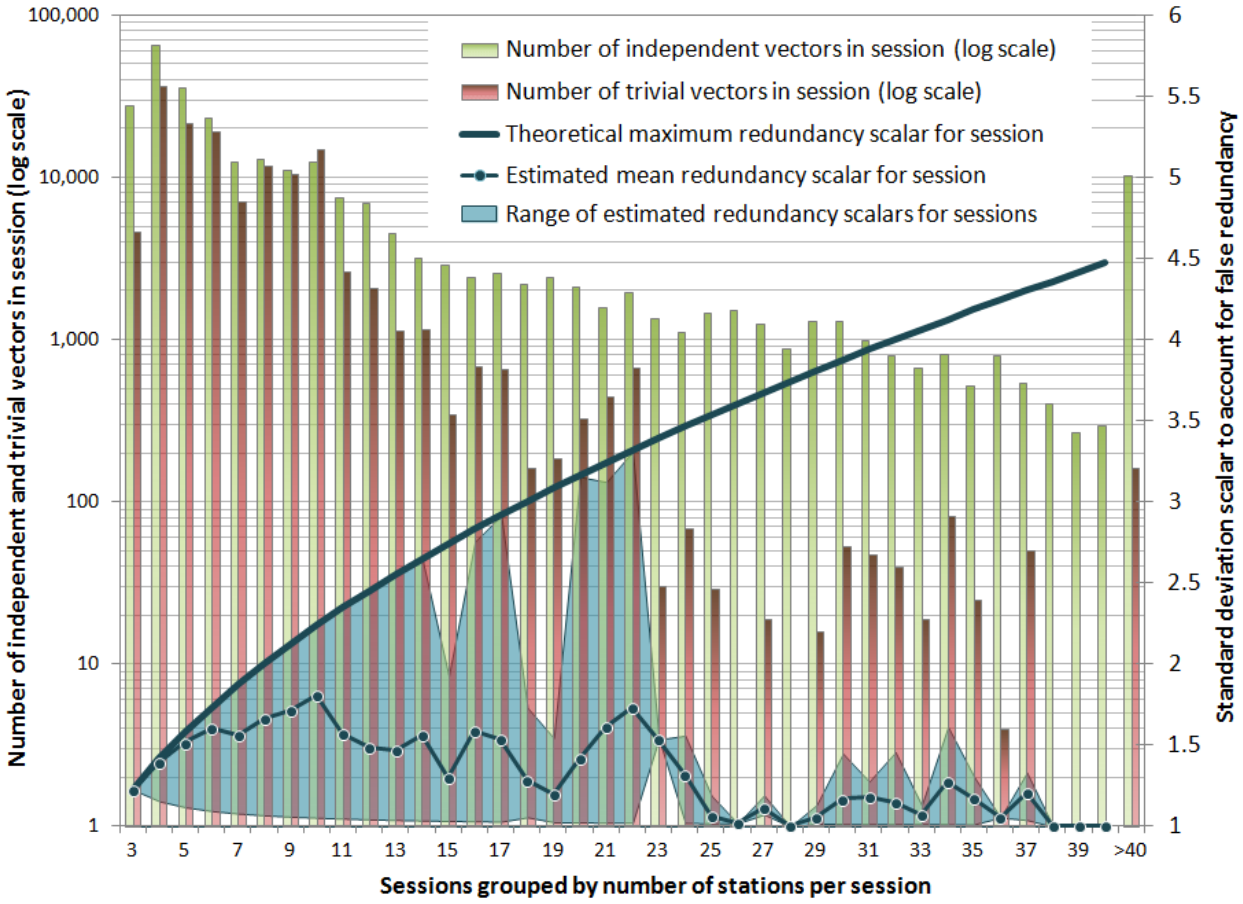

Figure 5.5. Number of trivial vectors in sessions and corresponding redundancy scalars.

Figure 5.5 shows the number of trivial vectors in sessions (left vertical axis) and the standard deviation scalar to account for false redundancy (right vertical axis). Both are functions of sessions grouped by the number of marks per session, *n*. The left vertical axis is the number of independent and trivial vectors in a session group, and it corresponds to the bars in the graph (a log scale was used because of the high variability in the number of trivial vectors). There are a few session groups with no trivial vectors (groups with 28, 38, 39, and 40 marks). The session group with 26 marks has one trivial vector (although it appears to have none in the figure).

The rightmost pair of bars in Figure 5.5 is the total number of independent and trivial vectors for sessions with more than 40 marks (the maximum is 194 marks per session for all sessions and 108 for sessions that contain trivial vectors). Collectively, these sessions account for 10,220 independent vectors but only 161 trivial vectors. In addition, the maximum percentage of trivial

vectors to the total possible for all of these sessions is only 2.4%, therefore the false redundancy is likely negligible for all sessions with more than 40 marks (although it can be accounted for mathematically).

The right vertical axis in Figure 5.5 is the standard deviation scalar applied to vectors in a session to account for false redundancy due to trivial vectors. The bold upper blue curve is the theoretical case when all possible trivial vectors are used in a session, per Equation (5.1). The blue shaded region under the curve is the estimated range in the redundancy scalar based on the ratio of actual to total possible trivial vectors, computed using Equation (5.2) for the maximum and minimum number of trivial vectors in each session group. The blue line within the range is the estimated mean redundancy, where each point on the line was computed using Equation (5.3) for all sessions in that group (i.e., it represents the estimated mean contribution of false redundancy to all sessions, not just those with trivial vectors).

A number of things can be ascertained from Figure 5.5. One is that the proportion of trivial vectors is greatest for sessions with a relatively small number of marks. For sessions with ten marks, the number of trivial vectors (14,785) is actually greater than independent vectors (12,574), but in all other cases the number of trivial vectors is less than independent vectors: an average of 27% of vectors are trivial for sessions with 22 or less marks, versus 2.8% for sessions with more than 22 marks.

Figure 5.5 also shows that for many sessions there is a large range in the proportion of possible trivial vectors used. Except for sessions with 15, 18, and 19 marks, all groups with 22 or less marks include some sessions where all possible trivial vectors are used. In contrast, all sessions with more than 22 marks have a very low maximum percentage of possible trivial vectors; the maximum is 10.0% for sessions with 34 marks (corresponding to an approximate redundancy scalar of 1.61 versus a maximum theoretical of 4.12).

For many session groups there is also a significant range in the percentage of possible trivial vectors used and thus of the redundancy scalar. The only sessions where 100% of trivial vectors are used are those with three marks, as shown by the range of zero at a redundancy scalar of 1.22. As the number of marks per session increases, the minimum redundancy scalar generally decreases, as shown by the lower bound of the range in redundancy scalar. The minimum decreases to less than 5% of the theoretical maximum for sessions with ten or more marks (except for the single trivial session with 23 marks). The mean redundancy scalar per session also generally decreases with an increasing number of marks (this is not immediately obvious in Figure 5.5, because it is with respect to the maximum theoretical value, rather than the actual scalar value). For sessions with ten marks, the mean scalar is 65% of the maximum value; for all sessions with more than ten marks the mean is less than 50% of the maximum, and it is less than 10% for all sessions with 25 or more marks.

Figure 5.5 shows that the standard deviation redundancy scalar can be quite large for some sessions. The largest scalar based on actual trivial vectors in the NA2011 networks is 3.3, for two sessions with 22 marks, each with 209 trivial vectors (99.5% of the maximum of 210). The standard deviations of all 418 vectors in these two sessions should be scaled by a factor of 3.3 to

account for the false redundancy. However, there are 14 other sessions with 22 marks that have 0.5% to 68.6% of the maximum possible trivial vectors. This is indicated by the minimum and mean redundancy scalars of 1.02 and 1.73, respectively, in Figure 5.5.

The preceding discussion shows that a large number of trivial vectors exist in the NA2011 networks. It also shows that the impact of these trivial vectors on the uncertainties is highly variable. In some sessions the vector standard deviations should be scaled by a factor of 2 or greater. But in sessions containing a small percentage of possible trivial vectors, the scale factor is small (e.g., less than 1.1). Accounting for the false redundancy would thus scale vector uncertainties by amounts that vary from 1 (no scaling) to 3.3. This not only affects the final adjusted coordinate uncertainties but also the coordinates themselves, since it changes relative weights of the observations.

The analysis performed here did not take into account rejected vectors. Obviously, if a trivial vector is rejected it cannot contribute to false redundancy. However, removal of subsets of trivial vectors from a session does not merely affect the uncertainty of computed coordinates, it also alters the coordinates themselves. This is particularly a problem for automated rejection criteria based on the magnitude of vector residuals. In such cases there is a tendency for rejections to cluster around specific marks, for example marks connected by more vectors with large uncertainties than other marks. The end result can be a network where some marks have all (or nearly all) vectors enabled and other marks have nearly all vectors rejected. This skews results, and this can also occur when a session is reduced to an independent set of vectors by removing the vectors with the largest residuals.

Another more subtle source of false redundancy is from observations that occur on different days but at the same time of day. In such cases not only is the GNSS constellation repeated, but most of the signal multipath, as well. This can be a problem for observations that occur even several days later, since the constellation changes by only about four minutes per day. It is unclear how or whether anything should be done to account for this type of false redundancy.

It should be re-emphasized that the analysis performed in this chapter for determining the presence of false redundancy is to some degree arbitrary. For example, it is based on defining redundant time overlap as 50% or greater. To appropriately assess the presence of false redundancy—and methods for mitigating its effects—a more rigorous analysis should be performed. Nonetheless, the methods used in this chapter hopefully provide a reasonably accurate portrayal of false redundancy. It is expected that a more rigorous analysis would change the number of sessions—and thus trivial and repeat vectors—by less than a few percent. This estimated limited impact is based on the multiple iterative analyses performed for defining sessions in this report.

5.2.4. An example of applying trivial vector false redundancy to a specific state

Although a large proportion (36%) of the NA2011 sessions contain trivial vectors, the distribution and the degree of "trivialness" (i.e., ratio of actual trivial vectors to total possible) vary greatly, as shown in Figure 5.5. Wisconsin is an example of a state where a significant number of projects with trivial vectors are known to occur. An indication of this can be seen in

the maps of Figure 4.35 and Figure 4.37. These maps show the estimated network horizontal and ellipsoid height accuracies, respectively, for the CONUS Primary network. Wisconsin stands out because of its extremely small accuracy values, particularly noticeable for the horizontal accuracies (Figure 4.35). Upon examination, it was found that the number and degree of trivial sessions is much greater than is typical for the NA2011 sessions. Table 5.20 provides statistics comparing the occurrence of trivial vector sessions in Wisconsin to the entire NA2011 network. For the 2885 Wisconsin Primary sessions, the mean ratio of the actual number of trivial vectors to the total possible is 64%, compared to 41% for all NA2011 sessions. The mean trivial vector scalar of Wisconsin is 1.47, versus 1.15 for NA2011 overall. The medians provide a more striking comparison: the median ratio of actual to possible trivial vectors in Wisconsin is 100%, but it is 0% for NA2011. This median statistics means that at least half of the sessions in Wisconsin use all possible trivial vectors, whereas more than half of the NA2011 sessions have no trivial vectors. This is also reflected in the median trivial redundancy scalars, 1.41 for Wisconsin, versus 1.00 for NA2011. Thus, half the Wisconsin sessions should be scaled by at least 1.41, and Table 5.20 shows that a quarter should be scaled by 1.73, up to a maximum of 2.24. This indicates a significant portion of the vector standard deviations for Wisconsin should essentially be doubled. Note that the statistics in Table 5.20 do not take into account the presence of rejected vectors, which can reduce the contribution of trivial vectors to false redundancy. However, this has almost no effect on the trivial vector session scalars. Most of the statistics in Table 5.20 remain the same (at the precision displayed) even when rejected vectors are taken into account.

Table 5.20. Trivial vectors in sessions of the Wisconsin Primary G-file and the entire NA2011 network.

	Wisconsin Primary sessions (num = 2885)				All NA2011 sessions (num = 78,185)			
	Number vectors in session	Number trivial vectors	Ratio actual trivial to possible	Trivial vector session scalar	Number vectors in session	Number trivial vectors	Ratio actual trivial to possible	Trivial vector session scalar
Minimum	1	0	0%	**1**	1	0	0%	**1**
Maximum	62	36	100%	**2.24**	230	209	100%	**3.31**
Mean	14.3	8.7	64%	**1.47**	5.4	1.8	41%	**1.15**
Std deviation	±12.5	±10.9	±45%	**±0.42**	7.4	±4.6	±47%	**±0.24**
Percentiles								
5%	1	0	0%	**1.00**	1	0	0%	**1.00**
25%	6	0	0%	**1.00**	2	0	0%	**1.00**
50% (median)	**10**	**5**	**100%**	**1.41**	**3**	**0**	**0%**	**1.00**
75%	17	10	100%	**1.73**	6	3	100%	**1.32**
95%	45	36	100%	**2.24**	15	9	100%	**1.58**

5.3. Chapter 5 summary

Several issues were identified with GNSS vectors used as observations in the NA2011 networks. These are listed below in nine categories:

1. Unusually short vectors (length less than 20 cm)
2. Baselines with vectors that differ in length by more than 10 cm
3. Erroneous vector covariances
4. Duplicate vectors (i.e., identical components and standard deviations)
5. Erroneous or suspect session start and stop times
6. Questionable session durations: Unusually short (five minutes or less) and long (more than five days)
7. Incorrect reference system designations for vectors
8. Broadcast orbits used for post-processing
9. Sessions with "trivial" (dependent) vectors and repeated vectors

The first six issues above in aggregate affected less than 1.5% of the NA2011 vectors. Item number 7 above occurs for about a third of the vectors, but for a vast majority the effect is extremely small. Item number 8 impacts approximately half the vectors, and it likely has significant impact for about 5% of the vectors (all observed prior to May 2000 when GPS selective availability was on). Item number 9 occurs for about a third of all vectors, and the magnitude of the impact on results is variable.

Despite problems with some of the data used in the NA2011 Project, a large majority appear to be of high quality. The most significant problem is the presence of such a large number of trivial vectors. The primary likely impact of this is overly optimistic accuracy estimates. It is also likely that trivial vectors significantly affected coordinates for at least some marks (coordinates are impacted when trivial vectors alter the selection of rejected vectors).

This chapter identified methods for identifying trivial vectors and mitigating their impact on results. However, no attempt was made to account for false redundancy due to trivial vectors in the NA2011 adjustments. It is recommended a method be developed to address this issue in any future adjustments, by improving upon the methods introduced in this chapter. Doing so would produce more realistic accuracy estimates. It would also reduce coordinate skewing due to the clustering of rejections that can occur when trivial vectors are present.

It is important to restate that the issues discussed in this chapter are retrospective—they were identified *after* the adjustment was completed. Clearly it is preferable to have known about these issues and to manage them while the project was underway. Indeed, knowing about and acting upon them would likely have improved the NA2011 Project's results. Even in retrospect, however, an awareness of the data characteristics aids us in interpreting the results. More importantly, the information provided here will be useful should NGS perform similar adjustments of existing GNSS networks in the future, both in terms of quality and efficiency. It is also useful for other types of analyses and projects that make use of CORS coordinates and GNSS vectors stored in the NGSIDB.

Chapter 6. Conclusions and Recommendations

6.1. Summary and conclusions for the NA2011 Project

The intent of this report is to provide comprehensive documentation of the National Adjustment of 2011 (NA2011) Project. The report serves as a record of what was done, how it was done, the reasons for decisions made, problems encountered, interpretation of results, and recommendations on how to improve efficiency and quality for similar projects in the future. The report also provides information on items that are not strictly a part of the project, to provide context and a record that is not fully documented elsewhere in NGS reports. This additional information includes a brief history of NAD 83 up to the time of this project; a summary of methods and results of the initial Multi-Year CORS Solution (MYCS1); technical details of the method used for scaling error estimates of individual GPS projects before combining them to create the NA2011 networks; and a detailed assessment of the presence and impact of trivial (dependent) GNSS vectors.

A key driver in preparing the report was to present enough detail for it to serve as a solid foundation for future, similar projects. In short, it provides information that would have been useful in performing the project itself. A corollary to this objective is providing an in-depth assessment of the condition and quality of GNSS data in the NGS Integrated Data Base (IDB), including guidance on what can be done to correct or account for data irregularities. Such information should prove useful in migrating the data to a new, modernized NSRS database, and perhaps will provide insight into designing and determining the type of content for a future database.

National or regional adjustments performed in the future could achieve better results—and be accomplished more quickly—based on what was learned in analyzing the data, methods, and results for this report. Part of making that possible was the creation of tools and techniques for analysis, particularly through the use of GIS. That is not to say the results of the NA2011 Project are compromised or of marginal quality. Quite the contrary—the overall results are excellent, as shown in Chapter 4, despite the presence of some outliers. Improved results would mainly be in the form of reducing the number and magnitude of outliers, which, although important, has little impact on the aggregate statistics. Indeed, the accuracy estimates for the NA2011 passive marks are on par with the formal accuracies reported for MYCS1. The 50th (median) and 95th percentile accuracy estimates (at 95% confidence) of each are listed in Table 6.1.

Table 6.1. Network accuracies of NA2011 and MYCS1 marks, cm (95% confidence).

	Horizontal		Ellipsoid height	
	NA2011	MYCS1	NA2011	MYCS1
50th percentile (median)	0.9	1.1	1.5	3.5
95th percentile	3.2	3.8	7.1	13.1
Number	77,560	1,309	77,560	1309

Granted, the NA2011 accuracy estimates are likely somewhat optimistic, and the MYCS1 accuracies may be somewhat pessimistic, as discussed in Chapter 4. Taking that into account (and considering other NA2011 accuracy metrics from vector residual and loop closure analyses), the accuracy estimates are quite comparable. Such results should give pause to those who insist on the superiority of CORSs, and by inference that NA2011 passive marks are by comparison deficient as geodetic control. The evidence indicates otherwise.

6.2. Recommendations

Recommendations based on this report are divided into three sections. The first concerns additional tasks associated with the NA2011 Project itself, and these can be done with little or no change to the NGSIDB and programs. The second set of recommendations requires the modification of existing NGS data holdings and software, modifications that range from minor to significant. The third set is for future national or large regional adjustments of GNSS networks.

The recommendations here are specific to the existing NGSIDB, software, products, and services. However, NGS is currently in the process of transitioning to four new terrestrial reference frames and a geopotential datum in 2022. This transition requires making changes to the NGS database, software, workflows, as well as how customers access and use NGS products and services. These changes are in various stages of development, and some are only in the planning stages. Nonetheless, such a situation means that the recommendations here run the risk of becoming obsolete shortly after publication of this report.

The first group of recommendations is intended for the near term and so (assuming they are followed) they would be unaffected by the changes underway at NGS. But the second and third groups are for the future, and they will likely be impacted by the changes. With that in mind, the intent here is that those recommendations be interpreted more broadly, even if they are written for the situation as it currently exists at NGS. It can hardly be done otherwise; details of the new database, software, and workflows have yet to be defined.

6.2.1. Recommendations for additional tasks associated with the NA2011 Project

The following recommendations are specific to the NA2011 Project and require no, or minor, modification of existing NGS data structures or software.

6.2.1.1. Readjustments of the Alaska and the Pacific networks

1. Perform readjustments of the Alaska and the Pacific networks using G-files updated with projects loaded in the database since March 29, 2012, along with the old Pacific project GPS415 that was accidentally excluded (as mentioned in Footnote 9). Newly available NAD 83 epoch 2010.00 CORS coordinates derived from the recently completed Multi-Year CORS Solution 2 (MYCS2) project (NGS, 2019a) should be used as constraints. This process benefits both networks, because there are now many more "computed" CORSs in Alaska, and new coordinates will be available for the CORS ASPA in American Samoa impacted by a major earthquake on September 29, 2009 and subsequent post-seismic deformation. In addition, tectonic modeling in Alaska has been significantly improved in *HTDP*, including the only implementation of a vertical component in *HTDP* (in central

Alaska). As discussed below in Section 6.2.1.3, using a more recent version of *HTDP* by itself resulted in better adjustment statistics, even with the same vectors and constraints as used for NA2011. And finally, the impact of Alaska and Pacific adjustments will better align the passive marks with CORSs in these tectonic active areas, at the same 2010.00 epoch currently used. These improvements can be accomplished without affecting other marks in the NSRS, since the networks are not connected to the CONUS networks. However, a new set of NAD 83 coordinates on passive control, so close to the planned 2022 replacement of NAD 83, could cause come customer concerns and/or complaints. That possibility should be considered before pursuing this recommendation.

2. Marks on Palau and Yap Island (located on the Philippine Sea plate) are referenced to the Mariana plate, as NAD 83 (MA11) epoch 2010.00. Whether or not a readjustment of the Pacific is performed, it is recommended the marks be referenced instead to the Pacific plate. NAD 83 (PA11) epoch 2010.00 coordinates already exist for marks on these islands, since both PA11 and MA11 coordinates were computed for all Pacific marks in the NA2011 adjustments. The reason for the change is that PA11 velocities on those islands are near zero, whereas MA11 velocities are approximately 6 cm/year. In addition, the MA11 shifts from previously published coordinates are very large (1.6 ***meters***).

6.2.1.2. Updates of data in the NGSIDB

1. Resolve GNSS vector errors and inconsistencies in the NGSIDB, as described in Section 2.4.2. Some of these can be fixed, others cannot. It would be possible to flag problematic vectors that cannot be fixed (such as trivial vectors), but that would require addition of one or more fields to the NGSIDB. This item should also include vectors with clearly erroneous sigmas, as discussed in Section 4.2.5 (i.e., vectors with sigmas that are constant or a linear function of length). That would require these vectors to be identified, but that could be accomplished fairly easily.

2. Allow export of unique identifiers in the NGSIDB for individual GNSS vectors that can be included in the G-file format (e.g., by placing them to the right column 90 for each vector C or F record). Having unique IDs makes it possible to easily cross-reference, thereby facilitating the finding and fixing of problems with vectors in the NGSIDB.

3. Allow the export of GNSS solution type (e.g., iono-free fixed double difference) from the NGSIDB, assuming it is stored. Those fields are part of the defined G-file format and are in G-files that are read for loading into the NGSIDB. If the solution type is not stored, there is no point in adding a field to the existing NGSIDB, since it would only apply to newly uploaded G-files. However, including that information in the new NSRS database is recommended.

4. Vector rejections in the G-files used for NA2011 are much different than those in the NGSIDB (recall that over 20,000 vectors rejected in the NGSIDB were enabled in the NA2011 Project). The NA2011 vector rejections should be adopted for the vectors in the NGSIDB, particularly since considerable effort went into manually identifying vector

rejections in specific areas. Although update of vector rejection status in the NGSIDB is recommended, it is recognized that doing so is problematic, since there is no simple means to correlate the NA2011 vectors with those in the NGSIDB (as mentioned in item number 2 above). In addition, creation of a new NSRS database and possible readjustment of historic vectors as part of the 2022 NSRS Modernization may provide a more efficient and timely means of managing vector status.

6.2.1.3. Improved adjustment results in Alaska using updated version of HTDP

During the NA2011 Project, a new version of *HTDP* (3.2.1) was released. That version included much improved crustal deformation models in Alaska. The updates in Alaska also included modeling of vertical displacements in central Alaska, the only area in *HTDP* models vertical deformation. For the NA2011 Project, *HTDP* v3.1.2 was used for transforming G-files, the same version as was used for computing coordinates and velocities for MYCS1 "modeled" CORSs. To evaluate the impact of this change, Alaska was readjusted using the same constraints and G-file as used for NA2011, except the G-file was transformed to NAD 83 (2011) epoch 2010.00 using *HTDP* v3.2.5, the latest available version at the time the readjustment was performed (September 2017). Even though the modeled CORS constraints were based on *HTDP* 3.1.2, using *HTDP* v3.2.5 significantly improved results. The adjustment statistics are provided in Table 6.2 (an adjustment without *HTDP* used is included for comparison).

Table 6.2. Comparison of Alaska adjustments for different versions of *HTDP* (includes adjustment with *HTDP* not used for comparison).

	Standard deviation of unit weight		Median network accuracies (cm)	
	Free	Constrained	Horizontal	Ellipsoid ht
HTDP not used	2.256	3.053	5.44	9.40
HTDP 3.1.2 (used for NA2011)	1.822	2.124	3.78	6.54
HTDP 3.2.5	1.719	2.011	3.58	6.19

The above figures show a significant improvement in results with the latest version 3.2.5 of *HTDP*, compared to version 3.1.2 used for NA2011 (although *HTDP* v3.2.7 is the version current at the time of this writing, the Alaska deformation grids have not been updated since v3.2.1). The improvement is particularly striking for both compared to when *HTDP* is not used at all, demonstrating the importance of *HTDP* in performing adjustments, in tectonically active areas especially. The coordinate shifts from v3.1.2 to v3.2.5 are surprising large: a maximum of 43 cm horizontal and 11 cm in height, with medians of 4 cm horizontally and 0.9 cm in absolute value of height. It is anticipated that the results would further improve by using the CORS coordinates from the MYCS2 reprocessing effort, as discussed above in Section 6.2.1.1. Similar advantages could also be realized by readjusting the Pacific network, and neither would affect other parts of the NSRS, because the networks are not connected. In both cases, if these

readjustments are done, the latest available observations should be added, since both networks have a large proportion of old observations and relatively poor connectivity.

6.2.2. Recommendations requiring modification of NGS products and services

6.2.2.1. NGS Bluebook, NGSIDB, and data-loading programs

1. Add a distance field to local accuracy to allow distance to be stored in the NGSIDB. A distance field would expedite Datasheet retrieval; it would no longer be necessary to compute distances during retrieval of local accuracies.
2. Add two additional fields to the network and local accuracies, for the north-up and east-up correlations. This would allow storage of the entire variance-covariance matrix.
3. Increase the number of decimal places available for storing network and local accuracy standard deviations from two to at least four, to avoid problems with the current 2-decimal place fixed-format (e.g., causes excessive occurrence of error ellipses with 45° rotations).
4. For all GPS projects submitted to NGS for including in the NGSIDB, require there be at least two independent occupations, each with at least one enabled vector tie, for all passive marks. Doing so will prevent creation of additional no-check marks in the NGSIDB. The purpose is to increase both vector tie and occupational redundancy, thereby improving both accuracy and reliability.

6.2.2.2. NGS Datasheets

1. Add the following information to Datasheets to help users assess the quality and suitability of GNSS control: Date of the most recent, as well as the oldest occupation (based on enabled vector ties), the number of occupations (counting only enabled vector ties), and the number of enabled vector ties. Note: this requires rejections in the NGSIDB to be consistent with the published coordinates, per item number 4 in Section 6.2.1.2.
2. Add NAD 83 mark velocity, as predicted by the current version of *HTDP*, and provide the *HTDP* version used. Showing model results on NGS Datasheets is similar to what is already done for the hybrid geoid, the Laplace correction, and modeled NAVD 88 gravity.
3. Add the deflection of the vertical components (in arcseconds). This is more useful for modern survey practice than the Laplace correction (e.g., for correcting total mark vertical angles to the ellipsoid normal).
4. Provide accuracy estimates for all quantities where NGS has existing estimates, as is currently being done for VERTCON. It should also be done for the hybrid geoid and NAVD 88 surface gravity (as this is part of the model).

6.2.2.3. Modifications of ADJUST (and NETSTAT)

1. Integrate *HTDP* with *ADJUST* so that *HTDP* is always used to transform a G-file prior to it being used in an adjustment. In addition to accounting for differential tectonic motion that is not modeled by a 14-parameter transformation, it also resolves the problem of the PA11 and

MA11 not existing in *ADJUST*. As well, it also reduced maintenance by no longer requiring that transformations in *ADJUST* be updated. Note that the latest version of *OPUS-Projects* is already incorporating this approach.

2. Add the ability in *ADJUST* to gracefully handle situations where the "VVHU" variance factor computation presently fails (e.g., when differencing causes a negative variance sum).
3. Output full network and local covariance matrices (i.e., include the north-up and east-up components).
4. Allow adjustments to be set up so that the minimally constrained (or unconstrained) adjustment is automatically followed by the constrained adjustment without user intervention. This would allow the automatic use of the F-test and the creation of coordinate comparisons between minimally constrained marks and control.
5. Compute and list constraint ratios from input-constrained coordinate sigmas and mark shifts.
6. Add the ability to automatically detect and handle trivial vectors (this will require some work, but it can be done with the information available).
7. Add the ability to perform unconstrained adjustments, rather than restricting a minimally constrained adjustment (e.g., by performing a pseudoinverse to handle normal matrix rank deficiency).
8. For *NETSTAT*, fix erroneous results for single-block adjustments and, if a future large adjustment is planned, modify it to perform parallel processing or make it compatible with rented supercomputer time or cloud-based computation. Note that with a supercomputer or cloud computing that Helmert blocking may be unnecessary, and this would simplify the setting up and managing of adjustments. The other previous pertinent recommendation for *ADJUST* should be implemented in *NETSTAT*, as well.

6.2.2.4. GIS tool for GNSS networks

1. As part of the NA2011 Project, GIS tools were created for visualization and analysis of results. Development of these tools continued after the final adjustments were completed, and they were used in performing analyses and creating figures for this report. The ArcGIS *NGS Toolbox* has evolved into a suite that includes not only tools for GNSS networks, but also tools for converting a variety of other NGS products into GIS features: leveling data, *HTDP* output, NGS grids (such as geoid models), and for creating velocity and displacement vectors. At the time of this writing (November 2019), the *NGS Toolbox* has not yet been released to the public as a beta product (the latest version is 4.3.4, last updated in July 2019). It is recommended that at least a beta release occur as soon as possible.
2. The utility of the ArcGIS *NGS Toolbox* could be improved by adding more attributes and features. Significant improvements that would have been helpful in performing the NA2011 Project have been added since project completion, including:
    a. Normalized and standardized vector residuals

b. Intravector (within vector) correlations
c. Vector 3D sigmas and sigma components rotated to north-east-up
d. Horizontal and vertical variance factors used in the adjustment
e. Vector sigma components scaled by horizontal and vertical variance factors
f. Vector midpoint coordinates
g. Mark constraint sigmas used for weighting constraints
h. Mark median local accuracies

Intervector (cross) correlations from simultaneous baseline processing would also be useful to capture, but this would require creation of an additional GIS feature indexed to the GNSS vector feature. It would also be useful to create a GIS feature with the overall adjustment statistics. The intent is to capture all information necessary to fully analyze, and even to perform, adjustments from GIS datasets.

6.2.3. Recommendations for future large adjustments of passive control

One of the main drivers for preparing this report was to provide detailed information on how to perform similar large adjustments efficiently and effectively. The assumption was that a similar NSRS-wide adjustment would be necessary to determine 2022 terrestrial reference frame coordinates on passive marks. It is unclear at this time whether that will occur, and if it does whether it will include all GNSS vectors in the NGSIDB or subsets. Even if there are no large adjustments associated with the new 2022 frames, other large adjustments may be performed in the near future (for example new adjustments of the Alaska and Pacific networks as recommended under Section 6.2.1.1, or future International Great Lakes Datum projects). The following recommendations are provided for future large adjustments of GNSS vectors.

6.2.3.1. Refinements of adjustment methods

1. Variance factors were computed (manually) for every GPS project before it was used in the NA2011 adjustments. But these variance factors change if the vector rejection status changes, and this certainly occurred in the iterative adjustments performed for vector enabling and rejecting. Project variance factors should be recomputed after every iteration, and the process should be automated.

2. Reconsider how GNSS data are grouped for variance factor calculation, rather than just as projects. Some projects are too variable for a single variance factor pair. Some projects last several years, some use different processing software. On the other hand, some projects are subdivided into parts when they should be more properly considered a single project. It is recommended that for variance factor computations GNSS data be grouped spatially, temporally, and by baseline processor, rather than by project.

3. The Helmert blocking strategy was based on the state where a project was nominally performed. But in reality, the situation was not so clear cut—projects in a state could actually span several states, as well as several months or years. It would be more logical, as described in the previous item, to create Helmert blocks in a manner similar to how variance component groups are defined, based largely on time and location, rather than on the state

where the project (nominally) was performed. This approach would also make it possible for block sizes to be more uniform, thus decreasing blocking complexity. It is not possible to equalize blocks by states when they vary as much as those defined for the District of Columbia and Minnesota.

4. Merge all CORS monuments for a single CORS ID into a single point. As performed for the NA2011 Project, every PID was treated as an independent mark. That means a single CORS could have multiple PIDs, one for its ARP, one for its external monument (if present), and one for the L1 phase center of every antenna ever used for that CORS. Treating these as separate marks is the same as treating every tripod setup over a single mark as individual marks; it simply does not make sense.
5. For the NA2011 Project, CONUS was split into a Primary and Secondary network, and at the time this seemed like the best available choice. However, this decision added complexity to an already difficult task, and it resulted in the creation of disconnected subnetworks that led to undetermined coordinates on some marks. Based on such difficulties, as well as on the results, it would be preferable to leave CONUS as a single network and instead determine an optimal means of appropriately weighting old observations to combine all into a single network, rather than splitting the network.
6. Improved outlier detection should be employed, beyond vector residual values. This could include rigorous independent loop misclosure analysis, the use of normalized residuals, and a robust application of vector component estimation.
7. Dependent ("trivial") vectors were identified in the GNSS vector dataset for this project. That information should be used to account for their false redundancy in future adjustments.
8. Improve how subsidence is handled. In the NA2011 Project, a fairly crude means of dealing with subsidence along the north Gulf Coast was employed. Better methods may be possible now that more observations have been made in subsidence areas. Such methods could include solving for velocities, rather than implying them from time-separated adjustments.
9. Revisit the idea of completely removing rejected vectors, rather than rejecting them by downweighting. Rejection by downweighting is useful for iterative adjustments that seek to reject enabled observations and re-enable rejected observations. But rejection by removal could be employed for the final adjustments, after most analysis has been completed.

6.2.3.2. Better coordination with future CORS reprocessing efforts

1. It is strongly recommended that the same epoch be used for NAD 83 as was used for the ITRF/IGS coordinates on which NAD 83 coordinates are based. The advantage for this is that the relationship between the frames is completely defined by a Helmert transformation. When the epochs differ, it is necessary to use crustal deformation models, such as those in *HTDP*, and this greatly complicates the situation for NGS customers. That problem is exacerbated because the deformation models can change with different versions of the

software, whereas this cannot occur if the epochs are the same (since the frame Helmert transformation parameters, once defined, are constant).

2. Ideally, future nationwide or large regional adjustments would include good coordination with the NGS group responsible for determining CORS coordinates (and their uncertainties). In the NA2011 Project, the CORSs and their formal uncertainties were simply provided without any feedback. As documented in Section 4.3.3, CORS sigmas were about 4 times greater than those estimated from the NA2011 adjustments (see Table 4.12). By working with the CORS group, perhaps a more consistent approach could be found for determining CORS and passive mark uncertainties, as well as how best to weight CORS coordinates in adjustments of passive marks. NGS policy requires that CORS coordinates and accuracies be determined independent of passive control, and given how CORSs are computed, this is a reasonable policy. However, one of the challenges is determining reliable uncertainties from the CORS reprocessing (such as done for MYCS1 and MYCS2). Including an evaluation of passive marks connected to CORSs could provide additional information on obtaining better estimates of CORS uncertainties, and could make them more consistent with one another.
3. Correctly identifying all the CORSs in the NA2011 network was a surprisingly difficult task, as described in lurid detail in Section 2.2.2. This was particularly the case for older observations, and when CORS antenna L1 phase centers were used as the "monument." It would be helpful to work more closely with the CORS Team to ensure such CORSs are correctly identified.
4. The previous item mentioned CORS L1 phase center monuments, often used as the "monument" for older surveys. This is problematic because those antennas (and their associated PIDs) have usually been replaced. In addition, the vector reductions for such cases were performed using relative (rather than absolute) antenna calibrations. A method for handling such cases was used for NA2011 (as described in Section 2.2.2.3), but it would be helpful to work more closely with the CORS group to ensure the approach used is appropriate. It would also be helpful if the CORS group maintained records of the antenna type associated with the L1 phase center PIDs.

6.2.3.3. Nationwide adjustment of GNSS-derived orthometric heights

Shortly after the completion of the NA2011 Project, the intent was to follow with a nationwide adjustment to determine GNSS-derived orthometric heights using the latest hybrid geoid model along with the geometric coordinates determined in the NA2011 adjustments. The advantage of such an adjustment is that it would provide more consistent GNSS-derived orthometric heights throughout the nation. The analysis and results could also give insight into developing a transformation model between NAVD 88 and the new geopotential datum. However, such an adjustment proved a more complex and difficult task than anticipated, and it could not be accomplished in a timely manner. Given that the 2022 NSRS Modernization will soon be performed, a nationwide vertical GNSS adjustment will not be pursued.

6.3. Implementation and digital deliverables

6.3.1. NGS Datasheets

The main implementation for this project was the loading of results into the NGSIDB to allow immediate access by the public via NGS Datasheets (NGS, 2019e). That occurred on June 27, 2012. Datasheets are available for download on the NGS website at geodesy.noaa.gov/datasheets/index.shtml through a variety of retrieval mechanisms. Datasheets can be obtained in standard ASCII text format or as Esri shapefiles. To illustrate content for an NA2011 mark, consider WHITMORE (PID GQ0372) in the Grand Canyon. This mark is shown in Figure 6.1 when it was occupied by the author in 2009. The datasheet for WHITMORE is shown in Figure 6.2, and its Accuracy Datasheet is shown in Figure 6.3. Portions of the content of both types of datasheet are described below.

Figure 6.1. Occupation of NGS control mark WHITMORE (PID GQ0372) in May, 2009.

Presently, NGS Datasheets provide NAD 83 (**11) epoch 2010.00 coordinates as current survey control for GNSS-derived coordinates. The quantity in parentheses is the datum tag (realization), either 2011, PA11, or MA11. For all marks determined in the NA2011 Project, the date of 6/27/2012 is provided on the same line as the current ellipsoid height. The Earth-

Centered, Earth-Fixed Cartesian coordinates are also provided (computed from latitude, longitude, and ellipsoid height based on the GRS 80 ellipsoid). All linear units are in meters.

For all NA2011 marks, the Datasheets also give coordinate network accuracies, and these are presented as horizontal and ellipsoid height accuracies in centimeters at the 95% confidence level, per Federal Geographic Data Committee standards (FGDC, 1998). The horizontal accuracy is given as the radius of a circle computed using the method of Leenhouts (1985). In addition to the accuracies are the north, east, and ellipsoid height standard deviations, also in centimeters, from which the accuracies were derived. The horizontal correlation coefficient is also given, and it is used as part of the horizontal accuracy computation. Local accuracies are not given on the Datasheet directly; instead, a link is provided immediately below the network accuracies. This link generates an accuracy Datasheet for the mark listing all the individual local accuracies, as well as the median local accuracy for the mark. For CORSs, local accuracies are not provided, and network accuracies are only available for "computed" CORSs.

The Datasheet also states that the NAD 83 coordinates are in a frame affixed to its relevant stable tectonic plate. For 2011 that is the North American plate, for PA11 it is the Pacific plate, and for MA11 it is the Mariana plate.

State Plane Coordinate System of 1983 (SPCS 83) coordinates corresponding to the current geodetic coordinates are also given in meters (to 3 decimal places). If the state where the mark is located has selected either the U.S. survey or international foot for geodetic control, SPCS 83 coordinates are also given in that version of the foot (to 2 decimal places). The SPCS 83 grid point scale factor, ellipsoid height ("elevation") factor, combined factor, and convergence angle are also given.

Previously published geodetic coordinates are also given in the superseded section of the datasheet, if they exist for the mark. The superseded coordinates are useful for comparison to previously determined values. For geometric control, they consist of latitude and longitude, as well as ellipsoid height (if available). Superseded accuracies and SPCS 83 coordinates are not given.

6.3.2. GIS datasets for the NA2011 Project

Providing comprehensive catalogs and records of the data and results of the NA2011 Project within the body of this report is not feasible, even in very large appendices—there is simply far too much information. Rather, the data and results are provided in digital format, mainly as attribute-rich GIS features. The advantage of using GIS features is the added spatial component to what would otherwise simply be tables. If the tables are related, such GIS datasets can be used as spatially-enabled databases. Such spatial content greatly enhances analysis power and flexibility, and it provides a useful means for visualization. Essentially all of the analysis in this report, including the creation of tables and charts (and of course maps) was done using data created, edited, and interconnected using GIS. The importance of GIS in successfully carrying out the NA2011 Project cannot be overstated, including the adjustments and this report. The project could scarcely have been done in such a short time with so few people without GIS.

The NGS Data Sheet

See file dsdata.pdf for more information about the datasheet.

```
PROGRAM = datasheet95, VERSION = 8.12.5.4
1        National Geodetic Survey,   Retrieval Date = NOVEMBER 11, 2019
 GQ0372 ***********************************************************************
 GQ0372  HT_MOD      -  This is a Height Modernization Survey Station.
 GQ0372  DESIGNATION -  WHITMORE
 GQ0372  PID         -  GQ0372
 GQ0372  STATE/COUNTY-  AZ/MOHAVE
 GQ0372  COUNTRY     -  US
 GQ0372  USGS QUAD   -  WHITMORE POINT (1967)
 GQ0372
 GQ0372                         *CURRENT SURVEY CONTROL
 GQ0372
 GQ0372* NAD 83(2011) POSITION- 36 10 54.03918(N) 113 15 41.08473(W)   ADJUSTED
 GQ0372* NAD 83(2011) ELLIP HT-  1650.420 (meters)        (06/27/12)   ADJUSTED
 GQ0372* NAD 83(2011) EPOCH   -  2010.00
 GQ0372* NAVD 88 ORTHO HEIGHT -  1674.88  (meters)     5495.0   (feet) GPS OBS
 GQ0372
 GQ0372  NAVD 88 orthometric height was determined with geoid model    GEOID09
 GQ0372  GEOID HEIGHT    -        -24.438 (meters)                     GEOID09
 GQ0372  GEOID HEIGHT    -        -24.388 (meters)                     GEOID18
 GQ0372  NAD 83(2011) X  - -2,036,027.987 (meters)                     COMP
 GQ0372  NAD 83(2011) Y  - -4,736,382.090 (meters)                     COMP
 GQ0372  NAD 83(2011) Z  -  3,745,456.210 (meters)                     COMP
 GQ0372  LAPLACE CORR    -          0.14  (seconds)                    DEFLEC18
 GQ0372
 GQ0372  Network accuracy estimates per FGDC Geospatial Positioning Accuracy
 GQ0372  Standards:
 GQ0372         FGDC (95% conf, cm)     Standard deviation (cm)     CorrNE
 GQ0372            Horiz  Ellip           SD_N   SD_E   SD_h      (unitless)
 GQ0372  ------------------------------------------------------------------
 GQ0372  NETWORK    0.27   0.55           0.12   0.10   0.28      0.03899909
 GQ0372  ------------------------------------------------------------------
 GQ0372  Click here for local accuracies and other accuracy information.
 GQ0372
 GQ0372
 GQ0372.The horizontal coordinates were established by GPS observations
 GQ0372.and adjusted by the National Geodetic Survey in June 2012.
 GQ0372
 GQ0372.NAD 83(2011) refers to NAD 83 coordinates where the reference frame has
 GQ0372.been affixed to the stable North American tectonic plate. See
 GQ0372.NA2011 for more information.
 GQ0372
 GQ0372.The horizontal coordinates are valid at the epoch date displayed above
 GQ0372.which is a decimal equivalence of Year/Month/Day.
 GQ0372
 GQ0372.The orthometric height was determined by GPS observations and a
 GQ0372.high-resolution geoid model using precise GPS observation and
 GQ0372.processing techniques.
 GQ0372
 GQ0372.Significant digits in the geoid height do not necessarily reflect accuracy.
 GQ0372.GEOID18 height accuracy estimate available here.
 GQ0372
 GQ0372.Click here to see if photographs exist for this station.
 GQ0372
 GQ0372.The X, Y, and Z were computed from the position and the ellipsoidal ht.
 GQ0372
 GQ0372.The Laplace correction was computed from DEFLEC18 derived deflections.
 GQ0372
 GQ0372.The ellipsoidal height was determined by GPS observations
 GQ0372.and is referenced to NAD 83.
  ...
```

(continued on next page)

(continued from previous page)

```
...
 GQ0372
 GQ0372. The following values were computed from the NAD 83(2011) position.
 GQ0372
 GQ0372;                    North         East     Units Scale Factor Converg.
 GQ0372;SPC AZ W     -   574,799.722   257,308.826   MT  0.99995712   +0 17 18.4
 GQ0372;SPC AZ W     - 1,885,825.86    844,189.06   iFT  0.99995712   +0 17 18.4
 GQ0372;UTM  12      - 4,006,469.402   296,636.645   MT  1.00010960   -1 20 07.7
 GQ0372
 GQ0372!             -  Elev Factor  x  Scale Factor =   Combined Factor
 GQ0372!SPC AZ W     -   0.99974104  x   0.99995712  =   0.99969817
 GQ0372!UTM  12      -   0.99974104  x   1.00010960  =   0.99985061
 GQ0372
 GQ0372:                Primary Azimuth Mark                     Grid Az
 GQ0372:SPC AZ W     -  WHITMORE AZ MK                           334 30 11.7
 GQ0372:UTM  12      -  WHITMORE AZ MK                           336 07 37.8
 GQ0372
 GQ0372_U.S. NATIONAL GRID SPATIAL ADDRESS: 12STF9663606469(NAD 83)
 GQ0372
 GQ0372|-----------------------------------------------------------------------|
 GQ0372| PID    Reference Object                    Distance      Geod. Az   |
 GQ0372|                                                          dddmmss.s  |
 GQ0372| CH4551 WHITMORE RM 1                        5.920 METERS 10227      |
 GQ0372| CH4550 WHITMORE AZ MK                                    3344730.1  |
 GQ0372|-----------------------------------------------------------------------|
 GQ0372
 GQ0372                          SUPERSEDED SURVEY CONTROL
 GQ0372
 GQ0372  NAD 83(2007)-  36 10 54.03863(N)    113 15 41.08491(W) AD(2007.00) A
 GQ0372  ELLIP H (09/10/11) 1650.438  (m)                       GP(2007.00) 4 1
 GQ0372  NAD 83(1992)-  36 10 54.03155(N)    113 15 41.08718(W) AD(       ) 3
 GQ0372  NAD 83(1986)-  36 10 54.02484(N)    113 15 41.08518(W) AD(       ) 3
 GQ0372  NAD 27      -  36 10 54.07500(N)    113 15 38.33700(W) AD(       ) 3
 GQ0372  NGVD 29 (07/19/86) 1674.6    (m)          5494.     (f) VERT ANG
 GQ0372
 GQ0372.Superseded values are not recommended for survey control.
 GQ0372
 GQ0372.NGS no longer adjusts projects to the NAD 27 or NGVD 29 datums.
 GQ0372.See file dsdata.pdf to determine how the superseded data were derived.
 GQ0372
 GQ0372_MARKER: DS = TRIANGULATION STATION DISK
 GQ0372_SETTING: 66 = SET IN ROCK OUTCROP
 GQ0372_STAMPING: WHITMORE 1953
 GQ0372_MARK LOGO: CGS
 GQ0372_STABILITY: A = MOST RELIABLE AND EXPECTED TO HOLD
 GQ0372+STABILITY: POSITION/ELEVATION WELL
 GQ0372_SATELLITE: THE SITE LOCATION WAS REPORTED AS SUITABLE FOR
 GQ0372+SATELLITE: SATELLITE OBSERVATIONS - May 27, 2013
 GQ0372
 GQ0372  HISTORY     - Date     Condition        Report By
 GQ0372  HISTORY     - 1953     MONUMENTED       CGS
 GQ0372  HISTORY     - 1965     GOOD             CGS
 GQ0372  HISTORY     - 20090525 GOOD             GRANCN
 GQ0372  HISTORY     - 20090601 GOOD             GEOANA
 GQ0372  HISTORY     - 20130527 GOOD             USGS
...
```

(station description and recovery information below is not shown)

Figure 6.2. An NGS Datasheet with NA2011 results for mark WHITMORE (PID GQ0372).

The Local and Network Accuracy Data Sheet

```
Program lna_ret Version 2.7.12 Date September 10, 2019
National Geodetic Survey, Retrieval Date = NOVEMBER 11, 2019
 GQ0372 ***********************************************************************
 GQ0372  ACCURACIES  -  Complete network and local accuracy information.
 GQ0372  HT_MOD      -  This is a Height Modernization Survey Station.
 GQ0372  DESIGNATION -  WHITMORE
 GQ0372  PID         -  GQ0372
 GQ0372
 GQ0372  Horiz and Ellip are the horizontal and ellipsoid height accuracies
 GQ0372  at the 95% confidence level per Federal Geographic Data Committee
 GQ0372  Geospatial Positioning Accuracy Standards.  SD_N, SD_E and SD_h are
 GQ0372  the standard deviations (one sigma) of the coordinates (NETWORK) or
 GQ0372  of the difference in the coordinates (LOCAL) in latitude, longitude
 GQ0372  and ellipsoid height.  CorrNE is the (unitless) correlation
 GQ0372  coefficient between the latitude and longitude components of either
 GQ0372  the coordinate (NETWORK) or coordinate difference (LOCAL).  Dist is
 GQ0372  the three-dimensional straight-line slope distance, in km, between
 GQ0372  station GQ0372 and the corresponding local station.  Local stations
 GQ0372  are stations processed simultaneously in a session regardless of
 GQ0372  distance.
 GQ0372
 GQ0372  Accuracy and standard deviation values are given in cm.
 GQ0372
 GQ0372  Type/PID  Horiz  Ellip  Dist(km)  SD_N   SD_E   SD_h         CorrNE
 GQ0372  ------------------------------------------------------------------
 GQ0372  NETWORK   0.27   0.55             0.12   0.10   0.28    +0.03899909
 GQ0372  ------------------------------------------------------------------
 GQ0372  LOCAL (019 points):
 GQ0372  AI5115    0.27   0.55    21.08    0.12   0.10   0.28    +0.03309554
 GQ0372  DN3648    0.36   0.71    40.01    0.16   0.13   0.36    +0.04245308
 GQ0372  DN3649    0.45   0.90    42.87    0.20   0.16   0.46    +0.03372403
 GQ0372  DG5949    0.33   0.65    47.30    0.15   0.12   0.33    +0.03937943
 GQ0372  FR0993    0.46   0.90    55.36    0.21   0.16   0.46    +0.05449020
 GQ0372  GQ0305    0.36   0.71    64.58    0.16   0.13   0.36    +0.03417117
 GQ0372  FR0404    0.33   0.71    65.77    0.15   0.12   0.36    +0.03814450
 GQ0372  GR0381    0.32   0.61    71.08    0.14   0.12   0.31    +0.03925330
 GQ0372  GQ0298    0.31   0.67    81.36    0.14   0.11   0.34    +0.02278449
 GQ0372  DG5946    0.27   0.53    98.01    0.12   0.10   0.27    +0.04533029
 GQ0372  AI8807    0.25   0.49   112.57    0.11   0.09   0.25    +0.06329431
 GQ0372  AI8822    0.25   0.49   118.37    0.11   0.09   0.25    +0.03166725
 GQ0372  AJ5640    0.35   0.71   129.84    0.16   0.12   0.36    +0.03271501
 GQ0372  AM7015    0.26   0.53   130.08    0.12   0.09   0.27    +0.05025666
 GQ0372  AJ5639    0.30   0.57   130.87    0.13   0.11   0.29    +0.06127733
 GQ0372  DN3645    0.38   0.76   141.38    0.17   0.14   0.39    +0.05388496
 GQ0372  DG5953    0.36   0.76   166.76    0.16   0.13   0.39    +0.05339158
 GQ0372  DK8419    0.31   0.61   180.16    0.14   0.11   0.31    +0.09441316
 GQ0372  DL1882    0.29   0.55   183.11    0.13   0.10   0.28    +0.00276841
 GQ0372
 GQ0372  MEDIAN    0.32   0.65    98.01
 GQ0372  ------------------------------------------------------------------
```

Figure 6.3. An NGS Accuracy Datasheet with NA2011 results for mark WHITMORE (PID GQ0372).

To extend such visualization and analysis capabilities to NGS customers, the data and results of the NA2011 Project (and this report) are available for downloading from the NGS website (https://geodesy.noaa.gov/). The report is available in the NGS Publications Library

(https://geodesy.noaa.gov/library/pdfs/NOAA_TR_NOS_NGS_0065.pdf), and data are available from a publicly accessible FTP folder (ftp://geodesy.noaa.gov/pub/NA2011/). A "ReadMe.pdf" file in the root of the FTP directory describes its contents and organization.

The GIS data are provided as four feature classes, in both ArcGIS geodatabase and shapefile formats. With these datasets, nearly all of the analyses performed for this report can be reproduced—and many other analyses can be performed, as well. A complete description of the field attributes for the five GIS datasets is provided in the following appendices:

- **Appendix A.** Properties of NA2011 Adjusted Mark GIS Feature Classes
- **Appendix B.** Properties of NA2011 GNSS Vector GIS Feature Classes
- **Appendix C.** Properties of the NA2011 Constrained MYCS1 CORSs GIS Feature Class
- **Appendix D.** Properties of the NA2011 GPS Project GIS Feature Class

The GIS features essentially consist of spatially enabled tables. For those who prefer accessing the data in tabular format, or do not have access to necessary software, each of the GIS features is provided as an *Excel* spreadsheet. These spreadsheets have the same fields as the GIS tables, therefore the descriptions of content in appendices A through D apply to the spreadsheets, as well. However, some of the spreadsheets are quite large. The spreadsheet containing the NA2011 vectors has 426,573 records and is approximately 250 megabytes in size (because of its size, it can only exist in the *.xlsx format, and not the older *.xls format). Data in both GIS and spreadsheet format were used for the analyses, tables, and figures this report. Each format (and the software used to exploit that format) has its advantages.

One of the greatest challenge in preparing this report was managing the extremely large and complex datasets. The final task for the report was organizing and assembling of the datasets in appendices A through D to provide them for public access. The intent is that these datasets serve as useful resources within NGS, as well as for NGS customers and stakeholders.

As crucial as GIS was for the NA2011 Project, even more important is how it may be used for future NGS projects, as well as for organization-wide data management and analysis, beyond individual projects. Because tools can be customized and created using Python scripting languages, the options and functionality are essentially limitless, and this applies not only to NGS internally but also to NGS customers. It is worth stating—again—that GIS is essentially a *spatially enabled database*. That means GIS can be used as a portal for accessing the future NSRS database NGS is in the process of building. Hopefully the role of GIS in the NA2011 Project can serve as an inspiration and example for achieving that vision.

References

Armstrong, M.L., Schenewerk, M. S., Mader, G., Martin, D., Stone, B., and Foote, R., 2015. *OPUS Projects: Online Positioning User Service Baseline Processing and Adjustment Software User Instructions and Technical Guide*, Ver. 2.5, National Oceanic and Atmospheric Administration, National Geodetic Survey, Silver Spring, MD. <https://geodesy.noaa.gov/corbin/class_description/OPUS-Projects_UI_TG_v2.5_Approved_8-05-15.pdf> (Nov 11, 2019)

Bird, P., 2003. An updated digital model of plate boundaries, *Geochemistry, Geophysics, Geosystems*, Vol 4, No 3, 52 pp. <https://agupubs.onlinelibrary.wiley.com/doi/10.1029/2001GC000252> (Oct 3, 2018)

Bossler, J. D., 1984. *Standards and Specifications for Geodetic Control Networks*, Federal Geodetic Control Committee (now the Federal Geodetic Control Subcommittee), 25 pp. <www.ngs.noaa.gov/FGCS/tech_pub/1984-stds-specs-geodetic-control-networks.pdf> (Oct 3, 2018)

Bossler, J. D., 1987. "Geodesy solves 900,000 equations simultaneously," *Eos Trans. AGU*, 68(23), 569– 569, doi:10.1029/EO068i023p00569 <https://agupubs.onlinelibrary.wiley.com/doi/epdf/10.1029/EO068i023p00569> (Nov 15, 2019)

Craymer, M., and Beck, N., 1992. "Session versus single-baseline GPS processing." Proc., ION GPS-92, Institute of Navigation, Alexandria, Va., 995–1004.

DeMets, C., Gordon, R. G., Argus, D. F., and Stein, S., 1994. "Effect of recent revisions to the geomagnetic reversal time scale on estimates of current plate motions." Geophys. Res. Lett., 21(20), 2191-2194.

Dixon, T.H., Amelung, F., Ferretti, A., Novali, F., Rocca, F., Dokka, R., Sella, G., Kim, S.-W., Wdowinski, S., and Whitman, D., 2006. "Subsidence and flooding in New Orleans," Brief Communications, *Nature*, Vol 441. < https://geodesy.noaa.gov/CORS/Articles/441587a.pdf> (Oct 3, 2018)

Eckl, M. C., Snay, R. A., Soler T., Cline, M. W., and Mader, G. L., 2001. "Accuracy of GPS-derived relative positions as a function of interstation distance and observing-session duration." *J. Geod.*, 75(12), 633-640.

FGDC (Federal Geographic Data Committee), 1998. *Geospatial Positioning Accuracy Standards*, FGDC-STD-007.2-1998, Federal Geographic Data Committee, Reston, Virginia, USA, 128 pp., <www.fgdc.gov/standards/projects/FGDC-standards-projects/accuracy/> (Oct 3, 2018) [includes Reporting Methodology (Part 1), Standards for Geodetic Networks (Part 2), National Standard for Spatial Data Accuracy (Part 3), Standards for Architecture, Engineering, Construction (A/E/C) and Facility Management (Part 4), and Standards for Nautical Charting Hydrographic Surveys (Part 5)].

Gillins, D., and Eddy, M. J., 2016. "Comparison of GPS Height Modernization Surveys Using OPUS-Projects and Following NGS-58 Guidelines." *J. Surv. Eng.*, 10.1061/(ASCE)SU.1943-5428.0000196, 05016007.

Griffiths, J., 2012. Personal communication. National Geodetic Survey.

Han, S., and Rizos, C., 1995. "Selection and scaling of simultaneous baselines for GPS network adjustment, or correct procedures for processing trivial baselines." Geomatics Res. Australasia, 63, 51–68.

Hofmann-Wellenhof, B., Lichtenegger, H., and Collins, J., 2001. *GPS—Theory and Practice*, 5th ed. Springer Verlag, New York.

Holdahl, S.R., Holzschuh, J.C., and Zilkoski, D.B., 1989. "Subsidence at Houston, Texas 1973-87," *NOAA Technical Report NOS 131 NGS 44*, National Geodetic Survey, Silver Spring, MD. <https://geodesy.noaa.gov/PUBS_LIB/Subsidence_at_Houston_Texas_TR_NOS131_NGS44.pdf> (Oct 3, 2018)

IGS (International GNSS Service), 2019. "Figures and Statistics for Broadcast Orbits wrt IGS Rapid Orbits," <http://www.igs.org/analysis/gps-broadcast> (Nov 19, 2019)

Institut Géographique National, 2016. International Terrestrial Reference Frame, Transformation parameters, <itrf.ign.fr/trans_para.php> (Oct 3, 2018)

International Earth Rotation and Reference Systems Service, 2015. "The International Terrestrial Reference Frame (ITRF)." <www.iers.org/IERS/EN/Home/home_node.html> (Oct 3, 2018)

Kashani, I., Wielgosz, P., and Grejner-Brzezinska, D.A., 2004. "On the reliability of the VCV Matrix: A case study based on GAMIT and Bernese GPS Software." *GPS Solutions*, (2004)8:193-199. DOI 10.1007/s10291-004-0103-9.

Leenhouts, P. P., 1985. "On the Computation of Bi-Normal Radial Error," *Navigation*, 32 (1), 16-28.

Leick, A., Rapoport, L., and Tatarnikov, D., 2015. *GPS Satellite Surveying* (4th Edition), John Wiley & Sons, New York, New York, USA, 807 pp.

Lucas, J.R., 1985. "A variance component estimation method for sparse matrix applications." *NOAA Technical Report* NOS 111 NGS 33. National Geodetic Survey, NOAA, Silver Spring, MD.

Mader, G., Schenewerk, M., Weston, N., Evjen, J., Tadepalli, K., and Neti, J., 2012. "Interactive web-based GPS network processing and adjustment using NGS' OPUS-Projects." In: *Proceedings of the FIG working week 2012*, Rome, Italy.

Milbert, D.G. and Kass, W.G., 1987. "*ADJUST*: The Horizontal Observation Adjustment Program," *NOAA Technical Memorandum NOS NGS- 47*, <https://geodesy.noaa.gov/PUBS_LIB/Adjust_TheHorizontalObservationAdjustmentProgram_TM_NOS_NGS_47.pdf> (Oct 3, 2018)

Milbert, D.G., 2009. An Analysis of the NAD 83 (NSRS2007) National Readjustment, National Geodetic Survey, Silver Spring, MD, USA, <https://geodesy.noaa.gov/PUBS_LIB/NSRS2007/NSRS2007Analysis.pdf> (Oct 3, 2018)

NGS (National Geodetic Survey), 1986. *Geodetic Glossary*, National Geodetic Survey, Rockville, Maryland, USA, 274 pp. <https://geodesy.noaa.gov/CORS-Proxy/Glossary/xml/NGS_Glossary.xml> (Oct 3, 2018) *[online version last updated in 2009]*

NGS (National Geodetic Survey), 2012. "Data Submission Policy," *NGS Policy 06-2012*, National Oceanic and Atmospheric Administration, National Geodetic Survey, Silver Spring, Maryland. <https://geodesy.noaa.gov/INFO/Policy/files/062012_Data_Submission_Policy.pdf> (Oct 3, 2018)

NGS (National Geodetic Survey), 2013a. *The National Geodetic Survey Ten-Year Strategic Plan: 2013-2023***,** National Geodetic Survey, Silver Spring, Maryland, 48 pp. <https://geodesy.noaa.gov/web/news/Ten_Year_Plan_2013-2023.pdf> (Oct 3, 2018)

NGS (National Geodetic Survey), 2013b. *MYCS1 CORS Coordinates*, National Geodetic Survey, Silver Spring, Maryland <https://geodesy.noaa.gov/CORS/MYCS1.shtml> (Nov 14, 2019)

NGS (National Geodetic Survey), 2018a. *ADJUST Supplemental Documentation*. National Oceanic and Atmospheric Administration, National Geodetic Survey, Silver Spring, MD. <http://www.ngs.noaa.gov/PC_PROD/ADJUST/adjust_supplemental.txt> (Nov 19, 2019).

NGS (National Geodetic Survey), 2018b. *Constrained Adjustment Guidelines*. National Oceanic and Atmospheric Administration, National Geodetic Survey, Silver Spring, Maryland. <https://geodesy.noaa.gov/PC_PROD/ADJUST/adjustment_guidelines.pdf> (Nov 19, 2019)

NGS (National Geodetic Survey), 2019a. *Multi-Year CORS Solution 2 (MYCS2) Coordinates*, National Geodetic Survey, Silver Spring, Maryland. <https://geodesy.noaa.gov/CORS/coords.shtml> (Nov 14, 2019)

NGS (National Geodetic Survey), 2019b. *National Geodetic Survey Strategic Plan: 2019-2023***,** National Geodetic Survey, Silver Spring, Maryland, 60 pp. <https://www.ngs.noaa.gov/web/about_ngs/info/documents/ngs-strategic-plan-2019-2023.pdf> (Nov 13, 2019)

NGS (National Geodetic Survey), 2019c. *NOAA Technical Report NOS NGS 67***,** "Blueprint for 2022, Part 3: Working in the Modernized NSRS," National Geodetic Survey, Silver Spring, Maryland, 77 pp. <https://geodesy.noaa.gov/PUBS_LIB/NOAA_TR_NOS_NGS_0067.pdf> (Nov 14, 2019)

NGS (National Geodetic Survey), 2019d. *Input Formats and Specifications of the National Geodetic Survey Data Base*, Volume I. Horizontal Control Data (and Annexes A-P), Federal Geodetic Data Committee, National Geodetic Survey, Silver Spring, Maryland. <https://geodesy.noaa.gov/FGCS/BlueBook/> (Nov 14, 2019)

NGS (National Geodetic Survey), 2019e. *The DSDATA Format*, National Geodetic Survey, Silver Spring, Maryland, 46 pp. <https://geodesy.noaa.gov/DATASHEET/dsdata.pdf> (Nov 11, 2019)

Øvstedal, O., 2000. "Single Processed Independent and Trivial Vectors in Network Analysis," *Journal of Surveying Engineering*, Vol. 126, No. 1, pp. 18-25.

Pearson, C., and Snay, R., 2007. "Updating *HTDP* for two recent earthquakes in California." Surv. Land Inf. Sci., 67(3), 149e158.

Pearson, C., and Snay, R., 2013. "Introducing *HTDP* 3.1 to transform coordinates across time and spatial reference frames." GPS Solutions, 17:1–15.

Pearson, C., McCaffrey, R., Elliot, J. L., and Snay, R., 2010. "*HTDP* 3.0: Software for coping with the coordinate changes associated with crustal motion." J. Surv. Eng., 136(2), 80-90.

Petit, G. and Luzum, B., eds., 2010. "IERS Conventions 2010," *IERS Technical Note No. 36*, International Earth Rotation and Reference Systems Service. <ftp://tai.bipm.org/iers/conv2010/tn36.pdf> (Nov 19, 2019)

Pursell, D.G. and Potterfield, M., 2008. NAD 83 (NSRS2007) National Readjustment Final Report, *NOAA Technical Report NOS NGS 60*, National Geodetic Survey, Silver Spring, MD, USA, 75 pp, <https://geodesy.noaa.gov/PUBS_LIB/NSRS2007/NOAATRNOSNGS60.pdf> (Oct 3, 2018)

Schenewerk, M., Dillinger, W., and Hilla, S., 1999), *Program for Adjustment of GPS Ephemerides* (*PAGES*). < https://geodesy.noaa.gov/GRD/GPS/DOC/pages/pages.html> (Oct 3, 2018)

Schwarz, C.R., ed., 1989. North American Datum of 1983, *NOAA Professional Paper NOS 2*, U.S. Department of Commerce, National Oceanic and Atmospheric Administration, National Geodetic

Survey, Rockville, Maryland, USA, 256 pp., <https://geodesy.noaa.gov/PUBS_LIB/NADof1983.pdf> (Oct 3, 2018)

Scripps Orbit and Permanent Array Center, 2017. *SECTOR: Scripps Epoch Coordinate Tool and Online Resource*, Scripps Orbit and Permanent Array Center, Scripps Institution of Oceanography. <sopac.ucsd.edu/sectorREADME.html> (Oct 3, 2018)

Shinkle, K.D. and Dokka, R.K., 2004. "Rates of vertical displacement at benchmarks in the lower Mississippi Valley and the Northern Gulf Coast," *NOAA Technical Report NOS NGS 50*, National Geodetic Survey, Silver Spring, MD, USA. <https://geodesy.noaa.gov/heightmod/NOAANOSNGSTR50.pdf> (Oct 3, 2018)

Smith, D.A., and Bilich, A., 2017. "NADCON 5.0: Geometric Transformation Tool for points in the National Spatial Reference System," *NOAA Technical Report NOS NGS 63*, National Oceanic and Atmospheric Administration, National Geodetic Survey, Silver Spring, Maryland. <https://geodesy.noaa.gov/library/pdfs/NOAA_TR_NOS_NGS_0063.pdf> (Oct 3, 2018)

Smith, D.A., and Bilich, A., 2019. "The VERTCON 3.0 Project: Creating vertical transformations for points in the National Spatial Reference System, including VERTCON 3.0 release 20190601," *NOAA Technical Report NOS NGS 68*, National Oceanic and Atmospheric Administration, National Geodetic Survey, Silver Spring, Maryland. <https://geodesy.noaa.gov/library/pdfs/NOAA_TR_NOS_NGS_0068.pdf> (Nov 19, 2019)

Snay, R. A., 1999. "Using the *HTDP* software to transform spatial coordinates across time and between reference frames." Surv. Land Inf. Sys., 59(1), 15-25. <https://geodesy.noaa.gov/TOOLS/Htdp/Using_HTDP.pdf > (Oct 3, 2018)

Snay, R. A., 2003. "Introducing two spatial reference frames for regions of the Pacific Ocean." Surv. Land Inf. Sci., 63(1), 5-12.

Snay, R. A., and Soler, T., 2008. "Continuously operating reference mark (CORS): History, applications, and future enhancements." J. Surv. Eng., 134(4), 95-104.

Snay, R.A., 2003. Introducing two spatial reference frames for regions of the Pacific Ocean. *Surv Land Inf Sci* 63:5–12.

Snay, R.A., 2006. *HTDP—Horizontal Time Dependent Positioning*, National Geodetic Survey, Silver Spring, Maryland, <https://geodesy.noaa.gov/TOOLS/Htdp/Htdp.shtml> (Oct 3, 2018)

Snay, R.A., 2012. Evolution of NAD 83 in the United States: Journey from 2D toward 4D, *Journal of Surveying Engineering*, American Society of Civil Engineers, Vol. 138, No. 4, pp. 161-171.

Soler, T. and Snay, R.A., 2004. Transforming Positions and Velocities between the International Terrestrial Reference Frame of 2000 and North American Datum of 1983, *Journal of Surveying Engineering*, American Society of Civil Engineers, Vol. 130, No. 2, pp. 49-55, <geodesy.noaa.gov/CORS/Articles/SolerSnayASCE.pdf> (Oct 3, 2018)

Soler, T., 2014. *CORS Coordinates*, National Geodetic Survey, Silver Spring, Maryland, <https://geodesy.noaa.gov/CORS/coords.shtml> (Oct 3, 2018)

Weston, N.D., Mader, G.L., and Soler, T., 2007. "OPUS Projects – A Web-based application to administer and process multi-day GPS campaign data." *Proc. of FIG (International Federation of Surveyors) Working Week*, FIG, Hong Kong, China.

Zilkoski, D.B. and Middleton, C., 2011. *Results of the February 2011 Harris Galveston Subsidence District Subsidence Study*, unpublished report, Harris-Galveston Subsidence District, Friendswood, TX.

Zilkoski, D.B. and Reese, S.M., 1986. "Subsidence in the Vicinity of New Orleans as Indicated by Analysis of Geodetic Leveling Data", *NOAA Technical Report NOS 120 NGS 38*, National Geodetic Survey, Silver Spring, MD. <https://geodesy.noaa.gov/PUBS_LIB/SubsidenceInTheVicinityOfNewOrleans_TR_NOS120_NGS38.pdf> (Oct 3, 2018)

Zilkoski, D.B., Hall L.W., Mitchell, G.J., Kammula, V., Singh, A., Chrismer, W.M., and Neighbors, R.J., 2003. *The Harris-Galveston Coastal Subsidence District/National Geodetic Survey Automated Global Positioning System Subsidence Monitoring Project*., Harris-Galveston Subsidence District, Friendswood, TX <http://hgsubsidence.org/wp-content/uploads/2014/07/GPS-Project.pdf> (July 19, 2020)

Appendix A. Properties of NA2011 Adjusted Mark GIS Feature Classes

The NA2011 adjusted mark GIS feature classes are point features provided in Esri file geodatabase format version 10.7, available at ftp://geodesy.noaa.gov/pub/NA2011/. Because the data are referenced to three different NAD 83 frames, the features are separated into three feature datasets corresponding to that particular frame. An ArcMap v10.7 document (*.mxd file) that reference the features are included. A "ReadMe.pdf" file in the root of the folder describes the contents and organization.

Feature classes are also provided in Esri shapefile formats with the same field names and attributes. However, shapefiles do not support a date field that also includes time, so time is stored in its own field separate from the date. In addition, shapefiles do not support null fields or relationships between feature classes. Numeric null fields in shapefiles are populated with a value of -9999.

The features are also provided in Microsoft *Excel* format, with all three NAD 83 frames combined into in a single file.

Note: Adjusted CORS coordinates in this dataset are not the same as the published values that were used as constraints, because stochastic constraints were used. See Appendix C for the constrained CORS coordinates determined in the MYCS1.

General characteristics of the NA2011 adjusted control mark GIS feature classes

- Feature geometry: Point
- Number of features: 81,055 points split into three feature classes based on the NAD 83 frame of the coordinates, all at epoch 2010.00 (January 1, 2010):
  - NAD 83 (2011): Referenced to the North America tectonic plate (80,515 points)
  - NAD 83 (PA11): Referenced to the Pacific tectonic plate (363 points)
  - NAD 83 (MA11): Referenced to the Mariana tectonic plate (177 points)
- Number of fields: 60 (defined in Table A1)
- Data types: Short integer, Float, Double, Date/time, Text
- Domains used for 9 text fields (defined in Table A2)
- Geometry does not support M values (route data) or Z values (3D data)
- Shapefile versions have time in separate field from date

Table A1. Data field attribute definitions of the NA2011 adjusted control mark GIS feature classes.

Field name	Field alias	Data type	Field description
PID	Permanent ID	Text (6)	NGS permanent identifier for the mark
Mark_name	Mark name (designation)	Text (40)	Name of mark (also called designation)
Mark_type	Mark type	Text (7)	Type of mark in context of adjustment (2 domain values; see description in table below)
NAD83frame	NAD 83 frame	Text (13)	NAD 83 frame of the coordinates (3 domain values; see description in table below)
Lat_DMS	Latitude (DMS)	Text (13)	Final adjusted latitude (degrees-minutes-seconds); ***NOT*** the same as published values for CORSs
Lon_DMS	Longitude (DMS)	Text (14)	Final adjusted longitude (degrees-minutes-seconds); ***NOT*** the same as published values for CORSs
Lat_DecDeg	Latitude (dec deg)	Double	Final adjusted latitude (decimal degrees); ***NOT*** the same as published values for CORSs
Lon_DecDeg	Longitude (dec deg)	Double	Final adjusted latitude (decimal degrees); ***NOT*** the same as published values for CORSs
Elpsd_ht	Ellipsoid height (m)	Double	Final adjusted ellipsoid height (meters); ***NOT*** the same as published values for CORSs
Acc95_hor	Accuracy hor 95% conf (cm)	Float	Horizontal (circular) accuracy at 95% confidence (cm)
Acc95_eht	Accuracy eht 95% conf (cm)	Float	Ellipsoid height accuracy at 95% confidence (cm)
Acc95_3D	Accuracy 3D 95% conf (cm)	Float	3D accuracy at 95% confidence (cm)
Err_a_axis	Error a axis 95% conf (cm)	Float	Semi-major (a) axis of error ellipse, scaled to 95% confidence (cm)
Err_b_axis	Error b axis 95% conf (cm)	Float	Semi-minor (b) axis of error ellipse, scaled to 95% confidence (cm)
Ratio_a_b	Ratio a/b (elongation)	Float	Ratio of error ellipse axes (a/b) or ellipse elongation (unitless)
Err_azimth	Error azimuth (deg)	Float	Azimuth of semi-major (a) axis of error ellipse (decimal degrees)
Sigma_N	Sigma north (cm)	Float	Standard deviation in latitude (cm)
Sigma_E	Sigma east (cm)	Float	Standard deviation in longitude (cm)
Sigma_U	Sigma up (cm)	Float	Standard deviation in ellipsoid height (cm)
Correl_NE	Correlation north-east	Double	Horizontal (north-east) correlation coefficient (unitless)
Shift_N	Shift north (cm)	Float	Shift (change) in latitude from previously published value (cm)
Shift_E	Shift east (cm)	Float	Shift (change) in longitude from previously published value (cm)
Shift_U	Shift up (cm)	Float	Shift (change) in ellipsoid height from previously published value (cm)
ShiftU_ABS	ABS shift up (cm)	Float	Absolute value of shift (change) in ellipsoid height from previously published value (cm)
Shift_hor	Shift horz (cm)	Float	Horizontal shift (change) from previously published value (cm)
Shift_az	Shift azimuth (deg)	Float	Azimuth of horizontal shift (change) from previously published value (decimal degrees)
Shift_3D	Shift 3D (cm)	Float	3D shift (change) from previously published value (cm)

Field name	Field alias	Data type	Field description
VecsEnable	Num vectors enabled	Short integer	Number of enabled vectors connected to the mark
VecsReject	Num vectors rejected	Short integer	Number of rejected vectors connected to the mark
VecsTotal	Num vectors total	Short integer	Total number of vectors connected to the mark
No_check	No check	Text (4)	Coordinates determined by a single vector (2 domain values; see description in table below)
NumOccAll	Num occupations all	Short integer	Total number of times mark was occupied (based on all vectors)
NumOccEnab	Num occupations enabled	Short integer	Number of times mark was occupied (based only on enabled vectors)
DateFrstOc*	Date time first occupied*	Date/time	Start date and time of first occupation of the mark (based on all vectors)
DateLastOc*	Date time last occupied*	Date/time	End date and time of last occupation of the mark (based on all vectors)
DateFrstEn*	Date time first enabled*	Date/time	Start date and time of first occupation of the mark (based only on enabled vectors)
DateLastEn*	Date time last enabled*	Date/time	End date and time of last occupation of the mark (based only on enabled vectors)
EpocFrstOc*	Epoch first occupied*	Double	Start epoch (decimal year) of first occupation of the mark (based on all vectors)
EpocLastOc*	Epoch last occupied*	Double	End epoch (decimal year) of last occupation of the mark (based on all vectors)
EpocFrstEn*	Epoch first enabled occup*	Double	Start epoch (decimal year) of first occupation of the mark (based only on enabled vectors)
EpocLastEn*	Epoch last enabled occup*	Double	End epoch (decimal year) of last occupation of the mark (based only on enabled vectors)
CORS_ID	CORS ID	Text (4)	4-character CORS identification code
MYCS_type	MYCS type	Text (8)	Type of MYCS1 coordinate (2 domain values; see description in table below)
CORSsource	CORS ID source	Text (10)	Source used to identify MYCS1 CORS ID (4 domain values; see description in table below)
ConstrNet	Constraint network	Text (9)	Network to which constraint was applied (4 domain values; see description in table below)
ConstrType	Constraint type	Text (9)	Type of mark used as a constraint (2 domain values; see description in table below)
SigConstrN	Sigma constr north (cm)	Float	Standard deviation in latitude used for constraint weight (cm)
SigConstrE	Sigma constr east (cm)	Float	Standard deviation in longitude used for constraint weight (cm)
SigConstrU	Sigma constr up (cm)	Float	Standard deviation in ellipsoid height used for constraint weight (cm)
State	State	Text (2)	2-letter abbreviation of state or territory where mark located
Block	Helmert block	Text (8)	Helmert block code based on GPS project location ("Multiple" means mark in more than 1 block)
Num_blocks	Num blocks	Short integer	Number of Helmert blocks in which mark occurs
Network	Network	Text (20)	Network where final coordinates were determined (9 domain values; see description in table below)
PrimSubnet	Primary subnetwork	Short integer	Number assigned to CONUS Primary subnetworks (none for Alaska or Pacific networks)
SecSubnet	Secondary subnetwork	Short integer	Number assigned to CONUS Secondary subnetworks (none for Alaska or Pacific networks)
GulfSubsid	Gulf Coast subsidence	Text (1)	Indicates whether mark is in Gulf Coast subsidence region as identified for this project ("Y" or "N")
Not_pub	Not published	Text (20)	Populated for marks not published by NGS (6 domain values; see description in table below)

Field name	Field alias	Data type	Field description
Excluded	Excluded	Text (1)	Indicates whether coordinates for a mark were excluded from final adjustments ("Y" or "N")
CommentCon	Comments on constraints	Text (60)	Comments about constraints used in adjustments (12 unique comments shown in table below)
CommentGen	Comments general	Text (60)	General comments about a mark (15 unique comments shown in table below)

*Time zone unknown; assume GPS time was used for most cases.

Table A2. Domains of text data field attributes and free-form text fields for control mark feature classes.

Count	Field name and text attributes (for defined domains and free-form text)	
	Mark_type *(domain)*	**Domain description**
79,860	Passive	Mark with no MYCS1 coordinates (coordinates determined in project)
1,195	CORS	Mark identified as a CORS (constrained MYCS1 coordinates)
	NAD83frame *(domain)*	**Domain description**
80,515	NAD 83 (2011)	Referenced to the North America tectonic plate
363	NAD 83 (PA11)	Referenced to the Pacific tectonic plate
177	NAD 83 (MA11)	Referenced to the Mariana tectonic plate
	No_check *(domain)*	**Domain description**
333	Soft	Multiple vector connections but only one enabled vector
1,801	Hard	Only a single vector connection total (no rejected vectors available)
	MYCS_type *(domain)*	**Domain description**
973	Computed	Coordinates based on velocities computed from GPS data
222	Modeled	Coordinates based on velocities modeled using NGS HTDP software
	CORSsource *(domain)*	**Domain description**
1,019	MYCS	MYCS1 CORS ID obtained directly from MYCS results
90	NGSIDB	MYCS1 CORS ID determined from NGSIDB
134	Inferred	MYCS1 CORS ID inferred from location, designation, or other information
1	Not a CORS	IGS station not part of CORS network and not included in MYCS1

Count	Field name and text attributes (for defined domains and free-form text)	
	ConstrNet *(domain)*	**Domain description**
1,096	Primary	CORS constrained only in CONUS Primary network
5,233	Secondary	CORS or passive mark constrained only in CONUS Secondary network
29	Both	CORS constrained in both CONUS Primary and Secondary networks
58	Alaska	CORS constrained in Alaska network
24	Pacific	CORS constrained in both Pacific networks (for Pacific and Mariana plates)
	ConstrType *(domain)*	**Domain description**
1,195	CORS MYCS	Constrained to NAD 83 coordinates determined in MYCS1
5,245	Passive	Constrained to passive coordinates determined in the Primary Network
	Network *(domain)*	**Domain description**
56,895	CONUS Primary	Coordinates determined by vectors only in CONUS Primary network
17,148	CONUS Secondary	Coordinates determined by vectors only in CONUS Secondary network
5,129	CONUS Both_Primary	Coordinates determined by vectors in both networks from Primary network adjustment
192	CONUS Both_Secondary	Coordinates determined by vectors in both networks from Secondary network adjustment
969	Alaska	Coordinates determined by vectors in Alaska network
363	Pacific_PA11	Coordinates determined by vectors in Pacific network, with NAD 83 (PA11) constraints
177	Pacific_MA11	Coordinates determined by vectors in Pacific network, with NAD 83 (MA11) constraints
148	CONUS Primary_post	Coordinates of Primary mark not determined because connected only to Secondary marks
34	CONUS Secondary_post	Coordinates of Secondary mark not determined because connected only to Primary marks
	Not_pub *(domain)*	**Domain description**
4,795	FAA mark	Airport features not suitable as geodetic control (such as runway endpoints)
93	Canada	Mark located outside United States (Canada)
8	Mexico	Mark located outside United States (Mexico)
1	Colombia	Mark located outside United States (Colombia)
1	French Guiana	Mark located outside United States (French Guiana)
1	IGS station only	IGS station not an NGS CORS and no description (not publishable from NGSIDB)

	CommentCon *(all unique text strings in free-form comment field)*
5,212	Primary passive constrained in secondary network
74	Only constrained in free adjustment (Secondary network)
28	Passive mark constrained in subnetwork with no CORS
24	CORS not constrained
11	No MYCS coordinates available, so not constrained
9	Constrained to CORS coordinates determined in April 2012
8	CORS not constrained (added to CORS network after project)
7	CORS not constrained (rejected as constraint)
5	CORS constrained in Secondary (but not in Primary)
1	Constrained to MYCS CORS ID = GOL2
1	Constrained to MYCS CORS ID = SHK1
1	Constrained to MYCS CORS ID = NJTW
	CommentGen *(all unique text strings in free-form comment field)*
229	Caribbean or South America mark
103	No-check in Primary (not no-check in Secondary)
74	Disconnected subnetwork in Primary (used Secondary)
34	All Secondary vectors rejected
34	Very large error due to being in disconnected subnetwork
13	Large error in Primary; used Secondary results
13	Not counted as hard no check because constrained as CORS
8	Results superseded (mark incorporated into CORS network)
2	Published as passive mark
2	Used superseded datasheet ellipsoid height for height shift
2	New PID due to merging with leveled mark
1	Mark not tied in Pacific network (in Alaska project)
1	All Primary vectors rejected
1	No ellipsoid height prior to NA2011 adjustment
1	PID merged with AI4496 (MYCS PID is for ORVB mon)

Appendix B. Properties of NA2011 GNSS Vector GIS Feature Classes

The NA2011 GNSS vector GIS feature classes are line features provided in Esri file geodatabase format version 10.7, available at ftp://geodesy.noaa.gov/pub/NA2011/. Because the data are referenced to three different NAD 83 frames, the features are separated into three feature datasets corresponding to that particular frame. An ArcMap v10.7 document (*.mxd file) that reference the features are included. A "ReadMe.pdf" file in the root of the folder describes the contents and organization.

Feature classes are also provided in Esri shapefile formats with the same field names and attributes. However, shapefiles do not support a date field that also includes time, so time is stored in its own field separate from the date. In addition, shapefiles do not support null fields or relationships between feature classes. Numeric null fields in shapefiles are populated with a value of -9999.

The features are also provided in Microsoft *Excel* format, with all three NAD 83 frames combined into in a single file.

Note: Vectors in the Pacific PA11 and MA11 networks are represented twice in the spreadsheet, because they same set of vectors was used for both Pacific networks. Constraints referenced to NAD 83 (PA11) were used for the PA11 vectors, and constraints referenced to NAD 83 (PA11) were used for the PA11 vectors. The vectors are therefore referenced to these respective frames and have slightly different residuals (and unique vector IDs).

General characteristics of the NA2011 GNSS vector GIS feature classes

- Feature geometry: Line
- Number of features: 426,573 lines split into three feature classes based on the NAD 83 frame of the coordinates, all at epoch 2010.00 (January 1, 2010):
  - NAD 83 (2011): Referenced to the North America tectonic plate (422,869 lines)
  - NAD 83 (PA11): Referenced to the Pacific tectonic plate (1,852 lines)
  - NAD 83 (MA11): Referenced to the Mariana tectonic plate (1,852 lines)
- Number of fields: 73 (defined in Table B1)
- Data types: Short integer, Long integer, Float, Double, Date/time, Text
- Domains used for 5 text fields (defined in Table B2)
- Geometry does not support M values (route data) or Z values (3D data)
- Shapefile versions have time in separate field from date

Table B1. Data field attribute definitions of the NA2011 GNSS vector GIS feature classes.

Field name	Field alias	Data type	Field description
UniqueID	Unique ID	Text (16)	Unique ID created from network and G-file name and line number
Network	Network	Text (15)	Network in which vectors were adjusted (5 domain values; see description in table below)
NAD83frame	NAD 83 frame	Text (13)	NAD 83 frame of the vectors (3 domain values; see description in table below)
Prom_PID	From mark PID	Text (6)	PID of "from" mark of vector (origin or stand point)
To_PID	To mark PID	Text (6)	PID of "to" mark of vector (head or fore point)
From_SSN	From G-file SSN	Text (4)	Station Serial Number used in G-file for "from" mark
To_SSN	To G-file SSN	Text (4)	Station Serial Number used in G-file for "to" mark
From_mark	From mark name	Text (40)	Name (designation) of "from" mark of vector (origin or stand point)
To_mark	To mark name	Text (40)	Name (designation) of "to" mark of vector (head or fore point)
BaselineID	Baseline ID	Text (13)	Unique ID of baseline between two marks (created from endpoint PIDs)
Num_vec_BL	Num vecs per baseline	Short integer	Number of vectors representing the baseline
NumDupVecs	Num duplicate vecs	Short integer	Number of duplicate vectors (represented more than once); zero means no duplicates
Vector_dX	Vector dX (m)	Double	Delta X component of vector in Earth-Centered, Earth-Fixed (ECEF) Cartesian coordinates (m)
Vector_dY	Vector dY (m)	Double	Delta Y component of vector in Earth-Centered, Earth-Fixed (ECEF) Cartesian coordinates (m)
Vector_dZ	Vector dZ (m)	Double	Delta Z component of vector in Earth-Centered, Earth-Fixed (ECEF) Cartesian coordinates (m)
Sigma_X	Sigma X (m)	Float	Standard deviation of X component of vector (m)
Sigma_Y	Sigma Y (m)	Float	Standard deviation of Y component of vector (m)
Sigma_Z	Sigma Z (m)	Float	Standard deviation of Z component of vector (m)
Correl_XY	Correlation XY	Double	XY correlation coefficient of vector variance-covariance matrix (unitless)
Correl_XZ	Correlation XZ	Double	XZ correlation coefficient of vector variance-covariance matrix (unitless)
Correl_YZ	Correlation YZ	Double	YZ correlation coefficient of vector variance-covariance matrix (unitless)
Sigma_N	Sigma north (m)	Float	Standard deviation of north component of vector (m)
Sigma_E	Sigma east (m)	Float	Standard deviation of east component of vector (m)
Sigma_U	Sigma up (m)	Float	Standard deviation of up component of vector (m)
Sigma_3D	Sigma 3D (m)	Float	3D standard deviation of vector (m)
s3D_scaled	Sigma 3D scaled (m)	Float	3D standard deviation of vector scaled by GPS project 3D variance factor (m)
Vec_length	Vector length (m)	Double	Length of vector, mark-to-mark (m)

Field name	Field alias	Data type	Field description
Time_start*	Date time session start*	Date/time	Start date and time of first vector session processing
Time_end*	Date time session end*	Date/time	End date and time of first vector session processing
EpochMidpt*	Epoch midpoint (dec yr)*	Double	Epoch of midpoint time of vector processing session (decimal year)
Year_midpt	Year of midpoint	Short integer	Year corresponding to midpoint time of vector processing session
DurationHr	Duration (hr)	Float	Duration of vector processing session (hours)
G_sess_num	G-file session num	Long integer	Number assigned to processing session as given in the vector G-file
Gvecs_sess	Num vecs in G-file session	Short integer	Number of vectors in processing session as given in the vector G-file
NumVecCalc	Num vecs in calcd session	Short integer	Number of vectors in processing session, calculated from all vectors in NA2011 project
Sesion_ID	Unique calcd session ID	Text (11)	Unique ID assigned to session, based on year, day of year, and calculated session number
Soln_type	Processing solution type	Text (15)	Type of baseline processing in session (5 domain values; see description in table below)
Num_marks	Num marks in session	Short integer	Number of marks in processing session, calculated from all vectors in NA2011 project
NumTrivial	Num triv vecs in session	Short integer	Actual number of trivial vectors in processing session (assuming all vectors enabled)
TrivPossbl	Num triv vecs possible	Short integer	Maximum number of trivial vectors possible in session (assuming all vectors enabled)
Repeat_vec	Num repeat vecs	Short integer	Number of vectors represented more than once in session (based on >= 50% time overlap)
TrvScalAll**	Triv vec scalar all**	Float	Scalar to apply to sigmas to account for trivial vector false redundancy (for all vectors enabled)
TrvScalEna**	Triv vec scalar enabled**	Float	Scalar to apply to sigmas to account for trivial vector false redundancy (for all vectors enabled)
Status	Status	Text (1)	Status of vector used in final adjustments (2 domain values; see description in table below)
N_res_free	N resid free (cm)	Float	North component of vector residual in final free (minimally constrained) adjustment (cm)
E_res_free	E resid free (cm)	Float	East component of vector residual in final free (minimally constrained) adjustment (cm)
U_res_free	U resid free (cm)	Float	Up component of vector residual in final free (minimally constrained) adjustment (cm)
ABS_U_free	ABS U resid free (cm)	Float	Absolute value of up component of vector residual in final free adjustment (cm)
HorResFree	Horz resid free (cm)	Float	North component of vector residual in final free (minimally constrained) adjustment (cm)
3D_ResFree	3D resid free (cm)	Float	3D vector residual in final free (minimally constrained) adjustment (cm)
N_res_cnst	N resid constr (cm)	Float	North component of vector residual in final constrained adjustment (cm)
E_res_cnst	E resid constr (cm)	Float	East component of vector residual in final constrained adjustment (cm)
U_res_cnst	U resid constr (cm)	Float	Up component of vector residual in final constrained adjustment (cm)
ABS_U_cnst	ABS U constr (cm)	Float	Absolute value of up component of vector residual in final constrained adjustment (cm)
HorResCnst	Hor resid constr (cm)	Float	North component of vector residual in final constrained adjustment (cm)
3D_ResCnst	3D resid constr (cm)	Float	3D vector residual in final constrained adjustment (cm)
ConFreeRes	Ratio constr 3D res to free	Float	Ratio of constrained 3D residual to free 3D residual (unitless)

Field name	Field alias	Data type	Field description
Software	Processing software	Text (15)	GNSS processing software used, as given in G-file (400 unique strings)
OrbSource	Orbit source	Text (5)	Source of orbits used in processing (15 domain values; see description in table below)
RefSysOrig	Orig ref system	Short integer	Original vector coordinate system code, before transforming to NAD 83 (25 unique values)
Agency	Agency	Text (6)	Agency or organization that performed processing (234 unique abbreviations)
Proj_ID	GPS project ID	Text (11)	GPS Project ID as assigned by NGS
GfileName	G-file name	Text (21)	Name assigned to G-file created from NGS Integrated Data Base
Gfile_line	G-file line number	Long integer	Line number of vector in G-file
SubsidRate	Subsidence rate (mm/yr)	Float	Subsidence rate estimated for Gulf Coast subsidence region
SubsidTime	Subsidence time span (yr)	Float	Time span between vector time midpoint and 2010.00 for Gulf Coast subsidence region
Subsid_est	Estimated subsidence (m)	Float	Estimated total subsidence (used for down-weighting up-component of vector)
Lat_midpnt	Latitude midpoint	Double	Approximate vector midpoint latitude (mean of latitude endpoints)
Lon_midpnt	Longitude midpoint	Double	Approximate vector midpoint longitude (mean of longitude endpoints)
Excluded	Excluded	Text (1)	Indicates whether vectors were excluded from all final adjustments ("Y" or "N")
CommentGen	Comments general	Text (45)	General comments about vectors (6 unique comments, as shown in table below)
Comment_BL	Comments baseline lengths	Text (45)	Baselines with large differences in vector lengths (6 unique comments, as shown in table below)
ComentTime	Comments date and time	Text (45)	Date & time issues, indicating whether edited (9 unique comments, as shown in table below)

*Time zone unknown; assume GPS time was used for most cases.
**Scalar is for combined effect of trivial and repeat vectors; scalars were not applied to vectors in this dataset or those used in actual adjustments.

Table B2. Domains of text data field attributes and free-form text fields of GNSS vector feature classes.

Count	Field name and text attributes (for defined domains and free-form text)	
	Network *(domain)*	**Domain description**
335,530	CONUS Primary	Vectors in CONUS Primary network
84,493	CONUS Secondary	Vectors in CONUS Secondary network
2,846	Alaska	Vectors in Alaska network
1,852	Pacific_PA11	Vectors in Pacific network, with NAD 83 (PA11) residuals
1,852	Pacific_MA11	Vectors in Pacific network, with NAD 83 (MA11) residuals

Count	Field name and text attributes (for defined domains and free-form text)	
	NAD83frame *(domain)*	**Domain description**
80,515	NAD 83 (2011)	Referenced to the North America tectonic plate
363	NAD 83 (PA11)	Referenced to the Pacific tectonic plate
177	NAD 83 (MA11)	Referenced to the Mariana tectonic plate
	Soln_type *(domain)*	**Domain description**
314,042	Sequential	All vectors processed sequentially
59,586	Simultaneous	All vectors processed simultaneously
20,045	Seq and simult	Both sequential and simultaneous processing
18,285	Single vector	Single vector in session (sequential)
14,615	Multiple simult	Two or more simultaneous sets in session
	Status *(domain)*	**Domain description**
404,912	E	Vector enabled
21,661	R	Vector rejected (by downweighting)
	OrbSource *(domain)*	**Domain description**
201,879	BROAD	Broadcast orbits
137,210	IGS	International GNSS Service
43,271	PCISE	Precise (source not specified)
36,326	NGS	National Geodetic Survey
41	NGS-P	National Geodetic Survey
386	PNGS	National Geodetic Survey
171	PNGSP	National Geodetic Survey
92	PNGSX	National Geodetic Survey
25	PNGSL	National Geodetic Survey
3,830	NSWC	Naval Surface Warfare Center
1,441	DMA	Defense Mapping Agency
380	SIO	Scripps Institution of Oceanography
311	JPL	Jet Propulsion Laboratory
579	AEROS	Software-specific (Aeros AIMS)
452	BIOA	Software-specific (Trimble TRIMVEC)
179	<NULL>	No orbit source provided

Count	Field name and text attributes (for defined domains and free-form text)
	CommentGen *(all unique text strings in free-form comment field)*
3,165	Constrained 3D residual > 4X larger than free
145	TBC vectors with erroneous covariance values
8	Vector excluded (from 1 mark in AK to CONUS)
2	Vector excluded (from 1 mark in AK to Hawaii)
5	Null geometry (endpoints have same coords)
32	Vector line crosses 180 degrees longitude
	Comment_BL *(all unique text strings in free-form comment field)*
3,741	Baseline vector lengths differ by 0.1-0.5 m
440	Baseline vector lengths differ by 0.5-1 m
350	Baseline vector lengths differ by 1-10 m
80	Baseline vector lengths differ by 10-100 m
53	Baseline vector lengths differ by 100-1000 m
6	Baselines vector lengths differ by > 1000 m
	ComentTime *(all unique text strings in free-form comment field)*
528	Time value suspect (hr > 24 or min > 60)
210	Time value suspect (duration <= 3 min)
67	Time value suspect (duration > 5 days)
68	Time value suspect; Edited start & stop time
18	Time value suspect; Edited start time
1	Time value suspect; Edited stop time
139	Date value suspect; Edited end date
34	Date value suspect; Edited start & stop date
9	Date value suspect; Edited start date

Appendix C. Properties of NA2011 Constrained MYCS1 CORSs GIS Feature Classes

The NA2011 constrained MYCS1 CORSs GIS feature classes are point features provided in Esri file geodatabase format version 10.7, available at ftp://geodesy.noaa.gov/pub/NA2011/. Because the data are referenced to three different NAD 83 frames, the features are separated into three feature datasets corresponding to that particular frame. An ArcMap v10.7 document (*.mxd file) that reference the features are included. A "ReadMe.pdf" file in the root of the folder describes the contents and organization.

Feature classes are also provided in Esri shapefile formats with the same field names and attributes. However, shapefiles do not support null fields or relationships between feature classes. Numeric null fields in shapefiles are populated with a value of -9999.

The features are also provided in Microsoft *Excel* format, with all three NAD 83 frames combined into in a single file.

Note: The constrained MYCS1 CORS coordinates in this dataset are the same as the values published at the time these coordinates were originally determined. They are not the same as the adjusted values, because stochastic constraints were used. Although the adjusted coordinates of the constrained MYCS1 CORSs were not published, they are available (see Appendix A).

General characteristics of the constrained MYCS1 CORSs GIS feature classes

- Feature geometry: Point
- Number of features: 1195 points split into three feature classes based on the NAD 83 frame of the coordinates, all at epoch 2010.00 (January 1, 2010):
  - NAD 83 (2011): Referenced to the North America tectonic plate (1171 points)
  - NAD 83 (PA11): Referenced to the Pacific tectonic plate (18 points)
  - NAD 83 (MA11): Referenced to the Mariana tectonic plate (6 points)
- Number of fields: 27 (defined in Table C1)
- Data types: Short integer, Float, Double, Text
- Domains used for 6 text fields (defined in Table C2)
- Geometry does not support M values (route data) or Z values (3D data)

Table C1. Data field attribute definitions of NA2011 constrained MYCS1 CORS GIS feature classes.

Field name	Field alias	Data type	Field description
CORS_ID	CORS ID	Text (4)	4-character CORS identification code
PID	Permanent ID	Text (6)	NGS permanent identifier for the mark
Mark_name	Mark name (designation)	Text (40)	Name of mark (also called designation)
NAD83frame	NAD 83 frame	Text (13)	NAD 83 frame of the coordinates (3 domain values; see description in table below)
Lat_DMS	Latitude (DMS)	Text (13)	Published MYCS1 latitude (degrees-minutes-seconds)
Lon_DMS	Longitude (DMS)	Text (14)	Published MYCS1 longitude (degrees-minutes-seconds)
Lat_DecDeg	Latitude (dec deg)	Double	Published MYCS1 latitude (decimal degrees)
Lon_DecDeg	Longitude (dec deg)	Double	Published MYCS1 longitude (decimal degrees)
Elpsd_ht	Ellipsoid height (m)	Double	Published MYCS1 ellipsoid height (meters)
Acc95_hor	Accuracy hor 95% conf (cm)	Float	Horizontal (circular) accuracy at 95% confidence (cm)
Acc95_eht	Accuracy eht 95% conf (cm)	Float	Ellipsoid height accuracy at 95% confidence (cm)
Sigma_N	Sigma north (cm)	Float	Standard deviation in latitude (cm)
Sigma_E	Sigma east (cm)	Float	Standard deviation in longitude (cm)
Sigma_U	Sigma up (cm)	Float	Standard deviation in ellipsoid height (cm)
Correl_NE	Correlation north-east	Double	Horizontal (north-east) correlation coefficient (unitless)
vN_cm_yr	Vel north (cm/yr)	Float	Velocity north (cm per year)
vE_cm_yr	Vel east (cm/yr)	Float	Velocity east (cm per year)
vU_cm_yr	Vel up (cm/yr)	Float	Velocity up (cm per year)
State	State	Text (2)	2-letter abbreviation of state or territory where station located
Network	Network	Text (15)	Network where MYCS1 coordinates used as constraints (6 domain values; see description in table below)
MYCS_type	MYCS type	Text (8)	Type of MYCS1 coordinate (2 domain values; see description in table below)
CORSsource	CORS ID source	Text (10)	Source used to identify MYCS1 CORS ID (3 domain values; see description in table below)
CORS_RefPt	CORS reference point	Text (8)	Physical point where MYCS1 coordinates referenced (3 domain values; see description in table below)
Mon_offset	Mon to ARP offset (m)	Float	Offset from ARP to external monument (m); positive if below ARP
RefPtBasis	Reference point basis	Text (16)	Basis of reference point source for MYCS1 coordinates (4 domain values; see description in table below)
Num_RefPts	Num ref points used	Short integer	Number of different reference points used for each MYCS1 CORS ID
Comments	Comments	Text (40)	Miscellaneous comments (5 unique comments shown in table below)

Table C2. Domains of text data field attributes and free-form text fields of MYCS1 feature classes.

Count	Field name and text attributes (for defined domains and free-form text)	
	NAD83frame *(domain)*	**Domain description**
1,171	NAD 83 (2011)	Referenced to the North America tectonic plate
18	NAD 83 (PA11)	Referenced to the Pacific tectonic plate
6	NAD 83 (MA11)	Referenced to the Mariana tectonic plate
	Network *(domain)*	**Domain description**
1,068	CONUS Primary	MYCS1 coordinates used as constraints only for CONUS Primary network
16	CONUS Secondary	MYCS1 coordinates used as constraints only for CONUS Secondary network
29	CONUS Both	MYCS1 coordinates used as constraints only for both CONUS networks
58	Alaska	MYCS1 coordinates used as constraints for Alaska network
18	Pacific_PA11	MYCS1 coordinates used as constraints for PA11 coordinates in Pacific network
6	Pacific_MA11	MYCS1 coordinates used as constraints for MA11 coordinates in Pacific network
	MYCS_type *(domain)*	**Domain description**
973	Computed	Coordinates based on velocities computed from GPS data
222	Modeled	Coordinates based on velocities modeled using NGS HTDP software
	CORSsource *(domain)*	**Domain description**
1,019	MYCS	MYCS1 CORS ID obtained directly from MYCS results
73	NGSIDB	MYCS1 CORS ID determined from NGSIDB
103	Inferred	MYCS1 CORS ID inferred from location, designation, or other information
	CORS_RefPt *(domain)*	**Domain description**
865	ARP	MYCS1 coordinates referenced to Antenna Reference Point
175	Monument	MYCS1 coordinates referenced to external monument
155	L1 APC	MYCS1 coordinates referenced to L1 antenna phase center
	RefPtBasis *(domain)*	**Domain description**
1,016	MYCS CORS	Based on PID associated with MYCS1
78	Previous PID	Based on PID previously used for CORS
96	Old antenna	Based on PID of antenna previously used for CORS
5	IGS station only	Based on PID for IGS station that was not part of CORS network

Count	Field name and text attributes (for defined domains and free-form text)
	Comments *(all unique text strings in free-form comment field)*
9	Coordinates determined in April 2012
1	PID associated with CORS ID = GOL0
1	PID associated with CORS ID = LROC
1	PID associated with CORS ID = SHK0

Appendix D. Properties of the NA2011 GPS Project GIS Feature Classes

The NA2011 GPS project GIS feature classes are point features provided in Esri file geodatabase format version 10.7, available at ftp://geodesy.noaa.gov/pub/NA2011/. Because the data are referenced to three different NAD 83 frames, the features are separated into three feature datasets corresponding to that particular frame. The GPS project feature classes referenced to NAD 83 (PA11) and NAD 83 (MA11) are identical, because the same projects (and vectors) were used in both the PA11 and MA11 networks (but with different constraints). An ArcMap v10.7 document (*.mxd file) that reference the features are included. A "ReadMe.pdf" file in the root of the folder describes the contents and organization.

Feature classes are also provided in Esri shapefile formats with the same field names and attributes. However, shapefiles do not support a date field that also includes time, so time is stored in its own field separate from the date. In addition, shapefiles do not support null fields or relationships between feature classes. Numeric null fields in shapefiles are populated with a value of -9999.

The features are also provided in Microsoft *Excel* format, with all three NAD 83 frames combined into in a single file. The Pacific frames NAD 83 (PA11) and (MA11) are shown as "NAD 83 (PA11/MA11)" to indicate that these projects are used in both frames.

General characteristics of the NA2011 adjusted control mark GIS feature classes

- Feature geometry: Point
- Number of features: 4267 points in three feature classes based on the NAD 83 frame of the coordinates, all at epoch 2010.00 (January 1, 2010):
  - NAD 83 (2011): Referenced to the North America tectonic plate (4228 points)
  - NAD 83 (PA11): Referenced to the Pacific tectonic plate (39 points); identical to NAD 83 (MA11) feature class except for spatial reference
  - NAD 83 (MA11): Referenced to the Mariana tectonic plate (39 points); identical to NAD 83 (PA11) feature class except for spatial reference
- Number of fields: 36 (defined in Table D1).
- Data types: Short integer, Float, Double, Date/time, Text
- Domains used for 3 text fields (defined in Table D2)
- Geometry does not support M values (route data) or Z values (3D data)
- Shapefile versions have time in separate field from date

Table D1. Data field attribute definitions of the NA2011 GPS project GIS feature classes.

Field name	Field alias	Data type	Field description
Project_ID*	GPS project ID*	Text (11)	Unique GPS project identifier, usually as "GPS" appended with sequential project number
Proj_num*	Proj number*	Short integer	Numerical part of GPS project ID, following the abbreviation "GPS" for most projects
Proj_part	Proj part	Text(4)	Letter or number proceeded by "/" and appended to project ID when project split into parts
Block	Helmert block	Text(14)	Helmert block code based on nominal GPS project location by state or part of state (69 total)
Date_start	Date/time start	Date/time	Start date and time of first occupation in project (based on vector sessions)
Date_end	Date/time end	Date/time	End date and time of last occupation in project (based on vector sessions)
Duration_d	Duration (days)	Double	Duration of project (days)
Date_midpt	Date/time midpoint	Date/time	Midpoint date and time of all vector processing session in project
EpochMidpt	Epoch midpoint (dec yr)	Double	Epoch of midpoint time of all vector processing session in project (decimal year)
Year_start	Year start	Short integer	Year corresponding to start date and time of project
Year_end	Year end	Short integer	Year corresponding to end date and time of project
Year_midpt	Year midpoint	Short integer	Year corresponding to midpoint of project
NAD83frame	NAD 83 frame	Text (13)	NAD 83 frame of project (3 domain values; see description in table below)
Lat _proj	Project mean lat (dec deg)	Double	Project latitude based on mean latitude of vector midpoints (decimal degrees)
Lon _proj	Project mean lon (dec deg)	Double	Project longitude based on mean longitude of vector midpoints (decimal degrees)
Num_marks	Num marks	Short integer	Total number of marks observed in project
VecsEnable	Num vectors enabled	Short integer	Number of enabled vectors in project
VecsReject	Num vectors rejected	Short integer	Number of rejected vectors in project
VecsTotal	Num vectors total	Short integer	Total number of vectors in project
FracReject	Fraction vecs rejected	Float	Proportion of rejected vectors (ratio of rejected to total number of vectors)
VecLenMed	Median vector length (m)	Double	Median vector length for project, mark-to-mark (meters)
VecLenMean	Mean vector length (m)	Double	Mean vector length for project, mark-to-mark (meters)
VecLenMin	Min vector length (m)	Double	Minimum vector length for project, mark-to-mark (meters)
VecLenMaz	Max vector length (m)	Double	Maximum vector length for project, mark-to-mark (meters)
DurMed_hr	Median session dur (hr)	Float	Median duration of vector processing session for project (hours)
DurMean_hr	Mean session dur (hr)	Float	Mean duration of vector processing session for project (hours)
DurMin_hr	Min session dur (hr)	Float	Minimum duration of vector processing session for project (hours)

Field name	Field alias	Data type	Field description
DurMax_hr	Max session dur (hr)	Float	Maximum duration of vector processing session for project (hours)
Agency	Agency	Text (6)	Lead agency or organization that performed processing for project (226 unique abbreviations)
2007status	2007 status	Text (21)	Status of project for 2007 national adjustment (5 domain values; see description in table below)
VS_horiz	Variance scalar horiz	Float	Horizontal variance scalar (factor) applied to vector standard deviations for project
VS_vert	Variance scalar vert	Float	Vertical variance scalar (factor) applied to vector standard deviations for project
VS_3D	Variance scalar 3D	Float	3D variance scalar (factor) computed from horizontal and vertical scalars
VS_HVratio	VS horz/vert ratio	Float	Ratio of horizontal to vertical variance scalar for project
Network**	Network**	Text (9)	Network in which project was adjusted (4 domain values; see description in table below)
Comments	Comments	Text (40)	Various comments about GPS projects (8 unique comments, as shown in table below)

*NGS now uses a 4-digit number for projects, with zero-padding for project numbers of less than 1000.
**Pacific not split into PA11 and MA11 networks, because all Pacific projects were in both networks (different constraints were used)

Table D2. Domains of text data field attributes and free-form text fields of GPS project feature classes.

Count	Field name and text attributes (for defined domains and free-form text)	
	NAD83frame *(domain)*	**Domain description**
4,228	NAD 83 (2011)	Referenced to the North America tectonic plate
39	NAD 83 (PA11)	Referenced to the Pacific tectonic plate
39	NAD 83 (MA11)	Referenced to the Mariana tectonic plate
	2007status *(domain)*	**Domain description**
3,417	Used in 2007	Project also used in 2007 national adjustment
810	After 2007 cutoff	Project not used in 2007 national adjustment because received after cutoff date
1	Skipped in 2007	Project available but not used in 2007 national adjustment
38	Not in 2007 (Pacific)	Project not used in 2007 national adjustment because located in the Pacific
1	Used GPS1753	Project GPS1753 was replaced by reprocessed version GPS1753/C for NA2011
	Network *(domain)*	**Domain description**
3,472	Primary	GPS projects in CONUS Primary network
614	Secondary	GPS projects in CONUS Secondary network
142	Alaska	GPS projects in Alaska network
39	Pacific	GPS projects in Pacific network (both PA11 and MA11)

Count	Field name and text attributes (for defined domains and free-form text)
	Comments *(all unique text strings in free-form comment field)*
116	Moved to Secondary
16	Moved to Primary
34	Accidentally skipped; later restored
11	Project added 2011-Dec
4	Project added 2012-Feb
28	Project added 2012-Mar
1	Removed 7952 of 9953 vectors
2	Used reprocessed version for NA2011

Appendix E. Software used to process GNSS vectors stored in the NGSIDB

Table E1. Software used to perform GNSS baseline processing for vectors used in the NA2011 Project.

GNSS processing software	Year of earliest use	Year of latest use	Number of vectors	Percent of vectors
Trimble GPSurvey	1990	2011	126,747	29.842%
Trimble Geomatics Office	2000	2011	84,582	19.915%
Trimble TRIMVEC	1986	1997	69,970	16.474%
PAGES	1996	2011	62,289	14.666%
OMNI	1987	1999	26,467	6.232%
Leica Geomatics Office	2004	2010	13,355	3.144%
Leica SKI Pro	1992	2007	12,044	2.836%
LINECOMP	1989	1997	8,820	2.077%
Ashtech Solutions	2002	2010	3,738	0.880%
Topcon Tools	2003	2009	3,122	0.735%
GAMIT	1991	2000	2,488	0.586%
PINNACLE	1999	2005	2,409	0.567%
GPPS	1987	1996	1,100	0.259%
AIMS	1986	1990	1,010	0.238%
PHASER	1984	1988	818	0.193%
Geohydro	1983	1987	780	0.184%
Trimble WAVE	1993	2001	780	0.184%
Trimble Total Control	2003	2011	722	0.170%
PNAV	1997	1998	582	0.137%
K & RS	1992	1992	496	0.117%
Remondi	1995	1995	459	0.108%
MAGNET	1985	1988	376	0.089%
SONAP	1990	1991	260	0.061%
Geodetics RTD	2000	2002	256	0.060%
PRISM	1995	1998	213	0.050%
LSQ	1983	1986	200	0.047%
TSS	1995	1996	153	0.036%
MGPS	1995	1995	144	0.034%
AOS	1997	1998	138	0.032%
GeoGenius	1998	1998	78	0.018%
Trimble Business Center	2011	2011	65	0.015%
DIPOP	1986	1986	40	0.009%
POPS	1990	1990	17	0.004%
RSGPS	2007	2007	3	0.001%